NOVEL INSIGHTS INTO INSECT ANTIVIRAL IMMUNITY

EDITED BY: Liang Jiang, Xiao-Qiang Yu and Luc Swevers
PUBLISHED IN: Frontiers in Immunology and Frontiers in Physiology

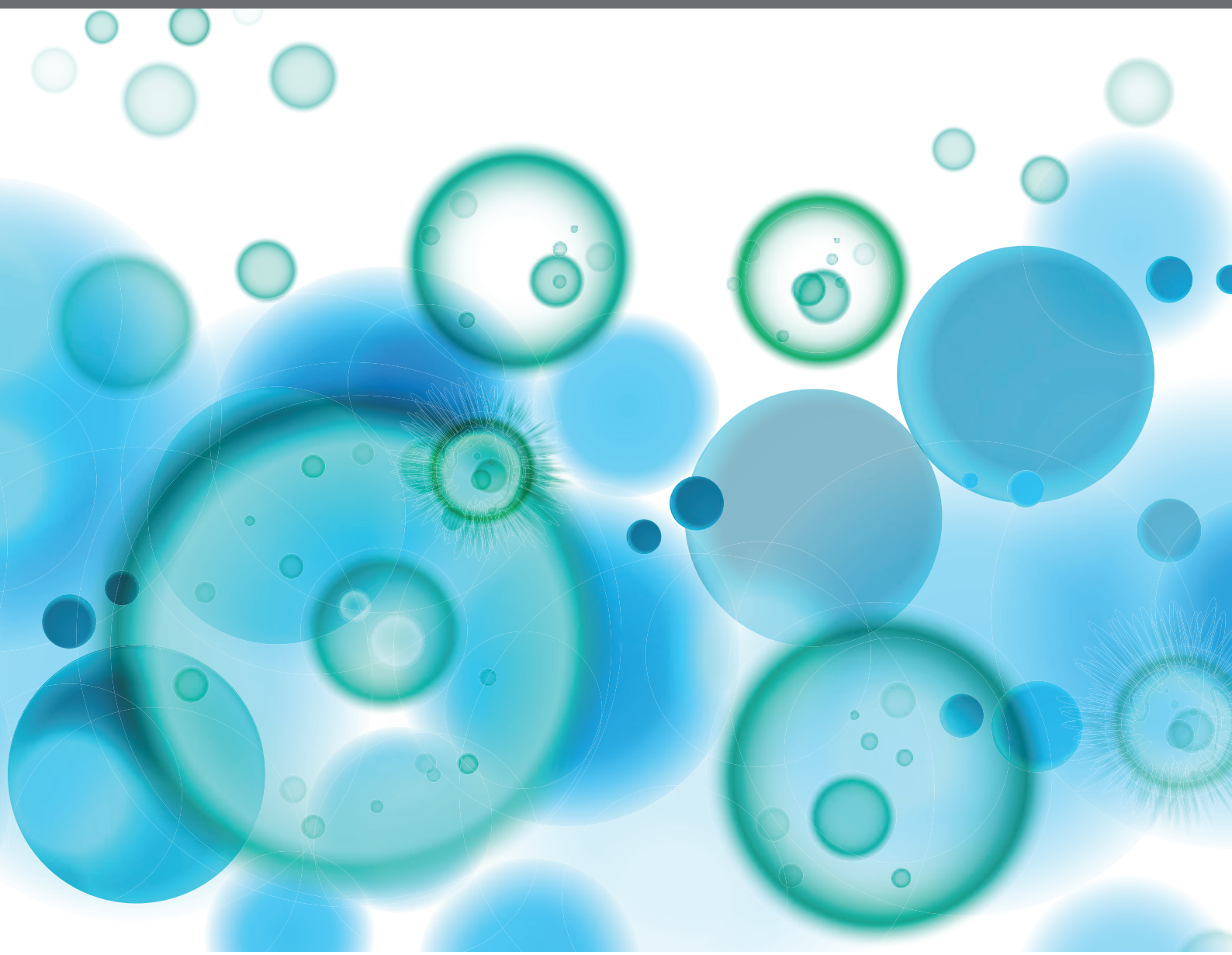

frontiers Research Topics

ISSN 1664-8714
ISBN 978-2-88974-410-7
DOI 10.3389/978-2-88974-410-7

About Frontiers

Frontiers is more than just an open-access publisher of scholarly articles: it is a pioneering approach to the world of academia, radically improving the way scholarly research is managed. The grand vision of Frontiers is a world where all people have an equal opportunity to seek, share and generate knowledge. Frontiers provides immediate and permanent online open access to all its publications, but this alone is not enough to realize our grand goals.

Frontiers Journal Series

The Frontiers Journal Series is a multi-tier and interdisciplinary set of open-access, online journals, promising a paradigm shift from the current review, selection and dissemination processes in academic publishing. All Frontiers journals are driven by researchers for researchers; therefore, they constitute a service to the scholarly community. At the same time, the Frontiers Journal Series operates on a revolutionary invention, the tiered publishing system, initially addressing specific communities of scholars, and gradually climbing up to broader public understanding, thus serving the interests of the lay society, too.

Dedication to Quality

Each Frontiers article is a landmark of the highest quality, thanks to genuinely collaborative interactions between authors and review editors, who include some of the world's best academicians. Research must be certified by peers before entering a stream of knowledge that may eventually reach the public - and shape society; therefore, Frontiers only applies the most rigorous and unbiased reviews.
Frontiers revolutionizes research publishing by freely delivering the most outstanding research, evaluated with no bias from both the academic and social point of view. By applying the most advanced information technologies, Frontiers is catapulting scholarly publishing into a new generation.

What are Frontiers Research Topics?

Frontiers Research Topics are very popular trademarks of the Frontiers Journals Series: they are collections of at least ten articles, all centered on a particular subject. With their unique mix of varied contributions from Original Research to Review Articles, Frontiers Research Topics unify the most influential researchers, the latest key findings and historical advances in a hot research area! Find out more on how to host your own Frontiers Research Topic or contribute to one as an author by contacting the Frontiers Editorial Office: frontiersin.org/about/contact

NOVEL INSIGHTS INTO INSECT ANTIVIRAL IMMUNITY

Topic Editors:
Liang Jiang, Southwest University, China
Xiao-Qiang Yu, University of Missouri–Kansas City, United States
Luc Swevers, National Centre of Scientific Research Demokritos, Greece

Citation: Jiang, L., Yu, X.-Q., Swevers, L., eds. (2022). Novel Insights Into Insect Antiviral Immunity. Lausanne: Frontiers Media SA. doi: 10.3389/978-2-88974-410-7

Table of Contents

frontiers in Immunology

EDITORIAL
published: 10 January 2022
doi: 10.3389/fimmu.2021.740989

Editorial: Novel Insights Into Insect Antiviral Immunity

Liang Jiang[1,2*†], *Xiao-Qiang Yu*[3,4†] *and Luc Swevers*[5†]

[1] State Key Laboratory of Silkworm Genome Biology, Chongqing Key Laboratory of Sericultural Science, Chongqing Engineering And Technology Research Center for Novel Silk Materials, Southwest University, Chongqing, China, [2] Biological Science Research Center, Southwest University, Chongqing, China, [3] Guangdong Provincial Key Laboratory of Insect Developmental Biology and Applied Technology, Institute of Insect Science and Technology, School of Life Sciences, South China Normal University, Guangzhou, China, [4] Division of Cell Biology and Biophysics, School of Biological and Chemical Sciences, University of Missouri-Kansas City, Kansas City, MO, United States, [5] Insect Molecular Genetics and Biotechnology, Institute of Biosciences and Applications, National Centre for Scientific Research Demokritos, Athens, Greece

Keywords: insect, virus, infection, immunity, antiviral

Editorial on the Research Topic

Novel Insights into Insect Antiviral Immunity

Insects are the largest group of animals distributed throughout the earth, including economically important insects (e.g. silkworms, honeybees, pollinators), agricultural and forestry pests (e.g. locusts, stink bugs, armyworms, weevils), virus vectors (e.g. mosquitoes, midges, blackflies), and model organisms (e.g. *Drosophila* in genetics and developmental biology). Viruses are the major pathogens of insects; however, the mechanism of viral infection and antiviral insect immunity is not fully understood. The 15 articles of this Research Topic highlight the latest advances regarding insect antiviral immunity.

Five contributions refer to the interaction between baculovirus and insect host. Jiang et al. reviewed the arms race between silkworm and baculovirus, including the baculovirus invasion mechanism, the silkworm immune response and the viral immune evasion mechanism, and surveyed strategies for the enhancement of host antiviral capacity. The authors also discussed outstanding major issues and future directions of research on silkworm antiviral immunity. Melanization is mediated by the prophenoloxidase (PPO) pathway, which is an important humoral response for killing invading pathogens in insects. Wang et al. identified a conserved PPO activation pathway in *Helicoverpa armigera* and confirmed that the three-step SP41/cSP1/cSP6 cascade can convert PPO into active phenoloxidase (PO), and that the cofactors cSPH11 and cSPH50 can enhance PO activity activated by cSP6. An *in vitro* reconstituted PPO activation cascade can block baculovirus infection, indicating the importance of melanization in controlling baculovirus infection. Baculovirus is characterized by a restricted host range: the silkworm is permissive for BmNPV infection but is a non-permissive host for AcMNPV. Lin et al. found that adenosine signaling was upregulated to enhance host energy levels after infection with non-permissive AcMNPV, and that inhibition of the adenosine receptor (*AdoR*), glycolysis and adenosine transport can decrease ATP content and increase AcMNPV proliferation in BmN cells, suggesting that *AdoR* modulates permissiveness of baculovirus infection *via* regulation of energy metabolism in the silkworm. Viruses also regulate the development and protein modifications of their hosts. Previous studies have shown that newly exuviated fifth instar silkworms infected with BmNPV exhibit delayed maturation. Results from Xu et al. further indicated that day-4 fifth instar larvae infected with BmNPV showed an increase in

OPEN ACCESS

Edited and reviewed by:
Miki Nakao,
Kyushu University, Japan

***Correspondence:**
Liang Jiang,
jiangliang@swu.edu.cn

†These authors have contributed equally to this work

Specialty section:
This article was submitted to Comparative Immunology, a section of the journal Frontiers in Immunology

Received: *14 July 2021*
Accepted: *20 December 2021*
Published: *10 January 2022*

Citation:
Jiang L, Yu X-Q and Swevers L (2022) Editorial: Novel Insights Into Insect Antiviral Immunity. Front. Immunol. 12:740989. doi: 10.3389/fimmu.2021.740989

ecdysone titer and precocious maturation, and RNA-seq was further used to analyze the candidate genes involved in this process. Mao et al. investigated the effect of HSC70-4 deacetylation on BmNPV infection. The authors found that lysine 77 (K77) deacetylation promoted the stability and nuclear import of HSC70-4 and viral proliferation, and that this process may be modulated by the ubiquitin proteasome system.

Some insects serve as vectors to transmit viruses, which adversely affect agricultural production (for plant viruses) and spread human diseases (for arboviruses). Five papers focus on the molecular mechanisms underlying the interactions between viruses and insect vectors. Zhao et al. investigated the proteomic interactions between tomato yellow leaf curl virus (TYLCV) and its whitefly vector and found that the whitefly protein Tid interacted with the coat protein of TYLCV. Tid protein content was increased following viral acquisition, and inhibition of Tid resulted in increased TYLCV replication in whitefly, suggesting the inhibitory role of Tid on viral infection. He et al. found that Toll pathway core genes (*Toll*, *MyD88*, and *Dorsal*) were upregulated in the planthopper vector after infection with rice stripe virus (RSV), and observed direct interactions between the viral nucleocapsid protein and the Toll receptor. RNAi of *Toll* led to increased RSV proliferation and mortality in planthoppers, indicating the antiviral defense of the Toll pathway against the plant virus in the planthopper vector. Many flaviviruses are arboviruses and major human pathogens, including Dengue virus (DENV), Zika virus (ZIKV), West Nile virus, and Yellow Fever virus. Harsh and Eleftherianos summarized recent studies about flavivirus infections and antiviral immune mechanisms and discussed the host tissue homeostasis and pathophysiological defects in mosquitoes and the model insect *Drosophila*. Leite et al. investigated the distinct functional roles of hemocytes at different stages of infection by DENV and ZIKV in mosquitoes. The authors showed that hemocytes were recruited to the midgut in response to virus and that blocking phagocytosis led to decreased viral replication in the midgut. By contrast, phagocytosis by hemocytes was essential to restrict viral dissemination during systemic infection. Results from Weng et al. showed that *TEP1* transcription was induced in mosquitoes following DENV infection, and silencing of *TEP1* resulted in decreased expression of the transcription factor Rel2 and certain antimicrobial peptides (AMPs) as well as increased viral content, suggesting that TEP1 regulates the immune response and consequently limits DENV infection in mosquitoes.

Four other contributions have topics that deal more generally with antiviral pathways and effector molecules. The first topic highlights intracellular and extracellular degradation as crucial for restricting viral infection. Jiang reviewed the main antiviral immune pathways and the virus-modulated signaling pathways in the silkworm; the former includes RNAi and signaling pathways mediated by NF-κB, Imd, STING and JAK/STAT while the latter includes the PPO, PI3K/Akt, and ERK pathways. Targeting these virus-modulated pathways by gene editing or inhibitors can enhance host antiviral capacity. Feng et al. reviewed the roles of (both validated and potential) AMPs in insect antiviral immune response and their possible mechanisms of synthesis and action. A second topic emphasizes the requirement for intercellular communication to mount systemic immune responses. Wang summarized the intercellular communications in insect antiviral immunity, including protein-based and virus-derived RNA-based cell-cell communications, and focusing on the signaling pathway that induces the production of potential cytokines. Another article focuses on the symbiont *Wolbachia*, a maternally transmitted bacterium in insects, which was recently discovered to protect insects against RNA viruses. Pimentel et al. described the main advances and possible mechanisms of the antiviral effect of *Wolbachia*. The authors also discussed the potential antiviral effect of *Wolbachia* in wild insect populations and its ecological relevance.

A final article presented by Lin et al. also adds a piece of interesting data on the regulation of host genes by virus-encoded miRNAs. The authors showed that the expression levels of BmCPV-miR-1 and BmCPV-miR-3 were increased while their common target host gene *BmRan* was inhibited in silkworms infected with cypovirus. It is proposed that the two miRNAs can inhibit *BmRan* expression and promote viral proliferation.

In summary, all published articles describe exciting new data of insect immunity against viral infection and provide new mechanisms of resistance and targets for pest control that can also have relevance for antiviral research in humans.

AUTHOR CONTRIBUTIONS

All authors listed have made a substantial, direct and intellectual contribution to the work, and approved it for publication.

FUNDING

This work was funded by the National Natural Science Foundation of China (No. 32170524 and No. 31970474) and the Natural Science Foundation of Chongqing, China (cstc2020jcyj-cxttX0001). Luc Swevers acknowledges support of this work by the project 'An Open-Access Research Infrastructure of Chemical Biology and Target-Based Screening Technologies for Human and Animal Health, Agriculture and the Environment (OPENSCREEN-GR)' (MIS 5002691) which is implemented under the Action 'Reinforcement of the Research and Innovation Infrastructure', funded by the Operational Programme 'Competitiveness, Entrepreneurship and Innovation' (NSRF 2014-2020) and co-financed by Greece and the European Union (European Regional Development Fund).

frontiers in Immunology

ORIGINAL RESEARCH
published: 28 April 2020
doi: 10.3389/fimmu.2020.00763

Adenosine Receptor Modulates Permissiveness of Baculovirus (Budded Virus) Infection via Regulation of Energy Metabolism in *Bombyx mori*

Yu-Hsien Lin[1,2†], Chia-Chi Tai[3†], Václav Brož[1], Cheng-Kang Tang[3], Ping Chen[3], Carol P. Wu[3], Cheng-Hsun Li[3] and Yueh-Lung Wu[3]*

[1] Biology Centre of the Czech Academy of Science, Institute of Entomology, Ceske Budejovice, Czechia, [2] Faculty of Science, University of South Bohemia, Ceske Budejovice, Czechia, [3] Department of Entomology, National Taiwan University, Taipei, Taiwan

OPEN ACCESS

Edited by:
Liang Jiang,
Southwest University, China

Reviewed by:
Wolfgang Ernst,
University of Natural Resources and Life Sciences Vienna, Austria
Bergmann Morais Ribeiro,
University of Brasilia, Brazil
Steven Reid,
University of Queensland, Australia

***Correspondence:**
Yueh-Lung Wu
runwu@ntu.edu.tw

† These authors have contributed equally to this work

Specialty section:
This article was submitted to Comparative Immunology, a section of the journal Frontiers in Immunology

Received: *09 January 2020*
Accepted: *03 April 2020*
Published: *28 April 2020*

Citation:
Lin Y-H, Tai C-C, Brož V, Tang C-K, Chen P, Wu CP, Li C-H and Wu Y-L (2020) Adenosine Receptor Modulates Permissiveness of Baculovirus (Budded Virus) Infection via Regulation of Energy Metabolism in Bombyx mori. Front. Immunol. 11:763. doi: 10.3389/fimmu.2020.00763

Although the modulation of host physiology has been interpreted as an essential process supporting baculovirus propagation, the requirement of energy supply for host antivirus reactions could not be ruled out. Our present study showed that metabolic induction upon AcMNPV (budded virus) infection of *Bombyx mori* stimulated virus clearance and production of the antivirus protein, gloverin. In addition, we demonstrated that adenosine receptor signaling (AdoR) played an important role in regulating such metabolic reprogramming upon baculovirus infection. By using a second lepidopteran model, *Spodoptera frugiperda* Sf-21 cells, we demonstrated that the glycolytic induction regulated by adenosine signaling was a conservative mechanism modulating the permissiveness of baculovirus infection. Another interesting finding in our present study is that both BmNPV and AcMNPV infection cause metabolic activation, but it appears that BmNPV infection moderates the level of ATP production, which is in contrast to a dramatic increase upon AcMNPV infection. We identified potential *AdoR* miRNAs induced by BmNPV infection and concluded that BmNPV may attempt to minimize metabolic activation by suppressing adenosine signaling and further decreasing the host's anti-baculovirus response. Our present study shows that activation of energy synthesis by adenosine signaling upon baculovirus infection is a host physiological response that is essential for supporting the innate immune response against infection.

Keywords: glycolysis, baculovirus, adenosine signaling, gloverin, *Bombyx mori*, *Spodoptera frugiperda*

INTRODUCTION

Baculoviruses are double-stranded circular DNA viruses with genomes of ∼80–180 kb. Baculoviruses can infect many species of arthropods, among which lepidopteran larvae are the most common host (1, 2). *Autographa californica* nucleopolyhedrovirus (AcMNPV) is the most thoroughly studied baculovirus, and it has been established as the primary baculovirus expression system since the 1980's (3). Another commonly studied baculovirus is *Bombyx mori* nucleopolyhedrovirus (BmNPV), which is also used to express

exogenous recombinant proteins (4). Although AcMNPV and BmNPV have highly similar genetic structures, they have very different host ranges (5, 6). AcMNPV is able to infect the broader range of lepidopteran larvae but has a lower capacity to infect *B. mori*, whereas BmNPV can only infect *B. mori* and is not capable of infecting the larvae of other Lepidoptera species (1, 7, 8).

Baculovirus infection has significant impacts on host physiology, establishing optimal conditions for successful propagation. Several virus-encoded proteins or microRNAs that regulate the host cell cycle, apoptosis, cytoskeleton rearrangement, immune responses, and membrane receptors have been reported for different baculoviruses (9). In addition, virus growth relies heavily on host resources, and the distribution and transfer of energy in hosts are important factors that affect viral replication. Studies of BmNPV and AcMNPV have demonstrated that baculovirus infection significantly increases the oxygen consumption and tricarboxylic acid (TCA) cycle activity in the permissive host (10–12). Increased expression of metabolic pathway genes, such as citrate synthase and pyruvate dehydrogenase, as well as genes involved in mitochondrial respiration, has been observed in AcMNPV- and BmNPV-infected cells (13).

Although intensification of host biosynthesis by viruses can provide sufficient substrates for virus replication, the host can also modulate its own metabolic activity to restrict viral propagation. For example, expression of *samhd1* in human myeloid cells decreases the dNTP pool, limiting reverse transcription and suppressing virus replication (14), and induction of interferon upon virus infection disrupts sterol biosynthesis and suppresses viral replication (15). In addition, increased metabolic activity during infection might prompt the immune response against pathogens. Transcriptomic and biochemical studies in fruit fly, tobacco budworm, cockroach, and mosquito demonstrate that genes involved in energy synthesis, detoxification, and carbohydrate metabolism are upregulated upon bacterial or fungal infection and that inhibition of host carbohydrate metabolism decreases the immune response against pathogens (16–20). The molecular mechanism involved in the systematic switch of metabolic homeostasis upon infection was described recently in *Drosophila melanogaster*. Upon bacterial and parasitic wasp infection, *Drosophila* immune cells release adenosine as a signal to activate metabolic reprogramming, which shifts energy distribution from developmental processes toward the immune response (19, 21).

Although previous studies have reported that energy production is induced after infection in both BmNPV-infected BmN cells and AcMNPV-infected Sf-9 cells, it is unclear whether this phenomenon is restricted to permissive infection conditions (11, 12). Moreover, it could not be ruled out that metabolic induction might contribute to the host immune response against virus infection. Therefore, in this study, we compared the metabolic responses of BmN cells and *B. mori* larvae upon non-permissive (by AcMNPV) and permissive (by BmNPV) infection conditions. We also performed functional analysis by inhibiting glycolysis with 2-deoxy-D-glucose (2DG) treatment and examined the baculovirus infective capacity. Furthermore, through reverse genetic and pharmaceutical approaches, we identified that adenosine signaling is a conserved mechanism that regulates metabolic activation and gloverin expressions upon AcMNPV infection.

MATERIALS AND METHODS

B. mori Larvae, and Cells

B. mori strain is a tetramolted hybrid of (Kou × Fu) × (Nung × Feng) generated by Taiwan Sericultural Improvement Station, Miaoli, Taiwan. Larvae were fed mulberry leaves and housed in a growth chamber at a constant temperature of 26°C with a photoperiod of 16 h of light and 8 h of darkness (22).

The *S. frugiperda* cell line IPLB-Sf-21 and *B. mori* larval ovarian cell line BmN were cultured in TC-100 insect medium containing 10% fetal bovine serum (Gibco BRL) in an incubator at 26°C (1).

Titration of Budded Virus

Sf-21 and BmN cells were used for the reproduction of recombinant AcMNPV and BmNPV budded virus carrying the enhanced green fluorescent protein gene, respectively, TCID50 (50% tissue culture infectious dose) values and real-time quantitative PCR (RT-qPCR) were used to estimate viral titers (1, 23).

Nucleic Acid Extraction

RNA from infected cells (2×10^5 cells/well) or larvae was extracted using the TRIzol reagent (Invitrogen). Two third-instar larvae were pooled together for homogenization. OD values and RNA concentrations were detected using a microvolume spectrophotometer (Nanodrop 2000; Thermo Scientific) (24, 25). cDNA was synthesized using the PrimeScript™ RT reagent kit (Takara). Briefly, 500 ng of RNA was dissolved in ddH_2O (total volume of 6.5 μL), after which 2 μL of 5 × PrimeScript™ buffer, 0.5 μL of RT enzyme mix, 0.5 μL of oligo dT primers and 0.5 μL of random 6-mers (total volume, 10 μL) were added according to the manufacturer's instructions. The mixture was incubated at 37°C for 15 min for reverse transcription, after which the reaction was terminated by heating at 85°C for 5 s. The obtained product was stored at 4°C for subsequent analysis (1). The cDNA was quantified using a Nanodrop 2000 spectrophotometer.

Analysis of Gene Expression by RT-qPCR

RT-qPCR carried out with SYBR green (Bioline) and the ABI PlusOne real-time system (StepOnePlusTM, Applied Biosystems) was used for relative target gene quantification. Each sample contained 10 μL of SYBR green, 0.8 μL of primer, 1 μL of cDNA, and ddH_2O to adjust the total volume to 20 μL. A list of primer sequences used in this study is given in **Table S1**.

siRNA Cell Transfection

siRNAs were synthesized by MDBio Co. (siRNA-AdoR sequence: 5′-GCGUCU UGUUAGCUGCUUU-3′; siRNA-control sequence: 5′-AAUUCUCCGAACGUGUC ACGU-3′). BmN cells were seeded into a 24-well plate at a density of 2 × 105 cells per well and the cells were transfected with siRNAs (100 pmol) using the Lipofectamine RNAiMAX Reagent

(Invitrogen). RT-PCR analysis was carried out to determine the inhibition efficiency of siRNA-transfected cells at 48 h post transfection (hpt). After transfection for 24 h, AcMNPV and BmNPV infections were separately carried out at a multiplicity of infection (MOI) of 1. The cells and supernatants were harvested to detect viral titers and ATP levels at 48 h postinfection (1).

Pharmacological Treatment of BmN Cells, Sf-21 Cells, and Larvae

BmN and Sf-21 cells (2×10^5) were preincubated for 2 h with Dipy (20 μM), 2DG (10 mM), or adenosine (100 μM). Subsequently, the cells were infected with AcMNPV or BmNPV at a MOI of 1. Third-instar larvae were injected with AcMNPV (1×10^6 PFU/5 μL) and Dipy (20 mM, 5 μL) or AcMNPV (1×10^6 PFU/5 μL) and 2DG (0.5 mM, 5 μL). The supernatants or hemolymphs were harvested to detect viral titers and ATP levels at 48 h postinfection.

To assess the cytotoxicity, we treated the BmN and Sf-21 cells (2×10^5) with DMSO (0.05%), 2DG (10 mM), Dipy (20 μM) and adenosine (10 mM) for 24, 48, and 72 h in 12 well-pates, and cells were stained with propidium iodide (50 μg/mL). for labeling the dead cells. The quantification of live and dead cells was conducted by flow cytometry in the 585 ± 40 nM channel using ACEA NovoCyte™ 3,000, and 10,000 events were quantified for comparison. The results were shown in **Figure S1**.

B. mori Hemolymph Collection

Late third-instar larvae of *B. mori* were first placed in a −20°C freezer for 2 min to prevent the secretion of defensive fluids. The larval prolegs were cut off, and 10 μL hemolymph from one late third-instar larva was collected with a pipette and transferred to 1.5-mL centrifuge tubes. Hemocytes were removed by centrifugation at 3,000 × *g* for 1 min (26), after which the supernatant was collected to measure the ATP level. For the glucose, trehalose, and adenosine measurements, 10 μL hemolymph (without hemocyte) was first mixed with 40 μL of PBS, and 5 μL of hemolymph solution was used for analysis. Protein concentration of each sample was measured by Nanodrop (A280).

Glucose, Trehalose, and Adenosine Measurements

The levels of glucose, trehalose, and adenosine were determined in *B. mori* hemolymph using colorimetric methods with a glucose assay kit (Cell Biolabs, Inc.), trehalose microplate assay kit (Cohesion Biosciences, Ltd.), and adenosine assay kit (Fluorometric), respectively. The detailed procedures have been described previously (19).

ATP Analysis

The level of ATP in the samples was assessed using an ATP determination kit (Molecular Probes). Virus-infected BmN cells (2×10^5) were collected by centrifugation at 7,500 × g at 4°C for 1 min. Cells were lysed with 200 μL of cell culture lysis reagent (25 mM Tris-phosphate (pH 7.8), 2 mM DTT, 2 mM 1,2-diaminocyclohexane-N,N,N,N -tetraacetic acid, 10% glycerol, 1% Triton® X-100) and centrifuged at 14,000 rpm for 3 min to remove cell debris. To quantify ATP, 10 μL of collected supernatant or hemolymph was transferred to a 96-well black opaque plate that contained 90 μL of the standard assay solution. Standard solutions of ATP were prepared in the same manner. The reaction was carried out at 28°C, after which the relative light units (RLUs) of the sample and standard solution were simultaneously measured using a SpectraMax Gemini EM Microplate Reader at a maximum emission of 560 nm. A standard curve was plotted using the measured RLUs.

Statistical Analysis

The Ct values obtained from the RT-qPCR assay were normalized using the $2^{-\Delta\Delta Ct}$ method; the 18 S ribosomal RNA (rRNA) gene was used as the reference gene (27). Comparisons between two groups were performed using Student's *t*-test, with $P < 0.05$ indicating a significant difference (marked with an * in the figures). Significance between three groups was analyzed by ANOVA with Tukey's HSD *post-hoc* test, and different letters indicate significant differences ($P < 0.05$).

RESULTS

Different Responses of Glycolytic Gene Expressions and ATP Synthesis Upon Permissive and Non-permissive Infections

It is known that AcMNPV and BmNPV have similar genomic compositions but different host tropisms. To verify their infection capabilities in the present study, Sf-21 and BmN cells were infected with both viruses, and virus titers were calculated after 48 h of infection. The results showed that increased amounts of the viruses were only observed in the BmNPV-infected BmN cells or AcMNPV-infected Sf-21 cells (**Figure 1A**). Viral titers increased by ∼100-fold compared with the non-permissive infection at 48 h after infection. The results also showed that under *in vivo* conditions, increased viral titer were only observed in *Bombyx mori* larvae injected with BmNPV but not in those injected with AcMNPV (**Figure 1B**).

To assess the response of glycolytic gene expressions under permissive and non-permissive infection, the transcription levels of genes involved in glycolysis were evaluated by real-time quantitative polymerase chain reaction (qPCR) after infecting BmN cells with AcMNPV or BmNPV (**Figure 1C**). Notably, expression of *treh* was induced by AcMNPV or BmNPV infection, but the induction level in AcMNPV-infected cells was significantly higher than that in BmNPV-infected cells (**Figure 1D**). No difference between the control and both baculovirus-infected cells was found for other glycolytic genes, including *pfk*, *tpi*, *gadph,* and *pglym*; *eno* showed increased transcription after infection, but with no difference between AcMNPV and BmNPV infection. In addition, ATP production after AcMNPV infection significantly increased from 24 to 72 h post infection (**Figure 1E**). Comparing to AcMNPV infection, BmNPV infection only significantly induced ATP level at 48 h post infection. These results indicated that the expression of a glycolytic gene, *treh*, as well as the production of ATP, was significantly induced by infection with both

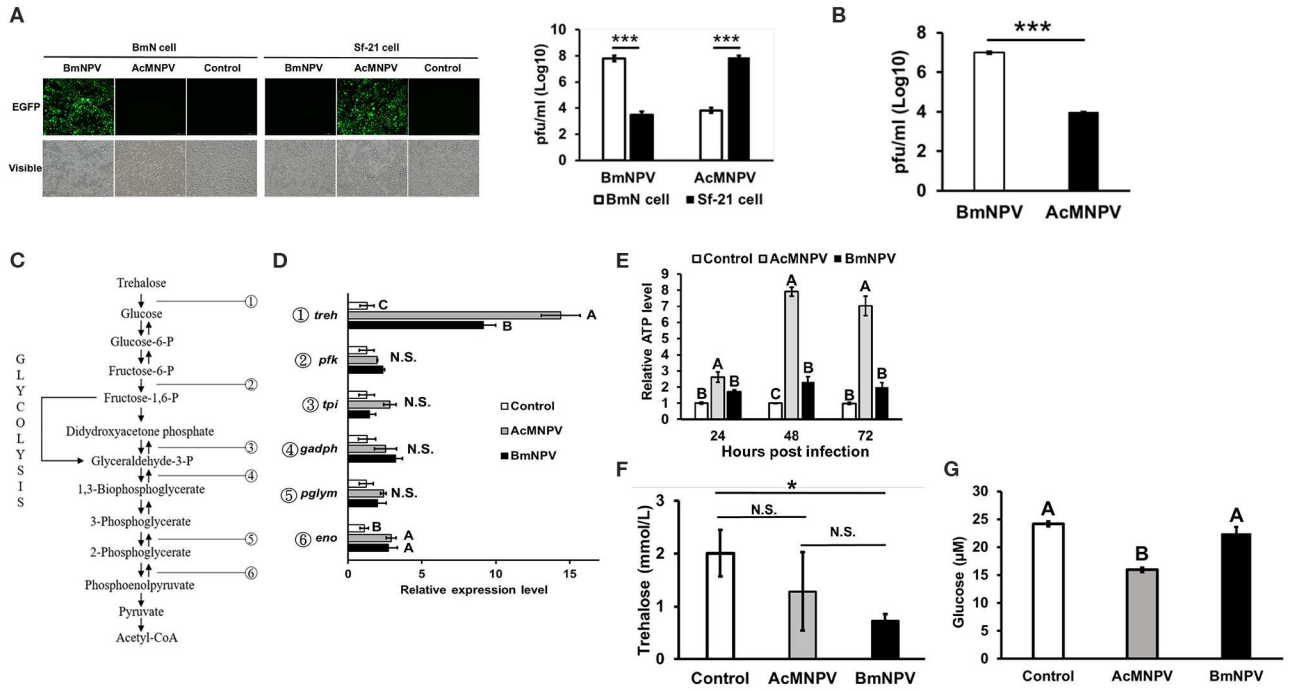

FIGURE 1 | Virus-host tropisms and host glycolytic activities upon AcMNPV and BmNPV infection. **(A)** Virus titers were determined by fluorescence intensity and by qPCR analysis at 48 hpi in BmN and Sf-21 cells infected with AcMNPV or BmNPV. **(B)** Virus titers quantification by qPCR in AcMNPV- or BmNPV infected *B. mori* larvae at 48 hpi **(C)** Summary of glycolytic and citrate cycle enzymes in insects. **(D)** RT-qPCR analysis of glycolytic genes trehalase-2 (*treh*), phosphofructokinase (*pfk*), triose phosphate isomerase (*tpi*), glyceraldehyde 3-phosphate dehydrogenase (*gapdh*), phosphoglyceromutase (*pglym*), and enolase (*eno*) in BmN cells at 48 h after infection with AcMNPV or BmNPV. All of the results were normalized to expression of the 18 S rRNA gene and non-infected control (ΔΔCt). **(E)** ATP levels were measured at 48 hpi in AcMNPV- or BmNPV-infected cells. All of the results were normalized to those in the non-infected control. Hemolymph trehalose **(F)** and glucose **(G)** levels in *B. mori* larvae were measured at 48 hpi; control larvae were injected with 1X PBS. All the values are the mean ± SEM of three **(A,C,G)** or four **(E,F)** replicates. Significances of D, E, F, and G were determined by one-way ANOVA with Tukey's HSD *post-hoc* analysis; different letters for the treatment group indicate significant differences at $P < 0.05$. Student's *t*-test was used for the analysis of A, B, F, $^{*}P < 0.05$, $^{***}P < 0.001$.

baculoviruses but was relatively higher in non-permissive AcMNPV-infected cells.

To further confirm these *in vitro* results, we compared circulating trehalose and glucose levels in infected larvae. Although no significant difference by ANOVA was observed for circulating trehalose between PBS-injected larvae and both virus-infected larvae ($P = 0.07$), the level of released trehalose in BmNPV-infected larvae tended to be lower than that in PBS-injected groups (**Figure 1F**, $P < 0.05$ *t*-test). In addition, the level of glucose was lowest in AcMNPV-infected larvae compared to in BmNPV-infected larvae or the PBS treatment control (**Figure 1G**). These *in vivo* results demonstrate different glycolytic activities between permissive and non-permissive infection conditions.

Inhibition of Glycolysis Enhances AcMNPV Replication in a Non-permissive Host

Because BmN cells displayed higher ATP production upon AcMNPV infection, we sought to understand whether such metabolic induction is a host physiological response for enhancing the antiviral immunity against AcMNPV replication or is induced by virus infection for virus replication. To address this issue, we treated AcMNPV-infected BmN cells with the glycolytic inhibitor 2-deoxy-D-glucose (2DG) (28). The results showed that 2DG successfully suppressed ATP production in AcMNPV-infected cells (**Figure 2A**), and such suppression increased the AcMNPV titer in non-permissive BmN cells, though infection capacity was still lower than in BmNPV infection (**Figure 2B**). To confirm the *in vitro* results, we conducted the same experiment under *in vivo* conditions. We first confirmed that AcMNPV infection induced higher ATP production than did BmNPV infection (**Figure 2C**) in larvae, which was shown in BmN cells (**Figure 1E**), and that ATP production can be further decreased by 2DG treatment. Moreover, glycolysis suppression by 2DG injection resulted in a significant increase in AcMNPV titer in non-permissive *B. mori* larvae (**Figure 2D**). Notably, 2DG treatments did not influence the BmNPV titers in permissive BmN cells or larvae (**Figures 2B,D**). Our results show that this glycolytic activation in *B. mori* upon AcMNPV infection indeed plays an important role in preventing AcMNPV replication. Hence, suppression of glycolysis by 2DG treatment increased the AcMNPV replication capacity in its non-permissive host.

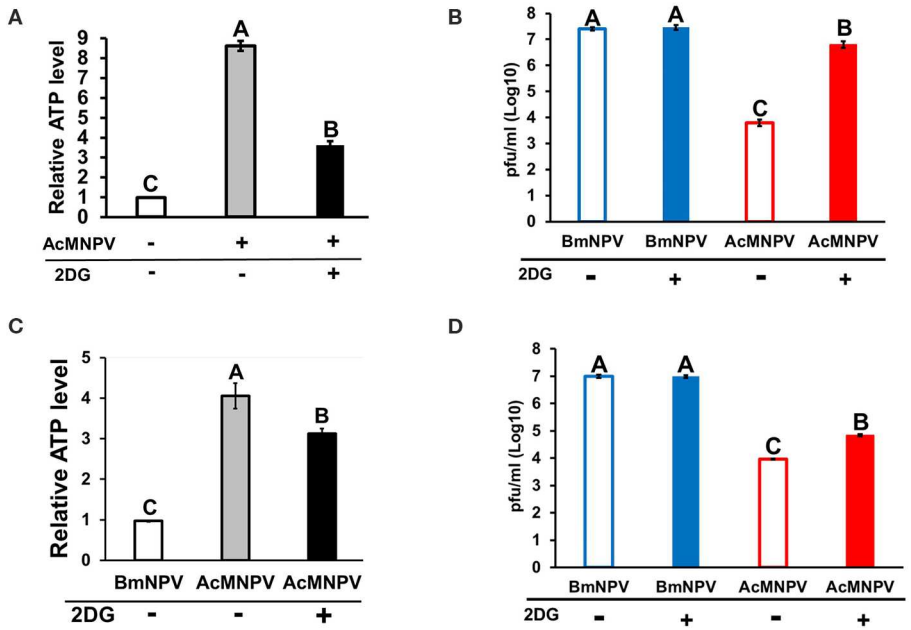

FIGURE 2 | Inhibition of glycolysis by 2-deoxy-D-glucose (2DG) treatment resulted in decreased ATP levels and increased AcMNPV replication in BmN cells and larvae. The ATP level was measured at 48 h postinfection (hpi) after 2DG treatment in BmN cells **(A)** and larvae **(C)**; the values were normalized to those in non-infected control BmN cells and BmNPV-infected larvae, respectively. Virus titers were estimated at 48 hpi in BmN cells **(B)** and larvae **(D)**; BmNPV treatment was used as the positive control. All values are shown as the mean ± SEM of four replicates for ATP measurements and three replicates for virus titer. Significance was determined by one-way ANOVA with Tukey's HSD *post-hoc* analysis; different letters for the treatment group indicate significant differences at $P < 0.05$.

Adenosine Signaling Is Involved in Metabolic Induction Upon Baculovirus Infection

Previous studies in *Drosophila* have demonstrated that adenosine signaling regulates glycolytic activity upon pathogenic infection (19, 21). We examined the temporal and spatial expression profiles of *Bombyx AdoR* by using SilkDB 3.0 database (https://silkdb.bioinfotoolkits.net) (29). We found that *AdoR* is expressed ubiquitously from larval to adult stages, and it is also detectable in immune organs including hemocyte, midgut and fat body. To confirm the involvement of adenosine signaling upon baculovirus infection, we compared the expression level of adenosine receptor (*AdoR*) after AcMNPV and BmNPV infection. *AdoR* expression showed no difference between non-infected larvae and AcMNPV-infected larvae, but both were higher than in BmNPV-infected larvae (**Figure 3A**). In BmN cells, *AdoR* expression increased after AcMNPV or BmNPV infection but was highest in AcMNPV-infected cells (**Figure 3B**). In addition, we examined the *AdoR* expression profiles in different immune organs (hemocyte, fat body, midgut), and results showed that BmNPV infection significantly suppressed AdoR expression in hemocyte (**Figure 3C**). Both virus infection significantly induced AdoR expressions in midgut but no impact on the AdoR expression in the fat body. The results revealed different profiles of *AdoR* transcription under *in vivo* and *in vitro* conditions, which might be due to different tissue-specific responses and the difference in complexity between whole larvae and BmN cells. Such transcriptional tissue-specific responses were also observed upon BmCPV infections in *Bombyx mori* (30). The lower *AdoR* expression in the hemocyte of BmNPV-infected larvae suggested that BmNPV suppresses the *AdoR* expression for compromising the host immune defense. Since *AdoR* in insect hemocyte has known playing the important roles on energy metabolism and cellular immune responses upon the bacterial and virus infections (21, 31) as well as hematopoiesis (32). Notably, the same patterns of *AdoR* expression in BmNPV-infected larvae and BmN cells always being lower than in AcMNPV infection were found. We further measured the extracellular adenosine level in the hemolymph of infected larvae but found no significant difference between the PBS injection control and AcMNPV- and BmNPV-infected larvae (**Figure 3D**). Our results indicate that adenosine signaling is lower under BmNPV infection than under AcMNPV infection.

To understand whether adenosine signaling regulates host metabolism and influences the capacity of AcMNPV replication in its non-permissive host, we inhibited *AdoR* expression by RNAi in AcMNPV-infected BmN cells and measured the ATP level and AcMNPV titer. *AdoR* transcription was successfully silenced after 48 h of transfection with *AdoR* siRNA (**Figure 4A**); moreover, induction of ATP levels upon AcMNPV infection was significantly decreased in BmN cells (**Figure 4B**). Notably, this metabolic suppression by *AdoR* RNAi significantly increased the AcMNPV titer compared with control siRNA treatment cells, but the titer was still lower than that in BmNPV infection (**Figure 4C**). The result was also visible by observing GFP (expressed from the viral sequence) signals under a fluorescence

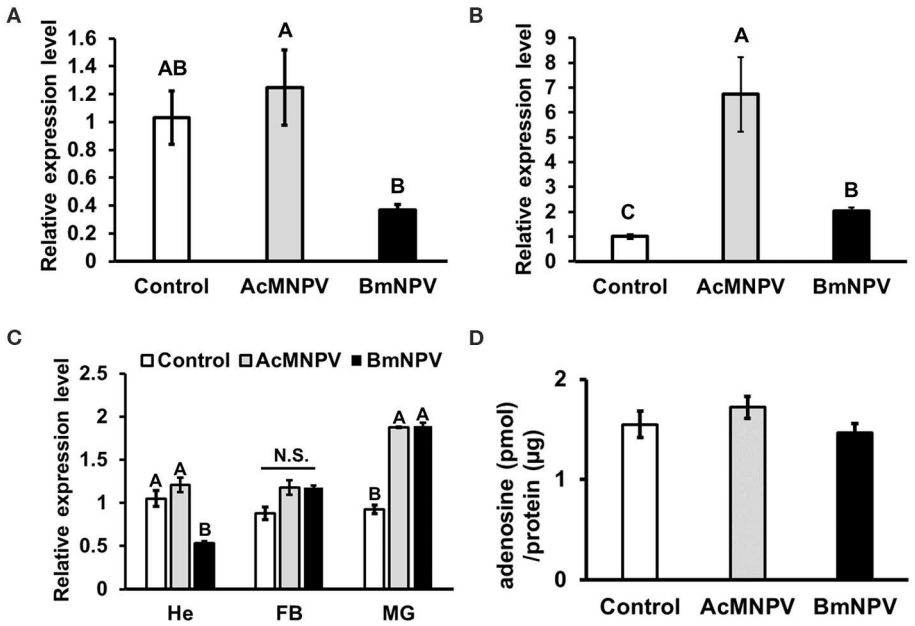

FIGURE 3 | Regulation of adenosine signaling upon AcMNPV and BmNPV infection. RT-qPCR analyses of *AdoR* expression in *B. mori* larvae **(A)** BmN cells **(B)** as well as in different immune organs **(C)** upon AcMNPV or BmNPV infection at 48 h postinfection (hpi). **(D)** Measurement of hemolymph adenosine levels of larvae injected with PBS (control), AcMNPV or BmNPV at 48 hpi. All values are shown as the mean ± SEM of three replicates for qPCR and four replicates for adenosine measurement. Significance was determined by one-way ANOVA with Tukey's HSD *post-hoc* analysis; different letters for the treatment group indicate significant differences at $P < 0.05$. MG, midgut; HE, hemocyte; FB, fat body.

microscope. The GFP signal in *AdoR* siRNA-treated cells was greater than that in control-treated cells (**Figure 4D**).

Inhibiting efflux transport of adenosine under stress conditions has been reported to decrease *AdoR* signaling (19, 33). To further confirm the RNAi results, we pharmaceutically blocked adenosine transport by treating cells with the equilibrative nucleoside transporter (ENT) inhibitor dipyridamole (Dipy). Blocking adenosine transportation suppressed ATP induction upon AcMNPV infection (**Figure 5A**) and significantly increased the AcMNPV titer in BmN cells (**Figure 5B**). We conducted the same experiment under *in vivo* conditions by injecting infected larvae with Dipy and observed the same results, whereby Dipy decreased ATP induction upon AcMNPV infection, increasing AcMNPV infective capacity in *B. mori* larvae (**Figures 5C,D**). We conclude that *AdoR* indeed regulates host metabolic induction upon AcMNPV infection and is essential for the host antivirus response.

Metabolic Activation Is Essential for the Antivirus Immune Response

Antimicrobial peptides (AMPs) have been reported to be involved in antivirus immune reactions in insects (13, 34). Of these, gloverin was shown that highly induced in the BmNPV-resistant strain of *B. mori* upon infection and suppressed by AcMNPV infection in *Spodoptera exigua* larvae (35, 36). Preincubation of Sf-9 cells with gloverin peptides also reduces the production of budded AcMNPV virus (37). In addition, suppression of gloverin expression by RNAi increased the AcMNPV replication in BmN cells (data not shown). To confirm that metabolic induction is an important factor enhancing the antivirus response to restrict AcMNPV permissiveness in *B. mori*, we inhibited glycolysis by injecting 2DG into infected larvae and assessed transcription of four *gloverin* genes (**Figures 6A–D**). The expression levels of the four *gloverin* genes were increased after infection by both baculoviruses but relatively higher with AcMNPV. Notably, 2DG treatment significantly decreased induction of all *gloverin* transcripts, confirming our hypothesis that metabolic activation upon AcMNPV infection is essential for supporting the immune response against infection. Furthermore, to again prove that adenosine signaling regulates host metabolic activation to support the antivirus response, we injected Dipy to block adenosine transport in infected larvae and measured expression of the four *gloverin* genes (**Figures 6E–H**). Except for *gloverin*-1, the other three *gloverins* showed similar results: Dipy injection significantly suppressed expression due to AcMNPV infection. Our results demonstrate that metabolic induction regulated by adenosine signaling is critical for the antiviral immune response in *B. mori*.

Adenosine Signaling Is a Conservative Mechanism Modulating the Permissiveness of Baculovirus Infection in *Spodoptera frugiperda* Cells

To demonstrate that our observations are not restricted to *B. mori*, we tested the role of adenosine signaling in another

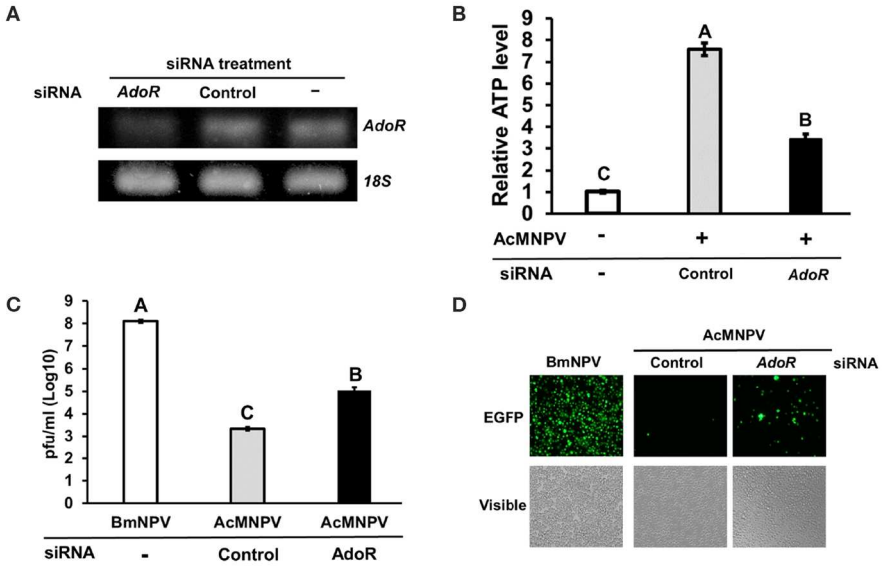

FIGURE 4 | *AdoR* RNAi suppressed ATP induction and increased AcMNPV titers in BmN cells. **(A)** Knockdown efficiency of *AdoR* siRNA treatment in BmN cells by RT-PCR analysis. **(B)** The ATP level was measured at 48 h postinfection (hpi) in *AdoR* and control siRNA-treated cells; values were normalized to those in the non-infected control. Virus titers were determined by qPCR **(C)** and fluorescence intensity **(D)** at 48 hpi in *AdoR*- and control siRNA-treated cells. All values are the mean ± SEM of four replicates for ATP level and three replicates for virus titer measurements. Significance was determined by one-way ANOVA with Tukey's HSD *post-hoc* analysis; different letters for the treatment group indicate significant differences at $P < 0.05$.

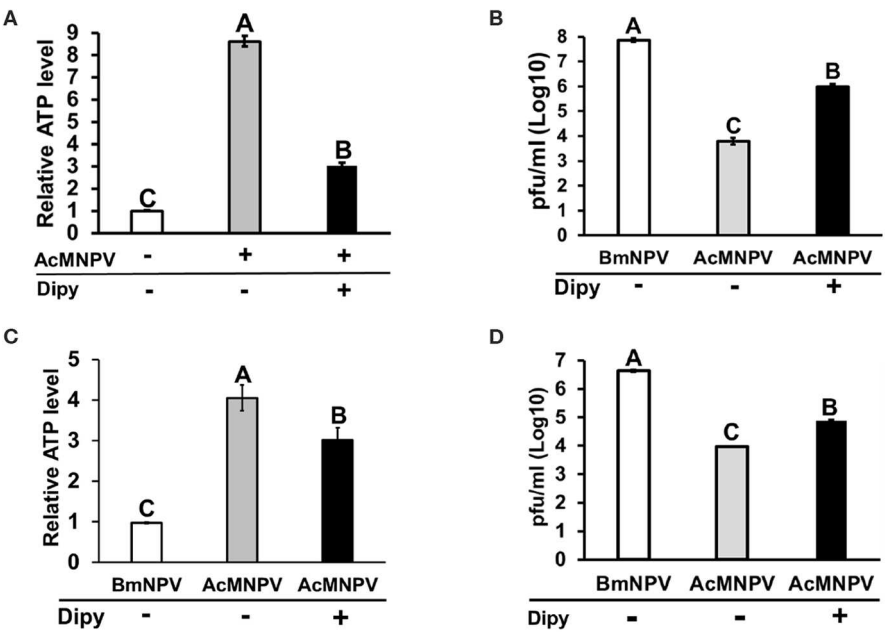

FIGURE 5 | Inhibition of adenosine transport by dipyridamole (Dipy) treatment decreased the ATP level, resulting in an increase in AcMNPV replication in BmN cells and larvae. The ATP level was measured at 48 h postinfection (hpi) with Dipy treatment in BmN cells **(A)** and larvae **(C)**; values were normalized to those in the non-infected control BmN cells and BmNPV-infected larvae, respectively. Virus titers were estimated at 48 hpi in BmN cells **(B)** and larvae **(D)**; BmNPV treatment represented the positive control. All values are shown as the mean ± SEM of four replicates for ATP level and three replicates for virus titer measurements. Significance was determined by one-way ANOVA with Tukey's HSD *post-hoc* analysis; different letters for the treatment group indicate significant differences at $P < 0.05$.

lepidopteran model, *S. frugiperda* Sf-21 cells. We obtained the same results, showing that inhibition of glycolysis and adenosine transport in Sf-21 cells increased the BmNPV replication in its non-permissive host (**Figure 7A**). Alternatively, enhancement of adenosine signaling in Sf-21 cells by applying adenosine led to a significant decrease in the AcMNPV infection capacity

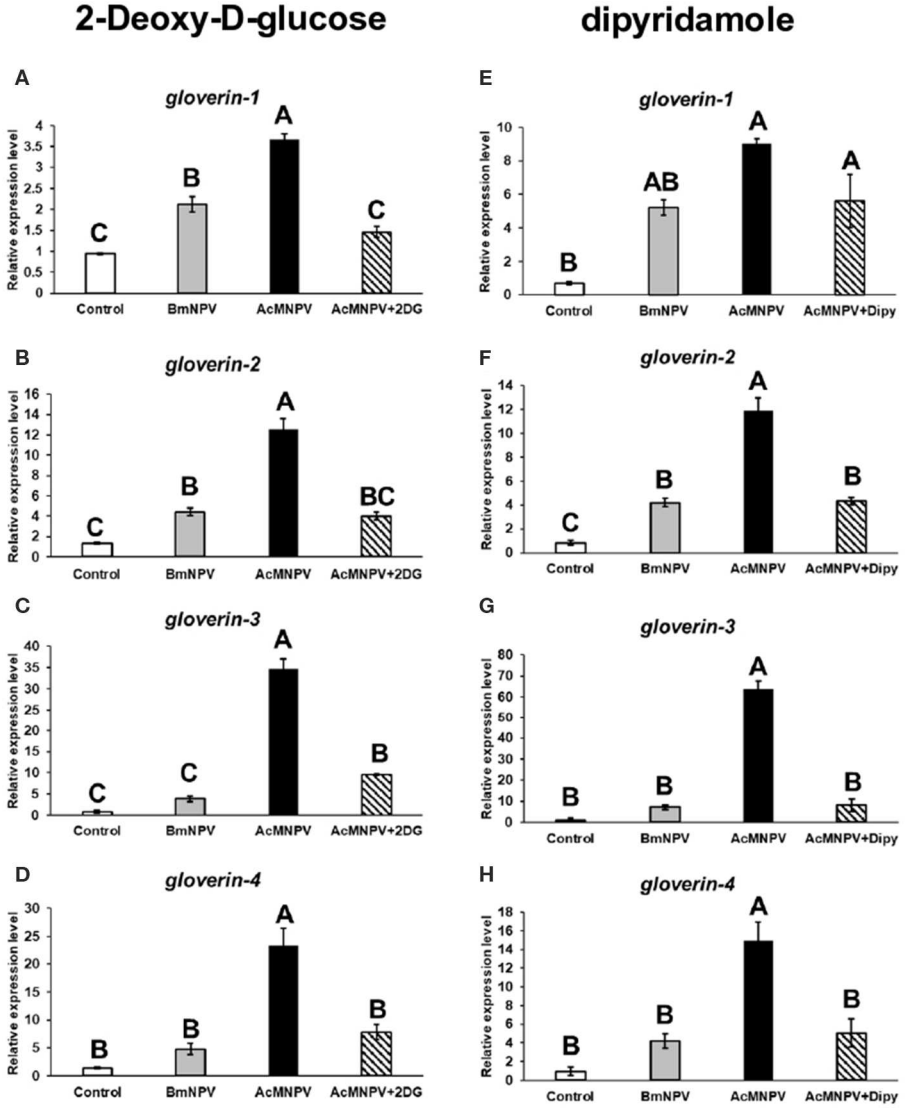

FIGURE 6 | Antivirus protein expression was regulated by *AdoR*-meditated metabolic activation upon AcMNPV infection. The expression levels of four gloverin genes were analyzed by RT-qPCR at 48 h postinfection (hpi) in larvae infected with BmNPV or AcMNPV and cotreated with 2DG **(A–D)** or Dipy **(E–H)**. Control larvae were injected with 1X PBS. All values are the mean ± SEM of three replicates. Significance was determined by one-way ANOVA with Tukey's HSD *post-hoc* analysis; different letters for the treatment group indicate significant differences at $P < 0.05$.

in its permissive host (**Figure 7B**). Our results indicated that inhibition of adenosine signaling resulted in a decreased glycolytic activity and antivirus reaction, which increased the baculovirus infective capacity in its non-permissive host; conversely, induction of adenosine signaling enhanced the host antivirus reaction, which decreased the AcMNPV propagation in Sf-21 cells.

DISCUSSION

AcMNPV has broader host range in comparing to BmNPV, which has only one permissive host, silkworm and its derived cell line Bm cells. Interestingly, despite having a wide range of host, AcMNPV is not able to achieve successful infection in Bm cells, making Bm cells non-permissive to AcMNPV (5, 7). Host tropism may be determined by the following factors: the ability of baculoviruses to enter host cells, to achieve normal viral gene expression during infection, and to utilize host cellular machinery to complete the infection procedure (6, 38). Many viral genes involved in host range determination have also been identified, including p143, p35, and hcf-1. Substitution of 2 amino acids in AcMNPV *p143* enabled AcMNPV replication in Bm5 cells. Blocking cell apoptosis and activating origin-specific DNA replication in AcMNPV can also alter host specificity, demonstrating that virus-host interactions can also alter host ranges in some baculoviruses. Baculoviruses produce two distinct

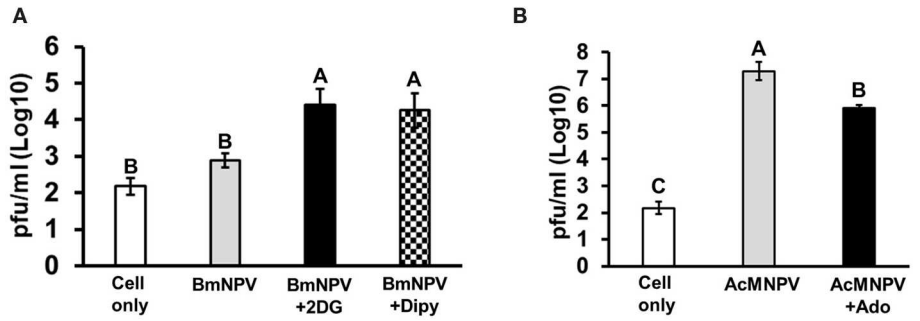

FIGURE 7 | Glycolysis and adenosine signaling in Sf-21 cells regulate the permissiveness of baculovirus infection. Sf-21 cells were preincubated with 2DG and Dipy **(A)** and adenosine (Ado) **(B)** before BmNPV or AcMNPV infection, respectively. The virus titers were estimated at 48 h postinfection. "Cell only" indicates cells without virus and drug treatments. All values are shown as the mean ± SEM of three replicates. Significance was determined by one-way ANOVA with Tukey's HSD *post-hoc* analysis; different letters for the treatment groups indicate significant differences at $P < 0.05$.

types of virions during the infection cycle: budded viruses (BV), which are responsible for systematic infection within hosts, and occlusion derived viruses (ODV), which are responsible for spreading infection to other susceptible species (39). Infective efficiency might be variable by oral delivery of ODV, since several antiviral proteins such as Bmlipase-1 and BmSP-2 are highly expressed in midgut, and virus also needs to passes through the host's peritrophic membrane for causing the systemic infection (39–41). Taking into consideration, our study mainly injected BV into the hemocoel of silkworms.

Previous studies on the regulation of host tropism of AcMNPV and BmNPV have mostly focused on how viruses modulate the cellular function of the host to establish successful propagation. Conversely, relatively few studies have investigated the host physiological response, which is important for anti-baculovirus reactions. Our results showed that expression of the glycolytic genes *treh* and *eno* as well as ATP production increased after BmNPV infected BmN cells (**Figure 1**). These results are consistent with previous observations on BmNPV-infected BmN cells or AcMNPV-infected Sf-9 cells, which showed increased citric acid expression, TCA cycle activity, and ATP levels after infection (11, 12). It was later concluded that virus induces metabolic activity of a permissive host due to the requirement of a large energy supply for baculovirus replication (9, 13). Regardless, the fact that the immune system of the host also requires a higher energy supply for antivirus immune responses should not be overlooked. In fact, our results showed that metabolic induction was more dramatic under non-permissive infection conditions. Both the *treh* expression level and ATP production in AcMNPV-infected BmN cells and larvae were significantly higher than under BmNPV infection (**Figures 1**, **2**). It was reported previously that AcMNPV infection of permissive host (Sf-9 cells) caused cell enlargements and resulted in increasing intracellular ATP level by 50–80% (42). In the present study, intracellular ATP level increased by 6 to 7-fold (600–700%) in AcMNPV infection of the non-permissive host (BmN cells). This increased ATP level was far more than that in the permissive cell line, suggesting that it was not likely contributed by cell enlargement after infection.

Trehalose circulation and consumption of glucose were also higher in AcMNPV-infected larvae (**Figure 1**). Moreover, instead of promoting virus infection, as in previous studies describing permissive infection, this metabolic induction under non-permissive infection appears to be a host physiological response against virus replication. Increased AcMNPV titers and suppressed *gloverin* induction were observed after applying the glycolytic inhibitor 2DG to infected BmN cells and larvae (**Figures 2**, **6**). In general, increased energy consumption upon pathogenic challenge is essential for supporting both cellular and humoral immune responses (18). In particular, the production of AMPs is usually dramatically and rapidly enhanced during infection, and it has been shown that activation of the IMD and Toll pathways as well as *drosomycin* overexpression have significant metabolic impacts in *Drosophila,* such as reduced glycogen and triglyceride stores (43–45). Our results show that activation and reallocation of energy supply toward the immune system is necessary for anti-baculovirus reactions.

Our results demonstrated that adenosine signaling is a key molecular mechanism regulating metabolic induction upon virus infection. Suppressing *AdoR* expression in BmN cells or inhibiting adenosine transport in BmN cells and larvae by RNAi affected ATP production and *gloverin* expression, resulting in increased AcMNPV-infected capability in non-permissive hosts (**Figures 4**–**6**). As a signaling molecule, adenosine is known to be involved in various stress responses, including immune reactions. Extracellular adenosine can be derived from the degradation of extracellular ATP or ADP release by damaged cells, or it can be converted from intracellular ATP and exported to the extracellular space via ENTs (46). Increased ATP synthesis under infection leads to higher extracellular adenosine levels, activating AdoR signaling, which regulates several immune responses, such as inflammatory cytokine production in mammals and hematopoiesis and phagocytosis in *Drosophila* (21, 47, 48). Additionally, our results are consistent with previous findings demonstrating that adenosine signaling regulates carbohydrate metabolism and energy distribution during bacterial and wasp infection in *Drosophila* (18, 19). Based on previous data and those from our present study, which used two different

lepidopteran models, we conclude that adenosine signaling may be a conserved mechanism that modulates host metabolism and immune reactions during pathogenic infection.

Notably, we discovered that *AdoR* expression (**Figure 3**), *treh* expression (**Figure 1D**), and ATP levels (**Figure 1E**) in BmNPV-infected cells or larvae were significantly lower than in AcMNPV infection. As our previous study demonstrated that BmNPV infection resulted in strong miRNA production in *B. mori* (1), we speculated that BmNPV infection may block host adenosine signaling by stimulating miRNA against *AdoR* expression, further suppressing metabolic activation and the antivirus response. We reexamined the transcriptome data from our previous study and found several potential miRNAs targeting *AdoR* (**Table S2**). Because induction of host miRNA expression by viral challenge may be a host antiviral response or it could be triggered by the virus for host physiology remodeling, further study will be needed to characterize the major miRNA involved in regulating *AdoR* signaling upon BmNPV infection.

Our experimental results confirm that adenosine signaling affects glycolytic and energy synthesis in *B. mori,* affecting the host antivirus immune response and restricting the host specificity of AcMNPV. Thus, our study provides a basis for future investigations on the association between host physiological responses and baculovirus infection, and the findings may also be relevant for pest control management.

DATA AVAILABILITY STATEMENT

The datasets analyzed in this article are not publicly available. Requests to access the datasets should be directed to runwu@ntu.edu.tw.

AUTHOR CONTRIBUTIONS

Y-HL, C-CT, VB, C-KT, PC, and Y-LW: guarantors of integrity of entire study, study concepts, and manuscript preparation. Y-HL, C-CT, C-KT, PC, C-HL, and Y-LW: study design, data acquisition/analysis, literature research, and manuscript preparation. Y-HL, C-CT, VB, CW, and Y-LW: data acquisition/analysis, manuscript editing, and revision. All authors reviewed the manuscript.

FUNDING

This research was funded by the grant MOST107-2311-B-002-024-MY3 to Y-LW from the Ministry of Science and Technology, Taiwan.

ACKNOWLEDGMENTS

We thank Dr. Eric C. Wu for kindly revising the manuscript. We thank Czech Academy of Sciences for supporting this cooperation activity (reference number: KAV-1832/OMS/2018) by the grants TWN-18-16 to Y-HL and TWN-18-15 to VB.

SUPPLEMENTARY MATERIAL

The Supplementary Material for this article can be found online at: https://www.frontiersin.org/articles/10.3389/fimmu.2020.00763/full#supplementary-material

Table S1 | List of qPCR primers.

Table S2 | List of predicted *AdoR* miRNAs in BmNPV-infected BmN cells.

Figure S1 | Cytotoxicity assessment of Dipy, 2DG and adenosine treatments. The BmN **(A)** and Sf-21 cells **(B)** were treated with DMSO (0.05%, labeled as control or ctr), 2-Deoxy-D-glucose (10 mM, labeled as 2DG), Dipyridamole (20 μM, labeled as Dipy) and adenosine (10 mM, labeled as Ado) for 24, 48, and 72 h, and cells were stained with propidium iodide (50 μg/mL) for labeling the dead cells. The quantification of live and dead cells was conducted by flow cytometry in the PE-A (585 ± 40 nM) channel using ACEA NovoCyteTM 3000, and 10,000 events were quantified for comparison. All values of bar graph are shown as the mean ± SEM of three replicates. Kruskal-Wallis test was used for statistical analysis, and results suggested that no significant difference of live or dead cell numbers among all the treatment in both cell line.

REFERENCES

1. Chen YW, Wu CP, Wu TC, Wu YL. Analyses of the transcriptome of bombyx mori cells infected with either BmNPV or AcMNPV. *J Asia Pac Entomol.* (2018) 21:37–45. doi: 10.1016/j.aspen.2017.10.009
2. Blissard GW, Rohrmann GF. Baculovirus diversity and molecular biology. *Annu Rev Entomol.* (1990) 35:127–55. doi: 10.1146/annurev.en.35.010190.001015
3. Smith GE, Summer MD, Fraser MJ. Production of human beta interferon in insect cells infected with a baculovirus expression vector. *Mol Cell Biol.* (1983) 2156–65. doi: 10.1128/MCB.3.12.2156
4. Yue W, Miao Y, Li X, Wu X, Zhao A, Nakagaki M. Cloning and expression of manganese superoxide dismutase of the silkworm, bombyx mori by Bac-to-Bac/BmNPV baculovirus expression system. *Appl Microbiol Biotechnol.* (2006) 73:181–6. doi: 10.1007/s00253-006-0462-y
5. Gomi S, Majima K, Maeda S. Sequence analysis of the genome of bombyx mori nucleopolyhedrovirus. *J Gen Virol.* (1999) 80:1323–37. doi: 10.1099/0022-1317-80-5-1323
6. Iwanaga M, Takaya K, Katsuma S, Ote M, Tanaka S, Kamita SG, et al. Expression profiling of baculovirus genes in permissive and nonpermissive cell lines. *Biochem Biophys Res Commun.* (2004) 323:599–614. doi: 10.1016/j.bbrc.2004.08.114
7. Woo SD, Roh JY, Choi JY, Jin BR. Propagation of bombyx mori nucleopolyhedrovirus in nonpermissive insect cell lines. *J Microbiol.* (2007) 45:133–8.
8. Martin O, Croizier G. Infection of a spodoptera frugiperda cell line with bombyx mori nucleopolyhedrovirus. *Virus Res.* (1997) 47:179–85. doi: 10.1016/S0168-1702(96)01412-8
9. Monteiro F, Carinhas N, Carrondo MJ, Bernal V, Alves PM. Toward system-level understanding of baculovirus-host cell interactions: from molecular fundamental studies to large-scale proteomics approaches. *Front Microbiol.* (2012) 3:391. doi: 10.3389/fmicb.2012.00391
10. Kamen AA, Bedard C, Tom R, Perret S, Jardin B. On-line monitoring of respiration in recombinant-baculovirus infected and uninfected insect cell bioreactor cultures. *Biotechnol Bioeng.* (1996) 50:36–48. doi: 10.1002/(SICI)1097-0290(19960405)50:1<36::AID-BIT5>3.0.CO;2-2
11. Iwanaga M, Shimada T, Kobayashi M, Kang W. Identification of differentially expressed host genes in bombyx mori nucleopolyhedrovirus infected cells by using subtractive hybridization. *Appl Entomol Zool.* (2007) 42:151–9. doi: 10.1303/aez.2007.151

12. Bernal V, Carinhas N, Yokomizo AY, Carrondo MJ, Alves PM. Cell density effect in the baculovirus-insect cells system: a quantitative analysis of energetic metabolism. *Biotechnol Bioeng*. (2009) 104:162–80. doi: 10.1002/bit.22364
13. Nguyen Q, Nielsen LK, Reid S. Genome scale transcriptomics of baculovirus-insect interactions. *Viruses*. (2013) 5:2721–47. doi: 10.3390/v5112721
14. Lahouassa H, Daddacha W, Hofmann H, Ayinde D, Logue EC, Dragin L, et al. SAMHD1 restricts the replication of human immunodeficiency virus type 1 by depleting the intracellular pool of deoxynucleoside triphosphates. *Nat Immunol*. (2012) 13:223–8. doi: 10.1038/ni.2236
15. Blanc M, Hsieh WY, Robertson KA, Watterson S, Shui G, Lacaze P, et al. Host defense against viral infection involves interferon mediated down-regulation of sterol biosynthesis. *PLoS Biol*. (2011) 9:e1000598. doi: 10.1371/journal.pbio.1000598
16. Bartholomay LC, Cho WL, Rocheleau TA, Boyle JP, Beck ET, Fuchs JF, et al. Description of the transcriptomes of immune response-activated hemocytes from the mosquito vectors aedes aegypti and *Armigeres subalbatus*. *Infect Immun*. (2004) 72:4114–26. doi: 10.1128/IAI.72.7.4114-4126.2004
17. Shelby KS, Popham HJ. RNA-Seq study of microbially induced hemocyte transcripts from larval heliothis virescens (lepidoptera: noctuidae). *Insects*. (2012) 3:743–62. doi: 10.3390/insects3030743
18. Dolezal T, Krejcova G, Bajgar A, Nedbalova P, Strasser P. Molecular regulations of metabolism during immune response in insects. *Insect Biochem Mol Biol*. (2019) 109:31–42. doi: 10.1016/j.ibmb.2019.04.005
19. Bajgar A, Kucerova K, Jonatova L, Tomcala A, Schneedorferova I, Okrouhlik J, et al. Extracellular adenosine mediates a systemic metabolic switch during immune response. *PLoS Biol*. (2015) 13:e1002135. doi: 10.1371/journal.pbio.1002135
20. Anderson RS, Holmes B, Good RA. Comparative biochemistry of phagocytizing insect hemocytes. *Comp Biochem Physiol B Comp Biochem*. (1973) 46:595–602. doi: 10.1016/0305-0491(73)90099-0
21. Bajgar A, Dolezal T. Extracellular adenosine modulates host-pathogen interactions through regulation of systemic metabolism during immune response in *Drosophila*. *PLoS Pathog*. (2018) 14:e1007022. doi: 10.1371/journal.ppat.1007022
22. Singh T, Singh PK, Sahaf KA. Egg diapause and metabolic modulations during embryonic development in the silkworm, bombyx mori L. *Ann Biol Res*. (2013) 4:12–21.
23. Lo H-R, Chao Y-C. Rapid titer determination of baculovirus by quantitative real-time polymerase chain reaction. *Biotechnol Prog*. (2004) 20:354–60. doi: 10.1021/bp034132i
24. Wu PC, Lin YH, Wu TC, Lee ST, Wu CP, Chang Y, et al. MicroRNAs derived from the insect virus HzNV-1 promote lytic infection by suppressing histone methylation. *Sci Rep*. (2018) 8:17817. doi: 10.1038/s41598-018-35782-w
25. Hu YT, Tang CK, Wu CP, Wu PC, Yang EC, Tai CC, et al. Histone deacetylase inhibitor treatment restores memory-related gene expression and learning ability in neonicotinoid-treated apis mellifera. *Insect Mol Biol*. (2018) 27:512–21. doi: 10.1111/imb.12390
26. Matsumoto Y, Ishii M, Sekimizu K. An *in vivo* invertebrate evaluation system for identifying substances that suppress sucrose-induced postprandial hyperglycemia. *Sci Rep*. (2016) 6:26354. doi: 10.1038/srep26354
27. Schmittgen TD, Livak KJ. Analyzing real-time PCR data by the comparative C-T method. *Nat Protoc*. (2008) 3:1101–8. doi: 10.1038/nprot.2008.73
28. Brown J. Effects of 2-deoxyglucose on carbohydrate metablism: review of the literature and studies in the rat. *Metabolism*. (1962) 11:1098–112.
29. Lu F, Wei Z, Luo Y, Guo H, Zhang G, Xia Q, et al. SilkDB 3.0: visualizing and exploring multiple levels of data for silkworm. *Nucleic Acids Res*. (2020) 48:D749–55. doi: 10.1093/nar/gkz919
30. Jiang L, Peng Z, Guo Y, Cheng T, Guo H, Sun Q, et al. Transcriptome analysis of interactions between silkworm and cytoplasmic polyhedrosis virus. *Sci Rep*. (2016) 6:24894. doi: 10.1038/srep24894
31. Chang Y, Tang CK, Lin YH, Tsai CH, Lu YH, Wu YL. Snellenius manilae bracovirus suppresses the host immune system by regulating extracellular adenosine levels in spodoptera litura. *Sci Rep*. (2020) 10:2096. doi: 10.1038/s41598-020-58375-y
32. Banerjee U, Girard JR, Goins LM, Spratford CM. Drosophila as a genetic model for hematopoiesis. *Genetics*. (2019) 211:367–417. doi: 10.1534/genetics.118.300223
33. Poernbacher I, Vincent JP. Epithelial cells release adenosine to promote local TNF production in response to polarity disruption. *Nat Commun*. (2018) 9:4675. doi: 10.1038/s41467-018-07114-z
34. Wu Q, Patocka J, Kuca K. Insect antimicrobial peptides, a mini review. *Toxins. (2*018) 10:461. doi: 10.3390/toxins10110461
35. Choi JY, Roh JY, Wang Y, Zhen Z, Tao XY, Lee JH, et al. Analysis of genes expression of spodoptera exigua larvae upon AcMNPV infection. *PLoS ONE*. (2012) 7:e42462. doi: 10.1371/journal.pone.0042462
36. Bao YY, Lv ZY, Liu ZB, Xue J, Xu YP, Zhang CX. Comparative analysis of bombyx mori nucleopolyhedrovirus responsive genes in fat body and haemocyte of B. mori resistant and susceptible strains. *Insect Mol Biol*. (2010) 19:347–58. doi: 10.1111/j.1365-2583.2010.00993.x
37. Moreno-Habel DA, Biglang-awa IM, Dulce A, Luu DD, Garcia P, Weers PM, et al. Inactivation of the budded virus of autographa californica M nucleopolyhedrovirus by gloverin. *J Invertebr Pathol*. (2012) 110:92–101. doi: 10.1016/j.jip.2012.02.007
38. Nagamine T, Sako Y. A role for the anti-viral host defense mechanism in the phylogenetic divergence in baculovirus evolution. *PLoS ONE*. (2016) 11:e0156394. doi: 10.1371/journal.pone.0156394
39. Jiang L, Xia Q. The progress and future of enhancing antiviral capacity by transgenic technology in the silkworm bombyx mori. *Insect Biochem Mol Biol*. (2014) 48:1–7. doi: 10.1016/j.ibmb.2014.02.003
40. Ponnuvel KM, Nakazawa H, Furukawa S, Asaoka A, Ishibashi J, Tanaka H, et al. A lipase isolated from the silkworm bombyx mori shows antiviral activity against nucleopolyhedrovirus. *J Virol*. (2003) 77:10725–9. doi: 10.1128/JVI.77.19.10725-10729.2003
41. Yao H, He F, Guo A, Cao C, Lu X, Wu X. Gene analysis of an antiviral protein SP-2 from Chinese wild silkworm, bombyx mandarina moore and its bioactivity assay. *Sci China C Life Sci*. (2008) 51:879–84. doi: 10.1007/s11427-008-0123-8
42. Tran TT, Dietmair S, Chan LC, Huynh HT, Nielsen LK, Reid S. Development of quenching and washing protocols for quantitative intracellular metabolite analysis of uninfected and baculovirus-infected insect cells. *Methods*. (2012) 56:396–407. doi: 10.1016/j.ymeth.2011.11.009
43. Rera M, Clark RI, Walker DW. Intestinal barrier dysfunction links metabolic and inflammatory markers of aging to death in *Drosophila*. *Proc Natl Acad Sci USA*. (2012) 109:21528–33. doi: 10.1073/pnas.1215849110
44. Roth SW, Bitterman MD, Birnbaum MJ, Bland ML. Innate immune signaling in *Drosophila* blocks insulin signaling by uncoupling $PI(3,4,5)P_3$ production and Akt activation. *Cell Rep*. (2018) 22:2550–56. doi: 10.1016/j.celrep.2018.02.033
45. Clark RI, Tan SW, Pean CB, Roostalu U, Vivancos V, Bronda K, et al. MEF2 is an *in vivo* immune-metabolic switch. *Cell*. (2013) 155:435–47. doi: 10.1016/j.cell.2013.09.007
46. Antonioli L, Csoka B, Fornai M, Colucci R, Kokai E, Blandizzi C, et al. Adenosine and inflammation: what's new on the horizon? *Drug Discov Today*. (2014) 19:1051–68. doi: 10.1016/j.drudis.2014.02.010
47. Mondal BC, Mukherjee T, Mandal L, Evans CJ, Sinenko SA, Martinez-Agosto JA, et al. Interaction between differentiating cell- and niche-derived signals in hematopoietic progenitor maintenance. *Cell*. (2011) 147:1589–600. doi: 10.1016/j.cell.2011.11.041
48. Lee JS, Yilmaz O. Unfolding role of a danger molecule adenosine signaling in modulation of microbial infection and host cell response. *Int J Mol Sci*. (2018) 19:199. doi: 10.3390/ijms19010199

Conflict of Interest: The authors declare that the research was conducted in the absence of any commercial or financial relationships that could be construed as a potential conflict of interest.

frontiers in Immunology

ORIGINAL RESEARCH
published: 05 May 2020
doi: 10.3389/fimmu.2020.00785

Identification of a Conserved Prophenoloxidase Activation Pathway in Cotton Bollworm *Helicoverpa armigera*

Qianran Wang[1,2], Mengyi Yin[1,2], Chuanfei Yuan[1,3], Xijia Liu[1], Zhihong Hu[1], Zhen Zou[2,3,4]* and Manli Wang[1]**

[1] State Key Laboratory of Virology, Center for Biosafety Mega-Science, Wuhan Institute of Virology, Chinese Academy of Sciences, Wuhan, China, [2] Savaid Medical School, University of Chinese Academy of Sciences, Beijing, China, [3] State Key Laboratory of Integrated Management of Pest Insects and Rodents, Institute of Zoology, Chinese Academy of Sciences, Beijing, China, [4] Key Laboratory of Tropical Translational Medicine, Laboratory of Medicine, School of Tropical Medicine, Ministry of Education, Hainan Medical University, Haikou, China

OPEN ACCESS

Edited by:
Liang Jiang,
Southwest University, China

Reviewed by:
Chengshu Wang,
Shanghai Institutes for Biological Sciences (CAS), China
Erjun Ling,
Shanghai Institutes for Biological Sciences (CAS), China

***Correspondence:**
Zhihong Hu
huzh@wh.iov.cn
Zhen Zou
zouzhen@ioz.ac.cn
Manli Wang
wangml@wh.iov.cn

Specialty section:
This article was submitted to Comparative Immunology, a section of the journal Frontiers in Immunology

Received: 17 February 2020
Accepted: 07 April 2020
Published: 05 May 2020

Citation:
Wang Q, Yin M, Yuan C, Liu X, Hu Z, Zou Z and Wang M (2020) Identification of a Conserved Prophenoloxidase Activation Pathway in Cotton Bollworm Helicoverpa armigera. Front. Immunol. 11:785. doi: 10.3389/fimmu.2020.00785

Melanization is a prominent insect humoral response for encapsulation of and killing invading pathogens. It is mediated by a protease cascade composed of a modular serine protease (SP), and clip domain SPs (cSPs), which converts prophenoloxidase (PPO) into active phenoloxidase (PO). To date, melanization pathway in cotton bollworm *Helicoverpa armigera*, an important agricultural pest, remains largely unclear. To biochemically reconstitute the pathway *in vitro*, the putative proteases along with modified proteases containing the factor Xa cleavage site were expressed by *Drosophila* S2 cell expression system. Purified recombinant proteins were used to examine their role in activating PPO. It is revealed that cascade is initiated by a modular SP-SP41, followed by cSP1 and cSP6. The three-step SP41/cSP1/cSP6 cascade could further activate PPO, and the PO activity was significantly enhanced in the presence of two cSP homologs (cSPHs), cSPH11 and cSPH50, suggesting the latter are cofactors for PPO activation. Moreover, baculovirus infection was efficiently blocked by the reconstituted PPO activation cascade, and the effect was boosted by cSPH11 and cSPH50. Taken together, we unraveled a conserved PPO activation cascade in *H. armigera*, which is similar to that exists in lepidopteran biochemical model *Manduca sexta* and highlighted its role in antagonizing viral infection.

Keywords: melanization, prophenoloxidase, serine protease, baculovirus, *Helicoverpa armigera*

Abbreviations: βGRP, β-glucan recognition proteins; β-ME, β-mercaptoethanol; AS, ammonium sulfate; CPC, cetylpyridinium chloride; cSP, clip domain serine protease; cSPH, clip-domain serine protease homolog; cSPH, cSP homologs; HearNPV, *Helicoverpa armigera* nucleopolyhedrovirus; HP, hemolymph protease; IEAR, acetyl-Ile-Glu-Ala-Arg-p-nitroanilide; LDLa, low-density lipoprotein receptor class A; MSP, modular serine protease; PAP, PPO activating protease; PO, phenoloxidase; PPAE, PPO activating enzyme; PPAF, PPO activating factor; PPO, prophenoloxidase; PRRs, pattern recognition receptors; SAE, SPE activating protease; SPE, Spätzle processing enzyme.

INTRODUCTION

Melanization is a prominent defense mechanism in arthropods that plays an essential role in wound healing, killing of microbes, and parasites encapsulation (1, 2). The key protease in melanization is phenoloxidase (PO), which can catalyze phenols to quinines, then form melanin. PO usually exists as the zymogen, prophenoloxidase (PPO). Its activation depends on the extracellular serine protease (SP) cascade triggered by invading microbes. The recognition of pathogen-associated molecular patterns, such as β-1,3-glucan from fungi, peptidoglycan from Gram-positive bacteria, or lipopolysaccharide from Gram-negative bacteria, by host pattern recognition receptors (PRRs) leads to the activation of modular proteases that sequentially cleave the downstream SPs and ultimately activate PPO (3).

The extracellular PPO activation pathway usually consists of a three-step proteolytic cascade initiated by one modular SP then followed by clip domain SPs (cSPs), which has been comprehensively revealed in a lepidopteran species *Manduca sexta* (4–7) and a coleopteran species *Tenebrio molitor* (8, 9). cSPs and the homologs are classified into four subfamilies (A–D) based on phylogenetic analysis (10, 11). Most PPO activating proteases that directly activate PPO belong to CLIPB, such as *M. sexta* PPO activating protease (PAP) 1-3 (12, 13) and *T. molitor* Spätzle processing enzyme (SPE) (8). The proteases that cleave CLIPB are generally derived from CLIPC. For example, *M. sexta* hemolymph protease (HP) 6 and HP21 activates PAP1 and PAP2/3, respectively (4, 7) and *T. molitor* SPE activating enzyme (SAE) cleaves SPE (8). The initiating modular SPs without clip domains that activate CLIPC members are characterized by containing low-density lipoprotein receptor class A (LDLa), Sushi and Wonton domains (14, 15). They could be autoactivated in the presence of pathogens, then cleaved the downstream proteases. In *M. sexta*, the modular SP, HP14, was stimulated to activate by its interaction with β-glucan recognition proteins (βGRP) 2 before cleaving HP21 (15). *T. molitor* modular SP (MSP) was also one modular SP which activated SAE (8). Alternatively, the initiating SP could be the CLIPD member. For example, *M. sexta* HP1, a member of CLIPD, was identified as a recognition protein of the melanization cascade which was activated without proteolytic cleavage (3, 16).

CLIPA are cSP homologs (cSPHs) that lost catalytic activity due to the replacement of catalytic triad residues (11). cSPHs seem to serve as cofactors that significantly increase PO activity (6, 12, 13). Although there were three PAPs in *M. sexta*, PO activity was very low in the absence of cofactors. Only in the presence of cSPH1 and cSPH2, PO activity was greatly enhanced (12). According to the crystal structure of *M. sexta* PPO, it has been suggested that the combination of cSPHs and PO might lead to the conformation change of the latter, enabling the substrate to be more accessible to the active site of PO (17).

Melanization has also been studied in other insects. In *Drosophila melanogaster*, Hayan, Sp7 and ModSP were verified to function during melanization (18, 19). In *Aedes aegypti*, immune melanization proteases (IMP-1 and IMP-2) were identifed to mediate the cleavage of PPO to combate the malaria parasite (20). In *Anopheles gambiae*, CLIPB9 directly cleaves and activates PPO, whereas CLIPB8 is also part of the PPO activation system (21, 22). In *Bombyx mori*, PGRP-S5 functions as a pattern recognition receptor during melanization (23) and BmSPH-1 interacts with PPO and PPO-activating enzyme (PPAE) (24). In *Ostrinia furnacalis*, SP105 could fucntionaly activate PPO (25). Overall, researches on melanization in other insects are not as comprehensive as those in *M. sexta* and *T. molitor*.

Several studies have suggested that melanization is involved in defense against virus infection. For examples, silencing PPO-I gene in *Armigeres subalbatus* increased Sindbis virus replication (26). Plasma PO of *Heliothis virescens* inhibited baculovirus infection (27). The melanin precursor 5,6-dihydroxyindole (DHI) showed broad-spectrum antiviral activity (28). PO activity in *Ae. aegypti* is required for innate immune response against Semliki Forest virus (SFV) infection (29). Recently, our study showed that melanization in *Helicoverpa armigera* is involved in baculovirus infection (30).

Cotton bollworm, *H. armigera*, is a worldwide distributed agricultural pest. It caused severe damage to many crops (31). Melanization in *H. armigera* plays an important role in defense against invading pathogens (30, 32–35). Previously transcriptomic and proteomic analyses showed that many SPs and homologs were up-regulated in response to the challenge of bacteria or fungi (34), however, they were down-regulated with baculovirus infection (30). At the same time, two negative regulators serpin-5 and serpin-9 of the pathway were sequentially induced by baculovirus infection to inhibit their target proteases, cSP4 and cSP6, respectively (30). Thus, baculoviruses have developed efficient strategies to suppress the host melanization response for their proper proliferation. Previous studies identified that there were two PPOs (PPO1 and PPO2) and at least 11 cSPs in *H. armigera* (34). These include procSP6, 7, and 8 belonging to CLIPB; procSP1, 2, 3, and 4 of CLIPC; and procSP5, 9, 10, and 29 belonging to CLIPD. In addition, three potential mudular SPs (proSP41, 42, and 43) were identified with the LDLa and sushi domains, while procSPH11, 49, and 50 were found to be cSP homologs. Furthermore, it has been verified that PPO can be proteolytically activated by cSP6, a member of the CLIPB subfamily (30). However, so far, the complete PPO activation pathway of *H. armigera* remains unclear.

In this study, we identified the members involved in PPO activation cascade step-by-step using biochemical methods and finally *in vitro* reconstructed a complete PPO activation pathway in *H. armigera*. Two cSPHs that could significantly enhanced PO activity were identified. The reconstructed PPO activation pathway efficiently antagonized viral infection *in vitro*. The cascade in *H. armigera* was conserved compared with that in *M. sexta*.

MATERIALS AND METHODS

Cells and Virus

The *Drosophila* S2 cell line was cultured in ESF921 medium (Expression Systems, Woodland, CA, United States) at 27°C.

The recombinant *Helicoverpa armigera* nucleopolyhedrovirus (HearNPV) expressing an *egfp* reporter gene (HearNPV-*egfp*) was previously constructed by our laboratory (36).

Expression of Recombinant Serine Proteases (SPs)

Total RNA was isolated from the fat body of the day-3 5th instar *H. armigera* larvae using TRIzol reagent (Invitrogen, Carlsbad, CA, United States). The entire coding region of proSPs (proSP41, procSP1, procSP6) and procSPHs (procSPH11, procSPH49 and procSPH50) (34) were amplified by reverse transcriptase polymerase chain reaction (RT-PCR) using the PrimeScript^{TM} RT reagent kit with gDNA Eraser (Takara Bio, Otsu, Japan) with the primers listed in **Supplementary Table S1**. The PCR products were cloned into the pMT-BiP/V5-HisA vector (Invitrogen). Overlap extension PCR was performed to prepare constructs designated as cSP_{Xa}, in which four residues at the putative activation site were replaced with tetrapeptide IEGR, a cleavage site of bovine coagulation factor Xa (37). The putative cleavage sites of proSP41, procSP1, procSP6, procSPH11, procSPH49 and procSPH50 are VDVL, TDKL, VGNK, ADLR, VSFI, and LDIR, respectively. The plasmids were transfected into *Drosophila* S2 cells along with pCoHygro hygromycin selection vector (Invitrogen) and stable cell lines were screened according to the manufacturer's instruction. The cell supernatants containing secreted recombinant proteases were harvested. Recombinant proteins were purified using nickel-charged resin (Roche Diagnostics, Basel, Switzerland), eluted with imidazole, and further concentrated by filtration through an Amicon Ultra 10K cartridge (Millipore, Billerica, MA, United States). The purified proteins were stored at −80°C before use.

Generation of Polyclonal Antibodies

procSP6, procSPH11, and procSPH50 for prokaryotic expression were subcloned into the pET-28a expression vector using the primers listed in **Supplementary Table S1**. Recombinant protein was expressed in *Escherichia coli* BL21 cells and purified with nickel-charged resin. procSP1 was expressed in *Drosophila* S2 cells as described above. The recombinant proteins were used to immune rabbit to generate the respective polyclonal antibodies as described previously (38). The polyclonal antibodies against PPO1 and PPO2 were generated as described previously (30).

Purification of PPO From Larval Hemolymph

Prophenoloxidase was purified from the hemolymph of day-3 5th instar *H. armigera* larvae according to the protocol reported described (30). Briefly, 10 ml hemolymph was collected from larval body and pooled into ice-cold saturated ammonium sulfate (AS). AS saturation (35-50%) was collected and loaded on column prepacked with Ceramic Hydroxyapatite (Bio-Rad, Hercules, CA, United States). The fractions with cetylpyridinium chloride (CPC) activated PO activity were combined and applied through Concanavalin A Sepharose column (Sigma-Aldrich, St. Louis, MO, United States). The flow-through fraction was applied to a Phenyl Sepharose 6 Fast Flow (low sub) column (GE Healthcare, Little Chalfont, United Kingdom). Fractions containing PO activity were applied to a Superdex 200 column (ÄKTApurifier; GE Healthcare). Purified PPO were stored at −80°C before analysis.

The Activation and Activity of Serine Protease and PPO

To activate $procSP_{Xa}$ with factor Xa, purified $procSP_{Xa}$ was incubated with bovine factor Xa (New England Biolabs, Ipswich, MA, United States) in buffer [20 mM Tris–HCl, 0.1 M NaCl, 2 mM CaCl (pH 8.0)] at 27°C for 5 h. Amidase activity of the reaction mixtures was measured using 200 μL, 50 μM acetyl-Ile-Glu-Ala-Arg-p-nitroanilide (IEAR) as the substrate (39). One unit of amidase activity was defined as ΔA405 of 0.001 in one minute. Factor Xa activated $procSP_{Xa}$ was incubated with procSP at 37°C for 1 h before immunoblot analysis under reducing conditions containing β-mercaptoethanol (β-ME) or non-reducing conditions. Mixtures containing sequentially activated SP cascade components ($cSP6_{Xa}$, $cSP1_{Xa}$/procSP6, and $SP41_{Xa}$/procSP1/procSP6) were incubated with purified PPO at room temperature for 10 min to detect PPO cleavage by immunoblotting. To measure PO activity, samples were transferred to 96-well plates, and 200 μL of 2 mM Dopa in 50 mM sodium phosphate buffer (pH 6.5) were added. The activity was determined by measuring the absorbance at 470 nm with a microplate reader (Synergy H1; BioTek, Winooski, VT, United States). One unit of PO activity was defined as ΔA470 of 0.001 in one minute (30).

Effects of *in vitro* Activated Melanization on Baculovirus Infection

HearNPV-*egfp* (MOI = 0.5 $TCID_{50}$ units/well) was mixed with the SP cascade ($SP41_{Xa}$ + procSP1 + procSP6), PPO and its substrate (PPO + Dopa), the cSPHs (procSPH11 + procSPH50), and the serine protease inhibitor (serpin-9) with different combinations. The amount of each agents were as follows: 200 ng PPO, 10 μL of 20 mM Dopa, 50 ng $SP41_{Xa}$, 50 ng procSP1, 100 ng procSP6, 200 ng procSPH11, 200 ng procSPH50, and 1 μg serpin-9. Then all of the mixtures were adjusted to a final volume of 100 μL and incubated at room temperature for 0, 1, and 3 h, respectively. The mixtures were added to HzAM1 cells in Grace's insect medium supplemented with 2% fetal bovine serum in 24-well plates and incubated for 2 h. The cells were washed three times with serum-free medium and incubated at 27°C for 24 h, and viral infection was examined under a fluorescence microscope using the EVOSTM FL Auto Imagine System (Thermo Fisher Scientific, Waltham, MA, United States).

Statistical Analysis

All statistical evaluations were determined using GraphPad Prism 5 software. Statistical differences between two groups were performed using the two-tailed Student's *t*-tests ($n \geq 3$ biological replicates) $^{*}p < 0.05$, $^{**}p < 0.01$, and $^{***}p < 0.001$.

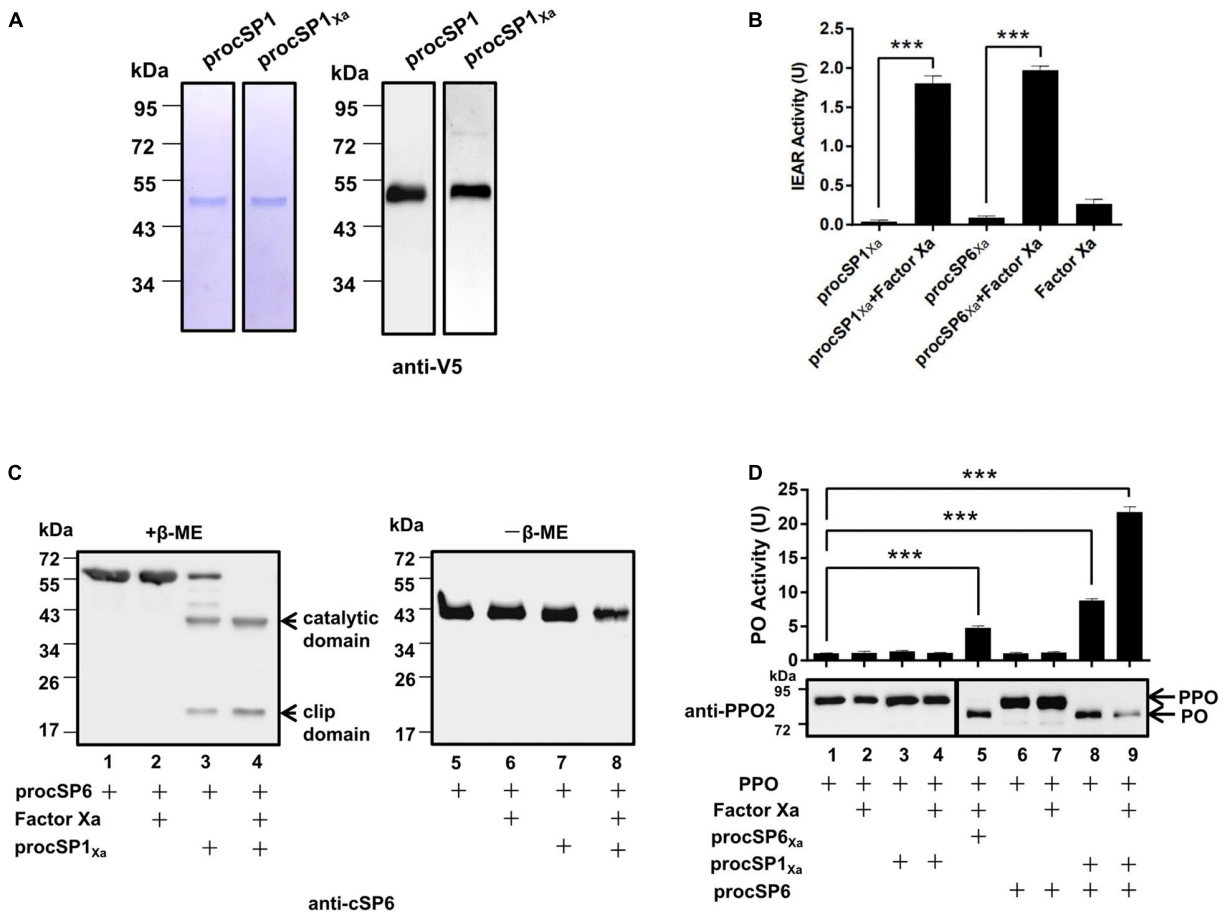

FIGURE 1 | Prophenoloxidase (PPO) is sequentially activated by cSP1/cSP6. **(A)** SDS-PAGE and immunoblot analysis of purified recombinant procSP1 and procSP1$_{Xa}$. Anti-V5 antibody was used to detect recombinant proteins by immunoblotting. **(B)** Amidase activity of cSP1$_{Xa}$. Catalytic activity of activated cSP1$_{Xa}$ (100 ng) and cSP6$_{Xa}$ (100 ng) were detected using IEAR as a substrate. ***$p < 0.001$. **(C)** Factor Xa activated procSP1$_{Xa}$ can cleave procSP6. procSP1$_{Xa}$ (50 ng) was processed by factor Xa, and then incubated with procSP6 (100 ng) for 1 h. To examine the effect of disulfide bonds on protein mobility, mixtures were treated with SDS sample buffer with (left panel) or without β-ME (right panel) and separated by SDS-PAGE followed by immunoblotting using an anti-cSP6 antibody. **(D)** PPO was sequentially activated by cSP1/cSP6. Activated cSP6 was incubated with PPO (100 ng) for 10 min, and analyzed by immunoblotting using an anti-PPO2 antibody (middle panel). Higher amount of PPO (300 ng) was used in detecting PO activity (upper panel), and PO activity was represented as mean ± SD of three independent experiments. ***$p < 0.001$.

Gene Accession Numbers

All sequence data that support the findings of this study are available in GenBank with the following accession numbers: proSP41 (MT182806), proSP42 (MT182807), proSP43 (MT182808), procSP1 (MT182805), procSP6 (KY680241), procSPH11 (MT182809), procSPH50 (MT182810), PPO1 (KY744277), PPO2 (KY744278), and serpin-9 (KY680239).

RESULTS

cSP1 Cleaves the PPO Activating Protease cSP6

We decided to *in vitro* re-constitute the PPO activation cascade of *H. armigera* using a "bottom-up" strategy. PPO was purified from the hemolymph of *H. armigera* larvae and, after a CPC-induced conformation changes, PO activity was confirmed by production of dopamine chrome (or dopachrome) from dopamine (or dopa) (**Supplementary Figure S1A**). Immunoblotting analysis further showed that purified PPO formed a heterodimer constituted of PPO1 and PPO2 (**Supplementary Figure S1B**). We previously identified that cSP6 served as a PPO activating enzyme (30). This was confirmed as evidenced by the cleavage and enzymatic activation of PPO by the factor Xa activated recombinant procSP6$_{Xa}$ (**Supplementary Figures S1C,D**).

According to the phylogenetic analysis, cSP1 of *H. armigera* was classified as a member of CLIPC subfamily, and showed close phylogenetic relationship to *M. sexta* HP21 (30), the upstream cSP of *M. sexta* PAP2/3 (7), implying that cSP1 might be the protease upstream of cSP6 in *H. armigera*. To characterize the function of cSP1, recombinant procSP1 and its modified form were expressed and purified using *Drosophila* S2 cells (**Figure 1A**). Activity of the cleaved cSP1 and cSP6 was detected as hydrolysis of the IEAR substrate (**Figure 1B**).

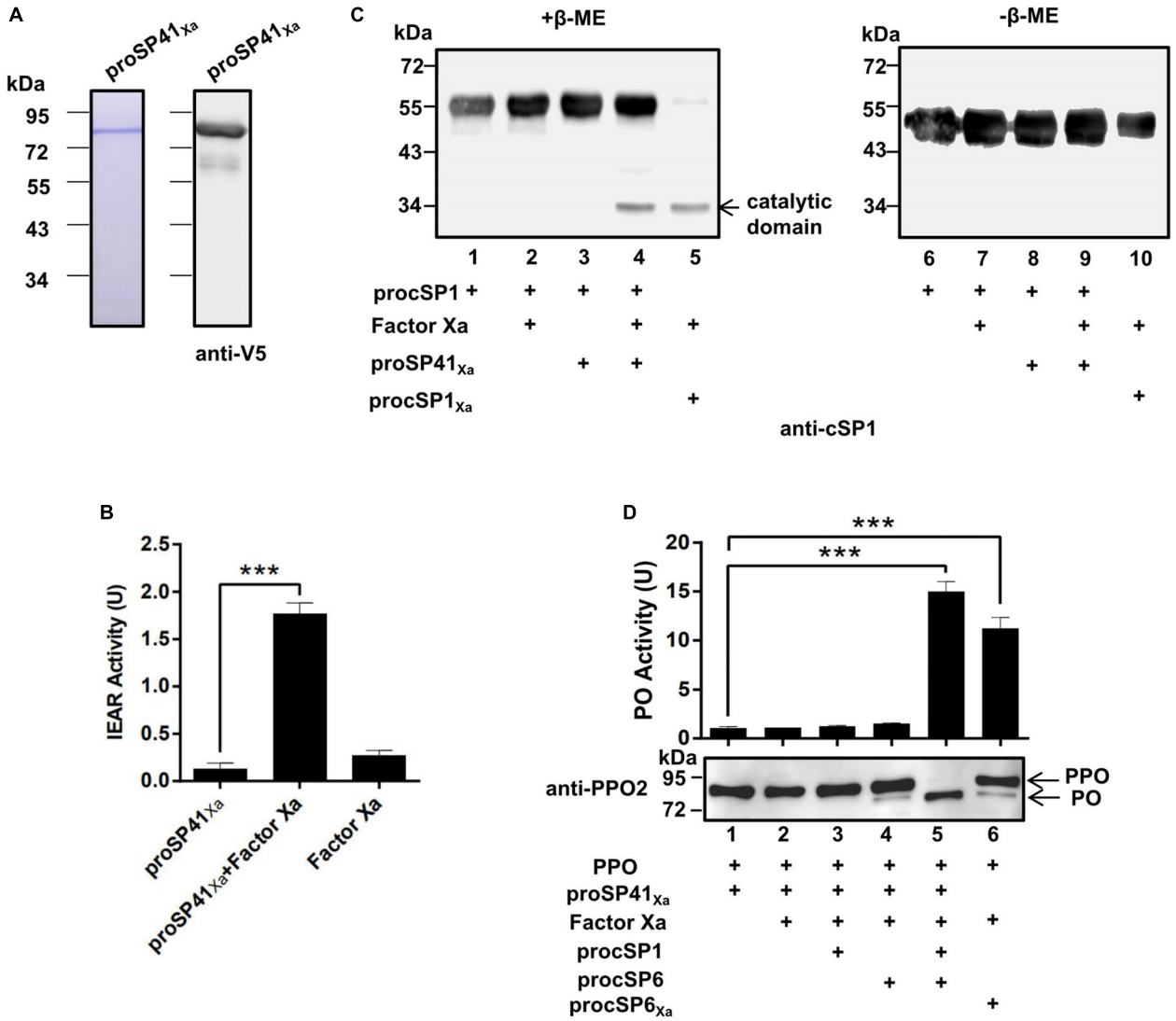

FIGURE 2 | Prophenoloxidase activation by the melanization cascade initiated by SP41. **(A)** SDS-PAGE and immunoblot analysis of purified recombinant proSP41 and proSP41$_{Xa}$. Anti-V5 antibody was used to detect recombinant proteins by immunoblotting. **(B)** Amidase activity of SP41$_{Xa}$. Catalytic activity of activated SP41$_{Xa}$ (300 ng) was detected using IEAR as a substrate. ***$p < 0.001$. **(C)** Activation of procSP1 by SP41$_{Xa}$. Factor Xa (50 ng) activated proSP41$_{Xa}$ was incubated with procSP1 (100 ng) for 1 h. To examine the effects of disulfide bonds on protein mobility, mixtures were treated with SDS sample buffer with (left panel) or without β-ME (right panel) and analyzed by immunoblotting using an anti-cSP1 antibody. **(D)** PPO activation by the melanization cascade initiated by SP41$_{Xa}$. Activated cSP1 in **(C)** was incubated with procSP6 (50 ng) for 1 h, and then mixed with 100 ng PPO with immunoblotting or 300 ng PPO with PO activity for another 10 min. Immunoblotting was performed using an anti-PPO2 antibody (middle panel). PO activity (upper panel) was represented as mean ± SD of three independent experiments. ***$p < 0.001$.

Then, procSP6 was incubated with factor Xa activated procSP1$_{Xa}$, and the result showed that cSP1$_{Xa}$ could cleave procSP6 (∼57 kDa), and the separated catalytic domain (∼38 kDa) and clip domain (∼19 kDa) were clearly detected with the anti-cSP6 antibody under reducing condition (**Figure 1C**, lane 4). Interestingly, procSP6 could be partially cleaved by procSP1$_{Xa}$ without activation (**Figure 1C**, lane 3). While under the non-reducing condition, the disulfide bond linked subdomains of cSP6 migrated to the same position as the procSP6 (**Figure 1C**, lanes 5–8), indicating that procSP6 was specifically cleaved by cSP1$_{Xa}$.

Next, PPO was added to the mixtures as described above and the cleavage of PPO was detected using immunoblotting. As expected, PPO was efficiently cleaved by cSP6 in the presence of procSP1$_{Xa}$ and factor Xa (**Figure 1D**, lane 9). Correspondingly, high PO activity was detected (**Figure 1D**, lane 9, upper panel). Interestingly, procSP1$_{Xa}$ and procSP6 mixed together were able to activate PPO in the absence of factor Xa (**Figure 1D**, lane 8), which was consistent with the finding that procSP6 was partially cleaved by procSP1$_{Xa}$ (**Figure 1C**, lane 3). We noticed that PO activity induced by cSP6 via activated cSP1 (**Figure 1D**, lane 9) was much higher than that by factor Xa activated cSP6$_{Xa}$

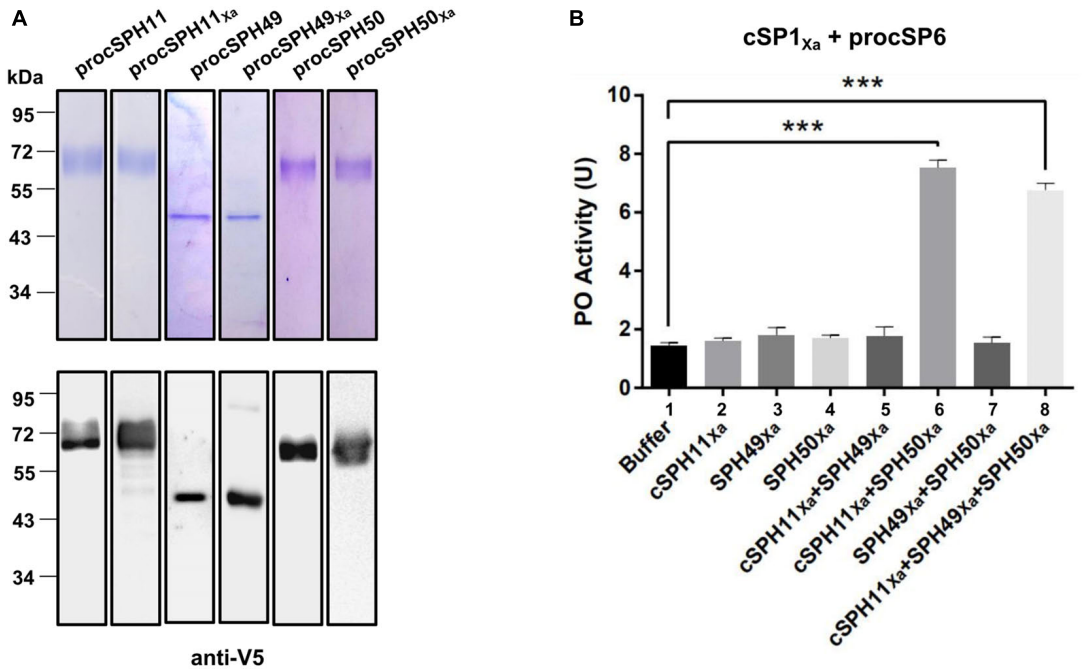

FIGURE 3 | Phenoloxidase (PO) activity is enhanced by $cSPH11_{Xa}$ and $cSPH50_{Xa}$. **(A)** SDS-PAGE and immunoblot analysis of recombinant procSPH11, $procSPH11_{Xa}$, procSPH49, $procSPH49_{Xa}$, procSPH50, and $procSPH50_{Xa}$. Anti-V5 antibody was used in immunoblotting. **(B)** PO activity increased significantly in the presence of $cSPH11_{Xa}$ and $cSPH50_{Xa}$. Factor Xa processed $procSP1_{Xa}$ (50 ng) was incubated with procSP6 (100 ng) for 1 h, respectively. At the same time, $procSPH11_{Xa}$, $procSPH50_{Xa}$ and $procSPH49_{Xa}$ (100 ng) were activated with factor Xa. Purified PPO (100 ng) was added to the mixture and PO activity was measured. PO activity was represented as mean ± SD of three independent experiments. ***$p < 0.001$.

(**Figure 1D**, lane 5), indicating that cSP6 activated at its native cleavage site has higher activity than the modified form. To be noted, PO activity induced by cSP6 via $procSP1_{Xa}$ (**Figure 1D**, lane 8) was also higher than that by factor Xa activated $cSP6_{Xa}$ (**Figure 1D**, lane 5), suggesting the self-activated $procSP1_{Xa}$ is likely to be able to active cSP6 at its native cleavage site. Thus, PPO can be activated by the cascade of cSP1/cSP6.

SP41 Is an Initiating SP of the PPO Activation Pathway

To find out the initiating SP in the PPO activation pathway of *H. armigera*, phylogenetic analysis (**Supplementary Figure S2A**) and domain architecture comparison (**Supplementary Figure S2B**) were performed. Three modular SPs (SP41, SP42, and SP43) in *H. armigera* showed homology (with the identities of 48, 58, and 44%, respectively) to *M. sexta* HP14, which is an initiating SP upstream of HP21 (14, 15), implying the possible role of the three SPs in activation of procSP1. To verify their functions, recombinant $proSP41_{Xa}$, $proSP42_{Xa}$, and $proSP43_{Xa}$ were expressed and purified using *Drosophila* S2 cells (**Supplementary Figures 2A, S3A**). The SP activity was measured using IEAR substrate, and the result showed that purified recombinant modular $SP41_{Xa}$ exhibited amidase activity (**Figure 2B**), so did $SP42_{Xa}$ and $SP43_{Xa}$ (**Supplementary Figure S3B**). Then $proSP41_{Xa}$, $proSP42_{Xa}$, and $proSP43_{Xa}$ were tested for their ability to cleave procSP1. Among the three cSPs, only $SP41_{Xa}$ cleaved procSP1 (**Figure 2C**, lane 4) and the catalytic domains of cSP1 migrated to the same position with procSP1 under non-reducing conditions, indicating that it was specifically cleaved (**Figure 2C**, lanes 6–10). In contrast, $proSP42_{Xa}$ and $proSP43_{Xa}$ failed to activate procSP1 (**Supplementary Figure S3C**).

We next investigated whether the entire pathway could activate PPO *in vitro*. The PO band was clearly detected after incubation of PPO with the mixtures of factor Xa, $proSP41_{Xa}$, procSP1, procSP6 (**Figure 2D**, lane 5), and PO activity was also increased (**Figure 2D**, lanes 5 and 6, upper panel). These results clearly showed that PPOs were enzymatically cleaved and activated by the cascade initiated from activated $SP41_{Xa}$. Thus, a complete PPO activation pathway in *H. armigera* was reconstructed *in vitro*.

PO Activity Is Enhanced in the Presence of cSPH11 and cSPH50

Phylogenetic analysis showed that three *H. armigera* cSPHs (cSPH11, cSPH49, and cSPH50) were homologs to *M. sexta* cSPH1 and cSPH2 (data not shown), suggesting that they may serve as potential cofactors for PPO activation. Therefore, we firstly expressed and purified recombinant procSPHs and their modified forms (**Figure 3A**). Then, the factor Xa activated procSPHs, either individually or in different combinations, were incubated with mixtures of PPO and $cSP1_{Xa}$ activated cSP6 before measuring of PO activity. Only in the presence of $cSPH11_{Xa}$ and $cSPH50_{Xa}$ simultaneously, a significant increase of PO activity

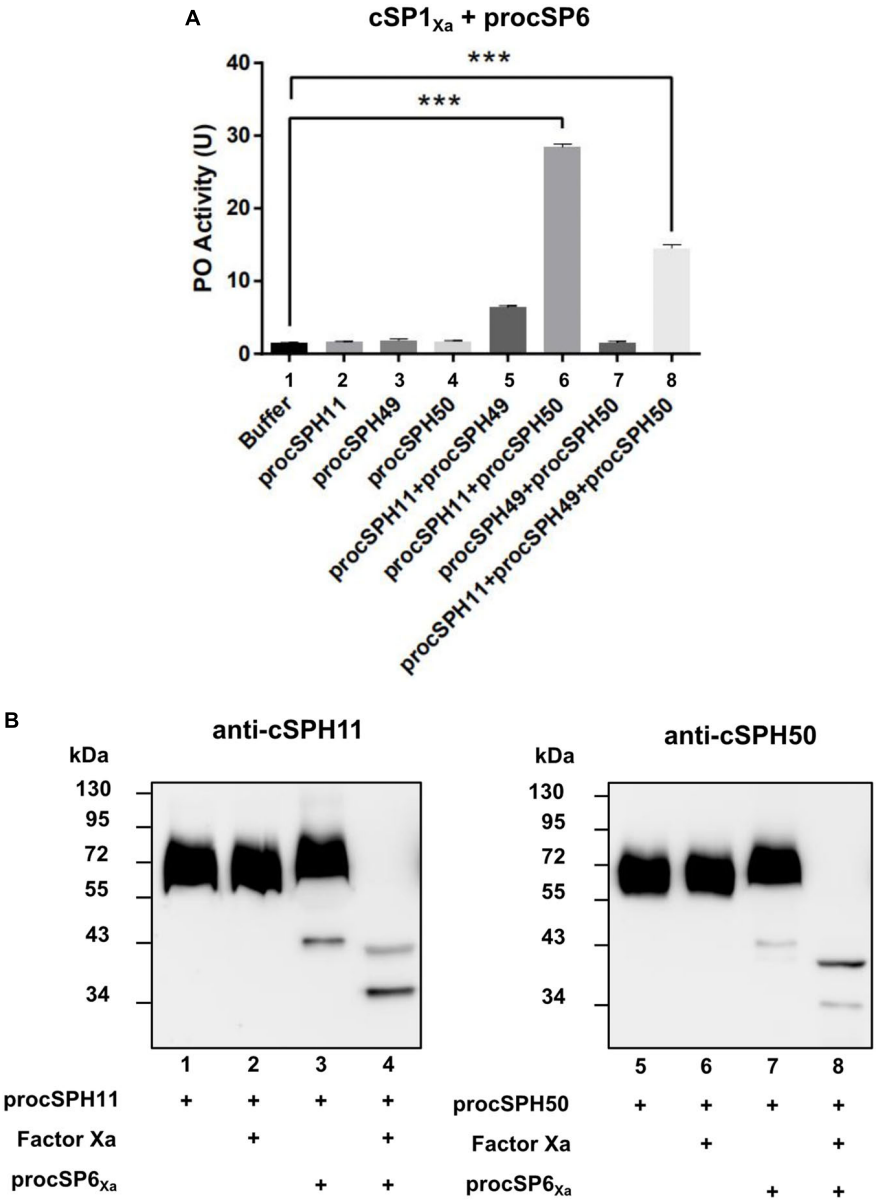

FIGURE 4 | cSPH11 and cSPH50 are cofactors in PPO activation. **(A)** PO activity was increased significantly in the presence of procSPH11 and procSPH50. The experimental groups were the same with **Figure 3B**, instead of factor Xa mutants, wild type procSPHs were used to measure PO activity (upper panel), which was represented as mean ± SD of three independent experiments. ***$p < 0.001$. **(B)** Proteolytic activation of procSPH11 and proSPH50 by $cSP6_{Xa}$. Factor Xa activated $cSP6_{Xa}$ (50 ng) was incubated with 100 ng procSPH11 (left panel) or procSPH50 (right panel) for 1 h. The mixtures were analyzed by immunoblotting using anti-cSPH11 or anti-cSPH50 antibody.

was detected (**Figure 3B**, lane 6 and 8), indicating that cSPH11 and cSPH50 acted in concert to synergize PO activity. To be noted, to better reflect the function of cSPHs, the amount of PPO used in this experiment (**Figure 3B**) was much lower than the above results when cSPHs were not present (**Figures 1D**, **2D**).

To further confirm this finding, we performed a similar experiment as **Figure 3B** by using purified wild type forms of procSPH11, procSPH49 and procSPH50 instead of the modified procSPHs activated with factor Xa. The result showed that PO activity was also increased in the presence of procSPH11 and procSPH50 (**Figure 4A**, lane 6), with even much higher activity (about fourfold greater) than those using the factor Xa activated cSPHs. Interestingly, the combination of cSPH11 and cSPH49 also increased PO activity (**Figure 4A**, lane 5) but the effect was less prominent than that induced by cSPH11 and cSPH50 (**Figure 4A**, lane 6).

In *M. sexta*, cSPHs could be cleaved by PAPs, which were PPO activating proteases (12). Therefore, we asked whether cSPHs would be cleaved by the PPO activating protease before functioning in *H. armigera*. To examine this hypothesis, factor

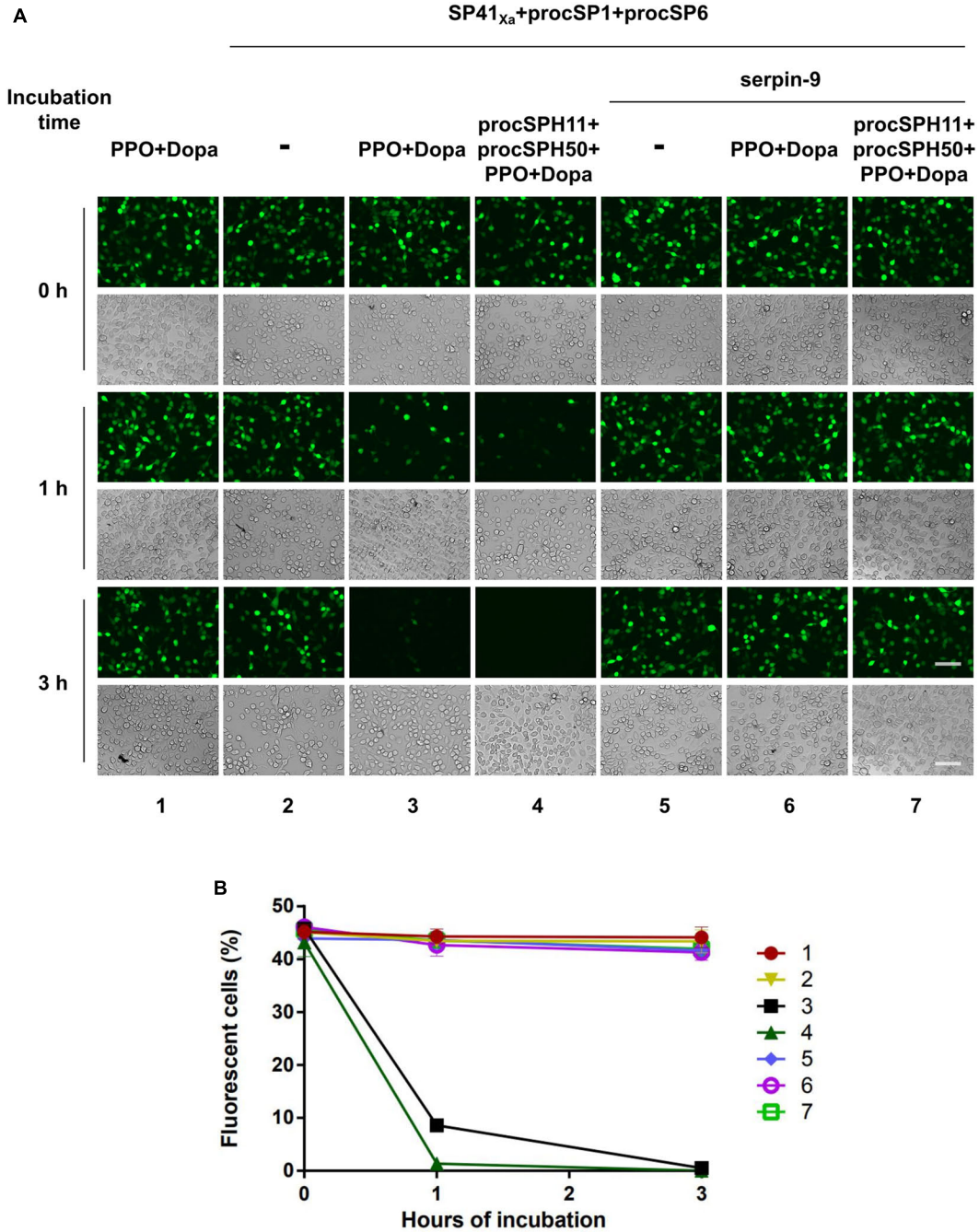

FIGURE 5 | Baculovirus infection is blocked by melanization cascade *in vitro*. **(A)** HearNPV-*egfp* was mixed with PPO and Dopa, SP cascade ($SP41_{Xa}$ + procSP1 + procSP6), the cSPHs (procSPH11 + procSPH50), and the serine protease inhibitor (serpin-9) with different combinations. These mixtures were incubated at room temperature for 0, 1, or 3 h before infecting HzAM1 cells. Fluorescence micrographs and normal imagines were acquired 24 h p.i. to assess the viability of the baculovirus. Scale bars represent 100 μm. **(B)** Quantification of fluorescent cells. Infected HzAM1 cells in images shown in **(A)** were counted. All data were represented as mean ± SD of three independent experiments. Labels 1–7 in the figure represented different treatments as indicated in **(A)**.

Xa activated $cSP6_{Xa}$ was incubated with procSPH11 (**Figure 4B**, left panel) or procSPH50 (**Figure 4B**, right panel) at 37°C for 1 h, and then analyzed using immunoblotting. As expected, cleaved bands corresponding to cSPH11 or cSPH50 were detected, when $cSP6_{Xa}$ was activated (**Figure 4B**, lanes 4 and 8).

In vitro PPO Activation Cascade Blocks Baculovirus Infection

Melanized hemolymph of *H. armigera* could inactivate the infectivity of HearNPV in cell cultures (30). Since hemolymph consists of complicated components, we would like to evaluate

whether our identified melanization cascade could directly block viral infection when activated *in vitro*. To this end, an *egfp* maker gene labeled HearNPV-*egfp* was incubated with purified PPO, the substrate Dopa, and selected cSP or SP for 0, 1, and 3 h at room temperature. Then, the mixtures were added to HzAM1 cells for 24 h before observation using fluorescence microscopy. When the HearNPV-*egfp* suspension was incubated with the mixtures of PPO and Dopa, the number of infected cells was similar among the 0, 1, and 3 h incubation groups (**Figure 5**, panel 1), suggesting that inactivated PPO and the substrate did not affect virus viability. Similarly, when the cascade components ($SP41_{Xa}$, procSP1, and procSP6) were incubated with the virus, respectively, the number of infected cells was similar at 0, 1, and 3 h post infection (h p.i.) (**Figure 5**, panel 2), indicating that these proteins alone had no effects on virus infectivity. However, in the presence of PPO and Dopa in addition to the cSP6 cascade components, much fewer infected cells were observed after 1 h, and almost no virus infection was observed after 3 h (**Figure 5**, panel 3), demonstrating that the cSP6 mediated PPO activation could block viral infection efficiently. When procSPH11 and procSPH50 were added to the above mixtures, a more potent inhibitory effect was observed after 1 h p.i., and no virus infected cells were detected (**Figure 5**, panel 4). Furthermore, when serpin-9, an inhibitor of cSP6 (30), was added to the mixtures, viral infection was substantially rescued (**Figure 5**, panel 6 and 7). These results demonstrated that the SP41/cSP1/cSP6 cascade can induce melanization and block baculovirus infection. Moreover, the inhibitory effect against baculovirus infection was enhanced in the presence of the cofactors and the inhibition could be rescued by serpin-9.

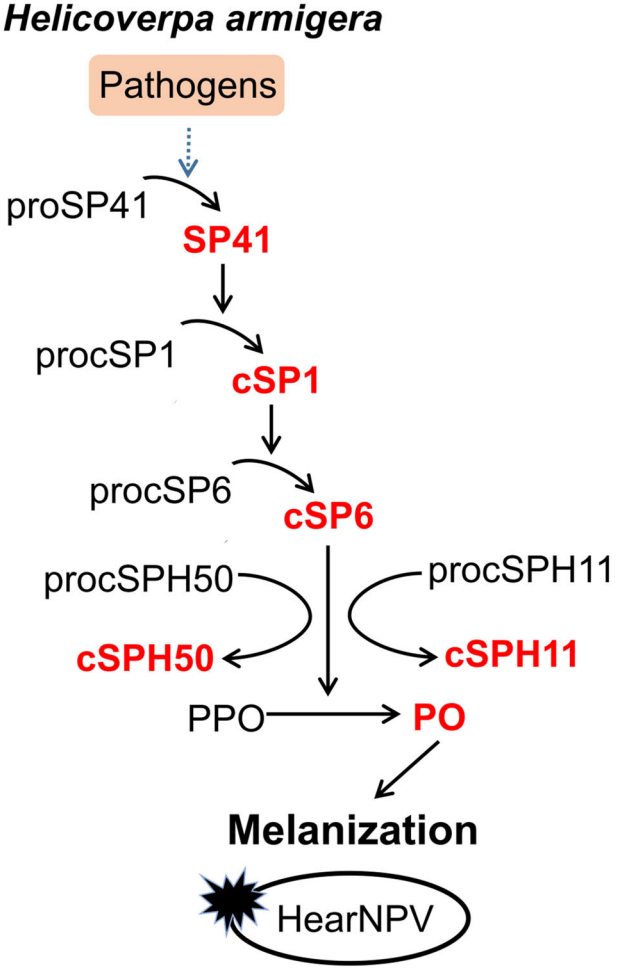

FIGURE 6 | Proposed PPO activation pathway in *H. armigera*. Initiation of SP41 sequentially cleaves cSP1/cSP6, resulting in PPO activation. The cofactors cSPH11 and cSPH50 can enhance PO activity activated by cSP6. Baculovirus infection can be blocked by melanization *in vitro*.

DISCUSSION

Although certain components of melanization cascade have been identified in many insects, such as *Ae. aegypti* (10, 20, 40, 41), *A. gambiae* (42–45), *D. melanogaster* (18, 46, 47), the complete PPO activation pathway was elucidated only in a few insects, for example *M. sexta* (4–7), and *T. molitor* (8, 9). To date, the complete pathway in *H. armigera* was unknown until this study. Transcriptome-based analysis revealed more than 60 SPs and homologs in *H. armigera*. Among these, at least 11 clip domain-containing members might be involved in PPO activation cascades (34). However, only cSP4 and cSP6 were confirmed to participate in *H. armigera* PPO activation pathway (30). Here, based on the PPO activating protease activity of cSP6, a PPO activation pathway composed of its activating protease cSP1 and the initiating protease SP41 was identified and reconstituted *in vitro* using biochemical methods. In addition, cSPH11 and cSPH50, which could be cleaved by the terminal cSP6, were characterized as the cofactors during PPO activation. The PPO pathway identified in *H. armigera* (**Figure 6**) resembles the HP14/HP21/PAP2/3 pathway of *M. sexta* (48, 49).

The initiating proteases of melanization are generally autoactivated upon binding of PRRs to pathogens (14, 15, 47, 49, 50). For *M. sexta* HP14, binding of β-1,3-glucan to βGRP2 results in a significant increase in affinity between the N-terminal LDLa domains of HP14 and βGRP2 (15). MSPs in other insects such as *D. melanogaster* (47) and *T. molitor* (8) are considered as initiating proteases in SP cascades and they also contain LDLa domains. Similarly, the three SPs (SP41-43) of *H. armigera* all have LDLa domains (**Supplementary Figure S2B**), however, only SP41 was able to induce melanization cascade (**Figure 2** and **Supplementary Figure S3**). In the domain structure, both SP41 and SP42 contain five LDLa domains and two Sushi domains at their N-termini, while SP43 has only four LDLa domains (**Supplementary Figure S2B**). Currently it is unclear why only SP41, but not the other two SPs serve as the initiating SP. Besides the modular SPs, cSPs may also function as the initiating SPs. *M. sexta* proHP1 utilizes a conventional mechanism to active its downstream protease which was not induced by proteolytic cleavage (16). Whether there exists another PPO activation cascade in *H. armigera* initiated by a clip domain SP remains to be determined.

Various mechanisms of PPO activation by the terminal cSPs and cofactors have been characterized in insects (2). In *B. mori*, PPO1 and PPO2 are cleaved by PPAE belonging to CLIPB, and the resulting large fragments of PO1 and PO2 directly exhibit PO activity (51). In *M. sexta*, cleavage of PPO1 and PPO2 by three PAPs (CLIPB) yielded large fragments of PPO1 and PPO2 with low PO activity, which was significantly enhanced by the SPH1 and SPH2 (CLIPA). During this process, SPHs must be cleaved by PAPs then to play their roles (6, 12, 13). In *Holotrichia diomphalia*, PPO-activating factor (PPAF)-I is a CLIPB protease which cleaves PPO-I to generate a 76 kDa fragment without PO activity; however, when PPAF-II (CLIPA) and PPAF-III (CLIPB) were further added, a new 60 kDa fragment with PO activity was produced (52). The crystal structure of PPAF-II showed that its clip domain adopted a novel conformation compared to CLIPB members then may serve as a module for binding the cleaved PO and forming active PO clusters (53). How PPAF-I, II and III act in concert to activate PPO remains to be determined. In *Ae. aegypti*. ten PPO genes were identified and a 50 kDa PO fragment was generated challenged by fungi, suggesting a complicated activation mechanism (40). In *H. armigera*, our results showed that the cofactors procSPH11 and procSPH50 were also cleaved by cSP6 (**Figure 4B**). There was low PO activity after PPO was cleaved by cSP6, and PO activity was significantly increased in the presence of cSPH11 and cSPH50 which are orthologs of *M. sexta* SPH1 and SPH2, respectively. Our results suggested that the mode of PPO activation in *H. armigera* was similar to that in *M. sexta*. It will be interesting to elucidate the mode of actions of the cofactors in insect melanization responses in the future.

Melanization is essential for combating pathogens in insects. In *Ae. aegypti*, PO activity was found to be required for defense against the SFV (29). Knocking down the only two PPO genes of *Penaeus monodon* led to the increased mortality by white spot syndrome virus (WSSV) infection (54). These suggest that melanization plays a crucial role in antiviral immunity. Correspondingly, viruses have evolved versatile strategies to inhibit or escape host melanization response for their proper survival, either by inhibiting the signal transduction of melanization or affecting PO activity directly. The polydnaviruses (PDV) carried by the *Microplitis demolitor* expresses Egf1.0 and Egf1.5 to inhibit the activity of PAP1 and PAP3 of *M. sexta* (55, 56). Infection of *Ae. aegypti* with Egf1.0-expressing SFV led to increased mortality and virus amplification (29). WSSV453, a non-structural viral protein, interacts with *P. monodon* proPPAE2 and interferes with its activation to active PPAE2 (57). In *H. armigera*, a transcriptomic analysis showed that cSP6 was markedly repressed during the late stage of baculovirus infection, and the inhibitor of cSP6 was up-regulated to suppress melanization (35). Although a previous study demonstrated that the melanized hemolymph of *H. armigera* could inactive virus (30), considering the complexity of hemolymph components, there might be other antiviral host factors involved in. Through the reconstruction of melanization *in vitro*, we demonstrated that activated melanization reaction itself could inhibit baculovirus infectivity (**Figure 5**). Thus, melanization response in *H. armigera* was confirmed to play an important and direct role in combating baculovirus infection. Baculovirus has a bilateral life cycle that it uses occlusion derived viruses (ODVs) to initiate midgut infection and budded viruses (BVs) for systemic infection. As melanization happens in hemolymph and it inactived BV infection *in vitro* (**Figure 5**), we propose melanization prevents systemic infection of baculovirus by inactivating BVs in the infected hemolymph.

Recently, a third PPO pathway comprising HP14/HP2/PAP2 was identified in *M. sexta*, largely activated in wandering larvae and pupae (58). Considering that there are two PPO activating proteases (cSP6 and cSP8) in *H. armigera* (30), it is possible that there might be at least two branches of melanization pathways in this species. The multiple melanization cascades may be involved in specific recognition of different pathogens and may provide a more complete protection of insects in combating against invading pathogens. Further efforts are required to characterize the complete melanization pathways/network in *H. armigera*. In addition, how virus interacts with PRRs or initiating SPs of PPO activation cascade is also worth further exploration. Taken together, our findings provide an important first step toward understanding the complicated melanization network in *H. armigera*.

DATA AVAILABILITY STATEMENT

All datasets generated for this study are included in the article/**Supplementary Material**.

AUTHOR CONTRIBUTIONS

QW, ZH, ZZ, and MW designed the experiments, interpreted the data, and wrote the manuscript. QW, MY, CY, and XL assisted with the experiments and provided critical reagents and intellectual input. ZH, ZZ, and MW supervised the study.

FUNDING

This work was supported by grants from the National Natural Science Foundation of China (grant numbers 31621061 and 31872298).

ACKNOWLEDGMENTS

We thank Ms. Xuefang An, Ms. Youling Zhu, Mr. Fan Zhang, and Mr. Yuzhou Xiao from the Experimental Animal Center, Wuhan Institute of Virology for helping in antibody preparation. We also thank Prof. Haobo Jiang from Oklahoma State University for valuable suggestions of the manuscript.

SUPPLEMENTARY MATERIAL

The Supplementary Material for this article can be found online at: https://www.frontiersin.org/articles/10.3389/fimmu.2020.00785/full#supplementary-material

REFERENCES

1. Cerenius L, Lee BL, Soderhall K. The proPO-system: pros and cons for its role in invertebrate immunity. *Trends Immunol.* (2008) 29:263–71. doi: 10.1016/j.it.2008.02.009
2. Lu A, Zhang Q, Zhang J, Yang B, Wu K, Xie W, et al. Insect prophenoloxidase: the view beyond immunity. *Front Physiol.* (2014) 5:252. doi: 10.3389/fphys.2014.00252
3. Yang F, Wang Y, He Y, Jiang H. In search of a function of Manduca sexta hemolymph protease-1 in the innate immune system. *Insect Biochem Mol Biol.* (2016) 76:1–10. doi: 10.1016/j.ibmb.2016.06.009
4. An C, Ishibashi J, Ragan EJ, Jiang H, Kanost MR. Functions of Manduca sexta hemolymph proteinases HP6 and HP8 in two innate immune pathways. *J Biol Chem.* (2009) 284:19716–26. doi: 10.1074/jbc.M109.007112
5. Jiang H, Wang Y, Yu XQ, Zhu Y, Kanost M. Prophenoloxidase-activating proteinase-3 (PAP-3) from Manduca sexta hemolymph: a clip-domain serine proteinase regulated by serpin-1J and serine proteinase homologs. *Insect Biochem Mol Biol.* (2003) 33:1049–60. doi: 10.1016/S0965-1748(03)00123-1
6. Yu XQ, Jiang H, Wang Y, Kanost MR. Nonproteolytic serine proteinase homologs are involved in prophenoloxidase activation in the tobacco hornworm. Manduca sexta. *Insect Biochem Mol Biol.* (2003) 33:197–208. doi: 10.1016/S0965-1748(02)00191-1
7. Gorman MJ, Wang Y, Jiang H, Kanost MR. Manduca sexta hemolymph proteinase 21 activates prophenoloxidase-activating proteinase 3 in an insect innate immune response proteinase cascade. *J Biol Chem.* (2007) 282:11742–9. doi: 10.1074/jbc.M611243200
8. Kim CH, Kim SJ, Kan H, Kwon HM, Roh KB, Jiang R, et al. A three-step proteolytic cascade mediates the activation of the peptidoglycan-induced toll pathway in an insect. *J Biol Chem.* (2008) 283:7599–607. doi: 10.1074/jbc.M710216200
9. Jiang R, Kim EH, Gong JH, Kwon HM, Kim CH, Ryu KH, et al. Three pairs of protease-serpin complexes cooperatively regulate the insect innate immune responses. *J Biol Chem.* (2009) 284:35652–8. doi: 10.1074/jbc.M109.071001
10. Waterhouse RM, Kriventseva EV, Meister S, Xi Z, Alvarez KS, Bartholomay LC, et al. Evolutionary dynamics of immune-related genes and pathways in disease-vector mosquitoes. *Science.* (2007) 316:1738–43. doi: 10.1126/science.1139862
11. Cao X, He Y, Hu Y, Zhang X, Wang Y, Zou Z, et al. Sequence conservation, phylogenetic relationships, and expression profiles of nondigestive serine proteases and serine protease homologs in Manduca sexta. *Insect Biochem Mol Biol.* (2015) 62:51–63. doi: 10.1016/j.ibmb.2014.10.006
12. Wang Y, Lu Z, Jiang H. Manduca sexta proprophenoloxidase activating proteinase-3 (PAP3) stimulates melanization by activating proPAP3, proSPHs, and proPOs. *Insect Biochem Mol Biol.* (2014) 50:82–91. doi: 10.1016/j.ibmb.2014.04.005
13. Gupta S, Wang Y, Jiang H. Manduca sexta prophenoloxidase (proPO) activation requires proPO-activating proteinase (PAP) and serine proteinase homologs (SPHs) simultaneously. *Insect Biochem Mol Biol.* (2005) 35:241–8. doi: 10.1016/j.ibmb.2004.12.003
14. Wang Y, Jiang H. Interaction of beta-1,3-glucan with its recognition protein activates hemolymph proteinase 14, an initiation enzyme of the prophenoloxidase activation system in Manduca sexta. *J Biol Chem.* (2006) 281:9271–8. doi: 10.1074/jbc.M513797200
15. Takahashi D, Garcia BL, Kanost MR. Initiating protease with modular domains interacts with beta-glucan recognition protein to trigger innate immune response in insects. *Proc Natl Acad Sci USA.* (2015) 112:13856–61. doi: 10.1073/pnas.1517236112
16. He Y, Wang Y, Yang F, Jiang H. Manduca sexta hemolymph protease-1, activated by an unconventional non-proteolytic mechanism, mediates immune responses. *Insect Biochem Mol Biol.* (2017) 84:23–31. doi: 10.1016/j.ibmb.2017.03.008
17. Li Y, Wang Y, Jiang H, Deng J. Crystal structure of Manduca sexta prophenoloxidase provides insights into the mechanism of type 3 copper enzymes. *Proc Natl Acad Sci USA.* (2009) 106:17002–6. doi: 10.1073/pnas.0906095106
18. Dudzic JP, Hanson MA, Iatsenko I, Kondo S, Lemaitre B. More than black or white: melanization and toll share regulatory serine proteases in *Drosophila*. *Cell Rep.* (2019) 27:1050–1061e3. doi: 10.1016/j.celrep.2019.03.101
19. Lemaitre B, Hoffmann J. The host defense of *Drosophila melanogaster*. *Annu Rev Immunol.* (2007) 25:697–743. doi: 10.1146/annurev.immunol.25.022106.141615
20. Zou Z, Shin SW, Alvarez KS, Kokoza V, Raikhel AS. Distinct melanization pathways in the mosquito *Aedes aegypti*. *Immunity.* (2010) 32:41–53. doi: 10.1016/j.immuni.2009.11.011
21. Zhang X, An C, Sprigg K, Michel K. CLIPB8 is part of the prophenoloxidase activation system in *Anopheles gambiae* mosquitoes. *Insect Biochem Mol Biol.* (2016) 71:106–15. doi: 10.1016/j.ibmb.2016.02.008
22. An C, Budd A, Kanost MR, Michel K. Characterization of a regulatory unit that controls melanization and affects longevity of mosquitoes. *Cell Mol Life Sci.* (2011) 68:1929–39. doi: 10.1007/s00018-010-0543-z
23. Chen K, Liu C, He Y, Jiang H, Lu Z. A short-type peptidoglycan recognition protein from the silkworm: expression, characterization and involvement in the prophenoloxidase activation pathway. *Dev Comp Immunol.* (2014) 45:1–9. doi: 10.1016/j.dci.2014.01.017
24. Lee KS, Kim BY, Choo YM, Jin BR. Dual role of the serine protease homolog BmSPH-1 in the development and immunity of the silkworm *Bombyx mori*. *Dev Comp Immunol.* (2018) 85:170–6. doi: 10.1016/j.dci.2018.04.011
25. Chu Y, Hong F, Liu Q, An C. Serine protease SP105 activates prophenoloxidase in Asian corn borer melanization, and is regulated by serpin-3. *Sci Rep.* (2017) 7:45256. doi: 10.1038/srep45256
26. Tamang D, Tseng SM, Huang CY, Tsao IY, Chou SZ, Higgs S, et al. The use of a double subgenomic Sindbis virus expression system to study mosquito gene function: effects of antisense nucleotide number and duration of viral infection on gene silencing efficiency. *Insect Mol Biol.* (2004) 13:595–602. doi: 10.1111/j.0962-1075.2004.00516.x
27. Shelby KS, Popham HJ. Plasma phenoloxidase of the larval tobacco budworm, Heliothis virescens, is virucidal. *J Insect Sci.* (2006) 6:1–12. doi: 10.1673/2006_06_13.1
28. Zhao P, Lu Z, Strand MR, Jiang H. Antiviral, anti-parasitic, and cytotoxic effects of 5,6-dihydroxyindole (DHI), a reactive compound generated by phenoloxidase during insect immune response. *Insect Biochem Mol Biol.* (2011) 41:645–52. doi: 10.1016/j.ibmb.2011.04.006
29. Rodriguez-Andres J, Rani S, Varjak M, Chase-Topping ME, Beck MH, Ferguson MC, et al. Phenoloxidase activity acts as a mosquito innate immune response against infection with Semliki Forest virus. *PLoS Pathog.* (2012) 8:e1002977. doi: 10.1371/journal.ppat.1002977
30. Yuan C, Xing L, Wang M, Wang X, Yin M, Wang Q, et al. Inhibition of melanization by serpin-5 and serpin-9 promotes baculovirus infection in cotton bollworm Helicoverpa armigera. *PLoS Pathog.* (2017) 13:e1006645. doi: 10.1371/journal.ppat.1006645
31. Tay WT, Soria MF, Walsh T, Thomazoni D, Silvie P, Behere GT, et al. A brave new world for an old world pest: helicoverpa armigera (Lepidoptera: Noctuidae) in Brazil. *PLoS One.* (2013) 8:e80134. doi: 10.1371/journal.pone.0080134
32. Wang P, Zhuo XR, Tang L, Liu XS, Wang YF, Wang GX, et al. C-type lectin interacting with beta-integrin enhances hemocytic encapsulation in the cotton bollworm, Helicoverpa armigera. *Insect Biochem Mol Biol.* (2017) 86:29–40. doi: 10.1016/j.ibmb.2017.05.005
33. Li YP, Xiao M, Li L, Song CX, Wang JL, Liu XS. Molecular characterization of a peptidoglycan recognition protein from the cotton bollworm, Helicoverpa armigera and its role in the prophenoloxidase activation pathway. *Mol Immunol.* (2015) 65:123–32. doi: 10.1016/j.molimm.2015.01.016
34. Xiong GH, Xing LS, Lin Z, Saha TT, Wang C, Jiang H, et al. High throughput profiling of the cotton bollworm Helicoverpa armigera immunotranscriptome during the fungal and bacterial infections. *BMC Genomics.* (2015) 16:321. doi: 10.1186/s12864-015-1509-1
35. Xing L, Yuan C, Wang M, Lin Z, Shen B, Hu Z, et al. Dynamics of the Interaction between cotton bollworm helicoverpa armigera and nucleopolyhedrovirus as revealed by integrated transcriptomic and proteomic analyses. *Mol Cell Proteomics.* (2017) 16:1009–28. doi: 10.1074/mcp.M116.062547
36. Song J, Wang R, Deng F, Wang H, Hu Z. Functional studies of per os infectivity factors of Helicoverpa armigera single nucleocapsid nucleopolyhedrovirus. *J Gen Virol.* (2008) 89(Pt 9):2331–8. doi: 10.1099/vir.0.2008/002352-0

37. Jenny RJ, Mann KG, Lundblad RL. A critical review of the methods for cleavage of fusion proteins with thrombin and factor Xa. *Protein Expr Purif.* (2003) 31:1–11. doi: 10.1016/S1046-5928(03)00168-2
38. Zou Z, Liu J, Wang Z, Deng F, Wang H, Hu Z, et al. Characterization of two monoclonal antibodies, 38F10 and 44D11, against the major envelope fusion protein of Helicoverpa armigera nucleopolyhedrovirus. *Virol Sin.* (2016) 31:490–9. doi: 10.1007/s12250-016-3831-4
39. Jiang H, Wang Y, Yu XQ, Kanost MR. Prophenoloxidase-activating proteinase-2 from hemolymph of Manduca sexta. A bacteria-inducible serine proteinase containing two clip domains. *J Biol Chem.* (2003) 278:3552–61. doi: 10.1074/jbc.M205743200
40. Wang Y, Jiang H, Cheng Y, An C, Chu Y, Raikhel AS, et al. Activation of *Aedes aegypti* prophenoloxidase-3 and its role in the immune response against entomopathogenic fungi. *Insect Mol Biol.* (2017) 26:552–63. doi: 10.1111/imb.12318
41. Wang YH, Chang MM, Wang XL, Zheng AH, Zou Z. The immune strategies of mosquito *Aedes aegypti* against microbial infection. *Dev Comp Immunol.* (2018) 83:12–21. doi: 10.1016/j.dci.2017.12.001
42. Volz J, Osta MA, Kafatos FC, Muller HM. The roles of two clip domain serine proteases in innate immune responses of the malaria vector *Anopheles gambiae*. *J Biol Chem.* (2005) 280:40161–8. doi: 10.1074/jbc.M506191200
43. Paskewitz SM, Andreev O, Shi L. Gene silencing of serine proteases affects melanization of *Sephadex beads* in *Anopheles gambiae*. *Insect Biochem Mol Biol.* (2006) 36:701–11. doi: 10.1016/j.ibmb.2006.06.001
44. Barillas-Mury C. CLIP proteases and Plasmodium melanization in Anopheles gambiae. *Trends Parasitol.* (2007) 23:297–9. doi: 10.1016/j.pt.2007.05.001
45. Yassine H, Kamareddine L, Chamat S, Christophides GK, Osta MA. A serine protease homolog negatively regulates TEP1 consumption in systemic infections of the malaria vector *Anopheles gambiae*. *J Innate Immun.* (2014) 6:806–18. doi: 10.1159/000363296
46. Ross J, Jiang H, Kanost MR, Wang Y. Serine proteases and their homologs in the *Drosophila melanogaster* genome: an initial analysis of sequence conservation and phylogenetic relationships. *Gene.* (2003) 304:117–31. doi: 10.1016/S0378-1119(02)01187-3
47. Buchon N, Poidevin M, Kwon HM, Guillou A, Sottas V, Lee BL, et al. A single modular serine protease integrates signals from pattern-recognition receptors upstream of the *Drosophila* Toll pathway. *Proc Natl Acad Sci USA.* (2009) 106:12442–7. doi: 10.1073/pnas.0901924106
48. Wang Y, Jiang H. Reconstitution of a branch of the Manduca sexta prophenoloxidase activation cascade in vitro: snake-like hemolymph proteinase 21 (HP21) cleaved by HP14 activates prophenoloxidase-activating proteinase-2 precursor. *Insect Biochem Mol Biol.* (2007) 37:1015–25. doi: 10.1016/j.ibmb.2007.05.013
49. Wang Y, Jiang H. Binding properties of the regulatory domains in *Manduca sexta* hemolymph proteinase-14, an initiation enzyme of the prophenoloxidase activation system. *Dev Comp Immunol.* (2010) 34:316–22. doi: 10.1016/j.dci.2009.11.001
50. Park JW, Kim CH, Kim JH, Je BR, Roh KB, Kim SJ, et al. Clustering of peptidoglycan recognition protein-SA is required for sensing lysine-type peptidoglycan in insects. *Proc Natl Acad Sci USA.* (2007) 104:6602–7. doi: 10.1073/pnas.0610924104
51. Yasuhara Y, Koizumi Y, Katagiri C, Ashida M. Reexamination of properties of prophenoloxidase isolated from larval hemolymph of the silkworm *Bombyx mori*. *Arch Biochem Biophys.* (1995) 320:14–23. doi: 10.1006/abbi.1995.1337
52. Kim MS, Baek MJ, Lee MH, Park JW, Lee SY, Soderhall K, et al. A new easter-type serine protease cleaves a masquerade-like protein during prophenoloxidase activation in Holotrichia diomphalia larvae. *J Biol Chem.* (2002) 277:39999–40004. doi: 10.1074/jbc.M205508200
53. Piao S, Song YL, Kim JH, Park SY, Park JW, Lee BL, et al. Crystal structure of a clip-domain serine protease and functional roles of the clip domains. *EMBO J.* (2005) 24:4404–14. doi: 10.1038/sj.emboj.7600891
54. Sutthangkul J, Amparyup P, Charoensapsri W, Senapin S, Phiwsaiya K, Tassanakajon A. Suppression of shrimp melanization during white spot syndrome virus infection. *J Biol Chem.* (2015) 290:6470–81. doi: 10.1074/jbc.M114.605568
55. Lu Z, Beck MH, Wang Y, Jiang H, Strand MR. The viral protein Egf1.0 is a dual activity inhibitor of prophenoloxidase-activating proteinases 1 and 3 from *Manduca sexta*. *J Biol Chem.* (2008) 283:21325–33. doi: 10.1074/jbc.M801593200
56. Lu Z, Beck MH, Strand MR. Egf1.5 is a second phenoloxidase cascade inhibitor encoded by *Microplitis demolitor* bracovirus. *Insect Biochem Mol Biol.* (2010) 40:497–505. doi: 10.1016/j.ibmb.2010.04.009
57. Sutthangkul J, Amparyup P, Eum JH, Strand MR, Tassanakajon A. Anti-melanization mechanism of the white spot syndrome viral protein, WSSV453, via interaction with shrimp proPO-activating enzyme, PmproPPAE2. *J Gen Virol.* (2017) 98:769–78. doi: 10.1099/jgv.0.000729
58. He Y, Wang Y, Hu Y, Jiang H. Manduca sexta hemolymph protease-2 (HP2) activated by HP14 generates prophenoloxidase-activating protease-2 (PAP2) in wandering larvae and pupae. *Insect Biochem Mol Biol.* (2018) 101:57–65. doi: 10.1016/j.ibmb.2018.08.001

Conflict of Interest: The authors declare that the research was conducted in the absence of any commercial or financial relationships that could be construed as a potential conflict of interest.

frontiers in Immunology

ORIGINAL RESEARCH
published: 04 August 2020
doi: 10.3389/fimmu.2020.01596

Proteomic Analyses of Whitefly-Begomovirus Interactions Reveal the Inhibitory Role of Tumorous Imaginal Discs in Viral Retention

*Jing Zhao†, Tao Guo†, Teng Lei, Jia-Chen Zhu, Fang Wang, Xiao-Wei Wang and Shu-Sheng Liu**

Ministry of Agriculture Key Laboratory of Molecular Biology of Crop Pathogens and Insects, Institute of Insect Sciences, Zhejiang University, Hangzhou, China

OPEN ACCESS

Edited by:
Xiao-Qiang Yu, University of Missouri–Kansas City, United States

Reviewed by:
Jesús Navas-Castillo, Institute of Subtropical and Mediterranean Horticulture La Mayora, Spain
Jun-Bo Luan, Shenyang Agricultural University, China

***Correspondence:**
Shu-Sheng Liu
shshliu@zju.edu.cn

†These authors have contributed equally to this work

Specialty section:
This article was submitted to Comparative Immunology, a section of the journal Frontiers in Immunology

Received: *10 February 2020*
Accepted: *16 June 2020*
Published: *04 August 2020*

Citation:
Zhao J, Guo T, Lei T, Zhu J-C, Wang F, Wang X-W and Liu S-S (2020) Proteomic Analyses of Whitefly-Begomovirus Interactions Reveal the Inhibitory Role of Tumorous Imaginal Discs in Viral Retention. Front. Immunol. 11:1596. doi: 10.3389/fimmu.2020.01596

In nature, plant viruses are mostly transmitted by hemipteran insects, such as aphids, leafhoppers, and whiteflies. However, the molecular mechanisms underlying the interactions between virus and insect vector are poorly known. Here, we investigate the proteomic interactions between tomato yellow leaf curl virus (TYLCV, genus *Begomovirus*, family *Geminiviridae*), a plant virus, and its vector whitefly (*Bemisia tabaci*) species complex. First, using a yeast two-hybrid system, we identified 15 candidate whitefly proteins interacting with the coat protein of TYLCV. GO and KEGG pathway analysis implicated that these 15 whitefly proteins are of different biological functions/processes mainly including metabolic process, cell motility, signal transduction, and response to stimulus. We then found that the whitefly protein tumorous imaginal discs (Tid), one of the 15 whitefly proteins identified, had a stable interaction with TYLCV CP *in vitro*, and the DnaJ_C domain of $Tid_{301-499aa}$ may be the viral binding site. During viral retention, the expression of whitefly protein Tid was observed to increase at the protein level, and feeding whiteflies with dsRNA or antibody against Tid resulted in a higher quantity of TYLCV in the whitefly body, suggesting the role of Tid in antiviral infection. Our data indicate that the induction of Tid following viral acquisition is likely a whitefly immune response to TYLCV infection.

Keywords: whitefly, TYLCV, interaction, Tid, antiviral infection

INTRODUCTION

Many plant viruses, such as species of the *Luteoviridae*, *Geminiviridae*, and *Nanoviridae* families, are transmitted by hemipteran insects in a persistent, circulative manner (1). During the long-term virus-vector interactions, insect vectors have developed two inevitable physical barriers to virus movement: midgut and salivary glands (1, 2). Initially, the vector ingests virions from virus-infected plants; then, virions enter the insect midgut lumen and subsequently cross through the midgut epithelial cells to be released into the hemolymph. Afterwards, virions move along with the hemolymph and reach the salivary glands from which they are injected into plants together with whitefly saliva secretion (1, 2). During this circulative journey, viruses need to interact with the

insect vector in a coordinated manner for successful transmission to occur; at the same time, viral infection may activate immune reactions from its vector (3, 4).

Begomoviruses (genus *Begomovirus*, family *Geminiviridae*) are a group of single-stranded circular DNA viruses, which are transmitted by whiteflies of the *Bemisia tabaci* species complex in a circulative manner (5, 6). Some begomoviruses are serious viral disease agents of many crops worldwide. For example, tomato yellow leaf curl virus (TYLCV) is transmitted by a notorious invading species of whitefly, provisionally named as Middle East–Asia Minor 1 (MEAM1), of the *B. tabaci* species complex and has caused enormous damage to the production of tomato and some other crops in many countries/regions in the last three decades (7–9). Similar to other begomoviruses and other circulatively transmitted viruses, ingested TYLCV moves along the path of stylet-midgut-hemolymph-salivary glands in whitefly vectors. During the movement, TYLCV depends on clathrin-mediated endocytosis to enter the midgut cells and then accumulates in intracellular vesicle-like structures (10–12). At the same time, a viral infection activates the whitefly autophagy pathway, which plays an important role in the antiviral response (13, 14).

Up to now, the coat protein (CP) is the only structural protein of begomoviruses known to be involved in viral movement in the vector (15). CP gene replacement results in dramatic changes in characteristics of viral acquisition and transmission by whitefly vector (16–19). However, so far, only a few whitefly proteins have been reported to interact with the viral CP. The heat shock protein 70 (HSP70) and vesicle-associated membrane protein–associated protein B (VAPB) show inhibitory roles in virus transmission (20, 21), and a peptidoglycan recognition protein BtPGRP acts in whitefly immunity (22). In contrast, GroEL produced by secondary endosymbionts *Hamiltonella* or *Arsenophonus* may protect the virus from degradation in vector hemolymph (23, 24), and the midgut protein, cyclophilin B and collagen protein may assist in viral transmission (25–27). Vitellogenin may enable transovarial transmission of virus to the next generation of whitefly (28). The putative roles of *Bt*HSP16, thioredoxin-like protein (TLP) and protein BtR242 produced by *Rickettsia* in the viral transmission are yet unclear (29–31). Despite this progress, the functions of some of the abovementioned proteins require further validation, and many more vector components remain to be discovered to achieve an adequate understanding of begomovirus-whitefly interactions.

In this study, first, using the yeast two hybrid (Y2H) system, we identified 15 candidate whitefly proteins interacting with TYLCV CP, including the evolutionarily highly conserved protein tumorous imaginal discs (Tid). As the mammalian homolog of whitefly Tid has been implicated for its role in a variety of signaling pathways and autophagy (32, 33), we then conducted a series of molecular experiments and bioassays to examine *in vitro* interaction between whitefly Tid and TYLCV CP. Following viral infection, increase of whitefly Tid at the protein level exerted constraints on viral retention. Our data provide novel insights into begomovirus-whitefly interactions, indicating the negative impact of Tid on viral retention.

MATERIALS AND METHODS

Virus, Plants, and Insects

TYLCV clone isolate SH2 (GenBank accession number: AM282874.1) was agro-inoculated into tomato plants (*Solanum lycopersicon* L. cv. Hezuo903) at the 3–4 true leaf stage. The tomato plants were then cultivated to the 7–8 true leaf stage, and plants showing typical symptoms were taken for use in experiments. Cotton plants (*Gossypium hirsutum* L. cv. Zhemian, 1793) were cultivated to the 6–7 true leaf stage for whitefly culture maintenance and experiments. A stock culture of MEAM1 whitefly was maintained in insect-proof cages on cotton plants at 26 ± 1°C, 60% relative humidity and 14 h light/10 h darkness.

Y2H Assay System

The Y2H assay based on the matchmaker gold yeast two-hybrid system (Cat. No. 630489; Clontech) was used to explore the interactions between whitefly proteins and TYLCV CP. The cDNA library of whitefly was constructed in the prey plasmid of SfiI-digested pGADT7. The full-length of TYLCV CP gene was cloned into the bait plasmid of pGBKT7 after Nde I and EcoR I restriction. Primers used for cloning are listed in **Supplementary Table 1**. We used the following procedure for the Y2H assay: (1) transform the recombinant plasmid pGBKT7-TYLCV CP into the Y2H Gold yeast strain; (2) select the yeast strain on synthetic defined minimal medium lacking tryptophan (S.D./-Trp); (3) extract the yeast protein by yeast total protein extraction kit (Cat. No.C500013; Sangon Biotech) and confirm the expression of TYLCV CP in yeast in a Western blot by anti-TYLCV CP antibody (provided by Professor Jian-Xiang Wu); (4) conduct the auto-activation detection; (5) transform the cDNA library of whitefly into the Y2HGold yeast strain containing the bait plasmid pGBKT7-TYLCV CP; (6) observe the growth of yeast strain on the double dropout medium (DDO: S.D./-Leu/-Trp) and triple dropout medium (TDO: S.D./-His/-Leu/-Trp) with 40 μg/ml X-alpha-Gal and 125 ng/ml aureobasidin A (AbA) (TDO/X/A), select the positive clones on TDO/X/A; (7) restreak these positive clones on quadruple dropout medium (QDO: S.D./Ade/-His/-Leu/-Trp) with 40 μg/ml X-alpha-Gal and 125 ng/ml AbA (QDO/X/A) to eliminate the false positives; (8) recover the prey plasmids from the positive clones and transform them into *Escherichia coli* strain DH5α, sequence, and identify their interactions with TYLCV CP again. The different fragments screened from the whitefly cDNA library were used in a BLAST search of the NCBI database (http://blast.st-va.ncbi.nlm.nih.gov/Blast.cgi), and the sequences of these fragments screening in the Y2H assay were deposited in GenBank.

Bioinformatic Analysis

Whitefly proteins identified from the Y2H assay system were categorized according to their gene ontology (GO) annotation using the Blast2GO software and then performed using the OmicShare tools, a free online platform for data analysis (http://www.omicshare.com/tools). The metabolic pathway analysis of these proteins was conducted according to the Kyoto Encyclopedia of Genes and Genomes (KEGG) pathway

annotation (https://www.kegg.jp/blastkoala/). Network diagrams were created using the database search tool for the retrieval of interacting genes/proteins (STRING 9.1; http://stringdb.org). All of these analyses were conducted by the full length of amino acid sequences.

Real-Time PCR

Quantitative (q) PCR was performed on CFX connect real-time PCR system (Bio-Rad, USA) using the SYBR Premix Ex Taq II (Cat. No. RR820A, Takara). β-Actin was used as an internal reference, and relative abundance of TYLCV or transcript was calculated by $2^{-\Delta\Delta Ct}$. Primers used for real-time PCR are listed in **Supplementary Table 1**.

dsRNA Synthesis

DNA templates with a T7 promoter at both ends of selected genes were used to synthesize dsRNA following the manufacturer's instruction of the T7 high-yield transcription kit (Cat. No.TR101-02; Vazyme). Then, dsRNA was purified using phenol: chloroform extraction, isopropanol precipitation, and resuspended in nuclease-free water. The size and quality of the dsRNA were confirmed by 1% agarose gel electrophoresis, and its quantity was measured using Nanodrop (Thermo Scientific, USA). ds*GFP* was used as a control. Primers used for DNA template synthesis are listed in **Supplementary Table 1**.

Membrane Feeding on dsRNA or Antibody

Whitefly adults within 7 days post-emergence were collected from cotton plants. A group of 250 adults were released into a glass tube 1.5 cm in diameter and 10 cm in length. According to Pan et al. (10), for dsRNA silencing, whiteflies were fed on 15% sucrose solution containing 200 ng/μl dsRNA for 48 h, and 15% sucrose solution with the same amount ds*GFP* was used as control. For antibody feeding, Tid polyclonal antibody (PcAb) was mixed with 15% sucrose solution with a dilution rate of 1:50 for 24 h, and 15% sucrose solution with the same dilution of rabbit pre-immune serum was set as control.

Viral Acquisition

For viral acquisition after ds*Tid* or ds*UBR7* feeding (ds*GFP* was used as control), whiteflies were caged with leaves from the same branch of TYLCV-infected tomato plants for 6, 12, or 24 h, respectively, and then transferred to feed on cotton for 48 h for viral retention. Female adults were collected in groups of 10 each and homogenized in 100 μL lysis buffer for relative viral quantity analysis (10). Three biological replicates were conducted for relative viral quantity analysis by real-time PCR. For the subsequent experiments of membrane feeding of dsRNA or antibody against Tid, whiteflies were caged with leaves of two symmetrical leaves of the same height on the same branch of TYLCV-infected tomato plants for 12 h and then transferred to feed on cotton for 48 h for viral retention. Three to five biological replicates were conducted for relative viral quantity analysis by real-time PCR.

Structural and Phylogenetic Analysis of Protein Tid

The amino acid sequence of Tid fragment screened from the Y2H assay (Tid-S, GenBank: MT505751) was aligned with the Tid full-length (Tid-FL, GenBank: MT505750) using Clustal X (2.0). Phylogenetic reconstruction was conducted using the maximum likelihood (ML) method and the global transvers time (GTR) model implemented in the MEGA v.6 program (34). Support for the internal nodes of the trees was evaluated using the bootstrap method with 10,000 replicates. The protein domain, transmembrane region, and signal peptide predictions were conducted using the NCBI conserved domain database (CDD) (http://www.ncbi.nlm.nih.gov/Structure/cdd/wrpsb.cgi), TMHMM Server v. 2.0 (http://www.cbs.dtu.dk/services/TMHMM/) and SignalP 4.1 Server (http://www.cbs.dtu.dk/services/SignalP/), respectively. The 3-D structure of protein Tid was predicted using swissmodel (http://swissmodel.expasy.org).

Full-Length Amplification, Protein Expression, and Antibody Production

The ORF of Tid-FL (GenBank: MT505750) was amplified from the whitefly cDNA using PrimerSTAR max DNA polymerase (Cat. No. R045A; Takara) and then cloned into pET28a plasmid for fusion with His tag. His-Tid-FL was expressed in inclusion bodies of *E. coli* strain *Rosetta*, and following renaturation and purification of inclusion body protein, His-Tid-FL was used to immunize rabbits to obtain a Tid-specific PcAb by HuaBio (China). Primers used in this experiment are listed in **Supplementary Table 1**. The specificity of Tid rabbit PcAb is shown in **Supplementary Figure 1**.

Glutathione-S-Transferase (GST) Pull-Down

Tid-S, $Tid_{76-138aa}$ (226-414 bp of *Tid-FL*, DnaJ domain), $Tid_{239-299aa}$ [715-897 bp of *Tid-FL*, four repeats of a CXXCXGX(G) motif], and $Tid_{301-419aa}$ (901-1,257 bp of *Tid-FL*, DnaJ_C domain) were cloned into pMAL-c5X for fusion with MBP tag, accordingly. TYLCV CP was cloned into pGEX-6p-1 for fusion with GST tag. These recombinant proteins were expressed in *E. coli* strain Rosetta and purified. GST-TYLCV CP was bound to glutathione agarose beads (Cat. No.17-5132-01; GE Healthcare) for 2–4 h at 4°C. Then the mixtures were centrifuged for 5 min at 1,000 rpm, and the supernatants were discarded. Agarose beads were washed five times with 1 × phosphate-buffer saline (PBS). Different purified and desalinated MBP-tag fusion proteins or the native whitefly proteins extracted by cytoplasmic extraction buffer (Cat. No.SC-003; Invent) were added to the beads, respectively, and incubated for 4 h at 4°C. These mixtures were centrifuged and washed five times with 1 × PBS, and the bead-bound proteins were eluted by boiling in PAGE buffer (Cat. No. FD 002; FDbio) for 10 min. Finally, these proteins were separated by SDS/PAGE gel electrophoresis and detected by Western blot using anti-MBP antibody (Cat. No.

TABLE 1 | Putative interacting proteins with TYLCV CP in whitefly by the Y2H screen.

No.	GenBank accession[a]	NCBI reference sequence[b]	Identity (%)[c]	Protein name
1	MT505752	XP_018911927.1	94	ATP synthase subunit beta, mitochondrial
2	MT505751	XP_018917603.1	54	Protein tumorous imaginal discs, mitochondrial-like
3	MT505753	XP_018912446.1	59	Gelsolin-like isoform X2
4	MT505754	XP_018903232.1	49	Actin-binding protein IPP-like
5	MT505755	XP_018902418.1	53	Eukaryotic translation initiation factor 4H isoform X2
6	MT505756	XP_018896959.1	65	Titin isoform X14
7	MT505757	XP_018903674.1	59	Twitchin isoform X10
8	MT505758	XP_018899978.1	59	Transcription initiation factor TFIID subunit 1-like
9	MT505759	XP_018904341.1	88	Translation elongation factor 2
10	MT505760	XP_018900124.1	48	NADH dehydrogenase [ubiquinone] 1 beta subcomplex subunit 9
11	MT505761	XP_018914181.1	61	Protein phosphatase 1B
12	MT505762	XP_018910197.1	35	Phospholipase A-2-activating protein
13	MT505763	XP_018905030.1	44	Putative E3 ubiquitin-protein ligase UBR7
14	MT505764	XP_018911353.1	65	Cathepsin L1
15	MT505765	XP_018904178.1	36	Activated CDC42 kinase 1

[a]*Sequences of whitefly genes obtained in this study, they were partial CDS which were deposited in GenBank.* [b]*NCBI reference full-length sequences of whitefly genes screening in Y2H assay. The full length of protein Tid was also obtained in this work (GenBank: MT505750), sharing 100% amino acid identity with its NCBI reference sequence (XP_018917603.1).* [c]*Identity: amino acid identity of whitefly proteins with Drosophila melanogaster counterpart.*

ab49923; Abcam) or anti-Tid antibody. Primers used are listed in **Supplementary Table 1**.

Expression Analysis of Tid

Whitefly adults within 7 days post-emergence from cotton were transferred to TYLCV-infected tomato for 12 h and then transferred to feed on cotton for 48 h. Un-infected tomato was used as a control. Whitefly adults (three biological replicates) were collected as groups of 30 adults for analyzing gene expression of *Tid* at the transcriptional level. Total RNA of whitefly was isolated with TRIzol (Cat. No. 15596-026; Invitrogen), and reverse transcription was done using the PrimeScript RT reagent kit (Cat. No. DRR037A; Takara). For translational-level analysis, 100 whitefly adults were collected as one sample for protein extraction by RIPA (Cat. No. P0013B; Beyotime). Then, we used the BCA protein assay (Cat. No. 23250; Thermo Scientific) to determine and unify the concentration of protein samples. Western blot analysis was conducted by anti-Tid antibody, using anti-β-actin antibody (Cat. No. E021020-01; Earthox) as a control. The translational-level analysis was repeated three times, and ImageJ was used to quantify the relative protein level, Following ds*Tid* membrane feeding, 12 h viral acquisition, and 48 h viral retention, the expressions of Tid at transcriptional and translational levels were analyzed as described above.

Statistical Analysis

Comparison of the relative abundance of virus in whitefly and expression levels of genes were performed using an independent *t*-test with $P < 0.05$ as the threshold of significant difference ($^{*}P < 0.05$, $^{**}P < 0.01$, and $^{***}P < 0.001$). All the statistical analyses were performed using SPSS 20.0 (SPSS Inc., USA).

RESULTS

Analysis of the Interactions Between Whitefly Proteins and TYLCV CP

As shown in **Supplementary Figure 2A**, the Y2H system was used to examine the interactions between whitefly proteins and TYLCV CP. The titer of the primary whitefly cDNA library was ∼5.0 × 10^6 cfu with an average insert size of 1 kb, meeting the requirements of a standard cDNA library (**Supplementary Figure 2B**). The fusion expression of TYLCV CP with GAL4 DNA-BD in the yeast (≈46 kDa) was verified using Western blot analysis (**Supplementary Figure 2C**). The auto-activation detection showed that the bait plasmid pGBKT7-TYLCV CP could be used in this Y2H system (**Supplementary Figure 2D**). After Y2H screening, 26 positive clones were isolated, and 15 unique whitefly proteins were identified (**Table 1**). To identify the one-to-one interaction between bait and prey protein, the interactions between these 15 screened whitefly proteins and TYLCV CP were validated using the Y2H assay (**Figure 1A**), combined with reported interactions between MEAM1 whitefly and TYLCV, and a protein interaction network was generated, including the predicted interactions among whitefly proteins (**Figure 1B**).

In silico Analysis of the Whitefly Proteins Screened by Y2H Assay

According to GO and KEGG analyses (**Figures 2**, **3**), the 15 interactors from the Y2H assay (**Table 1**) were classified into different groups, mainly including metabolic process, cell motility, signal transduction, and response to stimulus. The GO analysis suggests that the 15 proteins may be responsible for 17 different biological processes, mainly involved in cellular and metabolic processes with different distributions inside and

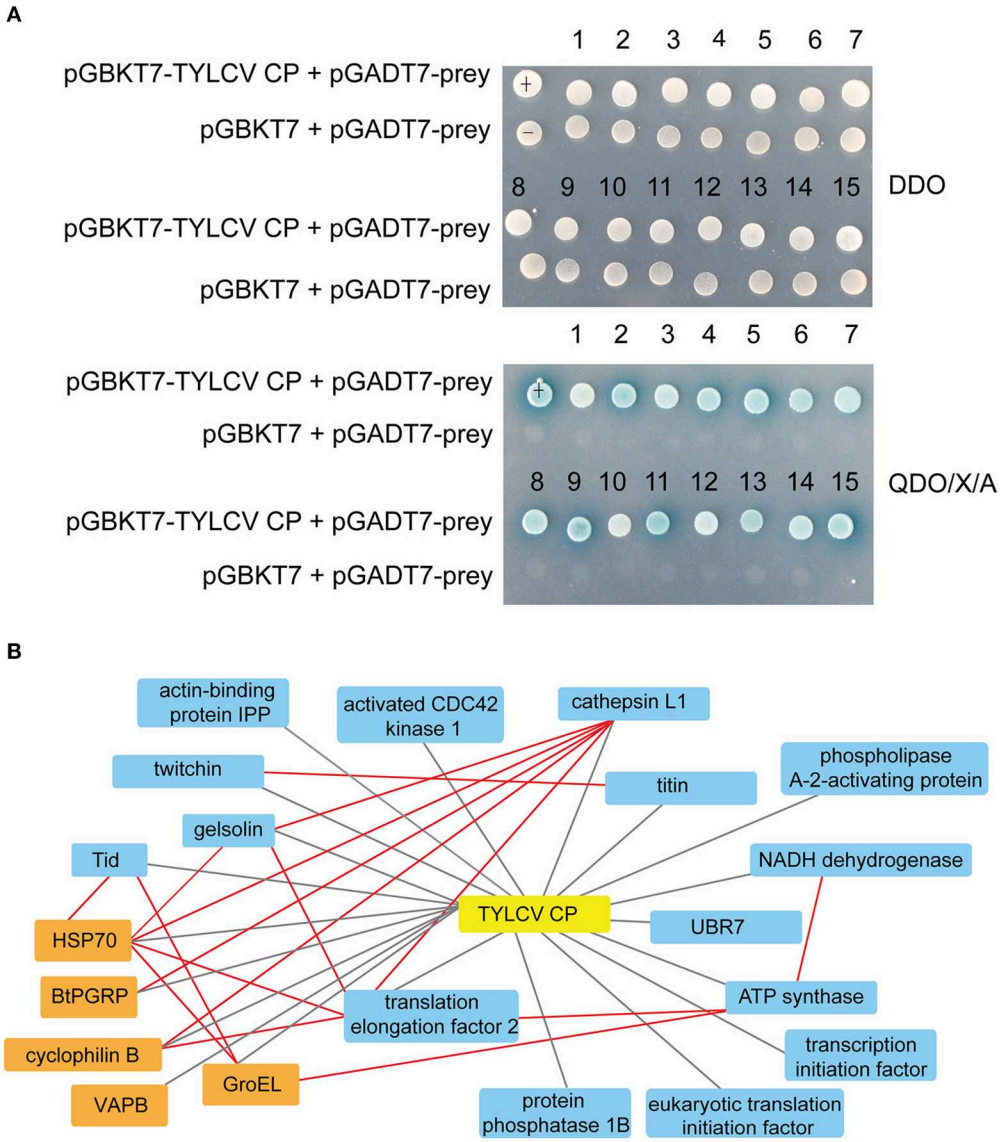

FIGURE 1 | Interactions between whitefly proteins and TYLCV CP. **(A)** Confirmed interactions between TYLCV CP and screened proteins of *B. tabaci* using Y2H assay. TYLCV CP and 15 respective prey proteins were used to cotransform yeast for growth on DDO and QDO/X/A selective medium. pGBKT7-p53 and pGADT7-LargeT were used as positive controls (+); pGBKT7-p53 and pGADT7 were used as negative controls (–). **(B)** Protein interaction network was constructed using TYLCV CP and 20 whitefly protein homologs of *Drosophila melanogaster;* 20 whitefly proteins include 15 candidate whitefly proteins (blue) obtained in this study and five other whitefly proteins (orange) available in the literature related to MEAM1 whitefly-TYLCV interactions. The red line means the interaction predicted from the database search tool for the retrieval of interacting genes/proteins (STRING 9.1; http://stringdb.org), the black line stands for the interaction supported by experiments.

outside of cells; most of them shared the binding activity, and about half of them possess catalytic activity (**Figure 2**). The KEGG pathway analysis suggests that the 15 proteins can be classified into 7 groups (**Figure 3**). For example, gelsolin-like isoform X2 belongs to the pathway of cell motility; protein phosphatase 1B as a member of the MAPK signaling pathway belongs to the group of signal transduction. The whitefly autophagy pathway and ubiquitin-proteasome system have been shown to play a role in antiviral response (13, 14, 35). Among the 15 whitefly proteins, there is a ubiquitin-protein ligase (UBR7) and a protein Tid related to macro-autophagy (33). Both of these two proteins belong to the biological process of response to stimulus (GO: 0050896).

Effects of dsRNA Interference of Tid and UBR7 on Viral Retention

To examine the role of proteins Tid and UBR7 on virus retention, whiteflies that had received dsRNA interference treatment were transferred to feed on a TYLCV-infected tomato for 6, 12, or 24 h, respectively, and then transferred to feed on cotton for

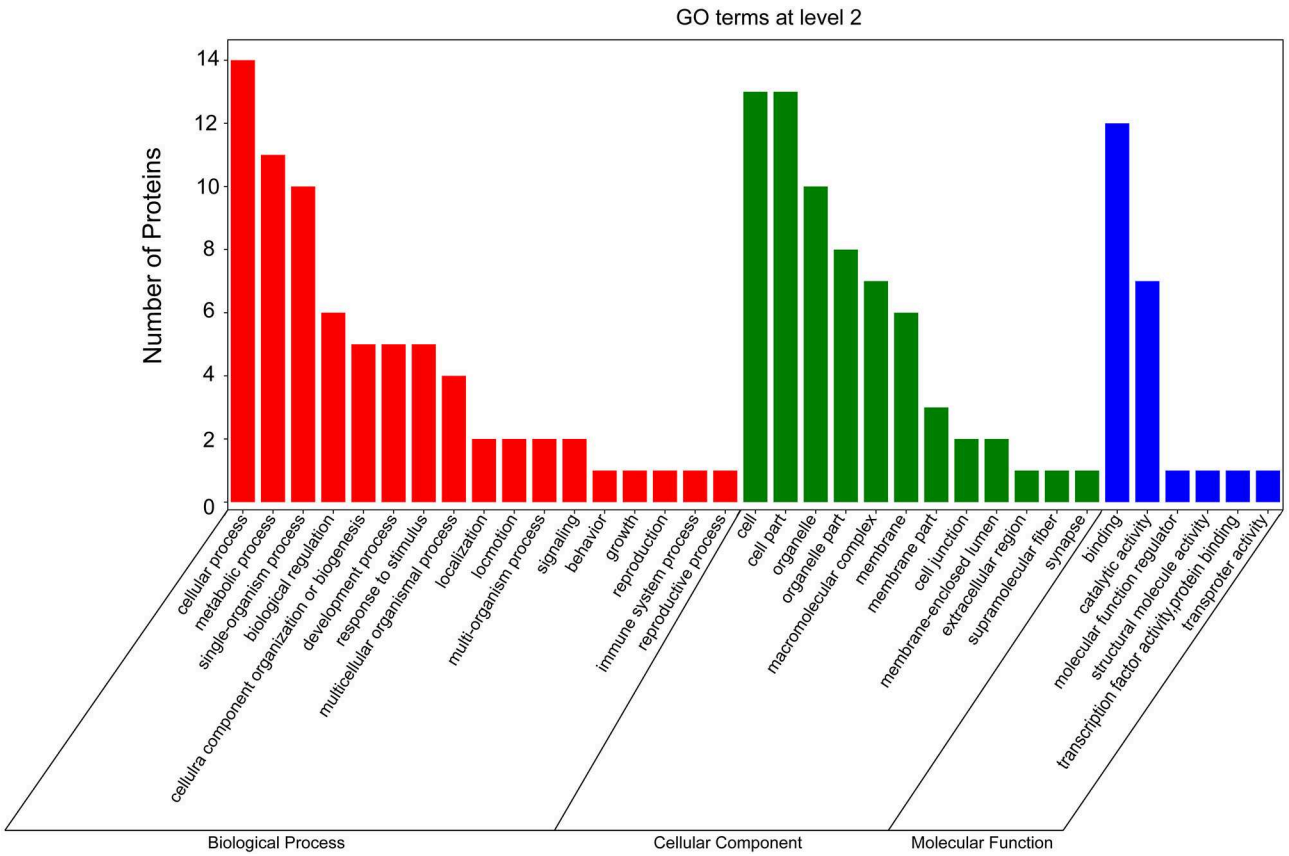

FIGURE 2 | GO analysis of the 15 putative interactors inferred via screening in the Y2H system. Different colors represent different GO categories. GO annotation was conducted by the Blast2GO software, and the figure was generated using the OmicShare tools, a free online platform for data analysis (http://www.omicshare.com/tools).

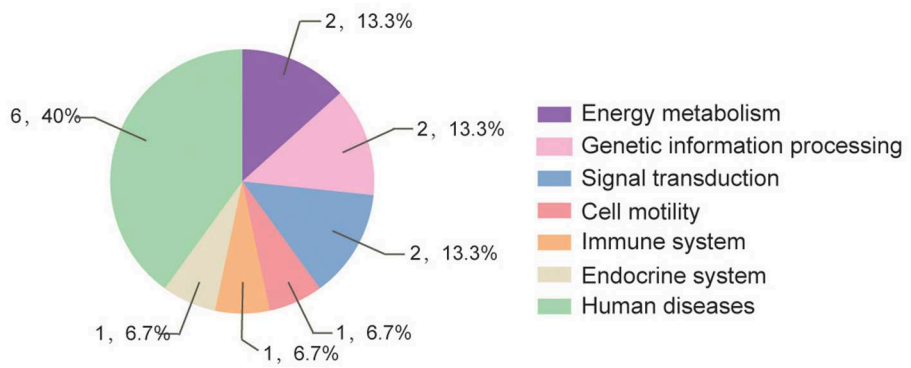

FIGURE 3 | Pathway distribution of the 15 putative interactors inferred via screening in the Y2H system. The metabolic pathway analysis of these proteins was conducted according to the Kyoto Encyclopedia of Genes and Genomes (KEGG) pathway annotation (https://www.kegg.jp/blastkoala/); in total, 15 pathways were identified for the 15 prey proteins.

48 h. At the end of each of the three time points, after ds*Tid* interference, the relative viral quantity in whiteflies significantly increased compared to the control (**Figures 4A–C**) although, for UBR7 dsRNA interference, following a viral acquisition access period for 12 h, the defense ability of the whitefly against TYLCV retention significantly decreased (**Figure 4B**). When the intervals of the viral acquisition access period lasted 6 or 24 h, the defense ability of the whitefly against TYLCV retention had

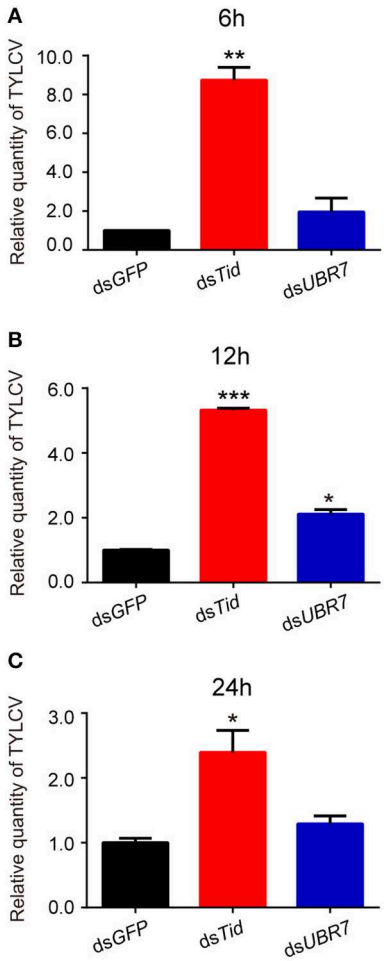

FIGURE 4 | Effects of dsRNA interference of *Tid* and *UBR7* on TYLCV retention. After dsRNA feeding, whiteflies of the interference treatments were caged to feed on leaves of the same branch of a TYLCV-infected tomato plant for 6 h **(A)**, 12 h **(B)**, or 24 h **(C)**, and then transferred to feed on cotton for 48 h to test the viral retention ability of the whitefly by qPCR. *GFP* was used as a control. Whitefly females were collected in groups of 10 each and homogenized in 100 μL lysis buffer for relative viral quantity analysis. In **(A)**, ds*Tid*: $n = 3$, $t = -11.716$, $P = 0.0072$; ds*UBR7*: $n = 3$, $t = -1.327$, $P = 0.3158$; in **(B)**, ds*Tid*: $n = 3$, $t = -66.018$, $P < 0.0001$; ds*UBR7*: $n = 3$, $t = -7.855$, $P = 0.0138$; and in **(C)**, ds*Tid*: $n = 3$, $t = -4.035$, $P = 0.0157$; ds*UBR7*: $n = 3$, $t = -2.058$, $P = 0.1087$. Independent *t*-test was used here and the differences between treatments were considered significant when $^*P < 0.05$; $^{**}P < 0.01$, $^{***}P < 0.001$.

non-significant decrease (**Figures 4A,C**). Based on these results, we selected Tid for the following experiments.

Structural and Phylogenetic Analysis of the Protein Tid

After sequencing the Tid prey plasmid screened from Y2H, we obtained an 855 bp long (285 aa) Tid-S sequence (GenBank: MT505751), having a 60% coverage (164–448aa) of Tid-FL. Tid-FL (GenBank: MT505750, ≈52 kDa) has a DnaJ domain (N-terminal, 76–138aa), a DnaJ_C domain (C-terminal, 301–419aa), and four repeats of a CXXCXGX(G) motif (239–299aa). Tid-S contains only the CXXCXGX(G) motifs and DnaJ_C domain (**Figure 5A**). Tid-FL has no transmembrane domain or signal peptide, and its 3-D structure model is shown in **Figure 5B**. Phylogenetic analysis of *B. tabaci* Tid and 16 other insect Tid proteins showed that *B. tabaci* Tid forms a monophyletic lineage with species of Hymenoptera and appears closely related to the genus *Drosophila* (**Figure 5C**). This DnaJ domain-containing protein is evolutionarily highly conserved; Tid in mammals and that of *Drosophila* show 54.9% identity in amino acid sequences (36), and the Tid of whitefly and that of *Drosophila melanogaster* show 54.0% identity in amino acid sequences.

In vitro Evidence Supports the Interaction Between Tid and TYLCV CP

TYLCV CP fused with GST and Tid-S tagged with MBP were used to verify their interaction through GST pull-down analysis (**Figure 6A**). Using the fusion protein GST-TYLCV CP as a bait protein and native whitefly proteins extracted by cytoplasmic extraction buffer (Cat. No.SC-003; Invent) as prey proteins, whitefly endogenous Tid could co-elute with GST-fused TYLCV CP but not with GST (**Figure 6B**). Further, we tested the interaction between TYLCV CP and different regions of Tid-FL mentioned above: $Tid_{76-138aa}$ (DnaJ domain), $Tid_{239-299aa}$ (four repeats of a CXXCXGX(G) motif), and $Tid_{301-419aa}$ (DnaJ_C domain). The results showed that $Tid_{76-138aa}$ and $Tid_{239-299aa}$ show no binding activity with TYLCV CP (**Figure 6C**); the binding site of TYLCV CP may be located in the C terminal of Tid-FL (**Figure 6D**).

The Increase of Tid at Protein Level During Viral Retention

Following viral infection, the expression of Tid at both transcriptional and translational levels was tested. Data demonstrates that there was no significant change of the expression of *Tid* at transcriptional level (**Figure 7A**). However, Western blot analysis showed TYLCV infection could significantly increase the expression of Tid at protein level (**Figure 7B**).

Effects of Tid Interference on TYLCV Retention

Following dsRNA feeding, the adults were transferred to feed on TYLCV-infected tomato plants for 12 h for virus acquisition and then were transferred to feed on cotton for 48 h for observation on virus retention. Data showed that the expression of *Tid* in whiteflies was effectively knocked down via dsRNA interference (**Figures 8A,B**), and knockdown of *Tid* expression resulted in significant increases of relative virus quantity in whiteflies (**Figure 8C**). In addition, blocking Tid function by anti-Tid antibody likewise resulted in significantly higher relative virus quantity in whiteflies during virus retention (**Figure 8D**).

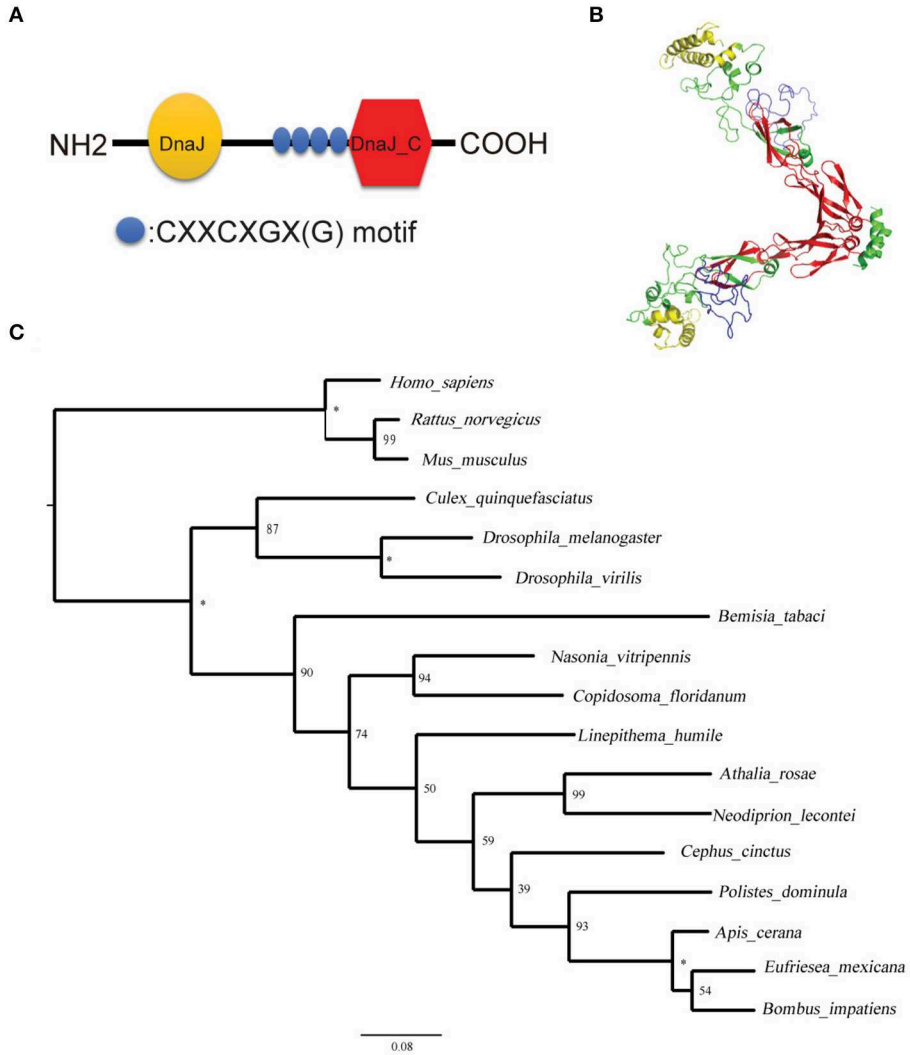

FIGURE 5 | Structural and phylogenetic analysis of the protein Tid. **(A)** Graphic presentation of the Tid structure. **(B)** 3-D structure of protein Tid. Asterisk indicates that the nodes were 100% supported. **(C)** Phylogenetic tree of *B. tabaci*-Tid and other arthropods and mammals were constructed using MEGA v.6 with the maximum likelihood (ML) method. Numbers next to the branches indicated bootstrap value of each internal branch in the phylogenetic tree nodes from 10000 replicates. Tid sequences include *Bemisia tabaci* (MT505750), *Homo sapiens* (NM 001286516), *Rattus norvegicus* (NM 001038596), *Mus musculus* (NM 001135112), *Culex quinquefasciatus* (XM 001848856), *Drosophila melanogaster* (NM 001259554), *Drosophila virilis* (XM 002059276), *Bemisia tabaci* (XP 018917603), *Nasonia vitripennis* (XM 016983982), *Copidosoma floridanum* (XM 014350678), *Linepithema humile* (XM 012379048), *Athalia rosae* (XM 012406140), *Neodiprion lecontei* (XM 015659368), *Cephus cinctus* (XM 015737810), *Polistes dominula* (XM 015322978), *Apis cerana* (XM 017059752), *Eufriesea mexicana* (XM 017897896), and *Bombus impatiens* (XM 012384798).

DISCUSSION

Investigation of the interactions between begomoviruses and whitefly proteins can provide new knowledge of the virus transportation journey in vector. In this study, 15 candidate whitefly proteins of various categories were detected that may interact with TYLCV CP. In further tests of Tid and UBR7, two of the 15 candidate proteins detected showed that both proteins posed an adverse effect on viral retention, and Tid had a stronger effect than UBR7. A stable interaction between whitefly Tid and TYLCV CP was then observed, and the C-terminal of Tid was observed to be the likely binding site. Viral infection could increase the expression of whitefly Tid at the protein level; feeding whiteflies with dsRNA or antibody against Tid resulted in a significantly higher quantity of TYLCV in the body of whiteflies following viral acquisition. Altogether, these data reveal one novel whitefly protein that may function in antiviral response.

The insect innate immune system incurs physical, cellular, and humoral responses to invaders (37), and it is common for insect vectors to take advantage of their immunity to fight against viral infection. Wang et al. (22) demonstrate that whitefly protein

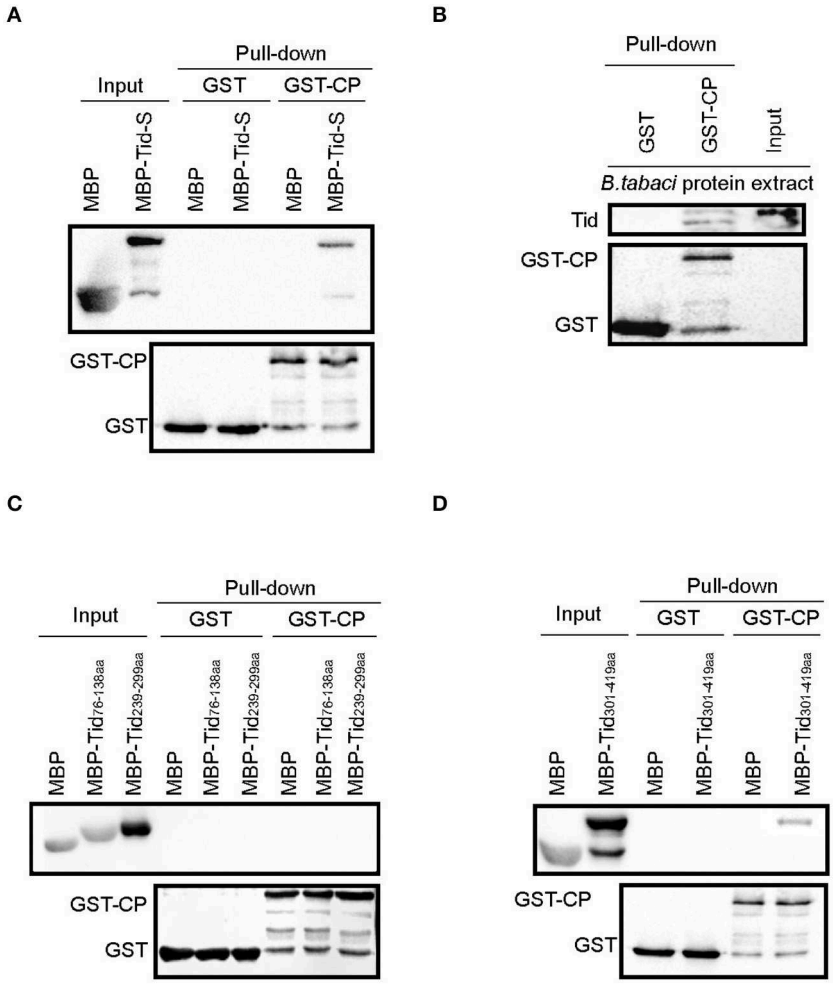

FIGURE 6 | Interaction analysis between Tid and TYLCV CP. GST-TYLCV CP was used as bait protein, **(A)** MBP-Tid-S was used as prey protein, confirmation of the interaction between GST-TYLCV CP and MBP-Tid-S using GST pull-down; **(B)** native whitefly proteins extracted by cytoplasmic extraction buffer (Cat. No.SC-003; Invent) were used as prey proteins, identification of the interaction between whitefly endogenous Tid and GST-TYLCV CP by GST pull-down; **(C)** MBP-Tid$_{76-138aa}$ and MBP-Tid$_{239-299aa}$ were, respectively, used as prey protein, the interactions between these two Tid regions and GST-TYLCV CP were conducted via GST pull-down. **(D)** The C terminal of Tid$_{301-419aa}$ was used as prey protein, identification of the interaction between Tid$_{301-419aa}$ and GST-TYLCV CP via GST pull-down.

*Bt*PGRP with antibacterial activity acts in multiple immune-response functions. Wang et al. (38) show that insect vectors could operate the c-Jun N-terminal kinase (JNK) signaling pathway for controlling viral transmission, causing a significant reduction in virus accumulation and transmission. The studies of Luan et al. (13) and Wang et al. (14) indicate that autophagy is involved in whitefly repression of begomovirus infection and triggers complex interactions between virus and insect vector. A previous study reported a mammalian homolog of whitefly Tid, which acted as a key regulator in mediating autophagy independently of HSP70 (33). Data available to date indicate that both Tid and HSP 70 play a role in repressing virus infection [(20); this study]; however, the relationships among whitefly autophagy, Tid, HSP70, and TYLCV CP remain unclear. Molecular mechanisms underlying the activation of autophagy pathway by TYLCV-infection in whiteflies warrant further investigation. Our findings provide clues for future studies on these issues.

Additionally, the roles of other candidate proteins detected in this study are also worth exploring. Gelsolin is a key regulator of actin filament assembly and disassembly (39), and actin has been shown to interact with several viral proteins and plays important roles in viral transmission. For example, interactions between non-structural protein Pns10 of rice dwarf virus and the cytoplasmic actin of leafhoppers is correlated with insect vector specificity (40); the non-structural protein P7-1 of reovirus southern rice black-streaked dwarf virus generates tubules and this tubules associate with the actin cytoskeleton in insect vector (*Sogatella furcifera*) cells (41, 42). In addition, MAPK signaling pathway is known to be activated by a diverse group of viruses and has important roles in viral replication (43), such as supporting assembly and maturation of West

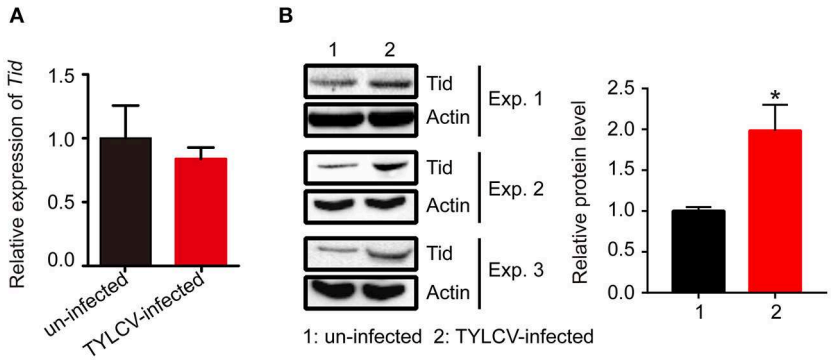

FIGURE 7 | The expression of Tid following TYLCV acquisition. **(A)** The change of the *Tid* expression following viral acquisition at transcriptional level was analyzed by qPCR analysis ($n = 3$, $t = 0.594$, $P = 0.5842$). **(B)** The expression of Tid following viral acquisition at protein level was analyzed by Western blot analysis; 100 whitefly adults were collected as one sample for protein extraction and BCA protein assay was used to determine and unify the concentration of protein samples. Three biological replicates were set, and the results were quantified by ImageJ, $t = -3.077$, $P = 0.0370$. Independent *t*-test was used here and the differences between treatments were considered significant when $^*P < 0.05$.

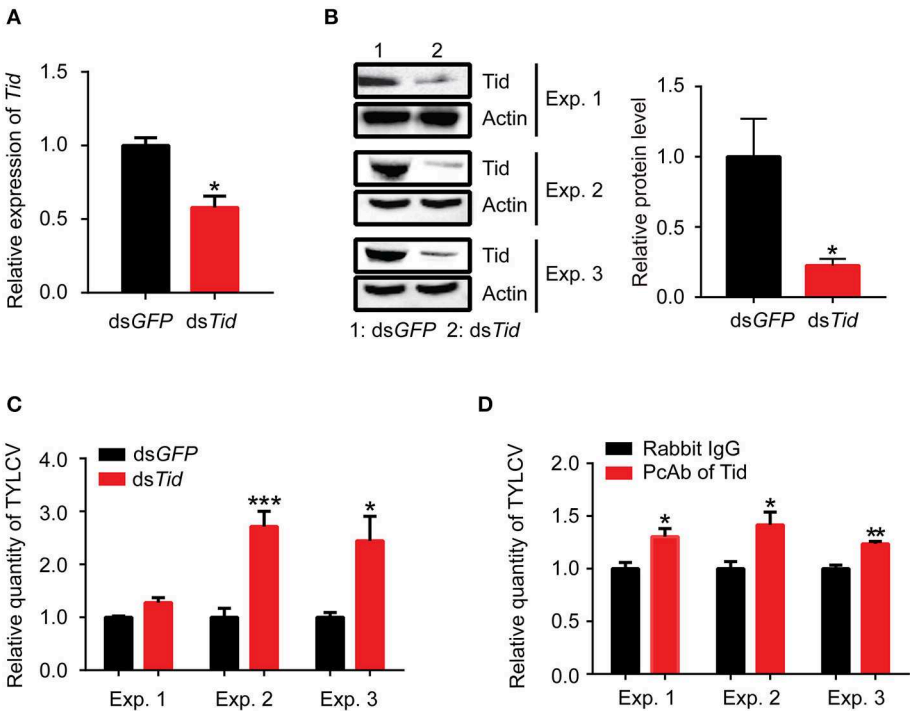

FIGURE 8 | Tid restricts viral retention in whiteflies. After feeding with dsRNA, **(A)** *Tid* mRNA levels after were analyzed by qPCR analysis. Whitefly adults were collected as groups of 30 adults for RNA isolation and cDNA synthesis ($n = 3$, $t = 4.46$, $P = 0.0111$); **(B)** Tid protein levels were analyzed by Western blot analysis; 100 whitefly adults were collected as one sample for protein extraction and BCA protein assay was used to determine and unify the concentration of protein samples. Three biological replicates were set and the results were quantified by ImageJ, $t = 2.82$, $P = 0.0478$. **(C)** After ds*Tid* interference and viral acquisition, TYLCV levels in whitefly whole body was analyzed by qPCR analysis. Whitefly females were collected in groups of 10 each and homogenized in 100 μL lysis buffer for relative viral quantity analysis (Exp. 1, $n = 4$–5, $t = -2.85$, $P = 0.0565$; Exp. 2, $n = 5$, $t = -5.12$, $P = 0.0009$; Exp. 3, $n = 3$, $t = -3.06$, $P = 0.0375$). **(D)** Effect of feeding whiteflies with an antibody against Tid: quantity of virus in the whole body (Exp. 1, $n = 5$, $t = -3.11$, $P = 0.0145$; Exp. 2, $n = 4$, $t = -2.96$, $P = 0.0252$; Exp. 3, $n = 3$–4, $t = -5.32$, $P = 0.0031$). Independent *t*-test was used here and the differences between treatments were considered significant when $^*P < 0.05$; $^{**}P < 0.01$, $^{***}P < 0.001$.

Nile virus and dengue virus (44, 45), regulating multiple steps of influenza A virus replication (46) and so on. In view of the potential role of protein phosphatase in regulating the life cycle of Simian Virus 40 (47), a study of the relationship of protein phosphatase 1B (a member of the MAPK signaling pathway) with TYLCV infection may be worthwhile. These

investigations may lead to a comprehensive recognition of whitefly binding partners of viral CP and better understanding of the complex interactions between begomoviruses and their whitefly vectors.

DATA AVAILABILITY STATEMENT

All datasets generated for this study are included in the article/**Supplementary Material**.

AUTHOR CONTRIBUTIONS

JZ and TG designed this study and conducted most experiments as well as data analysis. JZ drafted and revised the manuscript. TL did the qPCR analysis and participated in statistical analysis. J-CZ made bioinformatic analysis. FW participated in Y2H screening. X-WW participated in manuscript preparation. S-SL provided supervision for the study and participated in manuscript preparation and revision. All authors read and approved the final version of the manuscript.

FUNDING

This study was financially supported by the National Natural Science Foundation of China (Project Nos. 31930092 and 31925033).

ACKNOWLEDGMENTS

We thank Professor Jianxiang Wu, Institute of Biotechnology, Zhejiang University, for providing monoclonal antibodies of TYLCV CP. We also thank our lab engineer Gen-Hong Yan for his effort in plant growing and maintenance and Yuenan Zhou and Wenqiang Xia of our institute for their valuable discussions during this study.

SUPPLEMENTARY MATERIAL

The Supplementary Material for this article can be found online at: https://www.frontiersin.org/articles/10.3389/fimmu.2020.01596/full#supplementary-material

REFERENCES

1. Hogenhout SA, Ammar ED, Whitfield AE, Redinbaugh MG. Insect vector interactions with persistently transmitted viruses. *Annu Rev Phytopathol*. (2008) 46:327–59. doi: 10.1146/annurev.phyto.022508.092135
2. Gray S, Cilia M, Ghanim M. Circulative, "nonpropagative" virus transmission: an orchestra of virus-, insect-, and plant-derived instruments. *Adv Virus Res*. (2014) 89:141–99. doi: 10.1016/B978-0-12-800172-1.00004-5
3. Gray SM, Banerjee N. Mechanisms of arthropod transmission of plant and animal viruses. *Microbiol Mol Biol Rev*. (1999) 63:128–48. doi: 10.1128/MMBR.63.1.128-148.1999
4. Power AG. Insect transmission of plant viruses: a constraint on virus variability. *Curr Opin Plant Biol*. (2000) 3:336–40. doi: 10.1016/S1369-5266(00)00090-X
5. Harrison B, Robinson D. Natural genomic and antigenic variation in whitefly-transmitted geminiviruses (begomoviruses). *Annu Rev Phytophathol*. (1999) 37:369–98. doi: 10.1146/annurev.phyto.37.1.369
6. Ran R, Kanakala S, Kliot A, Pakkianathan BC, Farich BA, Santana-Magal N, et al. Persistent, circulative transmission of begomoviruses by whitefly vectors. *Curr Opin Virol*. (2015) 15:1–8. doi: 10.1016/j.coviro.2015.06.008
7. Li M, Hu J, Xu F, Liu SS. Transmission of *Tomato yellow* leaf curl virus by two invasive biotypes and a Chinese indigenous biotype of the whitefly *Bemisia tabaci*. *Int J Pest Manag*. (2010) 56:275–80. doi: 10.1080/09670871003743428
8. Moriones E, Navas-Castillo J. *Tomato yellow* leaf curl virus, an emerging virus complex causing epidemics worldwide. *Virus Res*. (2000) 71:123–34. doi: 10.1016/S0168-1702(00)00193-3
9. Rojas MR, Macedo M, Maliano MR, Soto-Aguilar M, Souza JO, et al. World management of geminiviruses. *Annu Rev Phytopathol*. (2018) 56:637–77. doi: 10.1146/annurev-phyto-080615-100327
10. Pan LL, Chen QF, Zhao JJ, Guo T, Wang XW, Hariton-Shalev A, et al. Clathrin-mediated endocytosis is involved in *Tomato yellow* leaf curl virus transport across the midgut barrier of its whitefly vector. *Virology*. (2017) 502:152–9. doi: 10.1016/j.virol.2016.12.029
11. Uchibori M, Hirata A, Suzuki M, Ugaki M. *Tomato yellow* leaf curl virus accumulates in vesicle-like structures in descending and ascending midgut epithelial cells of the vector whitefly, *Bemisia tabaci*, but not in those of nonvector whitefly Trialeurodes vaporariorum. *J Gen Plant Pathol*. (2013) 79:115–22. doi: 10.1007/s10327-012-0426-2
12. Xia WQ, Liang Y, Chi Y, Pan LL, Zhao J, Liu SS, et al. Intracellular trafficking of begomoviruses in the midgut cells of their insect vector. *PLoS Pathog*. (2018) 14:e1006866. doi: 10.1371/journal.ppat.1006866
13. Luan JB, Li JM, Varela N, Wang YL, Li FF, Bao YY, et al. Global analysis of the transcriptional response of whitefly to *Tomato yellow* leaf curl China virus reveals the relationship of coevolved adaptations. *J Virol*. (2011) 85:3330–40. doi: 10.1128/JVI.02507-10
14. Wang LL, Wang XR, Wei XM, Huang H, Wu JX, Chen XX, et al. The autophagy pathway participates in resistance to *Tomato yellow* leaf curl virus infection in whiteflies. *Autophagy*. (2016). 12:1560–74. doi: 10.1080/15548627.2016.1192749
15. Harrison BD, Swanson MM, Fargette D. Begomovirus coat protein: serology, variation and functions. *Mol Plant Pathol*. (2002) 60:257–71. doi: 10.1006/pmpp.2002.0404
16. Höfer P, Bedford ID, Markham PG, Jeske H, Frischmuth T. Coat protein gene replacement results in whitefly transmission of an insect nontransmissible geminivirus isolate. *Virology*. (1997) 236:288–95. doi: 10.1006/viro.1997.8751
17. Höhnle M, Höfer P, Bedford ID, Briddon RW, Markham PG, Frischmuth T. Exchange of three amino acids in the coat protein results in efficient whitefly transmission of a nontransmissible abutilon mosaic virus isolate. *Virology*. (2001) 290:164–71. doi: 10.1006/viro.2001.1140
18. Wei J, Zhao JJ, Zhang T, Li FF, Ghanim M, Zhou XP, et al. Specific cells in the primary salivary glands of the whitefly *Bemisia tabaci* control retention and transmission of begomoviruses. *J Virol*. (2014) 88:13460–8. doi: 10.1128/JVI.02179-14
19. Guo T, Zhao J, Pan LL, Geng L, Lei T, Wang XW, et al. The level of midgut penetration of two begomoviruses affects their acquisition and transmission by two species of *Bemisia tabaci*. *Virology*. (2018) 515:66–73. doi: 10.1016/j.virol.2017.12.004
20. Götz M, Popovski S, Kollenberg M, Gorovits R, Brown JK, Cicero JM, et al. Implication of Bemisia tabaci heat shock protein 70 in begomovirus-whitefly interactions. *J Virol*. (2012) 86:13241–52. doi: 10.1128/JVI.00880-12
21. Zhao J, Chi Y, Zhang XJ, Wang XW, Liu SS. Implication of whitefly vesicle associated membrane protein-associated protein B in the transmission of *Tomato yellow* leaf curl virus. *Virology*. (2019) 535:210–7. doi: 10.1016/j.virol.2019.07.007
22. Wang ZZ, Shi M, Huang YC, Wang XW, Stanley D, Chen XX. A peptidoglycan recognition protein acts in whitefly (*Bemisia tabaci*) immunity and involves in begomovirus acquisition. *Sci Rep*. (2016) 6:37806. doi: 10.1038/srep37806

23. Gottlieb Y, Zchorifein E, Mozesdaube N, Kontsedalov S, Skaljac M, Brumin M, et al. The transmission efficiency of *Tomato yellow* leaf curl virus by the whitefly *Bemisia tabaci* is correlated with the presence of a specific symbiotic bacterium species. *J Virol*. (2010) 84:9310–7. doi: 10.1128/JVI.00423-10
24. Rana VS, Sing ST, Priya NG, Kumar J, Rajagopal R. Arsenophonus GroEL interacts with CLCuV and is localized in midgut and salivary gland of whitefly *B. tabaci PLoS ONE*. (2012) 7:e42168. doi: 10.1371/journal.pone.0042168
25. Rana VS, Popli S, Saurav GK, Raina HS, Chaubey R, Ramamurthy VV, et al. A *Bemisia tabaci* midgut protein interacts with begomoviruses and plays a role in virus transmission. *Cell Microbiol*. (2015) 18:663–78. doi: 10.1111/cmi.12538
26. Kanakala S, Ghanim M. Implication of the whitefly *Bemisia tabaci* cyclophilin B protein in the transmission of *Tomato yellow* leaf curl virus. *Front Plant Sci*. (2016) 7:1702. doi: 10.3389/fpls.2016.01702
27. Rana VS, Popli S, Saurav GK, Raina HS, Jamwal R, Chaubey R, et al. Implication of the whitefly, *Bemisia tabaci*, collagen protein in begomoviruses acquisition and transmission. *Phytopathology*. (2019) 109:1481–93. doi: 10.1094/PHYTO-03-18-0082-R
28. Wei J, He YZ, Guo Q, Guo T, Liu YQ, Zhou XP, et al. Vector development and vitellogenin determine the transovarial transmission of begomoviruses. *Proc Natl Acad Sci USA*. (2017) 114:6747–51. doi: 10.1073/pnas.1701720114
29. Ohnesorge S, Bejarano ER. Begomovirus coat protein interacts with a small heat-shock protein of its transmission vector (*Bemisia tabaci*). *Insect Mol Biol*. (2010) 18:693–703. doi: 10.1111/j.1365-2583.2009.00906.x
30. Saurav GK, Rana VS, Popli S, Daimei G, Rajagopal R. A thioredoxin-like protein of *Bemisia tabaci* interacts with coat protein of begomoviruses. *Virus Genes*. (2019) 55:356–67. doi: 10.1007/s11262-019-01657-z
31. Lei T, Zhao J, Wang WL, Liu YQ, Liu S. Impact of a novel *Rickettsia* symbiont on the life history and virus transmission capacity of its host whitefly (*Bemisia tabaci*). *Insect Sci*. (2020). doi: 10.1111/1744-7917.12797. [Epub ahead of print].
32. Gaestel M. Molecular chaperones in signal transduction. *Handb Exp Pharmacol*. (2006) 172:93–109. doi: 10.1007/3-540-29717-0_4
33. Niu G, Zhang H, Liu D, Chen L, Belani C, Wang HG, et al. Tid1, the mammalian homologue of drosophila tumor suppressor tid56, mediates macroautophagy by interacting with beclin1-containing autophagy protein complex. *J Biol Chem*. (2015) 290:18102–10. doi: 10.1074/jbc.M115.665950
34. Tamura K, Stecher G, Peterson D, Filipski A, Kumar S. MEGA6: molecular evolutionary genetics analysis version 6.0. *Mol Biol Evol*. (2013) 30:2725–29. doi: 10.1093/molbev/mst197
35. Xia WQ, Liang Y, Liu YQ, Liu SS, Wang XW. Effects of ubiquitin-proteasome system on *Tomato yellow* leaf curl virus in whitefly *Bemisia tabaci* (Hemiptera: Aleyrodidae). *Acta Entomologica Sinica*. (2017) 60:1411–9. In Chinese with English abstract. doi: 10.16380/j.kcxb.2017.12.007
36. Schilling B, De-Medina T, Syken J, Vidal M, Münger K. A novel human dnaj protein, hTid-1, a homolog of the drosophila tumor suppressor protein Tid56, can interact with the human papillomavirus type 16 E7 oncoprotein. *Virology*. (1998) 247:74–85. doi: 10.1006/viro.1998.9220
37. Strand MR. In insect immunology. In: Beckage NE, editor. *Insect Immunity*. Amsterdam: Elsevier Academic Press (2008), p. 25–47.
38. Wang W, Zhao W, Li J, Luo L, Cui F. The c-jun n-terminal kinase pathway of a vector insect is activated by virus capsid protein and promotes viral replication. *eLife*. (2017) 6:e26591. doi: 10.7554/eLife.26591
39. Sun HQ, Yamamoto M, Mejillano M, Yin HL. Gelsolin, a multifunctional actin regulatory protein. *J Biol Chem*. (1999) 274:33179. doi: 10.1074/jbc.274.47.33179
40. Chen Q, Wang HT, Ren TY, Xie LH, Wei, TY. Interaction between non-structural protein Pns10 of rice dwarf virus and cytoplasmic actin of leafhoppers is correlated with insect vector specificity. *J. Gen. Virol.* (2015) 96:933–8. doi: 10.1099/jgv.0.000022
41. Liu Y, Jia DS, Che H, Chen Q, Xie LH, et al. The P7-1 protein of southern rice black-streaked dwarf virus, a fifijivirus, induces the formation of tubular structures in insect cells. *Arch Virol*. (2011) 156:1729–36. doi: 10.1007/s00705-011-1041-9
42. Jia DS, Mao QZ, Chen HY, Wang AM, Liu YY, Wang HT, et al. Virus-induced tubule: a vehicle for rapid spread of virions through basal lamina from midgut epithelium in the insect vector. *J Virol*. (2014) 88:10488–500. doi: 10.1128/JVI.01261-14
43. Kumar R, Khandelwal N, Thachamvally R, Tripathi BN, Barua S, Kashyap S, et al. Role of MAPK/MNK1 signaling in virus replication. *Virus Res*. (2018) 253:48–61. doi: 10.1016/j.virusres.2018.05.028
44. Hirsch AJ, Medigeshi GR, Meyers HL, DeFilippis V, Fruh K, Briese T, et al. The Src family kinase c-Yes is required for maturation of West Nile virus particles. *J Virol*. (2005) 79:11943–51. doi: 10.1128/JVI.79.18.11943-11951.2005
45. Chu JJ, Yang PL. C-src protein kinase inhibitors block assembly and maturation of dengue virus. *Proc Natl Acad Sci USA*. (2007) 104:3520–5. doi: 10.1073/pnas.0611681104
46. Kumar N, Liang Y, Parslow TG, Liang Y. Receptor tyrosine kinase inhibitors block multiple steps of influenza A virus replication. *J Virol*. (2011) 85:2818–27. doi: 10.1128/JVI.01969-10
47. Scheidtmann KH, Virshup DM, Kelly TJ. Protein phosphatase 2A dephosphorylates Simian virus 40 large T antigen specifically at residues involved in regulation of DNA-binding activity. *J Virol*. (1991) 65:2098. doi: 10.1128/JVI.65.4.2098-2101.1991

Conflict of Interest: The authors declare that the research was conducted in the absence of any commercial or financial relationships that could be construed as a potential conflict of interest.

The reviewer JN-C declared a past co-authorship with several of the authors SS-L and XW-W to the handling editor.

frontiers in Immunology

REVIEW
published: 02 September 2020
doi: 10.3389/fimmu.2020.02030

Antimicrobial Peptides as Potential Antiviral Factors in Insect Antiviral Immune Response

Min Feng[1,2], *Shigang Fei*[1], *Junming Xia*[1], *Vassiliki Labropoulou*[2], *Luc Swevers*[2]* and *Jingchen Sun*[1]*

[1] Guangdong Provincial Key Laboratory of Agro-Animal Genomics and Molecular Breeding, College of Animal Science, South China Agricultural University, Guangzhou, China, [2] Insect Molecular Genetics and Biotechnology, Institute of Biosciences and Applications, National Centre for Scientific Research Demokritos, Athens, Greece

Antimicrobial peptides (AMPs) with antiviral activity (antiviral peptides: AVPs) have become a research hotspot and already show immense potential to become pharmaceutically available antiviral drugs. AVPs have exhibited huge potential in inhibiting viruses by targeting various stages of their life cycle. Insects are the most speciose group of animals that inhabit almost all ecosystems and habitats on the land and are a rich source of natural AMPs. However, insect AVP mining, functional research, and drug development are still in their infancy. This review aims to summarize the currently validated insect AVPs, explore potential new insect AVPs and to discuss their possible mechanism of synthesis and action, with a view to providing clues to unravel the mechanisms of insect antiviral immunity and to develop insect AVP-derived antiviral drugs.

Keywords: antiviral peptides, antimicrobial peptides, insect, viruses, antiviral drugs

OPEN ACCESS

Edited by:
Katherine Buckley, Auburn University, United States

Reviewed by:
Robert Unckless, University of Kansas, United States
Ioannis Eleftherianos, George Washington University, United States

***Correspondence:**
Luc Swevers
swevers@bio.demokritos.gr
Jingchen Sun
cyfz@scau.edu.cn

Specialty section:
This article was submitted to Comparative Immunology, a section of the journal Frontiers in Immunology

Received: *16 June 2020*
Accepted: *27 July 2020*
Published: *02 September 2020*

Citation:
Feng M, Fei S, Xia J, Labropoulou V, Swevers L and Sun J (2020) Antimicrobial Peptides as Potential Antiviral Factors in Insect Antiviral Immune Response. Front. Immunol. 11:2030. doi: 10.3389/fimmu.2020.02030

INTRODUCTION

The role that insects have played as models in innate immunity research is unquestionable. Since the 1990's, the fruit fly *Drosophila melanogaster* emerged as an important paradigm of genetic analysis of innate immunity. Outstanding pioneering achievements were awarded the Nobel Prize, which has since greatly stimulated interest in this field (1, 2). Studies in insects initially focused on resistance to bacteria and fungi, and later slowly expanded into antiviral immunity. However, besides the discovery that RNA interference (RNAi) is crucial in insect antiviral immunity, knowledge of other antiviral pathways and antiviral factors is very limited (3–7). In contrast, in mammals, a diverse series of antiviral immune responses including virus recognition, downstream cascade reactions, and production of effectors were gradually unveiled (8–10). In particular, hundreds of interferon-stimulated genes (ISGs), which exert numerous antiviral effector functions, have been identified in multiple vertebrate species (11–15). This raises the question whether antiviral host factors, similar to interferon-stimulated effectors in mammals, also exist in insects.

In insects, antimicrobial peptides (AMPs) are a group of immune proteins that mainly function against bacteria and fungi (16, 17). A considerable number of AMP genes have been identified in *Drosophila*, the honey bee *Apis cerana* and the silkworm *Bombyx mori* (18–20). However, two antiviral screening experiments failed to show that AMPs are a class of antiviral factors in *Drosophila* (21, 22). Intriguingly, other data in the literature have indicated that AMPs have antiviral function in *Drosophila* and *B. mori* (23, 24). On the other hand, it should

be kept in mind that the interaction between host and virus is a complex process in which the immune response of the host is counteracted by the immune escape mechanisms of the virus. A recent study found that Kallithea virus (DNA virus of *D. melanogaster*) gp83 inhibits Toll signaling through the regulation of NF-κB transcription factors (25). The immunosuppression by Kallithea virus infection is also accompanied by the general down-regulation of AMP gene expression (25). Because the action of AMPs may be neutralized by the virus, simple tests cannot decide or exclude whether AMPs have antiviral activity. In fact, AMPs with antiviral activity (antiviral peptides: AVPs) have become a research hotspot and already show considerable potential to become pharmaceutically available antiviral drugs (26). AMPs and AVPs are usually derived from natural sources but they can be readily modified by adding non-natural amino acids or chemical groups to further enhance their stability and activity (27). Insects are an extremely successful and diverse group of animals that produce a wide range of AMPs which also could display potent antiviral activity. Accordingly, a review of insect antibacterial peptides with antiviral activity is considered timely to provide an assessment of the current knowledge as well as to stimulate efforts for the identification of additional insect-derived antiviral AMPs.

Herein, we will summarize the AMPs with antiviral activity reported in the database and literature and we will predict the antiviral activity of insect AMPs through AVP prediction software. This article aims to compile relevant information from insect AVPs as important components of insect antiviral innate immunity and to inspire the development of effective antiviral drugs.

DATABASES AND WEBSITES OF INSECT AVPS

AVPs are considered as a subset of AMPs which act as the first line of defense in many organisms as an innate immune response to viral infection. Compared to a hot field such as the development of antiviral and antitumor drugs in human medicine, the concept of AVP has not appeared often in the field of insect research, although the idea appeared more than 10 years ago (28, 29). With increasing interest for natural AMPs as potential new drugs, many databases, such as APD (30), AVPdb (31) and ParaPep (32), have been developed to centralize information about AMPs. Among AMP databases, a few databases integrate the AMPs with antiviral activity such as APD (30), AVPdb (31), DRAMP 2.0 (33), and dbAMP (34). The information incorporated in DRAMP 2.0 and dbAMP is relatively new and complete. The advantage of AVPdb is that it summarizes AVPs according to various anti-virus mechanisms. In addition, software for AVP prediction has been developed, e.g., AVPpred (35), AntiVPP 1.0 (36), and Meta-iAVP (37). Based on a series of concepts relevant to insect AVP research, we have cataloged several user-friendly and recently released databases and websites that are suitable for insect AVP research (**Table 1**). The data of known AVPs and prediction methods in this article also come from these databases and websites.

INSECT AMPS WITH ANTIVIRAL ACTIVITIES: THE INSECT AVPS IN PUBLIC DATABASES

The dbAMP was recently created as a useful resource for accumulating synthetic and natural AMPs from public AMP databases and scientific literature (34). In the dbAMP database, a total of 305 AVPs and 596 insect AMPs are collected (**Figure 1A**). Nine insect AVPs were obtained from the intersection of these two data sets in the dbAMP (**Figure 1A**). DRAMP 2.0 is an open-access comprehensive database containing general, patented and clinical AMPs (33). From this database, we identified 8 insect AVPs from a total 214 AVPs (**Figure 1B**). Integrating the insect AVPs information from the dbAMP and DRAMP 2.0 database, we obtained a total of 13 insect AVPs, which are shown in **Figure 1C**. Among hundreds of insect AMPs in the database, only 13 were associated with antiviral activity, which suggests that the research on insect AVP is still in in its infancy and requires more data. It can be assumed that many insect AMPs need to be explored for potential antiviral activity. Thus, the 596 insect AMPs in dbAMP database were further used to predict antiviral activity using Meta-iAVP (37). Unexpectedly, 392 insect AMPs were predicted as AVPs (predicted value >0.5) (**Supplementary File 1**). These predicted insect AVPs originated from *B. mori*, *Galleria mellonella*, *Aedes aegypti*, *Pachycondyla goeldii* (Ponerine ant), *Manduca sexta*, *D. melanogaster*, *Danaus plexippus*, *Anopheles gambiae*, *Apis mellifera* and others (**Figure 1D**). Based on this evidence, we have reason to believe that insect AMPs are a potential source for identification of AVPs, which is worthy of more in-depth study. However, at present, there is no special insect AMP database that can incorporate the latest review articles of insect AVPs. The existing databases continue to have omissions unless the information also becomes curated by professional insect researchers.

INSECT AMPS WITH ANTIVIRAL ACTIVITIES: THE INSECT AVPS IN PUBLISHED LITERATURE

Although the study of insect AVP as an important part of insect antiviral research was promoted more than 10 years ago (29), the available literature is still very limited. Surprisingly, until recently, few insect-derived AMPs were reported with documented antiviral activity. As shown in **Table 2**, ten insect AVPs were found to be involved in the antiviral response and the antiviral action was directed against both mammalian and insect viruses.

Cecropin-A was one of the first animal antimicrobial peptides to be isolated and fully characterized from the hemolymph of the moth *Hyalophora cecropia* (43, 44). Subsequent research confirmed that Cecropin-A has inhibitory activity against human immunodefciency virus 1 (HIV-1; *Retroviridae*), herpes simplex virus 1 and 2 (HSV; *Herpesviridae*) and against the arenavirus Junin virus (JV) (39, 40).

TABLE 1 | Databases and websites suitable for insect AVP research.

Name	Websites	Function	References
dbAMP	http://csb.cse.yzu.edu.tw/dbAMP/	Search for AVPs and insect-derived AMPs	(34)
DRAMP 2.0	http://dramp.cpu-bioinfor.org/	Search for insect AVPs	(33)
AVPdb	http://crdd.osdd.net/servers/avpdb/index.php	Antiviral mechanism of AVPs for reference	(31)
SignalP-5.0	http://www.cbs.dtu.dk/services/SignalP/	Prediction of AMPs signal peptide	(38)
Meta-iAVP	http://codes.bio/meta-iavp/	Prediction of AVPs	(37)

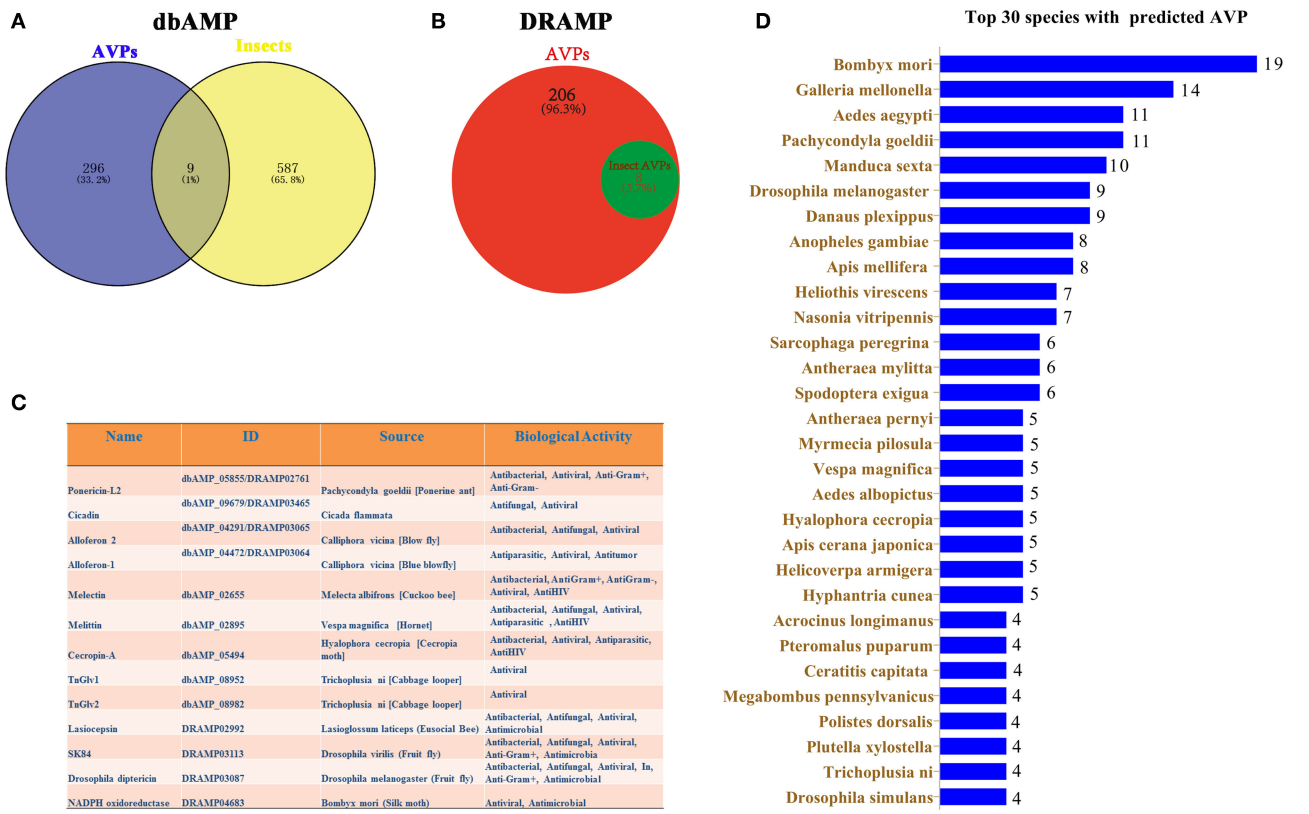

FIGURE 1 | Prediction of insect AVPs from published databases. **(A)** The intersection between AMPs with potential antiviral activity and insect AMPs in the dbAMP database. **(B)** Insect AMPs with predicted antiviral activity in the DRAMP 2.0 database. **(C)** Integration of information on predicted insect AVPs from the dbAMP and DRAMP 2.0 databases. **(D)** Top 30 insects with predicted AVPs that were identified using Meta-iAVP.

Melittin belongs to the class of bee venom-derived AVPs and was isolated from the honeybee *A. mellifera* (45). This AVP was also tested against HSV, HIV-1 and JV, showing inhibition of viral replication for all tested viruses (40, 46). In addition, melittin also curbs infectivity of a diverse array of viruses including Coxsackie Virus and other enteroviruses (*Picornaviridae*), Influenza A viruses (*Orthomyxoviridae*), Respiratory Syncytial Virus (RSV; *Pneumoviridae*), Vesicular Stomatitis Virus (VSV; *Rhabdoviridae*) and the plant virus tobacco mosaic virus (TMV; *Virgaviridae*) (47). More information about the antiviral activity of melittin can be found in a review by Memariani et al. (47).

The insect AMP alloferon 1 and 2, derived from the hemolymph of blow fly *Calliphora vicina*, showed antiviral activity against influenza virus A and influenza virus B (28). Additional research also found that alloferon 1 inhibits human herpes virus type 1 (HHV-1; *Herpesviridae*) and analogs were active against coxsackievirus *in vitro* using cell lines (48, 49). Despite the mechanism of antiviral activity of alloferon is still unknown, Alloferon 1 and its analogs are considered as promising candidates for the design of new AVPs (50).

The antiviral compound N-myristoylated-peptide containing only six amino acids with molecular weight of 916 Da was purified from larval hemolymph of the tobacco budworm *Heliothis virescens* (41). Insect myristoylated-peptide has been confirmed to be effective against HIV-1 and HSV-1 (41). The N-terminus of N-myristoylated-peptide contains the fatty acid myristoyl and the C-terminus contains histidine with two methyl groups giving the histidine a permanent positive charge (41). The

TABLE 2 | Insect AVP reported in the literature.

Insect AVP	Organism	Virus	References
Cecropin-A	*H. cecropia*	HSV-1/ HIV-1/ JV	(39, 40)
Melittin	*A. mellifera*	HSV-1/HIV-1/JV/ influenza A viruses/ RSV/VSV/TMV/ enterovirus/ coxsackievirus	(39, 40)
Alloferon 1	*C. vicina*	Influenza viruses A/B/ HHV-1	(28)
Alloferon 2	*C. vicina*	Influenza viruses A/B	(28)
Myristoylated-peptide	*H. virescens*	HIV-1/HSV-1	(41)
TnGlv1	*T. ni*	AcMNPV	(42)
TnGlv2	*T. ni*	AcMNPV	(42)
attC	*Drosophila*	SINV	(23)
dptB	*Drosophila*	SINV	(23)
C-lysozyme	*B. mori*	BmNPV	(24)

structure of the antiviral compound resembles the "myristate plus basic" motif present in particular viral proteins for binding to the cytoplasmic side of the plasma membrane to initiate virus assembly and budding from a host cell (41). It is speculated that the N-myristoylated-peptide is therefore able to specifically block or inhibit viruses like HIV-1 and HSV-1 that use this motif for exit from a host cell (41, 51).

Gloverin, a small cationic antibacterial protein, has been isolated from the hemolymph of various insects such as the giant silk moth *Hyalophora* (52) and the cabbage looper *Trichoplusia ni* (53). Two *T. ni* gloverin peptides named TnGlv1 and TnGlv2 showed resistance to the budded virus (BV) of *Autographa californica* multiple nucleopolyhedrovirus (AcMNPV; *Baculoviridae*) (42). The antiviral mechanism was speculated to be based on the accumulation of gloverin on the surface of BVs that may cause membrane strain or formation of pores that disrupt the BV envelope (42).

Two *Drosophila* AMP coding genes, diptericin B (dptB) and attacin C (attC), are upregulated in transgenic flies expressing a Sindbis virus (SINV) replicon. Silencing their expression led to a significant increase in SINV titers, suggesting that dptB and attC involved in *Drosophila* antiviral response to SINV (23). However, their mechanism of action remains to be elucidated.

Lysozyme is a ubiquitous peptide that is widely distributed in animals, plants, bacteria and viruses (54). The antibacterial, immunomodulatory and antiviral functions of lysozyme are well-known in vertebrates (55–57). More than fifty *lysozyme* genes have been identified from several insects (58), but the antiviral activity of insect lysozymes has not been widely investigated. In a recent study, the overexpression of *C-lysozyme* of *B. mori* could reduce *B. mori* nucleopolyhedrovirus (BmNPV) production and progeny virus virulence *in vivo* and *in vitro* (24). Further research is required to elucidate the antiviral mechanism of lysozyme peptides.

POTENTIAL AVPS IN FRUIT FLY, HONEYBEE AND SILKWORM

Insects are the most speciose group of animals that inhabit almost all ecosystems and habitats on the land (17, 59). Although insects are a rich source of natural AMPs (17), only few insect AMPs have been confirmed with antiviral activity (**Figure 1C**, **Table 2**). In this study we have predicted 392 potential AVPs from 596 insect AMPs in the dbAMP database (**Figure 1D**, **Supplementary File 1**). This information may stimulate researchers to carry out in-depth and extensive research on the activity of the predicted insect AVPs. Insects, especially *D. melanogaster*, has been widely used as model for the study of innate immunity and microbial pathogens and for assessing the *in vivo* efficacy of antimicrobial agents (60). The silkworm and honeybee are well-known representative economic insects. In the following section, we will elaborate on potential AVPs in the fruit fly *D. melanogaster*, the two honeybee species *A. mellifera* and *A. cerana* and the silkworm *B. mori*.

D. melanogaster

In general, seven well-characterized families including 21 inducible AMP/AMP-like genes have been identified in *Drosophila* (61, 62). The functions of *Drosophila* AMPs are not only involved in host defense, but expand also to gut microbiota homeostasis, tumor control, lifespan regulation and neurological processes (62, 63). However, to our knowledge, only two *Drosophila* AMPs, attC and dptB, have been reported to have antiviral function (23). Since the first animal AMP was discovered in insects (44), *D. melanogaster* has emerged as a powerful model for their characterization. Unfortunately, the research on antiviral immunity involving *Drosophila* AMPs has not received enough attention. After downloading the latest updated *Drosophila* AMP/AMP-like genes (including lysozyme) and their corresponding peptides from the NCBI database, their antiviral activity was predicted using Meta-iAVP (37). For AMP genes for which the mature peptide sequence was not determined, SignalP-5.0 was employed to predict the signal peptide and mature peptide (38).

Following this procedure, as shown in **Table 3**, a total of 23 potential AVPs were identified in *D. melanogaster*. We further analyzed these potential AVPs for their induction by viral infection in published transcriptome studies. Expression of *Defensin*, *Cecropin A1*, *Cecropin B*, *Andropin*, *Drosocin*, *Drosomycin*, *Metchnikowin*, *Lysozyme* S, *Attacin-B*, *Attacin-C*, *Diptericin A,* and *Lysozyme X* was found to be induced after viral infection in cell lines or adult flies (**Table 3**). Screening of transcriptome data for identification of key viral host factors is based on this concept (13). However, viruses may also interfere with the expression of antiviral factors as an immune escape strategy. Determination of antiviral activity based by induction of expression during viral infection is only indicative and cannot be considered as conclusive. But for screening of antiviral genes it can turn out to be a simple and effective method. Therefore, AMPs/AVPs that are up-regulated by a specific virus may be relatively reliable candidate host antiviral factors, for which further verification experiments have to be performed. It

TABLE 3 | Predicted AVPs in *Drosophila*.

Predicted AVP	Gene ID	Peptide ID	Value/ precursor	Value/mature	Up-regulated by virus
Defensin	36047	NP_523672.1	0.524	1	DCV (64, 65), DXV (64)
Cecropin A1	43596	NP_524588.1	0.908	0.946	DCV (66, 67), Sigma virus (64), CrPV (68)
Cecropin A2	43597	NP_524589.1	0.908	0.64	
Cecropin C	43599	NP_524591.1	1	0.744	
Cecropin B	43598	NP_524590.1	1	1	DCV (67)
Andropin	43595	NP_524587.1	0.762	0.524	DCV (67), FHV (69)
Drosocin	36635	NP_001246324.1/NP_523744.1	1	0.508	DXV (70), Sigma Virus (64)
Drosomycin	38419	NP_523901.1	0.992	0.524	DCV (64, 65, 71), DXV (64)
Drosomycin-like 5	38409	NP_647803.1	1	0.716	
Drosomycin-like 2	38408	NP_728860.2	1	0.946	
Drosomycin-like 3	317955	NP_728861.1	1	0.954	
Drosomycin-like 6	38416	NP_728873.1	0.92	0.892	
Drosomycin-like 1	326207	NP_728872.1	0.928	0.668	
Metchnikowin	36708	NP_523752.1	1	0.962	DCV (64, 65, 67, 71), DXV (64), SINV (23), CrPV (68)
Lysozyme P	38129	NP_476828.1	0.43(Non-AVP)	0.966	
Lysozyme S	38130	NP_476829.1	0.93	0.892	DCV (64), CrPV (68)
Attacin-B	36637	NP_001163152.1	0.64	0.07(Non-AVP)	DCV (66, 71), DXV (70), Sigma Virus (64), FHV (71), CrPV (68)
Attacin-C	36484	NP_523729.3	0.616	0(Non-AVP)	DCV (67, 71), SINV (23), FHV (71), CrPV (68)
Diptericin A	37183	NP_476808.1	0.86	0(Non-AVP)	Sigma Virus (64), CrPV (68)
Lysozyme B	38125	NP_001261245.1	0.986	0.282(Non-AVP)	
Lysozyme X	38122	NP_523881.1	0.774	0.272(Non-AVP)	FHV (71)
Lysozyme E	38128	NP_476827.2	1	0.008(Non-AVP)	

should also be noted that dptB has been shown to inhibit SINV replication (23), but it is not among the predicted candidate AVPs (**Table 3**). Thus, a strategy that screens virus-inducible genes clearly will not identify all potential AVPs.

In addition, some non-classical AMPs such as Bomanins (72), Daishos (73) and Listericin (74) in *Drosophila* have also attracted our attention. An effector peptide family encoded by twelve *Bomanin* (*Bom*) genes has been found to be essential for effective *Drosophila* Toll-mediated immune responses (72). Daisho peptides, a new class of innate immune effectors in *Drosophila*, were recently found to have humoral activity against a set of filamentous fungi (73). Currently, these *Drosophila* peptides have not been confirmed to have antiviral activity. Using Meta-iAVP (37) prediction, we found that BomS1, BomS4, BomS6, BomT1, BomBc2, and Listericin have potential AVPs activity (**Supplementary File 2**).

A. mellifera and *A. cerana*

Honeybees are important plant pollinators in both natural and agricultural ecosystems (75). Through pollination of flowering plants, honeybees do not only help to maintain biodiversity but in addition they also supply commodities such as honey, royal jelly, propolis (bee glue), pollen and wax. Viruses are significant threats to the health and well-being of the honeybee (76). Due to the abundance and economic importance of the honeybee, research on the interaction with bee viruses has received a lot of research interest. Honeybee antiviral defense mechanisms include RNAi, endocytosis, melanization, encapsulation, autophagy, pathogen-associated molecular pattern (PAMP)-triggered signal transduction cascades, and generation of reactive oxygen species (7, 77). There is currently no evidence that AMPs are involved in the antiviral response of honeybees (7, 77). However, melittin, the principal constituent in the venom of *A. mellifera*, has been demonstrated to be effective against the infectivity of a diverse array of mammalian viruses such as HIV and HSV (47). Venom-derived AMPs may not play a role in the antiviral response of its host, but the results of the antiviral experiments *in vitro* are an important reference of which the significance is not clear yet.

Following infection by pathogens, AMPs of four families comprising apidaecins (78), abaecins (79), hymenoptaecins (80), and defensins (81) are synthesized, representing a broad spectrum of antimicrobial activity in the haemolymph. Detailed comparison of these four AMP gene families between *A. mellifera* and *A. cerana* revealed that there are many similarities in the number and amino acid composition of the peptides in the abaecin, defensing, and apidaecin families, while many more hymenoptaecin peptides are found in *A. cerana* than in *A. mellifera* (19). Compared to *A. mellifera* that has a longer history of domestication, selection on *A. cerana* has favored

TABLE 4 | Predicted AVPs in *A. mellifera* and *A. cerana*.

Predicted AVP/ *A. mellifera*	Gene ID (NCBI)	Peptide ID	Value/ precursor	Value/mature	Up-regulated by virus
Defensin 1	406143	NP_001011616.2	0.966	0.772	DWV+SBV (82)
Defensin 2	413397	NP_001011638.1	0.916	0.43 (Non-AVP)	DWV+SBV (82)
Abaecin	406144	NP_001011617.1	1	0.64	DWV+SBV (82), BQCV (83)
Apisimin	406093	NP_001011582.1	0.586	0.974	DWV+SBV (82)
Hymenoptaecin	406142	NP_001011615.1	0.282 (Non-AVP)	0.542	DWV+SBV (82), IAPV (84), BQCV (83)
Lysozyme 1/2	724899	XP_026300526.1	0.078 (Non-AVP)	0.548	
lysozyme 3	409663	XP_393161.3	0.64	0.98	DWV+SBV (82)
A. cerana					
Defensin-2	108000415	XP_016916212.1	0.992	1	
Abaecin	108002218	XP_016919244.1	0.354 (Non-AVP)	0.906	CSBV (85)
Apidaecins type 22	108000468	XP_016916307.1	0.542	0.876	
Hymenoptaecin	107993492	XP_016905415.1	0.694	0 (Non-AVP)	CSBV (85)
Apisimin	108003250	XP_016920890.1	0.994	0.98	
AcDef7	EU727274	ACH96390.1	0.986	0.932	
AcHym3	EU727299	ACH96415.1	0.508	0.752	
AcHym16	EU727312	ACH96428.1	0.104 (Non-AVP)	0.536	
AcHym18	EU727314	ACH96430.1	0.696	0.028 (Non-AVP)	
AcHym1	EU727297	ACH96413.1	0.268 (Non-AVP)	0.696	
AcHym4	EU727300	ACH96416.1	0.716	0 (Non-AVP)	
AcHym7	EU727303	ACH96419.1	0.072 (Non-AVP)	0.876	
AcHym9	EU727305	ACH96421.1	0.694	0 (Non-AVP)	
AcHym25	EU835174	ACJ22829.1	0.508	0.752	
Lysozyme-like	108000169	XP_028523646.1	0.078 (Non-AVP)	1	
Lysozyme-like	114577830	XP_028523645.1	0.746	1	

the generation of more variable AMPs as protection against pathogens (19).

Using the predictive tools of Meta-iAVP (37), a total of 7 and 16 AVPs were obtained from *A. mellifera* and *A. cerana*, respectively (**Table 4**). Potential AVP genes of *A. mellifera* such as *defensin 1*, *defensin 2*, *abaecin*, *apisimin*, *hymenoptaecin,* and *lysozyme 3* were found to be up-regulated after infection with viruses such as Deformed wing virus (DWV), Sacbrood virus (SBV), black queen cell virus (BQCV), and Israeli acute paralysis virus (IAPV) in transcriptome data (**Table 4**). Almost all honeybee transcriptome studies that analyze virus infection are restricted to *A. mellifera* while little related research has been conducted on *A. cerana*. Recent research found that in *A. cerana* the predicted AVP genes *abaecin* and *hymenoptaecin* were significantly upregulated by Chinese Sacbrood virus (CSBV) infection (85). These potential AVPs, which are up-regulated by a specific honeybee virus, are important leads for future research on the antiviral immunity of honeybee AMPs.

B. mori

The domestic silkworm *B. mori*, is an important lepidopteran insect of high scientific and economic value (86). Like in apiculture, the viral disease can cause enormous economic loss in sericulture (87). For viral diseases of silkworm, currently there is no effective treatment. Although there exist specific strains of silkworm that are resistant to some viruses, the specific mechanism is unclear (88–90). Like other insects, RNAi was considered as the major defense strategy against viral infections in *B. mori* (91). However, the antiviral innate immune response of silkworm has not been systematically studied although specific antiviral molecules such as PP2A (92), BmSTING (93), BmAtlastin-n (94), BmNOX (95), Bmlipase-1 (96), were identified. In a review article the involvement of AMPs in the antiviral response of silkworm was claimed (6), but in fact very few specific cases of antiviral activity of silkworm AMPs are known, an exception being a recent article on inhibition of BmNPV by lysozyme (24). Interestingly, a study reported that *B. mori* peptidoglycan recognition protein S2 (BmPGRP-S2) overexpression could activate the Imd pathway and induce AMP upregulation, enhancing silkworm antiviral resistance (97).

Following the publication of the genome of the silkworm (86), 35 silkworm AMP genes were identified based on the silkworm genome sequence and expressed sequence tags databases (20). These silkworm AMP genes belong to six families including cecropins, moricins, gloverins, attacins, enbocins, and lebocin (20). Following analysis of updated

TABLE 5 | Predicted AVPs in *B. mori*.

Predicted AVP	Gene ID	Peptide ID	Value/ precursor	Value/mature	Up-regulated by virus
Attacin1	692555	NP_001037006.1	0.936	0.044 (Non-AVP)	BmNPV (98)
Attacin-like	101743224	XP_004926758.1	0.726	0.986	
Cecropin B	732858	NP_001096031.1	1	0.992	BmCPV (99)
Cecropin A	693029	NP_001037462.1	1	0.964	BmCPV (99)
Cecropin-like	101739821	NP_001037392.1	0.962	0.998	
Cecropin-D-like peptide	101740228	NP_001036924.2	1	0.694	
Cecropin D	692369	NP_001036833.1	0.988	0.892	
Cecropin CBM2	692583	NP_001037031.1	0.536	0.97	
Defensin	692778	NP_001037370.1	0.982	0.924	
Enbocin1	693035	NP_001037472.1	0.982	0.616	
Enbocin3	100101217	NP_001093310.1	0.854	0.998	
Gloverin 2	692527	NP_001037683.1	0.668	0.506	BmNPV (100)
Gloverin 3	692476	NP_001093312.1	0.068 (Non-AVP)	0.678	BmNPV (98, 100)
Gloverin 4	751090	NP_001037684.1	0.07 (Non-AVP)	0.81	BmNPV (98, 100)
Gloverin 4-like	692477	NP_001036932.1	0.038 (Non-AVP)	1	
Lebocin	100146108	NP_001119732.2	0.536	0.164 (Non-AVP)	BmNPV (98, 100)
Moricin	692365	NP_001036829.2	0.992	0.964	
Moricin-1-like	105842862	XP_012552566.1	0.536	0.908	
Moricin-1-like	101742278	XP_012551343.2	0.996	0.908	
Moricin-1-like	101742127	XP_012551345.2	0.554	0.818	
Lysozyme	693015	NP_001037448.1	0.968	0.678	BmNPV (100)

AMP gene data in the NCBI database, 21 potential silkworm AVPs (**Table 5**) were obtained using Meta-iAVP prediction (37). Among these potential AVP genes, *gloverin-2*, *gloverin-3*, *lebocin*, *attacin 1,* and *lysozyme* have been found to be induced by BmNPV infection in both resistant and susceptible silkworms (98, 100). It is worth noting that the expression of the potential AVP gene *gloverin-4* was significantly up-regulated only in BmNPV-infected resistant silkworm, while no changes were found in the BmNPV-infected susceptible silkworm and BmN cells, further suggesting that gloverin-4 is an AVP against BmNPV infection (98). The expression of the potential AVP gene *cecropin A* and *cecropin B* also tended to be up-regulated during infection with *B. mori* cytoplasmic polyhedrosis virus (BmCPV), but expression levels were too low to be considered as biologically important (99). Moreover, it is curious that although many omics data related to silkworm virus infection have been published, no more clues were obtained about the involvement of AMPs in the defense against *B. mori* bidensovirus (BmBDV), BmNPV and BmCPV infection (101–105).

THE PROGRAM OF AVP SYNTHESIS AND ITS MECHANISM OF ACTION IN INSECTS

Universally, after the virus invades the host, the host will initiate a recognition mechanism and induce a downstream antiviral cascade reaction. In vertebrates, during various viral infections, virus-associated PAMPs are recognized by pathogen recognition receptors (PRRs) such as Toll-like receptors (TLRs), retinoic acid-inducible gene I (RIG-I)-like receptors (RLRs), NOD-like receptors (12), interferon-γ-inducible protein 16 (IFI16), AIM2 (absent in melanoma 2) and cyclic GMP-AMP synthase (cGAS) that subsequently lead to the activation of inflammatory cytokines and chemokines as well as interferon (IFN) and ISG production through a cascade reaction (106). However, similar antiviral response systems have not been systematically studied in insects. At present, we have very limited knowledge of how insects recognize virus invasion and initiate cascade reactions to exert antiviral functions.

In insects, a number of actual and potential PRRs such as TLRs, peptidoglycan recognition proteins (PGRPs), Gram-negative bacteria-binding proteins (GNBPs), scavenger receptors (SRs), thioester-containing proteins (TEPs) and lectins have been identified (107, 108). Unfortunately, there is currently no evidence that any of the above-mentioned PRRs are involved in insect virus recognition, with the exception of the nucleic acid sensor Dicer-2 that can act as a PRR of double-stranded RNA in parallel to the RNAi pathway (107). Recently, *B. mori* cGAMP and PGRP2 were confirmed to be involved in host responses to BmNPV (93, 109). In *Drosophila*, Toll, IMD and JAK/STAT pathway may be involved in antiviral immunity (4, 65, 110). In addition, JAK/STAT pathway could also be activated by challenge with BmNPV and BmBDV (111). The classical innate immune pathways are also transcriptionally induced during pathogenic infection of Bm5 cells with RNA

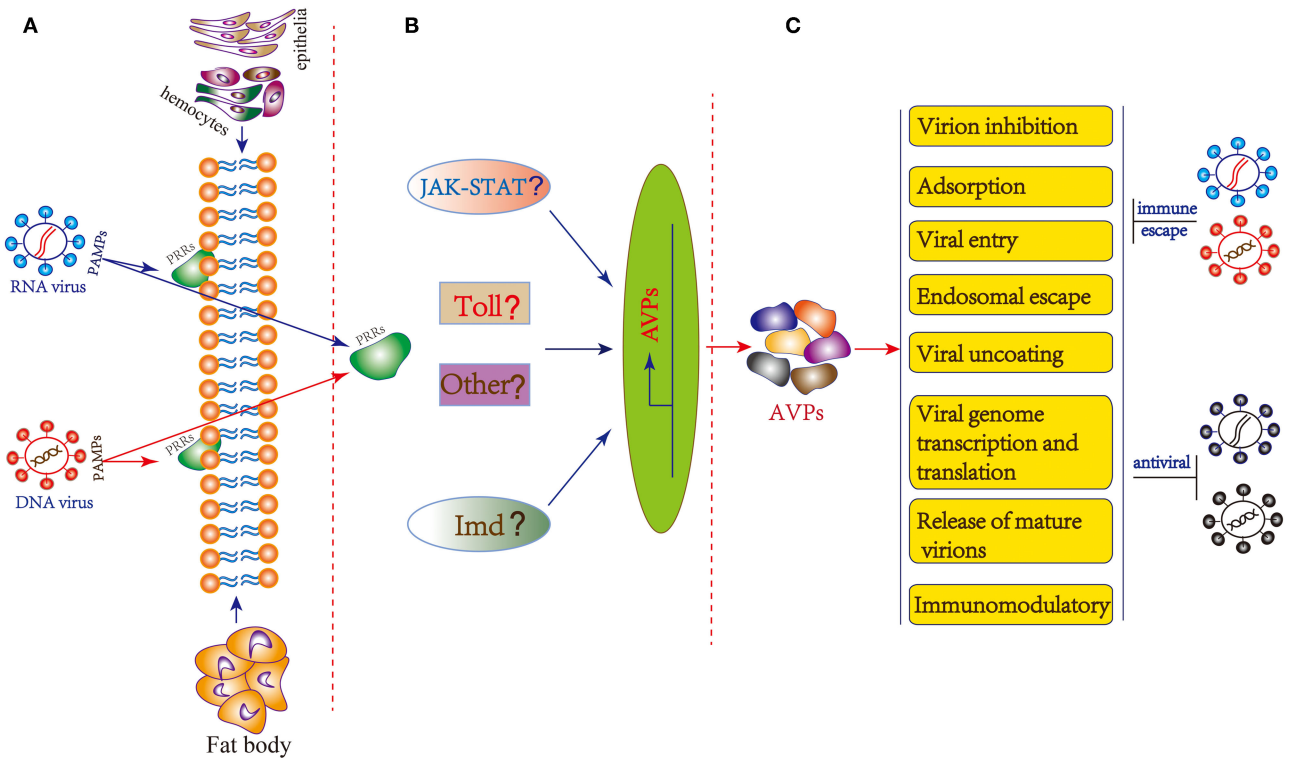

FIGURE 2 | General hypothesis of AVP synthesis and possible mechanism of action in insects. **(A)** Immune recognition of insect viruses. The PAMPs of insect RNA and DNA viruses are recognized by specific PRRs located in the cell membrane or cytoplasm of hemocytes, epithelia or fat body. **(B)** Potential downstream signaling cascade reactions including JAK-STAT, Toll, Imd, and other pathway to produce AVPs. **(C)** The mechanism of action of AVPs covers stages in almost the entire life cycle of the virus: virion inhibition; adsorption; viral entry; endosomal escape; viral uncoating; viral genome transcription and translation, and release of mature virions. Additionally, AVPs may inhibit viral infection by regulating the host immune system. As a counterdefense, insect viruses may employ several strategies to escape the antiviral effect of AVPs.

virus (112). However, the insect PRRs for viral recognition and signaling pathway activation have not been fully elucidated. Thus, there is currently no exact mechanism identified for the generation of AVPs and more in-depth research is needed. Based on evidence obtained in vertebrate (mammalian) systems, we can make the hypothesis that insect viral PAMPs are recognized by specific PRRs located in the cell membrane or cytoplasm of hemocytes, epithelia or fat body which then triggers downstream signaling cascades for the production of AVPs (**Figure 2**).

The AVPs possess diverse structures as well as might act according to different mechanisms. Based on the antiviral peptide database AVPdb (**Table 1**), a total of 45 virus targeting strategies employed by AVPs can be distinguished such as "Virus entry," "Virucidal on progeny virions," "Viral assembly," "Release," "Transcription," "Translation," "Transport," and "Replication" (31). The mechanism of action of AVPs summarized in the AVPdb database covers almost the entire life cycle of the virus (**Figure 2**). Additionally, AVPs may act against viral infection by regulating the host immune system (**Figure 2**). For instance AVP like alloferons from the blow fly are able to stimulate natural killer cells (NK) activity and interferon synthesis in animal and human models (28).

FUTURE RESEARCH

Many scientific questions about the identities of insect AVPs and their modes of action remain unresolved. Besides, viruses are the causative agents of various dreadful diseases in humans and animals. Recently, the testing and discovery of AVPs was accelerated because extraordinary advantages. Insects are considered an important source of natural AMPs, and their potential to act as AVPs is worthy of in-depth studies. In future research, the research on insect AVPs can mainly focus on the following key issues: (1) Identification of insect AVPs; (2) Recognition by PRRs and downstream cascade reactions involved in insect AVPs production; (3) Molecular mechanism of action of AVPs against insect viruses and vertebrate viruses; (4) AVP counter defense (immune escape) mechanisms by viruses; (5) Evaluation and application of insect AVPs as antiviral drugs.

AUTHOR CONTRIBUTIONS

MF participated in the design, collected and analyzed data, and drafted the manuscript. SF and JX helped with data collection. VL, LS, and JS participated in the design and coordination of the

study, and revised the manuscript. All authors read and approved the final manuscript.

FUNDING

This work was supported by the National Natural Science Foundation of China (31872426); Guangdong Natural Science Foundation (2018A030310210); the project Target Identification and Development of Novel Approaches for Health and Environmental Applications (MIS 5002514) which is implemented under the Action for the Strategic Development on the Research and Technological Sectors, funded by the Competitiveness, Entrepreneurship and Innovation (NSRF 2014-2020), and co-financed by Greece and the European Union (European Regional Development Fund); and Guangdong Provincial Promotion Project on Preservation and Utilization of Local Breed of Livestock and Poultry (No.2018-143).

SUPPLEMENTARY MATERIAL

The Supplementary Material for this article can be found online at: https://www.frontiersin.org/articles/10.3389/fimmu.2020.02030/full#supplementary-material

Supplementary File 1 | Antiviral activity prediction of all insect AMPs in the dbAMP database.

Supplementary File 2 | Antiviral activity prediction of Bomanins, Daishos, and Listericin in *Drosophila*.

REFERENCES

1. Lemaitre B, Nicolas E, Michaut L, Reichhart JM, Hoffmann JA. The dorsoventral regulatory gene cassette spatzle/Toll/cactus controls the potent antifungal response in Drosophila adults. *Cell*. (1996) 86:973–83. doi: 10.1016/S0092-8674(00)80172-5
2. Hoffmann JA, Kafatos FC, Janeway CA, Ezekowitz RA. Phylogenetic perspectives in innate immunity. *Science*. (1999) 284:1313–8. doi: 10.1126/science.284.5418.1313
3. Mussabekova A, Daeffler L, Imler JL. Innate and intrinsic antiviral immunity in *Drosophila*. *Cell Mol Life Sci*. (2017) 74:2039–54. doi: 10.1007/s00018-017-2453-9
4. Xu J, Cherry S. Viruses and antiviral immunity in *Drosophila*. *Dev Comp Immunol*. (2014) 42:67–84. doi: 10.1016/j.dci.2013.05.002
5. Swevers L, Liu J, Smagghe G. Defense mechanisms against viral infection in *Drosophila*: RNAi and Non-RNAi. *Viruses*. (2018) 10:230. doi: 10.3390/v10050230
6. Lu P, Pan Y, Yang Y, Zhu F, Li C, Guo Z, et al. Discovery of anti-viral molecules and their vital functions in *Bombyx mori*. *J Invertebr Pathol*. (2018) 154:12–8. doi: 10.1016/j.jip.2018.02.012
7. McMenamin AJ, Daughenbaugh KF, Parekh F, Pizzorno MC, Flenniken ML. Honey bee and bumble bee antiviral defense. *Viruses*. (2018) 10:395. doi: 10.3390/v10080395
8. Chen H, Jiang Z. The essential adaptors of innate immune signaling. *Protein Cell*. (2013) 4:27–39. doi: 10.1007/s13238-012-2063-0
9. Yan N, Chen ZJ. Intrinsic antiviral immunity. *Nat Immunol*. (2012) 13:214–22. doi: 10.1038/ni.2229
10. Schoggins JW. Interferon-stimulated genes: roles in viral pathogenesis. *Curr Opin Virol*. (2014) 6:40–6. doi: 10.1016/j.coviro.2014.03.006
11. Schoggins JW, Wilson SJ, Panis M, Murphy MY, Jones CT, Bieniasz P, et al. A diverse range of gene products are effectors of the type I interferon antiviral response. *Nature*. (2011) 472:481–5. doi: 10.1038/nature09907
12. Liu SY, Sanchez DJ, Aliyari R, Lu S, Cheng G. Systematic identification of type I and type II interferon-induced antiviral factors. *Proc Natl Acad Sci USA*. (2012) 109:4239–44. doi: 10.1073/pnas.1114981109
13. Xie T, Feng M, Dai M, Mo G, Ruan Z, Wang G, et al. Cholesterol-25-hydroxylase is a chicken ISG that restricts ALV-J infection by producing 25-hydroxycholesterol. *Viruses*. (2019) 11:498. doi: 10.3390/v11060498
14. Wang X, Li Y, Li LF, Shen L, Zhang L, Yu J, et al. RNA interference screening of interferon-stimulated genes with antiviral activities against classical swine fever virus using a reporter virus. *Antiviral Res*. (2016) 128:49–56. doi: 10.1016/j.antiviral.2016.02.001
15. Levraud JP, Jouneau L, Briolat V, Laghi V, Boudinot P. IFN-stimulated genes in zebrafish and humans define an ancient arsenal of antiviral immunity. *J Immunol*. (2019) 203:3361–73. doi: 10.4049/jimmunol.1900804
16. Yi HY, Chowdhury M, Huang YD, Yu XQ. Insect antimicrobial peptides and their applications. *Appl Microbiol Biotechnol*. (2014) 98:5807–22. doi: 10.1007/s00253-014-5792-6
17. Sheehan G, Farrell G, Kavanagh K. Immune priming: the secret weapon of the insect world. *Virulence*. (2020) 11:238–46. doi: 10.1080/21505594.2020.1731137
18. Imler JL, Bulet P. Antimicrobial peptides in *Drosophila*: structures, activities and gene regulation. *Chem Immunol Allergy*. (2005) 86:1–21. doi: 10.1159/000086648
19. Xu P, Shi M, Chen XX. Antimicrobial peptide evolution in the Asiatic honey bee *Apis cerana*. *PLoS ONE*. (2009) 4:e4239. doi: 10.1371/journal.pone.0004239
20. Cheng T, Zhao P, Liu C, Xu P, Gao Z, Xia Q, et al. Structures, regulatory regions, and inductive expression patterns of antimicrobial peptide genes in the silkworm *Bombyx mori*. *Genomics*. (2006) 87:356–65. doi: 10.1016/j.ygeno.2005.11.018
21. Liao JF, Wu CP, Tang CK, Tsai CW, Rouhova L, Wu YL. Identification of regulatory host genes involved in sigma virus replication using RNAi knockdown in *Drosophila*. *Insects*. (2019) 10:339. doi: 10.3390/insects10100339
22. Panda D, Rose PP, Hanna SL, Gold B, Hopkins KC, Lyde RB, et al. Genome-wide RNAi screen identifies SEC61A and VCP as conserved regulators of *Sindbis virus* entry. *Cell Rep*. (2013) 5:1737–48. doi: 10.1016/j.celrep.2013.11.028
23. Huang Z, Kingsolver MB, Avadhanula V, Hardy RW. An antiviral role for antimicrobial peptides during the arthropod response to alphavirus replication. *J Virol*. (2013) 87:4272–80. doi: 10.1128/JVI.03360-12
24. Chen TT, Tan LR, Hu N, Dong ZQ, Hu ZG, Jiang YM, et al. C-lysozyme contributes to antiviral immunity in *Bombyx mori* against nucleopolyhedrovirus infection. *J Insect Physiol*. (2018) 108:54–60. doi: 10.1016/j.jinsphys.2018.05.005
25. Palmer WH, Joosten J, Overheul GJ, Jansen PW, Vermeulen M, Obbard DJ, et al. Induction and suppression of NF-kappaB signalling by a DNA virus of *Drosophila*. *J Virol*. (2019) 93:e01443–18. doi: 10.1128/JVI.01443-18
26. Vilas Boas LCP, Campos ML, Berlanda RLA, de Carvalho Neves N, Franco OL. Antiviral peptides as promising therapeutic drugs. *Cell Mol Life Sci*. (2019) 76:3525–42. doi: 10.1007/s00018-019-03138-w
27. Gentilucci L, De Marco R, Cerisoli L. Chemical modifications designed to improve peptide stability: incorporation of non-natural amino acids, pseudo-peptide bonds, and cyclization. *Curr Pharm Des*. (2010) 16:3185–203. doi: 10.2174/138161210793292555
28. Chernysh S, Kim SI, Bekker G, Pleskach VA, Filatova NA, Anikin VB, et al. Antiviral and antitumor peptides from insects. *Proc Natl Acad Sci USA*. (2002) 99:12628–32. doi: 10.1073/pnas.192301899
29. Slocinska M, Marciniak P, Rosinski G. Insects antiviral and anticancer peptides: new leads for the future? *Protein Pept Lett*. (2008) 15:578–85. doi: 10.2174/092986608784966912
30. Wang G, Li X, Wang Z. APD3: the antimicrobial peptide database as a tool for research and education. *Nucleic Acids Res*. (2016) 44:D1087–93. doi: 10.1093/nar/gkv1278

31. Qureshi A, Thakur N, Tandon H, Kumar M. AVPdb: a database of experimentally validated antiviral peptides targeting medically important viruses. *Nucleic Acids Res*. (2014) 42:D1147–53. doi: 10.1093/nar/gkt1191
32. Mehta D, Anand P, Kumar V, Joshi A, Mathur D, Singh S, et al. ParaPep: a web resource for experimentally validated antiparasitic peptide sequences and their structures. *Database*. (2014) 2014:bau051. doi: 10.1093/database/bau051
33. Kang X, Dong F, Shi C, Liu S, Sun J, Chen J, et al. DRAMP 2.0, an updated data repository of antimicrobial peptides. *Sci Data*. (2019) 6:148. doi: 10.1038/s41597-019-0154-y
34. Jhong JH, Chi YH, Li WC, Lin TH, Huang KY, Lee TY. dbAMP: an integrated resource for exploring antimicrobial peptides with functional activities and physicochemical properties on transcriptome and proteome data. *Nucleic Acids Res*. (2019) 47:D285–97. doi: 10.1093/nar/gky1030
35. Thakur N, Qureshi A, Kumar M. AVPpred: collection and prediction of highly effective antiviral peptides. *Nucleic Acids Res*. (2012) 40:W199–204. doi: 10.1093/nar/gks450
36. Beltran Lissabet JF, Belen LH, Farias JG. AntiVPP 1.0: a portable tool for prediction of antiviral peptides. *Comput Biol Med*. (2019) 107:127–30. doi: 10.1016/j.compbiomed.2019.02.011
37. Schaduangrat N, Nantasenamat C, Prachayasittikul V, Shoombuatong W. Meta-iAVP: a sequence-based meta-predictor for improving the prediction of antiviral peptides using effective feature representation. *Int J Mol Sci*. (2019) 20:5743. doi: 10.3390/ijms20225743
38. Almagro Armenteros JJ, Tsirigos KD, Sonderby CK, Petersen TN, Winther O, Brunak S, et al. SignalP 5.0 improves signal peptide predictions using deep neural networks. *Nat Biotechnol*. (2019) 37:420–3. doi: 10.1038/s41587-019-0036-z
39. Wachinger M, Kleinschmidt A, Winder D, von Pechmann N, Ludvigsen A, Neumann M, et al. Antimicrobial peptides melittin and cecropin inhibit replication of human immunodeficiency virus 1 by suppressing viral gene expression. *J Gen Virol*. (1998) 79:731–40. doi: 10.1099/0022-1317-79-4-731
40. Albiol Matanic VC, Castilla V. Antiviral activity of antimicrobial cationic peptides against Junin virus and herpes simplex virus. *Int J Antimicrob Agents*. (2004) 23:382–9. doi: 10.1016/j.ijantimicag.2003.07.022
41. Ourth DD. Antiviral activity against human immunodeficiency virus-1 *in vitro* by myristoylated-peptide from *Heliothis virescens*. *Biochem Biophys Res Commun*. (2004) 320:190–6. doi: 10.1016/j.bbrc.2004.05.137
42. Moreno-Habel DA, Biglang-awa IM, Dulce A, Luu DD, Garcia P, Weers PM, et al. Inactivation of the budded virus of *Autographa californica* M nucleopolyhedrovirus by gloverin. *J Invertebr Pathol*. (2012) 110:92–101. doi: 10.1016/j.jip.2012.02.007
43. Hultmark D, Steiner H, Rasmuson T, Boman HG. Insect immunity. Purification and properties of three inducible bactericidal proteins from hemolymph of immunized pupae of *Hyalophora cecropia*. *Eur J Biochem*. (1980) 106:7–16. doi: 10.1111/j.1432-1033.1980.tb05991.x
44. Steiner H, Hultmark D, Engstrom A, Bennich H, Boman HG. Sequence and specificity of two antibacterial proteins involved in insect immunity. *Nature*. (1981) 292:246–8. doi: 10.1038/292246a0
45. Bazzo R, Tappin MJ, Pastore A, Harvey TS, Carver JA, Campbell ID. The structure of melittin. A 1H-NMR study in methanol. *Eur J Biochem*. (1988) 173:139–46. doi: 10.1111/j.1432-1033.1988.tb13977.x
46. Wachinger M, Saermark T, Erfle V. Influence of amphipathic peptides on the HIV-1 production in persistently infected T lymphoma cells. *FEBS Lett*. (1992) 309:235–41. doi: 10.1016/0014-5793(92)80780-K
47. Memariani H, Memariani M, Moravvej H, Shahidi-Dadras M. Melittin: a venom-derived peptide with promising anti-viral properties. *Eur J Clin Microbiol Infect Dis*. (2020) 39:5–17. doi: 10.1007/s10096-019-03674-0
48. Kuczer M, Dziubasik K, Midak-Siewirska A, Zahorska R, Luczak M, Konopinska D. Studies of insect peptides alloferon, Any-GS and their analogues. Synthesis and antiherpes activity. *J Pept Sci*. (2010) 16:186–9. doi: 10.1002/psc.1219
49. Kuczer M, Midak-Siewirska A, Zahorska R, Luczak M, Konopinska D. Further studies on the antiviral activity of alloferon and its analogues. *J Pept Sci*. (2011) 17:715–19. doi: 10.1002/psc.1388
50. Kuczer M, Majewska A, Zahorska R. New alloferon analogues: synthesis and antiviral properties. *Chem Biol Drug Des*. (2013) 81:302–9. doi: 10.1111/cbdd.12020
51. Resh MD. Fatty acylation of proteins: new insights into membrane targeting of myristoylated and palmitoylated proteins. *Biochim Biophys Acta*. (1999) 1451:1–16. doi: 10.1016/S0167-4889(99)00075-0
52. Axen A, Carlsson A, Engstrom A, Bennich H. Gloverin, an antibacterial protein from the immune hemolymph of *Hyalophora pupae*. *Eur J Biochem*. (1997) 247:614–9. doi: 10.1111/j.1432-1033.1997.00614.x
53. Lundstrom A, Liu G, Kang D, Berzins K, Steiner H. *Trichoplusia ni* gloverin, an inducible immune gene encoding an antibacterial insect protein. *Insect Biochem Mol Biol*. (2002) 32:795–801. doi: 10.1016/S0965-1748(01)00162-X
54. Gajda E, Bugla-Ploskonska G. Lysozyme–occurrence in nature, biological properties and possible applications. *Postepy Hig Med Dosw*. (2014) 68:1501–15. doi: 10.5604/17322693.1133100
55. Ragland SA, Criss AK. From bacterial killing to immune modulation: recent insights into the functions of lysozyme. *PLoS Pathog*. (2017) 13:e1006512. doi: 10.1371/journal.ppat.1006512
56. Singh IP, Bodiwala HS. Recent advances in anti-HIV natural products. *Nat Prod Rep*. (2010) 27:1781–800. doi: 10.1039/c0np00025f
57. Villa TG, Feijoo-Siota L, Rama JLR, Ageitos JM. Antivirals against animal viruses. *Biochem Pharmacol*. (2017) 133:97–116. doi: 10.1016/j.bcp.2016.09.029
58. Mohamed AA, Zhang L, Dorrah MA, Elmogy M, Yousef HA, Bassal TT, et al. Molecular characterization of a c-type lysozyme from the desert locust, *Schistocerca gregaria* (Orthoptera: acrididae). *Dev Comp Immunol*. (2016) 61:60–9. doi: 10.1016/j.dci.2016.03.018
59. Misof B, Liu S, Meusemann K, Peters RS, Donath A, Mayer C, et al. Phylogenomics resolves the timing and pattern of insect evolution. *Science*. (2014) 346:763–7. doi: 10.1126/science.1257570
60. Yamaguchi M, Yoshida H. *Drosophila* as a model organism. *Adv Exp Med Biol*. (2018) 1076:1–10. doi: 10.1007/978-981-13-0529-0_1
61. Hetru C, Troxler L, Hoffmann JA. *Drosophila melanogaster* antimicrobial defense. *J Infect Dis*. (2003) 187(Suppl. 2):S327–34. doi: 10.1086/374758
62. Hanson MA, Lemaitre B. New insights on *Drosophila* antimicrobial peptide function in host defense and beyond. *Curr Opin Immunol*. (2020) 62:22–30. doi: 10.1016/j.coi.2019.11.008
63. Loch G, Zinke I, Mori T, Carrera P, Schroer J, Takeyama H, et al. Antimicrobial peptides extend lifespan in *Drosophila*. *PLoS ONE*. (2017) 12:e0176689. doi: 10.1371/journal.pone.0176689
64. Tsai CW, McGraw EA, Ammar ED, Dietzgen RG, Hogenhout SA. *Drosophila melanogaster* mounts a unique immune response to the *Rhabdovirus sigma* virus. *Appl Environ Microbiol*. (2008) 74:3251–6. doi: 10.1128/AEM.02248-07
65. Dostert C, Jouanguy E, Irving P, Troxler L, Galiana-Arnoux D, Hetru C, et al. The Jak-STAT signaling pathway is required but not sufficient for the antiviral response of drosophila. *Nat Immunol*. (2005) 6:946–53. doi: 10.1038/ni1237
66. Roxstrom-Lindquist K, Terenius O, Faye I. Parasite-specific immune response in adult *Drosophila melanogaster*: a genomic study. *EMBO Rep*. (2004) 5:207–12. doi: 10.1038/sj.embor.7400073
67. Zhu F, Ding H, Zhu B. Transcriptional profiling of *Drosophila* S2 cells in early response to *Drosophila* C virus. *Virol J*. (2013) 10:210. doi: 10.1186/1743-422X-10-210
68. Merkling SH, Overheul GJ, van Mierlo JT, Arends D, Gilissen C, van Rij RP. The heat shock response restricts virus infection in *Drosophila*. *Sci Rep*. (2015) 5:12758. doi: 10.1038/srep12758
69. Castorena KM, Stapleford KA, Miller DJ. Complementary transcriptomic, lipidomic, and targeted functional genetic analyses in cultured *Drosophila* cells highlight the role of glycerophospholipid metabolism in flock house virus RNA replication. *BMC Genom*. (2010) 11:183. doi: 10.1186/1471-2164-11-183
70. Zambon RA, Nandakumar M, Vakharia VN, Wu LP. The toll pathway is important for an antiviral response in *Drosophila*. *Proc Natl Acad Sci USA*. (2005) 102:7257–62. doi: 10.1073/pnas.0409181102
71. Kemp C, Mueller S, Goto A, Barbier V, Paro S, Bonnay F, et al. Broad RNA interference-mediated antiviral immunity and virus-specific inducible responses in *Drosophila*. *J Immunol*. (2013) 190:650–8. doi: 10.4049/jimmunol.1102486

72. Clemmons AW, Lindsay SA, Wasserman SA. An effector peptide family required for *Drosophila* toll-mediated immunity. *PLoS Pathog.* (2015) 11:e1004876. doi: 10.1371/journal.ppat.1004876
73. Cohen LB, Lindsay SA, Xu Y, Lin SJH, Wasserman SA. The daisho peptides mediate *Drosophila* defense against a subset of filamentous fungi. *Front. Immunol.* (2020) 11:9. doi: 10.3389/fimmu.2020.00009
74. Goto A, Yano T, Terashima J, Iwashita S, Oshima Y, Kurata S. Cooperative regulation of the induction of the novel antibacterial listericin by peptidoglycan recognition protein LE and the JAK-STAT pathway. *J Biol Chem.* (2010) 285:15731–8. doi: 10.1074/jbc.M109.082115
75. Calderone NW. Insect pollinated crops, insect pollinators and US agriculture: trend analysis of aggregate data for the period 1992–2009. *PLoS ONE.* (2012) 7:e37235. doi: 10.1371/journal.pone.0037235
76. Chen YP, Siede R. Honey bee viruses. *Adv Virus Res.* (2007) 70:33–80. doi: 10.1016/S0065-3527(07)70002-7
77. Brutscher LM, Daughenbaugh KF, Flenniken ML. Antiviral defense mechanisms in honey bees. *Curr Opin Insect Sci.* (2015) 10:71–82. doi: 10.1016/j.cois.2015.04.016
78. Casteels P, Ampe C, Jacobs F, Vaeck M, Tempst P. Apidaecins: antibacterial peptides from honeybees. *EMBO J.* (1989) 8:2387–91. doi: 10.1002/j.1460-2075.1989.tb08368.x
79. Casteels P, Ampe C, Riviere L, Van Damme J, Elicone C, Fleming M, et al. Isolation and characterization of abaecin, a major antibacterial response peptide in the honeybee (*Apis mellifera*). *Eur J Biochem.* (1990) 187:381–6. doi: 10.1111/j.1432-1033.1990.tb15315.x
80. Casteels P, Ampe C, Jacobs F, Tempst P. Functional and chemical characterization of Hymenoptaecin, an antibacterial polypeptide that is infection-inducible in the honeybee (*Apis mellifera*). *J. Biol. Chem.* (1993) 268:7044–54.
81. Casteels-Josson K, Zhang W, Capaci T, Casteels P, Tempst P. Acute transcriptional response of the honeybee peptide-antibiotics gene repertoire and required post-translational conversion of the precursor structures. *J Biol Chem.* (1994) 269:28569–75.
82. Ryabov EV, Fannon JM, Moore JD, Wood GR, Evans DJ. The iflaviruses sacbrood virus and deformed wing virus evoke different transcriptional responses in the honeybee which may facilitate their horizontal or vertical transmission. *PeerJ.* (2016) 4:e1591. doi: 10.7717/peerj.1591
83. Doublet V, Paxton RJ, McDonnell CM, Dubois E, Nidelet S, Moritz RF, et al. Brain transcriptomes of honey bees (*Apis mellifera*) experimentally infected by two pathogens: black queen cell virus and *Nosema ceranae*. *Genom. Data.* (2016) 10:79–82. doi: 10.1016/j.gdata.2016.09.010
84. Galbraith DA, Yang X, Nino EL, Yi S, Grozinger C. Parallel epigenomic and transcriptomic responses to viral infection in honey bees (*Apis mellifera*). *PLoS Pathog.* (2015) 11:e1004713. doi: 10.1371/journal.ppat.1004713
85. Shan L, Liuhao W, Jun G, Yujie T, Yanping C, Jie W, et al. Chinese sacbrood virus infection in Asian honey bees (*Apis cerana* cerana) and host immune responses to the virus infection. *J Invertebr Pathol.* (2017) 150:63–9. doi: 10.1016/j.jip.2017.09.006
86. Xia Q, Zhou Z, Lu C, Cheng D, Dai F, Li B, et al. A draft sequence for the genome of the domesticated silkworm (*Bombyx mori*). *Science.* (2004) 306:1937–40. doi: 10.1126/science.1102210
87. Swevers L, Feng M, Ren F, Sun J. Antiviral defense against Cypovirus 1 (Reoviridae) infection in the silkworm, *Bombyx mori*. *Arch. Insect Biochem Physiol.* (2020) 103:e21616. doi: 10.1002/arch.21616
88. Li G, Zhou K, Zhao G, Qian H, Xu A. Transcriptome-wide analysis of the difference of alternative splicing in susceptible and resistant silkworm strains after BmNPV infection. *3 Biotech.* (2019) 9:152. doi: 10.1007/s13205-019-1669-9
89. Li G, Qian H, Luo X, Xu P, Yang J, Liu M, et al. Transcriptomic analysis of resistant and susceptible *Bombyx mori* strains following BmNPV infection provides insights into the antiviral mechanisms. *Int J Genomics.* (2016) 2016:2086346. doi: 10.1155/2016/2086346
90. Guo R, Wang S, Xue R, Cao G, Hu X, Huang M, et al. The gene expression profile of resistant and susceptible *Bombyx mori* strains reveals cypovirus-associated variations in host gene transcript levels. *Appl Microbiol Biotechnol.* (2015) 99:5175–87. doi: 10.1007/s00253-015-6634-x
91. Zografidis A, Van Nieuwerburgh F, Kolliopoulou A, Apostolou-Karampelis K, Head SR, Deforce D, et al. Viral Small-RNA analysis of *Bombyx mori* larval midgut during persistent and pathogenic cytoplasmic polyhedrosis virus infection. *J Virol.* (2015) 89:11473–86. doi: 10.1128/JVI.01695-15
92. Hu ZG, Dong ZQ, Dong FF, Zhu Y, Chen P, Lu C, et al. Identification of a PP2A gene in *Bombyx mori* with antiviral function against *B. mori* nucleopolyhedrovirus. *Insect Sci.* (2019) 27:687–96. doi: 10.1111/1744-7917
93. Hua X, Li B, Song L, Hu C, Li X, Wang D, et al. Stimulator of interferon genes (STING) provides insect antiviral immunity by promoting dredd caspase-mediated NF-kappaB activation. *J Biol Chem.* (2018) 293:11878–90. doi: 10.1074/jbc.RA117.000194
94. Liu TH, Dong XL, Pan CX, Du GY, Wu YF, Yang JG, et al. A newly discovered member of the Atlastin family, BmAtlastin-n, has an antiviral effect against BmNPV in *Bombyx mori*. *Sci Rep.* (2016) 6:28946. doi: 10.1038/srep28946
95. Selot R, Kumar V, Shukla S, Chandrakuntal K, Brahmaraju M, Dandin SB, et al. Identification of a soluble NADPH oxidoreductase (BmNOX) with antiviral activities in the gut juice of *Bombyx mori*. *Biosci Biotechnol Biochem.* (2007) 71:200–5. doi: 10.1271/bbb.60450
96. Ponnuvel KM, Nakazawa H, Furukawa S, Asaoka A, Ishibashi J, Tanaka H, et al. A lipase isolated from the silkworm *Bombyx mori* shows antiviral activity against nucleopolyhedrovirus. *J. Virol.* (2003) 77:10725–9. doi: 10.1128/JVI.77.19.10725-10729.2003
97. Zhao P, Xia F, Jiang L, Guo H, Xu G, Sun Q, et al. Enhanced antiviral immunity against *Bombyx mori* cytoplasmic polyhedrosis virus via overexpression of peptidoglycan recognition protein S2 in transgenic silkworms. *Dev Comp Immunol.* (2018) 87:84–9. doi: 10.1016/j.dci.2018.05.021
98. Bao YY, Tang XD, Lv ZY, Wang XY, Tian CH, Xu YP, et al. Gene expression profiling of resistant and susceptible *Bombyx mori* strains reveals nucleopolyhedrovirus-associated variations in host gene transcript levels. *Genomics.* (2009) 94:138–45. doi: 10.1016/j.ygeno.2009.04.003
99. Kolliopoulou A, Van Nieuwerburgh F, Stravopodis DJ, Deforce D, Swevers L, Smagghe G. Transcriptome analysis of *Bombyx mori* larval midgut during persistent and pathogenic cytoplasmic polyhedrosis virus infection. *PLoS ONE.* (2015) 10:e0121447. doi: 10.1371/journal.pone.0121447
100. Bao YY, Lv ZY, Liu ZB, Xue J, Xu YP, Zhang CX. Comparative analysis of *Bombyx mori* nucleopolyhedrovirus responsive genes in fat body and haemocyte of *B. mori* resistant and susceptible strains. *Insect Mol Biol.* (2010) 19:347–58. doi: 10.1111/j.1365-2583.2010.00993.x
101. Sun Q, Guo H, Xia Q, Jiang L, Zhao P. Transcriptome analysis of the immune response of silkworm at the early stage of *Bombyx mori* bidensovirus infection. *Dev Comp Immunol.* (2020) 106:103601. doi: 10.1016/j.dci.2019.103601
102. Xue J, Qiao N, Zhang W, Cheng RL, Zhang XQ, Bao YY, et al. Dynamic interactions between *Bombyx mori* nucleopolyhedrovirus and its host cells revealed by transcriptome analysis. *J Virol.* (2012) 86:7345-7359. doi: 10.1128/JVI.07217-12
103. Sagisaka A, Fujita K, Nakamura Y, Ishibashi J, Noda H, Imanishi S, et al. Genome-wide analysis of host gene expression in the silkworm cells infected with *Bombyx mori* nucleopolyhedrovirus. *Virus Res.* (2010) 147:166–75. doi: 10.1016/j.virusres.2009.10.015
104. Gao K, Deng XY, Qian HY, Qin G, Guo XJ. Digital gene expression analysis in the midgut of 4008 silkworm strain infected with cytoplasmic polyhedrosis virus. *J. Invertebr Pathol.* (2014) 115:8–13. doi: 10.1016/j.jip.2013.10.016
105. Jiang L, Peng Z, Guo Y, Cheng T, Guo H, Sun Q, et al. Transcriptome analysis of interactions between silkworm and cytoplasmic polyhedrosis virus. *Sci Rep.* (2016) 6:24894. doi: 10.1038/srep24894
106. Feng M, Zhang X. Immunity to *Avian leukosis* virus: where are we now and what should we do? *Front Immunol.* (2016) 7:624. doi: 10.3389/fimmu.2016.00624
107. Wang X, Zhang Y, Zhang R, Zhang J. The diversity of pattern recognition receptors (PRRs) involved with insect defense against pathogens. *Curr Opin Insect Sci.* (2019) 33:105–10. doi: 10.1016/j.cois.2019.05.004
108. Lu Y, Su F, Li Q, Zhang J, Li Y, Tang T, et al. Pattern recognition receptors in *Drosophila* immune responses. *Dev Comp Immunol.* (2020) 102:103468. doi: 10.1016/j.dci.2019.103468
109. Jiang L, Liu W, Guo H, Dang Y, Cheng T, Yang W, et al. Distinct functions of *Bombyx mori* peptidoglycan recognition protein 2 in immune responses to bacteria and viruses. *Front Immunol.* (2019) 10:776. doi: 10.3389/fimmu.2019.00776

110. Lamiable O, Imler JL. Induced antiviral innate immunity in *Drosophila*. *Curr Opin Microbiol*. (2014) 20:62–8. doi: 10.1016/j.mib.2014.05.006
111. Liu W, Liu J, Lu Y, Gong Y, Zhu M, Chen F, et al. Immune signaling pathways activated in response to different pathogenic micro-organisms in *Bombyx mori*. *Mol Immunol*. (2015) 65:391–7. doi: 10.1016/j.molimm.2015.02.018
112. Wang L, Cappelle K, Santos D, Vanden Broeck J, Smagghe G, Swevers L. Short-term persistence precedes pathogenic infection: infection kinetics of cricket paralysis virus in silkworm-derived Bm5 cells. *J Insect Physiol*. (2019) 115:1–11. doi: 10.1016/j.jinsphys.2019.03.004

Conflict of Interest: The authors declare that the research was conducted in the absence of any commercial or financial relationships that could be construed as a potential conflict of interest.

frontiers in Immunology

OPINION
published: 30 November 2020
doi: 10.3389/fimmu.2020.618801

Flavivirus Infection and Regulation of Host Immune and Tissue Homeostasis in Insects

Sneh Harsh[1,2] *and Ioannis Eleftherianos*[1]*

[1] Infection and Innate Immunity Lab, Department of Biological Sciences, Institute for Biomedical Sciences, The George Washington University, Washington, DC, United States, [2] Department of Biochemistry and Molecular Pharmacology, New York University School of Medicine, New York, NY, United States

Keywords: flavivirus, mosquito, *Drosophila*, immunity, homeostasis, pathophysiology

OPEN ACCESS

Edited by:
Luc Swevers,
National Centre of Scientific Research Demokritos, Greece

Reviewed by:
Berlin L. Londono-Renteria, Kansas State University, United States
Doug Brackney, Connecticut Agricultural Experiment Station, United States
Humberto Lanz-Mendoza, National Institute of Public Health, Mexico

***Correspondence:**
Ioannis Eleftherianos
ioannise@gwu.edu

Specialty section:
This article was submitted to Comparative Immunology, a section of the journal Frontiers in Immunology

Received: *18 October 2020*
Accepted: *16 November 2020*
Published: *30 November 2020*

Citation:
Harsh S and Eleftherianos I (2020) Flavivirus Infection and Regulation of Host Immune and Tissue Homeostasis in Insects. Front. Immunol. 11:618801. doi: 10.3389/fimmu.2020.618801

BACKGROUND

Flaviviruses are enveloped single-stranded RNA viruses and major human pathogens. They are responsible for causing outbreaks and therefore they represent a serious health issue worldwide (1). Because of the clinical significance of flaviviruses and the severity of epidemics they cause globally, developing efficient vaccines and drugs is critical for the success of disease control measures. Importantly, many flaviviruses, including Dengue virus (DENV), Japanese Encephalitis virus (JEV), West Nile virus (WNV), Yellow Fever virus (YFV), and Zika virus (ZIKV), are vectored though arthropods (arboviruses), mainly mosquitoes and ticks (2). Although most previous efforts have primarily focused on advancing the design of therapeutic strategies for alleviating the disease symptoms caused by flaviviruses, it is equally significant to also be able to interpret the molecular nature of the interactions that take place between flaviviruses and the insect vector and determine whether these interactions affect pathophysiological processes during infection and transmission.

Interactions between mosquito vectors and flaviviruses have been studied in several occasions (3). For instance, ZIKV is mainly transmitted by *Aedes aegypti* mosquitoes and recent studies have begun to examine vector-virus relationships and transmission dynamics of this virus pathogen (4). *Ae. aegypti* mosquitoes infected with ZIKV activate the RNA interference (RNAi) mechanism by upregulating several virus-produced short interfering RNAs (siRNAs), piwi-interacting RNAs and microRNAs. Many of the latter are also regulated by DENV and WNVs, but not by the alphavirus Chikungunya, indicating conservation in the mosquito response to flavivirus infection (5). Flavivirus infection in mosquito vectors activates innate immune signaling, which promotes the induction of antiviral response through the production of effector molecules (6). Activation of JAK/STAT together with Toll signaling elevates the *Ae. aegypti* resistance to ZIKV infection, silencing the Toll pathway adaptor MyD88 increases DENV infection in the *Ae. aegypti* midgut, and DENV infection in this mosquito vector decreases the signaling activity of immune deficiency (Imd) pathway (7–9). Interestingly, the secreted protein Vago limits WNV replication in *Culex* mosquito cells through induction of JAK/STAT signaling (10). Studies in mosquitoes are expected to contribute toward developing efficient procedures for preventing the spread of flaviviruses.

Results from research with insect vectors further stress the need for insect immunologists studying antiviral immunity to draw more attention to the outcome of flavivirus infection in insects rather than focusing exclusively on the replication efficacy of the virus. Therefore, this opinion article aims at highlighting recent studies that have started to dissect the interaction between

antiviral immune mechanisms and flavivirus tropism as well as host tissue homeostasis and pathophysiological defects in mosquitoes and the model insect *Drosophila*. Such information is critical because it has the potential to lead to the development of novel therapeutics that will be directed against the ability of flaviviruses to multiply in certain insect organs. This will be valuable knowledge for understanding and potentially predicting the severity and extent of flavivirus infection and the efficiency of transmission.

FLAVIVIRUS INTERACTION WITH MOSQUITO IMMUNE AND METABOLIC ORGANS

The insect fat body is a diffused organ that functions similarly to the mammalian liver and is responsible for metabolism and storage of nutrients as well as the production and secretion of antimicrobial peptides and other immune factors (11). Flaviviruses present in the mosquito hemocoel (the insect body cavity) replicate in the abdominal and thoracic fat body before they disseminate to the salivary glands and other insect tissues (12). For instance, WNV replicates primarily in the fat body of *Culex pipiens quinquefasciatus* (13), but DENV replication has not been associated with this tissue in *Aedes albopictus* and *Ae. aegypti* mosquitoes (14, 15). However, more recent findings indicate that DENV replication in the fat body cells of *A. albopictus* alters the expression of Actin and alpha Tubulin (16), and downregulates the transcription of Toll pathway related genes in *Ae. aegypti* (8). In *Ae. aegypti*, YFV replicates in the fat body and other organs and feeding mosquitoes with a DENV-infected blood meal leads to activation of autophagy in the this tissue and the midgut and increases the expression of genes related to apoptosis such as the effector caspase *Casps7* (17–19). Notably, activation of JAK/STAT signaling specifically in the fat body of *Ae. aegypti* restrains DENV efficiently but fails to restrict ZIKV infection, and priming of these mosquitoes with inactive DENV induces the activation of Notch signaling upon infection with active DENV and reduces viral propagation in the midgut and carcass (20, 21). Flaviviruses transmitted by mosquitoes are taken up through a blood meal and migrate to the mosquito gut before they move to the salivary glands in order to be passed on to another vertebrate host and maintain their lifecycle (22). Main barriers to systemic infection include the midgut infection barrier, midgut escape barrier, salivary gland infection barrier, and salivary gland escape barrier (23). In the gut, flavivirus infection triggers the induction of antiviral pathways through interaction with receptors in the midgut epithelial cells (24). Interfering with the expression of certain RNAi signaling components in *Ae. aegypti* adult mosquitoes reduces DENV titers in the midgut following oral infection (25). Although Toll signaling plays a crucial role in the anti-DENV response in the midgut of *Ae. aegypti* (26, 27), the involvement of this pathway in the mosquito immune response against WNV and YFV is not fully determined yet (28). Also, Imd signaling activity participates in the induction of anti-DENV immune functions in the mosquito gut, because inhibition of this pathway leads to higher DENV load in *Ae. aegypti* midgut (29). Similar role has further been demonstrated for two DENV restriction factors, which are regulated by the JAK/STAT pathway and their expression lowers viral titers in the *Ae. aegypti* midgut (30). Apoptosis events have been found to occur in the midgut of *C. pipiens* and *Ae. aegypti* refractory strains during infection with WNV or DENV, respectively, indicating a potential role in restricting virus propagation by these mosquito vectors (31, 32). Strikingly, the presence of gut microbiota in *Ae. aegypti* can have a direct or indirect influence on DENV infection and spread either by enhancing the mosquito innate immune response or suppressing virus replication through the secretion of unknown molecules [(24, 33) and references therein]. DENV infection in *Ae. aegypti* can be affected by the midgut-inhabiting bacterium *Serratia odorifera* or the fungus *Talaromyces*, which both increase mosquito sensitivity to this virus. This is achieved through the production of a bacterial polypeptide that interacts with the virus or the modification of trypsin enzyme activity by the fungus. Both microbially mediated effects lead to considerable changes in mosquito physiology (34, 35). Interestingly, variation in *Wolbachia*-mediated DENV blocking in *Ae. aegypti* has been previously attributed to the production of nitric oxide or other free radicals (36). Also, serum ion can be utilized by the *Ae. aegypti* iron metabolism pathway to strengthen reactive oxygen species activity in the gut epithelium in order to oppose DENV infection (37). In addition, expression of the redox-sensing gene *nuclear factor erythroid-derived factor 2* (*Nrf2*) limits ZIKV infection by maintaining midgut homeostasis through modulation of reactive oxygen species in the midgut as well as microbiota growth and stem cell proliferation (38).

The association between flavivirus infection and lipid droplet regulation in mammalian cells has been previously reported (39–41). For example, infection of BHK-21, HepG2, and C6/36 cells by DENV increases markedly the number of lipid droplets per cell. This interaction possibly occurs between lipid droplets and various conserved residues in the core protein of the virus and probably indicates a link between viral replication and modulation of lipid metabolism (42). Also, during DENV infection of the hepatocyte derived cellular carcinoma cell line Huh7, HMG-CoA reductase activity increases, leading to higher cholesterol levels in the endoplasmic reticulum necessary for virus replication complex formation (43). In a similar fashion, infection of the *Ae. aegypti* cell line Aag2 with DENV increases lipid droplet accumulation (44). This phenotype in the DENV infected cells is associated with substantial upregulation of transcript levels of genes encoding factors related to lipid droplet biogenesis and lipid storage. These effects are connected with changes in immune signaling regulation, given that ectopic activation of Toll or Imd pathways further result in higher numbers of lipid droplets in the midgut.

LESSONS FROM THE *DROSOPHILA*-FLAVIVIRUS MODEL

Due to ZIKV outbreaks in several countries over the past five years, recent research has used the *Drosophila* model for leveraging the powerful genetic and genomic tools in the fly in order to understand flavivirus pathogenesis (**Figure 1**). ZIKV possesses a positive-sense single-stranded RNA genome encoding three structural (capsid,

pre-membrane, envelope) and seven non-structural proteins (NS1, NS2A, NS2B, NS3, NS4A, NS4B, and NS5) (45). Expression of the ZIKV non-structural protein NS4A in the brain of *Drosophila* larvae induces apoptosis and leads to microcephaly, while expression of human *Ankyrin Repeat And LEM Domain Containing 2* (*ANKLE2*) gene, which is involved in brain development and has been previously implicated in hereditary microcephaly, in flies overexpressing ZIKV NS4A abolishes these defects. These results provide proof that ZIKV NS4A interacts physically with the ANKLE2 protein and causes microcephaly in an ANKLE2-dependent manner (46) (**Figure 1A**). More recently, these findings were extended by showing that mutations in *ANKLE2* gene perturbs an asymmetric cell division pathway in *Drosophila* neuroblasts and causes neurological disease and microcephaly, whereas overexpression of ZIKV NS4A in neuroblasts produces a similar phenotype observed in *Ankle2* mutants (47).

Also, it has been shown that ZIKV infection induces antiviral autophagy in the brain of adult *Drosophila* and this process depends on the activity of the Imd transcription factor Relish (48). The fly ortholog of the mammalian polyubiquitin-binding scaffold protein p62, the autophagy cargo receptor Ref(2)P, is also directed against ZIKV in the brain and protection against this pathogen is not dependent on RNAi signaling activity (48). Interestingly, ZIKV also replicates in the fat body, crop and gut of the adult fly and this tissue tropism disrupts gut and fat body lipid droplet homeostasis (49) (**Figure 1B**). This tissue-specific phenotype is further intensified in loss-of-function flies mutant for *Dicer-2*, the RNase of the RNAi pathway and is accompanied by reduced insulin signaling activity that leads to increased ZIKV replication and fly sensitivity to the infection (49). A genetic screen using naturally derived *Drosophila* lines revealed the insulin-like receptor InR as essential for fly survival to arbovirus infection (50). Insulin signaling was further found to suppress RNAi activity, but priming with mammalian insulin enhances the immune response to control ZIKV and DENV infection through induction of genes regulated *via* the JAK/STAT pathway.

Recently, it was demonstrated that ZIKV infection in *Drosophila* adult flies upregulates several gene targets that act as negative regulators of the JAK/STAT pathway and expression of certain ZIKV structural and non-structural proteins in different tissues of transgenic flies results in restricted eye growth, which is due to reduced rate of proliferation in eye imaginal epithelia (45). In particular, overexpression of ZIKV *NS4A*, a dominant negative form of *domeless*, and co-expression of dominant negative form of *domeless* and *NS4A* driven under an eye-specific promoter induces restricted eye phenotype in a JAK/STAT dependent manner. Of note, overexpression of ZIKV *NS4A* in the wing reduces the size of the pouch domain, an effect that is associated with decreased Notch signaling. This information points toward a relationship between ZIKV gene expression, JAK/STAT and Notch signaling activity which is necessary for *Drosophila* growth and development, and induction of pathological defects in the fly (**Figure 1A**). In a similar manner, expression of the DENV NS3 protein (which promotes virus replication) in *Drosophila* transgenic flies reduces their survival response to bacterial infection, but not to abiotic stress, indicating a link between DENV NS3 activity and antimicrobial immune capacity (51). Finally, a genome-wide RNAi screen in *Drosophila* cells has identified a large number of genes encoding cellular factors, many of which are able to restrict WNV infection. Intriguingly, all these genes are conserved in mosquitoes and the majority have human orthologs. Furthermore, a subset of those genes (e.g., dRUVBL1 and dXPO1) reduces flavivirus infection in adult flies demonstrating the power of *Drosophila* for the discovery of novel host molecules with anti-flavivirus activity (52).

CONCLUSIONS AND PERSPECTIVES

Flaviviruses have recently expanded globally by causing severe health impacts. Animal models are critical for understanding the molecular and physiological basis of host antiviral response and flavivirus pathogenesis. Because host innate immune responses are evolutionary conserved across many phyla, investigating the effect of flavivirus infection on the immune signaling and function of animal models is particularly informative because it can lead to the identification of anti-flavivirus immune processes in humans. Also, elucidating the scale of interactions between the host innate immune system and flaviviruses can lead to tissue-specific

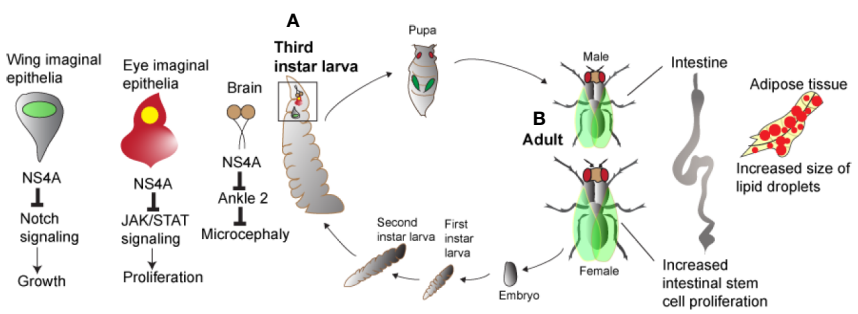

FIGURE 1 | Zika virus and host pathologies in *Drosophila*. Zika virus results in perturbed homeostasis of different organs in *Drosophila* larva and adult. **(A)** Overexpression of Zika virus NS4A results in microcephaly in brain and restricted growth of the wing and eye imaginal epithelia. In the wing and eye imaginal epithelia, Zika virus NS4A interacts with Notch and JAK/STAT signaling pathways while in case of the brain, Zika virus NS4A targets ANKLE2, a highly conserved mitotic regulator. **(B)** Infection of Zika virus in *Drosophila* adult flies results in perturbed intestinal and adipose tissue homeostasis marked by increased intestinal stem cell proliferation and increased size of the lipid droplets.

pathological deficits that modulate host functional changes associated with the disease. Probing the exact nature of interactions that take place during transmission of flaviviruses by mosquitoes and ticks and exploring the impact of the pathogens on tissue homeostasis during this process is considered a future research priority. Due to the close taxonomic relationship between mosquitoes and the common fruit fly (they are both members of the order Diptera), the use of *Drosophila* offers many advantages for studying these insect-borne viruses. Recent studies in *Drosophila* adult flies and larvae have been pivotal for the identification of fundamental mechanisms in insects that participate in the control of flaviviruses in the mosquito vector. If *Drosophila* factors interacting with flavivirus proteins are identified and characterized functionally, such findings could be extrapolated to mosquitoes after verification in the natural host (53). This approach could in turn put us in a better position to control the spread of flaviviruses in the mosquito vector, and thus enable us to prevent flavivirus dissemination to the human population.

AUTHOR CONTRIBUTIONS

SH wrote the original draft of the manuscript and IE revised and edited the paper. All authors contributed to the article and approved the submitted version.

ACKNOWLEDGMENTS

We would like to thank the Department of Biological Sciences and Columbian College of Arts and Science at The George Washington University for providing support to our research.

REFERENCES

1. Fernandez-Garcia M-D, Mazzon M, Jacobs M, Amara M. Pathogenesis of flavivirus infections: using and abusing the host cell. *Cell Host Microbe* (2009) 5:318–28. doi: 10.1016/j.chom.2009.04.001
2. Chong HY, Leow AB, Majeed ABA, Leow CH. Flavivirus infection-A review of immunopathogenesis, immunological response, and immunodiagnosis. *Virus Res* (2019) 274:197770. doi: 10.1016/j.virusres.2019.197770
3. Samuel GH, Adelman ZN, Myles KM. Antiviral Immunity and Virus-Mediated Antagonism in Disease Vector Mosquitoes. *Trends Microbiol* (2018) 26:447–61. doi: 10.1016/j.tim.2017.12.005
4. Plourde AR, Bloch EM. A Literature Review of Zika Virus. *Emerg Infect Dis* (2016) 22:1185–92. doi: 10.3201/eid2207.151990
5. Saldaña MA, Etebari K, Hart CE, Widen SG, Wood TG, Thangamani S, et al. Zika virus alters the microRNA expression profile and elicits an RNAi response in *Aedes aegypti* mosquitoes. *PloS Negl Trop Dis* (2017) 11: e0005760. doi: 10.1371/journal.pntd.0005760
6. Liu T, Xu Y, Wang X, Gu J, Yan G, Chen X-G. Antiviral systems in vector mosquitoes. *Dev Comp Immunol* (2018) 83:34–43. doi: 10.1016/j.dci.2017.12.025
7. Angleró-Rodríguez YII, MacLeod HJ, Kang S, Carlson JS, Jupatanakul N, Dimopoulos G. *Aedes aegypti* Molecular Responses to Zika Virus: Modulation of Infection by the Toll and Jak/Stat Immune Pathways and Virus Host Factors. *Front Microbiol* (2017) 8:2050. doi: 10.3389/fmicb.2017.02050
8. Ramirez JL, Dimopoulos G. The Toll immune signaling pathway control conserved anti-dengue defenses across diverse *Ae. aegypti* strains and against multiple dengue virus serotypes. *Dev Comp Immunol* (2010) 34:625–9. doi: 10.1016/j.dci.2010.01.006
9. Sim S, Dimopoulos G. Dengue virus inhibits immune responses in *Aedes aegypti* cells. *PloS One* (2010) 5:e10678. doi: 10.1371/journal.pone.0010678
10. Paradkar PN, Trinidad L, Voysey R, Duchemin J-B, Walker PJ. Secreted Vago restricts West Nile virus infection in *Culex* mosquito cells by activating the Jak-STAT pathway. *Proc Natl Acad Sci U S A* (2012) 109:18915–20. doi: 10.1073/pnas.1205231109
11. Li S, Yu X, Feng Q. Fat Body Biology in the Last Decade. *Annu Rev Entomol* (2019) 64:315–33. doi: 10.1146/annurev-ento-011118-112007
12. Huang YJ, Higgs S, Horne KM, Vanlandingham DL. Flavivirus-mosquito interactions. *Viruses* (2014) 6:4703–30. doi: 10.3390/v6114703
13. Girard YA, Klingler KA, Higgs S. West Nile virus dissemination and tissue tropisms in orally infected *Culex pipiens quinquefasciatus*. *Vector Borne Zoonotic Dis* (2004) 4:109–22. doi: 10.1089/1530366041210729
14. Linthicum KJ, Platt K, Myint KS, Lerdthusnee K, Innis BL, Vaughn DW. Dengue 3 virus distribution in the mosquito *Aedes aegypti*: an immunocytochemical study. *Med Vet Entomol* (1996) 10:87–92. doi: 10.1111/j.1365-2915.1996.tb00086.x
15. Sriurairatna S, Bhamarapravati N. Replication of dengue-2 virus in *Aedes albopictus* mosquitoes. An electron microscopic study. *Am J Trop Med Hyg* (1977) 26:1199–205. doi: 10.4269/ajtmh.1977.26.1199
16. Zhang M, Zheng X, Wu Y, Gan M, He A, Li Z, et al. Differential proteomics of *Aedes albopictus* salivary gland, midgut and C6/36 cell induced by dengue virus infection. *Virology* (2013) 444:109–18. doi: 10.1016/j.virol.2013.06.001
17. Ocampo CB, Caicedo PA, Jaramillo G, Ursic Bedoya R, Baron O, Serrato IM, et al. Differential expression of apoptosis related genes in selected strains of *Aedes aegypti* with different susceptibilities to dengue virus. *PloS One* (2013) 8: e61187. doi: 10.1089/vbz.2007.0269
18. Eng MW, van Zuylen MN, Severson DW. Apoptosis-related genes control autophagy and influence DENV-2 infection in the mosquito vector, *Aedes aegypti*. *Insect Biochem Mol Biol* (2016) 76:70–83. doi: 10.1016/j.ibmb.2016.07.004
19. McElroy KL, Girard YA, McGee CE, Tsetsarkin KA, Vanlandingham DL, Higgs S. Characterization of the antigen distribution and tissue tropisms of three phenotypically distinct yellow fever virus variants in orally infected *Aedes aegypti* mosquitoes. *Vector Borne Zoonotic Dis* (2008) 8:675–87. doi: 10.1089/vbz.2007.0269
20. Jupatanakul N, Sim S, Angleró-Rodríguez YII, Souza-Neto J, Das S, Poti KE, et al. Engineered *Aedes aegypti* JAK/STAT Pathway-Mediated Immunity to Dengue Virus. *PloS Negl Trop Dis* (2017) 11:e0005187. doi: 10.1371/journal.pntd.0005187
21. Serrato-Salas J, Izquierdo-Sánchez J, Argüello M, Conde R, Alvarado-Delgado A, Lanz-Mendoza H. *Aedes aegypti* antiviral adaptive response against DENV-2. *Dev Comp Immunol* (2018) 84:28–36. doi: 10.1016/j.dci.2018.01.022
22. Alonso-Palomares LA, Moreno-García M, Lanz-Mendoza H, Salazar MII. Molecular Basis for Arbovirus Transmission by *Aedes aegypti* Mosquitoes. *Intervirology* (2018) 61:255–64. doi: 10.1159/000499128
23. Franz AW, Kanor AM, Passarelli AL, Clem RJ. Tissue Barriers to Arbovirus Infection in Mosquitoes. *Viruses* (2015) 7:3741–67. doi: 10.3390/v7072795
24. Saraiva RG, Kang S, Simões ML, Angleró-Rodríguez YII, Dimopoulos G. Mosquito gut antiparasitic and antiviral immunity. *Dev Comp Immunol* (2016) 64:53–64. doi: 10.1016/j.tim.2017.12.005
25. Sánchez-Vargas I, Scott JC, Poole-Smith BK, Franz AWE, Barbosa-Solomieu V, Wilusz J, et al. Dengue virus type 2 infections of *Aedes aegypti* are modulated by the mosquito's RNA interference pathway. *PloS Pathog* (2009) 5:e1000299. doi: 10.1371/journal.ppat.1000299
26. Sim S, Ramirez JL, Dimopoulos G. Dengue virus infection of the *Aedes aegypti* salivary gland and chemosensory apparatus induces genes that modulate infection and blood-feeding behavior. *PloS Pathog* (2012) 8:e1002631. doi: 10.1371/journal.ppat.1002631
27. Xi Z, Ramirez JL, Dimopoulos G. The *Aedes aegypti* Toll pathway controls Dengue virus infection. *PloS Pathog* (2008) 4:e1000098. doi: 10.1371/journal.ppat.1000098
28. Colpitts TM, Cox J, Vanlandingham DL, Feitosa FM, Cheng G, Kurscheid S, et al. Alterations in the *Aedes aegypti* transcriptome during Infection with West Nile, Dengue and Yellow Fever viruses. *PloS Pathog* (2011) 7:e1002189. doi: 10.1371/journal.ppat.1002189
29. Sim S, Jupatanakul N, Ramirez JL, Kang S, Romero-Vivas CM, Mohammed H, et al. Transcriptomic profiling of diverse *Aedes aegypti* strains reveals increased basal-level immune activation in Dengue virus-refractory

populations and identifies novel virus-vector molecular interactions. *PloS Neglected Trop Dis* (2013) 7:e2295. doi: 10.1371/journal.pntd.0002295
30. Souza-Neto JA, Sim S, Dimopoulos G. An evolutionary conserved function of the JAK-STAT pathway in anti-dengue defense. *Proc Natl Acad Sci USA* (2009) 106:17841–6. doi: 10.1073/pnas.0905006106
31. Liu B, Behura SK, Clem RJ, Schneemann A, Becnel J, Severson DW, et al. P53-mediated rapid induction of apoptosis conveys resistance to viral infection in *Drosophila melanogaster*. *PloS Pathog* (2013) 9:e1003137. doi: 10.1371/journal.ppat.1003137
32. Vaidyanathan R, Scott T. Apoptosis in mosquito midgut epithelia associated with West Nile virus infection. *Apoptosis* (2006) 11:1643–51. doi: 10.1007/s10495-006-8783-y
33. Wu P, Sun P, Nie K, Zhu Y, Shi M, Xiao C, et al. A Gut Commensal Bacterium Promotes Mosquito Permissiveness to Arboviruses. *Cell Host Microbe* (2019) 25:101–112.e5. doi: 10.1016/j.chom.2018.11.004
34. Angleró-Rodríguez YII, Talyuli OA, Blumberg BJ, Kang S, Demby C, Shields A, et al. An *Aedes aegypti*-associated fungus increases susceptibility to dengue virus by modulating gut trypsin activity. *Elife* (2017) 6:e28844. doi: 10.7554/eLife.28844
35. Apte-Deshpande A, Paingankar M, Gokhale MD, Deobagkar DN. *Serratia odorifera* a midgut inhabitant of *Aedes aegypti* mosquito enhances its susceptibility to dengue-2 virus. *PloS One* (2012) 7:e40401. doi: 10.1371/journal.pone.0040401
36. Terradas G, Allen SL, Chenoweth SF, McGraw EA. Family level variation in *Wolbachia*-mediated dengue virus blocking in *Aedes aegypti*. *Parasitol Vectors* (2017) 10:622. doi: 10.1186/s13071-017-2589-3
37. Zhu Y, Tong L, Nie K, Wiwatanaratanabutr I, Sun P, Li Q, et al. Host serum iron modulates dengue virus acquisition by mosquitoes. *Nat Microbiol* (2019) 4:2405–15. doi: 10.1038/s41564-019-0555-x
38. Bottino-Rojas V, Talyuli OAC, Carrara L, Martins AJ, James AA, Oliveira PL, et al. The redox-sensing gene *Nrf2* affects intestinal homeostasis, insecticide resistance, and Zika virus susceptibility in the mosquito *Aedes aegypti*. *J Biol Chem* (2018) 293:9053–63. doi: 10.1074/jbc.RA117.001589
39. Carvalho FA, Carneiro FA, Martins IC, Assunção-Miranda I, Faustino AF, Pereira RM, et al. Dengue virus capsid protein binding to hepatic lipid droplets (LD) is potassium ion dependent and is mediated by LD surface proteins. *J Virol* (2012) 86:2096–108. doi: 10.1128/JVI.06796-11
40. Martins IC, Gomes-Neto F, Faustino AF, Carvalho FA, Carneiro FA, Bozza PT, et al. The disordered N-terminal region of dengue virus capsid protein contains a lipid-droplet-binding motif. *Biochem J* (2012) 444:405–15. doi: 10.1042/BJ20112219
41. Teoh PG, Huang ZS, Pong WL, Chen PC, Wu HN. Maintenance of dimer conformation by the dengue virus core protein α4-α4' helix pair is critical for nucleocapsid formation and virus production. *J Virol* (2014) 88:7998–8015. doi: 10.1128/JVI.00940-14
42. Samsa MM, Mondotte JA, Iglesias NG, Assunção-Miranda I, Barbosa-Lima G, Da Poian AT, et al. Dengue virus capsid protein usurps lipid droplets for viral particle formation. *PloS Pathog* (2009) 5:e1000632. doi: 10.1371/journal.ppat.1000632
43. Soto-Acosta R, Bautista-Carbajal P, Cervantes-Salazar M, Angel-Ambrocio AH, Del Angel RM. DENV up-regulates the HMG-CoA reductase activity through the impairment of AMPK phosphorylation: A potential antiviral target. *PloS Pathog* (2017) 13:e1006257. doi: 10.1371/journal.ppat.1006257
44. Barletta AB, Alves LR, Silva MC, Sim S, Dimopoulos G, Liechocki S, et al. Emerging role of lipid droplets in *Aedes aegypti* immune response against bacteria and Dengue virus. *Sci Rep* (2016) 6:19928. doi: 10.1038/srep19928
45. Harsh S, Fu Y, Kenney E, Han Z, Eleftherianos I. Zika virus non-structural protein NS4A restricts eye growth in *Drosophila* through regulation of JAK/STAT signaling. *Dis Model Mech* (2020) 13:dmm040816. doi: 10.1242/dmm.040816
46. Shah PS, Link N, Jang GM, Sharp PP, Zhu T, Swaney DL, et al. Comparative Flavivirus-Host Protein Interaction Mapping Reveals Mechanisms of Dengue and Zika Virus Pathogenesis. *Cell* (2018) 175:1931–45. doi: 10.1016/j.cell.2018.11.028
47. Link N, Chung H, Jolly A, Withers M, Tepe B, Arenkiel BR, et al. Mutations in ANKLE2, a ZIKA Virus Target, Disrupt an Asymmetric Cell Division Pathway in *Drosophila* Neuroblasts to Cause Microcephaly. *Dev Cell* (2019) 51:713–29. doi: 10.1016/j.devcel.2019.10.009
48. Liu Y, Gordesky-Gold B, Leney-Greene M, Weinbren NL, Tudor M, Cherry S. Inflammation-Induced, STING-Dependent Autophagy Restricts Zika Virus Infection in the *Drosophila* Brain. *Cell Host Microbe* (2018) 24:57–68e3. doi: 10.1016/j.chom.2018.05.022
49. Harsh S, Ozakman Y, Kitchen SM, Paquin-Proulx D, Nixon DF, Eleftherianos I. Dicer-2 Regulates Resistance and Maintains Homeostasis against Zika Virus Infection in *Drosophila*. *J Immunol* (2018) 201:3058–72. doi: 10.4049/jimmunol.1800597
50. Ahlers LRH, Trammell CE, Carrell GF, Mackinnon S, Torrevillas BK, Chow CY, et al. Insulin Potentiates JAK/STAT Signaling to Broadly Inhibit Flavivirus Replication in Insect Vectors. *Cell Rep* (2019) 29:1946–60. doi: 10.1016/j.celrep.2019.10.029
51. Querenet M, Danjoy ML, Mollereau B, Davoust N. Expression of dengue virus NS3 protein in *Drosophila* alters its susceptibility to infection. *Fly (Austin)* (2015) 9:1–6. doi: 10.1080/19336934.2015.1072662
52. Yasunaga A, Hanna SL, Li J, Cho H, Rose PP, Spiridigliozzi A, et al. Genome-wide RNAi screen identifies broadly-acting host factors that inhibit arbovirus infection. *PloS Pathog* (2014) 10:e1003914. doi: 10.1371/journal.ppat.1003914
53. Merkling SH, van Rij RP. Beyond RNAi: antiviral defense strategies in *Drosophila* and mosquito. *J Insect Physiol* (2013) 59:159–70. doi: 10.1016/j.jinsphys.2012.07.004

Conflict of Interest: The authors declare that the research was conducted in the absence of any commercial or financial relationships that could be construed as a potential conflict of interest.

frontiers in Immunology

ORIGINAL RESEARCH
published: 08 January 2021
doi: 10.3389/fimmu.2020.613957

Activation of Toll Immune Pathway in an Insect Vector Induced by a Plant Virus

Yu-Juan He[1,2†], Gang Lu[2†], Yu-Hua Qi[2], Yan Zhang[2], Xiao-Di Zhang[2], Hai-Jian Huang[2], Ji-Chong Zhuo[2], Zong-Tao Sun[2], Fei Yan[2], Jian-Ping Chen[1,2], Chuan-Xi Zhang[2*] and Jun-Min Li[2*]*

[1] College of Plant Protection, Nanjing Agricultural University, Nanjing, China, [2] State Key Laboratory for Managing Biotic and Chemical Threats to the Quality and Safety of Agro-products, Key Laboratory of Biotechnology in Plant Protection of MOA of China and Zhejiang Province, Institute of Plant Virology, Ningbo University, Ningbo, China

OPEN ACCESS

Edited by:
Xiao-Qiang Yu,
University of Missouri–Kansas City,
United States

Reviewed by:
Christine A. Jansen,
Utrecht University, Netherlands
Ioannis Eleftherianos,
George Washington University,
United States

***Correspondence:**
Jian-Ping Chen
jpchen2001@126.com
Chuan-Xi Zhang
chxzhang@zju.edu.cn
Jun-Min Li
lijunmin@nbu.edu.cn

[†]These authors have contributed equally to this work

Specialty section:
This article was submitted to Comparative Immunology, a section of the journal Frontiers in Immunology

Received: 04 October 2020
Accepted: 01 December 2020
Published: 08 January 2021

Citation:
He Y-J, Lu G, Qi Y-H, Zhang Y, Zhang X-D, Huang H-J, Zhuo J-C, Sun Z-T, Yan F, Chen J-P, Zhang C-X and Li J-M (2021) Activation of Toll Immune Pathway in an Insect Vector Induced by a Plant Virus. Front. Immunol. 11:613957. doi: 10.3389/fimmu.2020.613957

The Toll pathway plays an important role in defense against infection of various pathogenic microorganisms, including viruses. However, current understanding of Toll pathway was mainly restricted in mammal and some model insects such as *Drosophila* and mosquitoes. Whether plant viruses can also activate the Toll signaling pathway in vector insects is still unknown. In this study, using rice stripe virus (RSV) and its insect vector (small brown planthopper, *Laodelphax striatellus*) as a model, we found that the Toll pathway was activated upon RSV infection. In comparison of viruliferous and non-viruliferous planthoppers, we found that four Toll pathway core genes (*Toll*, *Tube*, *MyD88*, and *Dorsal*) were upregulated in viruliferous planthoppers. When the planthoppers infected with RSV, the expressions of *Toll* and *MyD88* were rapidly upregulated at the early stage (1 and 3 days post-infection), whereas *Dorsal* was upregulated at the late stage (9 days post-infection). Furthermore, induction of Toll pathway was initiated by interaction between a Toll receptor and RSV nucleocapsid protein (NP). Knockdown of *Toll* increased the proliferation of RSV in vector insect, and the ds*Toll*-treated insects exhibited higher mortality than that of ds*GFP*-treated ones. Our results provide the first evidence that the Toll signaling pathway of an insect vector is potentially activated through the direct interaction between Toll receptor and a protein encoded by a plant virus, indicating that Toll immune pathway is an important strategy against plant virus infection in an insect vector.

Keywords: Toll pathway, rice stripe virus, small brown planthopper, immune perception, protein interaction

INTRODUCTION

In invertebrates, host defense against pathogens, including bacteria, fungi, and viruses, is known to rely on innate immunity, while in vertebrates, the innate immune system provides the first defense line against pathogens before activation of acquired immune response (1). In insects, various evolutionarily conserved signaling pathways mediate antiviral immunity, including small RNA interference (RNAi), Toll, the immune deficiency (IMD), and JAK-STAT (2, 3). These pathways

mainly rely on different pattern recognition receptors (PRRs), which recognize signature molecules of pathogens, known as pathogen associated molecular patterns (PAMPs) and induce downstream effectors against viral infection (4, 5). Toll receptor superfamily, including invertebrate Tolls and vertebrate Toll-like receptors (TLRs), is important class of PRRs and the primary sensor of pathogens in all metazoans (6). The activation of Toll pathway in vertebrate is initiated by TLRs binding to various PAMPs, whereas in invertebrate, it is activated indirectly by Toll receptors binding to the cytokine-like molecule Spätzle (Spz) (7). Tolls and TLRs are characterized by an extracellular domain containing leucine-rich repeats (LRRs), a transmembrane domain, and a cytoplasmic tail that contains a conserved region called the Toll/IL-1 receptor (TIR) domain (8). The first identified Toll (Toll1) is the receptor of the Toll pathway, and to date, nine Toll genes have been identified in *Drosophila* (8). In invertebrate, pathogen infection is censored by extracellular recognition and the inactive precursor of the Spz is cleaved to active form. Then the activated Spz binds to Toll receptor and a cassette of proteins (MyD88, Tube and Pelle) are recruited to assemble a receptor-proximal oligomeric complex (9–11). In *Drosophila*, the complex further trigger the phosphorylation and degradation of Cactus, freeing Dorsal or Dif (Dorsal-related immunity factor) to transfer from the cytoplasm into the nucleus for the regulation of different antibacterial peptides (AMPs) expressions (12).

Although the importance of the Toll pathway against bacteria and fungi has been well demonstrated, accumulated evidences suggested that it also plays essential antiviral roles in invertebrate, such as the fly (*Drosophila*) and mosquitoes (*Culex*, *Aedes*, and *Anopheles*) (1, 13). The importance of Toll pathway against virus was firstly reported in *Drosophila* when challenged with *Drosophila* X virus (DXV) infection (1). Further studies indicated that the Toll pathway also mediate resistance to other RNA viruses including *Drosophila* C virus, cricket paralysis virus, flock house virus, and norovirus (14). In mosquito, Toll immune pathway was activated upon viral infection, and they controlled the conserved anti-dengue defenses across diverse *Aegypti* strains and against multiple dengue virus serotypes (13, 15). Interestingly, recent studies found that several members of Toll receptors can also act as PRRs analogous to the TLRs in mammal, triggering conventional or non-conventional Toll-Dorsal pathway. RNAi screening suggested that Toll-4 might be one of upstream PRR to detect white spot syndrome virus (WSSV) infection in shrimp, and thereby leading to conventional Toll-Dorsal pathway (16). Another example is three shrimp Tolls (Toll1-3) directly bind to PAMPs from bacterial infection, resulting in Dorsal translocation into nucleus to regulate the expression of different AMPs (17). In contrast, *Drosophila* Toll-7 can also act as a PRR and directly interact with vesicular stomatitis virus (VSV) at the plasma membrane, but induces antiviral autophagy independent of the canonical Toll-Dorsal signaling pathway (2).

Rice stripe virus (RSV) is a filamentous, negative-strand RNA virus of the genus *Tenuivirus* that causes rice stripe disease, one of the most severe rice diseases in East Asia (18–20). RSV is transmitted by the vector insect, small brown planthopper (SBPH, *Laodelphax striatellus*), in a persistent-propagative manner. RSV can replicate in *L. striatellus*, and can be transmitted to the progeny of the planthopper through infection of the embryos or germ cells in the female insects (21). The viral genome of RSV consists of four single-stranded RNA segments: RNA1-RNA4. RNA1 is negative-sense RNA and encodes a 337-kDa protein referred to as RNA-dependent RNA polymerase (22). The other three genomic segments exhibit ambisense coding features and each RNA encodes two proteins. Sense and antisense strands of RNA2 encode RNA silencing suppressor NS2 and the putative membrane glycoprotein NSvc2, respectively (23–25). RNA3 encodes a second viral suppressor NS3 (26), and complementary sense RNA3 (vcRNA3) encodes the nucleocapsid protein (NP) (27, 28). RNA4 encodes the disease-specific protein NS4 (29), and vcRNA4 encodes the movement protein (MP) (30, 31). Previous studies suggested the induced active response of *L. striatellus* during RSV infection. For example, analysis of viral-derived small interfering RNAs (siRNAs) revealed that RNAi-mediated antiviral response can successfully be induced by the infection of RSV and another reovirus, rice black-streaked dwarf virus (32). Activation of c-Jun N-terminal kinase (JNK) promoted RSV replication in *L. striatellus*, whereas JNK inhibition caused a significant reduction in virus production and thus delayed disease incidence in plants (33). In addition, silencing of the autophagy-related-8 (*Atg8*) expression of *L. striatellus* significantly decreased the phosphorylation of JNK in the midgut of the planthoppers, suggesting that ATG8 might activate the JNK machinery (34). Nevertheless, to date, whether the classical Toll-Dorsal pathway involved in antiviral response of *L. striatellus* or other plant virus vectors have never been investigated.

In this study, open reading frames (ORFs) of four core components from Toll pathway, including *Toll*, *Tube*, *MyD88*, and *Dorsal*, were identified from *L. striatellus* and their potential antiviral roles were further explored. Our results revealed that the Toll signaling pathway in *L. striatellus* is potentially induced through the direct interaction between Toll and RSV-NP. Knockdown of Toll increased the replication of RSV, indicating that Toll in insect vectors might act as PRR in perceiving plant viruses, similar to that of TLRs in mammalian.

MATERIALS AND METHODS

Insects

The planthopper populations are maintained on susceptive japonica rice seedlings (cv Wuyujing No. 3) in a temperature-controlled room at 25 ± 1°C, with 70–80% relative humidity, and a light/dark photoperiod of 14/10 h. The infection ratio of the viruliferous planthopper population (RSV-infected) was around 80% and monitored every 3–4 generations by reverse transcription polymerase chain reaction (RT-PCR) as described previously (32).

Gene Cloning and Phylogenetic Analysis

Four Toll pathway core genes (*Toll*, *Tube*, *MyD88*, and *Dorsal*) were obtained from transcriptome of *L. striatellus* (Accession Number: SRR4020768) by homology search based on the corresponding genes of *Nilaparvata lugens* as query sequences (nlToll, XP_022198839; nlTube, XP_022207725; nlMyD88, XP_022187892; nlDorsal, XP_022195378). Conserved protein domains were predicted using NCBI conserved domains database (https://www.ncbi.nlm.nih.gov/Structure/cdd/wrpsb.cgi). Phylogenetic trees were constructed based on the deduced amino-acid sequences in MEGA 6.0 using the maximum likelihood (ML) algorithm with 1,000 bootstrap replications. The full-length ORFs of the four identified genes were amplified with the respective primer pairs (**Supplementary Table 1**) from planthoppers using RT-PCR and further confirmed by Sanger sequencing (Sangon, China).

Yeast Two-Hybrid Assay

For the yeast two-hybrid assay (Y2H) interaction assay, the full-length of RSV NS2, NSvc2-C (C-terminal of glycoprotein), NSvc2-N (N-terminal of glycoprotein), NS3, NP, NS4, and MP were cloned into the DNA-binding domain of the vector pGBK-T7 to create bait plasmids. The full-length ORF of *Toll* was cloned into the activation domain of the yeast vector pGAD-T7. Yeast cells (AH109) were co-transformed with RSV protein libraries and pGAD-T7-*Toll*. Positive clones were selected on quadruple dropout medium (SD/-Leu/-Trp/-His/-Ade).

Bimolecular Fluorescence Complementation Assays

To further confirm the protein interactions, the full-length genes of RSV proteins NS2, NSvc2-C, NSvc2-N, NS3, NP, NS4, and MP were amplified and cloned into pCV-nYFP expression vector, respectively. The full-length ORF of *Toll* was cloned into pCV-cYFP expression vector. Constructed vector pCV-cYFP-*Toll* were then transformed into *Agrobacterium tumefaciens* GV3101 by heat transfer method, and co-transformed with pCV-nYFP-*NS2*, pCV-nYFP-*NSvc2-C*, pCV-nYFP-*NSvc2-N*, pCV-nYFP-*NS3*, pCV-nYFP-*NP*, pCV-nYFP-*NS4*, and pCV-nYFP-*MP*, into *Nicotiana benthamiana*, respectively. YFP fluorescence signal was observed under Nikon confocal (Nikon, Japan).

Total RNA Extraction and Quantitative Real-Time PCR

The total RNA was extracted using TRIzol (Invitrogen, USA) according to the manufacturer's instructions. The concentration and quality of total RNA was determined using a NanoDrop spectrophotometer (Thermo Scientific, USA). The first strand of complementary DNA (cDNA) from 1,000 ng of total RNA was synthesized with HiScript ®II Q RT SuperMix for qPCR (+gDNA wiper) (Vazyme, China) following the manufacturer's protocol. In brief, quantitative real-time PCR (qPCR) was performed in 10 μl-reaction agent containing 0.5 μl of template cDNA and 5 μl of Hieff ® qPCR SYBR Green PCR Master Mix (YESEN, China), 0.2 μl of 1 μM forward and reverse primers, and 4.1 μl of ddH_2O on LightCycler® 480 II (Roche, Switzerland). The thermal cycling conditions were 95°C for 5 min, 40 cycles of 95°C for 30 s, 60°C for 30 s, and 70°C for 30 s, followed by melting curve analysis. The data were analyzed using the $2^{-\Delta\Delta CT}$ method and statistically significant differences at $P < 0.05$ (*) and $P < 0.01$ (**) level are indicated according to one-way analysis of variance (ANOVA) test.

Expression Profiles of the Four Toll Pathway Genes

Planthopper samples of different developmental stages (eggs, 1st to 5th instar nymphs, female adults, and male adults) and various tissues (salivary gland, gut, ovary of female adult, epidermis, hemolymph, fat body, and testis of male adult) from non-viruliferous *L. striatellus* were collected. For the collection of hemolymph and fat body, the PBS solution after the dissect of planthoppers was centrifuged at 5,000 × *g* for 5 min at 4°C, and the hemolymph in supernatant and fat body in precipitate were separately collected, respectively. Five independent replicates were used in this experiment. For the collection of different developmental stages, various numbers of insects were obtained according to the sample size for each replicate. While for tissues, each replicate contains different tissues derived from approximately 40–50 individual adult planthoppers.

To determine the expression of *Toll*, *Tube*, *MyD88*, and *Dorsal* in response to RSV infection, approximately 20 adult planthoppers from non-viruliferous and viruliferous cultures were collected for RNA extraction individually. In addition, to further investigate the response of Toll pathway core gene expressions during the whole process of RSV infection, approximately 1,000 2nd instar nymphs of non-viruliferous planthoppers were transferred and feeding onto RSV-infected rice seedlings for 2 days. Then the planthoppers were transferred to healthy rice seedlings and collected at various time points (1, 3, 6, 9, or 12 days post-infection). About 20 planthoppers were collected at each time point and expressions of Toll pathway genes were determined from individual insect by qPCR as described above.

Double-Stranded RNA Synthesis and Delivery

Toll, *Tube*, *MyD88*, and *Dorsal* fragments of *L. striatellus* were amplified using gene-specific primer ligated with a T7-promoter sequence, and the green fluorescent proteins (*GFP*) fragment was used as a negative control. The primers used for the amplification were listed in **Supplementary Table 1**. The double-stranded RNA (dsRNA) was synthesized using the T7 RiboMAX Express RNAi System (Promega, USA) following the manufacturer's instructions. The quality of synthesized dsRNA was evaluated using agarose gel electrophoresis. Each planthopper was injected with 40 nl of dsRNA into the insect ventral thorax with a glass needle (35).

Quantification of Rice Stripe Virus Proliferation

Adult planthoppers from viruliferous culture were collected and injected with ds*Toll*, ds*Tube*, ds*MyD88*, and ds*Dorsal*,

respectively. ds*GFP* was used as a negative control. Each of the injected planthopper was used for RNA extraction and the RNAi efficiency was determined at 48 h post-injection using qPCR. The accumulation level of RSV was quantified by qPCR as described above with specific primer pairs for RSV-NP.

Accumulation of Rice Stripe Virus and Mortality of Planthoppers During Rice Stripe Virus Infection

Second instar planthoppers from non-viruliferous culture were injected with ds*Toll* individually and maintained in healthy rice seedling for 2 days. The injected planthoppers were then transferred onto RSV-infected rice seedlings for another 2 days for virus acquisition. Finally, the planthoppers were moved to healthy rice seedling again and collected at various time points for the detection of virus accumulation. ds*GFP* was used as a negative control. Each of the injected planthopper was used for RNA extraction at 0, 1, 3, 9 days post-RSV acquisition. The expression of RSV-NP was measured by qPCR after silencing of *Toll*. Approximately 20 planthoppers were used for the detection at each time point. Meanwhile, the mortality rate of ds*Toll* injected planthoppers was investigated. Three biological replicates were performed for each treatment in this experiment.

RESULTS

Identification of the Toll Pathway Core Genes in *Laodelphax striatellus*

To explore the potential antiviral roles of classic Toll pathway in *L. striatellus*, full ORF of Toll pathway core genes (*Toll*, *Tube*, *MyD88*, and *Dorsal*) were identified and cloned. The ORF of *Toll* consists of 3336 bp nucleotides encoding a predicted protein of 1,111 amino-acid residues with a calculated molecular mass of 125.82 kDa. The predicted Toll protein contains five conserved domains including a PRK15370 super family (type III secretion system effector E3 ubiquitin transferase SlrP), a LRR_8 (Leucine rich repeat), a PCC super family (polycystin cation channel protein), a LRR, and a TIR (Toll—interleukin 1—resistance) (**Figure 1A**); *Tube* contains a 1,500 bp ORF, encoding a predicted protein of 499 amino-acid residues with a calculated molecular mass of 55.58 kDa. The putative Tube protein contains a Death_Tube domain and a PKc (protein kinases) domain (**Figure 1B**); *MyD88* consists of 1,230 bp and encodes a predicted protein of 409 amino acids. The putative MyD88 protein contains two conserved domains Death_MyD88 and TIR_2 (a family of bacterial TLRs) (**Figure 1C**). *Dorsal* contains a continuous 2,712 bp ORF, encoding a predicted protein of 903 amino-acid residues. The putative Dorsal protein contains domains including a Dorsal_Dif, a RHD_dimer (Rel homology dimerization), and an AidA superfamily (**Figure 1D**). The full ORF sequences of *Toll*, *Tube*, *MyD88*, and *Dorsal* were submitted to GenBank with the accession numbers of MW048393, MW048395, MW048396, and MW048394.

Homology analysis showed that the predicted amino acids of the four Toll pathway proteins of *L. striatellus* share highest homologies to the other two rice planthoppers, *N. lugens* and *Sogatella furcifera*, with identities of 88.44 and 88.07% for Toll, 70.18 and 60.39% for Tube, 77.64 and 31.05% for MyD88, 65.11 and 49.77% for Dorsal, respectively. Phylogenetic analysis based on the putative amino-acid sequences suggested the four proteins of *L. striatellus* clustered together with the other two planthoppers (*N. lugens* and *S. furcifera*) with high strap value support (**Figure 1**).

Interaction Between *Laodelphax striatellus* Toll and Rice Stripe Virus-NP

To investigate the potential interaction between Toll and RSV proteins, seven viral proteins (NS2, NSvc2-C, NSvc2-N, NS3, NP, NS4, and MP) were used as baits to screen against the *L. striatellus* Toll. We found that Toll interacted with RSV-NP protein, but not the other six RSV proteins, and similar results were found when Toll was used as a bait and RSV-NP as a prey (**Figure 2A**, and **Figure S1**). In addition, yeast two-hybrid assay result showed that Toll could not interact directly with SPZ family including SPZ1, SPZ2, SPZ3, SPZ4, SPZ5, and SPZ6 proteins in SD/–Leu/–Trp/–His/–Ade medium (**Figure S2**). To confirm the interaction between planthopper Toll and RSV-NP, bimolecular fluorescence complementation (BiFC) assays were further performed in *N. benthamiana*. When pCV-cYFP-*Toll* and pCV-nYFP-*NP* were transiently co-expressed in *N. benthamiana* leaves, strong YFP fluorescence signals were observed in the cytomembrane, whereas no visible signal was detected in the negative control of pCV-cYFP–*Toll* and pCV–nYFP (**Figure 2B**). Similar results were found when pCV-cYFP-*NP* and pCV-nYFP-*Toll* were transiently co-expressed (**Figure 2B**). These results indicated that Toll and RSV-NP proteins interact directly and the *L. striatellus* Toll might act as PRR in recognizing signaling molecules of pathogen.

Temporal and Spatial Expression of *Laodelphax striatellus* Toll

To explore the expression pattern of Toll receptors, non-viruliferous planthopper samples from eight developmental stages and seven tissues were collected and quantified by qPCR. The results showed that *Toll* was ubiquitously expressed in all collected developmental stages and tissues of *L. striatellus* (**Figures 3A, B**). Messenger RNA (mRNA) of Toll was most abundant in the first instar nymphs of non-viruliferous planthopper, followed by eggs (**Figure 3A**). Furthermore, highest expression of *Toll* was observed in salivary glands compared with the other tissues of non-viruliferous planthoppers (**Figure 3B**).

Active Response of the Canonical Toll Pathway During Rice Stripe Virus Infection

To illustrate the potential roles of Toll signaling pathway in RSV infection, the expressions of *Toll*, *Tube*, *MyD88*, and *Dorsal* were compared between viruliferous planthopper and non-viruliferous planthopper. Significantly increased expressions of

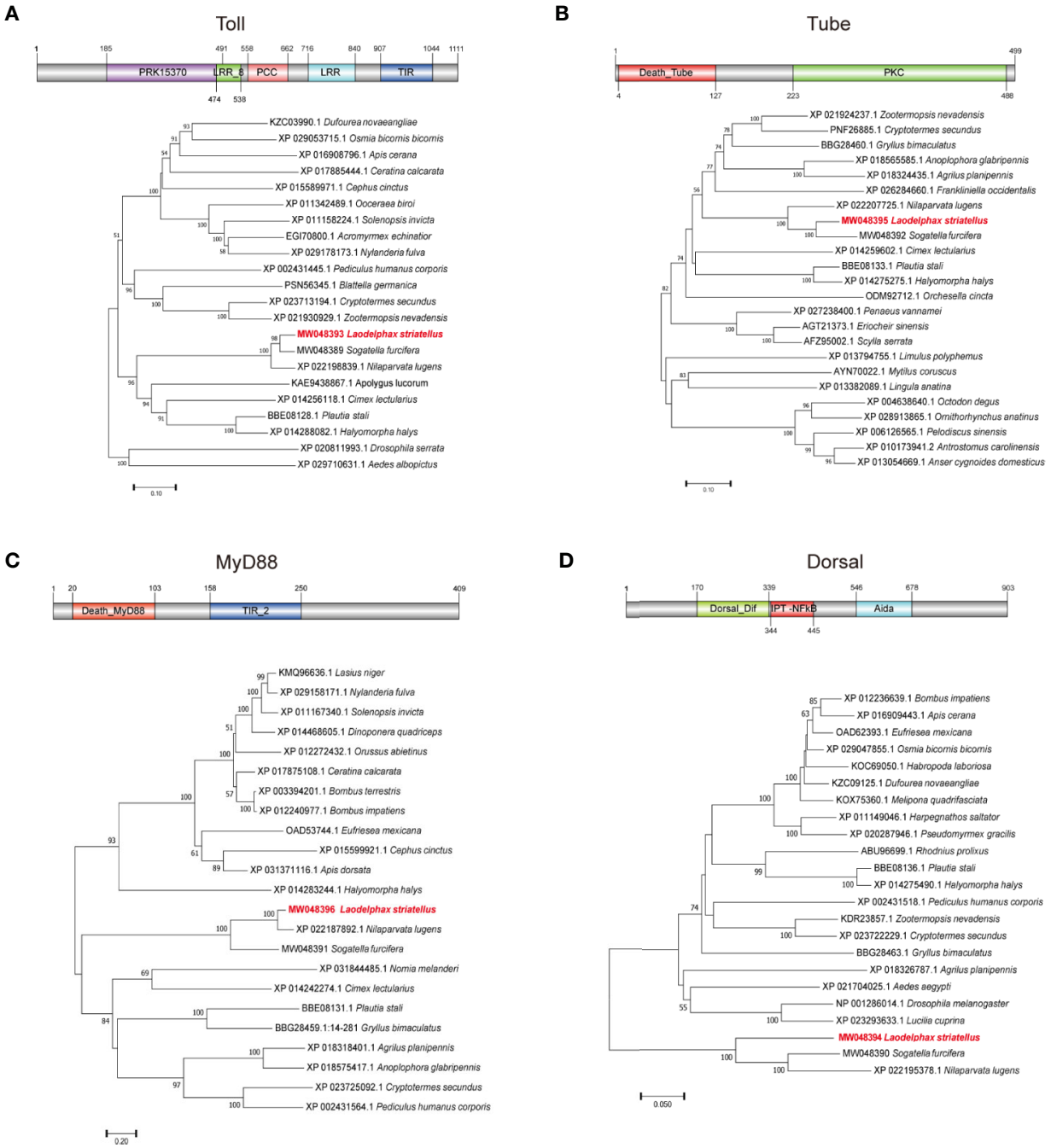

FIGURE 1 | The architecture and phylogenetic analysis of *Toll*, *Tube*, *MyD88*, and *Dorsal*. **(A)** *Toll* contains five conserved domains: PRK15370, TIR, LRR_8, leucine-rich repeat (LRR), and PCC. **(B)** *Tube* contains two conserved domains: Death and S_TKC. **(C)** *MyD88* contains two conserved domains: Death_MyD88 and TIR_2. **(D)** *Dorsal* contains three conserved domains: Dorsal_Dif, RHD_dimer, and AidA. Phylogenetic tree analysis with the maximum likelihood method was based on homologous amino-acid sequences of *Laodelphax striatellus* and other insects.

all the four genes were observed in viruliferous planthopper population (**Figures 3C–F**), suggesting that Toll pathway might be actively involved in the stable maintenance of RSV in planthopper.

Moreover, previous studies demonstrated that virus infection activated the Toll pathway within a short period (16). Considering the remarkable upregulation of *Toll*, *Tube*, *MyD88*, and *Dorsal* in viruliferous planthopper, how the Toll

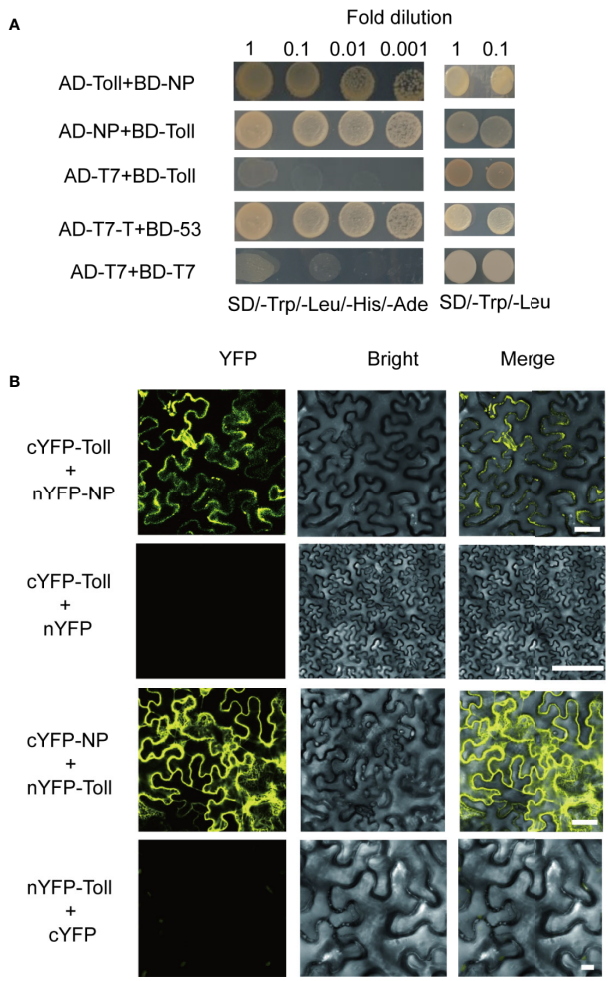

FIGURE 2 | Protein-protein interaction analysis of Toll and rice stripe virus (RSV)-NP. **(A)** Yeast two-hybrid assay result showed that Toll interacted with RSV-NP protein in SD/–Leu/–Trp/–His/–Ade medium. **(B)** Bimolecular fluorescence complementation assays showed that pCV-cYFP–*Toll* and pCV–nYFP–*RSV-NP*, pCV–cYFP–*RSV–NP* and pCV–nYFP–*Toll* fluorescent strong YFP signals in the cytomembrane but there were no detectable signals in the negative control combinations pCV-cYFP–*Toll* and pCV–nYFP, pCV–cYFP, and pCV–nYFP–*Toll*. Bars, 50 μm.

pathway of non-viruliferous planthoppers responded to RSV infection is of interest. As a result, *Toll*, *Tube*, and *MyD88*, but not *Dorsal*, were actively responded during early stage of RSV infection (**Figure 4**). The expressions of *MyD88* and *Toll* were significantly increased after 1 and 3 days post-infection (dpi) (**Figures 4A, C**), whereas *Tube* was notably decreased after 1 dpi compare to that of the control (0 dpi) (**Figure 4B**). No significant change was detected after 6 dpi of RSV infection for both *Toll*, *Tube*, and *MyD88*. However, all of the four Toll pathway core genes were up-regulated after 9 and 12 dpi (at the late stage) of RSV infection (**Figure 4**). These dynamic expressions of *Toll*, *Tube*, *MyD88*, and *dorsal* imply the active and complexed involvement of the canonical Toll signaling pathway in response to the infection process of RSV.

Potential roles of the Toll Pathway in the Maintenance of Rice Stripe Virus Proliferation

To investigate the potential roles of *Toll*, *Tube*, *MyD88*, and *Dorsal* in RSV infected planthoppers, dsRNA fragments corresponding to these four genes were synthesized and injected into the viruliferous planthoppers. Assessment of silencing efficient indicated the significant transcripts reduction (70%) for all of the four genes after 2 dpi (**Figures 5A, C, E, G**). Meanwhile, significant increase in titer of RSV was observed in ds*Toll*- and ds*Dorsal*-treated planthoppers (**Figures 5B, H**), whereas RNA level of RSV-NP was notably reduced for ds*Tube*-injected insects when compared with that of the control (ds*GFP*) (**Figure 5D**). In contrast, no significant difference was detected in RSV-NP between ds*MyD88* and ds*GFP*-treated planthoppers (**Figure 5F**).

The Toll Pathway Is Involved in the Anti-Rice Stripe Virus Defense

In view of the direct interaction between Toll and RSV-NP, the accumulation of RSV-NP transcripts was further examined in ds*Toll*-treated planthoppers when non-viruliferous planthoppers were infected by RSV. Injection of ds*Toll* successfully and stably inhibits the *Toll* expression in planthoppers after RSV acquisition for various days (**Figure 6A**). The effects of ds*Toll*-injection on the RSV proliferation in planthoppers were further determined. Significant increase in RSV-NP transcripts were observed in ds*Toll* injected planthopper compared to that of the control (ds*GFP*) at various infected time point (1, 3, and 9 dpi) (**Figure 6B**). Additionally, the mortality of RSV-infected planthopper was significantly higher after ds*Toll* treatment in 3 and 9 dpi than that of ds*GFP* control (**Figure 6C**). These data suggested that Toll might play an essential role in restricting RSV proliferation.

DISCUSSION

Accumulated evidence demonstrated that the innate immune system plays an important role in defense against viruses in mammal and some model insects such as *Drosophila* and mosquitoes (1, 13–16). However, whether the canonical pathway of vector insects also involved in defense against plant viruses remained unknown. In this study, we found that RSV activated the Toll immune pathway of *L. striatellus* through direct interaction between Toll protein and RSV-NP. Knockdown of *Toll* significantly increased the proliferation of RSV in vector insect, and the ds*Toll*-treated insects exhibited higher mortality than that of ds*GFP*-treated ones. Our results suggested a potential role of Toll pathway in restrict plant virus infection.

Activation of immune pathways relies on an array of PRRs to recognize the PAMPs, and subsequently induce an appropriate effector response to clear the infection (36). For Toll pathway, this process was mainly accomplished by Toll, which is the upstream receptor of this pathway. In *Drosophila*, Toll-7 is a PRR that

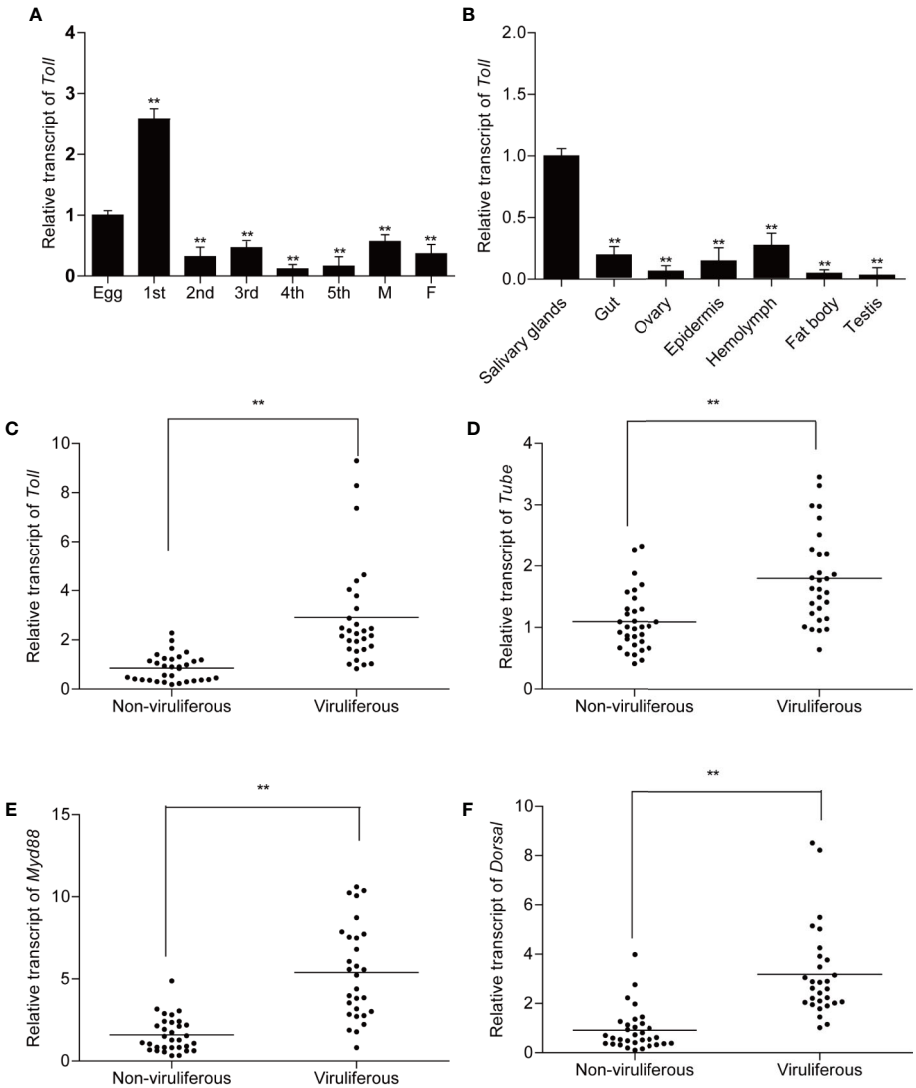

FIGURE 3 | Expression patterns of *Toll* and relative transcript levels of *Toll*, *Tube*, *MyD88*, and *Dorsal* in non-viruliferous and viruliferous planthopper. For qPCR detection of *Toll*, samples from different developmental stages (eggs, nymphs from 1st to 5th instars, female and male adults) **(A)** and different tissues (salivary gland, gut, ovary, epidermis, hemolymph, fat body, and testicle) **(B)** were collected from non-viruliferous planthoppers. Five biological replicates were performed. For analysis of relative transcript levels of *Toll* **(C)**, *Tube* **(D, E)** *MyD88* **(E)**, and *Dorsal* **(F)**, non-viruliferous and viruliferous planthopper samples were collected individually. Actin gene was used as housekeeping gene. Each point represents a biological replicate. Statistically significant differences at $P < 0.01$ (**) level are indicated according to one-way analysis of variance (ANOVA) test.

interacted with VSV at the plasma membrane and induced antiviral autophagy (2). In shrimp, knockdown of Toll4 results in elevated viral loads and renders shrimp more susceptible to WSSV infection. Furthermore, Toll4 could act as an upstream PRR to detect WSSV, and lead to nuclear translocation and phosphorylation of Dorsal for the trigger of AMP production against the virus (16). Our study identified a strong interaction between Toll and RSV-NP, indicating that Toll in *L. striatellus* might be an upstream receptor to recognize RSV, and Toll pathway was associated with plant virus infection in insect vector.

Toll pathways is the major constitute of insect immune pathways that activate a battery of immune proteins in response to various microorganism invasion. Remarkable upregulation in Toll pathway genes were reported in *Aedes aegypti* challenged with *Plasmodium gallinaceum* (37), *Drosophila* challenged with Vesicular stomatitis virus (2), and *Litopenaeus vannamei* challenged with WSSV (16). Our study demonstrated that *Toll*, *Tube*, and *MyD88* were actively responded during early stage of RSV oral infection (**Figure 4**), in accordance of previous work. For the transcription factor *Dorsal*, it is stable expressed at the early stage of viral infection, but significantly upregulated at the late stage (**Figure 4**). Since *Toll*, *Tube*, *MyD88*, and *Dorsal* are the four core genes of the canonical Toll-Dorsal signaling pathway, the upregulation of

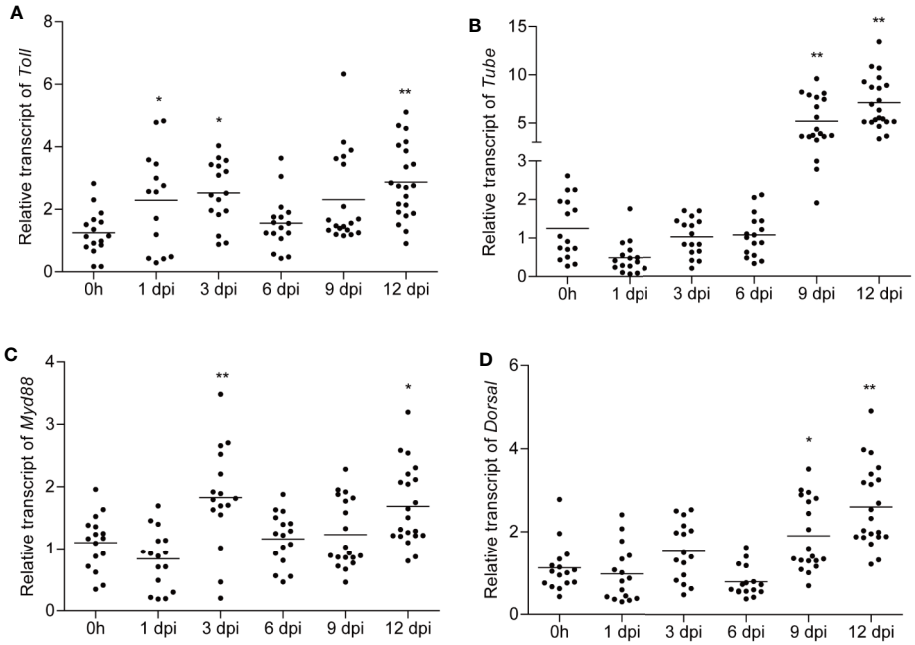

FIGURE 4 | The expression pattern of *Toll*, *Tube*, *MyD88*, and *Dorsal* when non-viruliferous planthoppers were infected with rice stripe virus (RSV). Non-viruliferous planthoppers were fed on RSV-infected rice seedlings, and the samples were collected at 1, 3, 6, 9, and 12 days post-infection (dpi). Relative transcript levels of *Toll* **(A)**, *Tube* **(B)**, *MyD88* **(C)**, and *Dorsal* **(D)** at the indicated time points were analyzed by qPCR. The non-viruliferous planthopper that did not contact with RSV was used as a control. Actin gene was used as housekeeping gene. Each point represents a biological replicate. Statistically significant differences at $P < 0.05$ (*) and $P < 0.01$ (**) level are indicated according to one-way ANOVA test.

these four genes at various stages during RSV infection (**Figure 4**), the interaction between Toll and RSV-NP (**Figure 2**), as well as the increased viral titers observed in ds*Toll*-treated planthoppers (**Figure 6**), implying that this classical pathway was actively involved in response to RSV infection. Nevertheless, more studies are needed to further investigate on the detail of downstream antiviral response, such as how does Dorsal translocate from cytoplasm into the nucleus, and which downstream effectors are regulated by Dorsal induced with RSV infection. In addition, for viruliferous planthopper, they can harbor the viruses for several generations, and no significant phenotype can be found in the RSV-infected insects. In this study, it is interesting to find that the expression level of four Toll pathway core genes were significantly higher in viruliferous planthopper than that in non-viruliferous one (**Figure 3**). Sustained activation of defense pathway inevitably consumes extra resources, which is detrimental to insects (38). We presumed that it might be more important for planthoppers to restrict RSV infection than other physiological metabolisms. Interestingly, higher mortality rate was recognized in ds*Toll*-treated viruliferous planthoppers (**Figure 6C**), suggesting that *dsToll*-treatment might interfere with the established delicate balance between innate immunity of planthopper and persistent RSV infection, as described in mosquitoes (39). Our results also consist with the previous report that TLR4 knockdown mice exhibited greater viral replication (Vaccinia virus) and mortality compared to the wild-type mice following respiratory infection (40), indicating that the Toll signaling pathway of the host might be essential for the virus persistent infection.

Involvement of Toll pathway in restrict virus infection has been well documented in previous work. In *Drosophila*, *Toll* and *Dif* mutant lines showed increased susceptibility to *Drosophila* X virus (1), and *Toll-7* depletion promoted vesicular stomatitis virus replication (2). In shrimps, silencing of *Toll-4* resulted in high WSSV titers, with the average viral DNA burden approximately 150 times higher than that of the control (16). In *A. aegypti*, silencing of *MyD88* led to a significant increase in dengue virus titers, demonstrating the importance of this innate immune pathway in the defense against different dengue virus serotypes at the early stages of infection (13). Our study demonstrated that *Toll*-inhibition and *Dorsal*-inhibition significantly increased the RSV titer, suggesting the potential antiviral roles of Toll pathway against plant virus. However, for ds*MyD88*-treatment viruliferous planthoppers, no significant change in RSV titer was observed when compared to the control (ds*GFP*) (**Figure 5F**), which is inconsistent with the previous studies in mosquitoes (13) and mice (41). Considering the increased expression of *MyD88* in response to RSV infection (**Figure 4C**), we presume that *MyD88* might play more important roles during the process of RSV infection, rather than the maintenance of RSV persistent infection in planthoppers. Furthermore, unexpectedly, RSV titer in ds*Tube*-

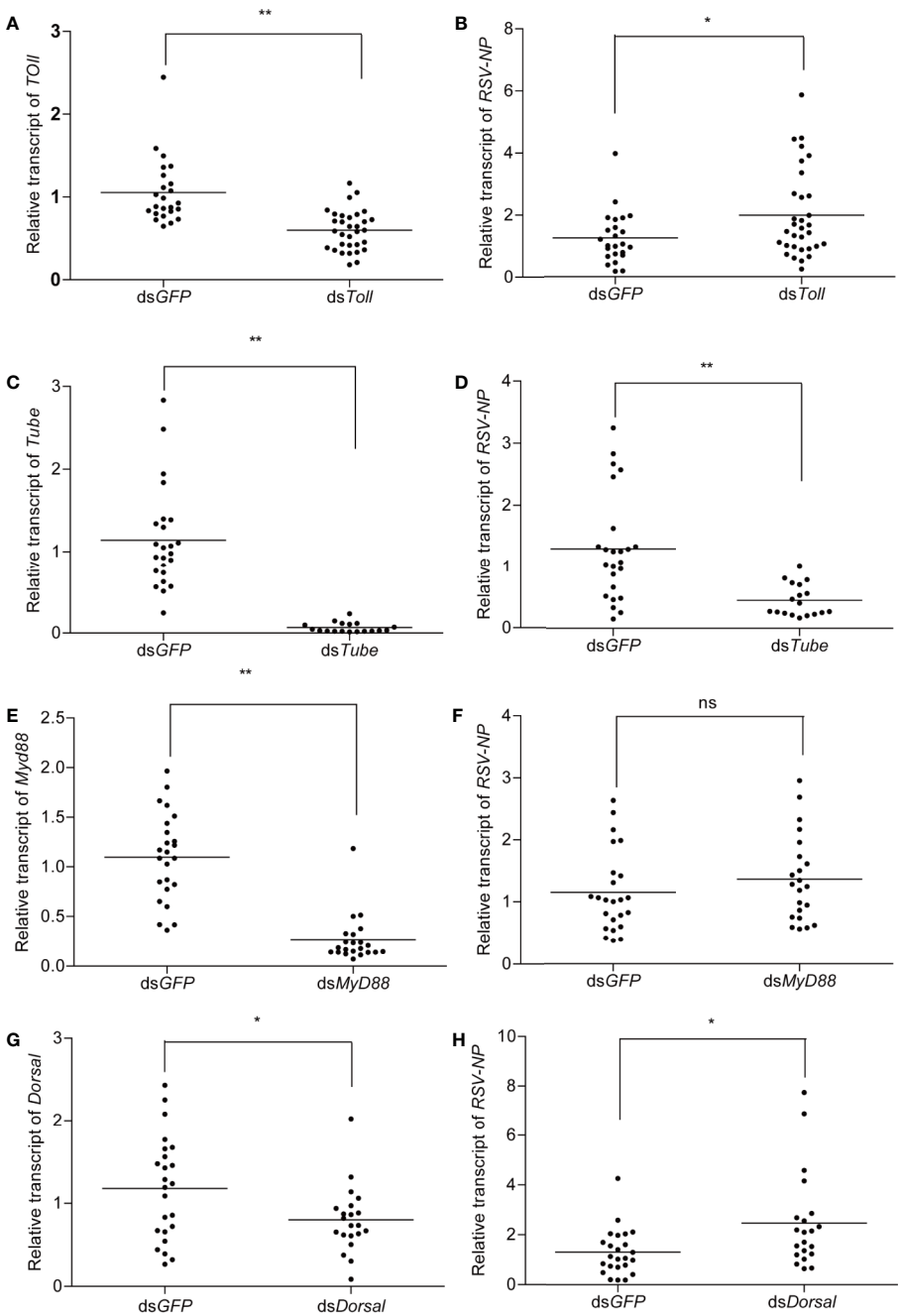

FIGURE 5 | The influence of double-stranded RNA (dsRNA) treatment on viruliferous planthoppers. Approximately 25 viruliferous planthopper were injected with ds*Toll*, ds*Tube*, ds*MyD88*, and ds*Dorsal*. The silencing efficiency of *Toll* **(A)**, *Tube* **(C)**, *MyD88* **(E)**, and *Dorsal* **(G)** were determined. Meanwhile, the relative transcript level of RSV-NP after silencing of *Toll* **(B)**, *Tube* **(D)**, *MyD88* **(F)**, and *Dorsal* **(H)** were analyzed by qPCR. Planthopers treated with ds*GFP* were used as a negative control. Each point represents a biological replicate. Statistically significant differences at $P < 0.05$ (*) and $P < 0.01$ (**) level are indicated according to one-way ANOVA test. ns, not significant.

treatment was significantly decreased compare to control (ds*GFP*) (**Figure 5D**). It will be interesting to further explore the possibility that whether Tube can interact directly with the protein of RSV and might be hijacked by the virus to promote its proliferation.

CONCLUSION

In summary, we found that Toll pathway was activated upon RSV infection, and the viruliferous planthopper exhibited higher level of *Toll*, *Tube*, *MyD88*, and *Dorsal*. More intriguing, unlike

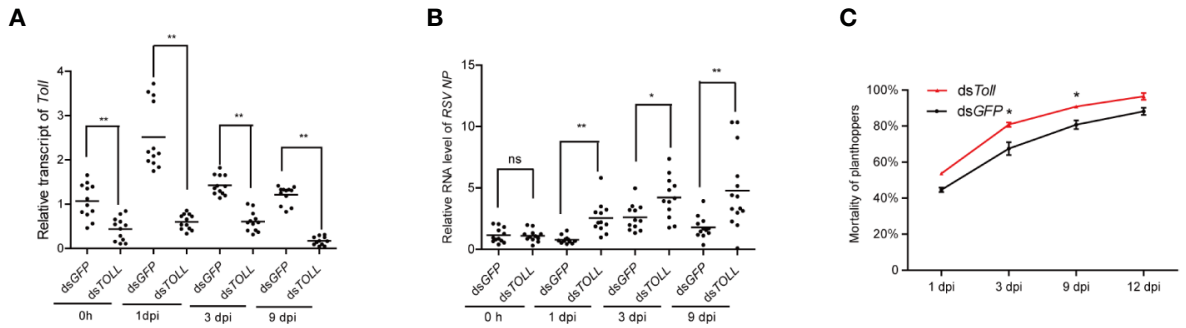

FIGURE 6 | The influence of double-stranded RNA (dsRNA) treatment on non-viruliferous planthoppers that orally infected with rice stripe virus (RSV). The non-viruliferous planthopper were treated with ds*Toll* or ds*GFP*. Two days later, the insects were provided with RSV-infected rice seedlings, and the RNAi efficiency **(A)** and the amount of RSV in vector insects **(B)** were determined by qPCR at the indicated time point. Each point represents a biological replicate. **(C)** The mortality of RSV-infected planthopper after ds*Toll* and ds*GFP* treatments. Three biological replicates were performed. Statistically significant differences at $P < 0.05$ (*) and $P < 0.01$ (**) level are indicated according to one-way ANOVA test. ns, not significant.

the classical Toll signaling pathway which rely on the Spz binding to the Toll receptor, our study provide the first evidence that the antiviral Toll signaling pathway of *L. striatellus* is potentially activated through the direct interaction between Toll receptor and PAMPs (RSV-NP), suggesting that Toll immune pathway is an important strategy against plant viruses in insect vectors.

DATA AVAILABILITY STATEMENT

The datasets presented in this study can be found in online repositories. The names of the repository/repositories and accession number(s) can be found below: https://www.ncbi.nlm.nih.gov/genbank/, MW048393 https://www.ncbi.nlm.nih.gov/genbank/, MW048395 https://www.ncbi.nlm.nih.gov/genbank/, MW048396 https://www.ncbi.nlm.nih.gov/genbank/, MW048394.

AUTHOR CONTRIBUTIONS

J-ML, J-PC, and C-XZ conceived the study and designed the project. Y-JH, GL, YZ, Y-HQ, Z-TS, X-DZ, and J-CZ performed the experiment, analyzed the data, and drafted the manuscript. H-JH, FY, and J-ML helped to revise the manuscript. All authors contributed to the article and approved the submitted version.

FUNDING

Present research was financially supported by the National Natural Science Foundation of China (32000121), Ningbo Science and Technology Innovation 2025 Major Project (2019B10004) and Commonweal Project (202002N3004, 202002N3008). This work was sponsored by K.C. Wong Magna Fund in Ningbo University.

SUPPLEMENTARY MATERIAL

The Supplementary Material for this article can be found online at: https://www.frontiersin.org/articles/10.3389/fimmu.2020.613957/full#supplementary-material

SUPPLEMENTARY FIGURE 1 | Protein-protein interaction between Toll and RSV NS2, NSvc2-C, NSvc2-N, NS3, NS4, and MP.

SUPPLEMENTARY FIGURE 2 | Protein-protein interaction between Toll and SPZ family of planthopper.

REFERENCES

1. Zambon RA, Nandakumar M, Vakharia VN, Wu LP. The Toll pathway is important for an antiviral response in *Drosophila*. *Proc Natl Acad Sci U S A* (2005) 102(20):7257–62. doi: 10.1073/pnas.0409181102
2. Nakamoto M, Moy RH, Xu J, Bambina S, Yasunaga A, Shelly SS, et al. Virus Recognition by Toll-7 Activates Antiviral Autophagy in *Drosophila*. *Immunity* (2012) 36(4):658–67. doi: 10.1016/j.immuni.2012.03.003
3. Janeway CAJr, Medzhitov R. Innate Immune Recognition. *Annu Rev Immunol* (2002) 20:197–216. doi: 10.1146/annurev.immunol.20.083001.084359
4. Palmer WH, Varghese FS, van Rij RP. Natural Variation in Resistance to Virus Infection in Dipteran Insects. *Viruses* (2018) 10(3):118. doi: 10.3390/v10030118
5. Kumar H, Kawai T, Akira S. Toll-like receptors and innate immunity. *Biochem Biophys Res Commun* (2009) 388(4):621–5. doi: 10.1016/j.bbrc.2009.08.062
6. Chtarbanova S, Imler JL. Microbial Sensing by Toll Receptors - A Historical Perspective. *Arterioscler Thromb Vasc Biol* (2011) 31(8):1734–8. doi: 10.1161/atvbaha.108.179523
7. Weber AN, Tauszig-Delamasure S, Hoffmann JA, Lelièvre E, Gascan H, Ray KP, et al. Binding of the *Drosophila* cytokine Spätzle to Toll is direct and establishes signaling. *Nat Immunol* (2003) 4(8):794–800. doi: 10.1038/ni955
8. Kawai T, Akira S. Toll-like receptors and their crosstalk with other innate receptors in infection and immunity. *Immunity* (2011) 34(5):637–50. doi: 10.1016/j.immuni.2011.05.006
9. Schneider DS, Jin Y, Morisato D, Anderson KV. A processed form of the Spätzle protein defines dorsal-ventral polarity in the *Drosophila* embryo. *Development* (1994) 120(5):1243–50.

10. Horng T, Medzhitov R. *Drosophila* MyD88 is an adapter in the Toll signaling pathway. *Proc Natl Acad Sci U S A* (2001) 98(22):12654–8. doi: 10.1073/pnas.231471798
11. Sun H, Bristow BN, Qu G, Wasserman SA. A heterotrimeric death domain complex in Toll signaling. *Proc Natl Acad Sci U S A* (2002) 99(20):12871–6. doi: 10.1073/pnas.202396399
12. Towb P, Bergmann A, Wasserman SA. The protein kinase Pelle mediates feedback regulation in the *Drosophila* Toll signaling pathway. *Development* (2001) 128(23):4729–36.
13. Ramirez JL, Dimopoulos G. The Toll immune signaling pathway control conserved anti-dengue defenses across diverse *Ae. aegypti* strains and against multiple dengue virus serotypes. *Dev Comp Immunol* (2010) 34(6):625–9. doi: 10.1016/j.dci.2010.01.006
14. Ferreira ÁG, Naylor H, Esteves SS, Pais IS, Martins NE, Teixeira L. The Toll-Dorsal Pathway Is Required for Resistance to Viral Oral Infection in *Drosophila*. *PLoS Pathog* (2014) 10(12):e1004507. doi: 10.1371/journal.ppat.1004507
15. Xi Z, Ramirez JL, Dimopoulos G. The *Aedes aegypti* toll pathway controls dengue virus infection. *PLoS Pathog* (2008) 4(7):e1000098. doi: 10.1371/journal.ppat.1000098
16. Li H, Yin B, Wang S, Fu Q, Xiao B, Lǔ K, et al. RNAi screening identifies a new Toll from shrimp *Litopenaeus vannamei* that restricts WSSV infection through activating Dorsal to induce antimicrobial peptides. *PLoS Pathog* (2018) 14(9):e1007109. doi: 10.1371/journal.ppat.1007109
17. Sun JJ, Xu S, He ZH, Shi XZ, Zhao XF, Wang JX. Activation of Toll Pathway Is Different between Kuruma Shrimp and *Drosophila*. *Front Immunol* (2017) 8:1151. doi: 10.3389/fimmu.2017.01151
18. Falk BW, Tsai JH. Biology and molecular biology of viruses in the genus Tenuivirus. *Annu Rev Phytopathol* (1998) 36:139–63. doi: 10.1146/annurev.phyto.36.1.139
19. S Toriyama. Rice stripe virus: prototype of a new group of viruses that replicate in plants and insects. *Microbiol Sci* (1986) 3(11):347–51. doi: 10.1016/0166-0934(86)90035-2
20. Wei TY, Yang JG, Liao FL, Gao FL, Lu LM, Zhang XT, et al. Genetic diversity and population structure of rice stripe virus in China. *J Gen Virol* (2009) 90(Pt 4):1025–34. doi: 10.1099/vir.0.006858-0
21. Hogenhout SA, Ammar E-D, Whitfield AE, Redinbaugh MG. Insect Vector Interactions with Persistently Transmitted Viruses. *Annu Rev Phytopathol* (2008) 46(1):327–59. doi: 10.1146/annurev.phyto.022508.092135
22. Toriyama S, Takahashi M, Sano Y, Shimizu T, Ishihama A. Nucleotide sequence of RNA 1, the largest genomic segment of rice stripe virus, the prototype of the tenuiviruses. *J Gen Virol* (1994) 75(Pt 12):3569–79. doi: 10.1099/0022-1317-75-12-3569
23. Takahashi M, Toriyama S, Hamamatsu C, Ishihama A. Nucleotide sequence and possible ambisense coding strategy of rice stripe virus RNA segment 2. *J Gen Virol* (1993) 74(Pt 4):769–73. doi: 10.1099/0022-1317-74-4-769
24. Yao M, Liu X, Li S, Xu Y, Zhou Y, Zhou X, et al. Rice stripe tenuivirus NSvc2 glycoproteins targeted to the golgi body by the N-terminal transmembrane domain and adjacent cytosolic 24 amino acids via the COP I- and COP II-dependent secretion pathway. *J Virol* (2014) 88(6):3223–34. doi: 10.1128/JVI.03006-13
25. Zheng L, Du Z, Lin C, Mao Q, Wu K, Wu J, et al. Rice stripe tenuivirus p2 may recruit or manipulate nucleolar functions through an interaction with fibrillarin to promote virus systemic movement. *Mol Plant Pathol* (2015) 16 (9):921–30. doi: 10.1111/mpp.12220
26. Wu G, Wang J, Yang Y, Dong B, Wang Y, Sun G, et al. Transgenic rice expressing rice stripe virus NS3 protein, a suppressor of RNA silencing, shows resistance to rice blast disease. *Virus Genes* (2014) 48(3):566–9. doi: 10.1007/s11262-014-1051-2
27. Hayano Y, Kakutani T, Hayashi T, Minobe Y. Coding strategy of rice stripe virus major nonstructural protein is encoded in viral RNA segment 4 and coat protein in RNA complementary to segment 3. *Virology* (1990) 177(1):372–4. doi: 10.1016/0042-6822(90)90493-b
28. Kakutani T, Hayano Y, Hayashi T, Minobe Y. Ambisense segment 3 of rice stripe virus the first instance of a virus containing two ambisense segments. *J Gen Virol* (1991) 72(Pt 2):465–8. doi: 10.1099/0022-1317-72-2-465
29. Kong L, Wu J, Lu L, Xu Y, Zhou X. Interaction between Rice stripe virus disease-specific protein and host PsbP enhances virus symptoms. *Mol Plant* (2014) 7(4):691–708. doi: 10.1093/mp/sst158
30. Kakutani T, Hayano Y, Hayashi T, Minobe Y. Ambisense segment 4 of rice stripe virus possible evolutionary relationship with phleboviruses and uukuviruses (*Bunyaviridae*). *J Gen Virol* (1990) 71(Pt 7):1427–32. doi: 10.1099/0022-1317-71-7-1427
31. Xiong R, Wu J, Zhou Y, Zhou X. Identification of a movement protein of the tenuivirus rice stripe virus. *J Virol* (2008) 82(24):12304–11. doi: 10.1128/JVI.01696-08
32. Li J, Andika IB, Shen J, Lv Y, Ji Y, Sun L, et al. Characterization of Rice Black-Streaked Dwarf Virus- and Rice Stripe Virus-Derived siRNAs in Singly and Doubly Infected Insect Vector *Laodelphax striatellus*. *PLoS One* (2013) 8(6): e66007. doi: 10.1371/journal.pone.0066007
33. Wang W, Zhao W, Li J, Luo L, Kang L, Cui F. The c-Jun N-terminal kinase pathway of a vector insect is activated by virus capsid protein and promotes viral replication. *Elife* (2017) 6(e26591). doi: 10.7554/eLife.26591
34. Yu YL, Zhang MT, Huo Y, Tang JL, Liu Q, Chen XY, et al. *Laodelphax striatellus* Atg8 facilitates Rice stripe virus infection in an autophagy-independent manner. *Insect Sci* (2020) 00:1–15. doi: 10.1111/1744-7917.12771
35. Xu HJ, Xue J, Lu B, Zhang XC, Zhuo JC, He SF, et al. Two insulin receptors determine alternative wing morphs in planthoppers. *Nature* (2015) 519 (7544):464–7. doi: 10.1038/nature14286
36. Wang XL, Zhang YQ, Zhang R, Zhang JH. The diversity of pattern recognition receptors (PRRs) involved with insect defense against pathogens. *Curr Opin Insect Sci* (2019) 33:105–10. doi: 10.1016/j.cois.2019.05.004
37. Zou Z, Souza-Neto J, Xi Z, Kokoza V, Shin SW, Dimopoulos G, et al. Transcriptome Analysis of *Aedes aegypti* Transgenic Mosquitoes with Altered Immunity. *PLoS Pathog* (2011) 7(11):e1002394. doi: 10.1371/journal.ppat.1002394
38. Huang HJ, Cui JR, Hong XY. Comparative analysis of diet-associated responses in two rice planthopper species. *BMC Genomics* (2020) 21:565. doi: 10.1186/s12864-020-06976-2
39. Lee WS, Webster JA, Madzokere ET, Stephenson EB, Herrero LJ. Mosquito antiviral defense mechanisms: a delicate balance between innate immunity and persistent viral infection. *Parasit Vectors* (2019) 12(1). doi: 10.1186/s13071-019-3433-8
40. Hutchens MA, Luker KE, Sonstein J, Núñez G, Curtis JL, Luker GD. Protective Effect of Toll-like Receptor 4 in Pulmonary Vaccinia Infection. *PLoS Pathog* (2008) 4(9):e1000153. doi: 10.1371/journal.ppat.1000153
41. Butchi N, Kapil P, Puntambekar S, Stohlman SA, Hinton DR, Bergmann CC. Myd88 Initiates Early Innate Immune Responses and Promotes CD4 T Cells during Coronavirus Encephalomyelitis. *J Virol* (2015) 89(18):9299–312. doi: 10.1128/jvi.01199-15

Conflict of Interest: The authors declare that the research was conducted in the absence of any commercial or financial relationships that could be construed as a potential conflict of interest.

frontiers in Immunology

MINI REVIEW
published: 29 January 2021
doi: 10.3389/fimmu.2020.626329

The Antiviral Effects of the Symbiont Bacteria *Wolbachia* in Insects

*André C. Pimentel, Cássia S. Cesar, Marcos Martins and Rodrigo Cogni**

Department of Ecology, University of São Paulo, São Paulo, Brazil

Wolbachia is a maternally transmitted bacterium that lives inside arthropod cells. Historically, it was viewed primarily as a parasite that manipulates host reproduction, but more recently it was discovered that *Wolbachia* can also protect *Drosophila* species against infection by RNA viruses. Combined with *Wolbachia's* ability to invade insect populations due to reproductive manipulations, this provides a way to modify mosquito populations to prevent them transmitting viruses like dengue. In this review, we discuss the main advances in the field since *Wolbachia's* antiviral effect was discovered 12 years ago, identifying current research gaps and potential future developments. We discuss that the antiviral effect works against a broad range of RNA viruses and depends on the *Wolbachia* lineage. We describe what is known about the mechanisms behind viral protection, and that recent studies suggest two possible mechanisms: activation of host immunity or competition with virus for cellular resources. We also discuss how association with *Wolbachia* may influence the evolution of virus defense on the insect host genome. Finally, we investigate whether the antiviral effect occurs in wild insect populations and its ecological relevance as a major antiviral component in insects.

Keywords: antiviral, *Wolbachia*, insects, arboviruses, evolution, wild populations, review, endosymbiont

OPEN ACCESS

Edited by:
Luc Swevers,
National Centre of Scientific Research Demokritos, Greece

Reviewed by:
Zhiyong Xi,
Michigan State University, United States
Ioannis Eleftherianos,
George Washington University, United States

***Correspondence:**
Rodrigo Cogni
rodrigocogni@gmail.com

Specialty section:
This article was submitted to Comparative Immunology, a section of the journal Frontiers in Immunology

Received: *05 November 2020*
Accepted: *14 December 2020*
Published: *29 January 2021*

Citation:
Pimentel AC, Cesar CS, Martins M and Cogni R (2021) The Antiviral Effects of the Symbiont Bacteria Wolbachia in Insects. Front. Immunol. 11:626329. doi: 10.3389/fimmu.2020.626329

INTRODUCTION

Wolbachia pipientis is a maternally transmitted alphaproteobacterium that lives obligatorily within the cytoplasm of arthropod cells (1). Until recently it was viewed primarily as a parasite that manipulates host reproduction, most commonly by inducing cytoplasmic incompatibility (2, 3). Cytoplasmic incompatibility allows *Wolbachia* to invade insect populations by causing embryonic mortality when uninfected females mate with infected males, thus conferring a selective advantage to infected females (4, 5). In 2008, two studies discovered that *Wolbachia* can protect *Drosophila melanogaster* against RNA viruses (6, 7). Subsequently, it was discovered that *Wolbachia* can block dengue virus replication in mosquitoes (8, 9). These findings provided a new way in which *Wolbachia* can be used to control human arboviruses, since previous attempts relied on using cytoplasmic incompatibility as a transgene driver, or reduction of mosquito longevity by a virulent *Wolbachia* strain. *Wolbachia* lineages from different insects that were transferred to the mosquito *Aedes aegypti* can limit the replication of arboviruses such as Dengue virus (DENV), Chikungunya virus (CHIKV), Yellow Fever virus (YFV), Zika virus (ZIKV) and West Nile virus (WNV) (9–12). *Wolbachia* can spread quickly through mosquito populations by cytoplasmic incompatibility (13–15), and large field trials have been successful in reducing dengue prevalence in human populations (16, 17).

In this Mini Review, we discuss the main advances in the field since the *Wolbachia* antiviral effect was discovered 12 years ago, current research gaps, and potential future developments. First, we address the generality of the antiviral effect and how it depends on *Wolbachia* lineage and on virus identity. Second, we discuss the possible mechanisms of antiviral protection. Third, we discuss how association with *Wolbachia* may influence the evolution of virus defense on the insect host genome. Finally, we discuss the virus blocking ecological relevance by addressing if it occurs in wild insect populations.

GENERALITY: DIFFERENT VIRUSES AND DIFFERENT *WOLBACHIA* LINEAGES

After the first studies showing that *Wolbachia* protects flies and mosquitoes against RNA viruses (6–8) and its potential to control insect-born human diseases (8–10, 14), there was a great interest in the area. Many studies conducted on mosquitoes tested for their vector competence and revealed that *Wolbachia* reduces infection and, in some cases, the dissemination and transmission of diseases such as dengue, chikungunya, yellow fever, zika, and West Nile fever (**Table 1**). In flies, *Wolbachia* protects mostly against Flock House virus (FHV), and *Drosophila* C virus (DCV). However, DCV is not commonly found in wild *Drosophila* populations (41) and there is limited information on protection against viruses that are common in nature, such as Nora (6) and Kallithea virus (36) (**Table 1**). Although many studies report *Wolbachia* protection against different viruses, there are a few cases in which *Wolbachia* provides no protection or even increases the host susceptibility to viral infection (**Table 1**). Furthermore, only three studies investigated *Wolbachia* protection against DNA viruses (6, 36, 40) and none found evidence of protection (**Table 1**). Therefore, *Wolbachia* protection in insects is a general phenomenon only against RNA viruses.

The level of protection against viruses varies among *Wolbachia* strains and depends on their density within the host (22, 42). It is common to transfer high density strains into new hosts, such as mosquitoes, to test for protection against viruses (**Figure 1A**). Thus, protection generally occurs in host-*Wolbachia* interactions that are not natural, but artificial (43). For example, the virulent strain *w*MelPop, originally isolated from *D. melanogaster* (44, 45), protects against different viruses in *Aedes aegypti* (**Table 1**). However, *w*MelPop is a strain that was identified only in laboratory and there is no record of it in nature. Other *Wolbachia* strains commonly used in experiments that have broad protection against viruses are *w*Mel, *w*MelCS, both isolated from *D. melanogaster*, *w*Au, isolated from *D. simulans*, *w*AlbB, isolated from *Aedes albopictus*, and *w*Stri, isolated from the planthooper *Laodelphax striatellus* (**Table 1**). Martinez and colleagues investigated antiviral protection in many *Wolbachia* strains originated from different *Drosophila* species after transfer into the same genetic background of *D. simulans*. Interestingly, they found that protection is not determined by host genotype, but by *Wolbachia* strain (23). All these studies showing that different strains protect different hosts against many RNA viruses were conducted in the laboratory, and there is still little evidence of the *Wolbachia* antiviral effect in nature (see last section below).

Another issue is that most studies that test for virus protection by *Wolbachia* are carried out using only the adult stage. So far, only Graham et al. (40) tested for viral protection in larval stages of *Spodoptera exempta*, and we still have no information of protection on pupae. Moreover, these results may be affected by the inoculation method in the laboratory. All studies in flies use systemic infection (stabbing or microinjection), while in mosquitoes some studies use oral infection besides microinjection. Although methods such as microinjection allow greater viral dose precision, we know that in nature insects acquire many pathogens by feeding (46, 47). Therefore, although there is a general pattern of protection against viruses in laboratory studies, there are some limitations on the methods used. Further studies testing *Wolbachia's* antiviral protection in insect host using methods that approximate of how infections occur in nature, such as oral infection (46, 47), are essential to understanding the dynamics between *Wolbachia* and viruses in wild populations.

Wolbachia infects about 50% of all insect species (48), and we can hypothesize that the antiviral protection may be one of the reasons for *Wolbachia* being so widely spread among arthropods. However, studies on *Wolbachia*'s viral protection are still limited to flies and mosquitoes, with the exception of one study on a Lepidoptera host (40) and one study on a Hemiptera host (33). Thus, more studies on different insect families are essential to test if the antiviral effect also occurs in other insects, and how likely it may be one of the main reasons for the high prevalence of *Wolbachia* in natural insect populations.

THE POSSIBLE MECHANISMS

Since the discovery of *Wolbachia* antiviral protection different mechanisms of action have been proposed, but up to now, there is no consensus on the underlying mechanism [reviewed by Lindsey et al (49)]. Current studies work on two main hypotheses to explain *Wolbachia* interference in viral replication: the activation of host immunity and competition with virus for cellular resources (**Figure 1B**).

The first hypothesis is that *Wolbachia* can directly activate innate immunity of the host prior to virus infection (immune priming), interfering with virus replication. The presence of the bacterium in host cells leads to cellular stress, including oxidative stress that activates host immune pathways (50). *Wolbachia* preactivates mosquito innate immunity by the oxidative stress, upregulating Toll pathway genes, known to be responsible for protection against dengue virus (8, 9, 50). Immune effector genes upregulation in *A. aegypti* suggests that the protection due to immunity priming is responsible for the viral interference (8, 9). However, the upregulation in the immune pathway genes is variable in different species and it seems to be influenced by the time of host-*Wolbachia* coevolution. For instance, there is no

TABLE 1 | *Wolbachia* antiviral effect on insects.

Wolbachia effect	*Wolbachia* strain	Natural host species	Tested host species	Tested virus	Study
Protection	*w*AlbB	*Aedes albopictus*	*Aedes aegypti, Aedes polynesiensis*	DENV, SFV, ZIKV	Bian et al., 2010[b] (8), Bian et al., 2013[b] (18), Ant et al., 2018[b] (19), Joubert et al., 2016[b] (20)
	*w*AlbB + *w*Mel	*Aedes albopictus* + *Drosophila melanogaster*	*Aedes aegypti*	DENV	Joubert et al., 2016[b] (20)
	*w*AlbA + *w*AlbB	*Aedes albopictus*	*Aedes albopictus*	DENV	Mousson et al., 2012[b,e] (21)
	wC. quinquefasciatus	*Culex quiquenfasciatus*	*Culex quiquenfasciatus*	WNV	Glaser & Meola, 2010[b] (12)
	*w*Ana	*Drosophila ananassae*	*Drosophila simulans*	DCV, FHV	Martinez et al., 2014[a,b] (22), Martinez et al., 2017[a] (23)
	*w*Ara	*Drosophila arawakana*	*Drosophila simulans*	DCV, FHV	Martinez et al., 2014[a,b] (22)
	*w*Au	*Drosophila simulans*	*Aedes aegypti, Drosophila simulans*	DENV, ZIKV, SFV, DCV, FHV	Ant et al., 2018[b] (19), Martinez et al., 2014[a,b] (22), Martinez et al., 2017[a,b] (23), Osborne et al., 2009[a,b] (24)
	*w*Ha	*Drosophila simulans*	*Drosophila simulans*	DCV, FHV	Martinez et al., 2017[a] (23), Osborne et al., 2009[a] (24)
	*w*Mel	*Drosophila melanogaster*	*Aedes aegypti, Aedes albopictus, Drosophila simulans, Drosophila melanogaster*	CHIKV, DCV, DENV, FHV, Flavivirus OTU2, ZIKV, SFV, WNV	Amuzu et al., 2018[b] (25), Ant et al., 2018[b] (19), Blagrove et al., 2012[b] (26), Martinez et al., 2014[a,b] (22), Fraser et al., 2017[b] (27), Hussain et al., 2013[b,f] (28), Joubert et al., 2016[b] (20), Martinez et al., 2017[a,b] (23), Osborne et al., 2009[a,b] (24), Van den Hurk et al., 2012[b,c,e,g] (10), Walker et al., 2011[b,c] (14), Ye et al., 2016[b,c,e] (29), Rancés et al., 2012[b] (30)
	*w*MelCs	*Drosophila melanogaster*	*Aedes aegypti, Drosophila simulans, Drosophila melanogaster*	CHIKV, CrPV, DCV, DENV, FHV, WNV	Martinez et al., 2014[a,b] (22), Hedges et al., 2008[a] (7), Fraser et al., 2017[b] (27), Hussain et al., 2013[b] (28), Martinez et al., 2017[a,b] (23), Glaser & Meola, 2010[b] (12)
	*w*MelPop	*Drosophila melanogaster*	*Aedes aegypti, Drosophila melanogaster*	CHIKV, DCV, DENV, FHV, Nora virus, YFV	Hedges et al., 2008[a] (7), Joubert et al., 2016[b] (20), Martinez et al., 2017[a,b] (23), Teixeira et al., 2008[a,b] (6), Van den Hurk et al., 2012[b,c,e,h,i] (10), Walker et al., 2011[b,c] (14), Moreira et al., 2009[b,c] (9)
	*w*Stv	*Drosophila sturtevanti*	*Drosophila simulans*	DCV	Martinez et al., 2014[a,b] (22)
	*w*Tei	*Drosophila teissieri*	*Drosophila simulans, Drosophila teissieri*	DCV, FHV	Martinez et al., 2014[a,b] (22), Martinez et al., 2017[a] (23)
	*w*Tro	*Drosophila tropicalis*	*Drosophila simulans, Drosophila tropicalis*	DCV, FHV	Martinez et al., 2014[a] (22), Martinez et al., 2017[a,b] (23)
	*w*Ma	*Drosophila simulans*	*Drosophila simulans*	FHV	Martinez et al., 2014[a] (22), Martinez et al., 2017[a] (23)
	*w*Ri	*Drosophila simulans*	*Aedes aegypti, Drosophila simulans*	DCV, DENV, FHV	Fraser et al., 2017[b] (27), Martinez et al., 2017[a] (23), Osborne et al., 2009[a] (24)
	*w*Pro	*Drosophila prosaltans*	*Drosophila prosaltans, Drosophila simulans*	FHV	Martinez et al., 2017[a] (23)
	*w*Yak	*Drosophila yakuba*	*Drosophila simulans*	FHV	Martinez et al., 2014[b] (22)
	*w*Inn	*Drosophila innubila*	*Drosophila innubila*	FHV	Unckless and Jaenike et al., 2012[a] (31)
	*w*Suz	*Drosophila suzukii*	*Drosophila suzukii*	DCV, FHV	Cattel et al., 2016[a,b,d] (32)
	*w*Stri	*Laodelphax striatellus*	*Nilaparvata lugens*	RRSV	Gong et al., 2020[b] (33)

(Continued)

TABLE 1 | Continued

Wolbachia effect	*Wolbachia* strain	Natural host species	Tested host species	Tested virus	Study
No protection	*w*Pip	*Culex pipiens*	*Culex pipiens*	CpVD	Altinli et al., 2019[b] (34)
	*w*Noto	*Aedes notoscriptus*	*Aedes notoscriptus*	DENV	Skelton et al., 2016[b,c] (35)
	*w*Mel	*Drosophila melanogaster*	*Aedes aegypti, Drosophila melanogaster, Drosophila simulans*	CHIKV, DENV, Flavivirus OTU1, Flavivirus OTU3, Flavivirus OTU16, Flavivirus OTU25, Flavivirus OTU20, Flavivirus OTU21, FHV, ZIKV, WNV, YFV	Amuzu et al., 2018[b] (25), Ant et al., 2018[b] (19), Martinez et al., 2014[b] (22), Martinez et al., 2017[b] (23), Hussain et al., 2013[b,f] (28), Van den Hurk et al., 2012[b,c,e,g,h,i] (10), Ye et al., 2016[b,c,e] (29)
	*w*MelPop	*Drosophila melanogaster*	*Aedes aegypti, Drosophila melanogaster*	FHV, IIV-6, YFV	Teixeira et al., 2008[a,b] (6), Van den Hurk et al., 2012[b,c,e,h,i] (10)
	*w*MelCS	*Drosophila melanogaster*	*Drosophila melanogaster*	Kallithea virus, La Crosse virus	Palmer et al., 2018[a] (36), Glaser & Meola, 2010[b] (12)
	*w*AlbB	*Aedes albopictus*	*Aedes aegypti, Culex tarsalis*	CHIKV, DENV, WNV	Ant et al., 2018[b] (19)
	*w*AlbA	*Aedes albopictus*	*Aedes aegypti*	SFV	Ant et al., 2018[b] (19)
	*w*AlbA + *w*AlbB	*Aedes albopictus*	*Aedes albopictus*	CHIKV, DENV	Mousson et al., 2010[b] (37), Mousson et al., 2012[a,b,e] (21)
	Male-killing *wD. bifasciata*	*Drosophila bifasciata*	*Drosophila bifasciata*	DCV, FHV	Longdon et al., 2012[a] (38)
	*w*Bai	*Drosophila baimaii*	*Drosophila simulans*	DCV, FHV	Martinez et al., 2014[a,b] (22)
	*w*Bic	*Drosophila bicornuta*	*Drosophila simulans*	DCV, FHV	Martinez et al., 2014[a,b] (22)
	*w*Bor	*Drosophila borealis*	*Drosophila simulans*	DCV, FHV	Martinez et al., 2014[a,b] (22)
	*w*Ha	*Drosophila simulans*	*Drosophila simulans*	DCV, FHV	Martinez et al., 2014[a,b] (22), Martinez et al., 2017[b] (23), Osborne et al., 2009[b] (24)
	*w*Ri	*Drosophila simulans*	*Drosophila simulans*	DCV, FHV	Martinez et al., 2017[b] (23), Osborne et al., 2009[b] (24)
	*w*No	*Drosophila simulans*	*Drosophila simulans*	DCV, FHV	Martinez et al., 2017[a,b] (23), Osborne et al., 2009[a,b] (24)
	*w*Inn	*Drosophila innubila*	*Drosophila simulans*	DCV, FHV	Martinez et al., 2014[a,b] (22)
	*w*Ma	*Drosophila simulans*	*Drosophila simulans*	DCV, FHV	Martinez et al., 2014[a,b] (22), Martinez et al., 2017[b] (23)
	*w*Pro	*Drosophila prosaltans*	*Drosophila simulans, Drosophila prosaltans*	DCV, FHV	Martinez et al., 2014[a,b] (22), Martinez et al., 2017[b] (23)
	*w*San	*Drosophila santomea*	*Drosophila simulans*	DCV, FHV	Martinez et al., 2014[a,b] (22)
	*w*Sh	*Drosophila sechellia*	*Drosophila simulans, Drosophila sechellia*	DCV, FHV	Martinez et al., 2014[a,b] (22), Martinez et al., 2017[a,b] (23)
	*w*Tri	*Drosophila triauraria*	*Drosophila simulans, Drosophila triauraria*	DCV, FHV	Martinez et al., 2014[a,b] (22), Martinez et al.2017[a,b] (23)
	*w*Tei	*Drosophila teissieri*	*Drosophila simulans, Drosophila teissieri*	FHV	Martinez et al., 2017[b] (23)
	*w*Yak	*Drosophila yakuba*	*Drosophila simulans*	DCV, FHV	Martinez et al., 2014[a,b] (22)
	*w*Ana	*Drosophila ananassae*	*Drosophila simulans,*	FHV	Martinez et al., 2014[a,b] (22), Martinez et al., 2017[a,b] (23)

(Continued)

TABLE 1 | Continued

Wolbachia effect	*Wolbachia* strain	Natural host species	Tested host species	Tested virus	Study
			Drosophila ananassae		
	*w*Stv	*Drosophila sturtevanti*	*Drosophila simulans*, *Drosophila sturtevanti*	FHV	Martinez et al., 2014[a,b] (22), Martinez et al., 2017[a,b] (23)
	wA. subalbatus	*Armigeres subalbatus*	*Armigeres subalbatus*	JEV	Tsai et al., 2006[c] (39)
	*w*Tro	*Drosophila tropicalis*	*Drosophila simulans*, *Drosophila tropicalis*	DCV, FHV	Martinez et al., 2014[b] (22), Martinez et al., 2017[b] (23)
	*w*Suz	*Drosophila suzukii*	*Drosophila suzukii*	DCV, FHV	Cattel et al., 2016[a,b,d] (32), Martinez et al., 2017[a,b] (23)
Increase in susceptibility	*w*Mel	*Drosophila melanogaster*	*Aedes aegypti*	Flavivirus OTU1, Flavivirus OTU2, Flavivirus OTU3, Flavivirus OTU20, Flavivirus OTU21	Amuzu et al., 2018[b] (25)
	*w*Exe1	*Spodoptera exempta*	*Spodoptera exempta*	SpexNPV	Graham et al., 2012[a] (40)
	*w*Ha	*Drosophila simulans*	*Drosophila simulans*	DCV	Martinez et al., 2014[b] (22)
	*w*San	*Drosophila santomea*	*Drosophila simulans*	FHV	Martinez et al., 2014[b] (22)

Study measured: a) host survival, b) viral titer, c) infection rate.

Result varied among: d) host genotype, e) infection/transmission/dissemination, f) days post infection, g) infection type (oral or intratoraxic), h) virus strain, i) viral titer inoculated in the host. CHIKV, chikungunya virus; CrPV, cricket paralysis virus; CpVD, Culex pipiens densovirus; DCV, Drosophila C virus; DENV, dengue virus; FHV, Flock House virus; IIV-6, insect iridescent virus 6; JEV, japanese encephalitis virus, RRSV, rice ragged stunt virus SFV, Semliki Forest virus, SpexNPV, Spodoptera exempta nucleopolyhedrovirus; WNV, West Nile virus; YFV, yellow fever virus; ZIKV, zika virus.

For each Wolbachia strain tested we report if there was protection, no protection or increase in susceptibility to viral infection. We present the natural host species of the strains, the hosts species in which the strains were tested, and the virus that were tested in the hosts.

upregulation on Toll or IMD genes by *Wolbachia* in its native host *Aedes fluviatilis*, but other immune-related genes are indeed modulated, as oxidative stress-related genes (51). The generation of oxygen reactive species itself is an example of immune response that vary between novel and native host, ranging from triggering oxidative stress to redox homeostasis restoration [reviewed by Zug and Hammerstein (52)]. But there is evidence that *Wolbachia*-induced oxidative stress is involved in virus blocking both in transinfected mosquito and *Drosophila* with a natural *Wolbachia* infection (50, 53).

The second hypothesis is that resources shared by *Wolbachia* and the virus can represent a limitation for development of the latter when they are co-infecting their host. As discussed in the previous section, *Wolbachia* protects mainly against RNA viruses which depends on specific cellular resources, the integrity of intracellular membranes for replication, and the host translation apparatus for virus protein production (49). Any disturbance caused by *Wolbachia* on these cellular components presumably interferes with virus replication. For instance, depletion, reduction, or modification of certain host lipids affect virus replication (54, 55). In particular for cholesterol, providing or restoring its intracellular traffic recover virus replication in a *Wolbachia*-infected host, indicating both the role of cholesterol in virus development and *Wolbachia* interference in host lipid availability (55, 56). In another recent example, it was found that *Wolbachia* and virus have antagonistic effect in the host expression of *prat2*, a gene involved in nucleotide synthesis (57).

Additionally, several approaches have shown that antiviral protection occurs in host bearing high density of *Wolbachia*, with no detectable protection is host with low symbiont density (22, 24). The same result is obtained in experimental manipulation of *Wolbachia* density with antibiotics (58). The control of symbiont density is dependent on the symbiont genotype and, in the case of *Wolbachia* strains isolated from *D. melanogaster*, the genetic basis of density determination has been assigned to the Octomom region which presents several duplications, or a deletion of the entire region, in high-density symbionts (59–61). However, one recent study with controlled genetic background showed an intriguing example of *Wolbachia* with no antiviral action in *A. aegypti*, even in relatively high density (62). Other than density, host development stage and temperature seem to modulate *Wolbachia* antiviral properties (61, 63).

The mechanism behind *Wolbachia* antiviral protection became an active area of research. New experimental approaches, such as the forward genetic screens applicable on genetically intractable bacteria (61), are extremely promising to pursue this question. One example of how recent experimental advances can bring progress to long standing questions is the case of cytoplasmic incompatibility caused by *Wolbachia*. Cytoplasmic incompatibility has been studied since 1971, yet

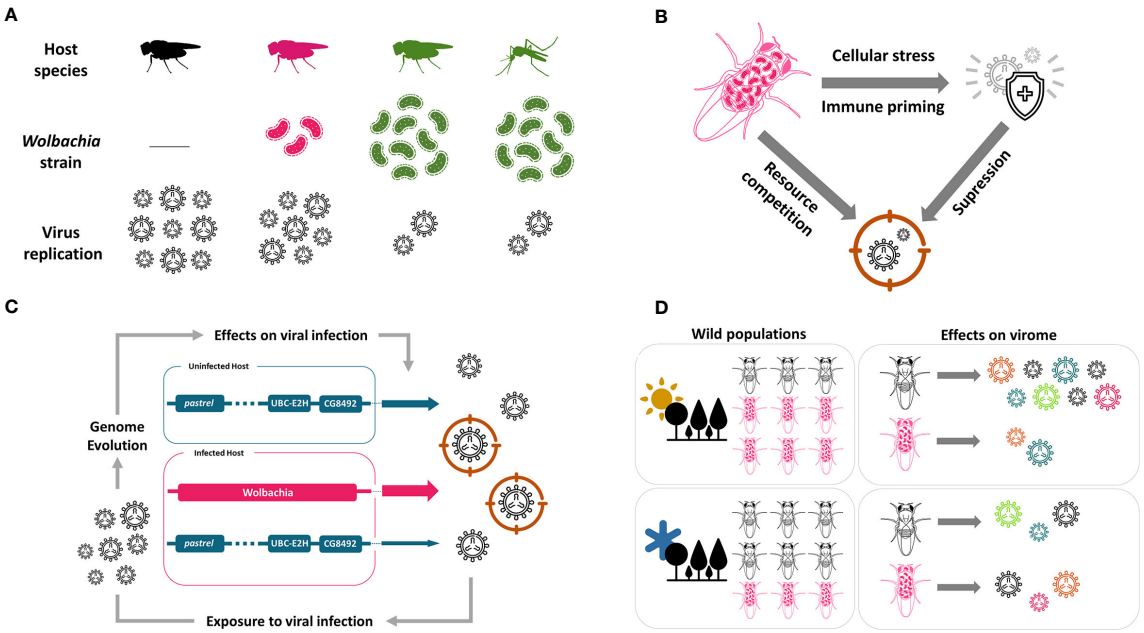

FIGURE 1 | *Wolbachia* antiviral effect in insects. **(A)** *Wolbachia* protects insects against RNA viruses. The protection is dependent on *Wolbachia* density, which varies between strains. Strains can be experimentally transferred to new hosts, such as mosquitoes. **(B)** *Wolbachia* can activate host immune system in some cases, but the mechanism of defense can also be related to competition with virus for cellular resources. The specific mechanism is not yet known. **(C)** Host immune response fight against virus, but its action and evolution are slowed down in the presence of *Wolbachia*. Colored arrows and their width represent genome and its participation in antiviral effect, respectively. **(D)** Environmental conditions, as temperature, determine *Wolbachia* antiviral response. In hot climate, *Wolbachia* may have a more important role protecting the host, and this can lead to higher *Wolbachia* prevalence on hot climate regions. But it is not yet known if *Wolbachia* reduces the virome in wild insect populations. This figure is made in conjunction with icons provided by thenounproject.com. The icons are: "Bacteria" by farra nugraha; "Virus" by KonKapp; "Immune System" by Bartama Graphic; "Immunity" by Timofey Rostilov; "Forest" by ProSymbols; "Sun" by Alice Design; and, "Cold" by Landan Lloyd.

only recently its mechanism was uncovered (1, 64, 65). The cytoplasmic incompatibility is controlled by two phage WO genes, *cifAwMel* and *cifBwMel*, present in the *Wolbachia* genome (66). Similar advances are likely to figure out the specific antiviral mechanism in the following years.

INFLUENCE ON EVOLUTION OF HOST "INTRINSIC" IMMUNOLOGICAL RESISTANCE MECHANISMS

Although *Wolbachia* confers viral protection to insects, natural insect populations have other means to fight against viruses (67, 68). Insects usually rely on the mechanisms of RNA interference, apoptosis, NF-κB pathways and translation control from its innate immune system to get along viral pathogens (69). Nevertheless, the population's ability to resist the plethora of viruses present in nature lies on its standing genetic variation on these mechanisms or the sudden appearance of beneficial mutations (70). However, in the presence of *Wolbachia*, the extended mutualistic genotype could mask or even substitute host's intrinsic mechanisms of antiviral defenses, shifting its adaptive landscape (71) (**Figure 1C**). Some recent experimental evolution studies have addressed how the presence of *Wolbachia* can alter the evolution of intrinsic antiviral mechanisms in insects.

In a pioneer study, Martins and colleagues used an experimental evolution approach in which *Drosophila melanogaster* populations were subjected to continuous DCV injections for a few generations (72). Compared with control populations that were not exposed to the virus, infected populations showed increased survival after DCV infection, and also increased survival after infection by cricket paralysis virus (CrPV) and FHV (72). This increased resistance to viral infection was associated with three candidate genes on the fly's genome - *pastrel*, *Ubc-E2H* and *CG8492* (72). In another experimental evolution study, Martinez and colleagues directly tested how the presence of *Wolbachia* can alter evolution of intrinsic antiviral mechanisms (71). They focused on a polymorphism of the gene *pastrel* that explains most of the variation on DCV resistance in *D. melanogaster* populations (73, 74). They infected populations with and without *Wolbachia* for nine generations. Resistance to DCV and the frequency of the resistant *pastrel* allele increased in all populations exposed to the virus compared with virus-free control populations (71). Most interestingly, the frequency of the resistant *pastrel* allele after nine generations was lower in *Wolbachia* infected populations than in the symbiont-free populations. After experimentally removing *Wolbachia*, the populations that had *Wolbachia*

during the selection experiment was much less resistant to the virus than the *Wolbachia*-free populations. This experiment shows that the presence of *Wolbachia* resulted in weaker selection on the host intrinsic antiviral defenses, making the host addicted to the protection caused by the symbiont (71). Another study showed that DCV infection selected for a particular *Wolbachia* strain that enhances survival and fecundity in the presence of DCV (75). Finally, Faria and colleagues showed that intrinsic antiviral defenses can replace symbiont protection (72, 76). They used previously selected populations for increased virus resistance (72), and removed the symbiont from these populations. They first observed a severe drop in survival after DCV infection, but resistance significantly increased in subsequent generations reaching the same levels as seen in the presence of *Wolbachia* after 20 generations (76).

These studies show that *Wolbachia* can change the strength of selection on host antiviral mechanisms, leading to evolutionary addiction (71, 72, 75, 76). Because *Wolbachia* prevalence varies in natural populations, this may be one mechanism that maintains genetic variation in intrinsic antiviral resistance in populations (76). One interesting interplay is that different *Drosophila* clades respond differently to viral infections (77), therefore, variation in resistance and susceptibility of hosts could be mirrored by the success and establishment of *Wolbachia* in some clades but not others in nature (78). In addition, it would be remarkably interesting to investigate how the presence of *Wolbachia* in some clades may affect the evolution of host-shifts by viruses (79).

IMPORTANCE IN WILD POPULATIONS

The *Wolbachia* antiviral effects were intensely studied in the last decade because of its importance in the field of public health. However, their ecological importance in wild populations has rarely being addressed. Around 50% of insect species may carry one or more strains of *Wolbachia* (48), meaning that almost 3 million insect species are infected. Therefore, *Wolbachia* may be a major component of antiviral defenses in nature (43). But just recently some studies started to test if *Wolbachia* can confer protection against viruses in wild insect populations. The antiviral effects of *Wolbachia* may mean that in nature it is frequently a mutualist that protects its host against infection. This may explain why *Wolbachia* strains that do not cause cytoplasmic incompatibility and have no obvious phenotypic effect can invade and be maintained in populations (80). Theory predicts that cytoplasmic incompatibility can only invade when local infection frequencies becomes sufficiently high to offset imperfect maternal transmission and infection costs (81, 82). However, recent data suggested that *Wolbachia* can spread from arbitrarily low frequencies (80). In this scenario, there appears to be a fitness advantage for the host caused by *Wolbachia* in natural populations (83). This fitness advantage may be *Wolbachia* antiviral effects. This is expected by the studies carried out in the laboratory showing the antiviral effect, but just now some studies started to test this in wild populations. It is interesting to notice that *Wolbachia* can also protect insects against bacteria and entomopathogenic fungi (84–86), and this can also add to the possible mutualistic effect in natural populations.

Drosophila flies have been used as the main model to study insect virus interactions, but until recently we knew extraordinarily little about the virus community that infect wild *Drosophila* populations. This is changing rapidly with recent studies using metagenomic approaches (87). In 2015, Webster and colleagues used metagenomic techniques in more than 2000 wild collect *Drosophila melanogaster* flies and discovered more than 20 new viruses (41). They found a high prevalence of virus infection with more than 30% of the wild collected individuals carrying a virus. There was also large variation in prevalence among the 17 sampled locations across the world. Because *Wolbachia* prevalence in these locations varied from 1.6% to 98% - with a mean of about 50% - they tested for associations between the prevalence of *Wolbachia* and the different viruses among and within populations. They could not find any association, indicating that *Wolbachia* is not an important determinant of virus incidence in the wild (41). However, as pointed by the authors, they had a small sample size per population resulting in low statistical power to detect an association. In addition, they looked only on the effect of *Wolbachia* on prevalence, but *Wolbachia* can also be influencing virus titer on infected flies.

In 2018, Shi and colleagues tested the effect of *Wolbachia* on viral abundance on six *D. melanogaster* populations sampled in Australia (88). They first sequenced total transcriptome of pools of *Wolbachia*-infected and *Wolbachia*-free lines to estimate viral abundance. Despite finding high RNA virus' abundance in all pools, they did not find any *Wolbachia* protective effect. They also sequenced the transcriptome of individual *Wolbachia*-infected and *Wolbachia*-free flies from one location, but again did not find any *Wolbachia* protective effect (88). These results should be interpreted with caution as well, since they sequenced only 122 flies in the pools, plus 40 individual flies. Given the large variation among pools in viral abundance and in the prevalence that varied from two to five viruses per pool, the statistical power to detect an effect was low. Additionally, they did not sequence wild collected flies, but F1 or F3 of laboratory cultured lines that were kept at 19°C. Unfortunately, it was discovered, very recently, that the antiviral effect of the *Wolbachia* strain wMel in *D. melanogaster* depends on temperature (63). The strong protection observed when flies develop from egg to adult at 25°C is greatly reduced or disappear when flies develop at 18°C (63). Therefore, the development conditions used by Shi et al. may have masked any possible *Wolbachia* protective effect.

Interestingly, the recent study on the effect of temperature on the *Wolbachia* antiviral effect (63) offers a hint on this puzzle. It is interesting that the *Wolbachia* antiviral effect observed at high development temperature is extremely reduced when flies develop at low temperatures. This was observed with different genotypes of *D. melanogaster*, different *Wolbachia* lineages, and different viruses, suggesting this is a general phenomenon (63).

These results suggest that in nature the mutualistic effect of virus protection will vary geographically and seasonally depending on climate, and this will result in the prevalence of *Wolbachia* being higher in tropical regions (**Figure 1D**). This is indeed what is observed in nature, where the frequency of *Wolbachia* is generally higher in populations from tropical regions (89). This pattern, although only a correlative suggestion, indicates that the antiviral protection may be the mutualistic effect in natural populations responsible for the widespread success of *Wolbachia*.

CONCLUSIONS

Since the *Wolbachia* antiviral effect in insects was discovered 12 years ago (6, 7), researchers have intensely studied this phenomenon. *Wolbachia* has even been successfully used to control the prevalence of human arboviruses, such as dengue, in mosquito populations (16, 17, 90). We learned a lot about the basic biology of the host-*Wolbachia*-virus interaction, but there are still many knowledge gaps. We now know the antiviral effect depends on *Wolbachia* strain, with only high-density strains having the antiviral effect. However, it is still unknown whether the antiviral effect occurs in insect species other than mosquitoes, flies and a planthopper. Importantly, the specific mechanism underlying antiviral protection has not been fully elucidated; upregulation of the host immune system or competition between *Wolbachia* and RNA viruses inside the host cell for some yet unknown resource necessary for virus replication are likely hypothesis (49, 52, 56). We have also learned that *Wolbachia* can alter the intensity of selection on host antiviral defenses, making the host more dependent on the symbiont for protection (71). We still do not know if the antiviral effect occurs in natural populations of insects and if it is the major mutualistic effect responsible for the extremely high prevalence of *Wolbachia* in insects. If it does, *Wolbachia* may be a major component of antiviral defense in nature.

AUTHOR CONTRIBUTIONS

AP, CC, MM, and RC wrote the paper. All authors contributed to the article and approved the submitted version.

FUNDING

Funding for this work was provided by São Paulo Research Foundation (FAPESP) (2013/25991-0, 2015/08307-3, 2018/01295-8 and 2019/03997-2), CNPq (154568/2018-0, 307015/2015-7 and 307447/2018-9), and a Newton Advanced Fellowship from the Royal Society.

ACKNOWLEDGMENTS

The authors thank Camila Beraldo and Murillo Rodrigues for suggestions on the manuscript.

REFERENCES

1. Werren JH. Biology of Wolbachia. *Annu Rev Entomol* (1997) 42:587–609. doi: 10.1146/annurev.ento.42.1.587
2. Bourtzis K, Nirgianaki A, Markakis G, Savakis C. Wolbachia infection and cytoplasmic incompatibility in Drosophila species. *Genetics* (1996).
3. Yen JH, Barr AR. The etiological agent of cytoplasmic incompatibility in Culex pipiens. *J Invertebr Pathol* (1973). doi: 10.1016/0022-2011(73)90141-9
4. Werren JH, Baldo L, Clark ME. Wolbachia: Master manipulators of invertebrate biology. *Nat Rev Microbiol* (2008). doi: 10.1038/nrmicro1969
5. Turelli M, Hoffmann AA. Rapid spread of an inherited incompatibility factor in California Drosophila. *Nature* (1991). doi: 10.1038/353440a0
6. Teixeira L, Ferreira Á, Ashburner M. The bacterial symbiont Wolbachia induces resistance to RNA viral infections in Drosophila melanogaster. *PloS Biol* (2008). doi: 10.1371/journal.pbio.1000002
7. Hedges LM, Brownlie JC, O'Neill SL, Johnson KN. Wolbachia and virus protection in insects. *Sci (80-)* (2008). doi: 10.1126/science.1162418
8. Bian G, Xu Y, Lu P, Xie Y, Xi Z. The endosymbiotic bacterium Wolbachia induces resistance to dengue virus in Aedes aegypti. *PloS Pathog* (2010) 6: e1000833. doi: 10.1371/journal.ppat.1000833
9. Moreira LA, Iturbe-Ormaetxe I, Jeffery JA, Lu G, Pyke AT, Hedges LM, et al. A Wolbachia Symbiont in Aedes aegypti Limits Infection with Dengue, Chikungunya, and Plasmodium. *Cell* (2009) 139:1268–78. doi: 10.1016/j.cell.2009.11.042
10. van den Hurk AF, Hall-Mendelin S, Pyke AT, Frentiu FD, McElroy K, Day A, et al. Impact of Wolbachia on Infection with Chikungunya and Yellow FeverViruses in the Mosquito Vector Aedes aegypti. *PloS Negl Trop Dis* (2012) 6:e1892. doi: 10.1371/journal.pntd.0001892
11. Aliota MT, Peinado SA, Velez ID, Osorio JE. The wMel strain of Wolbachia Reduces Transmission of Zika virus by Aedes aegypti. *Sci Rep* (2016). doi: 10.1038/srep28792
12. Glaser RL, Meola MA. The native Wolbachia endosymbionts of Drosophila melanogaster and Culex quinquefasciatus increase host resistance to west nile virus infection. *PloS One* (2010). doi: 10.1371/journal.pone.0011977
13. Hoffmann AA, Montgomery BL, Popovici J, Iturbe-Ormaetxe I, Johnson PH, Muzzi F, et al. Successful establishment of Wolbachia in Aedes populations to suppress dengue transmission. *Nature* (2011). doi: 10.1038/nature10356
14. Walker T, Johnson PH, Moreira LA, Iturbe-Ormaetxe I, Frentiu FD, McMeniman CJ, et al. The wMel Wolbachia strain blocks dengue and invades caged Aedes aegypti populations. *Nature* (2011). doi: 10.1038/nature10355
15. Xi Z, Khoo CCH, Dobson SL. Ecology: Wolbachia establishment and invasion in an Aedes Aegypti laboratory population. *Sci (80-)* (2005). doi: 10.1126/science.1117607
16. Ryan PA, Turley AP, Wilson G, Hurst TP, Retzki K, Brown-Kenyon J, et al. Establishment of wMel Wolbachia in Aedes aegypti mosquitoes and reduction of local dengue transmission in Cairns and surrounding locations in northern Queensland, Australia. *Gates Open Res* (2020). doi: 10.12688/gatesopenres.13061.2
17. Anders KL, Indriani C, Tantowijoyo W, Rancès E, Andari B, Prabowo E, et al. Reduced dengue incidence following deployments of Wolbachia-infected Aedes aegypti in Yogyakarta, Indonesia: A quasi-experimental trial using controlled interrupted time series analysis. *Gates Open Res* (2020). doi: 10.12688/gatesopenres.13122.1
18. Bian G, Joshi D, Dong Y, Lu P, Zhou G, Pan X, et al. Wolbachia invades Anopheles stephensi populations and induces refractoriness to Plasmodium infection. *Sci (80-)* (2013). doi: 10.1126/science.1236192
19. Ant TH, Herd CS, Geoghegan V, Hoffmann AA, Sinkins SP. The Wolbachia strain wAu provides highly efficient virustransmission blocking in Aedes aegypti. *PloS Pathog* (2018) 14:e1006815. doi: 10.1371/journal.ppat.1006815
20. Joubert DA, Walker T, Carrington LB, De Bruyne JT, Kien DHT, Hoang NLT, et al. Establishment of a Wolbachia Superinfection in Aedes aegypti

Mosquitoes as a Potential Approach for Future Resistance Management. *PloS Pathog* (2016) 12:e1005434. doi: 10.1371/journal.ppat.1005434
21. Mousson L, Zouache K, Arias-Goeta C, Raquin V, Mavingui P, Failloux AB. The Native Wolbachia Symbionts Limit Transmission of Dengue Virus inAedes albopictus. *PloS Negl Trop Dis* (2012) 6:e1989. doi: 10.1371/journal.pntd.0001989
22. Martinez J, Longdon B, Bauer S, Chan YS, Miller WJ, Bourtzis K, et al. Symbionts Commonly Provide Broad Spectrum Resistance to Viruses inInsects: A Comparative Analysis of Wolbachia Strains. *PloS Pathog* (2014) 10:e1004369. doi: 10.1371/journal.ppat.1004369
23. Martinez J, Tolosana I, Ok S, Smith S, Snoeck K, Day JP, et al. Symbiont strain is the main determinant of variation inWolbachia-mediated protection against viruses across Drosophila species. *MolEcol* (2017) 26:4072–84. doi: 10.1111/mec.14164
24. Osborne SE, Leong YS, O'Neill SL, Johnson KN. Variation in antiviral protection mediated by different Wolbachiastrains in Drosophila simulans. *PloS Pathog* (2009) 5:e1000656. doi: 10.1371/journal.ppat.1000656
25. Amuzu HE, Tsyganov K, Koh C, Herbert RI, Powell DR, McGraw EA. Wolbachia enhances insect-specific flavivirus infection in Aedes aegypti mosquitoes. *Ecol Evol* (2018) 8:5441–54. doi: 10.1002/ece3.4066
26. Blagrove MSC, Arias-Goeta C, Failloux A-B, Sinkins SP. Wolbachia strain wMel induces cytoplasmic incompatibility and blocks dengue transmission in Aedes albopictus. *Proc Natl Acad Sci* (2012) 109:255–60. doi: 10.1073/pnas.1112021108
27. Fraser JE, De Bruyne JT, Iturbe-Ormaetxe I, Stepnell J, Burns RL, Flores HA, et al. Novel Wolbachia-transinfected Aedes aegypti mosquitoes possess diverse fitness and vector competence phenotypes. *PloS Pathog* (2017) 13: e1006751. doi: 10.1371/journal.ppat.1006751
28. Hussain M, Lu G, Torres S, Edmonds JH, Kay BH, Khromykh AA, et al. Effect of Wolbachia on Replication of West Nile Virus in a MosquitoCell Line and Adult Mosquitoes. *J Virol* (2013)87:851–8. doi: 10.1128/JVI.01837-12
29. Ye YH, Carrasco AM, Dong Y, Sgrò CM, McGraw EA. The effect of temperature on Wolbachia-mediated dengue virusblocking in Aedes aegypti. *Am J Trop Med Hyg* (2016)94:812–9. doi: 10.4269/ajtmh.15-0801
30. Rancès E, Ye YH, Woolfit M, McGraw EA, O'Neill SL. The relative importance of innate immune priming inWolbachia-mediated dengue interference. *PloS Pathog* (2012) 8:e1002548. doi: 10.1371/journal.ppat.1002548
31. Unckless RL, Jaenike J. Maintenance of a male-killing wolbachia in drosophila innubila by male-killing dependent and male-killing independent mechanisms. *Evol (N Y)* (2012) 66:678–89. doi: 10.1111/j.1558-5646.2011.01485.x
32. Cattel J, Martinez J, Jiggins F, Mouton L, Gibert P. Wolbachia-mediated protection against viruses in the invasive pest Drosophila suzukii. *Insect Mol Biol* (2016) 25:595–603. doi: 10.1111/imb.12245
33. Gong JT, Li Y, Li TP, Liang Y, Hu L, Zhang D, et al. Stable Introduction of Plant-Virus-Inhibiting Wolbachia intoPlanthoppers for Rice Protection. *Curr Biol* (2020)30:4837–45. doi: 10.1016/j.cub.2020.09.033
34. Altinli M, Soms J, Ravallec M, Justy F, Bonneau M, Weill M, et al. Sharing cells with Wolbachia: the transovarian vertical transmission of Culex pipiens densovirus. *Environ Microbiol* (2019). doi: 10.1111/1462-2920.14511
35. Skelton E, Rancès E, Frentiu FD, Kusmintarsih ES, Iturbe-Ormaetxe I, Caragata EP, et al. A native Wolbachia endosymbiont does not limit dengue virus infection in the mosquito Aedes notoscriptus (Diptera: Culicidae). *J Med Entomol* (2016). doi: 10.1093/jme/tjv235
36. Palmer WH, Medd NC, Beard PM, Obbard DJ. Isolation of a natural DNA virus of Drosophila melanogaster, and characterisation of host resistance and immune responses. *PloS Pathog* (2018). doi: 10.1371/journal.ppat.1007050
37. Mousson L, Martin E, Zouache K, Madec Y, Mavingui P, Failloux AB. Wolbachia modulates Chikungunya replication in Aedesalbopictus. *Mol Ecol* (2010)19:1953–64. doi: 10.1111/j.1365-294X.2010.04606.x
38. Longdon B, Fabian DK, Hurst GDD, Jiggins FM. Male-killing Wolbachia do not protect Drosophila bifasciata againstviral infection. *BMC Microbiol* (2012) 12:1–6. doi: 10.1186/1471-2180-12-S1-S8
39. Tsai K-H, Huang C-G, Wu W-J, Chuang C-K, Lin C-C, Chen W-J. Parallel infection of Japanese encephalitis virus and Wolbachia within cells of mosquito salivary glands. *J Med Entomol* (2006) 43:752–6. doi: 10.1093/jmedent/43.4.752
40. Graham RI, Grzywacz D, Mushobozi WL, Wilson K. Wolbachia in a major African crop pest increases susceptibility toviral disease rather than protects. *Ecol Lett* (2012) 15:993–1000. doi: 10.1111/j.1461-0248.2012.01820.x
41. Webster CL, Waldron FM, Robertson S, Crowson D, Ferrari G, Quintana JF, et al. The discovery, distribution, and evolution of viruses associated with drosophila melanogaster. *PloS Biol* (2015). doi: 10.1371/journal.pbio.1002210
42. Martinez J, Ok S, Smith S, Snoeck K, Day JP, Jiggins FM. Should Symbionts Be Nice or Selfish? Antiviral Effects of Wolbachia Are Costly but Reproductive Parasitism Is Not. *PloS Pathog* (2015). doi: 10.1371/journal.ppat.1005021
43. Zug R, Hammerstein P. Bad guys turned nice? A critical assessment of Wolbachia mutualisms in arthropod hosts. *Biol Rev Camb Philos Soc* (2015). doi: 10.1111/brv.12098
44. Min KT, Benzer S. Wolbachia, normally a symbiont of Drosophila, can be virulent, causing degeneration and early death. *Proc Natl Acad Sci USA* (1997). doi: 10.1073/pnas.94.20.10792
45. Carrington LB, Leslie J, Weeks AR, Hoffmann AA. The popcorn wolbachia infection of drosophila melanogaster: Can selection alter wolbachia longevity effects? *Evol (N Y)* (2009). doi: 10.1111/j.1558-5646.2009.00745.x
46. Gupta V, Stewart CO, Rund SSC, Monteith K, Vale PF. Costs and benefits of sublethal Drosophila C virus infection. *J Evol Biol* (2017). doi: 10.1111/jeb.13096
47. Siva-Jothy JA, Prakash A, Vasanthakrishnan RB, Monteith KM, Vale PF. Oral bacterial infection and shedding in Drosophilamelanogaster. *J Vis Exp* (2018) 135:e57676. doi: 10.3791/57676
48. Weinert LA, Araujo-Jnr EV, Ahmed MZ, Welch JJ. The incidence of bacterial endosymbionts in terrestrial arthropods. *Proc R Soc B Biol Sci* (2015) 282:20150249. doi: 10.1098/rspb.2015.0249
49. Lindsey ARI, Bhattacharya T, Newton ILG, Hardy RW. Conflict in the intracellular lives of endosymbionts and viruses: A mechanistic look at Wolbachia-mediated pathogen-blocking. *Viruses* (2018) 10:1–29. doi: 10.3390/v10040141
50. Pan X, Zhou G, Wu J, Bian G, Lu P, Raikhel AS, et al. Wolbachia induces reactive oxygen species (ROS)-dependent activationof the Toll pathway to control dengue virus in the mosquito Aedes aegypti.*Proc Natl Acad Sci USA* (2012) 109:23–31. doi: 10.1073/pnas.1116932108
51. Caragata EP, Pais FS, Baton LA, Silva JBL, Sorgine MHF, Moreira LA. The transcriptome of the mosquito Aedes fluviatilis (Diptera:Culicidae), and transcriptional changes associated with its native Wolbachiainfection. *BMC Genomics* (2017)18:1–19. doi: 10.1186/s12864-016-3441-4
52. Zug R, Hammerstein P. Wolbachia and the insect immune system: What reactive oxygen species can tell us about the mechanisms of Wolbachia-host interactions. *Front Microbiol* (2015). doi: 10.3389/fmicb.2015.01201
53. Wong ZS, Brownlie JC, Johnson KN. Oxidative stress correlates with Wolbachia-mediated antiviralprotection in Wolbachia-Drosophila associations. *Appl EnvironMicrobiol* (2015) 81:3001–5. doi: 10.1128/AEM.03847-14
54. Molloy JC, Sommer U, Viant MR, Sinkins SP. Wolbachia modulates lipid metabolism in Aedes albopictus mosquito cells. *Appl Environ Microbiol* (2016) 82:3109–20. doi: 10.1128/AEM.00275-16
55. Geoghegan V, Stainton K, Rainey SM, Ant TH, Dowle AA, Larson T, et al. Perturbed cholesterol and vesicular trafficking associated withdengue blocking in Wolbachia-infected Aedes aegypti cells. *NatCommun* (2017) 8:1–10. doi: 10.1038/s41467-017-00610-8
56. Caragata EP, Rancès E, Hedges LM, Gofton AW, Johnson KN, O'Neill SL, et al. Dietary Cholesterol Modulates Pathogen Blocking byWolbachia. *PloS Pathog* (2013) 9:e1003459. doi: 10.1371/journal.ppat.1003459
57. Lindsey AR, Bhattacharya T, Hardy R, Newton IL. Wolbachia and virus alter the host transcriptome at the interface of nucleotide metabolism pathways. *bioRxiv* (2020) 1–38. doi: 10.1101/2020.06.18.160317
58. Lu P, Bian G, Pan X, Xi Z. Wolbachia induces density-dependent inhibition to dengue virus in mosquito cells. *PloS Negl Trop Dis* (2012) 6:1–8. doi: 10.1371/journal.pntd.0001754
59. Chrostek E, Marialva MSP, Esteves SS, Weinert LA, Martinez J, Jiggins FM, et al. Wolbachia Variants Induce Differential Protection to Viruses in Drosophila melanogaster: A Phenotypic and Phylogenomic Analysis. *PloS Genet* (2013). doi: 10.1371/journal.pgen.1003896
60. Chrostek E, Teixeira L. Mutualism Breakdown by Amplification of Wolbachia Genes. *PloS Biol* (2015). doi: 10.1371/journal.pbio.1002065

61. Duarte EH, Carvalho A, Verde UDC, Lisboa U. Regulation of Wolbachia proliferation by the amplification and deletion of an addictive genomic island. *bioRxiv* (2020). doi: 10.1101/2020.09.08.288217
62. Fraser JE, O'Donnell TB, Duyvestyn JM, O'Neill SL, Simmons CP, Flores HA. Novel phenotype of Wolbachia strain wPip in Aedes aegypti challenges assumptions on mechanisms of Wolbachia-mediated dengue virus inhibition. *PloS Pathog* (2020) 16:1–21. doi: 10.1371/journal.ppat.1008410
63. Chrostek E, Martins NE, Marialva MS, Teixeira L. Wolbachia-conferred antiviral protection is determined by developmental temperature. *bioRxiv* (2020). doi: 10.1101/2020.06.24.169169
64. Le Page DP, Metcalf JA, Bordenstein SR, On J, Perlmutter JI, Shropshire JD, et al. Prophage WO genes recapitulate and enhance Wolbachia-induced cytoplasmic incompatibility. *Nature* (2017) 543:243–7. doi: 10.1038/nature21391
65. Yen JH, Barr AR. New hypothesis of the cause of cytoplasmic incompatibility in Culexpipiens L. [31]. *Nature* (1971) 232:657–8. doi: 10.1038/232657a0
66. Shropshire JD, Bordenstein SR. Two-by-one model of cytoplasmic incompatibility: Synthetic recapitulation by transgenic expression of cifa and cifb in drosophila. *PloS Genet* (2019). doi: 10.1371/journal.pgen.1008221
67. Palmer WH, Varghese FS, Van Rij RP. Natural variation in resistance to virus infection in dipteran insects. *Viruses* (2018). doi: 10.3390/v10030118
68. Cogni R, Cao C, Day JP, Bridson C, Jiggins FM. The genetic architecture of resistance to virus infection in Drosophila. *Mol Ecol* (2016). doi: 10.1111/mec.13769
69. Marques JT, Imler JL. The diversity of insect antiviral immunity: Insights from viruses. *Curr Opin Microbiol* (2016). doi: 10.1016/j.mib.2016.05.002
70. Duxbury EML, Day JP, Vespasiani DM, Thüringer Y, Tolosana I, Smith SCL, et al. Host-pathogen coevolution increases genetic variation in susceptibility to infection. *Elife* (2019). doi: 10.7554/eLife.46440
71. Martinez J, Cogni R, Cao C, Smith S, Illingworth CJR, Jiggins FM. Addicted? Reduced host resistance in populations with defensive symbionts. *Proc R Soc B Biol Sci* (2016). doi: 10.1098/rspb.2016.0778
72. Martins NE, Faria VG, Nolte V, Schlötterer C, Teixeira L, Sucena É, et al. Host adaptation to viruses relies on few genes with different cross-resistance properties. *Proc Natl Acad Sci USA* (2014). doi: 10.1073/pnas.1400378111
73. Magwire MM, Fabian DK, Schweyen H, Cao C, Longdon B, Bayer F, et al. Genome-Wide Association Studies Reveal a Simple Genetic Basis of Resistance to Naturally Coevolving Viruses in Drosophila melanogaster. *PloS Genet* (2012). doi: 10.1371/journal.pgen.1003057
74. Cao C, Cogni R, Barbier V, Jiggins FM. Complex coding and regulatory polymorphisms in a restriction factor determine the susceptibility of Drosophila to viral infection. *Genetics* (2017). doi: 10.1534/genetics.117.201970
75. Faria VG, Martins NE, Magalhães S, Paulo TF, Nolte V, Schlötterer C, et al. Drosophila Adaptation to Viral Infection through Defensive Symbiont Evolution. *PloS Genet* (2016). doi: 10.1371/journal.pgen.1006297
76. Faria VG, Martins NE, Schlötterer C, Sucena É. Readapting to DCV infection without Wolbachia: Frequency changes of Drosophila antiviral alleles can replace endosymbiont protection. *Genome Biol Evol* (2018). doi: 10.1093/gbe/evy137
77. Longdon B, Hadfield JD, Day JP, Smith SCL, McGonigle JE, Cogni R, et al. The Causes and Consequences of Changes in Virulence following Pathogen Host Shifts. *PloS Pathog* (2015). doi: 10.1371/journal.ppat.1004728
78. Mateos M, Castrezana SJ, Nankivell BJ, Estes AM, Markow TA, Moran NA. Heritable endosymbionts of Drosophila. *Genetics* (2006) 174:363–76. doi: 10.1534/genetics.106.058818
79. Pimentel AC, Beraldo CS, Cogni R. Host-shift as the cause of emerging infectious diseases: Experimental approaches using Drosophila -virus interactions. *Genet Mol Biol* (2021) 44:e20200197. doi: 10.1590/1678-4685-gmb-2020-0197
80. Kriesner P, Hoffmann AA, Lee SF, Turelli M, Weeks AR. Rapid Sequential Spread of Two Wolbachia Variants in Drosophilasimulans. *PloS Pathog* (2013) 9:e1003607. doi: 10.1371/journal.ppat.1003607
81. Hoffmann AA, Turelli M. Unidirectional incompatibility in Drosophila simulans: inheritance, geographic variation and fitness effects. *Genetics* (1988). doi: 10.1093/genetics/119.2.435
82. Hoffmann AA, Hercus M, Dagher H. Population dynamics of the Wolbachia infection causing cytoplasmic incompatibility in Drosophila melanogaster. *Genetics* (1998).
83. Harcombe W, Hoffmann AA. Wolbachia effects in Drosophila melanogaster: In search of fitness benefits. *J Invertebr Pathol* (2004). doi: 10.1016/j.jip.2004.07.003
84. Panteleev DY, Goryacheva II, Andrianov BV, Reznik NL, Lazebny OE, Kulikov AM. The endosymbiotic bacterium Wolbachia enhances the nonspecific resistance to insect pathogens and alters behavior of Drosophila melanogaster. *Russ J Genet* (2007). doi: 10.1134/S1022795407090153
85. Ye YH, Woolfit M, Rancès E, O'Neill SL, McGraw EA. Wolbachia-Associated Bacterial Protection in the Mosquito Aedes aegypti. *PloS Negl Trop Dis* (2013). doi: 10.1371/journal.pntd.0002362
86. Pan X, Pike A, Joshi D, Bian G, McFadden MJ, Lu P, et al. The bacterium Wolbachia exploits host innate immunity to establish a symbiotic relationship with the dengue vector mosquito Aedes aegypti. *ISME J* (2018). doi: 10.1038/ismej.2017.174
87. Zhang YZ, Shi M, Holmes EC. Using Metagenomics to Characterize an Expanding Virosphere. *Cell* (2018). doi: 10.1016/j.cell.2018.02.043
88. Shi M, White VL, Schlub T, Eden JS, Hoffmann AA, Holmes EC. No detectable effect of Wolbachia wMel on the prevalence and abundance of the RNA virome of Drosophila melanogaster. *Proc R Soc B Biol Sci* (2018). doi: 10.1098/rspb.2018.1165
89. Kriesner P, Conner WR, Weeks AR, Turelli M, Hoffmann AA. Persistence of a Wolbachia infection frequency cline in Drosophila melanogaster and the possible role of reproductive dormancy. *Evol (N Y)* (2016). doi: 10.1111/evo.12923
90. Nazni WA, Hoffmann AA, NoorAfizah A, Cheong YL, Mancini MV, Golding N, et al. Establishment of Wolbachia Strain wAlbB in Malaysian Populations ofAedes aegypti for Dengue Control. *Curr Biol* (2019) 29:4241–8. doi: 10.1016/j.cub.2019.11.007

Conflict of Interest: The authors declare that the research was conducted in the absence of any commercial or financial relationships that could be construed as a potential conflict of interest.

frontiers in Immunology

REVIEW
published: 09 February 2021
doi: 10.3389/fimmu.2021.628151

Advances in the Arms Race Between Silkworm and Baculovirus

Liang Jiang[1,2*], *Marian R. Goldsmith*[3] *and Qingyou Xia*[1,2]

[1] State Key Laboratory of Silkworm Genome Biology, Southwest University, Chongqing, China, [2] Biological Science Research Center, Southwest University, Chongqing, China, [3] Department of Biological Sciences, University of Rhode Island, Kingston, RI, United States

Insects are the largest group of animals. Nearly all organisms, including insects, have viral pathogens. An important domesticated economic insect is the silkworm moth *Bombyx mori*. *B. mori nucleopolyhedrovirus* (BmNPV) is a typical baculovirus and a primary silkworm pathogen. It causes major economic losses in sericulture. Baculoviruses are used in biological pest control and as a bioreactor. Silkworm and baculovirus comprise a well-established model of insect–virus interactions. Several recent studies have focused on this model and provided novel insights into viral infections and host defense. Here, we focus on baculovirus invasion, silkworm immune response, baculovirus evasion of host immunity, and enhancement of antiviral efficacy. We also discuss major issues remaining and future directions of research on silkworm antiviral immunity. Elucidation of the interaction between silkworm and baculovirus furnishes a theoretical basis for targeted pest control, enhanced pathogen resistance in economically important insects, and bioreactor improvement.

Keywords: antiviral immunity, baculovirus, *Bombyx mori nucleopolyhedrovirus*, immune evasion, silkworm

OPEN ACCESS

Edited by:
Humberto Lanz-Mendoza, National Institute of Public Health, Mexico

Reviewed by:
Jorge Cime-Castillo, National Institute of Public Health, Mexico
Jorge Contreras-Garduño, National Autonomous University of Mexico, Mexico
Jiaping Xu, Anhui Agricultural University, China

***Correspondence:**
Liang Jiang
jiangliang@swu.edu.cn

Specialty section:
This article was submitted to Comparative Immunology, a section of the journal Frontiers in Immunology

Received: *11 November 2020*
Accepted: *04 January 2021*
Published: *09 February 2021*

Citation:
Jiang L, Goldsmith MR and Xia Q (2021) Advances in the Arms Race Between Silkworm and Baculovirus. Front. Immunol. 12:628151. doi: 10.3389/fimmu.2021.628151

INTRODUCTION

Insects are globally distributed and play vital roles in the biosphere. Lepidoptera is a major insect taxon with an estimated 150,000 to 180,000 described species (1, 2). Many lepidopterans are pests that adversely affect agricultural production. However, the silkworm moth *Bombyx mori*, the only fully domesticated insect, is an economically important lepidopteran used for silk production in many developing countries (3, 4). China is the largest producer of silkworm cocoons, with an annual value for the output of the silk industry of about 200 billion Yuan (about 30 billion USD) (3). Pathogenic viruses are severe threats to all organisms and silkworm viruses cause losses of almost 16% of potential cocoon production each year. *Bombyx mori nucleopolyhedrovirus* (BmNPV) is a primary silkworm pathogen. This typical baculovirus causes major economic losses in sericulture (3). Baculovirus is also used as a biological control agent against insect pests and as a bioreactor. The Silkworm Genome Project was completed >10 years ago (5–8) and promoted *B. mori* to model insect status in basic and applied research (9). Here, we present a broad overview of silkworm–baculovirus interactions. We also discuss the major challenges and future directions of research in silkworm antiviral immunity.

BACULOVIRUS HOST INVASION MECHANISM

Baculovirus consists of a circular double-stranded DNA genome that combines with capsid proteins to form an enveloped nucleocapsid (3, 10). *Autographa californica multiple nucleopolyhedrovirus* (AcMNPV) is a close relative of BmNPV and the most well studied baculovirus (11, 12). Both NPVs are models for basic molecular research which have been used to elucidate the baculovirus infection cycle. The baculovirus replication cycle includes two virion phenotypes, an occlusion-derived virus (ODV) and a budded virus (BV). ODVs are packaged in occlusion bodies and induce host infection, whereas BVs spread throughout the host after infection (12, 13). ODVs and BVs have the same nucleocapsids but different envelopes. BVs mature early during infection and acquire their envelopes from modified host cell membranes. In contrast, ODVs mature late in infection and form their envelopes within host nuclei (14, 15). BVs and ODVs interact differently with host cells: ODVs fuse with the midgut epithelial cell membrane, whereas BVs are internalized by adsorptive endocytosis (15).

Baculovirus occurs in the environment in the form of occlusion bodies. For infection, it invades insect larvae mainly by ingestion (3). ODVs are released after these occlusion bodies dissociate in the alkaline environment of larval gut juice. They pass through the peritrophic membrane, invade the midgut, and cause primary infection (**Figure 1**) (11–13). Several envelope proteins known as *per os* infectivity factors (PIFs) are unique to ODVs. They mediate specific ODV binding to midgut columnar epithelial cells and initiate oral infection by binding to receptors (16–19), after which nucleocapsids enter the epithelial cells *via* envelope-mediated membrane fusion (3, 11). Viral DNA is then released from the nucleocapsids and used as a template to generate new DNA and mRNA (3, 11).

Baculoviral gene expression occurs in four phases: immediate early, delayed early, late, and very late. In an infected cell, viral DNA replication starts at 8 h post infection (hpi) and represents the transition from the early stage to the late stage (20, 21). During early infection, host RNA polymerase transcribes the viral DNA and produces the elements required for its replication (15). Viral DNA replication and transcription then form nucleocapsid progeny that acquire envelopes by budding from the host cell membrane. The latter is modified mainly by virally encoded fusion protein GP64 to generate a BV, which causes systemic infection *via* the host tracheal system (13, 22, 23). At the latter infection stages, progeny ODVs acquire envelopes in the nucleus, possibly derived from nuclear membranes modified by several viral proteins (24), are subsequently assembled into occlusion bodies and released into the environment after host disintegration (11, 22).

BmNPV BV utilizes multiple strategies to invade host cells (**Figure 1**). Binding and penetration into host cells by BV of both BmNPV and AcMNPV are mediated by the GP64 envelope glycoprotein which is specific to BV (12, 25, 26). GP64 contains a cholesterol recognition amino acid consensus (CRAC) domain which is known to be essential for fusion between the BV envelope and mammalian cell membrane (26, 27). The BmN and BmE cell lines are derived from the ovary and embryonic cells of silkworm, respectively. Various endocytic inhibitor assays disclosed that BmNPV BV penetrates BmN cells by clathrin-independent macropinocytic endocytosis mediated by cholesterol on the cell membrane (28). The cholesterol transporter BmNPC1 interacts with GP64. Its deficiency inhibits viral penetration rather than viral binding to BmE cells (29). In contrast, BmNPV BV uses clathrin- and dynamin-dependent endocytosis pathways to penetrate BmN cells. Successful BV entry also requires low pH (25). A number of studies were performed to identify the host receptor of GP64 (12). The membrane protein BmREEPa is not a direct NPV receptor but interacts with GP64 and may participate in BV attachment or binding (30). Yeast two-hybrid and coimmunoprecipitation (Co-IP) assays demonstrated that the silkworm protein SINAL10 binds GP64, is concentrated near the cell membrane, and stimulates BmNPV proliferation in BmN cells (14). Nevertheless, to date, unequivocal identification of a receptor for GP64 remains elusive (12).

Baculovirus encodes some auxiliary genes to enhance its infection in insect larvae, including viral fibroblast growth factor (*vfgf*), ecdysteroid (UDP)-glucosyltransferase (*egt*), and *p35* (31). Horizontal gene transfer (HGT) between host and pathogen might augment pathogen survival and propagation. Several BmNPV auxiliary genes were acquired from the silkworm genome *via* HGT. These include *egt*, *vfgf*, and protein tyrosine phosphatase (*ptp*) (32). BmNPV PTP is a virus-associated structural protein which might have originated from insect *ptp-h* (32). Deleting it reduces production of progeny in larval silkworm hosts; moreover, the mutation can be rescued by inserting *Bmptp-h* into BmNPV ptp-deleted virus (33), and overexpression of *Bmptp-h* accelerates BmNPV multiplication in BmE host cells (34). Other experiments involving deletion and insertion of *ptp* and *egt* (34, 35) showed that HGT-derived genes are dispensable for virus production in certain cell lines but affect progeny contents and may control host physiology.

SILKWORM IMMUNE RESPONSE TO BACULOVIRUS

Innate immune responses in insects control and clear pathogens following infection (36, 37). Lepidopteran insects have several

Abbreviations: AcMNPV, *Autographa californica multiple nucleopolyhedrovirus*; AMP, antimicrobial peptide; *B. mori*, *Bombyx mori*; BEVS, baculovirus expression vector system; BmEGFR, *B. mori* epidermal growth factor receptor; *Bmhsp19.9*, *B. mori* heat shock protein 19.9; BmNPV, *Bombyx mori nucleopolyhedrovirus*; BV, budded virus; Co-IP, coimmunoprecipitation; CRAC, cholesterol recognition amino acid consensus; cSPs, clip-domain serine proteases; ECs, effector caspases; egt, ecdysteroid (UDP)-glucosyltransferase; GM, genetically modified; HGT, horizontal gene transfer; hpi, h post infection; IAP, inhibitor of apoptosis; iap-A, iap-antagonist; ICs, initiator caspases; miRNA, microRNA; ODV, occlusion-derived virus; PGRP, peptidoglycan recognition protein; PIF, *per os* infectivity factor; piRNA, PIWI-associated RNA; PO, phenoloxidase; PPO, prophenoloxidase; pre-miRNA, precursor miRNA; ptp, protein tyrosine phosphatase; RFPs, red fluorescent proteins; RGs, reference genes; RNAi, RNA interference; ROS, reactive oxygen species; siRNAs, short interfering RNAs; SPs, serine proteases; vfgf, viral fibroblast growth factor; VSRs, viral suppressors of RNAi.

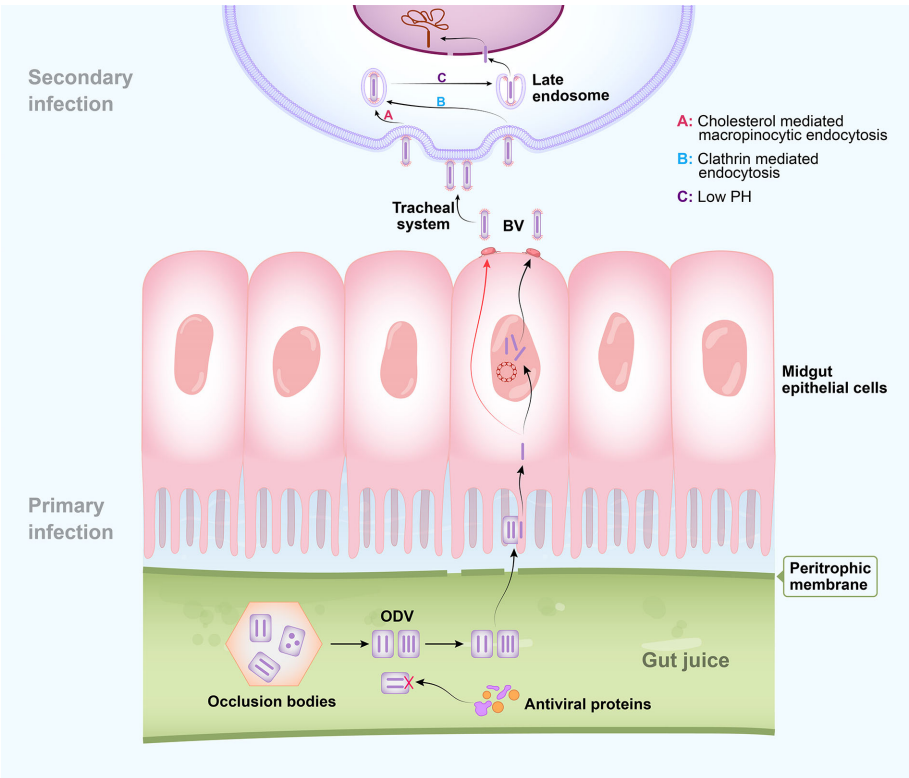

FIGURE 1 | Schematic diagram of baculovirus entry. Occlusion-derived viruses (ODVs) are released from occlusion bodies in the alkaline environment of larval gut juice after ingestion. Several insect gut juice proteins have strong antiviral capacity against ODVs. Intact ODVs pass through the peritrophic membrane and nucleocapsids enter the midgut epithelial cells *via* envelope-mediated membrane fusion to cause primary infection. Progeny budded viruses (BVs) spread through the host *via* the tracheal system to cause secondary infection. Binding and penetration into host cells by BV of both *Bombyx mori nucleopolyhedrovirus* (BmNPV) and *Autographa californica multiple nucleopolyhedrovirus* (AcMNPV) are mediated by the GP64 envelope glycoprotein which is specific to BV. BmNPV BV penetrates nonmidgut host cells by multiple strategies, including clathrin-independent macropinocytic endocytosis mediated by cholesterol on the cell membrane and clathrin- and dynamin-dependent endocytosis pathways. Successful BV entry also requires low pH. Nucleocapsid uncoating in the nucleus results in the subsequent virus infection process.

antiviral immune responses which they use against baculovirus infections. These include global protein synthesis shutdown, rRNA degradation, inactivation by gut juice antiviral proteins, melanization, apoptosis, RNAi-based antiviral response, and host gene-encoded resistance (**Figure 2**) (3, 36–39). Among these immune responses, there are relatively few studies on the mechanisms of the first two processes. After AcMNPV infection of *B. mori* cells, rRNA degradation is triggered by six amino acid residues (positions 514 and 599) of viral protein P143 as a primary antiviral response. Global protein synthesis shutdown then follows viral DNA replication, resulting in abortive infection (38, 40). The latter processes are more clearly delineated, and each process is described in turn here.

The insect midgut is the first tissue to be infected after baculovirus ingestion. Hence, it is an important immune organ which acts as a first line of defense against pathogens (41, 42). Several insect gut juice proteins secreted from the midgut have strong antiviral capacity. The antiviral proteins Bmlipase-1 (43), BmSP-2 (44), BmNOX (45), red fluorescent proteins (RFPs) (46), Bmtryp (47), and BmLHA (48) have been isolated from silkworm larva gut juice, which inhibit BmNPV at an initial infection stage. The activation of energy synthesis by adenosine signaling following baculovirus infection is a physiological response in the silkworm that supports its innate immunity (49). Melanization is a prominent humoral response in insects. It consists of a cascade of clip-domain serine proteases (cSPs) that converts zymogen prophenoloxidase (PPO) into active phenoloxidase (PO), which is negatively regulated by serpins. PO catalyzes melanin formation to encapsulate and kill invading pathogens (50, 51). Baculovirus infection is efficiently blocked by the PPO activation cascade (50). *Bmserpin2* knockdown increases PO activity and decreases viral DNA content in silkworm haemolymph infection with BmNPV (52). The stage of infection at which melanization inhibits baculovirus infection needs further exploration.

Apoptosis is a genetically controlled process that removes unwanted or damaged cells. It serves as an important antiviral defense mechanism in insects (15, 37, 53–55). The apoptotic caspase cascade comprises upstream initiator caspases (ICs) and downstream effector caspases (ECs) (15, 53) (**Figure 3**). To

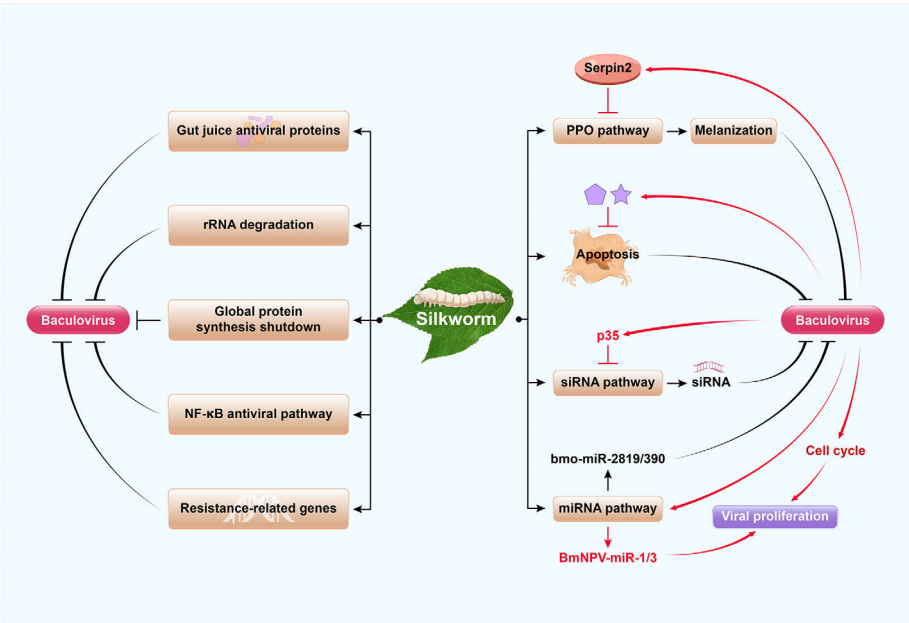

FIGURE 2 | Model of the arms race of silkworm and baculovirus. Silkworms have several antiviral immune responses which they use against baculovirus infections. These include global protein synthesis shutdown, rRNA degradation, inactivation by gut juice antiviral proteins, host gene-encoded resistance, NF-κB antiviral pathway, apoptosis, melanization, and RNAi-based antiviral response. The prophenoloxidase (PPO) activation cascade causes melanization to block baculovirus infection, which is negatively regulated by serpins. RNAi antiviral defense of insects includes the major mechanism of the siRNA pathway and the minor contribution of the miRNA pathway. The silkworm-encoded miRNA bmo-miR-2819 and bmo-miRNA-390 inhibit BmNPV proliferation by downregulating viral genes. As a confrontation, baculovirus have developed several strategies to escape host immunity and promote their own replication and proliferation, including inhibition of antiviral apoptosis, melanization, RNAi and regulation of the cell cycle. For example, *Bombyx mori nucleopolyhedrovirus* (BmNPV) induces *Bmserpin2* to inhibit host melanization. Meanwhile, *Autographa californica multiple nucleopolyhedrovirus* (AcMNPV) p35 inhibits siRNA pathway. Additionally, baculoviruses exploit the miRNA pathway to encode their own miRNAs (such as BmNPV-miR-1 and BmNPV-miR-3) for viral propagation.

initiate apoptosis, ECs are activated by ICs, and then cleave other signaling proteins (56). In lepidopterans, caspase-1, caspase-2, and caspase-3 are ECs while caspase-5 (Dronc) and caspase-6 (Dredd) are ICs (57). A cellular inhibitor of apoptosis (IAP) binds caspases, blocks their function, and prevents apoptosis activation in normal cells (15, 58). In BmN cells, *B. mori* iap1 (BmIAP1) interacts with BmDronc and Bmcaspase-1 and downregulates apoptosis (58). Apoptotic signaling, which is initiated upon baculovirus infection, promotes iap-antagonist (iap-A) binding to cellular IAP and releases free caspases to facilitate apoptosis (15, 53). The host p53 protein is pro-apoptotic and triggers antiviral apoptosis upon viral DNA replication. It elevates caspase-3-like protease activity and enhances BmDronc processing in BmN cells after BmNPV infection (53) (**Figure 3**). Nevertheless, a DNA damage response, which is elicited upon viral DNA replication, depletes cellular IAP protein, activates apoptosis, and promotes baculovirus multiplication in infected cells (59–61). Although apoptotic pathways and their associated viral and cellular factors play important roles in regulating the outcome of baculovirus infection in insect cells, their mechanisms and interactions are complex and remain to be fully elucidated.

RNA interference (RNAi) is an ancient post-transcriptional antiviral regulatory process in insects (36, 62) whereby the host RNAi response degrades baculovirus transcripts (63). In this process, viral infections generate dsRNAs that trigger the RNAi machinery and process them into viral short interfering RNAs (vsiRNAs) that target viral RNA sequences and inhibit viral proliferation (64). Another RNAi response involves the microRNA (miRNA) pathway in which precursor miRNA (pre-miRNA) is cleaved into mature miRNA that regulates gene expression by targeting specific mRNAs (65). Cellular miRNAs also affect viral infections and play important roles in host–pathogen interactions. The silkworm-encoded miRNA bmo-miR-2819 is upregulated at the delayed early stage in infection, and its overexpression inhibits BmNPV proliferation by downregulating viral *ie-1* (66). Similarly, bmo-miRNA-390 downregulates the expression of BmNPV-*cg30* (67). The PIWI-associated RNA (piRNA) pathway is also involved in an antiviral response but little information is reported in silkworm (68). Results from published reports reveal that the siRNA pathway is the major mechanism, whereas the contribution of the miRNA pathway is minor in RNAi antiviral defense of insects (**Figure 2**).

Innate immune signaling pathways and resistance-related genes play an important role in antiviral defense. The Imd and Toll signaling pathways participate in the antiviral immune response (36, 54) but do not seem to play roles in the silkworm BmNPV response. BmNPV infection induces

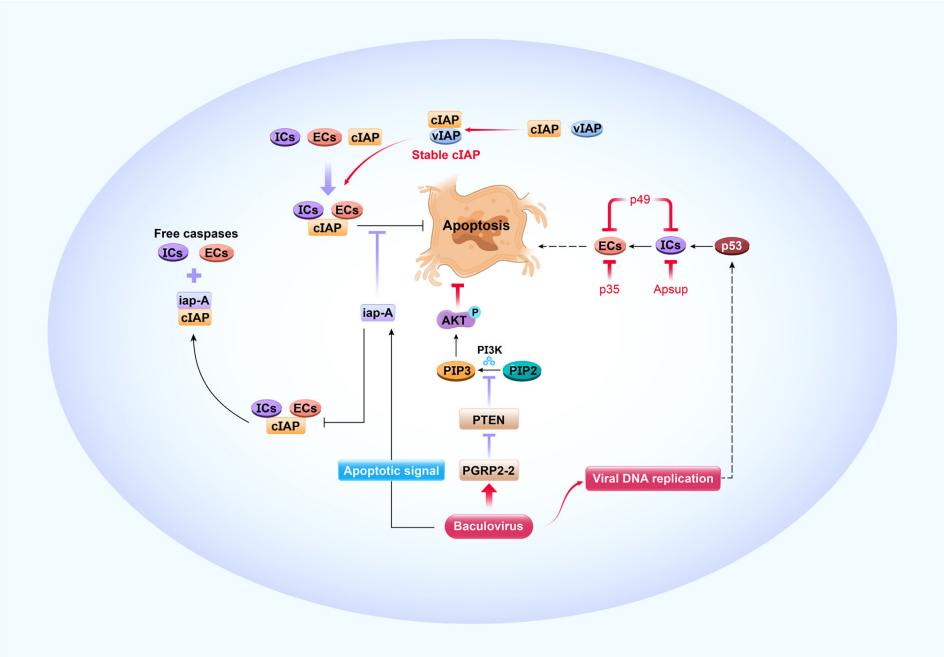

FIGURE 3 | Antiviral apoptosis and its modification by baculoviruses. The apoptotic caspase cascade comprises upstream initiator caspases (ICs) and downstream effector caspases (ECs). The cellular inhibitor of apoptosis (cIAP) binds caspases and blocks apoptosis in normal cells. Apoptotic signaling is initiated upon baculovirus infection, which causes iap-Antagonist (iap-A) to bind cIAP and release free caspases that facilitate apoptosis. Viral DNA replication triggers host p53 pro-apoptosis, which accelerates IC and EC activity. Progression of antiviral apoptotic signaling cascades is prevented by baculovirus-encoded apoptosis suppressors such as viral IAP (vIAP), p35, p49, and Apsup. When the apoptotic signal is initiated, vIAP blocks apoptosis by interacting with unstable cIAP such that the cIAP levels and antiapoptotic activity are maintained. Viral p35 binds ECs and p49 binds ICs and ECs to block apoptosis. Apsup inhibits apoptosis by preventing IC activity. BmNPV induces the pattern recognition receptor protein *PGRP2-2* to suppress *PTEN* and prevent it from inhibiting PI3K/Akt signaling and activating p-Akt. In this manner, cell apoptosis is inhibited. The resultant increase in cell survival is conducive to NPV proliferation.

cGAMP production in BmE cells and BmSTING responds to the cGAMP and activated Dredd caspase-mediated NF-κB antiviral signaling pathways (69). Antimicrobial peptides (AMPs), humoral immunity, and reactive oxygen species (ROS) may also be involved in the antiviral response (45, 70). Dozens of candidate genes regulating the silkworm immune response to baculovirus have been screened *via* multi-omics using various resistant hosts. However, the functions of only a few of them are verified in cells or individuals. For example, the BmLHA level in the digestive juice of resistant silkworm strains is relatively higher than that of susceptible silkworms, and recombinant BmLHA inhibits BmNPV proliferation in silkworm larvae (48). Similarly, *BmAtlastin-n* is highly expressed in resistant BmE-SWU2 cells but not in BmE-SWU1 cells susceptible to BmNPV, and *BmAtlastin-n* overexpression inhibits BmNPV reproduction in BmE-SWU1 cells and transgenic silkworms (71). Additionally, *B. mori* heat shock protein 19.9 (*Bmhsp19.9*) is upregulated at the late stage after BmNPV challenge in BmE cells and silkworms, and its overexpression markedly inhibits BmNPV proliferation in the hosts (72). Finally, overexpression of lysozyme *BmC-LZM*, which is upregulated at the very late stage of BmNPV infection in BmE cells, inhibits BmNPV virus in BmE cells but does not decrease mortality in silkworm larvae (73). The anti-BmNPV mechanisms of the aforementioned resistance-related genes are unclear and merit further investigation.

VIRAL IMMUNE EVASION MECHANISM

Viruses have developed several strategies to escape host immunity and promote their own replication and proliferation, including inhibition of antiviral melanization, autophagy, apoptosis, RNAi and regulation of the cell cycle (**Figure 2**). Baculoviruses can suppress host melanization so that they can proliferate. Several SPs (serine proteases) and their homologs are upregulated in response to bacterial or fungal challenge but downregulated in response to baculovirus infection (50, 51). For example, when serpins 5 and 9 are induced by HearNPV in *Helicoverpa armigera*, they inhibit SPs and melanization and promote viral infection (51). Similarly, *Bmserpin2* is upregulated and PO activity is diminished in haemolymph following BmNPV infection in silkworm. Hence, BmNPV inhibits host melanization by regulating *Bmserpin2* expression (**Figure 2**) (52). Additionally, several potential resistance-related genes such as *BmPP2A* (74) and *BmPEPCK-2* (75) are downregulated by BmNPV to allow robust viral proliferation.

Autophagy is a catabolic biological process in the body, which has antiviral efficacy by targeting viruses and sending them to the lysosome for phagocytosis and degradation. At the same time, viruses can also use autophagy to enhance their own replication (76). However, little is known about the association between BmNPV and autophagy. *Atg 6*, *Atg 7*, *Atg 8*, and *Atg 13*, proteins involved in various stages of autophagy, are all upregulated in BmN-SWU1 cells (77) but downregulated in BmE cells (75) following BmNPV infection, possibly because of the relative differences among cell lines and internal reference genes used in these experiments. Understanding the roles and mechanisms of such immuno-suppressive processes during BmNPV infection is clearly important for future applications to enhance their impact (for pests) or protecting their hosts (for beneficials) and merit further examination.

Baculoviruses can inhibit host antiviral apoptosis through a variety of strategies (**Figure 3**). The progression of apoptotic signaling cascades is prevented by virus-encoded apoptosis suppressors such as viral IAPs, p35, p49, and Apsup (55, 78, 79). Six IAPs (*iap1-6*) have been identified in baculoviruses that inhibit apoptosis in insects (78–80). Unlike their cellular counterparts, they lack an N-terminal instability motif (81) and stabilize cellular IAPs (82). In a model mechanism, Op-IAP3 derived from OpMNPV blocks apoptosis by interacting with an unstable auto-ubiquitinating host IAP such that cellular IAP levels and antiapoptotic activity are maintained (82). Similarly, IAP1 and IAP2 from BmNPV interact with BmIAP, and both BmIAP and viral IAPs increase BmNPV proliferation in infected silkworm cells (80). Numerous studies have shown that viral protein p35 blocks apoptosis by binding ECs (79, 83, 84), and p49 protein binds ICs and ECs and blocks apoptosis (85, 86). Additionally, Apsup from LdMNPV inhibits apoptosis by preventing proteolytic Dronc (IC) processing (87). Recently, our research demonstrated that peptidoglycan recognition protein (PGRP) is regulated by virus to inhibit host antiviral apoptosis, which is well known to recognize invading bacteria and fungi to activate host immune defenses (54). For example, BmNPV induces *BmPGRP2-2* to suppress *PTEN* and the inhibition of PI3K/Akt signaling, increase p-Akt production and activation, and inhibit cell apoptosis (54). Clearly, enhanced host cell survival is beneficial for viral proliferation (**Figure 3**).

Viruses have evolved strategies to circumvent host antiviral RNAi (siRNA and miRNA pathways). Almost all plant viruses and some insect viruses encode viral suppressors of RNAi (VSRs) to counteract the host siRNA pathway and inhibit vsiRNA production (88, 89). AcMNPV p35 is responsible for the suppression of RNAi in various insect cells; its VSR activity acts downstream in the RNAi pathway and is not associated with its antiapoptotic activity (89). The identification of BmNPV VSRs and clarification of their modes of action require further research. On the other hand, it is evident that baculoviruses exploit the miRNA pathway for their own propagation, suppress cellular miRNAs after infection, encode their own miRNAs, and disrupt host defense mechanisms that interfere with viral propagation (90–92). For example, BmNPV-miR-1 suppresses host miRNA biogenesis by regulating the exportin-5 cofactor Ran and enhancing viral multiplication (92). Simultaneously, BmNPV-miR-3 facilitates viral infection by modulating the expression of P6.9 and other late BmNPV genes (91) (**Figure 2**). Several miRNAs have been predicted in the BmNPV genome; however, only four miRNAs (BmNPV-miR-1, BmNPV-miR-2, BmNPV-miR-3, and BmNPV-miR-4) have been empirically identified (90) and biological functions of only two miRNAs have been uncovered thus far. Deciphering viral miRNA targets and functions remains a challenging task.

Virus regulation of the host cell cycle might be an important immune evasion strategy and could promote its proliferation. The normal insect cell life cycle is characterized by a complex series of events ranging from cell growth to replication, but this process is disrupted during infection (15). Baculovirus infection arrests the cell cycle at S or G2/M. The AcMNPV protein EC27 arrests the host cell cycle in the G2/M phase, and this arrest enables ODV maturation (93, 94). ERK regulates cell proliferation, differentiation, and apoptosis and is conserved among different species (95). The ERK signaling pathway is activated during the late phase of BmNPV infection *via* the *B. mori* epidermal growth factor receptor (BmEGFR). The latter inhibits cell proliferation and increases viral replication by increasing the G2/M phases of the cell cycle (96). *BmSpry* is a negative feedback regulator of the BmEGFR-ERK cascade; its inhibitory activity is upstream of ERK. It is downregulated by BmNPV to elevate ERK phosphorylation (p-ERK), thereby enhancing viral reproduction (95, 97). The modification mechanisms of cell cycle phases during baculovirus infection are only partially elucidated and need more experimentation.

ENHANCEMENT OF HOST ANTIVIRAL CAPACITY

No fundamental strategies have been established to cope with BmNPV during sericulture; instead, this industry mainly relies on thorough disinfection and strict breeding operation techniques to prevent virus infectivity. Breeding resistant host insect strains would help contend with baculovirus infection in sericulture (3, 98, 99). However, enhancing pathogen resistance in the host is usually accomplished at the expense of economically important traits, which is a major constraint in traditional silkworm breeding methods. This compromise may be avoided by applying transgenic and gene editing techniques (3). The antiviral capacity of transgenic silkworms could be enhanced using strategies based on the BmNPV infection process such as inhibiting BmNPV at the initial infection stage *via Bmlipase-1* overexpression (100), targeting BmNPV mRNA with RNAi (21), inhibiting BmNPV protein synthesis by *hycu-ep32* overexpression (101), and suppressing BmNPV by regulating the host immune pathway (54). Antiviral capacity could be further increased by optimizing and integrating the aforementioned anti-BmNPV strategies (41, 42, 102). Transgenic CRISPR/Cas9 system-mediated mutagenesis randomly targeting and inactivating the viral genome has been studied as a potential approach against BmNPV infection in silkworm (103).

Theoretically the inhibitory effect of the CRISPR/Cas9 system (knock out) on the virus should be higher than that of the RNAi system (knock down) when targeting the same viral genes. However, silkworms with inserted DNA fragments expressing dsRNA (21) or gRNA (103) are all transgenic strains and security assessment is an unavoidable challenge under the conditions of mass rearing practiced in sericulture.

Several drugs have been evaluated for their antiviral activity against BmNPV. The bacterial secondary metabolite prodigiosin inhibits BmNPV in BmN cells and is a potential antiviral compound (104). However, its antiviral efficacy must be tested in insect larvae. The single-crystal compound seselin extracted from *Aegle marmelos* (a kind of citrus fruit) shows antiviral activity against BmNPV in silkworm larvae (105). AZD8835, AMG319, HS173, AS605240, GDC0941, BEZ235 are PI3K inhibitors and afuresertib is an Akt inhibitor. These seven drugs target the PI3K/Akt pathway to decrease p-Akt and all inhibit BmNPV in BmE cells; nevertheless, only AMG319 and AZD8835 inhibit viral proliferation in silkworm larvae. Of these two, AZD8835 exhibits a stronger antiviral efficacy which might be due to lower drug toxicity in larvae and stronger inhibition of p-Akt (106). The development of drugs with high antiviral capacity in silkworms could decrease mortality in sericulture. However, their absorption and utilization efficiency, inhibitory efficacy, and cost-effectiveness must be increased while their cytotoxicity is decreased (106).

MAJOR ISSUES IN SILKWORM ANTIVIRAL STUDIES

Several conflicting results have been reported for the same genes in previous studies on the interaction between silkworm and baculovirus. These discrepancies may be explained by the use of different silkworm strains and cell lines as well as inappropriate internal reference genes (RGs). RGs must not be affected by experimental conditions and should be expressed at the same constant level in all samples. Unsuitable RGs lead to the incorrect interpretation of gene expression patterns and functions (107). As a widely used example, actin participates in baculovirus proliferation and expression after viral infection in silkworms (107). Hence, *actin* cannot serve as the RG for mRNA and protein detection in studies involving the interaction between silkworms and viruses. In contrast, *TIF-4A* is an appropriate RG for gene expression analysis (107) and GAPDH (54) is an appropriate internal reference for protein content measurements following viral challenges in silkworms.

Transgenic silkworms with high antiviral capacity have been constructed (102, 103, 108, 109). Nevertheless, their commercial application still faces great challenges. Security assessment must be performed on transgenic silkworms before they are commercialized (3). There are operational guidelines for safety assessments of genetically modified (GM) vertebrates and plants but not for insects, including silkworms. Thus, safety evaluations are difficult to execute on transgenic silkworms. Based on GM animal safety assessment guidelines, we conducted a preliminary evaluation of transgenic silkworms in our laboratory. A classical genetic analysis and molecular characterization of 11 successive generations showed that an inserted foreign DNA fragment was stably inherited in transgenic silkworms (110). The disposition of the inserted DNA in transgenic silkworms fed to chickens was also examined, with no apparent transfer of transgenic DNA from silkworms to chickens (111). A subacute toxicity test comprising a 28 d feeding study in rats showed that transgenic silkworms are toxicologically equivalent to normal silkworms and are safe for rats (112). Transgenic silkworms are unable to survive and reproduce in the field and would not cause environmental risks of competition with other insects, and no interspecific hybridization of transgenic silkworms and *Bombyx mandarina* was observed in nature, so transgenic silkworms have no risks to biodiversity (113). The transgenic silkworms that produce green fluorescent silk have been reared in a sericulture farm in Japan since 2017 (113). Nevertheless, the design of safety assessment procedures and identification of transgenic antiviral silkworm indicators are urgently required as they cannot be the same as those already implemented for GM vertebrates. A notable difference in appropriate safety assessment design is that although GM vertebrates are used for food and feed, transgenic silkworms are used only in silk production.

FUTURE DIRECTIONS OF SILKWORM ANTIVIRUS RESEARCH

Current research on the mechanisms by which baculovirus penetrates its host has focused mainly on BVs and insect cell lines (25, 28–30). Some of the constraints of investigations into the interactions between individual insects and baculovirus include limitations in insect genetic manipulation, long experimental periods, and intensive labor. The PIFs of ODV envelopes form complexes that mediate viral invasion in the insect midgut (16–19). The receptors involved in ODV invasion may also be part of a complex. Screening and identifying ODV receptor genes in the silkworm midgut are difficult exercises. The process of ODV entry must first be clarified in order to develop methods to block BmNPV infection in silkworm. Earlier studies reported that the resistance of silkworms to BmNPV is controlled by major genes and modified by minor genes (98); however, a major resistance gene has not yet been identified despite numerous attempts using various methods. Identification of resistance genes and analysis of silkworm antiviral mechanisms against BmNPV merit further investigation. In future experiments, we will screen for negative regulatory factors in the immune pathway using genome-wide CRISPR (114) and identify the host proteins that bind the virus by use of inhibitors. The target genes will be knocked out *via* gene editing to improve silkworm resistance. Immune priming is a new strategy to increase host antiviral capacity (115, 116) and we will clarify its mechanism of action in silkworm. The influences of gut microbes, heat shock response, and DNA methylation on viral silkworm infections will also be evaluated.

The baculovirus expression vector system (BEVS) is a bioreactor for the production of recombinant proteins and

vaccines. Several vaccines produced by BEVS have been approved for human and/or veterinary use (15, 117, 118). The BEVS was invented using AcMNPV in combination with an insect cell system (117). However, the cost of silkworm rearing is much lower than that of insect cell culture, promoting the use of BmNPV to generate foreign proteins using silkworm larvae as bioreactors. Understanding the baculovirus infection mechanism including modification of host and viral proteins will facilitate application of a combined BmNPV-silkworm system in production of high value-added medical proteins. Explorations of the silkworm immune response to baculovirus will help construct silkworms less sensitive to BmNPV by inhibiting the host immune system and resistance genes, and in combination with BmNPV with attenuated virulence, further reduce the costs of foreign protein fabrication.

Baculoviruses have been applied worldwide as biopesticides for the control of various insect pests (119, 120). Compared to chemical pesticides, baculoviruses are environmentally safe. Nevertheless, their killing rates are low, and their host range is narrow (15, 31, 119). In the future, baculovirus should be modified to expand its target pest host range. Its antagonism against the host immune defense must be strengthened by accentuating viral host immune evasion mechanisms which will enable use of lower viral titers to kill pests faster. Less sensitive insect bioreactors for baculovirus-based biopesticides should be designed to reduce production costs. Further investigations into silkworm antiviral mechanisms will provide a reverse theoretical basis and reference for biological insect pest control.

CONCLUSION

Viruses exert strong selection pressure on their hosts to evolve resistance pathways. In turn, these genetic modifications enable viruses to escape host antiviral mechanisms. This arms race favors host defense diversification and the development of viral escape mechanisms (37). Several factors contribute to viral coevolution with its natural host. A complete elucidation of antiviral immunity and immune evasion is challenging as numerous complex pathways are involved (37). Hence, BmNPV research should focus on actual silkworms rather than cell lines and novel technologies such as gene editing and value-added protein biosynthesis. Studies involving the silkworm–baculovirus model are highly informative as they disclose original antiviral strategies, immune evasion mechanisms, and weaknesses of viruses. In this way, genetic antiviral improvement of silkworms may be achieved along with the development of more effective approaches to control lepidopteran and other insect pests. These applications, along with the realization of more productive and efficient bioreactors for novel baculovirus-insect-derived products, are promising applications for the future.

AUTHOR CONTRIBUTIONS

LJ: analyzed data, drew figure, drafted the article, and supervision. MG: review and editing. QX: supervision. All authors contributed to the article and approved the submitted version.

ACKNOWLEDGMENTS

We thank Prof. Zhihong Hu for critical reading of the manuscript. This work was funded by the National Natural Science Foundation of China (no. 31501875), the Fundamental Research Funds for the Central Universities (SWU120029, XDJK2020C006), and the Venture & Innovation Support Program for Chongqing Overseas Returnees (cx2019152).

REFERENCES

1. Kawahara AY, Plotkin D, Espeland M, Meusemann K, Toussaint EFA, Donath A, et al. Phylogenomics reveals the evolutionary timing and pattern of butterflies and moths. *Proc Natl Acad Sci U S A* (2019) 116(45):22657–63. doi: 10.1073/pnas.1907847116
2. Misof B, Liu S, Meusemann K, Peters RS, Donath A, Mayer C, et al. Phylogenomics resolves the timing and pattern of insect evolution. *Science* (2014) 346(6210):763–7. doi: 10.1126/science.1257570
3. Jiang L, Xia Q. The progress and future of enhancing antiviral capacity by transgenic technology in the silkworm *Bombyx mori*. *Insect Biochem Mol Biol* (2014) 48:1–7. doi: 10.1016/j.ibmb.2014.02.003
4. Goldsmith MR, Shimada T, Abe H. The genetics and genomics of the silkworm, *Bombyx mori*. *Annu Rev Entomol* (2005) 50:71–100. doi: 10.1146/annurev.ento.50.071803.130456
5. Xia Q, Zhou Z, Lu C, Cheng D, Dai F, Li B, et al. A draft sequence for the genome of the domesticated silkworm (*Bombyx mori*). *Science* (2004) 306 (5703):1937–40. doi: 10.1126/science.1102210
6. Mita K, Kasahara M, Sasaki S, Nagayasu Y, Yamada T, Kanamori H, et al. The genome sequence of silkworm, *Bombyx mori*. *DNA Res An Int J Rapid Publ Rep Genes Genomes* (2004) 11(1):27–35. doi: 10.1093/dnares/11.1.27
7. International Silkworm Genome, C. The genome of a lepidopteran model insect, the silkworm *Bombyx mori*. *Insect Biochem Mol Biol* (2008) 38 (12):1036–45. doi: 10.1016/j.ibmb.2008.11.004
8. Xia Q, Guo Y, Zhang Z, Li D, Xuan Z, Li Z, et al. Complete resequencing of 40 genomes reveals domestication events and genes in silkworm (Bombyx). *Science* (2009) 326(5951):433–6. doi: 10.1126/science.1176620
9. Xia Q, Li S, Feng Q. Advances in silkworm studies accelerated by the genome sequencing of *Bombyx mori*. *Annu Rev Entomol* (2014) 59:513–36. doi: 10.1146/annurev-ento-011613-161940
10. Gomi S, Majima K, Maeda S. Sequence analysis of the genome of *Bombyx mori* nucleopolyhedrovirus. *J Gen Virol* (1999) 80(Pt 5):1323–37. doi: 10.1099/0022-1317-80-5-1323
11. Keddie BA, Aponte GW, Volkman LE. The pathway of infection of Autographa californica nuclear polyhedrosis virus in an insect host. *Science* (1989) 243(4899):1728–30. doi: 10.1126/science.2648574
12. Blissard GW, Theilmann DA. Baculovirus Entry and Egress from Insect Cells. *Annu Rev Virol* (2018) 5:113–39. doi: 10.1146/annurev-virology-092917-043356
13. Rahman MM, Gopinathan KP. Systemic and in vitro infection process of *Bombyx mori* nucleopolyhedrovirus. *Virus Res* (2004) 101(2):109–18. doi: 10.1016/j.virusres.2003.12.027

14. Feng M, Kong X, Zhang J, Xu W, Wu X. Identification of a novel host protein SINAL10 interacting with GP64 and its role in *Bombyx mori* nucleopolyhedrovirus infection. *Virus Res* (2018) 247:102–10. doi: 10.1016/j.virusres.2018.02.005
15. Saxena A, Byram PK, Singh SK, Chakraborty J, Murhammer D, Giri L. A structured review of baculovirus infection process: integration of mathematical models and biomolecular information on cell-virus interaction. *J Gen Virol* (2018) 99(9):1151–71. doi: 10.1099/jgv.0.001108
16. Xiang X, Chen L, Guo A, Yu S, Yang R, Wu X. The *Bombyx mori* nucleopolyhedrovirus (BmNPV) ODV-E56 envelope protein is also a per os infectivity factor. *Virus Res* (2011) 155(1):69–75. doi: 10.1016/j.virusres.2010.08.024
17. Boogaard B, van Lent JWM, Theilmann DA, Erlandson MA, van Oers MM. Baculoviruses require an intact ODV entry-complex to resist proteolytic degradation of per os infectivity factors by co-occluded proteases from the larval host. *J Gen Virol* (2017) 98(12):3101–10. doi: 10.1099/jgv.0.000974
18. Wang X, Shang Y, Chen C, Liu SR, Chang M, Zhang N, et al. Baculovirus Per Os Infectivity Factor Complex: Components and Assembly. *J Virol* (2019) 93 (6):e02053-18. doi: 10.1128/JVI.02053-18
19. Boogaard B, van Oers MM, van Lent JWM. An Advanced View on Baculovirus per Os Infectivity Factors. *Insects* (2018) 9(3):84. doi: 10.3390/insects9030084
20. Huh NE, Weaver RF. Categorizing Some Early and Late Transcripts Directed by the Autographa-Californica Nuclear Polyhedrosis-Virus. *J Gen Virol* (1990) 71:2195–200. doi: 10.1099/0022-1317-71-9-2195
21. Jiang L, Zhao P, Wang GH, Cheng TC, Yang Q, Jin SK, et al. Comparison of factors that may affect the inhibitory efficacy of transgenic RNAi targeting of baculoviral genes in silkworm, *Bombyx mori*. *Antivir Res* (2013) 97(3):255–63. doi: 10.1016/j.antiviral.2012.12.020
22. Slack J, Arif BM. The baculoviruses occlusion-derived virus: Virion structure and function. *Adv Virus Res* (2007) 69:99–165. doi: 10.1016/S0065-3527(06)69003-9
23. Engelhard EK, Kammorgan LNW, Washburn JO, Volkman LE. The Insect Tracheal System - a Conduit for the Systemic Spread of Autographa-Californica-M Nuclear Polyhedrosis-Virus. *Proc Natl Acad Sci U S A* (1994) 91(8):3224–7. doi: 10.1073/pnas.91.8.3224
24. Braunagel SC, Summers MD. Molecular biology of the baculovirus occlusion-derived virus envelope. *Curr Drug Targets* (2007) 8(10):1084–95. doi: 10.2174/138945007782151315
25. Feng M, Zhang JJ, Xu WF, Wang HP, Kong XS, Wu XF. *Bombyx mori* nucleopolyhedrovirus utilizes a clathrin and dynamin dependent endocytosis entry pathway into BmN cells. *Virus Res* (2018) 253:12–9. doi: 10.1016/j.virusres.2018.05.020
26. Kataoka C, Kaname Y, Taguwa S, Abe T, Fukuhara T, Tani H, et al. Baculovirus GP64-Mediated Entry into Mammalian Cells. *J Virol* (2012) 86(5):2610–20. doi: 10.1128/JVI.06704-11
27. Luz-Madrigal A, Asanov A, Camacho-Zarco AR, Sampieri A, Vaca L. A Cholesterol Recognition Amino Acid Consensus Domain in GP64 Fusion Protein Facilitates Anchoring of Baculovirus to Mammalian Cells. *J Virol* (2013) 87(21):11894–907. doi: 10.1128/JVI.01356-13
28. Huang JS, Hao BF, Cheng C, Liang F, Shen XJ, Cheng XW. Entry of *Bombyx mori* nucleopolyhedrovirus into BmN cells by cholesterol-dependent macropinocytic endocytosis. *Biochem Bioph Res Co* (2014) 453(1):166–71. doi: 10.1016/j.bbrc.2014.09.073
29. Li ZH, Fan YP, Wei JH, Mei XOG, He Q, Zhang YH, et al. Baculovirus Utilizes Cholesterol Transporter NIEMANN-Pick C1 for Host Cell Entry. *Front Microbiol* (2019) 10:2825. doi: 10.3389/fmicb.2019.02825
30. Dong XL, Liu TH, Wang W, Pan CX, Wu YF, Du GY, et al. BmREEPa Is a Novel Gene that Facilitates BmNPV Entry into Silkworm Cells. *PLoS One* (2015) 10(12):e0144575. doi: 10.1371/journal.pone.0144575
31. Wang ML, Hu ZH. Cross-talking between baculoviruses and host insects towards a successful infection. *Philos T R Soc B* (2019) 374(1767):20180324. doi: 10.1098/rstb.2018.0324
32. Katsuma S, Kawaoka S, Mita K, Shimada T. Genome-wide survey for baculoviral host homologs using the Bombyx genome sequence. *Insect Biochem Mol Biol* (2008) 38(12):1080–6. doi: 10.1016/j.ibmb.2008.05.008
33. Katsuma S. Phosphatase activity of *Bombyx mori* nucleopolyhedrovirus PTP is dispensable for enhanced locomotory activity in B. mori larvae. *J Invertebr Pathol* (2015) 132:228–32. doi: 10.1016/j.jip.2015.11.002
34. Wang F, Xue RJ, Li XY, Hu CM, Xia QY. Characterization of a protein tyrosine phosphatase as a host factor promoting baculovirus replication in silkworm, *Bombyx mori*. *Dev Comp Immunol* (2016) 57:31–7. doi: 10.1016/j.dci.2015.12.002
35. Zhang X, Xue R, Cao G, Hu X, Wang X, Pan Z, et al. Effects of egt gene transfer on the development of *Bombyx mori*. *Gene* (2012) 491(2):272–7. doi: 10.1016/j.gene.2011.09.026
36. Kingsolver MB, Huang ZJ, Hardy RW. Insect Antiviral Innate Immunity: Pathways, Effectors, and Connections. *J Mol Biol* (2013) 425(24):4921–36. doi: 10.1016/j.jmb.2013.10.006
37. Marques JT, Imler JL. The diversity of insect antiviral immunity: insights from viruses. *Curr Opin Microbiol* (2016) 32:71–6. doi: 10.1016/j.mib.2016.05.002
38. Hamajima R, Saito A, Makino S, Kobayashi M, Ikeda M. Antiviral immune responses of *Bombyx mori* cells during abortive infection with Autographa californica multiple nucleopolyhedrovirus. *Virus Res* (2018) 258:28–38. doi: 10.1016/j.virusres.2018.09.014
39. Ikeda M, Yamada H, Hamajima R, Kobayashi M. Baculovirus genes modulating intracellular innate antiviral immunity of lepidopteran insect cells. *Virology* (2013) 435(1):1–13. doi: 10.1016/j.virol.2012.10.016
40. Hamajima R, Kobayashi M, Ikeda M. Identification of amino acid residues of AcMNPV P143 protein involved in rRNA degradation and restricted viral replication in BM-N cells from the silkworm *Bombyx mori*. *Virology* (2015) 485:244–51. doi: 10.1016/j.virol.2015.08.008
41. Jiang L, Cheng TC, Dang YH, Peng ZW, Zhao P, Liu SP, et al. Identification of a midgut-specific promoter in the silkworm *Bombyx mori*. *Biochem Bioph Res Co* (2013) 433(4):542–6. doi: 10.1016/j.bbrc.2013.03.019
42. Jiang L, Huang CL, Sun Q, Guo HZ, Cheng TC, Peng ZW, et al. The 5 '-UTR intron of the midgut-specific BmAPN4 gene affects the level and location of expression in transgenic silkworms. *Insect Biochem Mol Biol* (2015) 63:1–6. doi: 10.1016/j.ibmb.2015.05.005
43. Ponnuvel KM, Nakazawa H, Furukawa S, Asaoka A, Ishibashi J, Tanaka H, et al. A lipase isolated from the silkworm *Bombyx mori* shows antiviral activity against nucleopolyhedrovirus. *J Virol* (2003) 77(19):10725–9. doi: 10.1128/JVI.77.19.10725-10729.2003
44. Nakazawa H, Tsuneishi E, Ponnuvel KM, Furukawa S, Asaoka A, Tanaka H, et al. Antiviral activity of a serine protease from the digestive juice of *Bombyx mori* larvae against nucleopolyhedrovirus. *Virology* (2004) 321(1):154–62. doi: 10.1016/j.virol.2003.12.011
45. Selot R, Kumar V, Shukla S, Chandrakuntal K, Brahmaraju M, Dandin SB, et al. Identification of a soluble NADPH oxidoreductase (BmNOX) with antiviral activities in the gut juice of *Bombyx mori*. *Biosci Biotechnol Biochem* (2007) 71(1):200–5. doi: 10.1271/bbb.60450
46. Sunagar SG, Savanurmath CJ, Hinchigeri SB. The profiles of red fluorescent proteins with antinucleopolyhedrovirus activity in races of the silkworm *Bombyx mori*. *J Insect Physiol* (2011) 57(12):1707–14. doi: 10.1016/j.jinsphys.2011.09.009
47. Ponnuvel KM, Nithya K, Sirigineedi S, Awasthi AK, Yamakawa M. In Vitro Antiviral Activity of an Alkaline Trypsin from the Digestive Juice of *Bombyx Mori* Larvae against Nucleopolyhedrovirus. *Arch Insect Biochem* (2012) 81 (2):90–104. doi: 10.1002/arch.21046
48. Zhang SZ, Zhu LB, You LL, Wang J, Cao HH, Liu YX, et al. A Novel Digestive Proteinase Lipase Member H-A in *Bombyx mori* Contributes to Digestive Juice Antiviral Activity Against B. mori Nucleopolyhedrovirus. *Insects* (2020) 11(3):154. doi: 10.3390/insects11030154
49. Lin YH, Tai CC, Broz V, Tang CK, Chen P, Wu CP, et al. Adenosine Receptor Modulates Permissiveness of Baculovirus (Budded Virus) Infection via Regulation of Energy Metabolism in *Bombyx mori*. *Front Immunol* (2020) 11:763. doi: 10.3389/fimmu.2020.00763
50. Wang Q, Yin M, Yuan C, Liu X, Hu Z, Zou Z, et al. Identification of a Conserved Prophenoloxidase Activation Pathway in Cotton Bollworm Helicoverpa armigera. *Front Immunol* (2020) 11:785. doi: 10.3389/fimmu.2020.00785
51. Yuan CF, Xing LS, Wang ML, Wang X, Yin MY, Wang QR, et al. Inhibition of melanization by serpin-5 and serpin-9 promotes baculovirus infection in cotton bollworm Helicoverpa armigera. *PLoS Pathog* (2017) 13(9):e1006645. doi: 10.1371/journal.ppat.1006645
52. Toufeeq S, Wang J, Zhang SZ, Li B, Hu P, Zhu LB, et al. Bmserpin2 Is Involved in BmNPV Infection by Suppressing Melanization in *Bombyx mori*. *Insects* (2019) 10(11):399. doi: 10.3390/insects10110399

53. Makino S, Hamajima R, Saito A, Tomizaki M, Iwamoto A, Kobayashi M, et al. *Bombyx mori* homolog of tumor suppressor p53 is involved in apoptosis-mediated antiviral immunity of B-mori cells infected with nucleopolyhedrovirus. *Dev Comp Immunol* (2018) 84:133–41. doi: 10.1016/j.dci.2018.02.009
54. Jiang L, Liu WQ, Guo HZ, Dang YH, Cheng TC, Yang WY, et al. Distinct Functions of *Bombyx mori* Peptidoglycan Recognition Protein 2 in Immune Responses to Bacteria and Viruses. *Front Immunol* (2019) 10:776. doi: 10.3389/fimmu.2019.00776
55. Clem RJ. The role of apoptosis in defense against baculovirus infection in insects. *Curr Topics Microbiol Immunol* (2005) 289:113–29. doi: 10.1007/3-540-27320-4_5
56. Timmer JC, Salvesen GS. Caspase substrates. *Cell Death Differ* (2007) 14 (1):66–72. doi: 10.1038/sj.cdd.4402059
57. Courtiade J, Pauchet Y, Vogel H, Heckel DG. A comprehensive characterization of the caspase gene family in insects from the order Lepidoptera. *BMC Genomics* (2011) 12:357. doi: 10.1186/1471-2164-12-357
58. Hamajima R, Iwamoto A, Tomizaki M, Suganuma I, Kitaguchi K, Kobayashi M, et al. Functional analysis of inhibitor of apoptosis 1 of the silkworm *Bombyx mori*. *Insect Biochem Mol Biol* (2016) 79:97–107. doi: 10.1016/j.ibmb.2016.10.012
59. Huang N, Wu WB, Yang K, Passarelli AL, Rohrmann GF, Clem RJ. Baculovirus Infection Induces a DNA Damage Response That Is Required for Efficient Viral Replication. *J Virol* (2011) 85(23):12547–56. doi: 10.1128/JVI.05766-11
60. Mitchell JK, Friesen PD. Baculoviruses Modulate a Proapoptotic DNA Damage Response To Promote Virus Multiplication. *J Virol* (2012) 86 (24):13542–53. doi: 10.1128/JVI.02246-12
61. Vandergaast R, Schultz KLW, Cerio RJ, Friesen PD. Active Depletion of Host Cell Inhibitor-of-Apoptosis Proteins Triggers Apoptosis upon Baculovirus DNA Replication. *J Virol* (2011) 85(16):8348–58. doi: 10.1128/JVI.00667-11
62. Vogel E, Santos D, Mingels L, Verdonckt TW, Vanden Broeck J. RNA Interference in Insects: Protecting Beneficials and Controlling Pests. *Front Physiol* (2019) 9:1912. doi: 10.3389/fphys.2018.01912
63. Jayachandran B, Hussain M, Asgari S. RNA Interference as a Cellular Defense Mechanism against the DNA Virus Baculovirus. *J Virol* (2012) 86 (24):13729–34. doi: 10.1128/JVI.02041-12
64. van Mierlo JT, van Cleef KW, van Rij RP. Defense and counterdefense in the RNAi-based antiviral immune system in insects. *Methods Mol Biol* (2011) 721:3–22. doi: 10.1007/978-1-61779-037-9_1
65. Seitz H, Ghildiyal M, Zamore PD. Argonaute loading improves the 5' precision of both MicroRNAs and their miRNA* strands in flies. *Curr Biol* (2008) 18(2):147–51. doi: 10.1016/j.cub.2007.12.049
66. Wu P, Shang Q, Dweteh OA, Huang HL, Zhang SL, Zhong JB, et al. Over expression of bmo-miR-2819 suppresses BmNPV replication by regulating the BmNPV ie-1 gene in *Bombyx mori*. *Mol Immunol* (2019) 109:134–9. doi: 10.1016/j.molimm.2019.03.013
67. Kang LQ, Wang ML, Cao XL, Tang SM, Xia DG, Shen XJ, et al. Inhibition of expression of BmNPV cg30 by bmo-miRNA-390 is a host response to baculovirus invasion. *Arch Virol* (2018) 163(10):2719–25. doi: 10.1007/s00705-018-3912-9
68. Wang GH, Jiang L, Zhu L, Cheng TC, Niu WH, Yan YF, et al. Characterization of Argonaute family members in the silkworm, *Bombyx mori*. *Insect Sci* (2013) 20(1):78–91. doi: 10.1111/j.1744-7917.2012.01555.x
69. Hua X, Li B, Song L, Hu C, Li X, Wang D, et al. Stimulator of interferon genes (STING) provides insect antiviral immunity by promoting Dredd caspase-mediated NF-kappaB activation. *J Biol Chem* (2018) 293(30):11878–90. doi: 10.1074/jbc.RA117.000194
70. Lu P, Pan Y, Yang YH, Zhu FF, Li CJ, Guo ZJ, et al. Discovery of anti-viral molecules and their vital functions in *Bombyx mori*. *J Invertebr Pathol* (2018) 154:12–8. doi: 10.1016/j.jip.2018.02.012
71. Liu TH, Dong XL, Pan CX, Du GY, Wu YF, Yang JG, et al. A newly discovered member of the Atlastin family, BmAtlastin-n, has an antiviral effect against BmNPV in *Bombyx mori*. *Sci Rep-Uk* (2016) 6:28946. doi: 10.1038/srep28946
72. Jiang L, Xie EY, Guo HZ, Sun Q, Liuli HY, Wang YM, et al. Heat shock protein 19.9 (Hsp19.9) from *Bombyx mori* is involved in host protection against viral infection. *Dev Comp Immunol* (2021) 114:103790. doi: 10.1016/j.dci.2020.103790
73. Chen TT, Tan LR, Hu N, Dong ZQ, Hu ZG, Jiang YM, et al. C-lysozyme contributes to antiviral immunity in *Bombyx mori* against nucleopolyhedrovirus infection. *J Insect Physiol* (2018) 108:54–60. doi: 10.1016/j.jinsphys.2018.05.005
74. Hu ZG, Dong ZQ, Dong FF, Zhu Y, Chen P, Lu C, et al. Identification of a PP2A gene in *Bombyx mori* with antiviral function against B. mori nucleopolyhedrovirus. *Insect Sci* (2020) 27(4):687–96. doi: 10.1111/1744-7917.12678
75. Guo HZ, Xu GW, Wang BB, Xia F, Sun Q, Wang YM, et al. Phosphoenolpyruvate carboxykinase is involved in antiviral immunity against *Bombyx mori* nucleopolyhedrovirus. *Dev Comp Immunol* (2019) 92:193–8. doi: 10.1016/j.dci.2018.11.015
76. Yin HC, Shao SL, Jiang XJ, Xie PY, Sun WS, Yu TF. Interactions between Autophagy and DNA Viruses. *Viruses-Basel* (2019) 11(9):776. doi: 10.3390/v11090776
77. Wang L, Xiao Q, Zhou XL, Zhu Y, Dong ZQ, Chen P, et al. *Bombyx mori* Nuclear Polyhedrosis Virus (BmNPV) Induces Host Cell Autophagy to Benefit Infection. *Viruses-Basel* (2018) 10(1):14. doi: 10.3390/v10010014
78. Clem RJ. Baculoviruses and apoptosis: the good, the bad, and the ugly. *Cell Death Differ* (2001) 8(2):137–43. doi: 10.1038/sj.cdd.4400821
79. Clem RJ. Baculoviruses and apoptosis: a diversity of genes and responses. *Curr Drug Targets* (2007) 8(10):1069–74. doi: 10.2174/138945007782151405
80. Chen P, Kang TT, Bao XY, Dong ZQ, Zhu Y, Xiao WF, et al. Evolutionary and functional analyses of the interaction between the *Bombyx mori* inhibitor of apoptosis (IAP) and nucleopolyhedrovirus IAPs. *Insect Sci* (2020) 27(3):463–74. doi: 10.1111/1744-7917.12664
81. Vandergaast R, Mitchell JK, Byers NM, Friesen PD. Insect Inhibitor-of-Apoptosis (IAP) Proteins Are Negatively Regulated by Signal-Induced N-Terminal Degrons Absent within Viral IAP Proteins. *J Virol* (2015) 89 (8):4481–93. doi: 10.1128/JVI.03659-14
82. Byers NM, Vandergaast RL, Friesen PD. Baculovirus Inhibitor-of-Apoptosis Op-IAP3 Blocks Apoptosis by Interaction with and Stabilization of a Host Insect Cellular IAP. *J Virol* (2016) 90(1):533–44. doi: 10.1128/JVI.02320-15
83. Bump NJ, Hackett M, Hugunin M, Seshagiri S, Brady K, Chen P, et al. Inhibition of Ice Family Proteases by Baculovirus Antiapoptotic Protein P35. *Science* (1995) 269(5232):1885–8. doi: 10.1126/science.7569933
84. Nakanishi T, Shimada T, Katsuma S. Characterization of a *Bombyx mori* nucleopolyhedrovirus mutant lacking both fp25K and p35. *Virus Genes* (2010) 41(1):144–8. doi: 10.1007/s11262-010-0492-5
85. Jabbour AM, Ekert PG, Coulson EJ, Knight MJ, Ashley DM, Hawkins CJ. The p35 relative, p49, inhibits mammalian and Drosophila caspases including DRONC and protects against apoptosis. *Cell Death Differ* (2002) 9(12):1311–20. doi: 10.1038/sj.cdd.4401135
86. Guy MP, Friesen PD. Reactive-site cleavage residues confer target specificity to baculovirus P49, a dimeric member of the P35 family of caspase inhibitors. *J Virol* (2008) 82(15):7504–14. doi: 10.1128/JVI.00231-08
87. Yamada H, Kitaguchi K, Hamajima R, Kobayashi M, Ikeda M. Novel Apoptosis Suppressor Apsup from the Baculovirus Lymantria dispar Multiple Nucleopolyhedrovirus Precludes Apoptosis by Preventing Proteolytic Processing of Initiator Caspase Dronc. *J Virol* (2013) 87 (23):12925–34. doi: 10.1128/JVI.02065-13
88. Ding SW, Voinnet O. Antiviral immunity directed by small RNAs. *Cell* (2007) 130(3):413–26. doi: 10.1016/j.cell.2007.07.039
89. Mehrabadi M, Hussain M, Matindoost L, Asgari S. The Baculovirus Antiapoptotic p35 Protein Functions as an Inhibitor of the Host RNA Interference Antiviral Response. *J Virol* (2015) 89(16):8182–92. doi: 10.1128/JVI.00802-15
90. Singh J, Singh CP, Bhavani A, Nagaraju J. Discovering microRNAs from *Bombyx mori* nucleopolyhedrosis virus. *Virology* (2010) 407(1):120–8. doi: 10.1016/j.virol.2010.07.033
91. Singh CP, Singh J, Nagaraju J. bmnpv-miR-3 facilitates BmNPV infection by modulating the expression of viral P6.9 and other late genes in *Bombyx mori*. *Insect Biochem Mol Biol* (2014) 49:59–69. doi: 10.1016/j.ibmb.2014.03.008
92. Singh CP, Singh J, Nagaraju J. A baculovirus-encoded MicroRNA (miRNA) suppresses its host miRNA biogenesis by regulating the exportin-5 cofactor Ran. *J Virol* (2012) 86(15):7867–79. doi: 10.1128/JVI.00064-12

93. Davy C, Doorbar J. G2/M cell cycle arrest in the life cycle of viruses. *Virology* (2007) 368(2):219–26. doi: 10.1016/j.virol.2007.05.043
94. Belyavskyi M, Braunagel SC, Summers MD. The structural protein ODV-EC27 of Autographa californica nucleopolyhedrovirus is a multifunctional viral cyclin. *Proc Natl Acad Sci U S A* (1998) 95(19):11205–10. doi: 10.1073/pnas.95.19.11205
95. Guo HZ, Sun Q, Wang BB, Wang YM, Xie EY, Xia QY, et al. Spry is downregulated by multiple viruses to elevate ERK signaling and ensure viral reproduction in silkworm. *Dev Comp Immunol* (2019) 98:1–5. doi: 10.1016/j.dci.2019.04.001
96. Jin S, Cheng T, Guo Y, Lin P, Zhao P, Liu C, et al. *Bombyx mori* epidermal growth factor receptor is required for nucleopolyhedrovirus replication. *Insect Mol Biol* (2018) 27(4):464–77. doi: 10.1111/imb.12386
97. Jin SK, Cheng TC, Jiang L, Lin P, Yang Q, Xiao Y, et al. Identification of a New Sprouty Protein Responsible for the Inhibition of the *Bombyx mori* Nucleopolyhedrovirus Reproduction. *PLoS One* (2014) 9(6):e99200. doi: 10.1371/journal.pone.0099200
98. Cheng Y, Wang XY, Du C, Gao J, Xu JP. Expression analysis of several antiviral related genes to BmNPV in different resistant strains of silkworm, *Bombyx mori*. *J Insect Sci* (2014) 14:76. doi: 10.1673/031.014.76
99. Chen TT, Hu N, Tan LR, Xiao Q, Dong ZQ, Chen P, et al. Resistant silkworm strain block viral infection independent of melanization. *Pestic Biochem Phys* (2019) 154:88–96. doi: 10.1016/j.pestbp.2018.12.012
100. Jiang L, Wang GH, Cheng TC, Yang Q, Jin SK, Lu G, et al. Resistance to *Bombyx mori* nucleopolyhedrovirus via overexpression of an endogenous antiviral gene in transgenic silkworms. *Arch Virol* (2012) 157(7):1323–8. doi: 10.1007/s00705-012-1309-8
101. Jiang L, Cheng TC, Zhao P, Yang Q, Wang GH, Jin SK, et al. Resistance to BmNPV via Overexpression of an Exogenous Gene Controlled by an Inducible Promoter and Enhancer in Transgenic Silkworm, *Bombyx mori*. *PLoS One* (2012) 7(8):e41838. doi: 10.1371/journal.pone.0041838
102. Jiang L, Zhao P, Cheng TC, Sun Q, Peng ZW, Dang YH, et al. A transgenic animal with antiviral properties that might inhibit multiple stages of infection. *Antivir Res* (2013) 98(2):171–3. doi: 10.1016/j.antiviral.2013.02.015
103. Chen SQ, Hou CX, Bi HL, Wang YQ, Xu J, Li MW, et al. Transgenic Clustered Regularly Interspaced Short Palindromic Repeat/Cas9-Mediated Viral Gene Targeting for Antiviral Therapy of *Bombyx mori* Nucleopolyhedrovirus. *J Virol* (2017) 91(8):e02465-16. doi: 10.1128/JVI.02465-16
104. Zhou W, Zeng C, Liu RH, Chen J, Li R, Wang XY, et al. Antiviral activity and specific modes of action of bacterial prodigiosin against *Bombyx mori* nucleopolyhedrovirus in vitro. *Appl Microbiol Biot* (2016) 100(9):3979–88. doi: 10.1007/s00253-015-7242-5
105. Somu C, Karuppiah H, Sundaram J. Antiviral activity of seselin from Aegle marmelos against nuclear polyhedrosis virus infection in the larvae of silkworm, *Bombyx mori*. *J Ethnopharmacol* (2019) 245:112155. doi: 10.1016/j.jep.2019.112155
106. Wang BB, Jiang L, Guo HZ, Sun Q, Wang YM, Xie EY, et al. Screening of PI3K-Akt-targeting Drugs for Silkworm against *Bombyx mori* Nucleopolyhedrovirus. *Molecules* (2019) 24(7):1260. doi: 10.3390/molecules24071260
107. Guo HZ, Jiang L, Xia QY. Selection of reference genes for analysis of stress-responsive genes after challenge with viruses and temperature changes in the silkworm *Bombyx mori*. *Mol Genet Genomics* (2016) 291(2):999–1004. doi: 10.1007/s00438-015-1125-4
108. Jiang L, Peng ZW, Guo HZ, Sun JC, Sun Q, Xia F, et al. Enhancement of antiviral capacity of transgenic silkworms against cytoplasmic polyhedrosis virus via knockdown of multiple viral genes. *Dev Comp Immunol* (2017) 77:138–40. doi: 10.1016/j.dci.2017.07.020
109. Sun Q, Jiang L, Guo HZ, Xia F, Wang BB, Wang YM, et al. Increased antiviral capacity of transgenic silkworm via knockdown of multiple genes on *Bombyx mori* bidensovirus. *Dev Comp Immunol* (2018) 87:188–92. doi: 10.1016/j.dci.2018.06.002
110. Jiang L, Sun Q, Liu WQ, Guo HZ, Peng ZW, Dang YH, et al. Postintegration stability of the silkworm piggyBac transposon. *Insect Biochem Mol Biol* (2014) 50:18–23. doi: 10.1016/j.ibmb.2014.03.006
111. Wang YM, Wang ZL, Guo HZ, Huang J, Li XY, Sun Q, et al. Potential of transferring transgenic DNA from silkworm to chicken. *Int J Biol Macromol* (2020) 142:311–9. doi: 10.1016/j.ijbiomac.2019.09.102
112. Jiang L, Wang YM, Guo HZ, Sun Q, Xie EY, Liuli HY, et al. Toxicological evaluation of transgenic silkworms. *Toxicol Res* (2020) 9(6):845–53. doi: 10.1093/toxres/tfaa089
113. Kômoto N, Tomita S. Risk Assessment of Transgenic Silkworms. *GMOs Topics Biodiversity Conserv 19*. (2020). doi: 10.1007/978-3-030-53183-6_10
114. Chang J, Wang R, Yu K, Zhang T, Chen X, Liu Y, et al. Genome-wide CRISPR screening reveals genes essential for cell viability and resistance to abiotic and biotic stresses in *Bombyx mori*. *Genome Res* (2020) 30(5):757–67. doi: 10.1101/gr.249045.119
115. Valdez A, Yepiz-Plascencia G, Ricca E, Olmos J. First Litopenaeus vannamei WSSV 100% oral vaccination protection using CotC::Vp26 fusion protein displayed on Bacillus subtilis spores surface. *J Appl Microbiol* (2014) 117 (2):347–57. doi: 10.1111/jam.12550
116. Tidbury HJ, Pedersen AB, Boots M. Within and transgenerational immune priming in an insect to a DNA virus. *P Roy Soc B-Biol Sci* (2011) 278 (1707):871–6. doi: 10.1098/rspb.2010.1517
117. Smith GE, Summers MD, Fraser MJ. Production of human beta interferon in insect cells infected with a baculovirus expression vector. *Mol Cell Biol* (1983) 3(12):2156–65. doi: 10.1128/MCB.3.12.2156
118. van Oers MM, Pijlman GP, Vlak JM. Thirty years of baculovirus-insect cell protein expression: from dark horse to mainstream technology. *J Gen Virol* (2015) 96(Pt 1):6–23. doi: 10.1099/vir.0.067108-0
119. Moscardi F. Assessment of the application of baculoviruses for control of Lepidoptera. *Annu Rev Entomol* (1999) 44:257–89. doi: 10.1146/annurev.ento.44.1.257
120. Lacey LA, Grzywacz D, Shapiro-Ilan DII, Frutos R, Brownbridge M, Goettel MS. Insect pathogens as biological control agents: Back to the future. *J Invertebr Pathol* (2015) 132:1–41. doi: 10.1016/j.jip.2015.07.009

Conflict of Interest: The authors declare that the research was conducted in the absence of any commercial or financial relationships that could be construed as a potential conflict of interest.

frontiers in Immunology

MINI REVIEW
published: 11 February 2021
doi: 10.3389/fimmu.2021.639092

Insights Into the Antiviral Pathways of the Silkworm *Bombyx mori*

Liang Jiang [1,2]*

[1] State Key Laboratory of Silkworm Genome Biology, Southwest University, Chongqing, China, [2] Biological Science Research Center, Southwest University, Chongqing, China

The lepidopteran model silkworm, *Bombyx mori,* is an important economic insect. Viruses cause serious economic losses in sericulture; thus, the economic importance of these viruses heightens the need to understand the antiviral pathways of silkworm to develop antiviral strategies. Insect innate immunity pathways play a critical role in the outcome of infection. The RNA interference (RNAi), NF-kB-mediated, immune deficiency (Imd), and stimulator of interferon gene (STING) pathways, and Janus kinase/signal transducer and activator of transcription (JAK/STAT) pathway are the major antiviral defense mechanisms, and these have been shown to play important roles in the antiviral immunity of silkworms. In contrast, viruses can modulate the prophenol oxidase (PPO), phosphatidylinositol 3-kinase (PI3K)/protein kinase B (Akt), and the extracellular signal-regulated kinase (ERK) signaling pathways of the host to elevate their proliferation in silkworms. In this review, we present an overview of the current understanding of the main immune pathways in response to viruses and the signaling pathways modulated by viruses in silkworms. Elucidation of these pathways involved in the antiviral mechanism of silkworms furnishes a theoretical basis for the enhancement of virus resistance in economic insects, such as upregulating antiviral immune pathways through transgenic overexpression, RNAi of virus genes, and targeting these virus-modulated pathways by gene editing or inhibitors.

Keywords: immunity, signaling pathway, virus, antivirus, insect, silkworm

OPEN ACCESS

Edited by:
Jun-ichi Hikima,
University of Miyazaki, Japan

Reviewed by:
Hiroshi Hamamoto,
Teikyo University, Japan
Kunlaya Somboonwiwat,
Chulalongkorn University, Thailand

***Correspondence:**
Liang Jiang
jiangliang@swu.edu.cn

Specialty section:
This article was submitted to Comparative Immunology, a section of the journal Frontiers in Immunology

Received: *08 December 2020*
Accepted: *26 January 2021*
Published: *11 February 2021*

Citation:
Jiang L (2021) Insights Into the Antiviral Pathways of the Silkworm Bombyx mori. Front. Immunol. 12:639092. doi: 10.3389/fimmu.2021.639092

INTRODUCTION

Virus infection poses a serious threat to human health and agricultural production. As the only fully domesticated insect, the lepidopteran model silkworm, *Bombyx mori*, is economically important for silk production. Sericulture is one of the main sources of income for farmers in many developing countries (1, 2). However, viral diseases have caused losses of nearly 16% of the potential cocoon production each year in sericulture, which are induced mainly by the *Bombyx mori nucleopolyhedrovirus* (BmNPV), *Bombyx mori cytoplasmic polyhedrosis virus* (BmCPV), or the *Bombyx mori bidensovirus* (BmBDV) (1).

Insects mainly rely on innate immunity to defend against invading pathogens, and immune pathways play an important role in this process. Although some host signaling pathways can be modulated by viruses to elevate virus proliferation, targeting these pathways can also inhibit virus infection. In this review, we present an overview of the main pathways involved in the antiviral mechanism of silkworms. Such knowledge could provide a theoretical basis for strategies for control of viral diseases in economic insects.

CHARACTERISTICS OF SILKWORM VIRUSES

Among the three major pathogenic viruses of silkworms, the BmNPV, a member of the Baculoviridae family having a circular double-stranded DNA genome (3), is the most prevalent threat to sericulture in almost all countries (1). The viral DNA combines with capsid proteins to form a nucleocapsid that is contained within an envelope (1, 3). The BmNPV replication cycle has two virion phenotypes: (1) the occlusion-derived virus that is transmitted among hosts, and packaged and protected in an occlusion body (4, 5), and (2) the budded virus that spreads throughout the host. The BmCPV belongs to the *Cypovirus* genus of the *Reoviridae* family, and its genome consists of ten discrete double-stranded RNA (dsRNA) segments (6, 7). The BmCPV particles contain nucleic acid and protein capsid, and they are non-enveloped and occluded within polyhedral bodies (6, 7). The BmBDV belongs to the *Bidensovirus* genus of *Bidnaviridae* family, and has two geographical variants, BmDNV-2 and BmDNV-Z (8–10). The BmBDV virions are non-enveloped and assembled by a protein capsid and nucleic acid, with their viral genome consisting of two linear non-homologous single-stranded DNA segments (8–10).

These viruses invade the silkworm larvae mainly via oral infection. The BmNPV can infect almost all tissues of the silkworm whereas the BmCPV and BmBDV can only infect the silkworm midgut (1). Some silkworm strains are resistant to the viruses at any viral dose (1, 9). For example, the *nsd-2* mutation is caused by a 6-kb deletion in the open reading frame of $+^{nsd-2}$ and imparts resistance to the BmDNV-2 (9). However, the receptor and major resistance genes to the BmNPV and BmCPV have not been identified in silkworm. The BmN and BmE are two cell lines commonly used in silkworm research, which are derived from the ovary and embryonic cells of silkworm, respectively. The BmNPV can infect the two cell lines, unlike the BmCPV and BmBDV; therefore, most silkworm antiviral research is focused on the BmNPV (11–17), a few on the BmCPV (18, 19), and very few on the BmBDV (20).

SILKWORM ANTIVIRAL IMMUNE PATHWAYS

The antiviral defense mechanism of silkworms mainly relies on innate immunity, including the RNA interference (RNAi), NF-kB-mediated pathways, and Janus kinase/signal transducer and activator of transcription (JAK/STAT) pathway (19, 21–24). Among these immune responses, RNAi is the major defense strategy against viruses in insects (23, 25).

RNAi Pathways

There are three RNAi-related pathways in insects, including the small interfering RNA (siRNA) pathway, microRNA (miRNA) pathway, and the PIWI-associated RNA (piRNA) pathway (26). When challenged with viruses, the siRNA pathway is activated by the dsRNA that is commonly generated as a byproduct of viral replication (27, 28). The Dicer2 enzyme recognizes viral dsRNA and processes the dsRNA into siRNAs. One strand of duplex siRNA is associated with Ago2 to form the RNA-induced silencing complex (RISC), and then directs RISC to the viral RNA target through base pairing. Subsequently, Ago2 cleaves the viral RNA, inhibiting viral replication (25, 27, 28) (**Figure 1A**). The expressions of both Ago2 and Dicer2 were not induced by silkworm viruses (21). However, the results of deep sequencing revealed that a large number of viral siNRA (∼20 nucleotides) was generated in insect hosts infected with baculovirus (29) and BmCPV (30), indicating that the RNAi response is an important antiviral defense of hosts. Overexpression of Ago2 and Dicer2 can improve the susceptibility of silkworm to dsRNA (31). Expression of dsRNA targeting the viral genes of BmNPV (13), BmCPV (18), and BmBDV (20) in transgenic silkworms substantially decreased the viral mRNA content and silkworm mortality after viral infection. The siRNA pathway is the predominant mechanism responsible for antiviral activity in insects (27, 28). For the applications and challenges of insect RNAi, please refer to the recent reviews (32, 33).

The miRNAs are small noncoding RNAs that can bind to target genes and regulate their expression (34). The miRNA pathway is involved in the interaction between silkworm and viruses (23, 35). Virus-encoded miRNA can facilitate viral multiplication. For example, BmNPV-miR-1 (35) and BmNPV-miR-3 (36) can enhance BmNPV infection via regulating the exportin-5 cofactor Ran and the viral *P6.9* expression, respectively; BmCPV-miR-1 could facilitate target gene *BmIAP* expression and BmCPV replication (37). Similarly, silkworm-encoded miRNA could be regulated to promote viral proliferation. For example, bmo-miR-274-3p, whose inhibition enhances target viral *NS5* expression and facilitates BmCPV replication, was downregulated in a BmCPV-infected silkworm midgut (38). Additionally, host miRNA can inhibit viral proliferation. For example, bmo-miR-2819 can downregulate the *ie-1* gene of BmNPV to suppress viral multiplication (39); although bmo-miR-278-3p could decrease target gene *IBP2* expression and increase BmCPV mRNA, it is downregulated and *IBP2* is upregulated in BmCPV-infected silkworms (40). The contribution of the miRNA pathway is minor in the RNAi antiviral defense of insects. In contrast to siRNAs and miRNAs, piRNAs are derived from single stranded RNA precursors (23). The role of the piRNA pathway in the antiviral response of insect models has been reviewed recently (41), however, of which the exact roles in the interaction between silkworm and its major pathogenic viruses are unclear, having few relevant reports so far (42, 43).

NF-kB-Mediated Antiviral Pathways

The Imd and Toll pathways are canonical NF-kB-dependent pathways involved in the innate immunity of insects, wherein they activate the downstream antimicrobial peptide (AMP) genes transcription mediated by two distinct orthologs of the NF-kB transcription factor (19, 25, 44). The NF-kB ortholog Relish is the terminal transcription factor for the Imd pathway, whereas the Dorsal and Dorsal-related immune factor (Dif) function in the Toll pathway (25). Toll pathway responds to Gram-positive bacteria and fungi infections, whereas Imd pathway

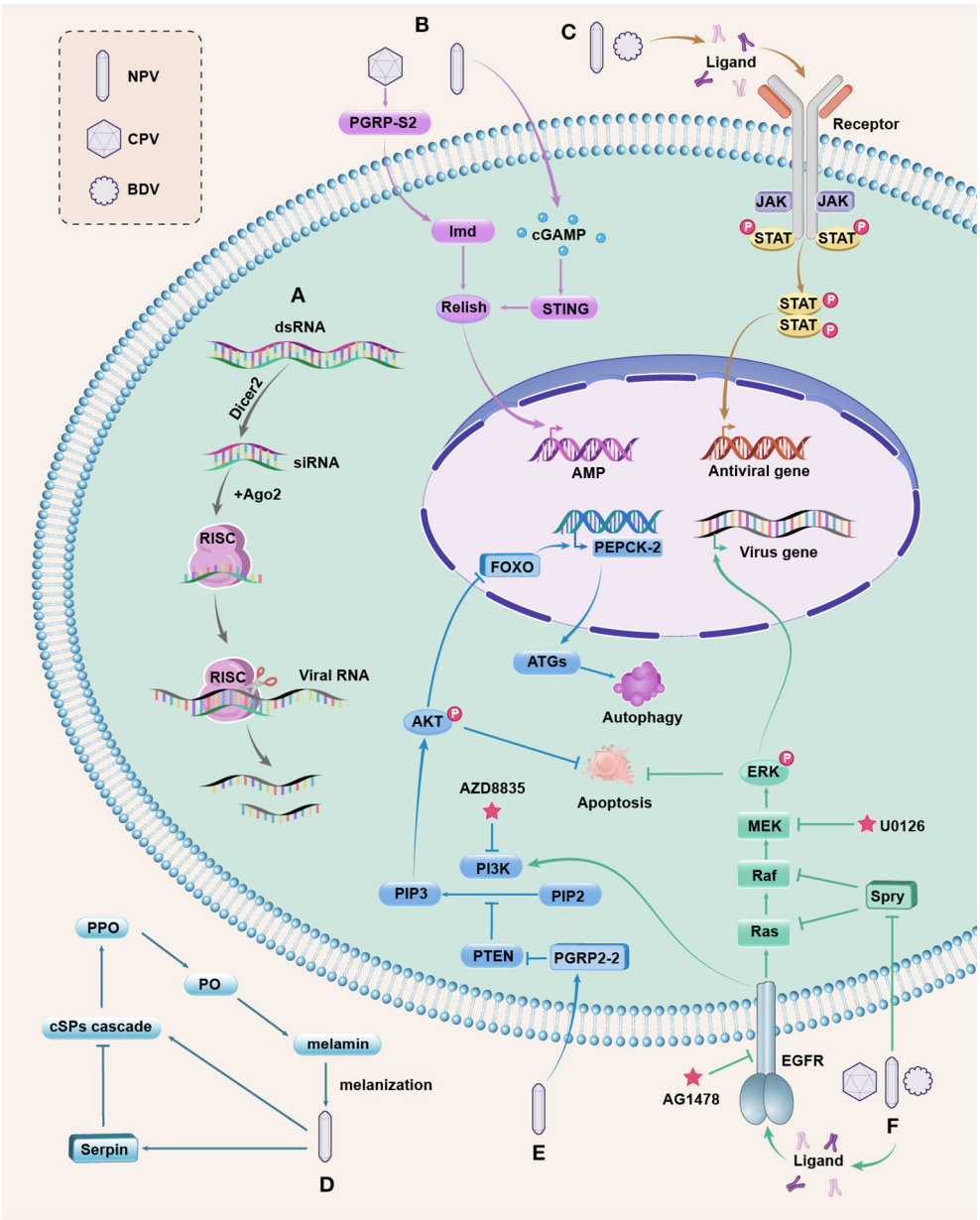

FIGURE 1 | Antiviral pathways in silkworm. **(A)** The siRNAi pathway is activated by viral dsRNA, which is cleaved into siRNAs by Dicer2. Ago2 is associated with one strand of siRNA to form RISC that can target and cleave the viral RNA to inhibit viral replication. **(B)** The NF-kB-mediated, Imd, and STING pathways. BmCPV induces the extracellular BmPGRP-S2 to active Imd and the downstream NF-kB ortholog Relish; BmNPV infection triggers the production of cGAMP to activate BmSTING for processing Relish. Activated Relish is translocated to the nucleus to initiate the transcription of AMP. Whether AMPs have antiviral function in silkworms needs further study. **(C)** The JAK/STAT pathway. The extracellular ligands bind to JAK associated receptors upon stimulation, leading to the activation of JAKs, and then cytosolic STATs are phosphorylated, forming the STAT dimers, which are translocated to the nucleus to regulate the expression of antiviral genes. **(D)** The PPO pathway is initiated by recognizing invading microbes, and then the extracellular cSP cascade is activated to convert the zymogen PPO to active PO. PO catalyzes the formation of melanin, resulting in melanization that kill the microbes. This pathway is negatively regulated by serpins, and baculovirus can induce serpins to suppress the melanization response of host insects for survival. **(E)** The PI3K/Akt pathway. Activated PI3K converts PIP2 into PIP3 to cause Akt phosphorylation (p-Akt). PTEN is a negative regulator of the PI3K/AKT pathway. BmNPV induces BmPGRP2-2 to suppress PTEN, resulting in increased p-Akt that inhibits cell apoptosis. Upregulated p-Akt also causes the inhibitory phosphorylation of the transcription factor FOXO, decreasing the expression of *BmPEPCK-2* and resulting in reduced autophagy genes (ATGs) expression, thereby blocking host autophagy. The inhibited apoptosis and autophagy are beneficial for viral replication. The PI3K inhibitor AZD8835 can decrease the mortality of silkworms infected with BmNPV. **(F)** The ERK pathway. Upon viral infection, the extracellular ligands activate EGFR (a receptor tyrosine kinase) to promote ERK phosphorylation (p-ERK) through the activation of Ras to the Raf/MEK/ERK phosphorylation cascade. p-ERK can regulate the transcription of viral genes and inhibit apoptosis. The Spry protein is a negative regulator of EGFR/ERK pathway that inhibits Ras or Raf, and both DNA and RNA viruses can downregulate Spry to increase p-ERK to ensure viral reproduction. AG1478 is a specific inhibitor of EGFR and U0126 binds to MEK to prevent p-ERK. The EGER also participates in the activation of PI3K by BmNPV. These pathways are integrated and are responsive to one another, which are complex and merit further investigation.

responds Gram-negative bacteria (19, 25). The transmembrane receptors peptidoglycan recognition protein (PGRP)-LC and the intracellular PGRP-LE sense the diaminopimelic acid-type peptidoglycan of Gram-negative bacteria, and transmit the signal to the adaptor molecule Imd, which is essential for the activation of Relish (25, 45). The Imd and Toll pathways have been shown to play a role in the antiviral immunity of *Drosophila* (25, 46–48). AMPs seems to have antiviral function in *Drosophila*, but their exact antiviral mechanisms are still unknown and more in-depth researches are needed (49).

Our research showed that *BmPGRP-S2* was induced by BmCPV in the silkworm midgut (7). Further experiments revealed that BmPGRP-S2 was a secreted protein, which may recognize a certain viral component and then transmit the signal to downstream molecules, and its overexpression increased the expression of *BmImd*, *BmRelish*, and *AMPs* and decreased silkworm mortality after BmCPV infection (19) (**Figure 1B**). These results indicate that the Imd pathway is involved in the defense against the RNA virus in silkworms. However, the function of this pathway in DNA virus-infected silkworms is not yet known. There have been few reports on the Toll pathway involved in antiviral immunity in silkworms. Recently, the stimulator of interferon genes (STING) has been reported to provide antiviral immunity against BmNPV in silkworms by promoting NF-kB activation (22). Production of cyclic guanosine monophosphate–adenosine monophosphate (cGAMP) is triggered upon BmNPV infection, inducing the BmSTING activation to process BmRelish, and then the activated BmRelish is translocated to the nucleus to initiate the transcription of AMP (22) (**Figure 1B**). The aforementioned result revealed that the NF-kB-mediated, Imd, and STING pathways play important roles in silkworm antiviral defense, but the antiviral mechanisms of the two pathways are only partially elucidated and need more experimentation. Deciphering the roles of Toll pathway in silkworm antiviral immunity remains a challenging task.

JAK/STAT Pathway

JAK/STAT signaling is an important pathway involved in multiple cellular processes such as cell proliferation and immune regulation in insects (21, 25). This pathway contains a diverse family of extracellular ligands such as cytokine and growth factors, transmembrane receptors, JAK tyrosine kinases that are associated with the intracellular part of the receptor, and STAT proteins (25, 50). Following stimulation, a ligand binds to the extracellular part of the JAK-associated receptors, leading to the activation of JAKs. Subsequently, cytosolic STATs are recruited to the JAK/receptor complex, and then phosphorylated, forming the STAT dimers, which are translocated into the nucleus and bound to the DNA promoters of the target genes to regulate their expression (25, 50) (**Figure 1C**).

The insect JAK/STAT pathway activation mechanism has been well-established in *Drosophila* and mosquito (25, 51–53). There has been growing evidence that the JAK/STAT pathway may be functionally analogous to the mammalian interferon system (51). The JAK/STAT pathway has been shown to respond to viral infections in *Drosophila* by regulating the production of downstream effector molecules, including the AMPs (25, 53). The BmNPV and BmBDV, unlike the BmCPV, induce the expression of *BmSTAT* in silkworms, implying that the JAK/STAT pathway could be activated by the DNA viruses in silkworms (21). Overexpression of *BmSTAT* in BmN cells increased the number of cells in the G2 phase of the cell cycle (54) and host resistance to BmNPV, but not to BmCPV (55). Additionally, inhibition of Hsp90 can cause upregulation of *BmSTAT* expression and suppression of BmNPV replication in the BmN cell (56), but it is not clear how Hsp90 can be linked to JAK/STAT. The extracellular ligand and effector molecules of this pathway in response to viral infection in silkworms have not been clearly identified and merit further investigation.

VIRUS-MODULATED HOST SIGNALING PATHWAYS

During the interaction between the insects and viruses, several host signaling pathways including the prophenol oxidase (PPO), phosphatidylinositol 3-kinase (PI3K)/protein kinase B (Akt), and the extracellular signal-regulated kinase (ERK) pathways have been reported to be modulated by viruses to elevate viral proliferation. For example, baculovirus induces *Bmserpin2* to inhibit the melanization reaction mediated by the PPO pathway, which also induces *BmPGRP2-2* to suppress *PTEN*, resulting in increased p-Akt that can inhibit cell apoptosis and autophagy. Meanwhile, silkworm viruses usurp the ERK pathway by downregulating *BmSpry* (57–60). It is noteworthy that targeting these hijacked host pathways can inhibit viral proliferation in silkworm.

PPO Pathway

Melanization reaction, mediated by the PPO pathway, is an important immune response in insect plasma and plays an essential role in the wound healing and killing of microbes (61, 62). This process is initiated by the recognition of invading microbes, and then the extracellular clip-domain serine protease (cSP) cascade is activated to convert the zymogen PPO to active phenoloxidase (PO). PO catalyzes the oxidation of phenols to form quinones and melanin, wherein the rapid polymerization of melanin at infection sites can kill and immobilize microbes (61–63) (**Figure 1D**). The melanization can kill baculovirus *in vitro* (64, 65). However, the PPO pathway is negatively regulated by serpins, and baculovirus can induce serpins to suppress the melanization response of host insects for survival (57, 64). *Bmserpin2* was upregulated in silkworms after BmNPV infection. Furthermore, knockdown of *Bmserpin2* can increase PO activity and decrease viral multiplication (57). The mechanism by which melanization contributes to the killing of pathogens remains elusive.

PI3K/Akt Pathway

The PI3K /Akt pathway plays an important role in regulating a number of cellular processes (66–68). Activation of PI3K can occur through the binding of a variety of ligands, including several growth factors to the receptor tyrosine kinases (RTKs). Activated PI3K then converts the substrate phosphatidylinositol

4, 5-bisphosphate (PIP2) into phosphatidylinositol (3,4,5)-trisphosphate (PIP3), and PIP3 causes the phosphorylation of Akt (p-Akt). Akt is considered a central mediator of the PI3K pathway. Active Akt drives cell proliferation, survival, apoptosis, and metabolism through the inhibitory phosphorylation of several substrates, including related kinases, signaling proteins, and the transcription factor forkhead box O (FOXO) (66, 69–71). BmFOXO directly upregulates *BmPEPCK-2*, and overexpression of *BmFOXO* and *BmPEPCK-2* can increase the expression of autophagy genes *ATG6/7/8* (17, 72). In addition, phosphatase and tensin homolog (PTEN) protein causes the dephosphorylation of PIP3, resulting in the suppression of the PI3K/AKT pathway (73).

A number of studies have demonstrated that many viruses can activate the PI3K/AKT pathway for their efficient proliferation (58, 66, 74, 75). The BmNPV induces the peptidoglycan recognition protein BmPGRP2-2 to suppress *PTEN*, resulting in increased p-Akt that can inhibit cell apoptosis (58). Meanwhile, the upregulation of p-Akt attenuates the activity of FOXO and decreases the expression of *BmPEPCK-2* and *ATG6/7/8*, thereby blocking host autophagy (17, 58, 72) (**Figure 1E**). The inhibited apoptosis and autophagy are beneficial for viral replication. However, which viral components are recognized by BmPGRP2-2 is unclear and needs further study. The PI3K/AKT pathway is a target for the treatment of many diseases (68, 70). The PI3K inhibitor AZD8835 can decrease the mortality of silkworms infected with BmNPV by blocking the p-Akt and suppressing viral proliferation (76), implying a promising antiviral strategy for silkworms.

ERK Pathway

ERKs are serine/threonine kinases activated by a variety of extracellular stimuli such as growth factors, environmental stresses, and microbial infections, and can transduce downstream cellular responses, including cell differentiation, survival, and apoptosis (77–80). Activation of the ERK pathway is required for efficient infection by many viruses (59, 80). One major class of ERK regulators is the RTK family. Upon stimulation, the extracellular ligands activate RTKs to promote the phosphorylation of ERK (p-ERK) by the activation of the small GTPase Ras to the Raf (MAP3K)/MEK (MAP2K)/ERK (MAPK) phosphorylation cascade. The ERKs then control transcription by phosphorylating various transcription factors in the nucleus or control targets in the cytoplasm (77, 78, 81, 82).

The epidermal growth factor receptor (EGFR) belongs to the RTK family (78, 81). The BmEGFR plays an important role in BmNPV infection, which participates in the activation of ERK and PI3K/Akt pathways by the virus. Moreover, activated ERK regulates the transcription of late viral genes and inhibits apoptosis (83). Additionally, Spry is a negative regulator of the EGFR/ERK pathway through the inhibition of Ras or Raf, and the overexpression of *BmSpry* suppressed p-ERK and BmNPV replication in BmE cells (84) (**Figure 1F**). Further research has found that *BmSpry* was decreased and p-ERK was increased in silkworms after infection with BmNPV, BmCPV, or BmBDV, and the knockdown of *BmSpry* in transgenic silkworms caused increased p-ERK, viral content, and mortality after infection with the three viruses, revealing that both DNA and RNA viruses usurp the ERK pathway to ensure viral reproduction (60). AG1478 is a specific inhibitor of EGFR tyrosine kinase activity (85) and the inhibitor U0126 binds to MEK to prevent p-ERK (86). The two inhibitors can inhibit p-ERK and BmNPV in BmE cells (83), but the inhibitory effect in silkworm larvae needs further test. The ERK pathway plays important roles in regulating the outcome of viral infection in silkworms, and the mechanisms remain to be fully elucidated.

CONCLUSIONS AND FUTURE PROSPECTS

Antiviral mechanisms are a worldwide problem and research hotspot. Insect-virus interactions may provide information on a vast repertoire of antiviral immune mechanisms (27). Results from the silkworm-virus model clearly show that there are multiple layers of antiviral defense that rely on conserved but also divergent pathways. For example, RNAi is a conserved antiviral mechanism among different insects, and it is the major antiviral response against both DNA and RNA viruses in silkworms. Meanwhile, NF-kB-mediated pathways are involved in antiviral immunity in silkworms but divergent responses to different viruses, such as BmCPV induces *BmPGRP-S2* and *Imd* to activate Relish whereas BmNPV activates cGAMP and STING to process Relish. Additionally, RNAi inhibits viral replication by cleaving the viral RNA while NF-kB-dependent antiviral immunity may based on AMPs. The multi-level response is beneficial to antiviral defense of host.

It is now apparent that these antiviral pathways are integrated and are responsive to one another, providing a pathogen-specific response. For example, the ERK and PI3K/Akt pathways have all been reported to interact with the JAK/STAT pathway (25), and the melanization and Toll pathways have also been found to interact (63). However, the integrated mechanisms of these pathways are complex, that is, the mechanisms by which baculovirus activate the ERK and PI3K/Akt pathways through EGFR may be different (83) and merit further investigation. Meanwhile, some mechanisms are tissue-specific or virus-specific, highlighting the importance of the investigation of virus–host interactions in the right context.

Coevolution between hosts and viruses favors the development of immune evasion mechanisms through modulation of the host signaling pathways by the pathogen (87). Targeting these hijacked pathways using inhibitors and knocking out their key regulators via gene editing would be a promising strategy to improve silkworm resistance. Meanwhile, RNAi of viral genes and overexpression of antiviral genes can enhance antiviral capacity of transgenic silkworms (1). Additionally, upregulation of antiviral immune pathways in transgenic silkworms is an available antiviral strategy. For the enhancement of host antiviral capacity and major issues in silkworm antiviral studies, please refer to our other review (87). These studies on antiviral pathways would be very instructive as they would reveal original antiviral strategies for the protection of beneficial insects and the target pathways hijacked by viruses for pest control.

AUTHOR CONTRIBUTIONS

LJ: drew figure, wrote the article, and supervision.

FUNDING

This work was funded by the National Natural Science Foundation of China (No. 32030103), the Fundamental Research Funds for the Central Universities (SWU120029, XDJK2020C006), and the Venture & Innovation Support Program for Chongqing Overseas Returnees (cx2019152).

ACKNOWLEDGMENTS

The author thanks Prof. Luc Swevers for critical reading of the manuscript and Prof. Qingyou Xia for inspiring discussion.

REFERENCES

1. Jiang L, Xia QY. The progress and future of enhancing antiviral capacity by transgenic technology in the silkworm *Bombyx mori*. *Insect Biochem Molec.* (2014) 48:1–7. doi: 10.1016/j.ibmb.2014.02.003
2. Goldsmith MR, Shimada T, Abe H. The genetics and genomics of the silkworm, *Bombyx mori*. *Annu Rev Entomol.* (2005) 50:71–100. doi: 10.1146/annurev.ento.50.071803.130456
3. Gomi S, Majima K, Maeda S. Sequence analysis of the genome of *Bombyx mori* nucleopolyhedrovirus. *J Gen Virol.* (1999) 80:1323–37. doi: 10.1099/0022-1317-80-5-1323
4. Blissard GW, Theilmann DA. Baculovirus entry and egress from insect cells. *Annu Rev Virol.* (2018) 5:113–39. doi: 10.1146/annurev-virology-092917-043356
5. Rahman MM, Gopinathan KP. Systemic and *in vitro* infection process of *Bombyx mori* nucleopolyhedrovirus. *Virus Res.* (2004) 101:109–18. doi: 10.1016/j.virusres.2003.12.027
6. Cao GL, Meng XK, Xue RY, Zhu YX, Zhang XR, Pan ZH, et al. Characterization of the complete genome segments from BmCPV-SZ, a novel *Bombyx mori* cypovirus 1 isolate. *Can J Microbiol.* (2012) 58:872–83. doi: 10.1139/w2012-064
7. Jiang L, Peng ZW, Guo YB, Cheng TC, Guo HZ, Sun Q, et al. Transcriptome analysis of interactions between silkworm and cytoplasmic polyhedrosis virus. *Sci Rep-Uk.* (2016) 6. doi: 10.1038/srep24894
8. Wang YJ, Yao Q, Chen KP, Wang Y, Lu J, Han X. Characterization of the genome structure of *Bombyx mori* densovirus (China isolate). *Virus Genes.* (2007) 35:103–8. doi: 10.1007/s11262-006-0034-3
9. Ito K, Kidokoro K, Sezutsu H, Nohata J, Yamamoto K, Kobayashi I, et al. Deletion of a gene encoding an amino acid transporter in the midgut membrane causes resistance to a Bombyx parvo-like virus. *Proc Natl Acad Sci USA.* (2008) 105:7523–7. doi: 10.1073/pnas.0711841105
10. Sun Q, Guo HZ, Xia QY, Jiang L, Zhao P. Transcriptome analysis of the immune response of silkworm at the early stage of *Bombyx mori* bidensovirus infection. *Dev Comp Immunol.* (2020) 106:601. doi: 10.1016/j.dci.2019.103601
11. Jiang L, Wang GH, Cheng TC, Yang Q, Jin SK, Lu G, et al. Resistance to *Bombyx mori* nucleopolyhedrovirus via overexpression of an endogenous antiviral gene in transgenic silkworms. *Arch Virol.* (2012) 157:1323–8. doi: 10.1007/s00705-012-1309-8
12. Jiang L, Cheng TC, Zhao P, Yang Q, Wang GH, Jin SK, et al. Resistance to BmNPV via overexpression of an exogenous gene controlled by an inducible promoter and enhancer in transgenic silkworm, *Bombyx mori*. *PLoS ONE.* (2012) 7:e41838. doi: 10.1371/journal.pone.0041838
13. Jiang L, Zhao P, Wang GH, Cheng TC, Yang Q, Jin SK, et al. Comparison of factors that may affect the inhibitory efficacy of transgenic RNAi targeting of baculoviral genes in silkworm, *Bombyx mori*. *Antivir Res.* (2013) 97:255–63. doi: 10.1016/j.antiviral.2012.12.020
14. Jiang L, Zhao P, Cheng TC, Sun Q, Peng ZW, Dang YH, et al. A transgenic animal with antiviral properties that might inhibit multiple stages of infection. *Antivir Res.* (2013) 98:171–3. doi: 10.1016/j.antiviral.2013.02.015
15. Chen SQ, Hou CX, Bi HL, Wang YQ, Xu J, Li MW, et al. Transgenic clustered regularly interspaced short palindromic repeat/Cas9-mediated viral gene targeting for antiviral therapy of *Bombyx mori* nucleopolyhedrovirus. *J Virol.* (2017) 91:16. doi: 10.1128/JVI.02465-16
16. Jiang L, Xie E, Guo H, Sun Q, Liuli H, Wang Y, et al. Heat shock protein 19.9 (Hsp19.9) from *Bombyx mori* is involved in host protection against viral infection. *Dev Comp Immunol.* (2021) 114:103790. doi: 10.1016/j.dci.2020.103790
17. Guo HZ, Xu GW, Wang BB, Xia F, Sun Q, Wang YM, et al. Phosphoenolpyruvate carboxykinase is involved in antiviral immunity against *Bombyx mori* nucleopolyhedrovirus. *Dev Comp Immunol.* (2019) 92:193–98. doi: 10.1016/j.dci.2018.11.015
18. Jiang L, Peng ZW, Guo HZ, Sun JC, Sun Q, Xia F, et al. Enhancement of antiviral capacity of transgenic silkworms against cytoplasmic polyhedrosis virus via knockdown of multiple viral genes. *Dev Comp Immunol.* (2017) 77:138–40. doi: 10.1016/j.dci.2017.07.020
19. Zhao P, Xia F, Jiang L, Guo H, Xu G, Sun Q, et al. Enhanced antiviral immunity against *Bombyx mori* cytoplasmic polyhedrosis virus via overexpression of peptidoglycan recognition protein S2 in transgenic silkworms. *Dev Comp Immunol.* (2018) 87:84–9. doi: 10.1016/j.dci.2018.05.021
20. Sun Q, Jiang L, Guo H, Xia F, Wang B, Wang Y, et al. Increased antiviral capacity of transgenic silkworm via knockdown of multiple genes on *Bombyx mori* bidensovirus. *Dev Comp Immunol.* (2018) 87:188–92. doi: 10.1016/j.dci.2018.06.002
21. Liu W, Liu J, Lu Y, Gong Y, Zhu M, Chen F, et al. Immune signaling pathways activated in response to different pathogenic micro-organisms in *Bombyx mori*. *Mol Immunol.* (2015) 65:391–7. doi: 10.1016/j.molimm.2015.02.018
22. Hua X, Li B, Song L, Hu C, Li X, Wang D, et al. Stimulator of interferon genes (STING) provides insect antiviral immunity by promoting Dredd caspase-mediated NF-kappaB activation. *J Biol Chem.* (2018) 293:11878–90. doi: 10.1074/jbc.RA117.000194
23. Swevers L, Feng M, Ren FF, Sun JC. Antiviral defense against Cypovirus 1 (Reoviridae) infection in the silkworm, *Bombyx mori*. *Arch Insect Biochem.* (2020) 103:3. doi: 10.1002/arch.21616
24. Wang LL, Cappelle K, Santos D, Vanden Broeck J, Smagghe G, Swevers L. Short-term persistence precedes pathogenic infection: infection kinetics of cricket paralysis virus in silkworm-derived Bm5 cells. *J Insect Physiol.* (2019) 115:1–1. doi: 10.1016/j.jinsphys.2019.03.004
25. Kingsolver MB, Huang ZJ, Hardy RW. Insect antiviral innate immunity: pathways, effectors, and connections. *J Mol Biol.* (2013) 425:4921–36. doi: 10.1016/j.jmb.2013.10.006
26. Kim VN, Han J, Siomi MC. Biogenesis of small RNAs in animals. *Nature reviews. Molecular cell biology.* (2009) 10:126–39. doi: 10.1038/nrm2632
27. Marques JT, Imler JL. The diversity of insect antiviral immunity: insights from viruses. *Curr Opin Microbiol.* (2016) 32:71–6. doi: 10.1016/j.mib.2016.05.002
28. Bronkhorst AW, van Rij RP. The long and short of antiviral defense: small RNA-based immunity in insects. *Curr Opin Virol.* (2014) 7:19–28. doi: 10.1016/j.coviro.2014.03.010
29. Jayachandran B, Hussain M, Asgari S. RNA interference as a cellular defense mechanism against the DNA virus baculovirus. *J Virol.* (2012) 86:13729–734. doi: 10.1128/JVI.02041-12
30. Zografidis A, Van Nieuwerburgh F, Kolliopoulou A, Apostolou-Karampelis K, Head SR, Deforce D, et al. Viral small-RNA analysis of *Bombyx mori* larval midgut during persistent and pathogenic cytoplasmic polyhedrosis virus infection. *J Virol.* (2015) 89:11473–86. doi: 10.1128/JVI.01695-15
31. You L, Zhang F, Huang S, Merchant A, Zhou X, Li Z. Over-expression of RNA interference (RNAi) core machinery improves susceptibility to RNAi in silkworm larvae. *Insect Mol Biol.* (2020) 29:353–62. doi: 10.1111/imb.12639
32. Leggewie M, Schnettler E. RNAi-mediated antiviral immunity in insects and their possible application. *Curr Opin Virol.* (2018) 32:108–14. doi: 10.1016/j.coviro.2018.10.004

33. Zhu KY, Palli SR. Mechanisms, applications, and challenges of insect RNA interference. *Ann Rev Entomol.* (2020) 65:293–311. doi: 10.1146/annurev-ento-011019-025224
34. Asgari S. MicroRNA functions in insects. *Insect Biochem Mol Biol.* (2013) 43:388–97. doi: 10.1016/j.ibmb.2012.10.005
35. Singh CP, Singh J, Nagaraju J. A baculovirus-encoded MicroRNA (miRNA) suppresses its host miRNA biogenesis by regulating the exportin-5 cofactor Ran. *J Virol.* (2012) 86:7867–9. doi: 10.1128/JVI.00064-12
36. Singh CP, Singh J, Nagaraju J. bmnpv-miR-3 facilitates BmNPV infection by modulating the expression of viral P6.9 and other late genes in *Bombyx mori*. *Insect Biochem Mol Biol.* (2014) 49:59–69. doi: 10.1016/j.ibmb.2014.03.008
37. Guo JY, Wang YS, Chen T, Jiang XX, Wu P, Geng T, et al. Functional analysis of a miRNA-like small RNA derived from *Bombyx mori* cytoplasmic polyhedrosis virus. *Insect science.* (2020) 27:449–62. doi: 10.1111/1744-7917.12671
38. Wu P, Jiang X, Sang Q, Annan E, Cheng T, Guo X. Inhibition of miR-274-3p increases BmCPV replication by regulating the expression of BmCPV NS5 gene in *Bombyx mori*. *Virus Genes.* (2017) 53:643–9. doi: 10.1007/s11262-017-1466-7
39. Wu P, Shang Q, Dweteh OA, Huang H, Zhang S, Zhong J, et al. Over expression of bmo-miR-2819 suppresses BmNPV replication by regulating the BmNPV ie-1 gene in *Bombyx mori*. *Mol Immunol.* (2019) 109:134–9. doi: 10.1016/j.molimm.2019.03.013
40. Wu P, Qin G, Qian H, Chen T, Guo X. Roles of miR-278-3p in IBP2 regulation and *Bombyx mori* cytoplasmic polyhedrosis virus replication. *Gene.* (2016) 575(2 Pt 1):264–9. doi: 10.1016/j.gene.2015.09.009
41. Kolliopoulou A, Santos D, Taning CNT, Wynant N, Vanden Broeck J, Smagghe G, et al. PIWI pathway against viruses in insects. *Wires Rna.* (2019) 10:6. doi: 10.1002/wrna.1555
42. Feng M, Kolliopoulou A, Zhou YH, Fei SG, Xia JM, Swevers L, et al. The piRNA response to BmNPV infection in the silkworm fat body and midgut. *Insect Sci.* (2020) doi: 10.1111/1744-7917.12796
43. Katsuma S, Kawamoto M, Shoji K, Aizawa T, Kiuchi T, Izumi N, et al. Transcriptome profiling reveals infection strategy of an insect maculavirus. *DNA Res.* (2018) 25:277–86. doi: 10.1093/dnares/dsx056
44. Hoffmann JA. The immune response of Drosophila. *Nature.* (2003) 426:33–8. doi: 10.1038/nature02021
45. Kaneko T, Yano T, Aggarwal K, Lim JH, Ueda K, Oshima Y, et al. PGRP-LC and PGRP-LE have essential yet distinct functions in the drosophila immune response to monomeric DAP-type peptidoglycan. *Nat Immunol.* (2006) 7:715–23. doi: 10.1038/ni1356
46. Mussabekova A, Daeffler L, Imler JL. Innate and intrinsic antiviral immunity in Drosophila. *Cell Mol Life Sci.* (2017) 74:2039–54. doi: 10.1007/s00018-017-2453-9
47. Zambon RA, Nandakumar M, Vakharia VN, Wu LP. The Toll pathway is important for an antiviral response in Drosophila. *Proc Natl Acad Sci USA.* (2005) 102:7257–62. doi: 10.1073/pnas.0409181102
48. Lamiable O, Kellenberger C, Kemp C, Troxler L, Pelte N, Boutros M, et al. Cytokine Diedel and a viral homologue suppress the IMD pathway in Drosophila. *Proc Natl Acad Sci USA.* (2016) 113:698–703. doi: 10.1073/pnas.1516122113
49. Feng M, Fei SG, Xia JM, Labropoulou V, Swevers L, Sun JC. Antimicrobial peptides as potential antiviral factors in insect antiviral immune response. *Front Immunol.* (2020) 11. doi: 10.3389/fimmu.2020.02030
50. Hombria JC, Brown S. The fertile field of Drosophila Jak/STAT signalling. *Curr Biol.* (2002) 12:R569–75. doi: 10.1016/S0960-9822(02)01057-6
51. Paradkar PN, Trinidad L, Voysey R, Duchemin JB, Walker PJ. Secreted Vago restricts West Nile virus infection in Culex mosquito cells by activating the Jak-STAT pathway. *Proc Natl Acad Sci USA.* (2012) 109:18915–20. doi: 10.1073/pnas.1205231109
52. Souza-Neto JA, Sim S, Dimopoulos G. An evolutionary conserved function of the JAK-STAT pathway in anti-dengue defense. *Proc Natl Acad Sci USA.* (2009) 106:17841–6. doi: 10.1073/pnas.0905006106
53. Dostert C, Jouanguy E, Irving P, Troxler L, Galiana-Arnoux D, Hetru C, et al. The Jak-STAT signaling pathway is required but not sufficient for the antiviral response of drosophila. *Nat Immunol.* (2005) 6:946–53. doi: 10.1038/ni1237
54. Hu X, Zhang X, Wang J, Huang M, Xue R, Cao G, et al. Transcriptome analysis of BmN cells following over-expression of BmSTAT. *Mol Gen Gen.* (2015) 290:2137–46. doi: 10.1007/s00438-015-1065-z
55. Zhang X, Guo R, Kumar D, Ma H, Liu J, Hu X, et al. Identification, gene expression and immune function of the novel Bm-STAT gene in virus-infected *Bombyx mori*. *Gene.* (2016) 577:82–8. doi: 10.1016/j.gene.2015.11.027
56. Shang Q, Wu P, Huang HL, Zhang SL, Tang XD, Guo XJ. Inhibition of heat shock protein 90 suppresses *Bombyx mori* nucleopolyhedrovirus replication in *B. mori*. *Insect Mol Biol.* (2020) 29:205–13. doi: 10.1111/imb.12625
57. Toufeeq S, Wang J, Zhang SZ, Li B, Hu P, Zhu LB, et al. Bmserpin2 is involved in BmNPV infection by suppressing melanization in *Bombyx mori*. *Insects.* (2019) 10(11). doi: 10.3390/insects10110399
58. Jiang L, Liu WQ, Guo HZ, Dang YH, Cheng TC, Yang WY, et al. Distinct functions of *Bombyx mori* peptidoglycan recognition protein 2 in immune responses to bacteria and viruses. *Front Immunol.* (2019) 10:776. doi: 10.3389/fimmu.2019.00776
59. Katsuma S, Mita K, Shimada T. ERK- and JNK-Dependent signaling pathways contribute to *Bombyx mori* nucleopolyhedrovirus infection. *J Virol.* (2007) 81:13700–9. doi: 10.1128/JVI.01683-07
60. Guo HZ, Sun Q, Wang BB, Wang YM, Xie EY, Xia QY, et al. Spry is downregulated by multiple viruses to elevate ERK signaling and ensure viral reproduction in silkworm. *Dev Comp Immunol.* (2019) 98:1–5. doi: 10.1016/j.dci.2019.04.001
61. Gonzalez-Santoyo I, Cordoba-Aguilar A. Phenoloxidase: a key component of the insect immune system. *Entomol Exp Appl.* (2012) 142:1–16. doi: 10.1111/j.1570-7458.2011.01187.x
62. Cerenius L, Lee BL, Soderhall K. The proPO-system: pros and cons for its role in invertebrate immunity. *Trends Immunol.* (2008) 29:263–71. doi: 10.1016/j.it.2008.02.009
63. Dudzic JP, Hanson MA, Iatsenko I, Kondo S, Lemaitre B. More than black or white: melanization and toll share regulatory serine proteases in Drosophila. *Cell Rep.* (2019) 27:1050. doi: 10.1016/j.celrep.2019.03.101
64. Yuan CF, Xing LS, Wang ML, Wang X, Yin MY, Wang QR, et al. Inhibition of melanization by serpin-5 and serpin-9 promotes baculovirus infection in cotton bollworm Helicoverpa armigera. *PLoS Pathog.* (2017) 13:6645. doi: 10.1371/journal.ppat.1006645
65. Wang QR, Yin MY, Yuan CF, Liu XJ, Hu ZH, Zou Z, et al. Identification of a conserved prophenoloxidase activation pathway in cotton bollworm *Helicoverpa armigera*. *Front Immunol.* (2020) 11:785. doi: 10.3389/fimmu.2020.00785
66. Xiao W, Yang Y, Weng QB, Lin TH, Yuan MJ, Yang K, et al. The role of the PI3K-Akt signal transduction pathway in *Autographa californica* multiple nucleopolyhedrovirus infection of *Spodoptera frugiperda* cells. *Virology.* (2009) 391:83–89. doi: 10.1016/j.virol.2009.06.007
67. Datta SR, Brunet A, Greenberg ME. Cellular survival: a play in three Akts. *Gene Dev.* (1999) 13:2905–27. doi: 10.1101/gad.13.22.2905
68. Fruman DA, Chiu H, Hopkins BD, Bagrodia S, Cantley LC, Abraham RT. The PI3K pathway in human disease. *Cell.* (2017) 170:605–35. doi: 10.1016/j.cell.2017.07.029
69. Vanhaesebroeck B, Guillermet-Guibert J, Graupera M, Bilanges B. The emerging mechanisms of isoform-specific PI3K signalling. *Nat Rev Mol Cell Bio.* (2010) 11:329–41. doi: 10.1038/nrm2882
70. Engelman JA. Targeting PI3K signalling in cancer: opportunities, challenges and limitations. *Nat Rev Cancer.* (2009) 9:550–62. doi: 10.1038/nrc2664
71. Jiramongkol Y, Lam EWF. FOXO transcription factor family in cancer and metastasis. *Cancer Metast Rev.* (2020) 39:681–709. doi: 10.1007/s10555-020-09883-w
72. Kang X, Wang Y, Liang W, Tang X, Zhang Y, Wang L, et al. *Bombyx mori* nucleopolyhedrovirus downregulates transcription factor BmFoxO to elevate virus infection. *Dev Comp Immunol.* (2020) 10:3904. doi: 10.1016/j.dci.2020.103904
73. Lee YR, Chen M, Pandolfi PP. The functions and regulation of the PTEN tumour suppressor: new modes and prospects. *Nat Rev Mol Cell Bio.* (2018) 19:547–62. doi: 10.1038/s41580-018-0015-0
74. Diehl N, Schaal H. Make yourself at home: viral hijacking of the PI3K/Akt signaling pathway. *Viruses-Basel.* (2013) 5:3192–212. doi: 10.3390/v5123192

75. Cooray S. The pivotal role of phosphatidylinositol 3-kinase-Akt signal transduction in virus survival. *J Gen Virol.* (2004) 85:1065–76. doi: 10.1099/vir.0.19771-0
76. Wang B, Jiang L, Guo H, Sun Q, Wang Y, Xie E, et al. Screening of PI3K-Akt-targeting drugs for silkworm against *Bombyx mori* nucleopolyhedrovirus. *Molecules.* (2019) 24:7. doi: 10.3390/molecules24071260
77. Shaul YD, Seger R. The MEK/ERK cascade: from signaling specificity to diverse functions. *Biochimica et biophysica acta.* (2007) 1773:1213–26. doi: 10.1016/j.bbamcr.2006.10.005
78. Hayashi S, Ogura Y. ERK signaling dynamics in the morphogenesis and homeostasis of Drosophila. *Curr Opin Genet Dev.* (2020) 63:9–15. doi: 10.1016/j.gde.2020.01.004
79. Johnson GL, Lapadat R. Mitogen-activated protein kinase pathways mediated by ERK, JNK, and p38 protein kinases. *Science.* (2002) 298:1911–2. doi: 10.1126/science.1072682
80. Bonjardim CA. Viral exploitation of the MEK/ERK pathway - A tale of vaccinia virus and other viruses. *Virology.* (2017) 507:267–75. doi: 10.1016/j.virol.2016.12.011
81. Morrison DK. MAP kinase pathways. *Csh Perspect Biol.* (2012) 4(11). doi: 10.1101/cshperspect.a011254
82. Buday L, Downward J. Epidermal growth-factor regulates P21(Ras) through the formation of a complex of receptor, Grb2 adapter protein, and sos nucleotide exchange factor. *Cell.* (1993) 73:611–20. doi: 10.1016/0092-8674(93)90146-H
83. Jin S, Cheng T, Guo Y, Lin P, Zhao P, Liu C, et al. *Bombyx mori* epidermal growth factor receptor is required for nucleopolyhedrovirus replication. *Insect Mol Biol.* (2018) 27:464–77. doi: 10.1111/imb.12386
84. Jin SK, Cheng TC, Jiang L, Lin P, Yang Q, Xiao Y, et al. Identification of a new sprouty protein responsible for the inhibition of the *Bombyx mori* Nucleopolyhedrovirus reproduction. *PLoS ONE.* (2014) 9:e99200. doi: 10.1371/journal.pone.0099200
85. Levitzki A, Gazit A. Tyrosine Kinase Inhibition - an Approach to Drug Development. *Science.* (1995) 267:1782–8. doi: 10.1126/science.7892601
86. Favata MF, Horiuchi KY, Manos EJ, Daulerio AJ, Stradley DA, Feeser WS, et al. Identification of a novel inhibitor of mitogen-activated protein kinase kinase. *J Biol Chem.* (1998) 273:18623–32. doi: 10.1074/jbc.273.29.18623
87. Jiang L, Goldsmith MR, Xia QY. Advances in the arms race between silkworm and baculovirus. *Front Immunol.* (2021) 12:628151. doi: 10.3389/fimmu.2021.628151

Conflict of Interest: The author declares that the research was conducted in the absence of any commercial or financial relationships that could be construed as a potential conflict of interest.

frontiers in Physiology

ORIGINAL RESEARCH
published: 19 February 2021
doi: 10.3389/fphys.2021.609674

Deacetylation of HSC70-4 Promotes *Bombyx mori* Nucleopolyhedrovirus Proliferation via Proteasome-Mediated Nuclear Import

*Fuxiang Mao[1,2], Xi Chen[1,2], Jonas Ngowo[1,2], Yajie Zhu[1,2], Jihai Lei[1,2], Xu Gao[1,2], Meng Miao[1,2], Yanping Quan[1,2] and Wei Yu[1,2]**

[1] Institute of Biochemistry, College of Life Sciences and Medicine, Zhejiang Sci-Tech University, Hangzhou, China, [2] Zhejiang Provincial Key Laboratory of Silkworm Bioreactor and Biomedicine, Hangzhou, China

OPEN ACCESS

Edited by:
Liang Jiang,
Southwest University, China

Reviewed by:
Victor Mikhailov,
Koltzov Institute of Developmental Biology, Russian Academy of Sciences, Russia
Jian Xu,
East China Normal University, China
Chengliang Gong,
Soochow University, China

***Correspondence:**
Wei Yu
mikkyu@163.com

Specialty section:
This article was submitted to Invertebrate Physiology, a section of the journal Frontiers in Physiology

Received: 24 November 2020
Accepted: 29 January 2021
Published: 19 February 2021

Citation:
Mao F, Chen X, Ngowo J, Zhu Y, Lei J, Gao X, Miao M, Quan Y and Yu W (2021) Deacetylation of HSC70-4 Promotes Bombyx mori Nucleopolyhedrovirus Proliferation via Proteasome-Mediated Nuclear Import. Front. Physiol. 12:609674. doi: 10.3389/fphys.2021.609674

Silkworm (*Bombyx mori*) is a model organism with great agricultural economic value that plays a crucial role in biological studies. *B. mori* nucleopolyhedrovirus (BmNPV) is a major viral pathogen found in silkworms, which leads to huge silk loss annually. In a recent lysine acetylome of silkworm infected with BmNPV, we focused on the heat shock cognate protein 70-4 (HSC70-4) lysine acetylation change due to the consequent nuclear accumulation and viral structure assembly. In this study, the genome replication, proliferation, and production of budded viruses (BVs) were arrested by HSP/HSC70 inhibitor treatment. However, HSC70-4 overexpression enhanced BmNPV reproduction. Furthermore, site-direct mutagenesis for acetylated mimic (K/Q) or deacetylated mimic (K/R) mutants of HSC70-4 demonstrated that lysine 77 (K77) deacetylation promotes HSC70-4 stability, viral DNA duplication, and HSC70-4 nuclear entry upon BmNPV challenge, and the nuclear propulsion of HSC70-4 after viral stimulus might be dependent on the interaction with the carboxyl terminus of HSC70-interacting protein (CHIP, an E3 ubiquitin ligase), followed by ubiquitin-proteasome system assistance. In this study, single lysine 77 deacetylation of HSC70-4 was deemed a part of the locomotive pathway for facilitating BmNPV proliferation and provided novel insights into the antiviral strategic development.

Keywords: HSC70-4, BmNPV, deacetylation, nuclear import, proteasome

INTRODUCTION

Silkworms play an essential role in the ancient Silk Road trade because of their derivative silk with high tremendous economic value, but are also of significance in research with respect to ease of rearing, acquisition of genome sequence, and availability of mutants from genetically homogeneous inbred lines (Xia et al., 2004). *Bombyx mori* nucleopolyhedrovirus (BmNPV), the primary pathogenic agent in silkworm viral disease, includes a large circular double-stranded DNA genome with putative 143 open reading frames (Shen et al., 2018). In addition, two distinct virion phenotypes are responsible for disseminating in insects or cells, respectively (Jiang and Xia, 2014).

One is the occlusion-derived virus (ODV), which contains numerous virions within a crystallized protein, called polyhedron, that promotes oral infection. The other is the budded virus (BV) that spreads between internal tissues. A detailed baculovirus invasion mechanism and silkworm immune response still need further understanding (Jiang et al., 2021a).

Heat shock proteins are involved in the interaction between baculovirus and silkworms (Mao et al., 2020; Shang et al., 2020; Jiang et al., 2021b). Heat shock protein 70 (HSP70) is conserved across evolution from archaebacteria to higher mammals (Lindquist and Craig, 1988). Differing from the HSP70 response to stress condition, heat shock cognate protein 70 (HSC70) is constitutively expressed to maintain the protein folding under normal conditions (Gething and Sambrook, 1992). Several investigations recently indicated that baculovirus infection induces *HSP/HSC70s* expression to promote viral genome replication, protein synthesis, and BV production (Lyupina et al., 2010, 2011, 2013, 2010; Breitenbach and Popham, 2013). For BmNPV and silkworm, HSC70 was found in the protein composition of ODV virion (Liu et al., 2008), and the transcriptional activity of the HSC70-4 promoter was elevated by the BmNPV homologous region 3 (Tang et al., 2005). In addition, HSC70-4 was accumulated in the nucleus at a very late BmNPV infection phase and identified the embedded assembly in ODV and BV structure, including the envelope and capsid (Iwanaga et al., 2014). During the polyhedrin aggregates/aggresomes formation upon BmNPV infection, HSP/HSC70s and ubiquitinated proteins colocalized with polyhedrin aggregates/aggresomes (Guo et al., 2015). Moreover, HSC70-4 interplays with the E3 ubiquitin ligase, carboxyl terminus of HSC70-interacting protein (CHIP), in *B. mori* (Ohsawa et al., 2016). Interestingly, BV production and polyhedrin expression of BmNPV is dependent on the intact ubiquitin-proteasome system (Katsuma et al., 2011). Based on the above reports, although HSC70-4 plays a crucial role in BmNPV infection, the elaborate molecular mechanisms need to be elucidated further.

Post-translational modifications, such as acetylation (Mawatari et al., 2015), phosphorylation (Muller et al., 2013), methylation (Gao et al., 2015), and ubiquitination (Kundrat and Regan, 2010), are essential for flexible regulation of HSP/HSC70s functional alternatives. Acetylation, which used to be studied in histone proteins, is also a commonly reversible molecule switch for non-histone proteins, affecting many cellular processes (Verdin and Ott, 2015). Currently, HSP/HSC70 acetylation has been widely studied in many aspects of cellular homeostasis, which is associated with protein folding, degradation, apoptosis, and autophagy (Yang et al., 2013; Wu et al., 2014; Seo et al., 2016; Park et al., 2017; Sun et al., 2019). For example, in the early stress period, the acetylated K77 lysine site of HSP70 led to increased protein refolding via interaction with HSP70/90 organizing protein (HOP) and HSP90; however, in the late stimulus phase, deacetylated K77 contributed to protein degradation by association with CHIP and HSP40 (Seo et al., 2016). In addition, K77 acetylation also hinders the caspase-dependent/independent apoptosis via interplay with Apaf1/AIF, respectively (Park et al., 2017). Similarly, HSP/HSC70s K88, K126, K159, and K246 acetylation-mediated protein-protein interaction, apoptosis, and autophagy have been widely investigated in cancer cells (Yang et al., 2013; Wu et al., 2014; Sun et al., 2019). Our previous proteomic profiling presented that BmN cellular histone deacetylase (HDAC) was upregulated upon BmNPV challenge (Mao et al., 2018). Nowadays, due to the analogous hydrophobic property, glutamine (Q) and arginine (R) are typically used for mimicking lysine (K) acetylation and deacetylation, respectively (Fujimoto et al., 2012; Huang et al., 2015). Nonetheless, how the HSP/HSC70s acetylation modulates viral proliferation is yet unknown.

Silkworm protein acetylation was studied in pro-survival, apoptosis, and autophagy (Zhou et al., 2016; Xue et al., 2019; Yang et al., 2020). Our recent acetylome upon BmNPV infection also stimulated a focus on HSC70-4 acetylation performance in baculovirus replication (Hu et al., 2018). In this study, we used the HSP/HSC70 inhibitor or overexpression of HSC70-4 to determine viral genome replication, propagation, and BV release. Furthermore, we detected several lysine sites by acetylation-mimic (K/Q) or deacetylation-mimic (K/R) in viral DNA duplication, and K77 deacetylation of HSC70-4 increased the number of viral genome copies by enhanced stability and nuclear import that may be dependent on the interaction with CHIP, followed by the ubiquitin-proteasome system for propulsion. This finding unveils the baculovirus-host interaction mechanism and provides novel insights into the antiviral strategy development.

MATERIALS AND METHODS

Plasmids, Cells, and Viruses

Bombyx mori BmN cell line, originated from the silkworm ovarian tissue, was preserved at 27°C in Sf-900 medium (Thermo Fisher Scientific, United States) supplemented with 10% fetal bovine serum (FBS; Corning, United States). BmNPV and the enhanced green fluorescent protein (EGFP)-tagged virus (BmNPV-EGFP), harboring the EGFP under the polyhedrin promoter without any protein fusion, were sustained in our laboratory with the multiplicity of infection (MOI) 10 for differently treated cells. The recombinant plasmid pET28a-*HSC70-4*(898-1801) for the induction of target protein expression and purification was constructed as described previously (Iwanaga et al., 2014). The transient expression vector in eukaryotic BmN cells with pIEx-1-*HSC70-4* was achieved for overexpression studies, and the target genes *HSC70-4*, *CHIP*, and *HOP* were amplified from the BmN cells. For this, RNA was isolated from BmN cells using TRIzol reagent (Thermo Fisher Scientific, United States), and the cDNA was reverse-transcribed by RevertAid First Strand cDNA Synthesis Kit (Thermo Fisher Scientific). Site-directed mutagenesis in HSC70-4 (K71Q, K71R, K77Q, K77R, K88Q, K88R, K126Q, K126R, K246Q, K246R, K524Q, and K524R) was carried out by overlapping polymerase chain reaction (PCR), as described previously (Ho et al., 1989). The method was also applied for fusing EGFP with HSC70-4

(wild-type, K77Q, K77R) followed by insertion into the pIEx-1 vector. Pairs of yeast two-hybrid plasmid pGBKT7-*HSC70-4/K77Q/K77R* and pGADT7-*CHIP/HOP* were constructed to test the protein-protein interaction. All primers are listed in **Supplementary Table 1**.

Antibodies, Reagents, and Transfection

pET28a-*HSC70-4*(898-1801) plasmid was transformed into *E. coli* (BL21 DE3) competent cells for recombinant HSC70-4 expression, induced by isopropyl-β-D-thiogalactopyranoside (IPTG), followed by the Ni-NTA column (Qiagen, Germany) purification. Subsequently, the refined protein was utilized for immunizing rabbits to obtain polyclonal antibodies (HuaAn Biotechnology, China). Gp64, His-tagged (Santa Cruz Biotechnology, United States), β-tubulin, and horseradish peroxidase (HRP)-conjugated secondary antibodies (Biosharp Life Sciences, China) were employed. VER155008 (VER) and MG132 were purchased from MedChemExpress (United States) and solubilized in dimethyl sulfoxide (DMSO) for the stock concentration of 50 mM. Transfection was performed as described previously (Xue et al., 2019) using SuperFectin^{TM}II *in vitro* DNA Transfection Reagent (Shanghai Pufei Biotechnology, China).

Chemicals Treatment and MTT Assay

After the chemical treatment with 1, 5, 10, and 20 μM VER for 24 or 48 h, the cells were harvested for cell viability assay. The MTT assay was performed as described previously (Yu et al., 2013b). Then, BmN cells were treated with 5 μM MG132 to bypass the cytotoxicity, based on the previous study (Katsuma et al., 2011).

Western Blotting

Disparate treated, transfected, or infected samples were collected and lysed for extraction of total protein in cell lysis buffer containing 0.5% NP40, 150 mM NaCl, 1 mM ethylenediaminetetraacetic acid (EDTA), 50 mM Tris pH 7.5, and protease inhibitor cocktail (Bimake, United States). After 30 min lysis on ice, the whole protein extract was subjected to centrifugation at 12000 rpm, 4°C for 15 min. The protein samples were quantified by Bradford assay, and an equivalent of 20 μg was resolved by 12% sodium dodecyl sulfate-polyacrylamide gel electrophoresis (SDS-PAGE), followed by electroblotting on polyvinyl difluoride (PVDF) membranes. Then, the membranes were blocked with 5% skim milk for 2 h and probed with the corresponding primary antibody. Subsequently, the membrane was incubated with a secondary antibody, and the immunoreactive bands were visualized using SignalFire ECL Reagent (Cell Signaling Technology, United States).

Viral Titer Determination

The viral titer of all the different groups was measured by the 50% tissue culture infective dose ($TCID_{50}$) of BmN cells. First, the cells were transfected with empty vector pIEx-1 or pIEx-1-*HSC70-4* or treated by VER (10 μM) or DMSO, respectively, and then infected with BmNPV at an MOI of 10 for 72 h. Subsequently, the virus in the supernatant was harvested and serially diluted 10-fold from 10^{-1} to 10^{-8}. A volume of 100 μL of the different gradient virus was inoculated into 96-well plates, and the titer was recorded at 0, 24, 48, 72, and 96 h p.i. by $TCID_{50}$ endpoint dilution assay.

Quantitative Analysis of Viral DNA Synthesis

qPCR was used to analyze viral DNA duplication as described previously (Yu et al., 2013a; Zhao et al., 2016). *gp41*, the viral gene, was applied to quantify viral DNA load and the specific primers used in qPCR to amplify the corresponding product. The qPCR was carried out using a GoTaq qPCR Master Mix kit (Promega, United States) on an ABI Prism 7500 Sequence Detection System (Applied Biosystems, United States). The PCR procedure was as follows: pre-denaturation at 95°C for 10 min, followed by 40 cycles of denaturation at 95°C for 10 s, annealing at 50°C for 10 s, and elongation at 72°C for 12 s. Each assay was carried out in biological triplicates.

Fluorescence Microscopy

Bombyx mori nucleopolyhedrovirus-EGFP was used for the determination of viral propagation under differentially transfected/treated BmN cells and were observed using an inverted fluorescence microscope (Eclipse, TE2000-U, Nikon, Japan). The EGFP-HSC70-4/K77Q/K77R subcellular nucleocytoplasmic distribution upon BmNPV infection was detected under a confocal microscope (IX81-FV1000, Olympus, Japan).

Yeast Two-Hybrid Assay

Recombinant pGBKT7-HSC70-4/K77Q/K77R and pGADT7-HOP/CHIP (2.5 μg each) constructs were simultaneously co-transformed into Y2HGold yeast competent cells AH109. The transformed yeasts (100 μL) were plated on SD-Trp/-Leu/-His/-Ade/X-α-gal nutrient-deficient medium for 3–5 days. A single colony of blue yeast was picked for another round of color observation.

Statistical Analysis

All experiments were independently repeated at least three times, and the data are shown as means ± standard deviation. The cell viability, viral DNA amount, and viral titer were determined using Student's *t*-test and GraphPad Prism 7. $^{*}p < 0.05$ indicates a statistically significant difference.

RESULTS

Impaired ATPase Activity of HSP70/HSC70 Interferes With Viral Proliferation

Based on previous studies about ATP-mimic molecule HSP/HSC70 specific inhibitor VER (**Figure 1A**) suppressing flavivirus (Taguwa et al., 2015, 2019), nairovirus (Surtees et al., 2016), and baculovirus (Lyupina et al., 2014;

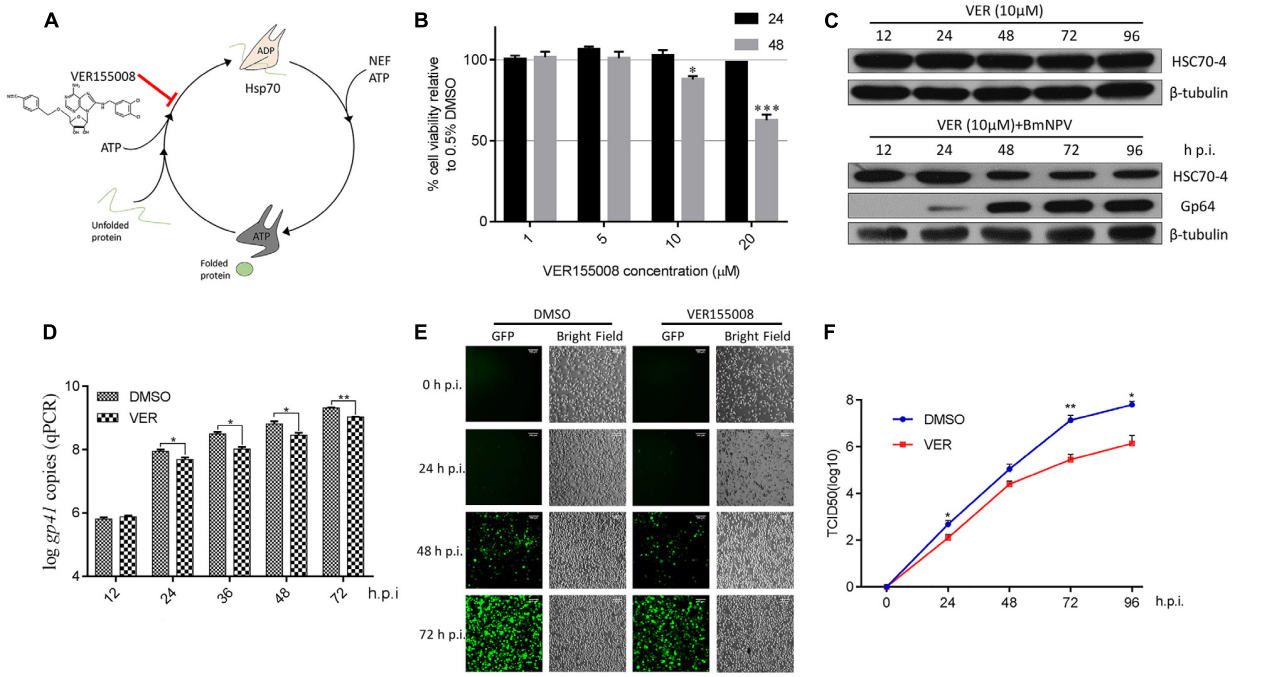

FIGURE 1 | The effect of HSP/HSC70s inhibitor VER for viral proliferation. **(A)** The schematic illustration of HSP/HSC70s inhibitor VER effect on intact nucleotides' binding cycle. **(B)** Determination of BmN cell viability by MTT assay with different concentrations (1, 5, 10, and 20 μM) inhibitor VER or DMSO incubation for 24 or 48 h in the absence of BmNPV. Cell viability is presented relative to the data of 0.5% DMSO. **(C)** Endogenous stability of HSC70-4 after inhibitor (10 μM) was added at 0 h post-infection (p.i.) or combined with inhibitor (10 μM) at 0 h p.i. and BmNPV treatment at several different time points and assessed by immunoblotting analysis. The viral structure protein Gp64 represented the BmNPV infectious process successfully. β-tubulin served as the loading control. **(D)** qPCR analysis of viral genome copies by HSP/HSC70s inhibition (10 μM) at 0 h p.i. in distinctive viral phases. DMSO groups were assessed as a negative control. **(E)** VER or DMSO-treated BmN cells were incubated with BmNPV-EGFP (enhanced green fluorescent protein). Infected cells (EGFP-positive) were detected at 0, 24, 48, and 72 h p.i. by fluorescence microscopy. Scale bar was 100 μm. The bright field represented the cell numbers and state control. **(F)** The yield of infectious BVs in the supernatants of corresponding treated cells was measured by $TCID_{50}$ endpoint dilution assay. Each data point represented the average titer of independent biological triplicates. *$p < 0.05$ indicated significant difference and **$p < 0.01$, ***$p < 0.005$ indicated extreme significant difference.

Mao et al., 2020), we also applied this inhibitor for determining the HSP/HSC70 ATPase activity for BmNPV reproduction. Initially, the BmN cell viability after VER treatment was measured (**Figure 1B**), showing that the different doses of chemicals had no cytotoxicity at the early stage of 24 h, but 10 μM inhibitor reduced cell survival after 48 h. However, during the BmNPV infectious phases, host cell viability was mainly governed by the virus rather than the inhibitor. Thus, considering relevant investigations about VER-treated Sf9 cells and AcMNPV (Lyupina et al., 2014), we consequently selected 10 μM for subsequent viral trials. We also assessed whether the stability of HSC70-4 was affected when the ATPase activity was blocked or combined with viral disruption. Consequently, the protein level did not show any obvious change by chemical treatment, but a gradual decline after simultaneous virus and HSP/HSC70 inhibitor stimulus was noted (**Figure 1C**). Next, we incubated the virus with VER or DMSO-treated BmN cells, and the different infectious stages were collected. The findings were consistent with the total viral DNA amount (**Figure 1D**), BmNPV propagation (**Figure 1E**), and BVs production (**Figure 1F**) that declines after HSP/HSC70s ATPase activity impairment with infection progress. The intact HSP/HSC70s played crucial roles in BmNPV proliferation.

Overexpression of HSC70-4 Facilitates BmNPV Infection

In this present study, the exogenous transient transfection indicated that overexpression of HSC70-4 is capable of being recognized explicitly as the endogenous cellular HSC70-4 by the customized polyclonal antibody (**Figure 2A**), and the overexpressed HSC70-4 reached a substantial level after 48 h post-transfection. Therefore, in the subsequent experiments, we adopted this time point for studying the overexpression of HSC70-4 effect in viral challenge. With this consequence, the viral genome replication (**Figure 2B**), BmNPV proliferation (**Figure 2C**), and BV yield (**Figure 2D**) were measured in empty vector or HSC70-4-transfected BmN cells, respectively. These data demonstrated that HSC70-4 enhances viral replication.

Potential Lysine Acetylation of HSC70-4 Upon Baculovirus Challenge

To study the acetylation of HSC70-4 in BmNPV, several lysine-acetylated sites (Kac) were identified in our previous relevant acetylome profiling post-BmNPV challenge (Hu et al., 2018). Also, some key Kacs, such as K71, K88, K126, K159, and K246, were investigated in recent studies (Yang et al., 2013;

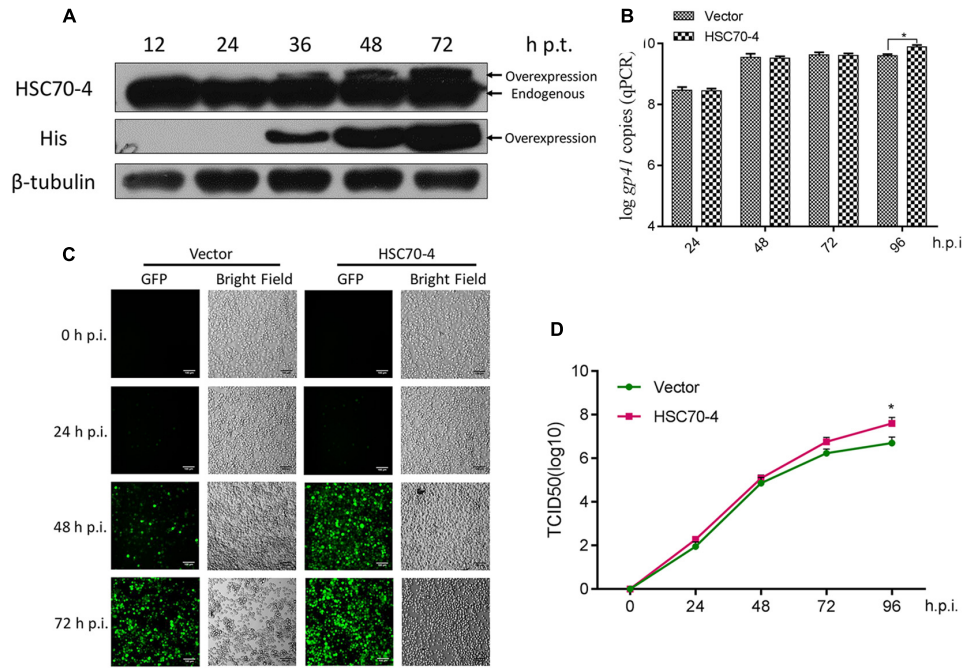

FIGURE 2 | Overexpression of HSC70-4 for viral proliferation. **(A)** The transient expression level of exogenously transfected BmN cells in the absence of BmNPV challenge was measured by immunoblotting analysis. **(B)** After 48 h transfection, empty vector or HSC70-4-transfected cells were incubated with BmNPV for 24, 48, 72, and 96 h infection. The viral genome replication of the corresponding treated cells was analyzed by qPCR. **(C)** At 48 h post-transfection of pIEx-1 or pIEx-1-HSC70-4 in BmN cells, BmNPV-EGFP was added, and the infected cells (EGFP-positive) were evaluated at 0, 24, 48, and 72 h post-infection by fluorescent microscope. Scale bar was 100 μm. **(D)** The collected infectious BVs in the supernatants of differentially transfected cells were determined by $TCID_{50}$ endpoint dilution assay. Each point was measured in biological triplicates. *$p < 0.05$ indicated a significant difference.

Wu et al., 2014; Seo et al., 2016; Park et al., 2017; Sun et al., 2019). Thus, the relatively comprehensive profile of Kac in different domains of HSC70-4 was created to represent a clear atlas (**Supplementary Figure 1A**). In the previous profile post-baculovirus challenge, five Kac sites were determined and analyzed by HPLC/MS/MS (**Supplementary Figure 1B**), while K77 and K246 in other species HSP/HSC70s had been investigated in-depth in protein folding/degradation, apoptosis, and autophagy (Wu et al., 2014; Seo et al., 2016). Related reports and the above results about HSC70-4 in BmNPV further prompted us to investigate whether the Kac response to viral stress plays functional roles in viral progress. Hence, we selected six conserved and well-studied lysine residues for further viral effects (**Figure 3A**). Then, overlapping PCR was employed for site-directed mutagenesis of lysine to mimic acetylation (glutamine, K/Q) or deacetylation (arginine, K/R) for viral genome replication analysis (**Figure 3B**). The results showed that acetylated K77 and K246 of HSC70-4 decrease the BmNPV genome copies but deacetylated K77 increases the number of copies (**Figure 3C**).

K77 Deacetylation Promotes HSC70-4 Stability and Nuclear Import Upon BmNPV

In order to explore if the acetylation of K77 affected HSC70-4 stability under normal conditions or viral stress, Western blot analysis was performed to observe the protein abundance after BmNPV 48 h transfection. Results showed that deacetylated K77 was able to increase the HSC70-4 level in the presence of a virus or a virus-free situation (**Figure 4A**), which might contribute to enhancing viral genome copy. Based on HSC70-4 nuclear accumulation upon BmNPV (Iwanaga et al., 2014), we deduced the differential modification of this protein that would make a difference in the nuclear movement by viral propulsion. The confocal microscopy (**Figure 4B**) confirmed the hypothesis that the deacetylated K77 residue is valuable for HSC70-4 nuclear import under BmNPV stimulation; however, the acetylated lysine 77 site is unable to accomplish the nucleus transportation. In conclusion, the results suggested that K77 deacetylation-mediated HSC70-4 stability and nuclear import potentially facilitates BmNPV replication.

K77 Deacetylation Is Crucial for HSC70-4 Interacting CHIP

A previous study reported that the K77 acetylation enhances the interplay between HSP70 and HOP, while K77 deacetylation contributes to HSP70 and CHIP interaction to implement the protein degradation (Seo et al., 2016). In *B. mori*, HSC70-4 was also capable of interacting with the E3 ubiquitin ligase CHIP (Ohsawa et al., 2016). Thus, we detected whether the K77 acetylation or deacetylation influenced the interplay between HSC70-4 and CHIP/HOP

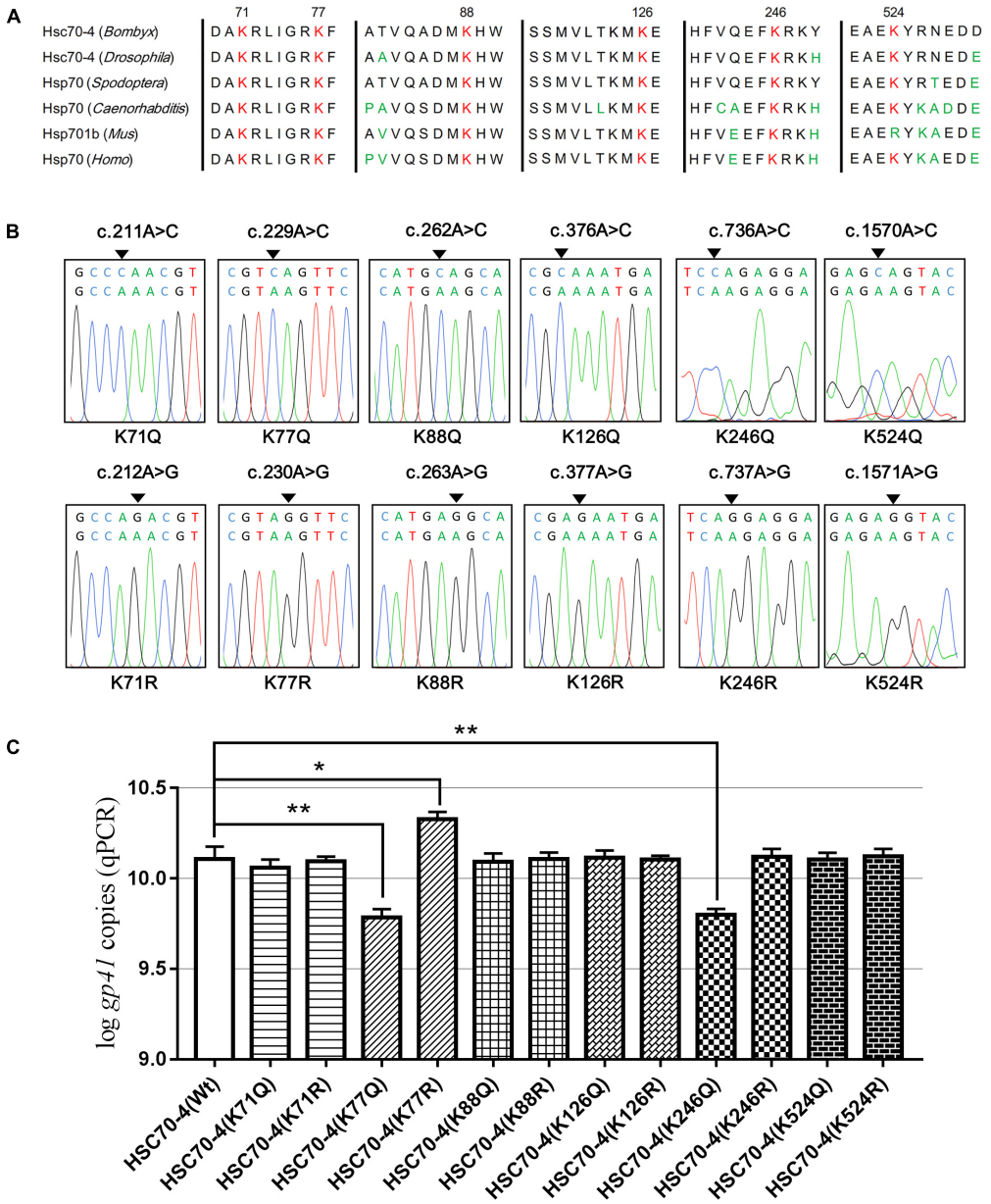

FIGURE 3 | Six conserved lysine residues mutated for viral genome analysis. **(A)** K71, K77, K88, K126, K246, and K524 conserved in *B. mori* HSC70-4 were aligned with their homologs in other species among *Drosophila melanogaster*, *Spodoptera frugiperda*, *Caenorhabditis elegans*, *Mus musculus*, and *Homo sapiens*. **(B)** Sequences of HSC70-4 site-mimic acetylation/deacetylation mutants were corrected by BLAST against GenBank. **(C)** Wild-type or 12 lysine acetylated/deacetylated mimic mutants of HSC70-4 48 h post-transfection were followed by BmNPV genome replication analysis after infection for 48 h. $^{*}p < 0.05$ represented a significant difference, and $^{**}p < 0.01$ indicated extreme significant difference.

by yeast two-hybrid assay. The findings revealed that K77 acetylation or deacetylation did not cause any difference in the association between HSC70-4 and HOP in yeast two-hybrid assay (**Supplementary Figure 2**); however, the wild-type and deacetylation-mimic HSC70-4 still maintained the interaction with CHIP, but the acetylation-mimic K77 hindered the association with CHIP (**Figure 5**). Consistently, these phenomena also reached a consensus with a previous report (Seo et al., 2016). The above trials showed that this lysine 77 residue deacetylation is essential for HSC70-4 and CHIP cooperation.

HSC70-4 Propulsion by K77 Deacetylation Requires the Ubiquitin-Proteasome System

The previous investigation demonstrated that the intact ubiquitin-proteasome system is crucial for BV production and

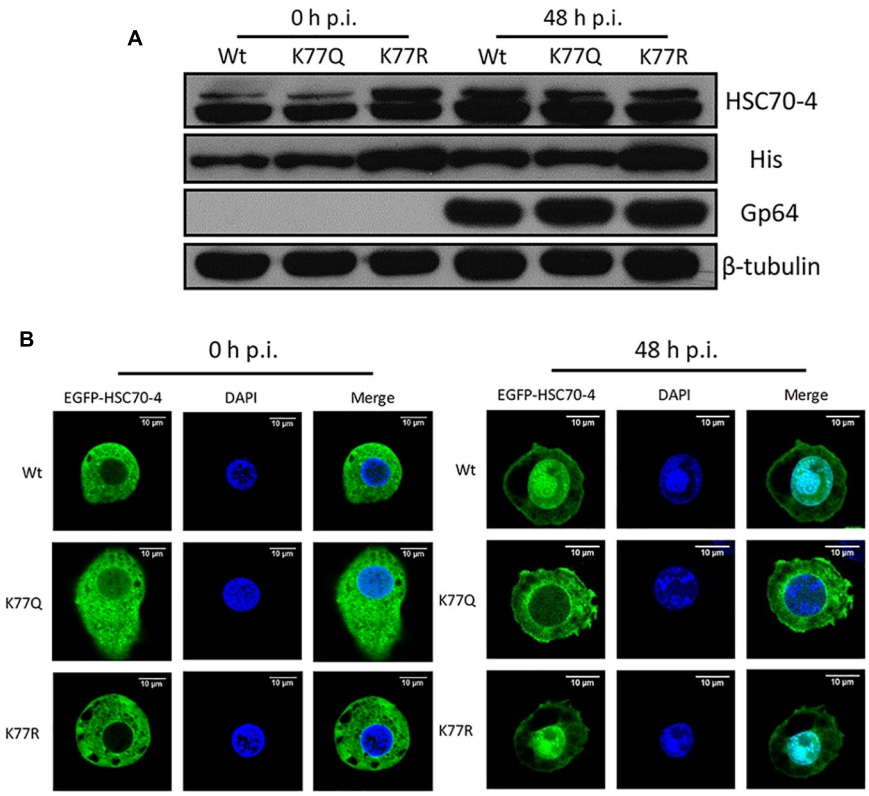

FIGURE 4 | K77 residue deacetylation is vital for HSC70-4 stability and nuclear import upon BmNPV. **(A)** After 48 h post-transfection of wild-type or mutant HSC70-4, virus-treated 48 h or virus-free 48 h for determining protein level. 6× His antibody was used for detecting exogenous HSC70-4 and mutants. HSC70-4 polyclonal antibody was used for confirming the His-tagged results. Tubulin was loading control, and Gp64 represented successful infection. **(B)** Confocal microscopy was applied to analyze the subcellular localization of EGFP-tagged HSC70-4/K77Q/K77R after the BmNPV challenge. Scale bar was 10 μm. DAPI was used for nuclear indication.

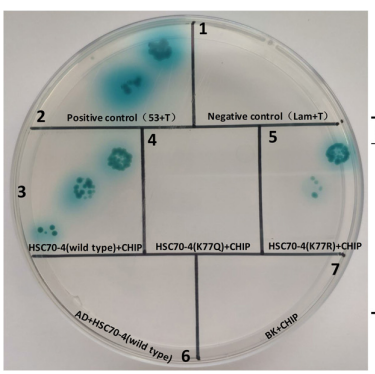

Samples	Plasmids	Interaction
1	pGBKT7-Lam/pGADT7-T	No
2	pGBKT7-53/pGADT7-T	Yes
3	pGBKT7-HSC70-4(Wt)/pGADT7-CHIP	Yes
4	pGBKT7-HSC70-4(K77Q)/pGADT7-CHIP	No
5	pGBKT7-HSC70-4(K77R)/pGADT7-CHIP	Yes
6	pGBKT7-HSC70-4(Wt)/pGADT7	No
7	pGBKT7/pGADT7-CHIP	No

FIGURE 5 | Preferential interaction between K77 deacetylation and CHIP. Yeast two-hybrid assay of the interaction between HSC70-4/K77Q/K77R and *B. mori* CHIP. pGBKT7-HSC70-4/K77Q/K77R and pGADT7-CHIP is the experimental group; pGBKT7-53 and pGADT7-T is a positive control; pGBKT7-Lam and pGADT7-T, pGBKT7 and pGADT7-CHIP, pGBKT7-HSC70-4/K77Q/K77R, and pGADT7 constitute the negative control.

polyhedrin expression during BmNPV infection (Katsuma et al., 2011). Combined with the K77 acetylation-induced difference between E3 ubiquitin ligase CHIP interaction and HSC70-4, we attempted to find if the ubiquitin-proteasome is a potential alternative pathway for HSC70-4 propulsion to the nucleus. Therefore, the application of proteasome inhibitor MG132 for analyzing BmNPV genome replication and proliferation manifested that the robust proteasome played vital roles in viral pathogenesis, such as genomic duplicates (**Figure 6A**) and propagation (**Figure 6B**), which was in agreement with the previous results (Katsuma et al., 2011). Furthermore, the damaged proteasome hampered HSC70-4 nuclear import

(**Figure 6C**), viral protein synthesis (**Figure 6D**), and viral genome copies (**Figure 6E**) after BmNPV invasion irrespective of whether it is acetylated or deacetylated. Although HSC70-4 is essential for the substrate degradation through the ubiquitin-proteasome system (Fernández-Fernández et al., 2017), the BmNPV utilized in this pathway demands more elucidation. These consistent consequences potentially indicated that HSC70-4 nuclear accumulation upon baculovirus challenge might be modulated by ubiquitin-mediated proteasome function.

DISCUSSION

Bombyx mori nucleopolyhedrovirus (BmNPV) is a pathogen that threatens the survival of silkworms; however, the baculovirus expression vector system could be used for the commercial manufacture of protein mass. Owing to the ambiguous mechanism between BmNPV and silkworm, we pursued the molecular machinery underlying this sophisticated process. Based on our previous BmN cellular acetylome upon BmNPV infection, five lysine residues with acetylated change were identified in HSC70-4 (Hu et al., 2018). This finding stimulated us to deduce whether this posttranslational modification played regulatory roles in the pathogenesis and development of baculovirus. In our study, K77 deacetylated HSC70-4 interacted with CHIP, assisted by the proteasome to accumulate in the nucleus for facilitating BmNPV genome replication.

Firstly, in the present study, we applied a wide-spectrum HSP/HSC70 inhibitor VER to test its function for BmNPV. VER was previously used to determine the *Autographa californica* multiple nucleopolyhedrovirus (AcMNPV) viral protein synthesis, genome replication, and BV production (Lyupina et al., 2014). In agreement with this phenomenon, VER also exerted an inhibitory role in BmNPV genome replication (**Figure 1D**), proliferation (**Figure 1E**), and BV yield (**Figure 1F**). Different from 20 μM or 100 μM VER treatment for Sf9 cells (Lyupina et al., 2014), the moderate application of 10 μM VER in BmN cells was able to diminish the cytotoxic effect (**Figure 1B**). Surprisingly, HSC70-4 protein level declined upon VER and BmNPV combined treatment (**Figure 1C**), which could be inferred as proper functions of HSC70-4 in baculovirus propagation.

Several studies investigated HSP/HSC70 in AcMNPV-infected Sf9 cells and reported that gene expression and protein abundance of HSP/HSC70 is upregulated in infected cells (Lyupina et al., 2010, 2011, 2013). However, Iwanaga et al. (2014) reported that HSC70-4 is steady during BmNPV invasion (Liu et al., 2008), which is consistent with our confirmation (**Supplementary Figure 3**). Combined with the above results of BmNPV and VER treatment, it is speculated that the inhibitor-impaired HSC70-4 would be degraded after the virus challenge, which possibly meant that BmNPV could distinguish the intact or damaged HSC70-4 for further utilization. The following data also supported that HSC70-4 is beneficial for baculovirus proliferation (**Figure 2C**), genome replication (**Figure 2B**), and BV release (**Figure 2D**).

In light of our recent silkworm cell acetylated profiling on baculovirus infection (Hu et al., 2018), several lysine residues (K77, K100, K246, K524, and K557) were identified in HSC70-4 with dynamic acetylation triggered by BmNPV (**Supplementary Figure 1B**). Hence, in association with the above results and other existing HSP70 acetylation reports (Yang et al., 2013; Wu et al., 2014; Seo et al., 2016; Park et al., 2017; Sun et al., 2019), we chose six relatively conserved lysine sites (K71, K77, K88, K126, K246, and K524) to continue the exploration of HSC70-4 in the virus progression (**Figure 3A**). After site-specific mimic acetylation (lysine/glutamine, K/Q) or deacetylation (lysine/arginine, K/R) mutation (**Figure 3B**), the viral genome analysis indicated that K77 and K246 acetylation of HSC70-4 showed a compromised effect in comparison to that of wild-type HSC70-4, while K77 deacetylation of HSC70-4 had a more robust influence than that of wild-type HSC70-4 (**Figure 3C**). Wu et al. (2014) investigated that K246 deacetylation of HSP70 was deacetylated by HDAC1 and HDAC7 that, in turn, inhibited autophagic cell death. Seo et al. (2016) demonstrated that HSP70 with K77 acetylation was effectuated by ARD1 acetyltransferase. The protein interacted with HSP90 and HOP for refolding as a response to early stress. In the late stimulus, HSP70 with K77 deacetylation tended to interplay with HSP40 and CHIP for protein degradation (Seo et al., 2016). Furthermore, deacetylated K77 would weaken HSP70 ATP hydrolysis and ATP binding ability, but the deacetylated K126 could enhance HSP70 ATP binding (Seo et al., 2016; Sun et al., 2019). Hence, in the subsequent study, K77 will be the superior target to unravel the role of HSC70-4 in BmNPV invasion. Also, K246 acetylation of HSC70-4 would still be our research goal for future baculovirus analysis about autophagy, and in a recent study, we reported that the autophagy-related gene 8 (*Atg8*) acetylation triggered by BmNPV regulates autophagy initiation (Xue et al., 2019).

Recent studies reported that the lysine acetylation could compete with ubiquitination to stabilize the protein (Ma et al., 2020). In the current study, different from VER-induced HSC70-4 degradation upon BmNPV stimulus, the deacetylation-mimic K77R blocked the ubiquitination of lysine, which might contribute to avoiding its degradation under normal circumstances (**Figure 4A**), which may be associated with allosteric conformational change failure of the ATP/ADP binding cycle (Seo et al., 2016). According to a previous study, HSC70-4 accumulated in the nucleus at the late infectious stage (Iwanaga et al., 2014). Similarly, the K77 deacetylation had a vital role in this nuclear import during BmNPV infection (**Figure 4B**), which might be associated with increased genome replication.

To detect whether the K77 acetylation affects the interacting partner of HSC70-4, we applied the yeast two-hybrid assay (Y2H). These results were consistent with those of a previous study that K77 acetylated HSP70 completely blocked its interaction with CHIP without any protein sequence mutation (Seo et al., 2016), and the consensus between HSP70 and HSC70 may provide novel insights into the categorization of these analogous molecules. HSC70-4, HSC70-3, HSC70-5, and HSC70-2 in *Bombyx mori* are constitutively expressed HSP70. HSC70-2 and HSC70-4 were located in the cytoplasm; HSC70-3 was in the endoplasmic reticulum. HSC70-5 was expressed in

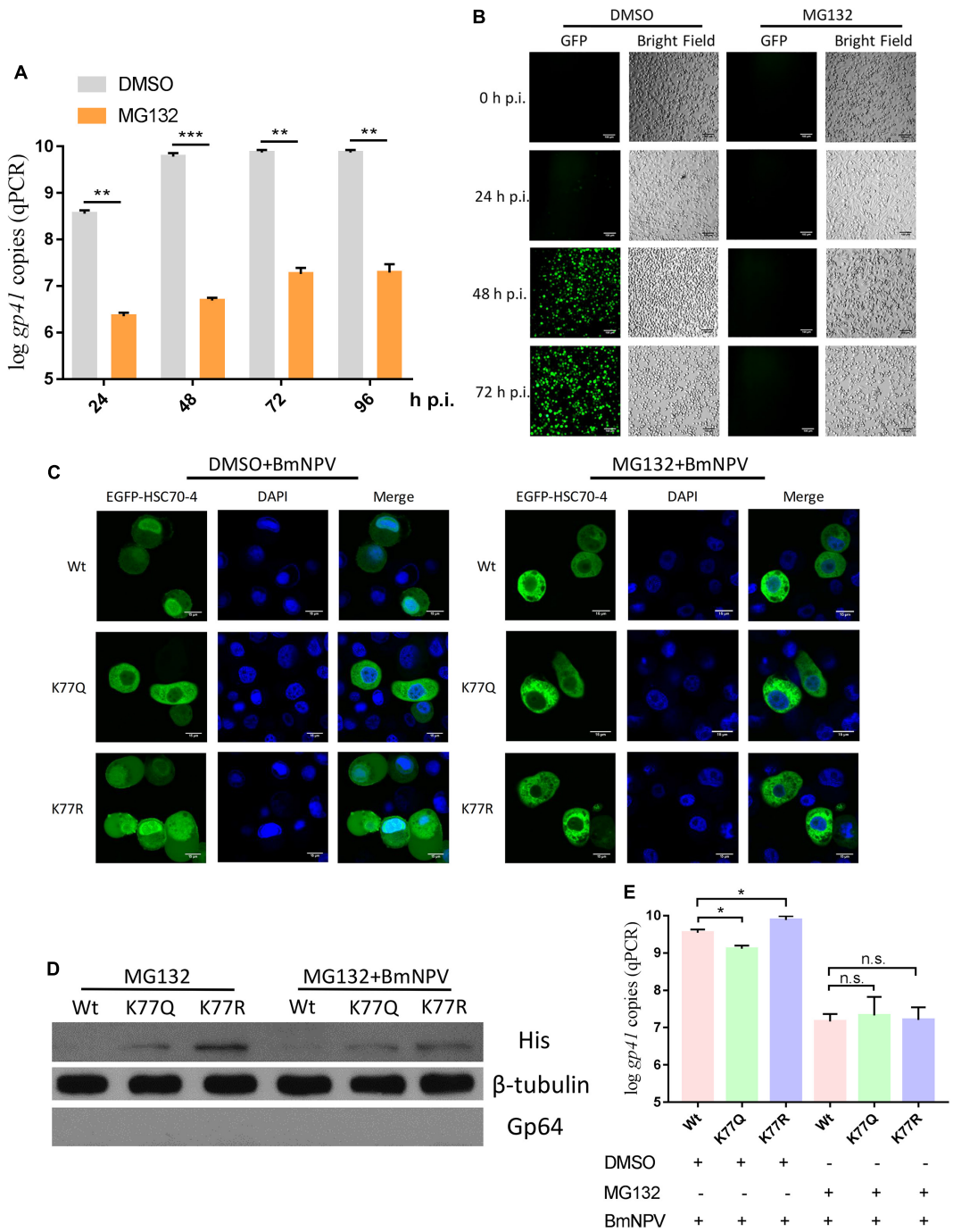

FIGURE 6 | Proteasome is required for HSC70-4 nuclear accumulation and viral DNA replication. **(A)** 5 μM proteasome inhibitor MG132 (0 h p.i.) effect for BmNPV genome copies at 24, 48, 72, and 96 h p.i. DMSO was used as the normal control. **(B)** BmNPV-EGFP proliferation upon MG132 treatment after 0, 24, 48, and 72 h p.i. was recorded by a fluorescence microscope. Bright field indicated the BmN cell number and cellular state. Scale bar was 100 μm. **(C)** After 48 h transfection of EGFP-HSC70-4/K77Q/K77R, MG132/DMSO (0 h p.i.), and BmNPV treatment, BmN cells were cultured for another 48 h post-infection and observed through confocal microscopy. DAPI was used to indicate the nucleus. Scale bar was 15 μm. **(D)** MG132 (0 h p.i.) or BmNPV was added simultaneously at 48 h post-transfection of wild-type or mutant HSC70-4 for 48 h incubation, followed by Western blot analysis. 6× His antibody was used for detecting exogenous HSC70-4 and mutants. Tubulin was used as a loading control. Gp64 represented viral infection progress. **(E)** Correspondingly, HSC70-4 or mutants at 48 h post-transfection were supplemented with inhibitor and virus to the transfected cells 48 h p.i. for the analysis of viral DNA amount. n.s. means non-significant difference. $^{*}p < 0.05$ represents significant difference and $^{**}p < 0.01$, $^{***}p < 0.005$ indicates extremely significant difference.

the mitochondria (Wang et al., 2012). Different cellular localization of HSP70 possibly decides the functional variety. A previous study showed differential effects of HSC70 and HSP70 on the intracellular trafficking and functional expression of epithelial sodium channels (Goldfarb et al., 2006), while the difference between HSC70 and HSP70 in baculovirus infection needs to be elucidated further.

In several investigations, the HSP/HSC70 colocalized with ubiquitinated proteins during the baculovirus infection (Lyupina et al., 2011, 2013; Guo et al., 2015). Linked to K77 deacetylation and interaction with E3 ubiquitin ligase CHIP, we found that the ubiquitin-proteasome system might contribute to the HSC70-4 nuclear import during the infectious process. A recent study also found that the ubiquitin-proteasome system is crucial for BmNPV polyhedrin expression and BV production (Katsuma et al., 2011). In the present study, the ubiquitin-proteasome is also required for viral genome replication (**Figure 6A**) and proliferation (**Figure 6B**) and can compromise K77 deacetylation-mediated HSC70-4 nuclear import (**Figure 6C**); also, the number of genome copies increase (**Figure 6E**) after BmNPV challenge. This phenomenon might imply that HSC70-4 nuclear accumulation is dependent on the ubiquitin-proteasome system for facilitating BmNPV replication.

DATA AVAILABILITY STATEMENT

The original contributions presented in the study are included in the article/**Supplementary Material**, further inquiries can be directed to the corresponding author.

AUTHOR CONTRIBUTIONS

FM, XC, and JN investigated the experiments, interpreted the data, and drafted the manuscript. YZ, JL, and XG provided critical data analysis and technical support. MM, YQ, and WY supervised the study. All authors reviewed the manuscript.

FUNDING

This work was financially supported by the National Natural Science Foundation of China (No. 31972623).

ACKNOWLEDGMENTS

The authors are thankful for Prof. Xijie Guo from Jiangsu University of Science and Technology, Zhenjiang, China for kindly providing yeast two-hybrid plasmids and technical support. The authors also thank Ms. Xue Bai from Zhejiang Sci-Tech University for kindly providing confocal microscopy technical support.

SUPPLEMENTARY MATERIAL

The Supplementary Material for this article can be found online at: https://www.frontiersin.org/articles/10.3389/fphys.2021.609674/full#supplementary-material

Supplementary Figure 1 | Kac sites of HSC70-4 response upon BmNPV stimulation. **(A)** The miniature architecture of HSC70-4 functional domains, including nucleotide-binding domain (blue section, 1–382 aa), substrate-binding domain (green section, 383–537 aa), and C-terminal domain (yellow section, 538–649 aa), was determined with a myriad of acetylated lysine sites in disparate segments (Kundrat and Regan, 2010; Muller et al., 2013; Gao et al., 2015; Verdin and Ott, 2015; Seo et al., 2016), and lysine sites in the red bar were identified in our previous profile. **(B)** Five Kac sites of HSC70-4 upon BmNPV trigger were identified by nano-HPLC/MS/MS.

Supplementary Figure 2 | K77 acetylation affects the interaction between HSC70-4 and HOP. Yeast two-hybrid assay of the interaction between HSC70-4/K77Q/K77R and *B. mori* HOP. pGBKT7-HSC70-4/K77Q/K77R and pGADT7-HOP is the experimental group; pGBKT7-53 and pGADT7-T are positive control; pGBKT7-Lam and pGADT7-T, pGBKT7 and pGADT7-HOP, pGBKT7-HSC70-4/K77Q/K77R, and pGADT7 are regarded as negative controls.

Supplementary Figure 3 | Stability of HSC70-4 upon BmNPV challenge. BmN cellular endogenous HSC70-4 stability dynamics after BmNPV infection were assessed at several different time points by immunoblotting assay. The viral structure protein Gp64 represented the BmNPV infectious process successfully. β-tubulin is used as loading control.

Supplementary Table 1 | The primers involved in this study.

REFERENCES

Breitenbach, J. E., and Popham, H. J. R. (2013). Baculovirus replication induces the expression of heat shock proteins *in vivo* and *in vitro*. *Arch Virol.* 158, 1517–1522. doi: 10.1007/s00705-013-1640-8

Fernández-Fernández, M. R., Gragera, M., Ochoa-Ibarrola, L., Quintana-Gallardo, L., and Valpuesta, J. M. (2017). Hsp70-a master regulator in protein degradation. *FEBS Lett.* 591, 2648–2660. doi: 10.1002/1873-3468.12751

Fujimoto, H., Higuchi, M., Koike, M., Ode, H., Pinak, M., Bunta, J. K., et al. (2012). possible overestimation of the effect of acetylation on lysine residues in KQ mutant analysis. *J. Comput. Chem.* 33, 239–246. doi: 10.1002/jcc.21956

Gao, W., Xiao, R., Peng, B., Xu, H., Shen, H., Huang, M., et al. (2015). Arginine methylation of HSP70 regulates retinoid acid-mediated RARβ2 gene activation. *Proc. Natl. Acad. Sci. U.S.A.* 122, E3327–E3336. doi: 10.1073/pnas.1509658112

Gething, M. J., and Sambrook, J. (1992). Protein folding in the cell. *Nature* 355, 33–45. doi: 10.1038/355033a0

Goldfarb, S. B., Kashlan, O. B., Watkins, J. N., Suaud, L., Yan, W., Kleyman, T. R., et al. (2006). Differential effects of Hsc70 and Hsp70 on the intracellular trafficking and functional expression of epithelial sodium channels. *Proc. Natl. Acad. Sci. U.S.A.* 103, 5817–5822. doi: 10.1073/pnas.0507903103

Guo, Z. J., Tao, L. X., Dong, X. Y., Yu, M. H., Tian, T., and Tang, X. D. (2015). Characterization of aggregate/aggresome structures formed by polyhedrin of *Bombyx mori* nucleopolyhedrovirus. *Sci. Rep.* 5:14601. doi: 10.1038/srep14601

Ho, S. N., Hunt, H. D., Horton, R. M., Pullen, J. K., and Pease, L. R. (1989). Site-directed mutagenesis by overlap extension using the polymerase chain reaction. *Gene* 77, 51–59. doi: 10.1016/0378-1119(89)90358-2

Hu, D., Xue, S., Zhao, C., Wei, M., Yan, H., Quan, Y., et al. (2018). Comprehensive profiling of lysine acetylome in baculovirus infected silkworm (*Bombyx mori*) cells. *Proteomics* 18:201700133. doi: 10.1002/pmic.201700133

Huang, R., Xu, Y., Wan, W., Shou, X., Qian, J., You, Z., et al. (2015). Deacetylation of nuclear LC3 drives autophagy initiation under starvation. *Mol. Cell* 57, 456–466. doi: 10.1016/j.molcel.2014.12.013

Iwanaga, M., Shibano, Y., Ohsawa, T., Fujita, T., Katsuma, S., and Kawasaki, H. (2014). Involvement of HSC70-4 and other inducible HSPs in *Bombyx mori* nucleopolyhedrovirus infection. *Virus Res.* 179, 113–118. doi: 10.1016/j.virusres.2013.10.028

Jiang, L., Goldsmith, M. R., and Xia, Q. (2021a). Advances in the arms race between silkworm and baculovirus. *Front. Immunol.* 12. doi: 10.3389/fimmu.2021.628151

Jiang, L., and Xia, Q. (2014). The progress and future of enhancing antiviral capacity by transgenic technology in the silkworm *Bombyx mori*. *Insect. Biochem. Mol. Biol.* 48, 1–7. doi: 10.1016/j.ibmb.2014.02.003

Jiang, L., Xie, E., Guo, H., Sun, Q., Liuli, H., Wang, Y., et al. (2021b). Heat shock protein 19.9 (Hsp19.9) from *Bombyx mori* is involved in host protection against viral infection. *Dev. Comp. Immunol.* 114:103790. doi: 10.1016/j.dci.2020.103790

Katsuma, S., Tsuchida, A., Matsuda-Imai, N., Kang, W., and Shimada, T. (2011). Role of the ubiquitin-proteasome system in *Bombyx mori* nucleopolyhedrovirus infection. *J. Gen. Virol.* 92, 699–705. doi: 10.1099/vir.0.027573-0

Kundrat, L., and Regan, L. (2010). Identification of residues on Hsp70 and Hsp90 ubiquitinated by the cochaperone CHIP. *J. Mol. Biol.* 395, 587–594. doi: 10.1016/j.jmb.2009.11.017

Lindquist, S., and Craig, E. A. (1988). The heat-shock proteins. *Annu. Rev. Genet.* 22, 631–677. doi: 10.1146/annurev.ge.22.120188.003215

Liu, X., Chen, K., Cai, K., and Yao, Q. (2008). Determination of protein composition and host-derived proteins of *Bombyx mori* nucleopolyhedrovirus by 2-dimensional electrophoresis and mass spectrometry. *Intervirology* 51, 369–376. doi: 10.1159/000193462

Lyupina, Y. V., Abaturova, S. B., Erokhov, P. A., Orlova, O. V., Beljelarskaya, S. N., and Mikhailov, V. S. (2013). Proteotoxic stress induced by *Autographa californica* nucleopolyhedrovirus infection of *Spodoptera frugiperda* Sf9 cells. *Virology* 436, 49–58. doi: 10.1016/j.virol.2012.10.018

Lyupina, Y. V., Dmitrieva, S. B., Timokhova, A. V., Beljelarskaya, S. N., Zatsepina, O. G., Evgen'ev, M. B., et al. (2010). An important role of the heat shock response in infected cells for replication of baculoviruses. *Virology* 406, 336–341. doi: 10.1016/j.virol.2010.07.039

Lyupina, Y. V., Orlova, O. V., Abaturova, S. B., Beljelskaya, S. N., Lavrov, A. N., and Mikhailov, V. S. (2014). Egress of budded virions of *Autographa californica* nucleopolyhedrovirus does not require activity of *Spodoptera frugiperda* HSP/HSC70 chaperones. *Virus Res.* 192, 1–5. doi: 10.1016/j.virusres.2014.08.002

Lyupina, Y. V., Zatsepina, O. G., Timokhova, A. V., Orlova, O. V., Kostyuchenko, M. V., Beljelarskaya, S. N., et al. (2011). New insights into the induction of the heat shock proteins in baculovirus infected insect cells. *Virology* 421, 34–41. doi: 10.1016/j.virol.2011.09.010

Ma, Y., Wu, C., Liu, J., Liu, Y., Lv, J., Sun, Z., et al. (2020). The stability and antiapoptotic activity of Bm30K-3 can be improved by lysine acetylation in the silkworm, *Bombyx mori*. *Arch. Insect. Biochem. Physiol.* 103:e21649. doi: 10.1002/arch.21649

Mao, F., Lei, J., Obeng, E., Wei, M., Zhao, C., Quan, Y., et al. (2018). Quantitative proteomics of *Bombyx mori* after BmNPV challenge. *J. Proteomics* 181, 142–151. doi: 10.1016/j.jprot.2018.04.010

Mao, F., Zhu, Y., Gao, X., Chen, X., Ngowo, J., Miao, M., et al. (2020). HSP/HSC70 activity is required for *Bombyx mori* nucleopolyhedrovirus replication at the early infectious phase. *Microb. Pathog.* 153:104647. doi: 10.1016/j.micpath.2020.104647

Mawatari, T., Ninomiya, I., Inokuchi, M., Harada, S., Hayashi, H., Oyama, K., et al. (2015). Valproic acid inhibits proliferation of HER2-expressing breast cancer cells by inducing cell cycle arrest and apoptosis through Hsp70 acetylation. *Int. J. Oncol.* 47, 2073–2081. doi: 10.3892/ijo.2015.3213

Muller, P., Ruckova, E., Halada, P., Coates, P. J., Hrstka, R., Lane, D. P., et al. (2013). C-terminal phosphorylation of Hsp70 and Hsp90 regulates alternate binding to co-chaperones CHIP and HOP to determine cellular protein folding/degradation balances. *Oncogene* 32, 3101–3110. doi: 10.1038/onc.2012.314

Ohsawa, T., Fujimoto, S., Tsunakawa, A., Shibano, Y., Kawasaki, H., and Iwanaga, M. (2016). Cloning and characterization of carboxyl terminus of heat shock cognate 70-interacting protein gene from the silkworm, *Bombyx mori*. *Comp. Biochem. Physiol. B Biochem. Mol. Biol.* 201, 29–36. doi: 10.1016/j.cbpb.2016.06.009

Park, Y. H., Seo, J. H., Park, J. H., Lee, H. S., and Kim, K. W. (2017). Hsp70 acetylation prevents caspase-dependent/independent apoptosis and autophagic cell death in cancer cells. *Int. J. Oncol.* 51, 573–578. doi: 10.3892/ijo.2017.4039

Seo, J. H., Park, J. H., Lee, E. J., Vo, T. T. L., Choi, H., Kim, J. Y., et al. (2016). ARD1-mediated Hsp70 acetylation balances stress-induced protein refolding and degradation. *Nat. Commun.* 7:12882. doi: 10.1038/ncomms12882

Shang, Q., Wu, P., Huang, H. L., Zhang, S. L., Tang, X. D., and Guo, X. J. (2020). Inhibition of heat shock protein 90 suppresses *Bombyx mori* nucleopolyhedrovirus replication in *B. mori*. *Insect. Mol. Biol.* 29, 205–213. doi: 10.1111/imb.12625

Shen, Y., Feng, M., and Wu, X. (2018). *Bombyx mori* nucleopolyhedrovirus ORF40 is essential for budded virus production and occlusion-derived virus envelopment. *J. Gen. Virol.* 99, 837–850. doi: 10.1099/jgv.0.001066

Sun, F., Jiang, X., Wang, X., Bao, Y., Feng, G., Liu, H., et al. (2019). Vincristine ablation of Sirt2 induces cell apoptosis and mitophagy via Hsp70 acetylation in MDA-MB-231 cells. *Biochem. Pharmacol.* 162, 142–153. doi: 10.1016/j.bcp.2018.10.021

Surtees, R., Dowall, S. D., Shaw, A., Armstrong, S., Hewson, R., Carroll, M. W., et al. (2016). Heat shock protein 70 family members interact with Crimean-Congo hemorrhagic fever virus and Hazara virus nucleocapsid proteins and perform a functional role in the Nairovirus replication cycle. *J. Virol.* 90, 9305–9316. doi: 10.1128/JVI.00661-16

Taguwa, S., Maringer, K., Li, X., Bernal-Rubio, D., Rauch, J. N., Gestwicki, J. E., et al. (2015). Defining Hsp70 subnetworks in Dengue virus replication reveals key vulnerability in flavivirus infection. *Cell* 163, 1108–1123. doi: 10.1016/j.cell.2015.10.046

Taguwa, S., Yeh, M. T., Rainbolt, T. K., Nayak, A., Shao, H., Gestwicki, J. E., et al. (2019). Zika virus dependence on host Hsp70 provides a protective strategy against infection and disease. *Cell Rep.* 26, 906–920. doi: 10.1016/j.celrep.2018.12.095

Tang, S., Zhao, Q., Yi, Y., Zhang, Z., and Li, Y. (2005). Homologous region 3 from *Bombyx mori* nucleopolyhedrovirus enhancing the transcriptional activity of heat shock cognate 70-4 promoter from *Bombyx mori* and *Bombyx mandarian* in vitro and in vivo. *Biosci. Biotechnol. Biochem.* 69, 1014–1017. doi: 10.1271/bbb.69.1014

Verdin, E., and Ott, M. (2015). 50 years of protein acetylation: from gene regulation to epigenetics, metabolism and beyond. *Nat. Rev. Mol. Cell Biol.* 16, 258–264. doi: 10.1038/nrm3931

Wang, L. L., Lin, H. J., Wang, Y., Li, Z., and Zhou, Z. Y. (2012). Chromosomal localization and expressional profile of heat shock protein 70 family genes in silkworm, *Bombyx mori*. *Sci. Sericul.* 38, 617–623. doi: 10.13441/j.cnki.cykx.2012.04.010

Wu, M. Y., Fu, J., Xiao, X., Wu, J., and Wu, R. C. (2014). MiR-34a regulates therapy resistance by targeting HDAC1 and HDAC7 in breast cancer. *Cancer Lett.* 354, 311–319. doi: 10.1016/j.canlet.2014.08.031

Xia, Q., Zhou, C., Lu, C., Cheng, D., Dai, F., Li, B., et al. (2004). A draft sequence for the genome of the domesticated silkworm (*Bombyx mori*). *Science* 306, 1937–1940. doi: 10.1126/science.1102210

Xue, S., Mao, F., Hu, D., Yan, H., Lei, J., Obeng, E., et al. (2019). Acetylation of BmAtg8 inhibits starvation-induced autophagy initiation. *Mol. Cell Biochem.* 457, 73–81. doi: 10.1007/s11010-019-03513-y

Yang, F., Zhu, B., Liu, J., Liu, Y., Jiang, C., Sheng, Q., et al. (2020). The effect of acetylation on the protein stability of BmApoLp-III in the silkworm, *Bombyx mori*. *Insect. Mol. Biol.* 29, 104–111. doi: 10.1111/imb.12613

Yang, Y., Fiskus, W., Yong, B., Atadja, P., Takahashi, Y., Pandita, T. K., et al. (2013). Acetylation hsp70 and KAP1-mediated Vps34 SUMOylation is required for autophagosome creation in autophagy. *Proc. Natl. Acad. Sci. U.S.A.* 110, 6841–6846. doi: 10.1073/pnas.1217692110

Yu, W., Du, C. Y., Quan, Y. P., Nie, Z. M., Chen, J., Lv, Z. B., et al. (2013a). Characterization of late gene expression factor LEF-10 from *Bombyx mori* nucleopolyhedrovirus. *Virus Res.* 175, 45–51. doi: 10.1016/j.virusres.2013.03.022

Yu, W., Li, Q., Yao, Y., Quan, Y., and Zhang, Y. (2013b). Two novel 30K proteins overexpressed in baculovirus system and their antiapoptotic effect in insect and mammalian cells. *Int. J. Genomics* 2013:323592. doi: 10.1155/2013/323592

Zhao, C., Zhang, C., Chen, B., Shi, Y., Quan, Y., Nie, Z., et al. (2016). A DNA binding protein is required for viral replication and transcription in *Bombyx mori* nucleopolyhedrovirus. *PLoS One* 11:e0159149. doi: 10.1371/journal.pone.0159149

Zhou, Y., Wu, C., Sheng, Q., Jiang, C., Chen, Q., Lv, Z., et al. (2016). Lysine acetylation stabilizes SP2 protein in the silkworm *Bombyx mori*. *J. Insect. Physiol.* 9, 56–62. doi: 10.1016/j.jinsphys.2016.06.008

Conflict of Interest: The authors declare that the research was conducted in the absence of any commercial or financial relationships that could be construed as a potential conflict of interest.

frontiers in Immunology

MINI REVIEW
published: 23 February 2021
doi: 10.3389/fimmu.2021.613729

Sending Out Alarms: A Perspective on Intercellular Communications in Insect Antiviral Immune Response

Fei Wang [1,2*]

[1] State Key Laboratory of Silkworm Genome Biology, Southwest University, Chongqing, China, [2] Biological Science Research Center, Southwest University, Chongqing, China

Viral infection triggers insect immune response, including RNA interference, apoptosis and autophagy, and profoundly changes the gene expression profiles in infected cells. Although intracellular degradation is crucial for restricting viral infection, intercellular communication is required to mount a robust systemic immune response. This review focuses on recent advances in understanding the intercellular communications in insect antiviral immunity, including protein-based and virus-derived RNA based cell-cell communications, with emphasis on the signaling pathway that induces the production of the potential cytokines. The prospects and challenges of future work are also discussed.

Keywords: insect, antiviral immunity, cytokine, Dicer-2, intercellular transfer

OPEN ACCESS

Edited by:
Luc Swevers,
National Centre of Scientific Research Demokritos, Greece

Reviewed by:
Humberto Lanz-Mendoza,
National Institute of Public Health, Mexico
Fangfang Li,
Chinese Academy of Agricultural Sciences, China
Eric Roberto Guimarães Rocha Aguiar,
Universidade Estadual de Santa Cruz, Brazil

***Correspondence:**
Fei Wang
massmoca@swu.edu.cn

Specialty section:
This article was submitted to Comparative Immunology, a section of the journal Frontiers in Immunology

Received: *03 October 2020*
Accepted: *12 January 2021*
Published: *23 February 2021*

Citation:
Wang F (2021) Sending Out Alarms: A Perspective on Intercellular Communications in Insect Antiviral Immune Response. Front. Immunol. 12:613729. doi: 10.3389/fimmu.2021.613729

INTRODUCTION

Viral infection has posed a significant threat to human and animal health, agricultural production and environmental safety. The frequent outbreaks of pandemics caused by viral infection taught us bitter lessons that the long-standing battles between the hosts and viruses are much rougher than expected. As obligate intracellular pathogens, viruses heavily rely on the host cell machinery and resources to replicate and propagate. Accordingly, host cells develop multiple strategies, including intrinsic antiviral response that directly restricts viral replication and assembly, and induced antiviral response that potentiates the antiviral activity of viral-restricting factors or cells to suppress and eliminate the invading pathogens (1–4).

Insects are the most abundant and diverse group of animals in the world. Some of them are regarded as model organisms, disease vectors, agriculture and household pests or industrial animals. A lot of studies have been carried out to investigate molecules, pathways and mechanisms that are involved in the immune response of different insects upon viral challenges. Among them, a few attentions are given to how extracellular signaling networks cooperate with intracellular pathways to mount a robust systemic immune response. Pieces of evidence have proposed that intricate intercellular communications occur in response to viral infection in insects, and helped us better understand the insect antiviral immunity in a systematic way.

The best characterized antiviral immune response in insects is RNA interference (RNAi) (3, 5). Three RNAi pathways have been identified in insects, including the small interfering RNA (siRNA) pathway, the microRNA (miRNA) pathway and the (PIWI-interacting RNA) piRNA pathway. Among them, siRNA has been most intensively studied as a potent antiviral defense strategy. siRNA

is initiated by recognition and cleavage of double-stranded RNA (dsRNA) produced either as viral replication intermediate or as base-pairing viral transcript by Dicer-2 in host cells. Dicer-2, an RNase III family endonuclease, processes dsRNA into 19-23-nucleotide (nt) long siRNA duplex, which is subsequently loaded onto Argonaute-2 (Ago-2) endonuclease and integrated into a multiple protein complex, RNA-induced silencing complex (RISC). siRNA duplex is then unwound to generate the guide strand, which targets viral mRNA or genomic RNA containing complementary sequence for degradation through the RNase activity of Ago-2, thereby restricting viral infection. miRNA pathway was previously charactered in post-transcriptional regulation of gene expression during development, in which a 22-nt duplex miRNA processed by RNase III enzyme Drosha and Dicer-1 sequentially forms miRNA programmed RNA induced silencing complex (miRISC) with Ago-1 protein. Recently, both virus derived miRNAs that regulate insect gene expression and insect-encoded miRNAs that target virus mRNA were reported, highlighting its role in host-virus interaction (6, 7). The antiviral role of piRNA which commonly involves in genomic control of transposable elements is controversial in *Drosophila* (8, 9), while in mosquito piRNAs that are derived from acquired viral cDNA with the characteristic size range of 24–30 nt and features of ping-pong amplification cycle were discovered to specifically inhibit viral replication (10, 11).

Besides RNAi, viral-induced apoptosis and autophagy also play important roles in restricting viral infection (12, 13). The expression level of several pro-apoptotic genes, such as *reaper*, *hid*, and *p53*, increased in response to virus-induced stress, while anti-apoptotic genes, such as *diap1* decreased, resulting in onset of apoptosis and subsequent phagocytosis of viral-infected cells by haemocytes (14–17). Interestingly, sometimes this antiviral apoptosis is suppressed by host protein, as evidence found in silkworm that peptidoglycan recognition protein (PGRP) 2-2, inhibited baculovirus-induced apoptosis *via* Akt activation, reflecting arms race between insect and virus (18, 19). Recently, a few studies found autophagy occurs after *Drosophila* infected with vesicular stomatitis virus (VSV), Rift Valley fever virus (RVFV) or Zika virus as evidenced by the elevation of lipidated Atg8 (Atg8-II) level and accumulation of Atg8 in autophagic punctae (20–24). Silencing core autophagy genes, such as *atg5* or *atg8*, led to significant increase of viral load. Plasma membrane receptor Toll-7 has also been demonstrated to activate autophagy upon sensing VSV glycoproteins or RVFV (24, 25), which is independent of transcription factor NF-κB, whereas eliminating Zika virus by autophagy in *Drosophila* appears to be NF-κB-dependent (23).

In addition, genome-wide RNAi screening and transcriptional profiling has revealed a plethora of genes involved in antiviral immune response. Some of them have broad antiviral activity. For instance, negative elongation factor (NELF) and positive elongation factor b (P-TEFb) collaboratively mediate transcriptional pausing to potentiate the rapid activation of some inducible genes and are required to restrict viral replication in adult flies and mosquito cells (26). Some have been reported to be involved in anti-microbial immunity with uncharacterized antiviral activity. For instance, two anti-microbial peptide (AMP) coding genes, *diptericinB* and *attacinC* were up-regulated in transgenic flies expressing a Sindbis virus (SINV) replicon (27). Knocking-down their expression led to a modest but significant increase in SINV load, confirming their antiviral functions. In mosquito cells, Dengue virus (DENV) infection up-regulated the expression of a cecropin-like peptide which does not only have anti-bacterial activity, but also have anti-DENV and anti-Chikungunya virus activity (28). The enhanced expression of *gloverin*, *lebocin*, *attacin* was also observed in silkworm larvae infected with *Bombyx mori* nucleopolyhedrovirus (BmNPV) (29). Based on these facts, the Toll and IMD pathways, which are the two canonical NF-κB pathways responsible for immune response against bacterial and fungi infection, are considered to be implicated in anti-viral immunity (30, 31). But most of viral-induced genes remain enigmas in terms of the molecular mechanism underling their antiviral activity. For instance, virus-induced RNA 1 (*vir-1*), a marker of the induction of anti-viral response, is mainly regulated by JAK/STAT pathway (32). Loss of function of JAK (named Hopscotch in *Drosophila*) caused decreased expression of *vir-1*, increased viral load and decreased survival after *Drosophila* C virus (DCV) infection. However, the molecular mechanism of antiviral activity of Vir-1 is unknown.

INTERCELLULAR COMMUNICATIONS

Although intracellular degradation is crucial to virus elimination, intercellular communication is believed to orchestrate and coordinate the cellular events. In the following, we will review the recent studies on extracellular signaling networks during antiviral immune response (**Figure 1**) and discuss the prospects and challenges of future work.

Protein Based Intercellular Communication: Cytokines

As a comparison, the potent antiviral immune response in mammalian cells is largely dependent on a group of secretory protein collectively named cytokines, which are produced and secreted by viral-infected cells, and bind specific receptors on its own, neighboring or distant cells to initiate intracellular signaling mainly *via* JAK/STAT pathway (33, 34). Cytokines are divided into several subgroups, including interferon, chemokine, interleukin and tumor necrosis factor, among which interferon is particularly important for the immune response to virus. Cells activated by interferon synthesize various molecules that inhibit virus entry, replication and assembly, or produce inflammatory reactions to initiate apoptosis, autophagy and necrosis (35). Although comparative genomic analysis and evolutionary study revealed that insects do not possess the homologous molecules to vertebrate cytokines, the core components of JAK/STAT pathway including Hopscotch (JAK), STAT92E (STAT), negative regulators SOCS and PIAS have been identified in insects, and parallels between gain-of-function studies with mammalian homologs suggests the functional similarity of insect JAK/STAT pathway to vertebrates. Thanks

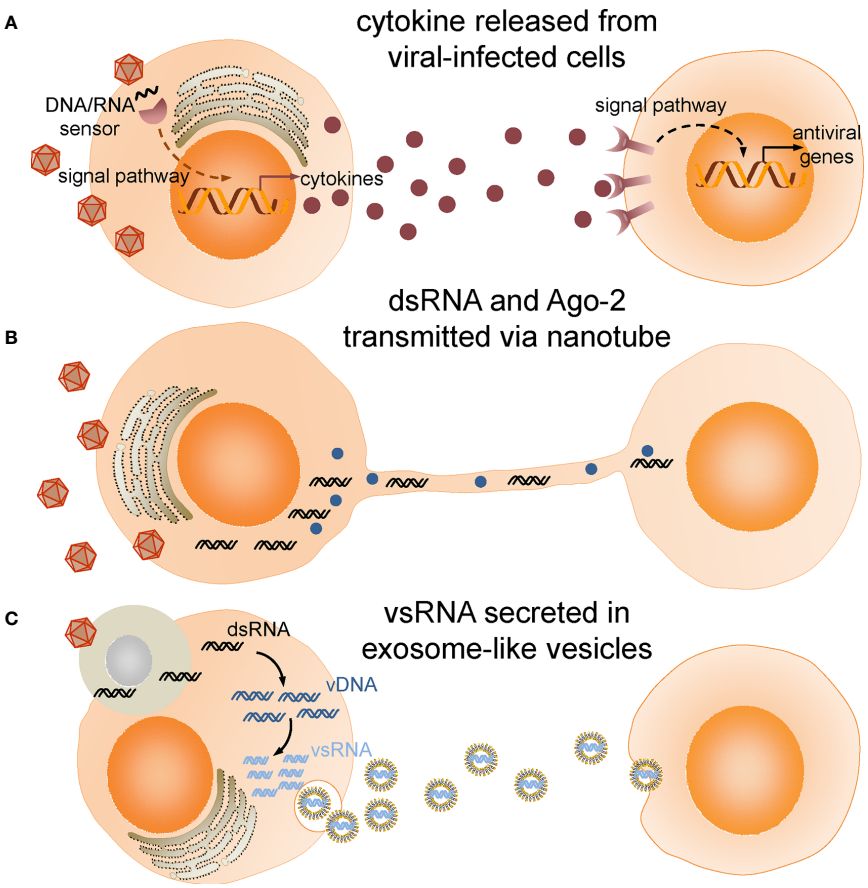

FIGURE 1 | Intercellular communications in insect antiviral immune response. **(A)** Cytokines produced and released from viral infected cells bind to receptors and activate antiviral immune response in target cells. **(B)** Double-stranded RNA (dsRNA) and Ago-2 is transferred through tunneling nanotubes bridging infected cells and neighboring cells. **(C)** Viral-derived dsRNAs (vsRNAs) produced in viral-infected cells engulfed by haemocytes are reverse-transcribed into vDNAs by endogenous transposon reverse transcriptase. vDNAs then serve as template for transcription of secondary vsRNAs which are secreted in exosome-like vesicles and processed into siRNA by cells taking up these vesicles.

to the genetic analysis of mutants defective in embryonic development, ligands and receptor of JAK/STAT pathway were first discovered in *Drosophila* (36). All three ligands, named unpaired (Upd), Upd2, and Upd3 bind the same receptor named Domelss (Dome) which shares sequence similarity with mammalian IL-6 receptor (37), but only Udp2 and Upd3 are induced by viral infection and provide protection from a viral infection (38). Notably, JAK/STAT pathway has been considered to be triggered in bystander cells rather than in infected cells, since *vir-1* was not induced in DCV-infected fat body and periovarian sheath, but was substantially induced in epithelial cells of the ventral epidermis or in the oviduct, in which no viral load was detected, suggesting that *vir-1* was induced after a signal generated by the DCV-infected cells (32).

The signaling pathways responsible for induction of mammalian cytokines may also give some clues to whether there exists any "cytokine" that transmits antiviral signals between insect cells. Viral nucleic acids in mammalian cells are recognized by diverse cytosolic RNA or DNA sensors, including toll-like receptors (TLRs), retinoic acid-inducible gene I (RIG-I), absent in melanoma 2 (AIM2), DNA-dependent activator of IFN-regulatory factors (DAI) and cyclic GMP-AMP synthase (cGAS) (39). The signal is eventually relayed to transcriptional factors, including interferon regulatory factor 3 (IRF3) and NF-κB *via* signaling adaptors, such as antiviral-signaling protein (MAVS) and stimulator of interferon genes (STING) to activate interferon expression (40, 41). Despite the fact that far less nucleic acids sensors have been identified in insects, STING-mediated antiviral immunity has been discovered in *Drosophila* and *Bombyx mori* recently (23, 42, 43). Epistatic analysis showed that dSTING acts upstream of IKKβ and NF-κB transcriptional factor Relish to regulate the expression of a set of antiviral molecules, including a putative transmembrane protein named Nazo. Flies bearing dSTING or Relish mutant displayed higher susceptibility to infection of DCV, VSV or Cricket paralysis virus (CrPV). Activation of Relish by BmSTING was also detected in silkworm cell as evidenced by the cleavage of Relish carboxy-terminal Ankyrin repetitive sequence, which releases Relish from sequestration in cytoplasm, when BmSTING was over-expressed. The evolutionary conservation in STING- and NF-κB-dependent

antiviral signaling pathway between insects and mammals suggests functional similarity in their downstream effectors. Indeed, a few years ago an antiviral factor Vago which bears no sequence homology to mammalian cytokines was first reported to be induced in the fat body of flies upon DCV infection, later its mosquito homologs that may act like interferon have been identified in *Culex*, *Aedes* and *Anopheles* (44, 45). CxVago was produced and secreted by West Nile virus (WNV)-infected cells. Incubating naïve cells with supernatant collected from Vago-expressing cells activated the JAK/STAT signaling pathway and induced the expression of *vir-1* in naïve cells independent of Dome. A NF-κB binding site was identified in CxVago promoter region afterwards, and *Culex* Rel2 which is a *Drosophila* Relish homolog has been demonstrated to be required for induction of CxVago subsequently. In addition, activation of Rel2 upon SINV infection was observed in mosquito cells (46). Intriguingly, after incubating with supernatants harvested from cells expressing Relish activated form, naïve silkworm cells displayed substantial resistance to BmNPV infection. Certain polypeptides purified from the supernatants of DNV-infected mosquito cells also acted like cytokines, conferring antiviral activity to naïve cells (47, 48).

Interestingly, in both flies and mosquito cells, induction of Vago has been characterized to be Dicer-2 dependent, since Dicer-2-mutant flies or Dicer-2-silenced mosquito cells had significantly lower levels of Vago induced by viral infection compared to Dicer-2-intact controls. But mutation of other RNAi key players, such as Ago-2 and R2D2 had no impact on Vago expression, indicating that induction of Vago is independent of RNAi pathway. Phylogenetic analysis revealed Dicer-2, which is a key player in RNAi, is closely related to mammalian RIG-I in terms of their DExD/H-box helicase domain (49, 50). Both of them belong to RIG-I-like receptor (RLR) family along with some other cytoplasmic RNA sensors, including MDA5 and Laboratory of Genetics and Physiology 2 (LGP2). More recently, Dicer-2 has been reported to modulate viral DNA production *via* acting as a pattern recognition receptor similar to RLR that senses defective viral genomes (DVGs) (51). The absence of RIG-I proteins in insects but presence of the activity of RNA sensing and induction of antiviral factors which is carried out in a Dicer-2 dependent manner suggests Dicer-2 may be the archetypal RLR that activates the antiviral signaling pathway in insects. It is worth exploring whether Dicer-2, STING and Relish constitute a signaling axis that leads to the production of antiviral effectors and contributes to cell-cell communication.

Apparently, not all viral-induced molecules potentiate antiviral immunity, some may promote host survival by preventing immune signaling from over-activation. Diedel has been characterized as an immunomodulatory cytokine in *Drosophila* that was strongly induced following infection with slowly replicating viruses, such as SINV and VSV (52). *diedel* mutant flies developed persistent inflammation as a few immune-related genes, most of which are considered to be controlled by the IMD pathway, were up-regulated in the absence of viral infection. They also showed reduced survival after immune challenges without an increase in viral load, suggesting the IMD pathway which may contribute to viral-induced pathogenesis is required to be down-regulated. Interestingly, Diedel homologs have also been identified in the genome of three different and unrelated families of DNA viruses that infect Lepidoptera, including Entomopoxvirinae, Baculoviridae, and Ascoviridae (53). Transcriptome analysis found elevated expression of ascovirus *diedel* in infected *Spodoptera frugiperda* larvae (54), and expression of the ascovirus *diedel* partially rescued the reduced viability of *diedel* mutant flies (52). The possible horizontal transfer of immunomodulatory genes from host to virus represents a strategy that virus exploits to manipulate host immune response in favor of its own replication and dissemination.

RNA Based Intercellular Communication: Transferring of Virus-Derived RNA Between Cells

Intercellular transferring of virus- or host-derived RNA, DNA and proteins from infected cells to neighboring cells are increasingly recognized as an important mean to mount a self-sustaining and even amplified innate immune response. Gap junctions, exosomes, microvesicles and plant plasmodesmata have been reported to deliver the substances originated from viral infected cells to immunize the other cells before arrival of the virus (55–58). Although the open circulatory system in insects is always believed to allow fast spread of virus in the hemolymph and migration beyond the primary site of replication, the possible cell-cell communication is supported by evidence of intercellular transferring of virus-derived RNA. Flies defective in dsRNA endocytosis or intracellular transport were hypersensitive to viral infection, and the high mortality was accompanied by hundredfold increase in viral titer, suggesting a systemic spread of dsRNA is required for antiviral immunity (59). Nanotube-like structures made of actin and tubulin were first reported in a study of the intercellular communication between *Drosophila* cells (60). Those membrane projections generated by viral-infected cells bridge neighboring cells for transferring of components of RNAi machinery, including Ago-2 and dsRNA between cells. A more recent study discovered that haemocytes acquire virus-derived dsRNA (vsRNA) by phagocytosing virus-infected cells and reverse-transcribe the viral RNA through endogenous transposon reverse transcriptases into DNA which serves as a template for transcription of secondary vsRNA in an Ago-2 dependent manner (61). The secondary vsRNA is secreted by haemocytes in exosome-like vesicles (ELVs) and spreads through the haemolymph. It is then processed into siRNA by cells taking up these ELVs and confers virus-specific immunity. Of note, this systemic antiviral potential of haemocyte-derived ELVs persists weeks after the onset of viral infection, thus it was proposed as an RNAi-based "adaptive immunity" in *Drosophila*.

DISCUSSION

Extracellular signaling network coordinates the systemic immune response through alarming or even arming the non-infected cells

with messages from viral infected cells. Although it is one of the most important parts of immune response, much less have we learnt about the molecules or vesicles secreted by viral infected cells, ways to deliver them or the pathways they influence. Integrated omics approaches might be required to characterize the soluble substances in the fractionated extracellular fluid of viral infected cells in the future research, screening of target genes under regulation of signaling pathways that are activated by viral sensors would also help to narrow down the candidates. Furthermore, the absence of viral loads in tissues expressing antiviral marker genes (32) or passive protection of naïve flies against viral challenges conferred by injection of purified ELVs from viral infected flies (61) suggests a tissue-targeted delivery or diffusion throughout the entire body, therefore identification of molecules that act as receptors or carriers of those extracellular substances will decipher how the antiviral signal is transmitted between cells, which tissues or organs are targeted and which intracellular pathways are activated.

Although the lack of sequence similarity between insect and vertebrate cytokines impedes a sequence-function relationship analysis, the structural features they share suggest they are functionally related. For example, one subdomain of Diedel, consisting of an antiparallel β-sheet covered by an α-helix, resembles certain CC or CXC chemokine family members (62), which modulate immune response by maintaining proliferative homeostasis and attenuating apoptosis. Interestingly, recombinant human IL-8 was reported to promote the phagocytic activity of *Drosophila* S2 cells and enhance the expression of Upd-3 as well as some AMP genes, including *defensin*, *cecropin A1*, and *diptericin* (63), implying that certain membrane bound molecule may function as receptor to ligand that resembles the structure of IL-8.

Some danger signals, such as metabolites produced by viral-infected cells or damage-associated molecular pattern (DAMP) released by dead or damaged cells, may also serve as mediator for systemic inflammatory response. For instance, in mammalian models nitric oxide (NO) generated through NO synthase (NOS) which is upregulated upon viral infection can diffuse freely across cell membranes and activate antiviral mechanisms in various ways, including direct and indirect damage to viral genomes (64, 65). In insects, it is well documented that NO regulates immune response to bacteria, nematode and parasites characterized by AMP expression and melanin production (66–68), and a cell-based assay showed that NO inhibits DENV replication partly through suppressing RNA-dependent RNA polymerase (69), although its role in insect antiviral immunity has not been characterized. Actin, an evolutionarily-conserved DAMP was reported to selectivity induce JAK/STAT target genes through cytokine Upd3 in *Drosophila*, whether it confers antiviral activity needs further investigation (70).

Antiviral immune response induced by different viruses varies, which might be another factor that complicates the understanding of insect antiviral immunity. For instance, Vago/Vago-like expression was down-regulated upon the infection of virulent virus but not with avirulent virus in bumblebee (71). Fast replicating viruses, such as DCV, CrPV and Flock House virus (FHV), unlike slowly replicating viruses, did not induce Diedel expression (52). In the mosquito midgut, transcriptional level of Rel2 and its canonical target genes, such as *diptericin* and *attancin*, was not induced by DENV (72), but the activation of Rel2 was detected on protein level and knockdown of Rel2 significantly increased WNV viral load (44). The seemingly disagreement on the involvement of certain molecules in antiviral immunity suggests a careful assessment of their general or specific functions is required.

In addition to their potential roles in the antiviral immune response, some molecules also participate in the defense against other microbial challenges. For example, knock-down of dSTING resulted in more susceptibility to *Listeria* infection (73) and mutation of BmSTING led to defective autophagy of microsporidia in silkworm larvae (74), suggesting insect STING mediates immune signaling pathways in response to various pathogens. However, some cytokines that have been identified in insect immune defenses against bacteria or parasites, such as growth blocking peptide (GBP) which has been characterized as a cytokine switching humoral and cellular immune response (75, 76), and TNF ortholog Eiger which promotes apoptotic cell death *via* JNK pathway and aids clearance of extracellular pathogens (77, 78), are not reported in the antiviral response. Therefore, it will be interesting to investigate whether there exist multifaceted mediators in insect innate immunity.

While studies on the viral-induced intercellular communication are still preliminary in insects, they provide valuable insights into artificial manipulation of host immune response. Insulin/insulin-like peptide has been recently reported to potentiate JAK/STAT pathway *via* ERK to broadly inhibit flavivirus replication in fly and mosquito cells, and insulin-supplemented meal effectively reduced WNV titers in infected *Culex* mosquitos (79, 80). Although the change in insulin level induced by viral infection was not yet reported in insects or even linked to antiviral immunity prior to this report, the decrease in insulin secretion was found to be common in mammals after viral infection. Research efforts aimed at characterizing the intercellular communication will not only provide a greater depth of knowledge regarding extracellular signaling networks, but also potential targets for pest or disease control based on interfering intercellular communication or priming insects with molecules transmitting antiviral messengers.

AUTHOR CONTRIBUTIONS

The author confirms being the sole contributor of this work and has approved it for publication.

FUNDING

This work is supported by grant of "National Natural Science Foundation of China" (No. 31672495) and Natural Science Foundation of Chongqing, China (cstc2020jcyj-msxmX0193).

ACKNOWLEDGMENTS

The author thanks Prof. Qingyou Xia and Yang Cao for inspiring discussion.

REFERENCES

1. Yan N, Chen ZJ. Intrinsic antiviral immunity. *Nat Immunol* (2012) 13:214–22. doi: 10.1038/ni.2229
2. Schneider WM, Chevillotte MD, Rice CM. Interferon-stimulated genes: A complex web of host defenses. *Annu Rev Immunol* (2014) 32:513–45. doi: 10.1146/annurev-immunol-032713-120231
3. Mussabekova A, Daeffler L, Imler J-L. Innate and intrinsic antiviral immunity in *Drosophila*. *Cell Mol Life Sci* (2017) 74:2039–54. doi: 10.1007/s00018-017-2453-9
4. Lamiable O, Imler J-L. Induced antiviral innate immunity in *Drosophila*. *Curr Opin Microbiol* (2014) 20:62–8. doi: 10.1016/j.mib.2014.05.006
5. Kemp C, Imler J-L. Antiviral immunity in *Drosophila*. *Curr Opin Immunol* (2009) 21:3–9. doi: 10.1016/j.coi.2009.01.007
6. Hussain M, Asgari S. MicroRNAs as mediators of insect host-pathogen interactions and immunity. *J Insect Physiol* (2014) 70:151–8. doi: 10.1016/j.jinsphys.2014.08.003
7. Asgari S. Role of microRNAs in insect host-microorganism interactions. *Front Physiol* (2011) 2:48:48. doi: 10.3389/fphys.2011.00048
8. Wu Q, Luo Y, Lu R, Lau N, Lai EC, Li W-X, et al. Virus discovery by deep sequencing and assembly of virus-derived small silencing RNAs. *Proc Natl Acad Sci USA* (2010) 107:1606–11. doi: 10.1073/pnas.0911353107
9. Petit M, Mongelli V, Frangeul L, Blanc H, Jiggins F, Saleh MC. piRNA pathway is not required for antiviral defense in *Drosophila melanogaster*. *Proc Natl Acad Sci USA* (2016) 113:E4218–E27. doi: 10.1073/pnas.1607952113
10. Tassetto M, Kunitomi M, Whitfield ZJ, Dolan PT, Sanchez-Vargas I, Garcia-Knight M, et al. Control of RNA viruses in mosquito cells through the acquisition of vDNA and endogenous viral elements. *Elife* (2019) 8:e41244. doi: 10.7554/eLife.41244
11. Varjak M, Leggewie M, Schnettler E. The antiviral piRNA response in mosquitoes? *J Gen Virol* (2018) 99:1551–62. doi: 10.1099/jgv.0.001157
12. Lamiable O, Arnold J, de Faria I, Olmo RP, Bergami F, Meignin C, et al. Analysis of the contribution of hemocytes and autophagy to *Drosophila* antiviral immunity. *J Virol* (2016) 90:5415–26. doi: 10.1128/jvi.00238-16
13. Nainu F, Shiratsuchi A, Nakanishi Y. Induction of apoptosis and subsequent phagocytosis of virus-infected cells as an antiviral mechanism. *Front Immunol* (2017) 8:1220. doi: 10.3389/fimmu.2017.01220
14. Makino S, Hamajima R, Saito A, Tomizaki M, Iwamoto A, Kobayashi M, et al. *Bombyx mori* homolog of tumor suppressor p53 is involved in apoptosis-mediated antiviral immunity of *B. mori* cells infected with nucleopolyhedrovirus. *Dev Comp Immunol* (2018) 84:133–41. doi: 10.1016/j.dci.2018.02.009
15. Mocarski E, Liu B, Behura SK, Clem RJ, Schneemann A, Becnel J, et al. P53-mediated rapid induction of apoptosis conveys resistance to viral infection in *Drosophila melanogaster*. *PloS Pathog* (2013) 9:e1003137. doi: 10.1371/journal.ppat.1003137
16. Settles EW, Friesen PD. Flock house virus induces apoptosis by depletion of *Drosophila* inhibitor-of-apoptosis protein DIAP1. *J Virol* (2008) 82:1378–88. doi: 10.1128/jvi.01941-07
17. Nainu F, Tanaka Y, Shiratsuchi A, Nakanishi Y. Protection of insects against viral infection by apoptosis-dependent phagocytosis. *J Immunol* (2015) 195:5696–706. doi: 10.4049/jimmunol.1500613
18. Jiang L, Liu W, Guo H, Dang Y, Cheng T, Yang W, et al. Distinct functions of *Bombyx mori* peptidoglycan recognition protein 2 in immune responses to bacteria and viruses. *Front Immunol* (2019) 10:776. doi: 10.3389/fimmu.2019.00776
19. Jiang L, Goldsmith MR, Xia Q. Advances in the arms race between silkworm and baculovirus. *Front Immunol* (2021). doi: 10.3389/fimmu.2021.628151
20. Delorme-Axford E, Klionsky DJ. Inflammatory-dependent sting activation induces antiviral autophagy to limit Zika virus in the *Drosophila* brain. *Autophagy* (2018) 15:1–3. doi: 10.1080/15548627.2018.1539585
21. Liu Y, Cherry S. Zika virus infection activates STING-dependent antiviral autophagy in the *Drosophila* brain. *Autophagy* (2018) 15:174–5. doi: 10.1080/15548627.2018.1528813
22. Shelly S, Lukinova N, Bambina S, Berman A, Cherry S. Autophagy is an essential component of *Drosophila* immunity against vesicular stomatitis virus. *Immunity* (2009) 30:588–98. doi: 10.1016/j.immuni.2009.02.009
23. Liu Y, Gordesky-Gold B, Leney-Greene M, Weinbren NL, Tudor M, Cherry S. Inflammation-induced, STING-dependent autophagy restricts Zika virus infection in the *Drosophila* brain. *Cell Host Microbe* (2018) 24:57–68. doi: 10.1016/j.chom.2018.05.022
24. Moy Ryan H, Gold B, Molleston Jerome M, Schad V, Yanger K, Salzano M-V, et al. Antiviral autophagy restricts Rift Valley fever virus infection and is conserved from flies to mammals. *Immunity* (2014) 40:51–65. doi: 10.1016/j.immuni.2013.10.020
25. Nakamoto M, Moy Ryan H, Xu J, Bambina S, Yasunaga A, Shelly Spencer S, et al. Virus recognition by Toll-7 activates antiviral autophagy in *Drosophila*. *Immunity* (2012) 36:658–67. doi: 10.1016/j.immuni.2012.03.003
26. Xu J, Grant G, Sabin Leah R, Gordesky-Gold B, Yasunaga A, Tudor M, et al. Transcriptional pausing controls a rapid antiviral innate immune response in *Drosophila*. *Cell Host Microbe* (2012) 12:531–43. doi: 10.1016/j.chom.2012.08.011
27. Huang Z, Kingsolver MB, Avadhanula V, Hardy RW. An antiviral role for antimicrobial peptides during the arthropod response to alphavirus replication. *J Virol* (2013) 87:4272–80. doi: 10.1128/JVI.03360-12
28. Diamond MS, Luplertlop N, Surasombatpattana P, Patramool S, Dumas E, Wasinpiyamongkol L, et al. Induction of a peptide with activity against a broad spectrum of pathogens in the *Aedes aegypti* salivary gland, following infection with Dengue virus. *PloS Pathog* (2011) 7:e1001252. doi: 10.1371/journal.ppat.1001252
29. Bao Y-Y, Tang X-D, Lv Z-Y, Wang X-Y, Tian C-H, Xu YP, et al. Gene expression profiling of resistant and susceptible *Bombyx mori* strains reveals nucleopolyhedrovirus-associated variations in host gene transcript levels. *Genomics* (2009) 94:138–45. doi: 10.1016/j.ygeno.2009.04.003
30. Merkling SH, van Rij RP. Beyond RNAi: Antiviral defense strategies in *Drosophila* and mosquito. *J Insect Physiol* (2013) 59:159–70. doi: 10.1016/j.jinsphys.2012.07.004
31. Xu J, Cherry S. Viruses and antiviral immunity in *Drosophila*. *Dev Comp Immunol* (2014) 42:67–84. doi: 10.1016/j.dci.2013.05.002
32. Dostert C, Jouanguy E, Irving P, Troxler L, Galiana-Arnoux D, Hetru C, et al. The Jak-STAT signaling pathway is required but not sufficient for the antiviral response of drosophila. *Nat Immunol* (2005) 6:946–53. doi: 10.1038/ni1237
33. Majoros A, Platanitis E, Kernbauer-Hölzl E, Rosebrock F, Müller M, Decker T. Canonical and non-canonical aspects of JAK–STAT signaling: lessons from interferons for cytokine responses. *Front Immunol* (2017) 8:29:29. doi: 10.3389/fimmu.2017.00029
34. Morris R, Kershaw NJ, Babon JJ. The molecular details of cytokine signaling via the JAK/STAT pathway. *Protein Sci* (2018) 27:1984–2009. doi: 10.1002/pro.3519
35. Schoggins JW, Rice CM. Interferon-stimulated genes and their antiviral effector functions. *Curr Opin Virol* (2011) 1:519–25. doi: 10.1016/j.coviro.2011.10.008
36. Zeidler MP, Bausek N. The *Drosophila* JAK-STAT pathway. *JAKSTAT* (2014) 2:e25353. doi: 10.4161/jkst.25353
37. Chen HW, Chen X, Oh SW, Marinissen MJ, Gutkins JS, Hou SX. Mom identifies a receptor for the *Drosophila* JAK/STAT signal transduction pathway and encodes a protein distantly related to the mammalian cytokine receptor family. *Gene Dev* (2002) 16:388–98. doi: 10.1101/gad.955202
38. Kemp C, Mueller S, Goto A, Barbier V, Paro S, Bonnay F, et al. Broad RNA interference–mediated antiviral immunity and virus-specific inducible responses in *Drosophila*. *J Immunol* (2013) 190:650–8. doi: 10.4049/jimmunol.1102486
39. Wu J, Chen ZJ. Innate immune sensing and signaling of cytosolic nucleic acids. *Annu Rev Immunol* (2014) 32:461–88. doi: 10.1146/annurev-immunol-032713-120156
40. Liu S, Cai X, Wu J, Cong Q, Chen X, Li T, et al. Phosphorylation of innate immune adaptor proteins MAVS, STING, and TRIF induces IRF3 activation. *Science* (2015) 347:aaa2630. doi: 10.1126/science.aaa2630
41. Ran Y, Shu H-B, Wang Y-Y. MITA/STING: a central and multifaceted mediator in innate immune response. *Cytokine Growth Factor Rev* (2014) 25:631–9. doi: 10.1016/j.cytogfr.2014.05.003
42. Hua X, Li B, Song L, Hu C, Li X, Wang D, et al. Stimulator of interferon genes (STING) provides insect antiviral immunity by promoting Dredd caspase–mediated NF-κB activation. *J Biol Chem* (2018) 293:11878–90. doi: 10.1074/jbc.RA117.000194

43. Goto A, Okado K, Martins N, Cai H, Barbier V, Lamiable O, et al. The kinase IKKβ regulates a STING- and NF-κB-dependent antiviral response pathway in *Drosophila*. *Immunity* (2018) 49:225–34.e4. doi: 10.1016/j.immuni.2018.07.013
44. Olson KE, Paradkar PN, Duchemin J-B, Voysey R, Walker PJ. Dicer-2-dependent activation of *Culex* Vago occurs via the TRAF-Rel2 signaling pathway. *PloS Negl Trop Dis* (2014) 8:e2823. doi: 10.1371/journal.pntd.0002823
45. Paradkar PN, Trinidad L, Voysey R, Duchemin JB, Walker PJ. Secreted Vago restricts West Nile virus infection in *Culex* mosquito cells by activating the Jak-STAT pathway. *Proc Natl Acad Sci USA* (2012) 109:18915–20. doi: 10.1073/pnas.1205231109
46. Avadhanula V, Weasner BP, Hardy GG, Kumar JP, Hardy RW. A novel system for the launch of alphavirus RNA synthesis reveals a role for the IMD pathway in arthropod antiviral response. *PloS Pathog* (2009) 5:e1000582. doi: 10.1371/journal.ppat.1000582
47. Wang F, Li X, Hua X, Xia Q. Screening and analysis of anti-BmNPV cytokines in silkworm (*Bombyx mori*). *Sci Agricult Sinica* (2018) 51:789–99. doi: 10.3864/j.issn.0578-1752.2018.04.018
48. Kanthong N, Laosutthipong C, Flegel TW. Response to Dengue virus infections altered by cytokine-like substances from mosquito cell cultures. *BMC Microbiol* (2010) 10:290. doi: 10.1186/1471-2180-10-290
49. Deddouche S, Matt N, Budd A, Mueller S, Kemp C, Galiana-Arnoux D, et al. The DExD/H-box helicase Dicer-2 mediates the induction of antiviral activity in drosophila. *Nat Immunol* (2008) 9:1425–32. doi: 10.1038/ni.1664
50. Paro S, Imler J-L, Meignin C. Sensing viral RNAs by Dicer/RIG-I like ATPases across species. *Curr Opin Immunol* (2015) 32:106–13. doi: 10.1016/j.coi.2015.01.009
51. Poirier EZ, Goic B, Tomé-Poderti L, Frangeul L, Boussier J, Gausson V, et al. Dicer-2-dependent generation of viral DNA from defective genomes of RNA viruses modulates antiviral immunity in insects. *Cell Host Microbe* (2018) 23:353–65.e8. doi: 10.1016/j.chom.2018.02.001
52. Lamiable O, Kellenberger C, Kemp C, Troxler L, Pelte N, Boutros M, et al. Cytokine Diedel and a viral homologue suppress the IMD pathway in *Drosophila*. *Proc Natl Acad Sci USA* (2016) 113:698–703. doi: 10.1073/pnas.1516122113
53. Gould A, Mlih M, Khericha M, Birdwell C, West AP. Karpac J. A virus-acquired host cytokine controls systemic aging by antagonizing apoptosis. *PloS Biol* (2018) 16:e2005796. doi: 10.1371/journal.pbio.2005796
54. Zaghloul HAH, Hice R, Arensburger P, Federici BA. Transcriptome analysis of the *Spodoptera frugiperda* ascovirus *in vivo* provides insights into how its apoptosis inhibitors and caspase promote increased synthesis of viral vesicles and virion progeny. *J Virol* (2017) 91:e00874–17. doi: 10.1128/JVI.00874-17
55. Rosas-Diaz T, Zhang D, Fan PF, Wang LP, Ding X, Jiang YL, et al. A virus-targeted plant receptor-like kinase promotes cell-to-cell spread of RNAi. *Proc Natl Acad Sci USA* (2018) 115:1388–93. doi: 10.1073/pnas.1715556115
56. Kalamvoki M, Du T, Roizman B. Cells infected with herpes simplex virus 1 export to uninfected cells exosomes containing STING, viral mRNAs, and microRNAs. *Proc Natl Acad Sci USA* (2014) 111:E4991–6. doi: 10.1073/pnas.1419338111
57. Baroja-Mazo A, Martin-Sanchez F, Gomez AI, Martinez CM, Amores-Iniesta J, Compan V, et al. The NLRP3 inflammasome is released as a particulate danger signal that amplifies the inflammatory response. *Nat Immunol* (2014) 15:738–48. doi: 10.1038/ni.2919
58. Patel SJ, King KR, Casali M, Yarmush ML. DNA-triggered innate immune responses are propagated by gap junction communication. *Proc Natl Acad Sci USA* (2009) 106:12867–72. doi: 10.1073/pnas.0809292106
59. Saleh M-C, Tassetto M, van Rij RP, Goic B, Gausson V, Berry B, et al. Antiviral immunity in *Drosophila* requires systemic RNA interference spread. *Nature* (2009) 458:346–50. doi: 10.1038/nature07712
60. Karlikow M, Goic B, Mongelli V, Salles A, Schmitt C, Bonne I, et al. *Drosophila* cells use nanotube-like structures to transfer dsRNA and RNAi machinery between cells. *Sci Rep* (2016) 6:27085. doi: 10.1038/srep27085
61. Tassetto M, Kunitomi M, Andino R. Circulating immune cells mediate a systemic RNAi-based adaptive antiviral response in *Drosophila*. *Cell* (2017) 169:314–25.e13. doi: 10.1016/j.cell.2017.03.033
62. Doucet D, Coste F, Kemp C, Bobezeau V, Hetru C, Kellenberger C, et al. Crystal structure of Diedel, a marker of the immune response of *Drosophila melanogaster*. *PloS One* (2012) 7:e33416. doi: 10.1371/journal.pone.0033416
63. Malagoli D, Sacchi S, Ottaviani E. Unpaired (upd)-3 expression and other immune-related functions are stimulated by interleukin-8 in *Drosophila melanogaster* SL2 cell line. *Cytokine* (2008) 44:269–74. doi: 10.1016/j.cyto.2008.08.011
64. Abdul-Cader MS, Amarasinghe A, Abdul-Careem MF. Activation of toll-like receptor signaling pathways leading to nitric oxide-mediated antiviral responses. *Arch Virol* (2016) 161:2075–86. doi: 10.1007/s00705-016-2904-x
65. Nappi AJ, Vass E, Frey F, Carton Y. Nitric oxide involvement in *Drosophila* immunity. *Nitric Oxide* (2000) 4:423–30. doi: 10.1006/niox.2000.0294
66. Eleftherianos I, More K, Spivack S, Paulin E, Khojandi A, Shukla S. Nitric oxide levels regulate the immune response of *Drosophila melanogaster* reference laboratory strains to bacterial infections. *Infect Immun* (2014) 82:4169–81. doi: 10.1128/Iai.02318-14
67. Foley E, O'Farrell PH. Nitric oxide contributes to induction of innate immune responses to gram-negative bacteria in *Drosophila*. *Gene Dev* (2003) 17:115–25. doi: 10.1101/gad.1018503
68. Herrera-Ortiz A, Martinez-Barnetche J, Smit N, Rodriguez MH, Lanz-Mendoza H. The effect of nitric oxide and hydrogen peroxide in the activation of the systemic immune response of *Anopheles albimanus* infected with *Plasmodium berghei*. *Dev Comp Immunol* (2011) 35:44–50. doi: 10.1016/j.dci.2010.08.004
69. Takhampunya R, Padmanabhan R, Ubol S. Antiviral action of nitric oxide on dengue virus type 2 replication. *J Gen Virol* (2006) 87:3003–11. doi: 10.1099/vir.0.81880-0
70. Srinivasan N, Gordon O, Ahrens S, Franz A, Deddouche S, Chakravarty P, et al. Actin is an evolutionarily-conserved damage-associated molecular pattern that signals tissue injury in *Drosophila melanogaster*. *Elife* (2016) 5:e19662. doi: 10.7554/eLife.19662
71. Niu J, Meeus I, Smagghe G. Differential expression pattern of Vago in bumblebee (*Bombus terrestris*), induced by virulent and avirulent virus infections. *Sci Rep* (2016) 6:34200. doi: 10.1038/srep34200
72. Xi Z, Ramirez JI, Dimopoulos G. The *Aedes aegypti* Toll pathway controls dengue virus infection. *PloS Pathog* (2008) 4:e1000098. doi: 10.1371/journal.ppat.1000098
73. Martin M, Hiroyasu A, Guzman RM, Roberts SA, Goodman AG. Analysis of *Drosophila* STING reveals an evolutionarily conserved antimicrobial function. *Cell Rep* (2018) 23:3537–50.e6. doi: 10.1016/j.celrep.2018.05.029
74. Hua X, Xu W, Ma S, Xia Q. STING-dependent autophagy suppresses *Nosema bombycis* infection in silkworms, *Bombyx mori*. *Dev Comp Immunol* (2020) 115:103862. doi: 10.1016/j.dci.2020.103862
75. Ishii K, Hamamoto H, Kamimura M, Nakamura Y, Noda H, Imamura K, et al. Insect cytokine paralytic peptide (PP) induces cellular and humoral immune responses in the silkworm *Bombyx mori*. *J Biol Chem* (2010) 285:28635–42. doi: 10.1074/jbc.M110.138446
76. Tsuzuki S, Matsumoto H, Furihata S, Ryuda M, Tanaka H, Jae Sung E, et al. Switching between humoral and cellular immune responses in *Drosophila* is guided by the cytokine GBP. *Nat Commun* (2014) 5:4628. doi: 10.1038/ncomms5628
77. Schneider DS, Ayres JS, Brandt SM, Costa A, Dionne MS, Gordon MD, et al. *Drosophila* eiger mutants are sensitve to extracellular pathogens. *PloS Pathog* (2007) 3:e24. doi: 10.1371/journal.ppat.0030041
78. Igaki T, Kanda H, Yamamoto-Goto Y, Kanuka H, Kuranaga E, Aigaki T, et al. Eiger, a TNF superfamily ligand that triggers the *Drosophila* JNK pathway. *EMBO J* (2002) 21:3009–18. doi: 10.1093/emboj/cdf306
79. Trammell CE, Goodman AG. Emerging mechanisms of insulin-mediated antiviral immunity in *Drosophila melanogaster*. *Front Immunol* (2019) 10:2973:2973. doi: 10.3389/fimmu.2019.02973
80. Ahlers LRH, Trammell CE, Carrell GF, Mackinnon S, Torrevillas BK, Chow CY, et al. Insulin potentiates JAK/STAT signaling to broadly inhibit flavivirus replication in insect vectors. *Cell Rep* (2019) 29:1946–60.e5. doi: 10.1016/j.celrep.2019.10.029

Conflict of Interest: The author declares that the research was conducted in the absence of any commercial or financial relationships that could be construed as a potential conflict of interest.

frontiers in Physiology

ORIGINAL RESEARCH
published: 10 May 2021
doi: 10.3389/fphys.2021.650972

Precocious Metamorphosis of Silkworm Larvae Infected by BmNPV in the Latter Half of the Fifth Instar

Ping-Zhen Xu[1,2], Mei-Rong Zhang[1,2], Xue-Yang Wang[1,2] and Yang-Chun Wu[1,2]**

[1] Jiangsu Key Laboratory of Sericultural Biology and Biotechnology, School of Biotechnology, Jiangsu University of Science and Technology, Zhenjiang, China, [2] Key Laboratory of Silkworm and Mulberry Genetic Improvement, Ministry of Agriculture, Sericultural Research Institute, Chinese Academy of Agricultural Sciences, Zhenjiang, China

The mulberry silkworm (*Bombyx mori*) is a model organism, and BmNPV is a typical baculovirus. Together, these organisms form a useful model to investigate host–baculovirus interactions. Prothoracic glands (PGs) are also model organs, used to investigate the regulatory effect of synthetic ecdysone on insect growth and development. In this study, day-4 fifth instar silkworm larvae were infected with BmNPV. Wandering silkworms appeared in the infected groups 12 h earlier than in the control groups, and the ecdysone titer in infected larvae was significantly higher than that of the control larvae. We then used RNA sequencing (RNA-seq) to analyze silkworm PGs 48 h after BmNPV infection. We identified 15 differentially expressed genes (DEGs) that were classified as mainly being involved in metabolic processes and pathways. All 15 DEGs were expressed in the PGs, of which *Novel01674*, *BmJing*, and *BmAryl* were specifically expressed in the PGs. The transcripts of *BmNGDN*, *BmTrypsin-1*, *BmACSS3*, and *BmJing* were significantly increased, and *BmPyd3*, *BmTitin*, *BmIGc2*, *Novel01674*, and *BmAryl* were significantly decreased from 24 to 72 h in the PGs after BmNPV infection. The changes in the transcription of these nine genes were generally consistent with the transcriptome data. The upregulation of *BmTrypsin-1* and *BmACSS3* indicate that these DEGs may be involved in the maturation process in the latter half of the fifth instar of silkworm larvae. These findings further our understanding of silkworm larval development, the interaction between BmNPV infection and the host developmental response, and host–baculovirus interactions in general.

Keywords: ***Bombyx mori*, *Bombyx mori* nucleopolyhedrovirus, prothoracic gland, transcriptome, 20-hydroxyecdysone**

OPEN ACCESS

Edited by:
Liang Jiang,
Southwest University, China

Reviewed by:
Jingchen Sun,
South China Agricultural University, China
Wei Yu,
Zhejiang Sci-Tech University, China

****Correspondence:***
Ping-Zhen Xu
xpz198249@just.edu.cn
Yang-Chun Wu
199400001939@just.edu.cn

Specialty section:
This article was submitted to Invertebrate Physiology, a section of the journal Frontiers in Physiology

Received: *08 January 2021*
Accepted: *06 April 2021*
Published: *10 May 2021*

Citation:
Xu P-Z, Zhang M-R, Wang X-Y and Wu Y-C (2021) Precocious Metamorphosis of Silkworm Larvae Infected by BmNPV in the Latter Half of the Fifth Instar. Front. Physiol. 12:650972. doi: 10.3389/fphys.2021.650972

INTRODUCTION

The mulberry silkworm (*Bombyx mori*) has been reared for the past 5,000 years in China due to its importance for silk production. In addition to this economic importance, *B. mori* has recently played an essential role as a model organism in scientific research, molecular biology, and genetics studies (Mita et al., 2004; Xia et al., 2004). *B. mori* undergoes complete (egg–larva–pupa–adult) metamorphosis within each generation; however, only the larval stage feeds. In general, silkworm larvae are tetramolters that proceed through four instars, molting between each instar. The durations of the larval instar stages are as follows: 3–4 days in the first instar, 2–3 days in

the second instar, 3–4 days in the third instar, 5–6 days in the fourth instar, and 6–8 days in the fifth instar. However, the duration of the larval stage depends on the silkworm strain and rearing temperature. Silkworm larvae grow rapidly, and the weight of a terminal fifth instar larva is ∼10,000 times that of a newly hatched larva (Xu et al., 2019). In particular, day 3 of the fifth instar larvae is the boundary for the larval stage, where the larvae feed and grow quickly from day 1 to day 3 of the fifth instar. The larvae then (in the gluttonous stage) greatly synthesize silk proteins in the silk gland (Xu et al., 2019), which indicates maturation and leads to spinning in the terminal fifth instar stage. After the completion of silk spinning, the silkworms proceed with larval–pupal metamorphosis.

Sericulture is one of the main sources of income for farmers in many developing countries, such as China, India, Brazil, Vietnam, and Thailand (Jiang and Xia, 2014). China produces almost 80% of cocoons worldwide. Sericulture faces biological challenges from pathogenic fungi, bacteria, and viruses, which can cause annual cocoon production losses of 20–30% (Jiang et al., 2013a). Although antibiotics are administered to silkworms to prevent and treat bacterial diseases, and fresh lime and chlorine-containing preparations are used to disinfect the rearing seat to prevent fungal diseases, there are no effective prevention and treatment methods for viral diseases. Viral diseases are responsible for almost 80% of the annual cocoon production losses, and *B. mori* nucleopolyhedrovirus (BmNPV) is one of the major pathogens and the most prevalent threat to sericulture in almost all countries worldwide (Jiang et al., 2013a; Jiang and Xia, 2014). BmNPV is an enveloped double-stranded DNA virus that presents a biphasic infection process throughout its viral life cycle, generating progeny with two different phenotypes, namely, occlusion-derived virus (ODV) and budded virus (BV) (Gomi et al., 1999). ODVs are packaged in occlusion bodies (OBs). Both forms play different roles during pathogenesis. The alkalinity of the silkworm midgut triggers the dissolution of OBs and the release of ODV in the midgut lumen. The ODV is responsible for the primary infection through oral transmission of the virus among silkworm larvae, while the BV is responsible for the secondary infection, causing systemic spreading all over the host within the infected silkworm larvae (Jiang, 2021).

Bombyx mori is a model organism, and BmNPV is a typical baculovirus (Gomi et al., 1999; Mita et al., 2004; Xia et al., 2004), and together, they present an important model to assess host–baculovirus interactions (Jiang and Xia, 2014). Insights from previous host studies revealed that innate antiviral immunity in lepidopteran insects plays important roles in host–baculovirus interactions (Jiang, 2021). Antiviral proteins, including red fluorescent proteins (RFPs) (Sunagar et al., 2011; Manjunatha et al., 2018), Bmlipase (Bmlipase-1 and Bmlipase member H-A) (Ponnuvel et al., 2003; Zhang S. Z. et al., 2020), serine proteases (SPs), and serine protease homologs (SPHs) (Nakazawa et al., 2004; Ponnuvel et al., 2012), show strong antiviral activity in the digestive juice of the silkworm. Moreover, heat shock protein 19.9 (*Bmhsp19.9*) is involved in antiviral immunity against BmNPV function (Jiang et al., 2021b). BmNPV has also evolved diverse mechanisms to counter host responses and ensure its replication. For example, BmNPV activates the expression of *BmPGRP2-2* to inhibit *phosphatase and tensin homolog* (*PTEN*), which relieves its suppression of the PI3K-Akt pathway and triggers an increase in Akt phosphorylation (p-Akt) to inhibit cell apoptosis; the resulting increased cell survival is beneficial for viral replication (Jiang et al., 2019). *BmSpry* is upstream of ERK and JNK and is downregulated by BmNPV to elevate p-ERK and ensure viral reproduction in the silkworm (Guo et al., 2019). BmNPV activates the host ERK and JNK signal pathways for efficient replication (Katsuma et al., 2007). The baculovirus ecdysteroid UDP-glucosyltransferase gene (*egt*) encoding the enzyme ecdysteroid UDP-glucosyltransferase catalyzes the transfer of glucose from UDP-glucose to ecdysteroid molting hormones, and the expression of this enzyme blocks the molting of infected larval insects (O'Reilly and Miller, 1989). The BmNPV *egt* gene prolongs the survival time of infected silkworms to increase virus reproduction (Katsuma and Shimada, 2015).

The expression of NPV genes occurs in four phases: immediate early phase (0–4 h post-infection, hpi), delayed early stage (5–7 hpi), late stage (8–18 hpi), and very late stage (>18 hpi). Viral DNA replication starts at 8 hpi and represents the transition from the early stage to the late stage (Huh and Weaver, 1990; Jiang et al., 2013b, 2021a). Global shutoff of host gene expression and protein synthesis in insect cells begins at the early stage at around 12–18 h after NPV infection (Du and Thiem, 1997; Shirata et al., 2010; Ikeda et al., 2013). However, previous studies that investigated the interactions between BmNPV and its hosts have mainly focused on newly exuviated fifth instar silkworm larvae infected by BmNPV and the systemic process of infection by BmNPV within 48 hpi (i.e., silkworm larvae in the first half of the fifth instar). Until now, no studies have investigated the interactions between BmNPV and silkworm larvae in the latter half of the fifth instar.

The use of next-generation sequencing technologies in genome-wide studies of silkworms and BmNPV interactions is a recent development and is rapidly advancing. Recently, several studies have reported on the transcriptional response of silkworm larvae against BmNPV infection in the major innate immune tissues of the fat body and midgut (Chen et al., 2019; Huang et al., 2019; Jiang et al., 2019; Toufeeq et al., 2019; Zhang X. et al., 2020). However, the gene expression of prothoracic glands (PGs) infected by BmNPV has not yet been analyzed.

In the present study, we first investigated the precocious molting and metamorphosis of silkworm larvae under BmNPV infection, and the ecdysone titer in infected larvae was significantly higher than that of the control larvae. We then used RNA sequencing (RNA-seq) to analyze silkworm PGs 48 h after BmNPV infection. The classifications of the 15 differentially expressed genes (DEGs) were mainly involved in the metabolic processes and pathways. The reverse transcription quantitative PCR (RT-qPCR) results of the DEGs in the PGs of BmNPV-infected larvae at 24, 48, and 72 h were generally consistent with the transcriptome data. The transcripts of *BmTrypsin-1* and *BmACSS3* were significantly increased from 24 to 72 h after BmNPV infection, indicating that they may be involved in the maturation process in the latter half of the fifth instar of silkworm larvae. This study was conducted to further our understanding

of the complex biological processes in the interactions between BmNPV and its precocious metamorphic insect hosts.

MATERIALS AND METHODS

Study Animals and Virus

Bombyx mori F_{50} strain larvae were reared on fresh mulberry leaves under a 12:12 h day/night cycle at 25 ± 1°C and 60% relative humidity. The majority of the fifth instar larvae started wandering on day 8, depending on the batch of the silkworm. The larvae underwent oral inoculation with a wild BmNPV T3 strain, and the OBs were obtained from the larvae hemolymph before the larvae died. The OBs were purified by repeated and differential centrifugation, as previously described (Rahman and Gopinathan, 2004).

Sample Collection

In total, 500 day-4 fifth instar larvae were orally infected with BmNPV using 2.0×10^6 OB/larva. Control larvae ($n = 500$) were fed the same volume of sterile distilled water. The larvae of the infected and control groups were maintained in isolation and reared under the same conditions. The PGs were entwined in pairs in the tracheal bush of the first spiracle (**Supplementary Figure 1**). The PGs were carefully removed from the larvae of the infected and control groups after 24, 48, and 72 h (**Supplementary Figure 2**). Hemolymph was collected from day 6 (48 hpi), day 6.5 (60 hpi), day 7 (72 hpi), and day 7.5 (84 hpi) fifth instar larvae of the infected and control groups for use in assays of the ecdysteroid titers among the different developmental stages.

Statistics of Precocious Maturation of Silkworms After BmNPV Infection

Day-4 fifth instar larvae were divided into 6 groups with 200 in each group. All 200 larvae used in each of the three independent experiments were orally infected with BmNPV using 2.0×10^6 OB/larva. The 200 control larvae used in each of the three independent experiments were fed with the same volume of sterile distilled water. The larvae of the infected and control groups were maintained in isolation and reared under the same conditions. Diseased and dead larvae were removed and counted during rearing. When the proportion of mature silkworms was > 5% (first gate), the statistics was started.

Cholesterol and 7-Dehydrocholesterol Feeding Experiments

As previously described (Wu et al., 2016), silkworm larvae were fed mulberry leaves supplemented with 8,000 mg/L of cholesterol and 7-dehydrocholesterol (7dC). Mulberry leaves supplemented with the same volume of sterile distilled water were used as the control. Day-5 fifth instar larvae were initially fed (first feed session) with cholesterol and 7dC supplemented leaves and then again 24 h later (second feed session). Replacement mulberry leaves were added 6 h after each feeding session. The proportion of mature vs. immature larvae was counted, and the second gate was determined to be the point at which the majority of the larvae had started maturing. The point at which all larvae (100%) had reached maturity defined the third gate. All experiments were repeated three times per group.

Assay of Ecdysteroid Titers in Hemolymph and Examination of Viral DNA in PGs

The hemolymph samples were homogenized in 50% MeOH (800 μl). The resultant homogenates were centrifuged, and the supernatant was used to assay the ecdysteroid titers using an Insect Ecdysone ELISA Kit (Shanghai MEILIAN Biotechnology Co., Ltd.) according to the manufacturer's instructions. RT-PCR was used to analyze the BmNPV virus replication level. The total DNA was extracted from the PGs of the BmNPV-infected larvae at 24, 48, and 72 h, as well as from the control larvae at 48 h. The DNA templates (10 ng) were PCR amplified using primers for the BmNPV *GP41* gene. The silkworm glyceraldehyde-3-phosphate dehydrogenase (*BmGAPDH*) was used as the internal control. The specific primers for each gene used in the RT-PCR are shown in **Supplementary Table 1**. The RT-PCR product of each gene was defined as previously described (Zhang et al., 2019).

Transcriptome Analysis

Total RNA was isolated from the PGs of the silkworm larvae using the TRIzol reagent (Invitrogen, New York, NY, United States) according to the manufacturer's instructions. RNA purity was quantified using a NanoDrop 2000 spectrophotometer (Thermo Fisher Scientific, New York, NY, United States). Poly(A)-tailed RNA prepared using magnetic oligo (dT) beads was broken into short fragments using a fragment buffer and was then reverse transcribed to synthesize first-strand complementary DNA (cDNA) with a random primer. DNA polymerase I was then mixed with RNase H, deoxyribonucleotide triphosphate (dNTP), and the buffer solution to synthesize the complementary strand. The libraries were constructed using the Illumina methods and protocols, following the manufacturer's instructions. The insert size and concentration of the cDNA library were both checked and quantified by an Agilent Bioanalyzer 2100 (Agilent Technologies, Inc., Santa Clara, CA) and Qubit® RNA Assay Kit (Life Technologies, CA, United States), respectively. RNA-seq was carried out using an Illumina HiSeq 2500 instrument (Illumina, San Diego, CA, United States). To obtain clean reads and ensure the quality of information analysis, the raw reads were filtered by removing the adapter sequences, empty reads, unknown nucleotides (ratio ≥ 10%), and low-quality reads with a basic mass value of $Q \leq 20$, which accounted for more than 50% of the whole read length. The clean read assembly was performed according to a previous report (Grabherr et al., 2011). The paired-end clean reads were mapped to the *B. mori* genome using the software package TopHat2 (version 2.0.12) (Kim et al., 2013). The genome sequences and annotation file were downloaded from SilkDB. The RNA-seq reads were aligned and then used to construct transcripts with Cufflinks (version 2.1.1) (Trapnell et al., 2012). HTSeq (version 0.6.1) was used to count the reads mapped to each gene to quantify the gene expression levels

(Anders et al., 2015). The fragments per kilobase of transcript per million mapped reads (FPKM) of each gene were then calculated based on the length of the gene and read count mapped to a given gene. Genes with a FPKM $\geq$ 1.0 were identified as "expressed." A ratio ($\log_2$ fold change) between the infected and control groups of $\geq$ 1.5 was identified as the determinant of the DEGs. The raw data have been submitted to the Gene Expression Omnibus (GEO) database with the accession number GSE167875. The functional annotation of DEGs was performed using the Gene Ontology (GO) assignments (Gotz et al., 2008) and Kyoto Encyclopedia of Genes and Genomes (KEGG) pathway enrichments (Kanehisa et al., 2012).

Tissue Expression Patterns of DEGs

The PGs are important endocrine organs that are significantly different from other tissues in both their morphology and function. In silkworms, the day-3 fifth instar is the boundary for the whole larval development stage (Xu et al., 2019). To analyze the tissue expression patterns of the identified DEGs in the PGs, the PGs, head, integument, midgut, fat body, hemocyte, ovary, testis, Malpighian tubule, trachea, anterior silk gland (ASG), median silk gland (MSG), and posterior silk gland (PSG) of day-3 fifth instar larvae were collected. We detected the expression patterns in the multiple tissues of day-3 fifth instar larvae. Total RNA was extracted using the TRIzol reagent (Invitrogen, Carlsbad, CA, United States). Total RNA concentrations were quantified, and single-stranded cDNAs were synthesized. The *BmGAPDH* gene was used as an intrinsic control.

RT-qPCR Analysis

The genes selected according to the RNA-seq results were compared by RT-qPCR. Total RNA was extracted from the PGs samples of the infected and control groups at 24, 48, and 72 h. The first-strand cDNA was synthesized using the PrimeScript Reverse Transcriptase kit (TaKaRa, Dalian, China) according to the manufacturer's instructions. RT-qPCR was performed as previously described (Xu et al., 2019). The *BmGAPDH* gene was used as an intrinsic control (Guo et al., 2016).

RESULTS

Statistics of Precocious Maturation of Silkworm After BmNPV Infection

The point when the proportion of mature silkworms was >5% was considered as the first gate, the point when the majority of larvae started maturing was considered as the second gate, and the point when all larvae had reached maturity (100%) was considered as the third gate. The duration of the fifth instar larval stage of the *B. mori* F_{50} strain was almost 8.5 days (**Figure 1**). The day-4 fifth instar larvae infected with BmNPV matured early. The times that both the first- and second-gate mature silkworms appeared in the infected groups were 12 h earlier than in the control groups (**Figure 1**). The weights of mature silkworms in the infected groups were significantly decreased when compared with the control groups (**Supplementary Table 2**). The spinning process was normal, and there was no difference between the infected groups and the control groups. Approximately half of the larvae in the infected groups died during the larval–pupal stage. Compared with the control groups, the cocoon sizes and the weights of the pupae (female and male) were observably reduced in the BmNPV-infected groups (**Supplementary Table 2**). The fifth instar larvae underwent precocious maturation after infection with BmNPV. Moreover, the day-5 fifth instar larvae were fed with 8,000 mg/L cholesterol and 7dC (via supplemented leaves). The results of feeding with cholesterol and 7dC were also shown to induce precocious maturation when compared to the control, where a certain number of larvae exhibited an anal prolapse in each group fed with cholesterol and 7dC (**Supplementary Table 3**).

Assay of Ecdysteroid Titers and RT-PCR Analysis of Viral DNA After BmNPV Infection

Based on the findings of precocious maturation of silkworms after BmNPV infection, the molting and metamorphosis of silkworm requires the presence of 20-hydroxyecdysone (20E). We speculated that the BmNPV infection would have some influences on the ecdysone titer. Thus, the titers of ecdysone in infected and control larvae were determined by ELISA. The results indicated that the ecdysone titers were significantly higher in infected larvae than in the control larvae (**Figure 2A**). Meanwhile, RT-PCR was used to analyze the virus genomic DNA copies in the PGs at 24, 48, and 72 h after BmNPV infection. The expression of the *BmNPV GP41* gene was detected in the PGs from 24 to 72 hpi (**Figure 2B**). The expression of the *GP41* gene was not detected in the PGs from the uninfected larvae at 48 h (**Figure 2B**). These results were useful for selecting the time point for the RNA-seq experiments.

General Information of RNA-Seq and DEGs

The square of the Pearson correlation coefficient (R^2) between the four samples was > 0.938 (**Supplementary Figure 3**). The Q20 values for the clean reads (for each group) were above 95% (**Supplementary Table 4**). The percentage of clean sequences located on the genome was > 80%. These results indicated that the transcriptome data were assembled with high quality and can be used for further research. The number of expressed genes was 10,152 in the control groups and 10,404 in the BmNPV-infected groups (**Supplementary Table 5**). In total, seven upregulated and eight downregulated DEGs were screened out (**Table 1** and **Supplementary Table 6**). The functions of the 15 DEGs were primarily located in the binding proteins of nucleic acids, ions, and proteins, and *BmTrypsin-1* had a serine-type endopeptidase activity (**Table 1**). The DEGs were then annotated by GO analysis to determine their involvement in biological processes, molecular functions, and cellular components (**Supplementary Figure 4**). The upregulated expression genes were related to biological processes that were mainly focused on metabolic and biological processes (**Supplementary Figure 4** and **Supplementary Table 7**). The

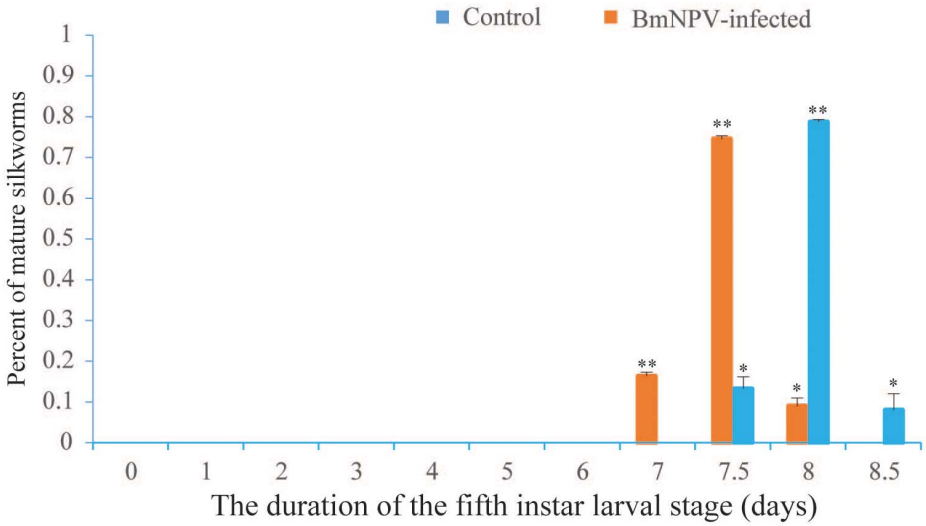

FIGURE 1 | Statistics of the duration of the fifth instar and precocious maturation for day-4 fifth instar silkworm larvae infected with BmNPV. Values represent means ± SDs of three independent investigations. Significant differences are indicated by (*$p < 0.05$) or (**$p < 0.01$).

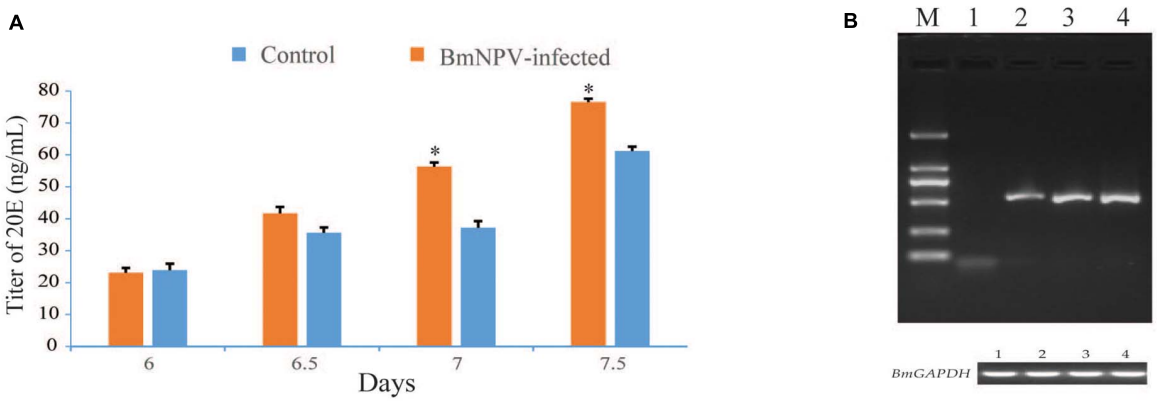

FIGURE 2 | Assay of ecdysteroid titers in hemolymph and examination of virus genomic DNA copies in the prothoracic glands (PGs). **(A)** ELISA analysis was repeated three times for each set of protein samples. Values represent the means ± SDs of three independent determinations. Significant difference is indicated by (*$p < 0.05$). **(B)** The expression of the BmNPV *GP41* gene was detected in the PGs of the BmNPV-infected silkworm larvae at 24, 48, and 72 h, as well as the control larvae at 48 h. M: DL2000 DNA marker; numbers 1–4 indicate the control group at 48 h and the BmNPV-infected groups at 24, 48, and 72 h, respectively.

downregulated expression genes were focused on biological and metabolic processes and respond to stress factors and stimuli in biological processes (**Supplementary Figure 4** and **Supplementary Table 7**). Regarding the cellular components, only the downregulated expression genes were involved in the membrane and integral components of the membrane, and the upregulated expression genes were not enriched (**Supplementary Figure 4** and **Supplementary Table 7**). Within the molecular function, the upregulated expression genes were primarily located in the catalytic activity, and the down regulated expression genes were involved in protein binding, hydrolase activity, and catalytic activity (**Supplementary Figure 4** and **Supplementary Table 7**). There were some differences in the GO functional annotations between the upregulated and downregulated genes (**Supplementary Figure 4**). The KEGG pathway enrichment analysis of the identified DEGs showed that the enriched genes were mainly involved in pathways, including metabolic pathways, propanoate metabolism, beta-alanine metabolism, drug metabolism with other enzymes, pyrimidine metabolism, and pantothenate and coenzyme A (CoA) biosynthesis (**Table 2** and **Supplementary Table 8**). The KEGG pathway enrichment analysis of *BmACSS3* revealed that acyl-coenzyme A (AcCoA) synthase activity and *BmACSS3* could be involved in the acyl-CoA to cholesterogenesis pathways.

Spatial Expression Patterns of the Identified DEGs

We investigated the spatial expression patterns of the identified DEGs in multiple tissues of the PGs, head, integument, midgut, fat body, hemocyte, ovary, testis, Malpighian tubule, trachea,

TABLE 1 | List of the differentially expressed genes in silkworm prothoracic glands with a 1.5-fold change after BmNPV infection.

	Gene name	Description	log_2 fold change	Function	ID in silkDB
Upregulated					
1	*BmNGDN*	Eukaryotic translation initiation factor 4E binding protein	1.92	EIF4E binding protein	BGIBMGA003191
2	*BmGag-p*	Gag-pol polyprotein	1.59	Retrotransposon protein	BGIBMGA004024
3	*BmNord*	Neuron-derived neurotrophic factor	2.78	N/A	BGIBMGA008935
4	*BmTrypsin-1*	Trypsin-1 serine protease	2.32	Serine-type endopeptidase activity	BGIBMGA008938
5	*BmACSS3*	Acyl-CoA synthetase short-chain family member 3	1.90	AMP-binging enzyme	BGIBMGA010070
6	*BmJing*	Zinc finger protein jing	3.10	Nucleic acid binding	Novel00232
7	*BmMar1*	Mariner transposon Bmmar1 transposase gene	2.35	DNA binding	Novel00602
Downregulated					
8	*BmPyd3*	Carbon–nitrogen hydrolase protein	−2.39	Carbon-nitrogen hydrolase	BGIBMGA001595
9	*BmTitin*	Muscle proteins	−2.82	Protein binding	BGIBMGA002033
10	*BmUnc-89*	Muscle M-line assembly protein unc-89	−2.93	Heterocyclic compound binding	BGIBMGA002034
11	*BmIGc2*	Immunoglobulin C-2 Type	−3.89	Hexosaminidase activity	BGIBMGA004546
12	*BmAryl*	Arylphorin subunit alpha	−1.51	N/A	BGIBMGA008860
13	*BmTitin2*	Muscle proteins	−4.06	protein binding	Novel00168
14	*BmKettin*	Muscle proteins	−5.98	Protein binding	Novel00554
15	*Novel01674*	Uncharacterized protein LOC105842185	−3.84	Ion binding	Novel01674

TABLE 2 | The Kyoto Encyclopedia of Genes and Genomes (KEGG) pathway enrichment analysis.

Number	Map_Name	KEGG_ID	Gene_ID	Definition	log_2 fold change
1	Metabolic pathways	bmor:100329149|	BGIBMGA001595	Beta-ureidopropionase	−2.39
		bmor:101743386|	BGIBMGA010070	Fatty acid CoA ligase	1.90
2	Propanoate metabolism	bmor:100329149|	BGIBMGA001595	Beta-alanine synthase	−2.39
3	Beta-alanine metabolism	bmor:101743386|	BGIBMGA010070	Acyl-CoA synthetase	1.90
4	Drug metabolism with other enzymes	bmor:100329149|	BGIBMGA001595	Cyanide hydratase	−2.39
5	Pyrimidine metabolism	bmor:100329149|	BGIBMGA001595	Beta-alanine synthase	−2.39
6	Pantothenate and CoA biosynthesis	bmor:100329149|	BGIBMGA001595	Pantetheine hydrolase	−2.39

ASG, MSG, and PSG of day-3 fifth instar larvae. Such findings can further our understanding of the PGs and elucidate the expression characteristics of DEGs. Expression signals of all of the 15 DEGs were detected in the PGs (**Figure 3**). The genes of *Novel01674*, *BmJing*, and *BmAryl* were expressed only in PGs (**Figure 3**). *BmACSS3* was expressed only in the PGs, head, and integument (**Figure 3**). The other 11 genes were expressed in multiple tissues (**Figure 3**).

Expression Analysis of the Identified DEGs

We used RT-qPCR to investigate the relative expression levels of nine randomly selected genes of the DEGs in the PGs of BmNPV-infected larvae at 24, 48, and 72 h. The expression levels of *BmNGDN*, *BmTrypsin-1*, *BmACSS3*, and *BmJing* were upregulated in the transcriptome data, i.e., their transcripts were significantly increased from 24 to 72 h after BmNPV infection (**Figures 4A–D**). Meanwhile, the expression levels of *BmPyd3*, *BmTitin*, *BmIGc2*, *Novel01674*, and *BmAryl* were downregulated in the transcriptome data, i.e., their transcripts were significantly decreased from 24 to 72 h after BmNPV infection (**Figures 4E–I**). The changes in the transcription of the nine genes were generally consistent with the transcriptome data.

DISCUSSION

The mulberry silkworm is one of the best models to study insect physiology and biochemistry, especially to better understand the relationship between induction factors (external and internal) and development. In general, the larvae of tetramolter silkworms proceed through five instars and undergo molting between each instar. The last instar larva completes the larval–pupal transition. The developmental speed of silkworm larvae has been shown to be regular and constant within the same silkworm strain and when maintained under the same rearing conditions. The day-3 fifth instar larval stage is considered to represent the boundary for the larval stage.

In this study, the day-4 fifth instar larvae infected with BmNPV (using 2.0×10^6 OB/larva) matured early, and the ecdysone titer in infected larvae was significantly higher than that of the control larvae. In addition, BmNPV infection (using 2.0×10^7 OB/larva) also caused larvae precocious maturation (only at the first gate), followed by illness and death (data not shown). Meanwhile, day-5 fifth instar larvae fed with cholesterol and 7dC also exhibited precocious maturation. Cholesterol and 7dC supplementation in the latter half of the fifth instar shortened the fifth instar period. In contrast, cholesterol and 7dC supplementation in the first half of the fifth instar (days 1–3)

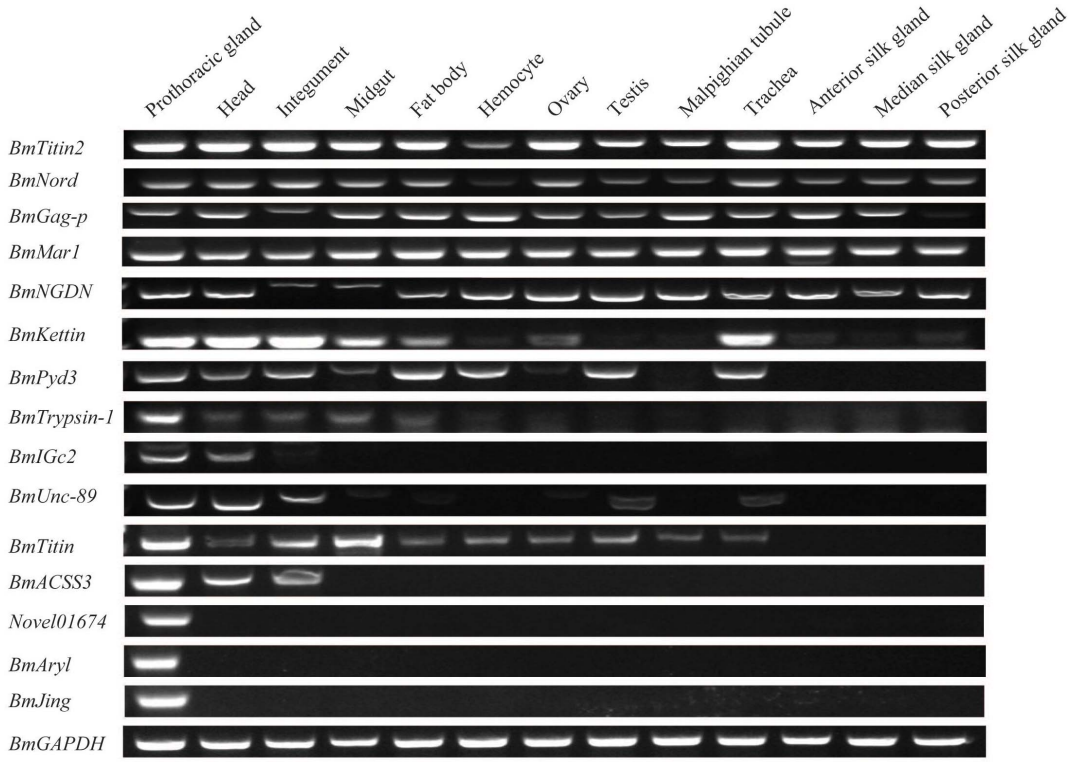

FIGURE 3 | Expression patterns of the differentially expressed genes (DEGs) in multiple tissues of day-3 fifth instar silkworm larvae. RT-PCR was performed, and the *BmGAPDH* gene was used as the internal control.

prolonged the fifth instar period, but no results were observed for BmNPV infection in the first half of the fifth instar because the larvae died. Briefly, the prothoracicotropic hormone (PTTH) secreted by the brain stimulates the PGs to release ecdysteroid, which in turn induces larval or metamorphic ecdysis depending on the presence of juvenile hormone (JH) secreted by the corpora allata. Throughout the latter half of the fifth instar, the first step of the ecdysteroid titer increased in a stepwise manner, the second step of the ecdysteroid titer showed a small increase (which led to the silkworms wandering) followed by a plateau, and the third step of the ecdysteroid titer showed an initially gradual but then steep increase to reach a peak 1 day later (Mizoguchi et al., 2001).

Insights from host studies reveal that baculoviruses manipulate host behavior to enhance transmission to new victims. For example, baculoviruses enable infected larvae to continue to seek foliage and prolong insect feeding after infection, thus resulting in an increased OBs production (O'Reilly and Miller, 1989). The *egt* gene of NPV, expressed immediately, encodes an enzyme that inactivates the molting hormone 20E by transferring a sugar moiety from a nucleotide sugar donor to a hydroxyl group on 20E (Hoover et al., 2011). The ecdysone blood level is reduced by up to 90% in silkworms as a result of the transgenic expression of the *egt* gene of BmNPV and because *egt* expression in *egt*-transgenic silkworms prolongs the duration of the larval and pupal stages resulting in the arresting of the pupal-to-adult metamorphosis (Zhang et al., 2012). Interestingly, in the present study, silkworm larvae infected with BmNPV in the latter half of the fifth instar showed precocious molting and metamorphosis and a higher level of hemolymph ecdysone titer. The *egt* gene of BmNPV is dispensable for normal virus production (Katsuma et al., 2008). The fast-killing phenotype is observed in the three *egt*-mutated BmNPVs only when the infection process progresses through silkworm larval–larval transition, but under infection in the middle stages of the fifth instar, the slow-killing phenotype is observed than that of the wild-type virus-infected larvae (Katsuma and Shimada, 2015). In particular, in the gluttonous stage, silkworms synthesize an enormous amount of silk proteins in the silk gland (Xu et al., 2019), and silk proteins are dispensable for normal silkworm development. A certain amount of silk proteins can remain in the body (incomplete spinning) that can lead to an incomplete larval–pupal transition. Silkworm and BmNPV interactions are largely dependent on the developmental stage of the host larvae infected by the virus. In addition, the overproduction of silkworm PTTH induces higher than normal levels of hemolymph ecdysteroids, which have been found to inhibit the pathogenicity of the virus, but did not have any observable effects on the development of infected *Spodoptera frugiperda* larvae (O'Reilly et al., 1995). Moreover, insect innate immunity can be activated by 20E and 20E, which induce antimicrobial peptide (AMP) gene expression and thus

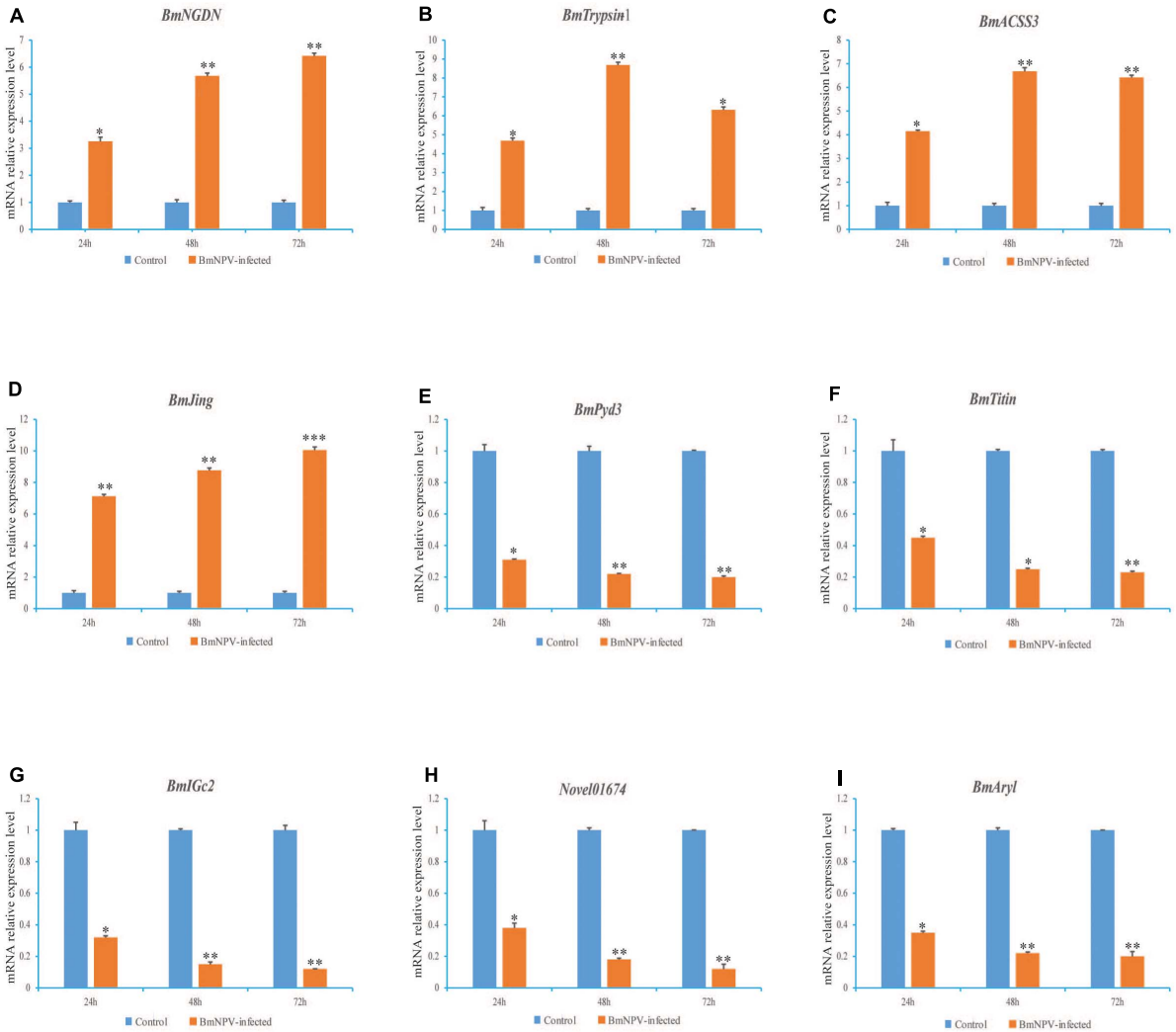

FIGURE 4 | Analysis of the nine randomly selected genes of the differentially expressed genes (DEGs) in the prothoracic glands (PGs) of BmNPV-infected silkworm larvae. The expression levels of *BmNGDN* **(A)**, *BmTrypsin-1* **(B)**, *BmACSS3* **(C)**, *BmJing* **(D)** were upregulated and the expression levels of *BmPyd3* **(E)**, *BmTitin* **(F)**, *BmIGc2* **(G)**, *Novel01674* **(H)**, *BmAryl* **(I)** were downregulated from 24 to 72 h after BmNPV infection, respectively. Here, *BmGAPDH* was used as the internal control. The experiments were repeated three times. Values represent the means ± SDs of three independent experiments. Significant differences are indicated by (*$p < 0.05$) or (**$p < 0.01$).

act as immune activators (Dimarcq et al., 1997; Roxstrom-Lindquist et al., 2005; Flatt et al., 2008). The ecdysteroid titer showed a small increase followed by a plateau that occurred 1 day before the silkworms started wandering. Thereafter, the titer increased gradually and then steeply to reach a peak (where the majority of silkworms had started wandering) the following day (Mizoguchi et al., 2001). Therefore, we speculated that BmNPV infection in the latter half of the fifth instar of silkworm larvae induced precocious molting and metamorphosis and a higher level of hemolymph ecdysone titer, which would enable infected larvae to complete their larval–pupal transition.

Briefly, PGs are an important endocrine organ with characteristically cholesterol-rich tissue as the main site of synthetic ecdysteroids (Igarashi et al., 2018). In this study, the RT-PCR results confirmed that the silkworm PGs were infected by BmNPV through oral inoculation. Seven upregulated and eight downregulated DEGs were identified from silkworm PGs sequenced by RNA-seq 48 h after BmNPV infection. The RT-qPCR results of the DEGs in the PGs of BmNPV-infected larvae at 24, 48, and 72 h were generally consistent with the transcriptome data. The classifications of the 15 DEGs were primarily located in binding activity of nucleic acids, ions, and proteins that were mainly involved in the metabolic processes and pathways. The spatial expression profiles of *Novel01674*, *BmAryl*, and *BmJing* indicated that they were specifically expressed in the silkworm PGs. The KEGG pathway enrichment analysis of *BmACSS3* (BGIBMGA010070) revealed that acyl-coenzyme A (AcCoA) synthase activity and *BmACSS3* could be involved in the acyl-CoA to cholesterogenesis pathways.

The acyl-coA synthetase catalyzes fatty acids to form a thioester with CoA, which is a common initial step of all fatty acid metabolic processes (Watkins, 1997). Fatty acids are the building blocks of many lipids, including triacylglycerol and cholesteryl esters. RNAi-mediated knockdown of the acyl-coenzyme A synthetase gene prolongs and extends the maximum lifespan (Eisenberg et al., 2014). Trypsin-1 serine protease (*BmTrypsin-1*) had serine-type endopeptidase activity. SPs play crucial roles in insect development and innate immunity. RNAi-mediated silencing of SPs results in severe molting defects, specifically by reducing the expression of genes in the 20E synthesis and signaling pathway, and increases larval sensitivity to bacteria (Broehan et al., 2010; Yang et al., 2019). In silkworm PGs, the transcripts of *BmTrypsin-1* and *BmACSS3* were significantly increased from 24 to 72 h after BmNPV infection. *BmTrypsin-1* and *BmACSS3* may be involved in the maturation process in the latter half of the fifth instar of silkworm larvae.

DATA AVAILABILITY STATEMENT

The datasets presented in this study can be found in online repositories. The names of the repository/repositories and accession number(s) can be found in the article/ **Supplementary Material**.

AUTHOR CONTRIBUTIONS

P-ZX performed the experiment and wrote the manuscript. M-RZ performed the literature review and analyzed the data. X-YW prepared the illustrations and collected the data. Y-CW suggested important research points. All authors have read and approved the final version of the manuscript.

FUNDING

This research was financially supported by the Jiangsu Provincial Natural Science Foundation of China (Grant No. BK2012273) and the National Natural Science Foundation of China (Grant Nos. 31302035 and 2735011802).

SUPPLEMENTARY MATERIAL

The Supplementary Material for this article can be found online at: https://www.frontiersin.org/articles/10.3389/fphys.2021.650972/full#supplementary-material

Supplementary Figure 1 | View of the prothoracic glands (PGs) entwined in the tracheal bush of the first spiracle.

Supplementary Figure 2 | View of the prothoracic glands (PGs) from a fifth instar silkworm larva.

Supplementary Figure 3 | Analysis of the correlation of RNA-seq data. **(A)** Diagram of the correlation coefficients between samples. **(B)** Correlation between C1 and C2. **(C)** Correlation between C1 and N1. **(D)** Correlation between C1 and N2. **(E)** Correlation between C2 and N1. **(F)** Correlation between C2 and N2. **(G)** Correlation between N1 and N2. C1 and C2 indicate the two independent biological experiments of transcriptome sequencing of prothoracic glands (PGs) in the control groups, respectively. N1 and N2 indicate the two independent biological experiments of transcriptome sequencing of PGs in the control groups, respectively.

Supplementary Figure 4 | GO enrichment analysis of the differentially expressed genes (DEGs). Genes were annotated by the biological process, cellular component, and molecular function.

Supplementary Table 1 | Primers of genes for RT-PCR and RT-qPCR.

Supplementary Table 2 | The weight of mature silkworms and pupae in BmNPV-infected and control groups.

Supplementary Table 3 | The results of feeding experiment with cholesterol, and 7-dehydrocholesterol (7dC), using water as control.

Supplementary Table 4 | Summary statistics of prothoracic gland of *Bombyx mori* genes based on transcriptome data.

Supplementary Table 5 | A list of genes with FPKM $\geq$ 1.0 between infected and control groups.

Supplementary Table 6 | A list of differential expression genes between infected and control groups.

Supplementary Table 7 | Infected vs. control DEG_GO_enrichment result.

Supplementary Table 8 | Infected vs. control all DEG_KEGG_pathway_enrichment result.

REFERENCES

Anders, S., Pyl, P. T., and Huber, W. (2015). HTSeq–a Python framework to work with high-throughput sequencing data. *Bioinformatics* 31, 166–169. doi: 10.1093/bioinformatics/btu638

Broehan, G., Arakane, Y., Beeman, R. W., Kramer, K. J., Muthukrishnan, S., and Merzendorfer, H. (2010). Chymotrypsin-like peptidases from *Tribolium castaneum*: a role in molting revealed by RNA interference. *Insect Biochem. Mol. Biol.* 40, 274–283. doi: 10.1016/j.ibmb.2009.10.009

Chen, T. T., Tan, L. R., Hu, N., Dong, Z. Q., Hu, Z. G., Qin, Q., et al. (2019). Specific genes related to nucleopolyhedrovirus in *Bombyx mori* susceptible and near-isogenic resistant strains through comparative transcriptome analysis. *Insect Mol. Biol.* 28, 473–484. doi: 10.1111/imb.12566

Dimarcq, J. L., Imler, J. L., Lanot, R., Ezekowitz, R. A., Hoffmann, J. A., Janeway, C. A., et al. (1997). Treatment of l(2)mbn *Drosophila tumorous* blood cells with the steroid hormone ecdysone amplifies the inducibility of antimicrobial peptide gene expression. *Insect Biochem. Mol. Biol.* 27, 877–886. doi: 10.1016/s0965-1748(97)00072-6

Du, X., and Thiem, S. M. (1997). Responses of insect cells to baculovirus infection: protein synthesis shutdown and apoptosis. *J. Virol.* 71, 7866–7872. doi: 10.1128/jvi.71.10.7866-7872.1997

Eisenberg, T., Schroeder, S., Andryushkova, A., Pendl, T., Kuttner, V., Bhukel, A., et al. (2014). Nucleocytosolic depletion of the energy metabolite acetyl-coenzyme a stimulates autophagy and prolongs lifespan. *Cell Metab.* 19, 431–444. doi: 10.1016/j.cmet.2014.02.010

Flatt, T., Heyland, A., Rus, F., Porpiglia, E., Sherlock, C., Yamamoto, R., et al. (2008). Hormonal regulation of the humoral innate immune response in *Drosophila melanogaster*. *J. Exp. Biol.* 211, 2712–2724. doi: 10.1242/jeb.014878

Gomi, S., Majima, K., and Maeda, S. (1999). Sequence analysis of the genome of *Bombyx mori* nucleopolyhedrovirus. *J. Gen. Virol.* 80(Pt 5), 1323–1337. doi: 10.1099/0022-1317-80-5-1323

Gotz, S., Garcia-Gomez, J. M., Terol, J., Williams, T. D., Nagaraj, S. H., Nueda, M. J., et al. (2008). High-throughput functional annotation and data mining with the Blast2GO suite. *Nucleic Acids Res.* 36, 3420–3435. doi: 10.1093/nar/gkn176

Grabherr, M. G., Haas, B. J., Yassour, M., Levin, J. Z., Thompson, D. A., Amit, I., et al. (2011). Full-length transcriptome assembly from RNA-Seq data without a reference genome. *Nat. Biotechnol.* 29, 644–U130.

Guo, H., Jiang, L., and Xia, Q. (2016). Selection of reference genes for analysis of stress-responsive genes after challenge with viruses and temperature changes in the silkworm *Bombyx mori*. *Mol. Genet. Genomics* 291, 999–1004. doi: 10.1007/s00438-015-1125-4

Guo, H. Z., Sun, Q., Wang, B. B., Wang, Y. M., Xie, E. Y., Xia, Q. Y., et al. (2019). Spry is downregulated by multiple viruses to elevate ERK signaling and ensure viral reproduction in silkworm. *Dev. Comp. Immunol.* 98, 1–5. doi: 10.1016/j.dci.2019.04.001

Hoover, K., Grove, M., Gardner, M., Hughes, D. P., McNeil, J., Slavicek, J., et al. (2011). A gene for an extended phenotype. *Science* 333, 1401–1401.

Huang, H. L., Wu, P., Zhang, S. L., Shang, Q., Yin, H. T., Hou, Q. R., et al. (2019). DNA methylomes and transcriptomes analysis reveal implication of host DNA methylation machinery in BmNPV proliferation in *Bombyx mori*. *BMC Genomics* 20:736. doi: 10.1186/s12864-019-6146-7

Huh, N. E., and Weaver, R. F. (1990). Categorizing some early and late transcripts directed by the *Autographa californica* nuclear polyhedrosis virus. *J. Gen. Virol.* 71(Pt 9), 2195–2200. doi: 10.1099/0022-1317-71-9-2195

Igarashi, F., Ogihara, M. H., Iga, M., and Kataoka, H. (2018). Cholesterol internalization and metabolism in insect prothoracic gland, a steroidogenic organ, via lipoproteins. *Steroids* 134, 110–116. doi: 10.1016/j.steroids.2018.01.012

Ikeda, M., Yamada, H., Hamajima, R., and Kobayashi, M. (2013). Baculovirus genes modulating intracellular innate antiviral immunity of lepidopteran insect cells. *Virology* 435, 1–13. doi: 10.1016/j.virol.2012.10.016

Jiang, L. (2021). Insights into the antiviral pathways of the silkworm *Bombyx mori*. *Front. Immunol.* 12:639092. doi: 10.3389/fimmu.2021.639092

Jiang, L., Goldsmith, M. R., and Xia, Q. Y. (2021a). Advances in the arms race between silkworm and *Baculovirus*. *Front. Immunol.* 12:628151. doi: 10.3389/fimmu.2021.628151

Jiang, L., Liu, W. Q., Guo, H. Z., Dang, Y. H., Cheng, T. C., Yang, W. Y., et al. (2019). Distinct functions of *Bombyx mori* peptidoglycan recognition protein 2 in immune responses to bacteria and viruses. *Front. Immunol.* 10:776. doi: 10.3389/fimmu.2019.00776

Jiang, L., and Xia, Q. (2014). The progress and future of enhancing antiviral capacity by transgenic technology in the silkworm *Bombyx mori*. *Insect. Biochem. Mol. Biol.* 48, 1–7. doi: 10.1016/j.ibmb.2014.02.003

Jiang, L., Xie, E. Y., Guo, H. Z., Sun, Q., Liuli, H. Y., Wang, Y. M., et al. (2021b). Heat shock protein 19.9 (Hsp19.9) from *Bombyx mori* is involved in host protection against viral infection. *Dev. Comp. Immunol.* 114:103790. doi: 10.1016/j.dci.2020.103790

Jiang, L., Zhao, P., Cheng, T. C., Sun, Q., Peng, Z. W., Dang, Y. H., et al. (2013a). A transgenic animal with antiviral properties that might inhibit multiple stages of infection. *Antivir. Res.* 98, 171–173. doi: 10.1016/j.antiviral.2013.02.015

Jiang, L., Zhao, P., Wang, G. H., Cheng, T. C., Yang, Q., Jin, S. K., et al. (2013b). Comparison of factors that may affect the inhibitory efficacy of transgenic RNAi targeting of baculoviral genes in silkworm, *Bombyx mori*. *Antivir. Res.* 97, 255–263. doi: 10.1016/j.antiviral.2012.12.020

Kanehisa, M., Goto, S., Sato, Y., Furumichi, M., and Tanabe, M. (2012). KEGG for integration and interpretation of large-scale molecular data sets. *Nucleic Acids Res.* 40, D109–D114.

Katsuma, S., Kawaoka, S., Mita, K., and Shimada, T. (2008). Genome-wide survey for baculoviral host homologs using the *Bombyx* genome sequence. *Insect. Biochem. Mol.* 38, 1080–1086. doi: 10.1016/j.ibmb.2008.05.008

Katsuma, S., Mita, K., and Shimada, T. (2007). ERK- and JNK-Dependent signaling pathways contribute to *Bombyx mori* nucleopolyhedrovirus infection. *J. Virol.* 81, 13700–13709. doi: 10.1128/jvi.01683-07

Katsuma, S., and Shimada, T. (2015). The killing speed of egt-inactivated *Bombyx mori* nucleopolyhedrovirus depends on the developmental stage of *B-mori* larvae. *J. Invertebr. Pathol.* 126, 64–70. doi: 10.1016/j.jip.2015.01.012

Kim, D., Pertea, G., Trapnell, C., Pimentel, H., Kelley, R., and Salzberg, S. L. (2013). TopHat2: accurate alignment of transcriptomes in the presence of insertions, deletions and gene fusions. *Genome Biol.* 14:R36.

Manjunatha, G. K. S., Peter, A., Naika, M. B. N., Niranjana, P., and Shamprasad, P. (2018). Identification of in-vitro red fluorescent protein with antipathogenic activity from the midgut of the silkworm (*Bombyx Mori* L.). *Protein Pept. Lett.* 25, 302–313. doi: 10.2174/0929866525666180115121853

Mita, K., Kasahara, M., Sasaki, S., Nagayasu, Y., Yamada, T., Kanamori, H., et al. (2004). The genome sequence of silkworm, *Bombyx mori*. *DNA Res.* 11, 27–35. doi: 10.1093/dnares/11.1.27

Mizoguchi, A., Ohashi, Y., Hosoda, K., Ishibashi, J., and Kataoka, H. (2001). Developmental profile of the changes in the prothoracicotropic hormone titer in hemolymph of the silkworm *Bombyx mori*: correlation with ecdysteroid secretion. *Insect. Biochem. Mol. Biol.* 31, 349–358. doi: 10.1016/s0965-1748(00)00127-2

Nakazawa, H., Tsuneishi, E., Ponnuvel, K. M., Furukawa, S., Asaoka, A., Tanaka, H., et al. (2004). Antiviral activity of a serine protease from the digestive juice of *Bombyx mori* larvae against nucleopolyhedrovirus. *Virology* 321, 154–162. doi: 10.1016/j.virol.2003.12.011

O'Reilly, D. R., Kelly, T. J., Masler, E. P., Thyagaraja, B. S., Robson, R. M., Shaw, T. C., et al. (1995). Overexpression of *Bombyx mori* prothoracicotropic hormone using baculovirus vectors. *Insect. Biochem. Mol. Biol.* 25, 475–485. doi: 10.1016/0965-1748(94)00087-f

O'Reilly, D. R., and Miller, L. K. (1989). A baculovirus blocks insect molting by producing ecdysteroid UDP-glucosyl transferase. *Science* 245, 1110–1112. doi: 10.1126/science.2505387

Ponnuvel, K. M., Nakazawa, H., Furukawa, S., Asaoka, A., Ishibashi, J., Tanaka, H., et al. (2003). A lipase isolated from the silkworm *Bombyx mori* shows antiviral activity against nucleopolyhedrovirus. *J. Virol.* 77, 10725–10729. doi: 10.1128/jvi.77.19.10725-10729.2003

Ponnuvel, K. M., Nithya, K., Sirigineedi, S., Awasthi, A. K., and Yamakawa, M. (2012). In vitro antiviral activity of an alkaline trypsin from the digestive juice of *Bombyx mori* larvae against nucleopolyhedrovirus. *Arch. Insect Biochem. Physiol.* 81, 90–104. doi: 10.1002/arch.21046

Rahman, M. M., and Gopinathan, K. P. (2004). Systemic and in vitro infection process of *Bombyx mori* nucleopolyhedrovirus. *Virus Res.* 101, 109–118. doi: 10.1016/j.virusres.2003.12.027

Roxstrom-Lindquist, K., Assefaw-Redda, Y., Rosinska, K., and Faye, I. (2005). 20-Hydroxyecdysone indirectly regulates Hemolin gene expression in *Hyalophora cecropia*. *Insect Mol. Biol.* 14, 645–652. doi: 10.1111/j.1365-2583.2005.00593.x

Shirata, N., Ikeda, M., and Kobayashi, M. (2010). Identification of a Hyphantria cunea nucleopolyhedrovirus (NPV) gene that is involved in global protein synthesis shutdown and restricted *Bombyx mori* NPV multiplication in a *B. mori* cell line. *Virology* 398, 149–157. doi: 10.1016/j.virol.2009.11.049

Sunagar, S. G., Savanurmath, C. J., and Hinchigeri, S. B. (2011). The profiles of red fluorescent proteins with antinucleopolyhedrovirus activity in races of the silkworm *Bombyx mori*. *J. Insect Physiol.* 57, 1707–1714. doi: 10.1016/j.jinsphys.2011.09.009

Toufeeq, S., Wang, J., Zhang, S. Z., Li, B., Hu, P., Zhu, L. B., et al. (2019). Bmserpin2 is involved in BmNPV infection by suppressing melanization in *Bombyx mori*. *Insects* 10:399. doi: 10.3390/insects10110399

Trapnell, C., Roberts, A., Goff, L., Pertea, G., Kim, D., Kelley, D. R., et al. (2012). Differential gene and transcript expression analysis of RNA-seq experiments with TopHat and Cufflinks. *Nat. Protoc.* 7, 562–578. doi: 10.1038/nprot.2012.016

Watkins, P. A. (1997). Fatty acid activation. *Prog. Lipid Res.* 36, 55–83.

Wu, F., Wang, P. Y., Zhao, Q. L., Kang, L. Q., Xia, D. G., Qiu, Z. Y., et al. (2016). Mutation of a cuticle protein gene, BmCPG10, is responsible for silkworm non-moulting in the 2nd instar mutant. *PLoS One* 11:e0153549. doi: 10.1371/journal.pone.0153549

Xia, Q., Zhou, Z., Lu, C., Cheng, D., Dai, F., Li, B., et al. (2004). sequence for the genome of the domesticated silkworm (*Bombyx mori*). *Science* 306, 1937–1940. doi: 10.1126/science.1102210

Xu, P., Zhang, M., Qian, P., Li, J., Wang, X., and Wu, Y. (2019). iTRAQ-based quantitative proteomic analysis of digestive juice across the first 48 hours of the fifth instar in silkworm larvae. *Int. J. Mol. Sci.* 20:6113. doi: 10.3390/ijms20246113

Yang, W. J., Chen, C. X., Yan, Y., Xu, K. K., and Li, C. (2019). Clip-domain serine protease gene (LsCLIP3) is essential for larval-pupal molting and immunity in *Lasioderma serricorne*. *Front. Physiol.* 10:1631. doi: 10.3389/fphys.2019.01631

Zhang, M. R., Xu, P. Z., Pang, H. L., Chen, T., and Zhang, G. Z. (2019). Expression analysis of mRNA decay of maternal genes during *Bombyx mori* maternal-to-zygotic transition. *Int. J. Mol. Sci.* 20:5651. doi: 10.3390/ijms20225651

Zhang, S. Z., Zhu, L. B., You, L. L., Wang, J., Cao, H. H., Liu, Y. X., et al. (2020). A novel digestive proteinase lipase member H-A in *Bombyx mori* contributes to digestive juice antiviral activity against *B. mori* nucleopolyhedrovirus. *Insects* 11:154. doi: 10.3390/insects11030154

Zhang, X., Xue, R. Y., Cao, G. L., Hu, X. L., Wang, X. J., Pan, Z. H., et al. (2012). Effects of egt gene transfer on the development of *Bombyx mori*. *Gene* 491, 272–277. doi: 10.1016/j.gene.2011.09.026

Zhang, X., Zhang, Y. S., Dai, K., Liang, Z., Zhu, M., Pan, J., et al. (2020). N-6-methyladenosine level in silkworm midgut/ovary cell line is associated with *Bombyx mori* nucleopolyhedrovirus infection. *Front. Microbiol.* 10:2988. doi: 10.3389/fmicb.2019.02988

Conflict of Interest: The authors declare that the research was conducted in the absence of any commercial or financial relationships that could be construed as a potential conflict of interest.

frontiers in Immunology

ORIGINAL RESEARCH
published: 13 May 2021
doi: 10.3389/fimmu.2021.660873

Distinct Roles of Hemocytes at Different Stages of Infection by Dengue and Zika Viruses in *Aedes aegypti* Mosquitoes

Thiago H. J. F. Leite[1†], *Álvaro G. A. Ferreira*[1,2†], *Jean-Luc Imler*[3] *and João T. Marques*[1,3*]

[1] Department of Biochemistry and Immunology, Instituto de Ciências Biológicas, Universidade Federal de Minas Gerais, Belo Horizonte, Brazil, [2] Mosquitos Vetores: Endossimbiontes e Interação Patógeno-Vetor, Instituto René Rachou – Fiocruz, Belo Horizonte, Brazil, [3] Université de Strasbourg, CNRS UPR9022, Inserm U1257, Strasbourg, France

Aedes aegypti mosquitoes are vectors for arboviruses of medical importance such as dengue (DENV) and Zika (ZIKV) viruses. Different innate immune pathways contribute to the control of arboviruses in the mosquito vector including RNA interference, Toll and Jak-STAT pathways. However, the role of cellular responses mediated by circulating macrophage-like cells known as hemocytes remains unclear. Here we show that hemocytes are recruited to the midgut of *Ae. aegypti* mosquitoes in response to DENV or ZIKV. Blockade of the phagocytic function of hemocytes using latex beads induced increased accumulation of hemocytes in the midgut and a reduction in virus infection levels in this organ. In contrast, inhibition of phagocytosis by hemocytes led to increased systemic dissemination and replication of DENV and ZIKV. Hence, our work reveals a dual role for hemocytes in *Ae. aegypti* mosquitoes, whereby phagocytosis is not required to control viral infection in the midgut but is essential to restrict systemic dissemination. Further understanding of the mechanism behind this duality could help the design of vector-based strategies to prevent transmission of arboviruses.

Keywords: Zika virus, dengue virus, cellular immunity, macrophage-like cells, *Aedes aegypti*, vector mosquitoes, hemocytes

OPEN ACCESS

Edited by:
Luc Swevers, National Centre of Scientific Research Demokritos, Greece

Reviewed by:
Emilie Pondeville, MRC-University of Glasgow Centre For Virus Research (MRC), United Kingdom
Ryan C. Smith, Iowa State University, United States

***Correspondence:**
João T. Marques
jtm@ufmg.br

[†]*These authors have contributed equally to this work*

Specialty section:
This article was submitted to Comparative Immunology, a section of the journal Frontiers in Immunology

Received: *29 January 2021*
Accepted: *30 April 2021*
Published: *13 May 2021*

Citation:
Leite THJF, Ferreira ÁGA, Imler J-L and Marques JT (2021) Distinct Roles of Hemocytes at Different Stages of Infection by Dengue and Zika Viruses in Aedes aegypti Mosquitoes. Front. Immunol. 12:660873. doi: 10.3389/fimmu.2021.660873

INTRODUCTION

Aedes aegypti mosquitoes are vectors for a wide variety of arthropod-borne viruses (arboviruses) (1). How these mosquitoes recognize and respond to viral infection is a central question that directly affects their vector competence. The understanding of antiviral responses in insects has greatly benefited from work in the fruit fly *Drosophila melanogaster* (2). Work in this model organism has identified many important antiviral defense mechanisms such as RNA interference (RNAi), Jak-STAT and STING (3–12). Later work in mosquitoes has shown that RNAi and Jak-STAT are important for the control of arbovirus infections (13–18). Interestingly, despite being widely conserved throughout evolution, STING has been lost in mosquitoes (19).

In addition to these well-known innate immunity pathways, the *Drosophila* model has also highlighted the role of circulating macrophage-like cells, referred to as hemocytes, in the control of

viral infection (20–22). Cellular immunity in insects includes phagocytosis of foreign bodies, nodulation, wound healing and the encapsulation of pathogens (23–27). Hemocytes can be freely circulating in the insect hemolymph or associated with tissues but these populations seem to be highly dynamic and interchangeable (28). Hemocytes are often recruited to infected tissues, which increases the chances of coming into contact with the pathogen to be cleared by phagocytosis (28, 29). A good example of hemocyte recruitment during an infection is in the case of *Plasmodium*, the malaria parasite. Invasion of the midgut of *Anopheles* mosquitoes by *Plasmodium* ookinetes promotes hemocyte recruitment and release of components of the mosquito complement system, promoting pathogen elimination (30–34). Despite the importance of hemocytes for the clearance of bacteria and *Plasmodium* in mosquitoes, little is known about their role during viral infections, particularly arboviruses such as dengue (DENV) and Zika (ZIKV) viruses. DENV and ZIKV belong to the *Flaviviridae* family and, together with the alphavirus chikungunya virus (CHIKV) are among the most important arboviruses transmitted by *Ae. aegypti* mosquitoes causing infections worldwide (1). Similar to the malaria parasite, arboviruses are acquired orally during blood feeding by mosquitoes, and the gut represents a physical barrier that hinders the passage of the viral particles to the mosquito hemocele (35). Reaching the hemocele is a necessary step for the virus to spread systemically and reach the salivary glands where it can be transmitted to a vertebrate host (21–23). During systemic infection, several tissues may host viral replication, including hemocytes themselves, but it is unclear how they contribute to amplification of the virus (36–38). Despite this increasing knowledge about the functions of hemocytes in mosquitoes, the role of cellular immunity in the antiviral defense remains largely unknown.

In this work, we investigated the involvement of hemocytes in the control of DENV and ZIKV in *Ae. aegypti* mosquitoes. Our results suggest a complex role for hemocytes. We show that hemocytes were recruited to the midgut in response to the presence of the virus but, once there, their phagocytic activity seems to facilitate viral replication although other functions my play a role in the antiviral defense. In contrast, during the systemic phase of the infection, inhibition of phagocytosis by hemocytes led to increased viral infection pointing to a more traditional role in antiviral immunity. Together our results indicate that hemocytes have dual roles in the control of arboviruses in *Ae. aegypti* mosquitoes depending on tissue affected and the stage of the infection in the vector.

MATERIALS AND METHODS

Indirect Immunofluorescence Assays

Mosquitoes were anaesthetized on ice and then were inject with 250 nanoliters of 20% paraformaldehyde for hemocyte fixation in midgut basal lamina. After 20 minutes, midguts were dissected in 4% paraformaldehyde diluted in phosphate-buffered saline (PBS) (13 mM NaCl, 0.7 mM Na2HPO4, 1 mM NaH2PO4 at pH 7.2) (PBS). The remaining midguts were fixed in the same solution for 20 minutes, and then washed three times in PBS and then incubated with blocking solution PBSBT (1× PBS + 1% BSA + 0.1% Triton X-100) for 15 minutes at room temperature. Samples were then incubated overnight with 4G2 monoclonal antibody for Flavivirus E protein (ATCC: HB-112, used at 1:50 in PBST) at 4°C. Midguts were washed three times with PBSBT (5 min each) and incubated for 2 h with constant rocking at 25°C with goat anti-mouse IgG antibody (Invitrogen). Midguts were washed three times with PBST (5 min each) and incubated for 15 min with DAPI (Molecular Probes, 1:500), and phalloidin-rhodamine (Molecular Probes, 1:500). Then the midguts were washed in PBS and placed onto slides. Images were obtained with an LSM 880 microscope (Zeiss).

Mosquito Perfusion to Obtain Circulating Hemocytes

Circulating hemocytes were obtained by perfusion of adult mosquitoes as described (39) with modifications. Briefly, mosquitoes were injected with 1 uL of anticoagulant buffer solution (70% PBS 1x (pH 7.0) + 30% citrate buffer (98 mM NaOH, 186 mM NaCl, 1.7 mM EDTA and 41 mM citric acid, buffer pH 4.5) and were incubated on a petri dish on ice for 10 min to let hemocytes dissociate from tissues. The last two segments of abdomen were cut to create an opening, which was positioned onto a microscope slide. Each individual mosquito was positioned vertically and then injected with 3 uL of the same anticoagulant buffer solution in the lateral side of torax using a microinjector (Nanoject III). The injection pressure forced the diluted hemolymph to exit the opening made in the final portion of the abdomen and onto the microscope slide. The hemolymph was incubated at room temperature for 20 min in order to let the hemocytes adhere to the slides. Hemocytes were fixed in 4% paraformaldehyde for 20 min, washed three times in PBS and then incubated with blocking solution PBSBT (1× PBS + 1% BSA + 0.1% Triton X-100) for 15 minutes at room temperature. Slides were incubated for 15 min with DAPI (Molecular Probes, 1:500) and phalloidin-rhodamine (Molecular Probes, 1:40), followed by 3 washes in PBS. Cells were visualized in a fluorescence microscope for counting. To visualize infected hemocytes, the 4G2 monoclonal antibody against Flavivirus E protein was used.

Hemocyte Labeling *In Vivo*

For *in vivo* hemocyte staining we used Vybrant™ CM-DiI Cell-Labeling Solution (Invitrogen™) essentially as described (29). Briefly, female mosquitoes were placed on petri dish on ice and injected with 150 nanoliters containing 100 μM CM-DiI, freshly prepared in sterile water, after blood or sugar meal at specific time points. Injections were done using a nano-injector Nanoject III (Drummond Scientific Company). After injections, mosquitoes are placed on cages at 28°C until specific time points for midguts dissections.

Quantification of the Infection Area in the Midgut

Area measurements and hemocyte counting were performed using ImageJ v1.53c (https://imagej.nih.gov/ij/). All images

were acquired under identical conditions, digitized, converted to RGB image and stored in an uncompressed tagged image file format (.tiff). Infection area computing was performed using ImageJ. The following steps were performed for all images to quantify the area of infection in the midgut, as shown in **Supplementary Figure 1**: step 1, color-deconvolution was used to isolate red, green and blue spectra and select the image corresponding to virus infection staining; step 2, a projection final image was generated using all acquired series of z-stack confocal images using the tool "Image > Stacks > Z-project function"; step 3, the projection image was processed into 8 bits image type; step 4, the midgut outline was delimited; step 5, the area outside of midgut delimitation was erased by using the "clear outside" function; steps 6 and 7, optical density was assessed by setting a threshold using the "threshold tool", and a maximum threshold was set; steps 8 and 9, the function "Measure" in the 'Analyze' tool menu was used to calculate the optical density and compute the midgut infection area.

Quantification of Hemocytes in the Midgut

Hemocyte numbers were quantified in the confocal microscopy images of midguts. The following steps were performed using ImageJ for all images: step 1, color-deconvolution was used to isolate red, green and blue spectra and select the images corresponding to hemocytes cell tracker and DNA staining; step 2, for each color, a projection final image was generated using all acquired series of z-stack confocal images using the tool "Image > Stacks > Z-project function"; step 3, the projection image was processed into 8 bits image type; step 4, the number of hemocytes was then counted using the ITCN (Image-based Tool for Counting Nuclei); step 5, for all hemocytes automatically identified in the hemocytes cell tracker color we additionally confirmed the presence of nuclei using the DNA staining image and reject the counts that do not presented a nucleus.

Inhibition of Phagocytosis by Injection of Latex Beads

To block the phagocytic activity of hemocytes in mosquitoes, we adapted protocols previously used for *Drosophila* (20). Adult mosquitoes were injected with 69 nanoliters of latex microspheres (CML Latex Beads, 4% w/v, 0.3 µm, ThermoFisher). Latex beads were washed and resuspended at a 2X concentration in PBS before injections. In order to quantify the inhibition of phagocytosis, we first injected regular latex beads followed by injection of red fluorescent beads (FluoSpheres ™ Carboxylate-Modified Microspheres, 0.2 µm, dark red fluorescent (660/680), 2% solids, ThermoFisher) two days later. Perfusions were done 4 and 8 days after the first injection and the total number of hemocytes was counted as well as the percentage of cells with red beads.

RT-qPCR

Total RNA (200 ng) extracted from individual insects or individual tissues was reverse transcribed using Moloney murine leukaemia virus reverse transcriptase. cDNA was subjected to quantitative PCR (qPCR) using the kit Power SYBR Green Master Mix (Applied Biosystems), following the manufacturer's instructions. Primers used for quantitative PCR (qPCR) were as follows: RPL32 (forward, 5′-ACTTCTTCGTC CGCTTCTTG-3′; reverse, 5′-AGCCGCGTGTTGTACTCTG-3′), DENV1 (forward, 5′-TCGGAAGCTTGCTTAACGTAG-3′; reverse, 5′ TCCGTTGGTTGTTCATCAGA-3′), ZIKV (forward, 5′-TCAAACGAATGGCAGTCAGTG-3′; reverse, 5′-GCTTGTTGAAGTGGTGGGAG-3′) as previously described (14).

Mosquito Rearing and Infections

All experiments were carried out using *Ae. aegypti* Bangkok strain. Mosquitoes were maintained in an incubator at 28°C and 70–80% relative humidity, in a 12:12 h light:dark photoperiod, and with 10% sucrose solution ad libitum. For mosquito infections, we used previously described models for flavivirus infections using mice or artificial membrane feeding. Isolates of DENV4 (H241 strain), DENV1 (MV09) and ZIKV (PE243/2015) were previously described (14). As a mouse model, we utilized DENV1 and ZIKV infection of interferon alpha/beta and gamma receptor-deficient (AG129) animals (14). Mice were injected intraperitoneally with 10^6 pfu/mL of virus. Infected mice were anaesthetized at 3 days post injection (peak of viraemia) using ketamine/xylazine (80/8 mg kg^{-1}) and placed on top of the netting-covered containers with 5- to 6-day-old adult mosquito females. For infections by artificial membrane feeding, 5-6 day old adult females were starved for 24h and fed with a mixture of blood and virus supernatant containing 10^7 pfu/mL of DENV4 or 10^6 pfu/mL of ZIKV utilizing a glass artificial feeding system covered with pig intestine membrane, essentially as described (14). Mosquitoes were allowed to feed for 1 h. After blood feeding, fully engorged females were selected and harvested individually for midgut dissection at different time points. For direct systemic infections by intrathoracic injections, mosquitoes were anaesthetized with CO2 and kept on ice during the whole procedure. 4-day-old females were intrathoracically injected with 69 nL of L15 media containing virus (5 or 50 pfu), using a nano-injector Nanoject III (Drummond Scientific Company). Mosquitoes were harvested at different days post injection for RNA extraction. Tissues or mosquitoes were ground in TRIzol (Invitrogen) using glass beads. Total RNA was extracted from individual mosquitoes or individual tissues according to the manufacturer's protocol.

RESULTS

DENV and ZIKV Trigger Accumulation of Hemocytes in the Mosquito Midgut

Hemocytes play an important role in mosquito immunity but their function in the antiviral response against arboviruses remains unclear. Here, we first analyzed whether hemocytes would respond to the presence of arboviruses, DENV and ZIKV, in the blood meal (**Figure 1A**). Others have observed that blood feeding induces an increase in the numbers of hemocytes in mosquitoes (40, 41). Here we observed that there is also an increase in the number of hemocytes associated with the midgut compared to mosquitoes that were kept on sugar at 4

and 8 days post feeding (**Figures 1B, C**). At the earlier time point, there was no significant difference between the number of hemocytes associated with the midgut of mosquitoes fed with blood or blood and virus (**Figure 1B**). However, at 8 days post feeding, numbers of midgut-associated hemocytes were significantly higher in the presence of DENV or ZIKV when compared to a control blood meal (**Figure 1C**). Notably, these hemocytes do not seem to be recruited to sites of viral replication. We observed that hemocytes were often found dispersed throughout the midgut and not necessarily concentrated around regions with staining of the viral E protein as an indication of infection (**Figures 1D–G**). These results suggest that the presence of virus particles in the blood meal increases the number of hemocytes associated to midgut possibly by providing signals for increased recruitment or longer retention of these cells in the organ. The delayed effect at later times post infection also suggests that the accumulation of hemocytes may require prolonged stimuli.

Phagocytosis by Hemocytes Does Not Contribute to the Control of DENV and ZIKV in the Midgut

Increased numbers of hemocytes in the midgut in response to arboviruses in the blood meal suggests that these cells may play a role in the antiviral defense. Phagocytosis is a major function of hemocytes. Indeed, blocking phagocytosis by hemocytes or complete genetic ablation of these cells leads to decreased resistance to viruses in *Drosophila* (20–22). Here, we decided to use injection of latex beads into mosquitoes, which is often used as a strategy to over-load hemocytes and inhibit their phagocytic capacity (20, 21, 42). In our experiments, we observed that injection of beads seemed to decrease the number of circulating hemocytes in the mosquito but that was not significant (**Supplementary Figure 2A**). The number of hemocytes was estimated in a fraction of the hemolymph obtained by perfusion of mosquitoes with a low volume of buffer. Although this strategy recovered smaller numbers of hemocytes compared to other methods (39, 40), it still allowed us to compare numbers of cells between two conditions, which was our objective. Using the same strategy, we observed that phagocytosis by hemocytes was significantly inhibited by latex beads 2 days after their injection into *Ae. aegypti* mosquitoes (**Supplementary Figure 2B**). We next analyzed the effect of latex beads in mosquitoes that were given a blood meal containing DENV or ZIKV 2 days later, during the time when phagocytosis is inhibited (**Figure 2A**). Blocking phagocytosis did not affect significantly the area of infection by DENV or ZIKV in the midgut at 4 days post feeding (**Figures 2B, C**). In contrast, at 8 days post feeding, we observed that midgut of mosquitoes injected with latex beads had a significantly decreased area of infection by DENV and ZIKV compared to controls (**Figures 2B–G**). Importantly, injection of latex beads did not significantly change the total size of the midgut at the same time point but affected the absolute infection area suggesting that the kinetics of viral replication itself was affected (**Supplementary Figure 3**). At 4 days post feeding, injection of beads caused a reduction in viral RNA levels in DENV and ZIKV infected mosquitoes, although it was only significant for the latter (**Supplementary Figure 4**). At 8 days post feeding, DENV and ZIKV RNA levels were also significantly decreased in midguts from mosquitoes injected with latex beads compared to controls (**Figures 2H, I**). These results suggest that blocking the phagocytic activity of hemocytes using latex beads led to decreased viral replication in the midgut of mosquitoes. Notably, we consistently observed that latex beads increased the number of midgut-associated hemocytes in sugar and blood fed mosquitoes, independent of virus infection (**Supplementary Figure 5**). Latex beads also increased numbers of hemocytes in the midgut of DENV and ZIKV infected mosquitoes at 4 and 8 days post feeding (**Figures 2J, K**). During viral infection, latex beads had a less striking effect on hemocyte numbers at later time points since infection itself led to accumulation of hemocytes in the midgut (**Figure 1C**). This increased accumulation of hemocytes in the midgut induced by latex beads preceded the reduction in viral levels. Thus, we cannot rule out that increased accumulation of hemocytes in the midgut induced by beads is helping control viral infection but this would have to occur independently of their phagocytic activity.

Phagocytosis by Hemocytes Is Required for Systemic Control of DENV and ZIKV

The above results suggest that phagocytosis is not involved in the control of viral infection in the midgut of *Aedes* mosquitoes. This contrasts with the well-known roles of phagocytosis by hemocytes in insect immunity especially in the antiviral defense of *Drosophila*. However, these cells have also been shown to host replication of arboviruses such as DENV, Sindbis and O'nyong'nyong virus, which could help explain a proviral function (36–38). We confirmed that hemocytes could be directly infected by ZIKV as indicated staining for the viral E protein (**Supplementary Figure 6**). Thus, phagocytosis of viral particles by hemocytes could help promote viral replication in mosquitoes. In order to look further into this possibility, we analyzed dissemination of DENV and ZIKV infection from the midgut to the carcass in mosquitoes injected with latex beads (**Figure 3A**). Although the midgut infection rate was significantly reduced when phagocytosis was inhibited (**Figures 2B–I**), this did not significantly affect the prevalence of mosquitoes with disseminated infection (**Figures 3B, C**). Nevertheless, we observed a significant increase in viral RNA levels in the carcass of mosquitoes infected with DENV and ZIKV when phagocytosis by hemocytes was inhibited (**Figures 3D, E**). Here we note that mosquitoes fed on viremic mice show over 80% prevalence of infection. Therefore, to further analyze a possible effect of latex beads on the dissemination, we decided to analyze a model of artificial blood feeding where virus concentrations could be more easily controlled to reach closer to 50% prevalence (**Figure 3F**). In this model, injection of beads into mosquitoes prior to blood feeding containing DENV or ZIKV lead to a significant decrease in the prevalence of infection (**Figures 3G, H**). At the same time, viral loads were not significantly different for DENV and were increased in ZIKV infected individuals when phagocytosis was inhibited (**Figures 3I, J**). This reinforces the idea that blocking phagocytosis by hemocytes leads to decreased midgut replication that results in lower systemic dissemination. In order to bypass the midgut and directly analyze the role of

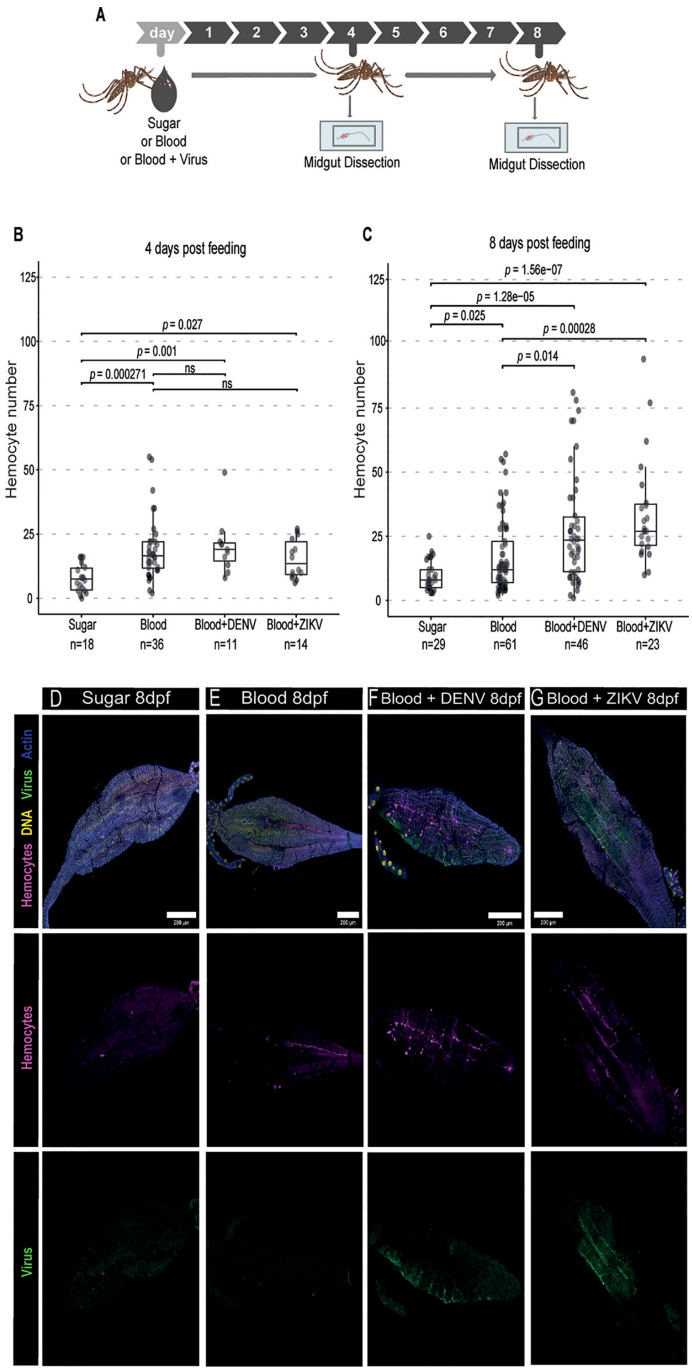

FIGURE 1 | Hemocyte accumulation in the midgut of *Ae. aegypti* mosquitoes in response to DENV and ZIKV. **(A)** Mosquitoes fed with sugar, blood or blood and virus were dissected at different times and their midgut was analyzed by confocal microscopy. Virus-infected mice were used as a source of blood. **(B, C)** Quantification of the number of midgut-associated hemocytes between mosquitoes fed with sugar, blood or blood and virus at 4 **(B)** and 8 **(C)** days post feeding. DENV and ZIKV were analyzed together. 2 independent experiments for each virus were pooled. Each dot represents an individual midgut. Total number of midguts tested is indicated below each box plot. Upper, middle and lower bars in the boxplot represent the 75th percentile, the median and the 25th percentile, respectively. Statistical analyses were performed using the Kruskal-Wallis test followed by Dunn's test to correct for multiple comparisons. ns, non-significant. **(D–G)** Representative confocal microscopy images of mosquito midguts showing CM-DiL stained hemocytes in magenta, DNA in yellow, viral E proteins in green and actin in blue. Midguts from mosquitoes fed with sugar **(D)**, blood **(E)**, blood + DENV **(F)** and blood + ZIKV **(G)** are shown at 8 days post feeding.

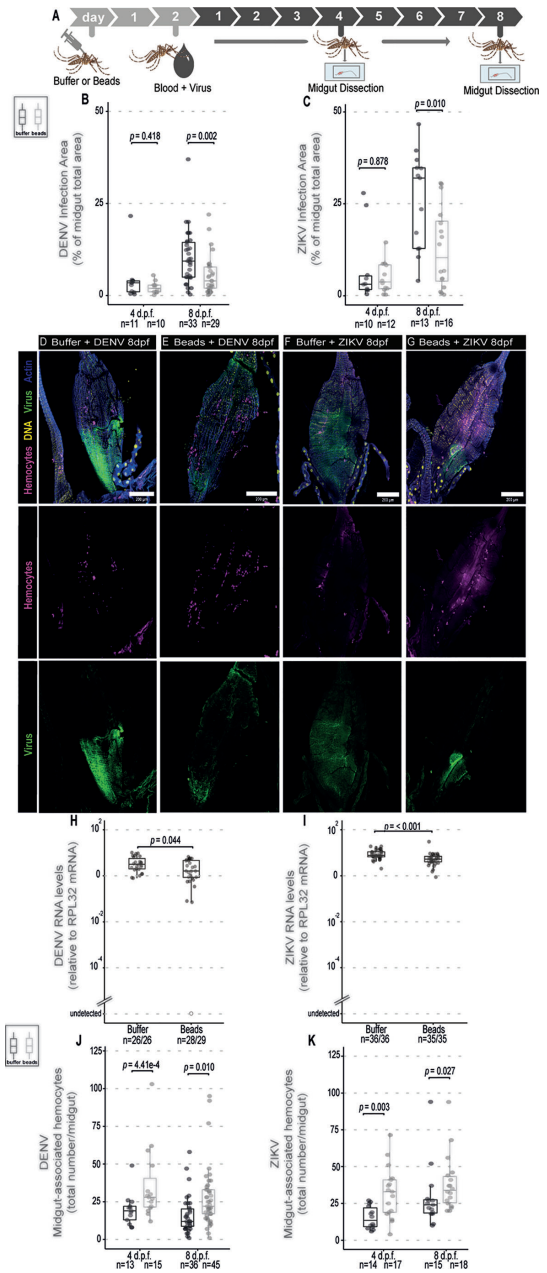

FIGURE 2 | Phagocytosis by hemocytes is not required to control DENV and ZIKV infection in the midgut of *Ae. aegypti* mosquitoes. **(A)** Mosquitoes injected with latex beads were fed 2 days later with blood + virus and dissected at different times to be analyzed. Virus-infected mice were used as a source of blood. **(B, C)** Percentage of total midgut infection area that shows staining for the viral protein at 4 and 8 days post infection was determined by immunofluorescence. Total number of midguts tested is indicated below each box plot. DENV **(B)** and ZIKV **(C)** were analyzed separately. 2 independent experiments for each virus were pooled. Each dot represents an individual midgut. **(D–G)** Representative confocal microscopy images of mosquito midguts showing CM-DiL stained hemocytes in magenta, DNA in yellow, viral E proteins in green and actin in blue. **(D, E)** Midguts from mosquitoes fed on blood + DENV. **(F, G)** Midguts from mosquitoes fed on blood + ZIKV. **(D, F)** Midguts from control mosquitoes injected with buffer; **(E, G)** Midguts from mosquitoes injected with latex beads. **(H)** DENV and **(I)** ZIKV RNA levels measured by RT-qPCR at 8 days post feeding. The number of positive midguts over the total tested is indicated below each boxplot. **(J, K)** Number of midgut-associated hemocytes in individual midguts from control and virus infected mosquitoes at 4 and 8 days post feeding. DENV **(J)** and ZIKV **(K)** were analyzed separately. Total number of midguts tested is indicated below each box plot. 2 independent experiments for each virus were pooled. **(B, C, H–K)** Each dot represents an individual midgut. Upper, middle and lower bars in the boxplot represent the 75th percentile, the median and the 25th percentile, respectively. Statistical analyses were performed using the Mann-Whitney-Wilcoxon test.

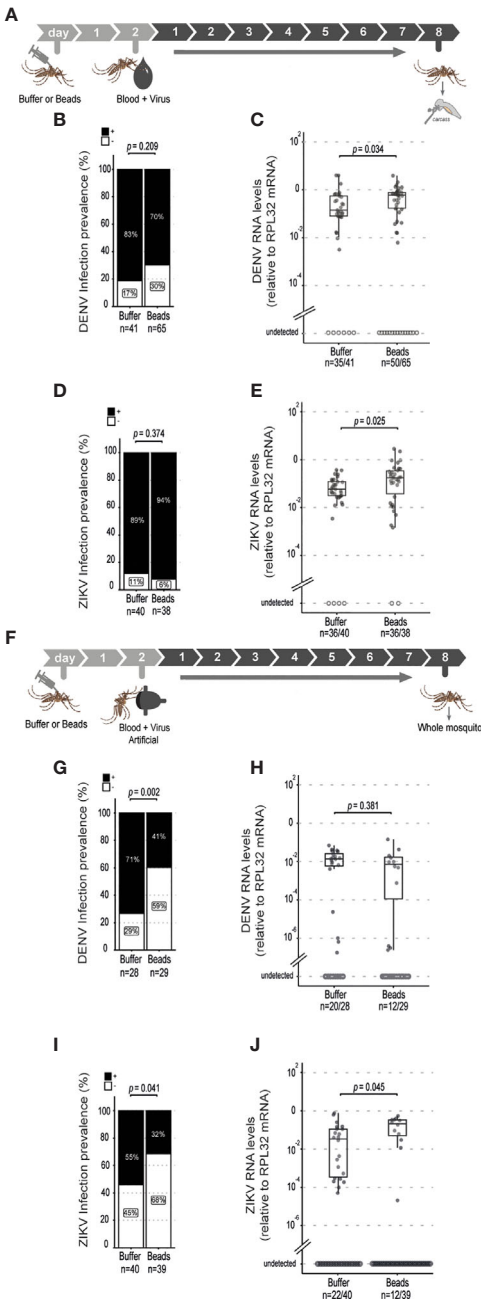

FIGURE 3 | Systemic dissemination of ZIKV and DENV infection is controlled by hemocyte phagocytosis. **(A)** Mosquitoes injected with latex beads were fed 2 days later with blood and virus and dissected at 8 days post feeding to be analyzed. Virus-infected mice were used as a source of blood. **(B, C)** Prevalence of DENV **(B)** and ZIKV **(C)** infection in the mosquito carcass at 8 days post feeding. The number of positive mosquitoes over the total tested is indicated below each column. One representative experiment is shown. This experiment was repeated 3 times for DENV and once for ZIKV. Statistical analyses were performed using two-tailed Fishers exact test. **(D, E)** Viral RNA levels at 8 days post feeding for DENV **(D)** and ZIKV **(E)**. One representative experiment is shown. This experiment was repeated 3 times for DENV and once for ZIKV. Each dot represents an individual mosquito. **(F)** Mosquitoes injected with latex beads were given an artificial blood meal with virus 2 days later and analyzed at 8 days post feeding. **(G, H)** Prevalence of DENV **(G)** and ZIKV **(H)** infection in mosquitoes injected with buffer or beads. The number of positive mosquitoes over the total tested is indicated below each column. One representative experiment is shown. This experiment was repeated twice for DENV and once for ZIKV. Statistical analyses were performed using two-tailed Fishers exact test. **(I, J)** DENV **(I)** and ZIKV **(J)** RNA levels in mosquitoes injected with buffer or beads. Each dot represents an individual mosquito. The number of positive mosquitoes over the total tested is indicated below each boxplot. One representative experiment is shown. This experiment was repeated twice for DENV and once for ZIKV. **(D, E, I, J)** Upper, middle and lower bars in the boxplot represent the 75th percentile, the median and the 25th percentile, respectively. Statistical analyses were performed using the Mann-Whitney-Wilcoxon test.

hemocytes during systemic viral replication, we used a model of intrathoracic injection of the virus (**Figure 4A**). Consistent with results using the oral infection models, we observed that inhibition of the phagocytic activity of hemocytes led to a clear increase in systemic viral replication after injection of DENV and ZIKV (**Figures 4B, C**). This effect was highly significant and did not depend on the dose of virus used or the kinetics of infection. Together, our data indicate that phagocytosis by hemocytes is essential to control systemic viral replication, which is consistent with their important roles in cellular immunity.

DISCUSSION

Here we have studied the role of phagocytosis by insect macrophage-like cells in the control of DENV and ZIKV in *Ae. aegypti* mosquitoes. These macrophage-like cells, known as hemocytes, are important components of the mosquito immune system (25). We and others have previously shown that phagocytosis by these cells plays an important function in the antiviral defense of *Drosophila* (20–22) but their role during viral infections in mosquitoes remain unclear.

Our results show that hemocytes accumulate in the midgut of *Ae. aegypti* mosquitoes in response to the presence of ZIKV and DENV in the blood meal. Interestingly, increased numbers of hemocytes in the midgut are not observed at 4 days post infection but only later at 8 days, suggesting it either requires continuous stimulation or is triggered only after certain levels of viral replication. Since the infection did not significantly change the number of circulating hemocytes, these results suggest that these cells were recruited or retained more efficiently in the midgut. Increased numbers of hemocytes in the midgut suggests an important role for these cells in the response to viral infection. However, our results were less clear regarding their possible function in the midgut. We observed that blocking phagocytosis by hemocytes using latex beads led to decreased virus replication in the midgut after 8 days post infection when these cells accumulate significantly. We show that phagocytosis is inhibited at 2 days post injection of latex beads at the time of viral infection in the midgut. Although it is unclear how long this inhibition lasts, these results suggest that phagocytosis by hemocytes has a proviral function during the early stages of DENV and ZIKV infection in the midgut. However, when phagocytosis was blocked by latex beads, we also observed increased numbers of hemocytes in the midgut of mosquitoes as early as 4 days post infection. This effect was independent of viral replication or blood feeding and could be related to lower motility of hemocytes after phagocytosis since we do observe a

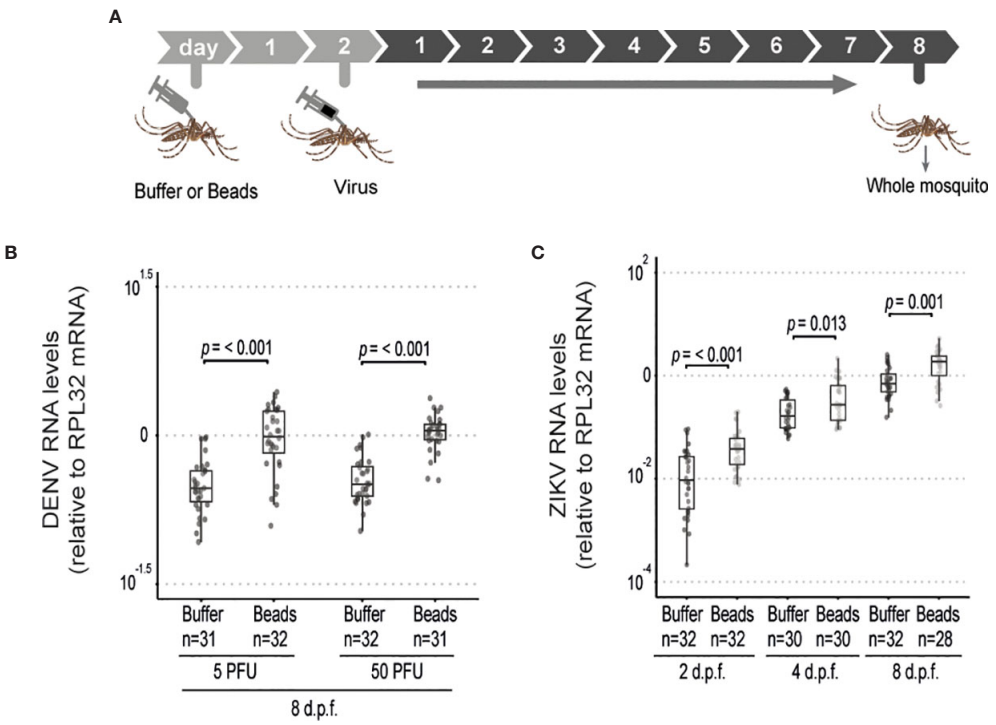

FIGURE 4 | Phagocytosis by hemocyte is required to inhibit systemic replication of ZIKV and DENV. **(A)** Mosquitoes injected with latex beads were subsequently injected with virus 2 days later and samples were analyzed at different time points. **(B)** Viral RNA levels in mosquitoes injected with 5 or 50 PFU of DENV at 8 days post injection. **(C)** Viral RNA levels in mosquitoes injected with 5 PFU of ZIKV at 2, 4 and 8 days post injection. One representative experiment is shown. This experiment was repeated twice for DENV and once for ZIKV. **(B, C)** Each dot represents an individual mosquito. The number of positive mosquitoes over the total tested is indicated above each boxplot. Upper, middle and lower bars in the boxplot represent the 75th percentile, the median and the 25th percentile, respectively. Statistical analyses were performed using the Mann-Whitney-Wilcoxon test.

tendency of decreased numbers of circulating hemocytes after injection of beads. Nevertheless, increased numbers of hemocytes in the midgut precede and could be responsible for the inhibition of viral replication independent of phagocytosis. Phagocytosis of latex beads does not seem to prime hemocytes for wound healing in *Drosophila* (26), which would suggest that these hemocytes in the mosquito midgut are not activated but rather inert. Our current data do not allow us to rule out that there are other antiviral functions by hemocytes triggered by latex beads (e.g. production of antiviral cytokines) but it is clear that phagocytosis is not required to control viral infection in the midgut of mosquitoes. Paradoxically, when the infection disseminates from the midgut, phagocytosis by hemocytes has an important role controlling systemic viral replication. Together, our data point to a dual role for phagocytosis by hemocytes in the antiviral response of *Ae. aegypti* mosquitoes against DENV and ZIKV. Phagocytosis does not affect virus replication in the midgut but is essential to control systemic infection. Notably, work by our groups and others have pointed to important differences in the requirements to control viral replication in the midgut compared to systemic infection in mosquitoes (14, 36). For example, RNA interference plays a major role during systemic infection but has little contribution to the control of viral replication in the midgut (14). Similarly, apoptosis, which is coupled to phagocytosis by hemocytes to restrict viral infection in *Drosophila* (20, 21), may not be efficiently induced in response to virus infection in the midgut epithelium of *Aedes* mosquitoes

The reason for contrasting roles of hemocytes during infection of the midgut compared to systemic dissemination of DENV and ZIKV suggests a complex scenario. It is possible that hemocytes might carry out immune functions that have opposing impacts over viral infection whether in the midgut or systemically. For example, phagocytosis might be important to clear viruses from the circulation but, in the midgut, could help virus dissemination. However, recent single cell analyses have indicated that hemocytes are composed of many subgroups that likely have distinct functions in immunity (43–46). Based on these data, it is possible that epithelial and systemic responses to viral infections mobilize different subtypes of hemocytes. Upon blood feeding, there is extensive damage to the basal lamina of the midgut and this is further exacerbated by infection by chikungunya virus (47, 48). ZIKV causes similar damage to the basal lamina (49) and that is likely true for other arboviruses. Damage to the basal lamina presumably leads to the recruitment of certain subtypes of hemocytes to these damaged regions with high concentration of the virus (47, 49). It is possible that hemocytes that are recruited to repair this damage become infected and help amplify local viral replication. Alternatively, these hemocytes could promote enterocyte survival or intestinal stem cell proliferation (50–53) and thus favor viral replication in the midgut. In contrast, during systemic dissemination of ZIKV and DENV, other subtypes of hemocytes would then play a more classical antiviral role by clearing particles and infected cells (20). Hemocytes may also participate in a systemic antiviral RNA interference of mosquitoes, as proposed in Drosophila (22), and this may not be functional in the midgut. Notably, recent work in *Anopheles* mosquitoes has suggested that subtypes of hemocytes may have different roles during specific stages of *Plasmodium* infection (34). These are pressing questions that we are currently investigating to elucidate the mechanism by which hemocytes contribute to the antiviral defense. Alternative methods for hemocyte depletion (34, 54) or genetic approaches to ablate or interfere with cell function in mosquitoes will be important tools for the field going forward. These studies will help understand how vector mosquitoes recognize and fight viral infections that could lead to novel strategies to control transmission of arboviruses.

DATA AVAILABILITY STATEMENT

The original contributions presented in the study are included in the article/**Supplementary Material**. Further inquiries can be directed to the corresponding author.

ETHICS STATEMENT

The animal study was reviewed and approved by Comissão de Ética no uso de animais - CEUA da UFMG (337/2016).

AUTHOR CONTRIBUTIONS

TL, AF, J-LI, and JM designed the experiments. TL and AF carried out the experiments and statistical analysis. TL, AF, J-LI, and JTM analyzed results. TL, AF, J-LI, and JM wrote the manuscript. All authors contributed to the article and approved the submitted version.

FUNDING

This work was funded by Conselho Nacional de Desenvolvimento Científico e Tecnológico (CNPq), Fundação de Amparo a Pesquisa do Estado de Minas Gerais (FAPEMIG), Rede Mineira de Imunobiologicos (grant # REDE-00140-16), Instituto Nacional de Ciência e Tecnologia de Vacinas (INCTV), the Institute for Advanced Studies of the University of Strasbourg (USIAS fellowship 2019) and the Investissement d'Avenir Programs (ANR-10-LABX-0036 and ANR-11-EQPX-0022). This study was financed in part by the Coordenação de Aperfeiçoamento de Pessoal de Nível Superior - Brasil (CAPES) - Finance Code 001.

ACKNOWLEDGMENTS

We would like to thank members of the Marques laboratory and research units CNRS UPR9022, Inserm U1257, in particular Dominique Ferrandon, for helpful discussions and suggestions.

Images in this work were obtained with the help of Gustavo Menezes and Hortência Oliveira from the Center for Gastrointestinal Biology at UFMG and also using equipment in the Centro de Aquisição e Processamento de Imagens from UFMG (CAPI- ICB/UFMG).

SUPPLEMENTARY MATERIAL

The Supplementary Material for this article can be found online at: https://www.frontiersin.org/articles/10.3389/fimmu.2021.660873/full#supplementary-material

REFERENCES

1. Shaw WR, Catteruccia F. Vector Biology Meets Disease Control: Using Basic Research to Fight Vector-Borne Diseases. *Nat Microbiol* (2019) 4:20–34. doi: 10.1038/s41564-018-0214-7
2. Marques JT, Imler J-L. The Diversity of Insect Antiviral Immunity: Insights From Viruses. *Curr Opin Microbiol* (2016) 32:71–6. doi: 10.1016/j.mib.2016.05.002
3. Deddouche S, Matt N, Budd A, Mueller S, Kemp C, Galiana-Arnoux D, et al. The DExD/H-box Helicase Dicer-2 Mediates the Induction of Antiviral Activity in Drosophila. *Nat Immunol* (2008) 9:1425–32. doi: 10.1038/ni.1664
4. Dostert C, Jouanguy E, Irving P, Troxler L, Galiana-Arnoux D, Hetru C, et al. The Jak-STAT Signaling Pathway is Required But Not Sufficient for the Antiviral Response of Drosophila. *Nat Immunol* (2005) 6:946–53. doi: 10.1038/ni1237
5. Goto A, Okado K, Martins N, Cai H, Barbier V, Lamiable O, et al. The Kinase Ikkβ Regulates a STING- and NF-κb-Dependent Antiviral Response Pathway in Drosophila. *Immunity* (2018) 49:225–34. doi: 10.1016/j.immuni.2018.07.013
6. Marques JT, Wang J-P, Wang X, de Oliveira KPV, Gao C, Aguiar ERGR, et al. Functional Specialization of the Small Interfering RNA Pathway in Response to Virus Infection. *PLoS Pathog* (2013) 9:e1003579. doi: 10.1371/journal.ppat.1003579
7. Cai H, Holleufer A, Simonsen B, Schneider J, Lemoine A, Gad HH, et al. 2'3'-cGAMP Triggers a STING- and NF-κb-Dependent Broad Antiviral Response in Drosophila. *Sci Signal* (2020) 13:eabc4537. doi: 10.1126/scisignal.abc4537
8. Kemp C, Mueller S, Goto A, Barbier V, Paro S, Bonnay F, et al. Broad RNA Interference-Mediated Antiviral Immunity and Virus-Specific Inducible Responses in Drosophila. *J Immunol* (2013) 190:650–8. doi: 10.4049/jimmunol.1102486
9. West C, Silverman N. p38b and JAK-STAT Signaling Protect Against Invertebrate Iridescent Virus 6 Infection in Drosophila. *PLoS Pathog* (2018) 14:e1007020. doi: 10.1371/journal.ppat.1007020
10. van Rij RP, Saleh M-C, Berry B, Foo C, Houk A, Antoniewski C, et al. The RNA Silencing Endonuclease Argonaute 2 Mediates Specific Antiviral Immunity in Drosophila Melanogaster. *Genes Dev* (2006) 20:2985–95. doi: 10.1101/gad.1482006
11. Merkling SH, Bronkhorst AW, Kramer JM, Overheul GJ, Schenck A, Van Rij RP. The Epigenetic Regulator G9a Mediates Tolerance to RNA Virus Infection in Drosophila. *PLoS Pathog* (2015) 11:e1004692. doi: 10.1371/journal.ppat.1004692
12. Wang X-H, Aliyari R, Li W-X, Li H-W, Kim K, Carthew R, et al. RNA Interference Directs Innate Immunity Against Viruses in Adult Drosophila. *Science* (2006) 312:452–4. doi: 10.1126/science.1125694
13. Souza-Neto JA, Sim S, Dimopoulos G. An Evolutionary Conserved Function of the JAK-STAT Pathway in Anti-Dengue Defense. *Proc Natl Acad Sci U S A* (2009) 106:17841–6. doi: 10.1073/pnas.0905006106
14. Olmo RP, Ferreira AGA, Izidoro-Toledo TC, Aguiar ERGR, de Faria IJS, de Souza KPR, et al. Control of Dengue Virus in the Midgut of Aedes Aegypti by Ectopic Expression of the dsRNA-binding Protein Loqs2. *Nat Microbiol* (2018) 3:1385–93. doi: 10.1038/s41564-018-0268-6
15. Sánchez-Vargas I, Scott JC, Poole-Smith BK, Franz AWE, Barbosa-Solomieu V, Wilusz J, et al. Dengue Virus Type 2 Infections of Aedes Aegypti Are Modulated by the Mosquito's RNA Interference Pathway. *PLoS Pathog* (2009) 5:e1000299. doi: 10.1371/journal.ppat.1000299
16. Morazzani EM, Wiley MR, Murreddu MG, Adelman ZN, Myles KM. Production of Virus-Derived Ping-Pong-Dependent piRNA-like Small RNAs in the Mosquito Soma. *PLoS Pathog* (2012) 8:e1002470. doi: 10.1371/journal.ppat.1002470
17. Khoo CC, Piper J, Sanchez-Vargas I, Olson KE, Franz AW. The RNA Interference Pathway Affects Midgut Infection- and Escape Barriers for Sindbis Virus in Aedes Aegypti. *BMC Microbiol* (2010) 10:130. doi: 10.1186/1471-2180-10-130
18. Khoo CCH, Doty JB, Heersink MS, Olson KE, Franz AWE. Transgene-Mediated Suppression of the RNA Interference Pathway in Aedes Aegypti Interferes With Gene Silencing and Enhances Sindbis Virus and Dengue Virus Type 2 Replication. *Insect Mol Biol* (2013) 22:104–14. doi: 10.1111/imb.12008
19. Wu X, Wu F-H, Wang X, Wang L, Siedow JN, Zhang W, et al. Molecular Evolutionary and Structural Analysis of the Cytosolic DNA Sensor cGAS and STING. *Nucleic Acids Res* (2014) 42:8243–57. doi: 10.1093/nar/gku569
20. Lamiable O, Arnold J, de Faria IJ da S, Olmo RP, Bergami F, Meignin C, et al. Analysis of the Contribution of Hemocytes and Autophagy to Drosophila Antiviral Immunity. *J Virol* (2016) 90:5415–26. doi: 10.1128/JVI.00238-16
21. Nainu F, Tanaka Y, Shiratsuchi A, Nakanishi Y. Protection of Insects Against Viral Infection by Apoptosis-Dependent Phagocytosis. *J Immunol* (2015) 195:5696–706. doi: 10.4049/jimmunol.1500613
22. Tassetto M, Kunitomi M, Andino R. Circulating Immune Cells Mediate a Systemic Rnai-Based Adaptive Antiviral Response in Drosophila. *Cell* (2017) 169:314–25.e13. doi: 10.1016/j.cell.2017.03.033
23. Hillyer J. The Antibacterial Innate Immune Response by the Mosquito Aedes Aegypti is Mediated by Hemocytes and Independent of Gram Type and Pathogenicity. *Microbes Infect* (2004) 6:448–59. doi: 10.1016/j.micinf.2004.01.005
24. Hillyer JF, Schmidt SL, Christensen BM. Rapid Phagocytosis and Melanization of Bacteria and Plasmodium Sporozoites by Hemocytes of the Mosquito Aedes Aegypti. *J Parasitol* (2003) 89:62–9. doi: 10.1645/0022-3395
25. Hillyer JF, Strand MR. Mosquito Hemocyte-Mediated Immune Responses. *Curr Opin Insect Sci* (2014) 3:14–21. doi: 10.1016/j.cois.2014.07.002
26. Weavers H, Evans IR, Martin P, Wood W. Corpse Engulfment Generates a Molecular Memory That Primes the Macrophage Inflammatory Response. *Cell* (2016) 165:1658–71. doi: 10.1016/j.cell.2016.04.049
27. Sanchez Bosch P, Makhijani K, Herboso L, Gold KS, Baginsky R, Woodcock KJ, et al. Adult Drosophila Lack Hematopoiesis But Rely on a Blood Cell Reservoir At the Respiratory Epithelia to Relay Infection Signals to Surrounding Tissues. *Dev Cell* (2019) 51:787–803.e5. doi: 10.1016/j.devcel.2019.10.017
28. King JG, Hillyer JF. Spatial and Temporal In Vivo Analysis of Circulating and Sessile Immune Cells in Mosquitoes: Hemocyte Mitosis Following Infection. *BMC Biol* (2013) 11:55. doi: 10.1186/1741-7007-11-55
29. King JG, Hillyer JF. Infection-Induced Interaction Between the Mosquito Circulatory and Immune Systems. *PLoS Pathog* (2012) 8:e1003058. doi: 10.1371/journal.ppat.1003058
30. Barletta ABF, Trisnadi N, Ramirez JL, Barillas-Mury C. Mosquito Midgut Prostaglandin Release Establishes Systemic Immune Priming. *iScience* (2019) 19:54–62. doi: 10.1016/j.isci.2019.07.012
31. Rodrigues J, Brayner FA, Alves LC, Dixit R, Barillas-Mury C. Hemocyte Differentiation Mediates Innate Immune Memory in *Anopheles gambiae* Mosquitoes. *Science* (2010) 329:1353–5. doi: 10.1126/science.1190689
32. Volohonsky G, Paul-Gilloteaux P, Štáfková J, Soichot J, Salamero J, Levashina EA. Kinetics of Plasmodium Midgut Invasion in Anopheles Mosquitoes. *PLoS Pathog* (2020) 16:e1008739. doi: 10.1371/journal.ppat.1008739
33. Castillo JC, Ferreira ABB, Trisnadi N, Barillas-Mury C. Activation of Mosquito Complement Antiplasmodial Response Requires Cellular Immunity. *Sci Immunol* (2017) 2:eaal1505. doi: 10.1126/sciimmunol.aal1505
34. Kwon H, Smith RC. Chemical Depletion of Phagocytic Immune Cells in Anopheles Gambiae Reveals Dual Roles of Mosquito Hemocytes in anti-Plasmodium Immunity. *Proc Natl Acad Sci U S A* (2019) 116:14119–28. doi: 10.1073/pnas.1900147116
35. Franz A, Kantor A, Passarelli A, Clem R. Tissue Barriers to Arbovirus Infection in Mosquitoes. *Viruses* (2015) 7:3741–67. doi: 10.3390/v7072795
36. Carissimo G, Pondeville E, McFarlane M, Dietrich I, Mitri C, Bischoff E, et al. Antiviral Immunity of Anopheles Gambiae is Highly Compartmentalized,

With Distinct Roles for RNA Interference and Gut Microbiota. *Proc Natl Acad Sci U S A* (2015) 112:E176–85. doi: 10.1073/pnas.1412984112
37. Salazar MI, Richardson JH, Sánchez-Vargas I, Olson KE, Beaty BJ. Dengue Virus Type 2 Replication and Tropisms in Orally Infected Aedes Aegypti Mosquitoes. *BMC Microbiol* (2007) 7:9. doi: 10.1186/1471-2180-7-9
38. Parikh GR, Oliver JD, Bartholomay LC. A Haemocyte Tropism for an Arbovirus. *J Gen Virol* (2009) 90:292–6. doi: 10.1099/vir.0.005116-0
39. Coggins SA, Estévez-Lao TY, Hillyer JF. Increased Survivorship Following Bacterial Infection by the Mosquito Aedes Aegypti as Compared to Anopheles Gambiae Correlates With Increased Transcriptional Induction of Antimicrobial Peptides. *Dev Comp Immunol* (2012) 37:390–401. doi: 10.1016/j.dci.2012.01.005
40. Castillo J, Brown MR, Strand MR. Blood Feeding and Insulin-like Peptide 3 Stimulate Proliferation of Hemocytes in the Mosquito Aedes Aegypti. *PLoS Pathog* (2011) 7:e1002274. doi: 10.1371/journal.ppat.1002274
41. Bryant WB, Michel K. Blood Feeding Induces Hemocyte Proliferation and Activation in the African Malaria Mosquito, Anopheles Gambiae Giles. *J Exp Biol* (2014) 217:1238–45. doi: 10.1242/jeb.094573
42. Nehme NT, Liégeois S, Kele B, Giammarinaro P, Pradel E, Hoffmann JA, et al. A Model of Bacterial Intestinal Infections in Drosophila Melanogaster. *PloS Pathog* (2007) 3:e173. doi: 10.1371/journal.ppat.0030173
43. Raddi G, Barletta ABF, Efremova M, Ramirez JL, Cantera R, Teichmann SA, et al. Mosquito Cellular Immunity At Single-Cell Resolution. *Science* (2020) 369:1128–32. doi: 10.1126/science.abc0322
44. Severo MS, Landry JJM, Lindquist RL, Goosmann C, Brinkmann V, Collier P, et al. Unbiased Classification of Mosquito Blood Cells by Single-Cell Genomics and High-Content Imaging. *Proc Natl Acad Sci U S A* (2018) 115:E7568–77. doi: 10.1073/pnas.1803062115
45. Cattenoz PB, Sakr R, Pavlidaki A, Delaporte C, Riba A, Molina N, et al. Temporal Specificity and Heterogeneity of Drosophila Immune Cells. *EMBO J* (2020) 39:e104486. doi: 10.15252/embj.2020104486
46. Tattikota SG, Cho B, Liu Y, Hu Y, Barrera V, Steinbaugh MJ, et al. A Single-Cell Survey of Drosophila Blood. *Elife* (2020) 9:e54818. doi: 10.7554/eLife.54818
47. Dong S, Balaraman V, Kantor AM, Lin J, Grant DG, Held NL, et al. Chikungunya Virus Dissemination From the Midgut of Aedes Aegypti is Associated With Temporal Basal Lamina Degradation During Bloodmeal Digestion. *PLoS Negl Trop Dis* (2017) 11:e0005976. doi: 10.1371/journal.pntd.0005976
48. Kantor AM, Grant DG, Balaraman V, White TA, Franz AWE. Ultrastructural Analysis of Chikungunya Virus Dissemination From the Midgut of the Yellow Fever Mosquito, Aedes Aegypti. *Viruses* (2018) 10:571. doi: 10.3390/v10100571
49. Cui Y, Grant DG, Lin J, Yu X, Franz AWE. Zika Virus Dissemination From the Midgut of Aedes Aegypti is Facilitated by Bloodmeal-Mediated Structural Modification of the Midgut Basal Lamina. *Viruses* (2019) 11:1056. doi: 10.3390/v11111056
50. Amcheslavsky A, Lindblad JL, Bergmann A. Transiently "Undead" Enterocytes Mediate Homeostatic Tissue Turnover in the Adult Drosophila Midgut. *Cell Rep* (2020) 33:108408. doi: 10.1016/j.celrep.2020.108408
51. Haller S, Franchet A, Hakkim A, Chen J, Drenkard E, Yu S, et al. Quorum-Sensing Regulator RhlR But Not its Autoinducer RhlI Enables Pseudomonas to Evade Opsonization. *EMBO Rep* (2018) 19:e44880. doi: 10.15252/embr.201744880
52. Ayyaz A, Li H, Jasper H. Haemocytes Control Stem Cell Activity in the Drosophila Intestine. *Nat Cell Biol* (2015) 17:736–48. doi: 10.1038/ncb3174
53. Chakrabarti S, Dudzic JP, Li X, Collas EJ, Boquete J-P, Lemaitre B. Remote Control of Intestinal Stem Cell Activity by Haemocytes in Drosophila. *PLoS Genet* (2016) 12:e1006089. doi: 10.1371/journal.pgen.1006089
54. Ramesh Kumar J, Smith JP, Kwon H, Smith RC. Use of Clodronate Liposomes to Deplete Phagocytic Immune Cells in Drosophila Melanogaster and Aedes Aegypti. *Front Cell Dev Biol* (2021) 9:627976. doi: 10.3389/fcell.2021.627976

Conflict of Interest: The authors declare that the research was conducted in the absence of any commercial or financial relationships that could be construed as a potential conflict of interest.

frontiers in Immunology

ORIGINAL RESEARCH
published: 13 May 2021
doi: 10.3389/fimmu.2021.670122

A Thioester-Containing Protein Controls Dengue Virus Infection in *Aedes aegypti* Through Modulating Immune Response

Shih-Che Weng[1], *Hsing-Han Li*[2], *Jian-Chiuan Li*[2], *Wei-Liang Liu*[2], *Chun-Hong Chen*[2,3]* *and Shin-Hong Shiao*[1]*

[1] Department of Tropical Medicine and Parasitology, College of Medicine, National Taiwan University, Taipei, Taiwan,
[2] National Institute of Infectious Diseases and Vaccinology, National Health Research Institutes, Miaoli, Taiwan,
[3] National Mosquito-Borne Diseases Control Research Center, National Health Research Institutes, Miaoli, Taiwan

OPEN ACCESS

Edited by:
Xiao-Qiang Yu,
University of Missouri–Kansas City,
United States

Reviewed by:
Salvador Hernández-Martínez,
National Institute of Public Health,
Mexico
Jorge Cime-Castillo,
National Institute of Public Health,
Mexico

***Correspondence:**
Shin-Hong Shiao
shshiao@ntu.edu.tw
Chun-Hong Chen
chunhong@gmail.com

Specialty section:
This article was submitted to Comparative Immunology, a section of the journal Frontiers in Immunology

Received: 20 February 2021
Accepted: 28 April 2021
Published: 13 May 2021

Citation:
Weng S-C, Li H-H, Li J-C, Liu W-L, Chen C-H and Shiao S-H (2021) A Thioester-Containing Protein Controls Dengue Virus Infection in Aedes aegypti Through Modulating Immune Response. Front. Immunol. 12:670122. doi: 10.3389/fimmu.2021.670122

Complement-like proteins in arthropods defend against invading pathogens in the early phases of infection. Thioester-containing proteins (TEPs), which exhibit high similarity to mammalian complement C3, are thought to play a key role in the innate immunity of arthropods. We identified and characterized anti-dengue virus (DENV) host factors, in particular complement-like proteins, in the mosquito *Aedes aegypti*. Our results indicate that TEP1 limits DENV infection in *Ae. aegypti.* We showed that *TEP1* transcription is highly induced in mosquitoes following DENV infection. Silencing *TEP1* resulted in the up-regulation of viral RNA and proteins. In addition, the production of infectious virus particles increased in the absence of *TEP1*. We generated a transgenic mosquito line with a TEP1 loss-of-function phenotype under a blood meal-inducible promoter. We showed that viral protein and titers increased in transgenic mosquitoes after an infectious blood meal. Interestingly, expression of transcription factor Rel2 and certain anti-microbial peptides (AMPs) were inhibited in transgenic mosquitoes. Overall, our results suggest that TEP1 regulates the immune response and consequently controls the replication of dengue virus in mosquitoes. This finding provides new insight into the molecular mechanisms of mosquito host factors in the regulation of DENV replication.

Keywords: *Aedes aegypti*, dengue virus, thioester-containing protein (TEP), innate immunity, transgenic mosquito

INTRODUCTION

Dengue fever is one of the most important arthropod-borne viral diseases. It is caused by four different serotypes of dengue virus (DENV1–4). DENV is a positive-stranded RNA virus that belongs to the *Flaviviridae* family and is transmitted to humans through the bite of infected *Aedes* genus mosquitoes. A current estimate suggests that more than 390 million DENV infections happen worldwide every year (1–3). DENV infection causes a range of symptoms, including undifferentiated fever, dengue fever (DF), and dengue hemorrhagic fever or dengue shock syndrome (DHF/DSS) (2, 4, 5). Dengue is spread through the bite of female mosquitoes, mainly *Aedes aegypti* and, to a lesser extent, *Aedes albopictus*. Mosquitoes acquire the virus when feeding on

the blood of an infected person. The virus then replicates within midgut epithelial cells, where it starts to disseminate *via* hemolymph three to five days post-infection (dpi) to infect other tissues, such as fat cells, the trachea, and nervous tissue. Finally, the virus reaches the salivary glands, where it replicates before transmission to another host (6, 7).

Mosquitoes have developed a complex innate immune response system for defense against invading pathogens (6, 8). Complement-like proteins in arthropods function as defense in the early phases of infection (9). Thioester-containing proteins (TEPs), which exhibit high similarity to the mammalian complement C3, are thought to play a key role in the innate immunity of arthropods (10–13). In vertebrates, TEP family members range from broad-spectrum serine protease inhibitors such as α2-macroglobulins to complement factors involved in the recognition and destruction of pathogens (9, 14). An *Anopheles* TEP, induced by *Plasmodium berghei*, was demonstrated to bind and kill ookinetes in the mosquito midgut (13, 15). TEPs in *Anopheles* were shown to play crucial roles in scavenging bacteria *via* phagocytosis (16). It has also been suggested that *Drosophila* TEPs are required for the efficient phagocytosis of Gram-positive or Gram-negative bacteria in S2 cells (17). Additionally, TEPs in the yellow fever mosquito *Ae. aegypti* were identified as key factors for the restriction of flaviviral infections (11, 18). Previous functional studies indicate that TEPs exert potent anti-DENV activity. Some studies also indicate that TEPs may play a role in DENV suppression through the activation of antimicrobial peptides (AMPs) (18). However, the relationship between TEPs and AMPs is still unclear.

AMPs are the effectors of innate immunity in insects and are regulated by a wide variety of signal transduction pathways in response to different microbial infections (6, 8, 19). To date, 17 AMPs have been discovered in the *Ae. aegypti* genome and are categorized into five independent groups: defensins (4), cecropins (10), attacin (1), diptericin (1), and gambicin (1) (19). The mechanisms involved in the regulation of AMPs *via* immune pathways have mainly been studied in *Drosophila* (6, 8, 19). In mosquitoes, Toll, Imd, and JAK-STAT pathways are activated during pathogen infection (6, 8, 19, 20). Pathogenic surface proteins are recognized by immune receptors and trigger downstream transcription factors, such as Rel1 (Toll pathway), Rel2 (Imd pathway), and STAT (JAK-STAT pathway) (21). Then, the activated transcription factors bind to specific regulatory elements for AMP gene transcription initiation (6, 8, 19). The JAK-STAT pathway has been shown to be activated by viral infection in mosquitoes (6, 8, 20). Previous studies also report that AMP expression may be induced by DENV infection in mosquitoes, and AMPs exhibit antiviral activity (6, 8, 18, 20).

In this study, we show that TEP1 limits DENV infection in *Ae. aegypti*. Silencing TEP1 using a reverse genetic approach resulted in an up-regulation of viral RNA and proteins in mosquitoes. In addition, the production of infectious viral particles increased in the absence of TEP1. We generated a midgut-specific TEP1 microRNA (TEP1-miR) expression mosquito with a TEP1 loss-of-function phenotype using the carboxypeptidase (CPA) promoter. We demonstrated that both the viral RNA and titer increased in mosquitoes from this line after an infectious blood meal. Interestingly, transgenic mosquitos with TEP1 loss-of-function inhibited the transcription factor Rel2 of the Imd pathway. Overall, our results suggest that TEP1 regulates the mosquito immune response and consequently controls the replication of dengue virus. These findings provide new insight into the molecular mechanisms of mosquito host factors in the regulation of DENV replication.

MATERIALS AND METHODS

Mosquitoes

UGAL/Rockefeller strain *Ae. aegypti* mosquitoes were kept at 28°C and 70% relative humidity under a light-dark cycle of 12:12 hours as previously described (22, 23). Hatched larvae were transferred to plastic containers with sufficient water and fed with yeast extract daily. Pupae were collected and transferred to a plastic container in an insect dorm. Emerged mosquitoes were fed using cotton balls soaked with a 10% sucrose solution. Female mosquitoes three to five days post- eclosion (PE) were used for our experiments. The sucrose-soaked cotton balls were removed at least 12 hours before blood feeding. Female mosquitoes were permitted to blood-feed on an anesthetized ICR strain mouse for 15 to 30 minutes. ICR strain mice were anesthetized with an intraperitoneal injection of Avertin at a dose of 0.2 mL per 10 g of weight. All animal procedures and experimental protocols were approved by AAALAC-accredited facility, the Committee on the Ethics of Animal Experiments of the National Taiwan University College of Medicine (IACUC approval No: 20200210).

Cell Culture and Virus

Ae. albopictus C6/36 cells were cultured in DMEM/MM (1:1) containing 2% heat-inactivated fetal bovine serum (FBS) and 1× penicillin–streptomycin solution. For virus production, cells were infected with the DENV2 strain 16681 at 0.01 multiplicity of infection (MOI). The culture supernatant was harvested at 7 dpi and stored at −80°C. To determine the viral titer, the virus stock was subjected to examination with a plaque assay, as previously described (24). Approximately 1.0×10^7 PFU/mL DENV2 was used to infect the mosquitoes.

RNA Extraction and Reverse Transcription (RT)

The whole bodies of three to five mosquitoes or the midguts of 20 to 30 mosquitoes were collected in 1.5 mL tubes containing 0.5 mL Trizol Reagent (Invitrogen). Tissue was homogenized with a rooter-stator homogenizer at room temperature for 5 minutes and centrifuged at 13000 rpm for 10 minutes at 4°C. After centrifugation, the supernatant was transferred to a new micro-tube with 0.1 mL chloroform (J. T. Baker) and mixed thoroughly at room temperature for 3 minutes. Samples were then centrifuged at 13000 rpm for 15 minutes at 4°C and the

supernatant was transferred carefully to a new micro-tube with 0.25 isopropanol (J. T. Baker). Samples were gently mixed and stored at −80°C for 30 minutes. After precipitation, the samples were once again centrifuged at 13000 rpm for 30 minutes at 4°C. The supernatant was discarded and 0.5 mL 75% ethanol (Taiwan Burnett International Co., Ltd) was used to wash the RNA pellet. All resulting samples were centrifuged at 8000 rpm for 5 minutes at 4°C and the supernatant was discarded. Finally, the RNA pellet was dried in a laminar flow hood and dissolved in DEPC-H_2O. After Baseline-ZEROTM DNase (Epicentre) treatment, the RNA sample was stored at −80°C.

The RNA concentration was quantified with a spectrophotometer (Nanodrop 2000, Thermo) and was diluted with DEPC-H_2O at a concentration of 1 μg/μL. The RNA samples were reverse-transcribed to cDNA with a High-Capacity cDNA Reverse Transcription Kit (Applied Biosystems). The cDNA samples were stored at −20°C for further use. Gene expression was analyzed with a polymerase chain reaction (PCR) using ProTaq Plus DNA Polymerase (Protech). The ribosomal protein S7 gene was used as an internal control.

Quantitative PCR (qPCR)

The qPCR system used in this study was the SYBR Green dye binding system. SYBR Green binds to the minor groove of DNA and the target gene is quantified by detecting the resulting fluorescence signal. The cDNA sample was quantified with the KAPA SYBR FAST Universal qPCR kit (KAPA) and the qPCR primers were designed using ABI Primer Expression Software. PCR consisted of an initial denaturation at 95°C for 3 minutes, followed by 40 cycles at 94°C for 3 seconds, and 40 seconds at 60°C. Fluorescence readings were measured at 72°C after each cycle. The target gene signal was detected and analyzed with the ABI 7900HT Fast Real-Time PCR System, and relative quantification results were normalized using the ribosomal protein S7 gene as an internal control.

Double-Stranded RNA (dsRNA) Preparation

RNAi primers were designed with the E-RNAi webservice (http://www.dkfz.de/signaling/e-rnai3//). The T7 promoter sequence (5′- TAATACGACTCACTATAGGG) was incorporated into all forward and reverse RNAi primers. The target gene fragment was amplified with Ex Taq DNA Polymerase (Takara). Fragments were amplified and cloned into a pCR 2.1-TOPO vector at 23°C for 30 minutes using a TOPO TA Cloning Kit (Invitrogen). The constructed plasmid was transformed into HIT-DH5α competent cells. Plasmids from positive colonies were purified using a FarvoPrep Plasmid DNA Extraction Mini Kit (Favogen) and sequenced to confirm that the cDNA was in frame.

The plasmid was digested by a restriction enzyme and fragments were separated using 1% agarose gel. Target fragments were isolated and purified from the gel using a FarvoPrep GEL/PCR Purification Kit (Favogen). The fragments were then amplified with Ex Taq DNA Polymerase (Takara) and purified with the FarvoPrep™ GEL/PCR Purification Kit (Favogen). The purified PCR product was used as the template for synthesizing the dsRNA *in vitro* using a T7-Scribe™ Transcription Kit (Epicentre). The reaction was performed at 37°C for 4 to 12 hours. A solution of 95 μL of DEPC-H_2O and ammonium acetate (stop solution) was added to stop the reaction and the supernatant was transferred into a new Eppendorf tube with 150 μL of a phenol/chloroform (AMRESCO) solution. Samples were centrifuged at 13000 rpm for 5 minutes at 4°C and the supernatant was transferred to a new Eppendorf tube with 150 μL of chloroform. After another centrifugation at 13000 rpm for 5 minutes at 4°C, the supernatant was transferred to a new Eppendorf tube with 110 μL isopropanol. Samples were gently mixed and stored at −80°C for 30 minutes. Finally, each sample was centrifuged at 13000 rpm for 30 minutes at 4°C. The dsRNA pellets were dried in a laminar flow hood and dissolved in DEPC-H_2O.

The dsRNA was diluted to a final concentration of 5 μg/μL. Between day three to five post-eclosion (PE), female mosquitoes were injected with 280 nL of dsRNA (5 μg/μL) using a Nanoject II AutoNanoliter Injecter (Drummond Scientific Company). dsRNA against LacZ was used as control dsRNA (dsLacZ). Silencing efficiency was confirmed by collecting the total RNA of mosquitoes three days post-injection for RT-PCR analysis.

Western Blot Analysis

The whole bodies of three to five mosquitoes or the midguts of 10 to 30 mosquitoes were collected in 1.5 mL Eppendorf tubes containing 100 μL of protein lysis buffer and homogenized with a rooter-stator homogenizer. Each homogenized sample was centrifuged at 13000 rpm for 30 minutes at 4°C and the supernatant was transferred to a QIAshredder column (QIAGEN). The eluted samples were collected and transferred to new Eppendorf tubes at −80°C. The protein concentration was quantified using the Bradford method with a Bio-Rad Protein Assay Dye Reagent (Bio-Rad Laboratories, Inc.). Each protein sample was mixed with the same volume of sample buffer, Laemmli 2× Concentrate (SIGMA), and adjusted to the same volume with 1× sample buffer. To denature proteins for electrophoresis, protein samples were incubated at 98°C for 18 minutes. The protein samples (10 μg in midguts or 60 μg in whole body mosquitoes per lane) were subjected to SDS-PAGE and blotted onto a PVDF membrane (Pall Corporation) for 1.5 hours. The membranes were blocked with 5% skim milk in PBST (1× phosphate-buffered saline, 0.4% tween 20) at room temperature for one hour. Afterwards, the membranes were incubated in the blocking solution with the primary antibody (Anti-NS1, anti-*Anopheles gambiae* TEP1, or Anti-GAPDH) overnight at 4°C. The anti-*Anopheles gambiae* TEP1 antibody used was a gift from Dr. Stephanie Blandin at the Institute of Molecular and Cellular Biology, French National Centre for Scientific Research (CNRS) in Strasbourg, France. Membranes were washed in a PBST solution and incubated with a secondary antibody (anti-rabbit IgG) in the blocking solution at room temperature for one hour. Finally, membranes were washed in PBST and developed using WesternBright Peroxide and ECL (Advansta Inc.) as the substrate for horseradish peroxidase following the manufacturer's instructions.

Immunofluorescence Assay

Mosquito midguts were dissected in PBS and fixed in 4% paraformaldehyde (Electron Microscopy, Hatfield, PA) for at least four hours. The fixative was then removed and the midguts were rinsed in PBS, incubated for one hour in 0.1% Triton X-100 in PBS for cell permeabilization, and blocked with a PAT blocking buffer (1% Bovine serum albumin (BSA), 0.5% Triton X-100 in PBS) for one hour. A monoclonal mouse anti-NS1 antibody (YH0023) (Yao-Hong Biotechnology Inc., Taipei, Taiwan) was used as the primary antibody to examine DENV antigens in the midguts. They were then incubated with a 1:500 dilution of goat anti-mouse antibody conjugated with Alexa-488 fluorochrome (Molecular Probes Inc., Eugene, OR). Finally, midguts were mounted with a DAPI-containing medium for confocal microscopy (ZEISS, LSM 510 META Confocal Microscope).

Plaque Assay

The whole bodies or midguts were collected from TEP1 silenced, dsLacZ-treated, or wild type (control) mosquitoes in 100 µL serum-free medium with antibiotics (penicillin–streptomycin) and stored at −80°C. C6/36 cells were seeded in a 24-well tissue culture plate and incubated at 28°C overnight. The homogenized suspensions of infectious mosquitoes were centrifuged at 18,928 × g for 30 minutes and kept on ice. The cell monolayers were rinsed with PBS and 200 µL of the 10-fold serial dilutions of infectious mosquito suspensions were added for two hours. After viral adsorption, 500 µL 1% methyl cellulose cell media with antibiotics (penicillin–streptomycin) was added and the plates were kept in an incubator at 28°C for five days. The plates were fixed with 4% formaldehyde for one hour at room temperature and stained with 1% crystal violet for 30 minutes. Plaques were quantified *via* manual counting (24).

Generation of Transgenic Mosquitoes

Female mosquitoes were allowed to lay eggs for 50 minutes three days after the blood meal. The DNA of donor and helper plasmids was mixed at the ratio of 500:300 ng/µL and diluted in a 1× injection buffer (2 mM KCl, 0.1 mM sodium phosphate, pH 6.8). Approximately 500 injected embryos were kept on the filter paper for four days before hatching. Each surviving male and female adult from the injected generation 0 (G0) was outcrossed with three control females or males at a male/female or female/male ratio of 1:3. eGFP fluorescence driven by the 3xp3 promoter manifests at the optic nerve and tracheal gills of G1 transgenic larvae, which were screened with the help of a stereoscopic fluorescent microscope (SZX10, Olympus) (25, 26).

pMOS1-AeCPA-miR-TEP1-2miR-3xp3-eGFP Vector

The functional stem-loop structure of the artificial mir-based RNAi_TEP1 miRNA was created through the first primer sets, AeTEP1-mir-1-1/Ae-TEP1-mir-1-2 or AeTEP1-mir-2-1/Ae-TEP1-mir-2-2, by PCR. This functional stem-loop miRNA was then extended and flanking sequences with restriction enzyme sites were added with the second primer set, Mir6.1_5′EcoRI/BglII and Mir6.1_3′BamHI/XhoI, to get the precursor TEP1 miRNA unit. The BglII and BamHI restriction enzyme sites of the precursor TEP1 miRNA unit were used for assembling TEP1-miR-1 and TEP1-miR-2 to generate the TEP1-2miRNA cassette (27). Based on the above, following double digestion by the restriction enzymes, EcoRI/BamHI-TEP1-miR-1 and BglII/XhoI-TEP1-miR-2 were integrated concurrently into the EcoRI and XhoI sites of pMOS1_AePUb-Den3-4miR_3xp3-eGFP (GenBank accession: MG603748) to generate a pMOS1_AePUb-miR-TEP1-2miR_3xP3-eGFP transition plasmid with a truncated AePUb promoter (26). The AeCPA promoter was amplified from *Ae. aegypti* genomic DNA by using the following primers: pMOS1_fusion_AeCPA-pr-F and pMOS1_fusion_AeCPA-pr-R (28). Finally, the AeCPA promoter fragments were cloned into the FseI and EcoRI double-digested pMOS1_AePUb-miR-TEP1-2miR_3xp3-eGFP transition plasmid with In-Fusion HD Cloning technology (Clontech), generating the pMOS1-AeCPA-miR-TEP1-2miR-3xp3-eGFP vector.

Statistical Analysis

All statistical analyses were performed using GraphPad Prism 5 software. Gene expression and fecundity data were analyzed using ANOVA for all independent experiments.

RESULTS

An Infectious Blood Meal Activates TEP1 Expression in the Mosquito Midgut

To identify the immune-responsive genes involved in DENV replication in mosquitoes, we selected several immune-responsive genes previously identified as potential inducible genes (29, 30). Total RNA was extracted from the midguts of mosquitoes at three and seven days after an infectious or normal blood meal. The transcriptional profiles of the immune-responsive genes from normal (BF) and infectious DENV2 blood-fed (DENV2) mosquito midguts were examined with qRT-PCR analysis. Interestingly, our results showed that transcription of TEP1 was significantly up-regulated three days post DENV2 infection (**Figure 1**). This indicates that TEP1 is sensitive to DENV infection in the mosquito midgut. Therefore, we investigated the role of TEP1 in DENV2 replication further.

TEP1 Is Involved in DENV Replication in the Midgut of Mosquitoes

First, we examined the expression profiles of TEP1 between normal and infectious DENV2 blood-fed in mosquito midguts. Midguts from female mosquitoes were collected 6, 12, 24, 48, and 72 hours after a normal or infectious blood meal. Equal amounts of total RNA from each group were used for cDNA synthesis. The transcriptional profiles of TEP1 were examined with qRT-PCR analysis. Our results showed that TEP1 RNA expression was higher in the midgut of the mosquito after a blood meal (**Figure 2A**). The RNA expression level was significantly higher after an infectious blood meal. In order to examine the translational

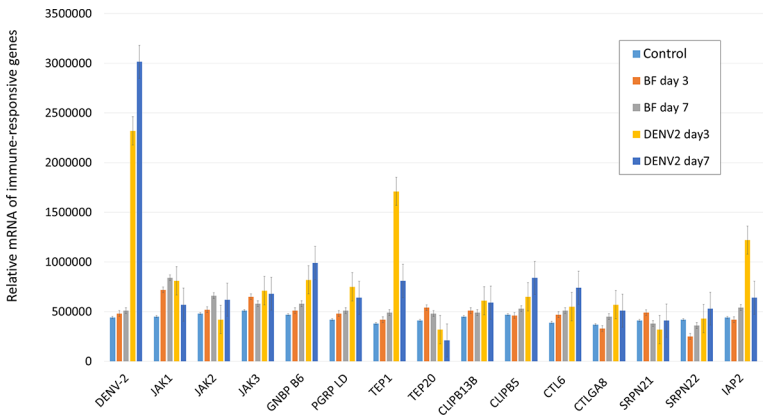

FIGURE 1 | Transcriptional Analysis of Immune-Responsive Genes in the Mosquito Midgut. The relative mRNA levels of the immune-responsive genes from three and seven days after normal (BF) and infectious DENV2 blood-fed (DENV2) mosquito midguts were examined with qRT-PCR analysis. Midguts of mosquitoes fed with non-infectious blood were used as controls. An equal amount of total RNA from each group was used for cDNA synthesis. Ribosomal protein S7 was used for normalization of relative target gene mRNA expression. Values are mean ± S.E. (error bars) of the copy number of each gene. At least three biological cohorts from each time point were used for analysis.

pattern of TEP1, total protein from the midgut of the mosquito was collected 6, 12, 24, 48, and 72 hours after a normal or infectious blood meal. Equal amounts of total protein from each group were used for western blot analysis. Our results show that TEP 1 was activated at 6 hours with a blood medium and decays at 12 hours after feeding, while the expression is higher at 6 hours when the blood includes virus and this was maintained up to 24 hours post infection (**Figure 2B**). To clarify the role of TEP1 in DENV2 replication, we used a reverse genetic approach by introducing TEP1 dsRNA into the mosquito to silence TEP1 expression. The viral genome and NS1 protein expression were activated in the absence of TEP1 (**Figures 2C, D**). These results indicate that TEP1 plays a crucial role in regulating DENV2 replication in the midgut of mosquitoes.

TEP1 miRNA-Mediated Loss-of-Function Transgenic Mosquitoes Enhance DENV Replication

To investigate the function of TEP1 in mosquitoes, we generated a TEP1 loss-of-function transgenic mosquito using anti-TEP1 miR expression (**Figure 3A**). The expression of anti-TEP1 miR was regulated by a mosquito midgut-specific CPA promoter, which is activated after a blood meal. First, we examined the efficiency of TEP1 silencing in the transgenic mosquitoes. The total RNA of wild type and anti-TEP1 miR-expressed transgenic mosquitoes was collected 6, 12, 24, 48, and 72 hours after a normal blood meal. The expression levels of both TEP1 (**Figure 3B**) and GFP (**Figure 3C**) were determined by qRT-PCR. Compared with wild type mosquito, our results indicate that the TEP1 mRNA level was down-regulated 24 and 48 hours after the blood meal in the transgenic mosquitoes (**Figure 3B**). GFP expression was used as a marker for anti-TEP1 miR-expressed transgenic mosquitoes (**Figure 3C**). To investigate the role of TEP1 in DENV2 replication in the mosquito midgut, replication efficacy in transgenic mosquitoes was examined. Total protein from wild type or anti-TEP1 miR-expressed transgenic mosquitoes were collected 1, 2, 4, 6, 8, and 10 days after a normal or infectious blood meal (**Figure 3D**). Expression of the viral proteins were significantly increased in the transgenic mosquitoes after an infectious blood meal compared to the wild type mosquitoes (**Figure 3D**). Combined, our results suggest that TEP1 is crucial for boosting DENV2 replication in the midgut of mosquitoes.

TEP1 Silencing Enhances DENV Particle Production in Mosquitoes

We examined the effect of TEP1 on infectious virus particle production by comparing the efficiency of particle production between wild type and anti-TEP1 miR-expressed transgenic mosquitoes. Whole body samples of wild type or transgenic mosquitoes were collected 2, 4, 6, 8, 10, and 14 days after an infectious blood meal. They were examined with a plaque assay for infectious virus particle quantification. Our results show that, in response to TEP1 silencing, infectious virus particle production efficiency was higher in transgenic mosquitoes than in wild type mosquitoes after the infectious blood meal (**Figure 4A**). This supports the notion that TEP1 plays a key role in DENV replication. In addition, we examined the effect of TEP1 on infectious virus particle production in the mosquito midgut with a plaque assay (**Figure 4B**). Combined, our results indicate that TEP1 serves as a negative regulator for DENV2 replication in the midgut of mosquitoes.

TEP1 Silencing Enhances AMP Expression in Mosquitoes

A previous study reported that a TEP-related protein, *Ae. aegypti* macroglobulin complement-related factor (AaMCR), is an essential factor in resisting flaviviral infection in *Ae. aegypti* (18). Moreover, AaMCR interacts with DENV through a

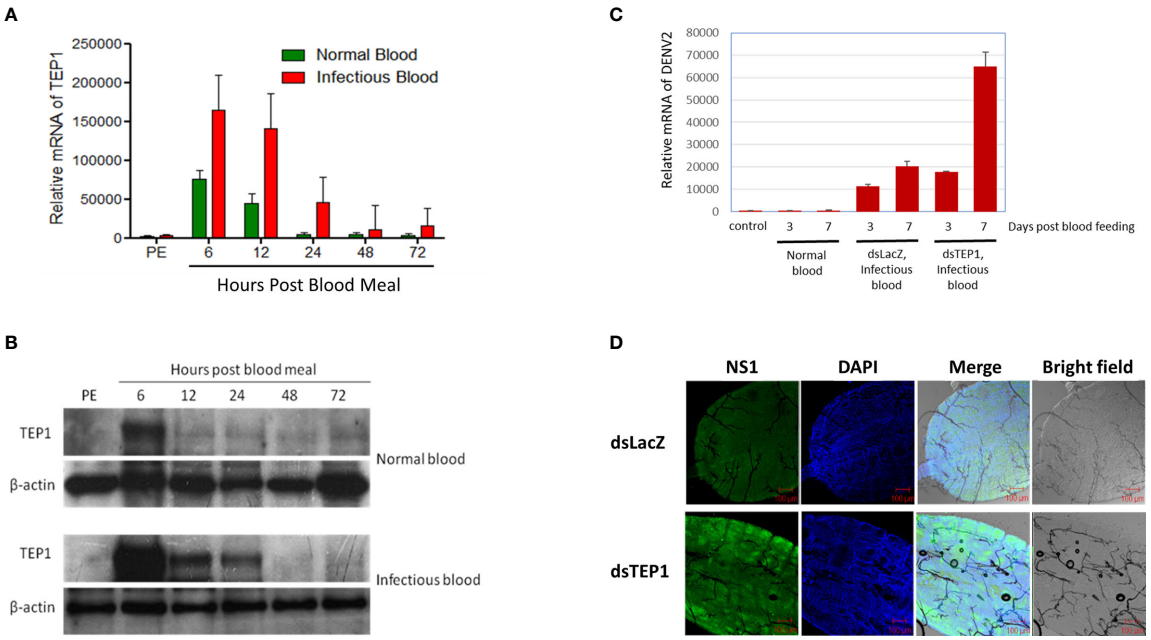

FIGURE 2 | TEP1 Silencing Resulted in an Increase in Viral Load. **(A)** The relative mRNA levels of thioester-containing protein 1 (TEP1) in the midgut of female mosquitoes were quantified by real-time PCR after a normal or dengue virus (DENV) infectious blood meal. Midguts were collected 6, 12, 24, 48, and 72 hours after a normal or infectious blood meal. Equal amounts of total RNA from each group were used for cDNA synthesis. Ribosomal protein S7 was used for normalization of relative target gene mRNA expression. Values are mean ± S.E. (error bars) of the copy number of TEP1. At least three biological cohorts from each time point were used for analysis. **(B)** Midguts were collected 6, 12, 24, 48, and 72 hours after a normal or infectious blood meal. Total protein was extracted and western blot analysis was performed using the polyclonal antibody against *Anopheles gambiae* TEP1. Anti-β-actin antibody was used as the loading control. **(C)** The midguts were collected three or seven days after a naïve blood meal or infectious blood meal. Midguts of 3-day-old, non-blood-fed female mosquitoes were used as controls. Midguts from female mosquitoes were collected and treated with TEP1 double-stranded RNA (dsRNA) three or seven days after an infectious blood meal. Total RNA was extracted and quantified, followed by cDNA synthesis and subjected to quantitative real-time PCR analysis with a specific primer for DENV2. Values are mean ± S.E. (error bars) of the copy number of DENV2. At least three biological cohorts from each time point were used for analysis. Ribosomal protein S7 was used for normalization of relative target gene mRNA expression. **(D)** Mosquitoes pre-treated with TEP1 dsRNA were collected for infectious DENV blood feeding. Mosquito midguts were dissected and collected seven days after feeding with infectious blood for immunofluorescent analysis. The anti-DENV NS1 protein antibody was used to detect the expression of DENV in the midgut of mosquitoes. Alexa Fluor 488 goat anti-mouse IgG was used as a secondary antibody. The images were analyzed by confocal microscopy with single planes presented. Mosquitoes pre-treated with LacZ dsRNA fed infectious blood were used as controls. PE means post-eclosion.

homologue of the scavenger receptor-C (AaSR-C), which interacts with DENV and AaMCR. The expression of AMPs is regulated by the AaSR-C/AaMCR complex for potent anti-DENV activity. Additionally, previous studies have also suggested that AMPs play crucial roles in mosquito immune defense against DENV (31–33). Therefore, we hypothesized that TEP1 controls DENV replication by regulating the expression of AMPs. To examine this hypothesis, total RNA was extracted from the midgut of either the wild type or anti-TEP1 miR-expressed transgenic mosquitoes 6, 12, 24, 48, and 72 hours after a normal blood meal. The transcriptional profiles of immune-responsive genes from normal blood-fed mosquitoes were examined with qRT-PCR analysis. Our results showed that Rel1 remained unchanged in TEP1 silenced mosquitoes (**Figure 5A**) whereas Rel2, and defensins were significantly suppressed in TEP1 silenced mosquitoes (**Figures 5B, C**). On the other hand, cecropins was also suppressed at PE stage in TEP1 silenced mosquitoes (**Figure 5D**). Our results point out the crucial role TEP1 plays in controlling immune response in *Ae. aegypti*.

DISCUSSION

Hosts have developed complex immune systems to defend themselves from invading pathogens before they cause significant physiological damage (6, 8). In mammals, both the innate and adaptive immune systems fight viral infections. In contrast, insects only rely on the innate immune and potentially cytokine-like responses for viral infection defense (6, 8, 15, 30). Without an antibody-based immune response, insects have developed a functional complement-like system to combat pathogens (14, 15). Previous studies on *Anopheles* mosquitoes have shown that TEPs bind to pathogens, such as the malaria parasite *Plasmodium berghei*, and activate phagocytosis to mitigate infection (10, 13, 16). TEP1, TEP3, and TEP4 promote phagocytosis to limit Gram-positive and Gram-negative bacterial infections, and both TEP1 and TEP3 are able to bind to the surface of malaria parasites and activate lysis and melanization (10, 13–16). In *Drosophila*, complement-like protein DmMCR has been shown to bind specifically to the surface of *Candida albicans* to opsonize and promote subsequent

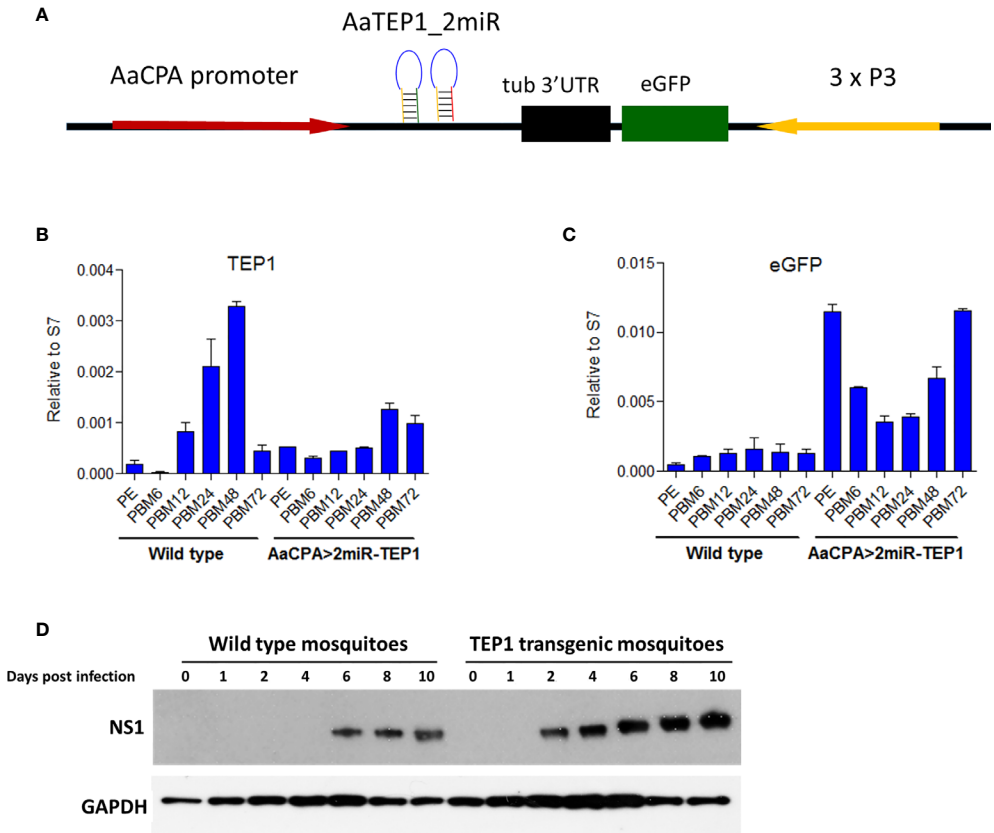

FIGURE 3 | Signal Pathways involved in Dengue Virus (DENV) Replication and Transmission in *Aedes aegypti*. **(A)** Development of a thioester-containing protein 1 (TEP1) loss-of-function transgenic mosquito line with a blood meal-inducible carboxypeptidase (CPA) promoter. Based on the mariner transposon system, the midgut-specific blood meal-inducible CPA promoter (AaCPA) was used for expressing the downstream synthetic miRNAs. AaCPA promoter, *Ae. aegypti* carboxypeptidase A promoter; AaTEP1_2miR, anti-TEP1 miRNA. **(B, C)** miRNA-mediated TEP1 silenced transgenic mosquitoes. The whole bodies of female wild type or transgenic mosquitoes (AaCPA>2miR-TEP1) were collected 6, 12, 24, 48, and 72 hours after a normal blood meal. Total RNA was extracted and quantified, followed by cDNA synthesis and subjected to quantitative real-time PCR analysis with a specific primer for TEP1 **(B)** or GFP **(C)**. Values are mean ± S.E. (error bars) of the ratio of each gene to ribosomal protein S7. At least three biological cohorts from each time point were used for analysis. Ribosomal protein S7 was used for normalization of the relative target gene mRNA expression. **(D)** Anti-DENV phenotype of transgenic mosquitoes. The whole bodies of female mosquitoes were collected 0, 1, 2, 3, 4, 6, 8, and 10 days after an infectious DENV blood meal. Total protein was extracted and western blot analysis was performed with the antibody against DENV NS1 protein. Anti-GAPDH antibody was used as the loading control. PE means post-eclosion.

phagocytosis (17). TEPs have been identified as key factors in the restriction of flaviviral infections (11, 18). Functional studies indicate that TEPs exert potent anti-DENV activity by regulating AMP activation (18). However, the detailed mechanisms underlying the TEPs-based complement-like system for regulating mosquito immunity against viral infections remain unclear.

More than 30 secreted and membrane-bound proteins have been identified in the human complement network (9, 14). Foreign antigens are recognized by pattern receptors, including C1q, ficolin, and mannose-binding C-type lectin (MBL), which subsequently activate a complement cascade (9). Recent reports have shown that mosquito extracellular C-type lectins, which are the putative homologues of the human MBL, rather than acting as antiviral pattern recognition receptors, act as cellular receptors facilitating West Nile virus and DENV infection (34, 35). We have demonstrated that *Ae. aegypti* TEP1 is highly expressed in the midgut of mosquitoes after an infectious blood meal at both the transcriptional and translational levels. In addition, viral titers were significantly higher in the absence of TEP1. Therefore, these results indicate that TEP1 is an important anti-DENV protein in mosquitoes. We have successfully developed a transgenic mosquito line with TEP1 loss-of-function phenotypes and a blood meal-inducible CPA promoter. The viral titer and RNA in transgenic mosquitoes were higher after an infectious blood meal, further confirming the anti-DENV role of TEP1.

We also demonstrated that TEP1 is an important factor in regulating the replication of DENV. This may be achieved by modulating the expression of AMPs in *Ae. aegypti*. AMPs in insects are effectors of innate immunity, and are regulated by a wide variety of signal transduction pathways in response to different microbial infections (6, 8, 19). To date, 17 AMPs have been discovered in the *Ae. aegypti* genome and they are categorized into five independent groups (defensins, cecropins,

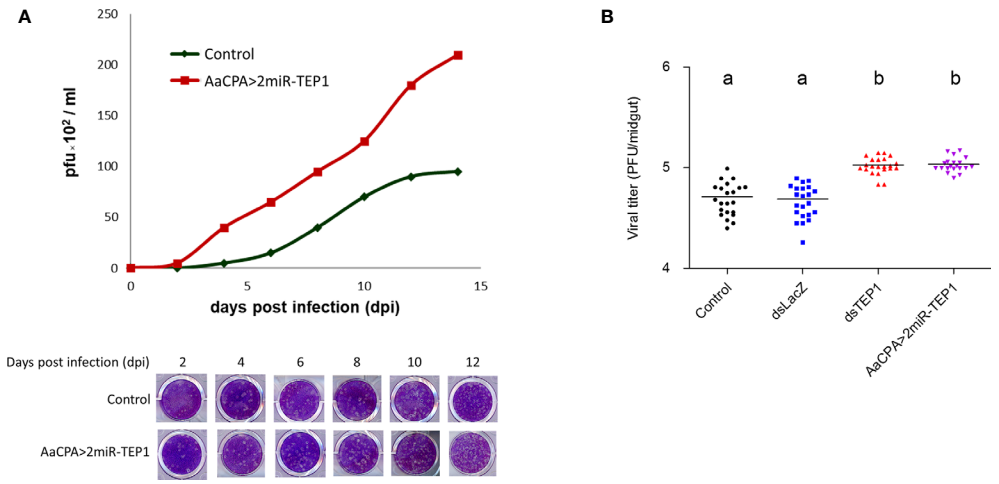

FIGURE 4 | Thioester-Containing Protein 1 (TEP1) Transgenic Mosquito Enhances Dengue Virus (DENV) Infection. **(A)** *Aedes aegypti* control and loss-of-function transgenic (AaCPA>2miR-TEP1) mosquitoes were fed an infectious DENV blood meal. The whole bodies of infected mosquitoes were collected 0, 2, 4, 6, 8, 10, and 12 days after the infectious blood meal and viral titers were determined and quantified with a plaque assay. **(B)** *Ae. aegypti* mosquitoes with silenced TEP1 or mosquitoes from the loss-of-function transgenic line were fed an infectious DENV blood meal. Midguts from infected mosquitoes were collected seven days after the infectious blood meal and the viral titers were determined by plaque assay. Letters indicate the statistical significance according to Tukey's multiple comparison test. There is no significant difference between them ($p > 0.05$). Control: *Aedes aegypti* UGAL/Rockefeller strain without any transgenic materials or dsRNA treatment.

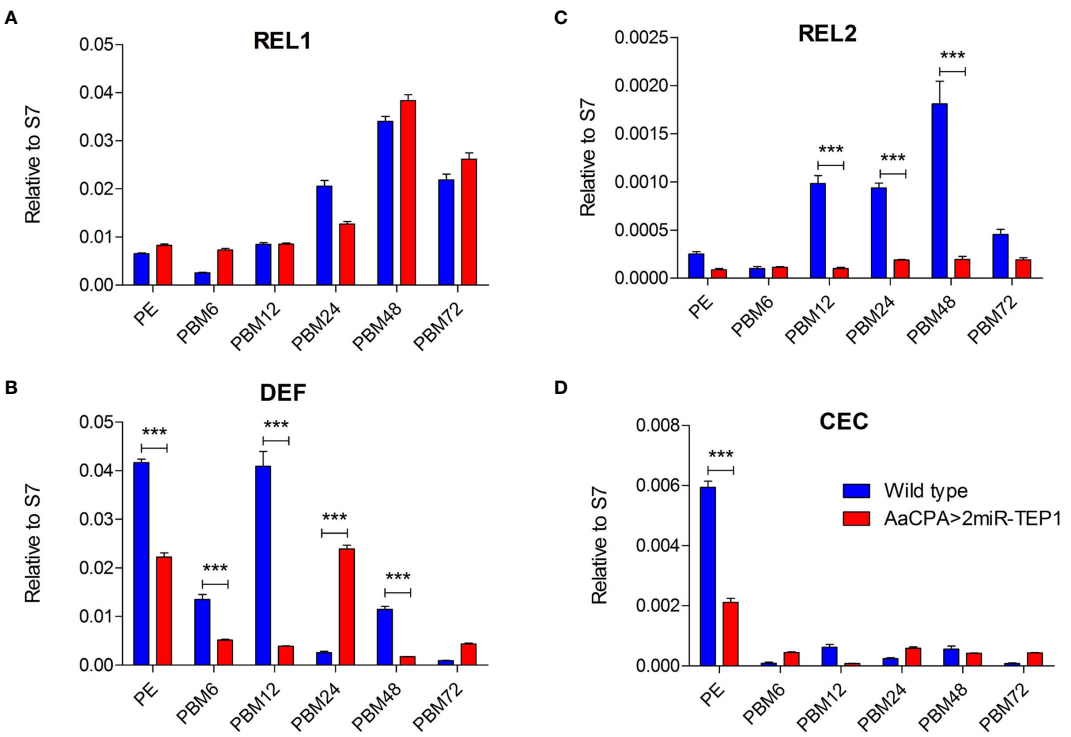

FIGURE 5 | Role of Defensins and Cecropins in Thioester-Containing Protein 1 (TEP1) Transgenic Mosquitoes after Blood Meals. **(A–D)** The whole bodies of female wild type or transgenic mosquitoes (AaCPA>2miR-TEP1) were collected 6, 12, 24, 48, and 72 hours after a normal blood meal. Total RNA was extracted and quantified, followed by cDNA synthesis and subjected to quantitative real-time PCR analysis with a specific primer for Rel1 **(A)**, Rel2 **(B)**, defensins **(C)**, and cecropins **(D)**. At least three biological cohorts from each time point were used for analysis. Ribosomal protein S7 was used for normalization of relative target gene mRNA expression. PE means post-eclosion.

attacin, diptericin, and gambicin) (19). The immune pathway mechanisms for AMP regulation have been mainly studied in *Drosophila* (6, 8, 19). In mosquitoes, Toll, Imd, and JAK-STAT pathways are activated upon pathogen infection (6, 8, 19, 20). Pathogenic cell surface proteins are recognized by immune receptors and trigger downstream transcription factors such as Rel1 (Toll pathway), Rel2 (Imd pathway), and STAT (JAK-STAT pathway). Previous studies have evaluated how the expression of AMPs are induced by DENV infection in mosquitoes, and they exhibit antiviral activities (6, 8, 18, 20). We further demonstrated that transgenic mosquitoes with TEP1 loss-of-function inhibited the expression of two AMPs and the transcription factor Rel2 of the Imd pathway. Our results indicated that, compared with wild type mosquitoes, the levels of AMPs expression are suppressed in TEP1-silenced mosquitoes after the mosquitoes take a blood meal. Similar results also descript in previous study. The study shows that mosquito blood meal results in robust activation of the GABAergic system through glutamate-derived GABA production from blood digestion. The enhancement of GABA signaling suppresses antiviral responses, such as AMP induction by the Imd signaling pathway (36). These results suggest that TEP1 play an important role in AMPs production. Our results coincide with previous findings reporting that TEP1 plays an important role in regulating the immune response of mosquitoes.

In conclusion, we demonstrated that TEP1 limits DENV infections in *Ae. aegypti*. Silencing TEP1 using a reverse genetic approach resulted in an up-regulation of viral RNA and proteins in mosquitoes. The production of infectious virus particles increased in the absence of TEP1. Next, we generated a midgut-specific TEP1-miR expression mosquito with a TEP1 loss-of-function phenotype through the CPA promoter. We showed that viral RNA and titer increased in this transgenic mosquito line after an infectious blood meal. Interestingly, transgenic mosquitoes with a TEP1 loss-of-function phenotype inhibited the transcription factor Rel2. Our current results suggest that TEP1 regulates the mosquito immune response and consequently controls DENV replication. These findings provide new insight into the molecular mechanisms of mosquito host factors in regulating DENV replication.

DATA AVAILABILITY STATEMENT

The datasets presented in this study can be found in online repositories. The names of the repository/repositories and accession number(s) can be found in the article/**Supplementary Material**.

ETHICS STATEMENT

All animal procedures and experimental protocols were approved by the AAALAC-accredited facility, the Committee on the Ethics of Animal Experiments of the National Taiwan University College of Medicine (IACUC approval No: 20200210).

AUTHOR CONTRIBUTIONS

S-CW, H-HL, C-HC, and S-HS contributed to conception and design of the study. S-CW, H-HL, J-CL, and W-LL performed the experiments and statistical analysis. S-CW and S-HS wrote the first draft of the manuscript. H-HL, and C-HC wrote sections of the manuscript. All authors contributed to the article and approved the submitted version.

FUNDING

This work was supported by the Ministry of Science and Technology (Taiwan) MOST 109-2320-B-002-062-MY3 and MOST 109-2327-B-400-004 to S-HS. This work was also supported by the National Health Research Institutes (Taiwan) 08A1-MRGP12-035 and 09A1-MRGP12-035 to C-HC.

SUPPLEMENTARY MATERIAL

The Supplementary Material for this article can be found online at: https://www.frontiersin.org/articles/10.3389/fimmu.2021.670122/full#supplementary-material

REFERENCES

1. Osman S, Preet R. Dengue, Chikungunya and Zika in GeoSentinel Surveillance of International Travellers: A Literature Review From 1995 to 2020. *J Travel Med* (2020). doi: 10.1093/jtm/taaa222
2. Wilder-Smith A, Ooi EE, Horstick O, Wills B. Dengue. *Lancet* (2019) 393 (10169):350–63. doi: 10.1016/S0140-6736(18)32560-1
3. Leta S, Beyene TJ, De Clercq EM, Amenu K, Kraemer MUG, Revie CW. Global Risk Mapping for Major Diseases Transmitted by Aedes Aegypti and Aedes Albopictus. *Int J Infect Dis* (2018) 67:25–35. doi: 10.1016/j.ijid.2017.11.026
4. Huang CC, Hsu CC, Guo HR, Su SB, Lin HJ. Dengue Fever Mortality Score: A Novel Decision Rule to Predict Death From Dengue Fever. *J Infect* (2017) 75 (6):532–40. doi: 10.1016/j.jinf.2017.09.014
5. Guo C, Zhou Z, Wen Z, Liu Y, Zeng C, Xiao D, et al. Global Epidemiology of Dengue Outbreaks in 1990-2015: A Systematic Review and Meta-Analysis. *Front Cell Infect Microbiol* (2017) 7:317. doi: 10.3389/fcimb.2017.00317
6. Mukherjee D, Das S, Begum F, Mal S, Ray U. The Mosquito Immune System and the Life of Dengue Virus: What We Know and Do Not Know. *Pathogens* (2019) 8(2). doi: 10.3390/pathogens8020077
7. Salazar MI, Richardson JH, Sanchez-Vargas I, Olson KE, Beaty BJ. Dengue Virus Type 2: Replication and Tropisms in Orally Infected Aedes Aegypti Mosquitoes. *BMC Microbiol* (2007) 7:9. doi: 10.1186/1471-2180-7-9
8. Cheng G, Liu Y, Wang P, Xiao X. Mosquito Defense Strategies Against Viral Infection. *Trends Parasitol* (2016) 32(3):177–86. doi: 10.1016/j.pt.2015.09.009
9. Shishido SN, Varahan S, Yuan K, Li X, Fleming SD. Humoral Innate Immune Response and Disease. *Clin Immunol* (2012) 144(2):142–58. doi: 10.1016/j.clim.2012.06.002
10. Levashina EA, Moita LF, Blandin S, Vriend G, Lagueux M, Kafatos FC. Conserved Role of a Complement-Like Protein in Phagocytosis Revealed by dsRNA Knockout in Cultured Cells of the Mosquito, Anopheles Gambiae. *Cell* (2001) 104(5):709–18. doi: 10.1016/s0092-8674(01)00267-7
11. Cheng G, Liu L, Wang P, Zhang Y, Zhao YO, Colpitts TM, et al. An *In Vivo* Transfection Approach Elucidates a Role for Aedes Aegypti Thioester-

Containing Proteins in Flaviviral Infection. *PloS One* (2011) 6(7):e22786. doi: 10.1371/journal.pone.0022786
12. Buresova V, Hajdusek O, Franta Z, Loosova G, Grunclova L, Levashina EA, et al. Functional Genomics of Tick Thioester-Containing Proteins Reveal the Ancient Origin of the Complement System. *J Innate Immun* (2011) 3(6):623–30. doi: 10.1159/000328851
13. Blandin S, Shiao SH, Moita LF, Janse CJ, Waters AP, Kafatos FC, et al. Complement-Like Protein TEP1 is a Determinant of Vectorial Capacity in the Malaria Vector Anopheles Gambiae. *Cell* (2004) 116(5):661–70. doi: 10.1016/s0092-8674(04)00173-4
14. Shokal U, Eleftherianos I. Evolution and Function of Thioester-Containing Proteins and the Complement System in the Innate Immune Response. *Front Immunol* (2017) 8:759. doi: 10.3389/fimmu.2017.00759
15. Blandin S, Levashina EA. Thioester-Containing Proteins and Insect Immunity. *Mol Immunol* (2004) 40(12):903–8. doi: 10.1016/j.molimm.2003.10.010
16. Moita LF, Wang-Sattler R, Michel K, Zimmermann T, Blandin S, Levashina EA, et al. In Vivo Identification of Novel Regulators and Conserved Pathways of Phagocytosis in a. *Gambiae Immun* (2005) 23(1):65–73. doi: 10.1016/j.immuni.2005.05.006
17. Stroschein-Stevenson SL, Foley E, O'Farrell PH, Johnson AD. Identification of Drosophila Gene Products Required for Phagocytosis of Candida Albicans. *PloS Biol* (2006) 4(1):e4. doi: 10.1371/journal.pbio.0040004
18. Xiao X, Liu Y, Zhang X, Wang J, Li Z, Pang X, et al. Complement-Related Proteins Control the Flavivirus Infection of Aedes Aegypti by Inducing Antimicrobial Peptides. *PloS Pathog* (2014) 10(4):e1004027. doi: 10.1371/journal.ppat.1004027
19. Zhang R, Zhu Y, Pang X, Xiao X, Zhang R, Cheng G. Regulation of Antimicrobial Peptides in Aedes Aegypti Aag2 Cells. *Front Cell Infect Microbiol* (2017) 7:22. doi: 10.3389/fcimb.2017.00022
20. Chowdhury A, Modahl CM, Tan ST, Wong Wei Xiang B, Misse D, Vial T, et al. JNK Pathway Restricts DENV2, ZIKV and CHIKV Infection by Activating Complement and Apoptosis in Mosquito Salivary Glands. *PloS Pathog* (2020) 16(8):e1008754. doi: 10.1371/journal.ppat.1008754
21. Ramirez JL, Dimopoulos G. The Toll Immune Signaling Pathway Control Conserved Anti-Dengue Defenses Across Diverse Ae. Aegypti Strains and Against Multiple Dengue Virus Serotypes. *Dev Comp Immunol* (2010) 34(6):625–9. doi: 10.1016/j.dci.2010.01.006
22. Weng SC, Shiao SH. Frizzled 2 is a key component in the regulation of TOR signaling-mediated egg production in the mosquito Aedes aegypti. *Insect Biochem Mol Biol* (2015) 61:17–24. doi: 10.1016/j.ibmb.2015.03.010
23. Chang CH, Liu YT, Weng SC, Chen IY, Tsao PN, Shiao SH. The non-canonical Notch signaling is essential for the control of fertility in Aedes aegypti. *PLoS Negl Trop Dis* (2018) 12(3):e0006307. doi: 10.1371/journal.pntd.0006307
24. Sri-In C, Weng SC, Chen WY, Wu-Hsieh BA, Tu WC, Shiao SH. A Salivary Protein of Aedes Aegypti Promotes Dengue-2 Virus Replication and Transmission. *Insect Biochem Mol Biol* (2019) 111:103181. doi: 10.1016/j.ibmb.2019.103181
25. Li HH, Cai Y, Li JC, Su MP, Liu WL, Cheng L, et al. C-Type Lectins Link Immunological and Reproductive Processes in Aedes Aegypti. *iScience* (2020) 23(9):101486. doi: 10.1016/j.isci.2020.101486
26. Yen PS, James A, Li JC, Chen CH, Failloux AB. Synthetic miRNAs Induce Dual Arboviral-Resistance Phenotypes in the Vector Mosquito Aedes Aegypti. *Commun Biol* (2018) 1:11. doi: 10.1038/s42003-017-0011-5
27. Chen CH, Huang H, Ward CM, Su JT, Schaeffer LV, Guo M, et al. A synthetic maternal-effect selfish genetic element drives population replacement in Drosophila. *Science* (2007) 316(5824):597–600. doi: 10.1126/science.1138595
28. Franz AW, Sanchez-Vargas I, Adelman ZN, Blair CD, Beaty BJ, James AA, et al. Engineering RNA Interference-Based Resistance to Dengue Virus Type 2 in Genetically Modified Aedes Aegypti. *Proc Natl Acad Sci USA* (2006) 103(11):4198–203. doi: 10.1073/pnas.0600479103
29. Xi Z, Ramirez JL, Dimopoulos G. The Aedes Aegypti Toll Pathway Controls Dengue Virus Infection. *PloS Pathog* (2008) 4(7):e1000098. doi: 10.1371/journal.ppat.1000098
30. Waterhouse RM, Kriventseva EV, Meister S, Xi Z, Alvarez KS, Bartholomay LC, et al. Evolutionary Dynamics of Immune-Related Genes and Pathways in Disease-Vector Mosquitoes. *Science* (2007) 316(5832):1738–43. doi: 10.1126/science.1139862
31. Chowdhury A, Modahl CM, Tan ST, Wong Wei Xiang B, Misse D, Vial T, et al. JNK pathway restricts DENV2, ZIKV and CHIKV infection by activating complement and apoptosis in mosquito salivary glands. *PLoS Pathog* (2020) 16(8):e1008754. doi: 10.1371/journal.ppat.1008754
32. Wang JM, Cheng Y, Shi ZK, Li XF, Xing LS, Jiang H, et al. Aedes aegypti HPX8C modulates immune responses against viral infection. *PLoS Negl Trop Dis* (2019) 13(4):e0007287. doi: 10.1371/journal.pntd.0007287
33. Liu WQ, Chen SQ, Bai HQ, Wei QM, Zhang SN, Chen C, et al. The Ras/ERK signaling pathway couples antimicrobial peptides to mediate resistance to dengue virus in Aedes mosquitoes. *PLoS Negl Trop Dis* (2020) 14(8):e0008660. doi: 10.1371/journal.pntd.0008660
34. Cheng G, Cox J, Wang PH, Krishnan MN, Dai JF, Qian F, et al. A C-Type Lectin Collaborates With a CD45 Phosphatase Homolog to Facilitate West Nile Virus Infection of Mosquitoes. *Cell* (2010) 142(5):714–25. doi: 10.1016/j.cell.2010.07.038
35. Liu Y, Zhang FC, Liu JY, Xiao XP, Zhang SY, Qin CF, et al. Transmission-Blocking Antibodies Against Mosquito C-Type Lectins for Dengue Prevention. *PloS Pathog* (2014) 10(2). doi: 10.1371/journal.ppat.1003931
36. Zhu Y, Zhang R, Zhang B, Zhao T, Wang P, Liang G, et al. Blood Meal Acquisition Enhances Arbovirus Replication in Mosquitoes Through Activation of the GABAergic System. *Nat Commun* (2017) 8(1):1262. doi: 10.1038/s41467-017-01244-6

Conflict of Interest: The authors declare that the research was conducted in the absence of any commercial or financial relationships that could be construed as a potential conflict of interest.

frontiers in Physiology

ORIGINAL RESEARCH
published: 04 August 2021
doi: 10.3389/fphys.2021.663482

Two Putative Cypovirus-Encoded miRNAs Co-regulate the Host Gene of GTP-Binding Nuclear Protein Ran and Facilitate Virus Replication

*Su Lin[1,2], Yongsheng Wang[1,2], Ze Zhao[1,2], Wanming Wu[1,2], Yun Su[1,2], Zhendong Zhang[1,2], Manman Shen[1,2], Ping Wu[1,2], Heying Qian[1,2] and Xijie Guo[1,2]**

[1] School of Biotechnology, Jiangsu University of Science and Technology, Zhenjiang, China, [2] Sericultural Research Institute, Chinese Academy of Agricultural Sciences, Zhenjiang, China

microRNA (miRNA) plays important roles in regulating various biological processes, including host-pathogen interaction. Recent studies have demonstrated that virus-encoded miRNAs can manipulate host gene expression to ensure viral effective multiplication. *Bombyx mori* cypovirus (BmCPV), a double-stranded RNA virus with a segmented genome, is one of the important pathogens for the economically important insect silkworm. Our present study indicated that two putative miRNAs encoded by BmCPV could promote viral replication by inhibiting the gene expression of *B. mori* GTP-binding nuclear protein Ran (*BmRan*), an essential component of the exportin-5-mediated nucleocytoplasmic transport of small RNAs. BmCPV-miR-1 and BmCPV-miR-3 are two of the BmCPV-encoded miRNAs identified in our previous studies. *BmRan* is a common target gene of them with binding sites all located in the 3′-untranslated region (3′-UTR) of its mRNA. The expression levels of the two miRNAs in the midgut of larvae infected with BmCPV gradually increased with the advance of infection, while the expression of the target gene *BmRan* decreased gradually. The miRNAs and the recombinant target gene consisting of reporter gene *mCherry* and 3′-UTR of *BmRan* mRNA were expressed in HEK293T cells for validating the interaction between the miRNAs and the target gene. qRT-PCR results revealed that BmCPV-miR-1 and BmCPV-miR-3 negatively regulate target gene expression not only separately but also cooperatively by binding to the 3′-UTR of *BmRan* mRNA. By transfecting miRNA mimics into BmN cells and injecting the mimics into the body of silkworm larvae, it was indicated that both BmCPV-miR-1 and BmCPV-miR-3 could repress the expression of *BmRan* in BmN cells and in the silkworm, and the cooperative action of the two miRNAs could enhance the repression of *BmRan* expression. Furthermore, the repression of *BmRan* could facilitate the replication of BmCPV genomic RNAs. It is speculated that BmCPV-miR-1 and BmCPV-miR-3 might reduce the generation of host miRNAs by inhibiting expression of *BmRan*, thus creating a favorable intracellular environment for virus replication. Our results are helpful to better understand the pathogenic mechanism of BmCPV to the silkworm, and provide insights into one of the evasion strategies used by viruses to counter the host defense for their effective multiplication.

Keywords: silkworm, cypovirus, microRNA, target gene, *BmRan*, virus replication

OPEN ACCESS

Edited by:
Liang Jiang,
Southwest University, China

Reviewed by:
Nguyen T. K. Vo,
University of Waterloo, Canada
Anna Kolliopoulou,
University of West Attica, Greece

***Correspondence:**
Xijie Guo
guoxijie@just.edu.cn

Specialty section:
This article was submitted to Invertebrate Physiology, a section of the journal Frontiers in Physiology

Received: *03 February 2021*
Accepted: *13 July 2021*
Published: *04 August 2021*

Citation:
Lin S, Wang Y, Zhao Z, Wu W, Su Y, Zhang Z, Shen M, Wu P, Qian H and Guo X (2021) Two Putative Cypovirus-Encoded miRNAs Co-regulate the Host Gene of GTP-Binding Nuclear Protein Ran and Facilitate Virus Replication. Front. Physiol. 12:663482. doi: 10.3389/fphys.2021.663482

INTRODUCTION

Bombyx mori cypovirus (BmCPV) is one of the important pathogens of the silkworm (Cao et al., 2012). It is a typical RNA virus belonging to the *Cypovirus* genus of *Reoviridae*. Its genome consists of 10 segmented double-stranded RNAs with a total length of more than 24 kbp, each encoding a structural or non-structural protein (Hagiwara et al., 2002; Hu et al., 2019). The virus infects only midgut epithelial cells in the silkworm and produces polyhedra in the cytoplasm. The intact virus particles are generally embedded in the polyhedra and must be released in the larval midgut to infect the silkworm. The infection of the virus to the silkworm always causes serious cytoplasmic polyhedrosis disease resulting in big losses to the commercial sericultural production. The mechanism of interaction between the virus and silkworm needs to be further explored for the development of effective strategies to control the occurrence and prevalence of the disease. In the silkworm, major antiviral defense mechanisms such as RNA interference (RNAi), NF-kB-mediated, Imd (immune deficiency), stimulator of interferon gene (STING), and Janus kinase/signal transducer and activator of transcription (JAK/STAT) pathways have been shown to play important roles in antiviral immunity (Jiang, 2021). In contrast, viruses can modulate prophenol oxidase (PPO), phosphatidylinositol 3-kinase (PI3K)/protein kinase B (Akt), and extracellular signal-regulated kinase (ERK) signaling pathways of the host to elevate their proliferation in the silkworm (Jiang, 2021). Transcriptome studies of silkworm have revealed a complex response against BmCPV infection. While, studies of deep sequencing of viral small RNAs have indicated the importance of the RNAi pathway in the control of cypovirus infection although many functional aspects still need to be elucidated and conclusive evidence is lacking (Swevers et al., 2020).

microRNA (miRNA) is a type of 19–25 nt single-stranded non-coding small RNAs, which is widely found in animals, plants, and nematodes, and regulates the expression of target genes at the post-transcriptional level (Filipowicz et al., 2008). A miRNA can target and regulate multiple target genes, and a target gene may also be regulated by multiple miRNAs. At the same time, studies have shown that the increase in the number of miRNA binding sites in mRNA 3′-untranslated region (3′-UTR) can enhance the translational repression of a target gene (Heiss et al., 2012). Similar studies also showed that co-operativity between two or more miRNA-binding sites enhanced repression of mRNA translation via an unknown mechanism when sites were separated by 13–35 nucleotides (Saetrom et al., 2007). Many viruses also encode miRNAs and 569 miRNAs of virus origin have been registered in the miRBase database version 22.1 (2018)[1]. Virus-encoded miRNAs play an important role in the intricate interaction between virus and hosts, including regulation of host immune response, evasion from recognition by the host immune system (Liang et al., 2014), inhibition of apoptosis (Zhao et al., 2011), regulation of cell cycle (Gottwein et al., 2007), mimicking host miRNAs (Grimson et al., 2007; Zhao et al., 2009), and so on. At present, most viral miRNAs reported are encoded by DNA viruses, but some RNA viruses can also encode functional miRNAs (Swaminathan et al., 2013; Qiu et al., 2018). Our previous deep sequencing of small RNA in the midgut of silkworm larvae infected by BmCPV virus identified some virus-derived non-coding RNA sequences similar to miRNA. Further study proved that a BmCPV-encoded miRNA can regulate the expression of host genes and affect the replication and proliferation of the virus (Guo et al., 2020).

The present work studies the functions of two putative BmCPV-encoded miRNAs, namely BmCPV-miR-1 and BmCPV-miR-3. Target gene prediction against the silkworm genome identified that the *B. mori* GTP-binding nuclear protein ran gene (*BmRan*) is the common target gene of the two miRNAs. Their regulation on the target gene and its influence on BmCPV virus replication were analyzed. Studying the BmCPV-encoded functional miRNAs and revealing their functions in the process of pathogen-host interaction would enrich the miRNA family encoded by viruses and help to reveal the miRNA-mediated new mechanism of regulation on RNA virus replication and proliferation.

MATERIALS AND METHODS

Silkworm Strain, Cell Lines, and Virus

The domesticated silkworm of strain 4008 used in this study was supplied by Silkworm Germplasm Conservation Center, Chinese Academy of Agricultural Sciences. BmCPV, BmN cell, and HEK293T cell (human embryonic kidney cells) lines were maintained in our laboratory. miRNA mimics, inhibitors, and negative controls (NCs) were synthesized and chemically modified by Shanghai GenePharma Co., Ltd. The pmCherry-N1 plasmid, lentiviral expression vector pLNHX, pLKO.3G, and packaging plasmids pVSV-G, pSPAX2, and pMD2.G were purchased from Wuhan MiaoLingBio Inc. and kept in our laboratory.

Virus Inoculation and Tissue Collection

Bombyx mori cypovirus polyhedra suspension at a concentration of 1.0×10^8 mL^{-1} was coated on fresh mulberry leaves cut into 5×3 cm. The leaves coated with the virus suspension were fed to the 5th instar silkworm larvae and the average amount of virus ingested by each larva was calculated to be about 1.0×10^6 polyhedra. Another group of larvae fed with mulberry leaves coated with sterile water were used as blank control. When the mulberry leaves coated with virus or water were all eaten up (about 6 h), the larvae were given fresh mulberry leaves and reared under the standard condition of 14 h light and 10 h darkness and relative humidity of about 90%.

The larvae were dissected at 12, 24, 48, 72, and 96 h, respectively after inoculation to collect midguts. The collected midgut was rinsed in DEPC water to remove the attached mulberry leaf pieces and put into a cryotube after the extra water was absorbed with tissue paper. The midguts of every five larvae were mixed as one sample and three samples were taken at each time point. Then the samples were stored at −80°C after quick freezing in liquid nitrogen.

[1] http://www.mirbase.org/

RNA Extraction

In this study, the expression level of both the virus-derived miRNAs and the host target gene, and the replication level of viral genome in the midgut of the silkworm larvae needed to be quantitatively detected, respectively. Therefore, total RNA was extracted with a classic manual method of the following steps. The frozen silkworm larval midguts were ground into fine powder with liquid nitrogen, put into an RNase free centrifuge tube. A total of 1 mL of lysate RL was added into the tube, and the mixture was shaken and mixed, then incubated at room temperature for 5 min. It was centrifuged at 4°C, 12000 rpm for 15 min. Then the supernatant was mixed with 200 μL of chloroform in a new tube, shaken sufficiently, and kept at room temperature for 10 min, followed by centrifugation at 4°C, 12000 rpm for 15 min. The upper aqueous phase was mixed with an equal volume of pre-cooled isopropanol in a new RNase free centrifuge tube, kept at 4°C for 10 min, then centrifuged at 4°C, 12000 rpm for 10 min. The supernatant was discarded, the pellet was washed with 1 mL of 75% ethanol and centrifuged at 4°C, 7500 rpm for 5 min. Then, the supernatant was discarded and the pellet was kept at room temperature for 5–10 min to allow the RNA pellet to dry. The RNA precipitate was dissolved with 30–50 μL of RNase-free water, and stored at −80°C after the concentration was measured.

cDNA Synthesis

cDNA was synthesized with a TaKaRa Primer Script^{TM} RT reagent kit for reverse transcription (Takara Biomedical Technology Co., Ltd., China) according to the manufacturer's instructions. For the first step, 2 μL of 5 × gDNA Eraser Buffer, 1 μL of gDNA Eraser, and 1 μg of RNA were mixed in the reaction tube to a total volume of 10 μL by adding ddH_2O, then kept at 42°C for reaction for 2 min. Then, 10 μL of the reaction solution, 4 μL of 5 × Prime Script Buffer 2, 1 μL of Prime Script RT Enzyme Mix I, 1 μL of RT Primer, and 4 μL of ddH_2O were mixed, and the reaction was performed with the program 37°C, 15 min, 85°C, 5 s, and 4°C + ∞. After the reaction, the synthesized cDNA was stored at −20°C. The cDNA for miRNA detection was synthesized with stem-loop RT primers. The stem-loop primers were designed with reference to literature (Chen et al., 2005) and the sequences are shown in **Table 1**.

qRT-PCR

Primer Premier 5.0 software was used to design quantitative primers (**Table 1**) for target gene *BmRan*, reporter gene *mCherry*, and internal reference gene β-*actin* (**Table 1**), and the stem-loop primers for miRNA quantitative detection were designed with reference to literature (Chen et al., 2005). The reaction system was prepared according to the instructions of the SYBR premix Ex Taq^{TM} kit (Takara Biomedical Technology Co., Ltd., China) (2 × SYBR Premix Ex Taq^{TM}: 10 μL, ROX Reference Dye: 0.4 μL, upstream primer: 0.8 μL, downstream primer: 0.8 μL, cDNA: 1 μL, ddH_2O: 7 μL, total volume: 20 μL). Three technical replicates were set for each quantitative reaction and the reaction was run on an ABI Prism fluorescence quantitative PCR instrument (Applied Biosystems, Foster City, CA, United States).

TABLE 1 | Primer sequences for qRT-PCR.

Primer name	Sequence (5′–3′)
Stem-loop reverse-transcribed PCR for BmCPV-miR-1	
	RT: GTCGTATCCAGTGCAGGGTCCGAGGT ATTCGCACTGGATACGACTAGTGT
	F: ACACTCCAGCTGGGGAAATGGACACAGGC
Stem-loop reverse-transcribed PCR for BmCPV-miR-3	
	RT: GTCGTATCCAGTGCAGGGTCCGAGGTATTCGCA CTGGATACGACATCAAGCC
	F: ACACTCCAGCTGGGTAGGAGAATTAGCGCGG
Universal	**R:** CCAGTGCAGGGTCCGAGGTA
mCherry	**F:** CTCAGTTCATGTACGGCTCCAAGG
	R: GGAGTCCTGGGTCACGGTCAC
Human β-actin	**F:** CTCCATCCTGGCCTCGCTGT
	R: GCTGTCACCTTCACCGTTCC
BmRan	**F:** GCCGTAACGACTTTGCTTTGGAAC
	R: TTGCCAGTACCACCATCTCCTACC
Genomic RNA S2	**F:** GTTGAGCGTCAGCAGTCAGATCG
	R: TGTTTACCCTGAGCAGCGTTATCG
Genomic RNA S5	**F:** CGCTTACAGGCAGTGGAATAGGAC
	R: GCTCTAACACATCGCTGGGCTAAG
Genomic RNA S10	**F:** ACCGTCAGTGATTGCTCGTGTAAC
	R: AGCGTCACCCTATCCGAAGACC
Bmβ-actin	**F:** CCGTATGAGAAAGGAAATCA
	R: TTGGAAGGTAGAGAGGGAGG

The reaction program was 95°C for 45 s followed by 45 cycles of 95°C for 5 s, and 60°C for 31 s. *Bm*β-*actin* and *BmTIF-4A* were used as internal reference genes for detection of target gene expression. The differences in gene expression levels were calculated using the relative quantitative $2^{-\Delta\Delta CT}$ method (Chang et al., 2009).

Target Gene Prediction

The target genes of BmCPV-miR-1 and BmCPV-miR-3 was predicted against the silkworm genome by the miRanda and Targetscan[2] software. The genes that could be predicted by both the two software programs and that mainly participated in immune response, escape of immune recognition, regulation of cell apoptosis, regulation of cell cycle, etc. were selected as the candidate target genes. The minimum free energy of hybridization between miRNA and target gene mRNA was calculated via software RNAhybrid[3].

Construction of Lentiviral Expression Vectors and Transfection of HEK293T Cells

To verify the miRNA regulation on target gene expression by binding to its target site in 3′-UTR of mRNA, the lentiviral expression vectors for expression of the target gene and the miRNAs were constructed respectively and transfected into HEK293T cells. The reporter gene *mCherry* sequence

[2]http://www.targetscan.org/vert_71/

[3]https://bibiserv.cebitec.uni-bielefeld.de/rnahybrid

(731 bp) was obtained from the plasmid pmCherry-N1. The 570 bp sequence encoding 3′-UTR of the target gene (*BmRan*) mRNA was amplified from the midgut cDNA of the experimental silkworm strain 4008. They were ligated into lentiviral vector pLNHX sequentially to construct the expression vectors pLNHX-mCherry-RanUTR, carrying a recombinant target gene consisting of the reporter gene *mCherry* and the 3′-UTR of *BmRan* mRNA. The *mCherry* gene serves not only as the reporter for successful transfection but also as the substituent target gene for miRNA regulation. At the same time, the miRNA binding sites on the target gene mRNA 3′-UTR were mutated by Mut Express II Fast Mutagenesis Kit V2 (Vazyme Biotech Co., Ltd., China) to construct the expression vector pLNHX-mCherry-RanUTR-mut, in which the miRNA binding sites were destroyed. On the other hand, the miRNA precursor sequence was cloned from the BmCPV genome and inserted into the lentiviral vector pLKO.3G (carrying EGFP reporter gene) to construct the expression vectors pLKO.3G-miR-1 and pLKO.3G-miR-3. The lentiviral vector inserts and primer sequences are shown in **Table 2**.

HEK293T cells were inoculated into a 60 mm cell culture dish in which the cell density should be over 60%, and the transfection was conducted 20 h later. In a 1.5 mL EP tube, 5.3 μg of expression plasmid pLNHX-mCherry-RanUTR or pLNHX-mCherry-RanUTR-mut and 2.7 μg of packaging plasmid pVSV-G were mixed to 125 μL with serum-free DMEM medium (Shanghai Thermo Scientific, China). In another EP tube, 20 μL of transfection reagent (Entranster^{TM}-H4000, Beijing Engreen, China) was mixed with 105 μL of serum-free medium and kept at room temperature for 5 min. Then the transfection reagent mixture was mixed thoroughly into the expression plasmid mixture and left to stand for 15 min. For transfection, the medium in the petri dish was removed and the above mixed solution was added to the cells then fresh medium was added up to 5 mL. At 6 h after the transfection, the culture medium was replaced by the fresh medium containing fetal bovine serum (FBS) (Shanghai Thermo Scientific) and the cells were cultured for 24–48 h before the next transfection. When the cells showing red fluorescence accounted for about 80%, they were inoculated into a six-well plate in which the cell density should be over 60%. In a 1.5 mL EP tube, 2 μg of pLKO.3G-miR-1 or pLKO.3G-miR-3, 1.5 μg of packaging plasmid pMD2.G, and 0.5 μg of packaging plasmid pSPAX2 were mixed with serum-free medium to 50 μL. At the same time, 10 μL of transfection reagent (Entranster^{TM}-H4000, Beijing Engreen) and 40 μL of serum-free culture medium were mixed in another EP tube and kept at room temperature for 5 min. Then the solution in the two tubes was mixed thoroughly and left to stand for 15 min. The medium in the cell culture was removed, the mixture was added to the cells, and then serum-containing medium was added up to 2 mL. The cells were collected 24 h and 48 h after transfection for RNA extraction and for detection of changes in the expression of reporter gene *mCherry* by qRT-PCR with human β-*actin* as the internal reference.

TABLE 2 | Sequences for construction of lentivirus expression vectors.

Name	Sequence (5′–3′)
Sequences for construction of lentivirus vectors	
*BmRan-3′*UTR	GTCGACGCACAAAATACTGCTCTTCCTGAGGAAGATGAAGACTTATAAATATGATCAACGGATGTACCCAGTGCCCATTTTGTGA TTGGAGGATCATGCAAATGTGTTCAGTGTAGCGTACACTAAATTTTTTCATTCCATTAGGTGATCGCAAATGAACATTATTTTAATAA CTTATTAAACCTTCAATCATTTGCTTTAATTAATGTAAAATCATTAGATAATTTAACACGTAGCTCCTCTAGTTTGAGTTTTATAAAACT GTAATTCTAAACTTTTATATTGAAAGGCAACAAAAATATGAGTATTATTTATGTGTAGTTCATTTTTGTTACAGTTGTCATAAAAACATT TTGCATTGATTGCCCAATATGTGTTAATGCCTATTTGGTCACTGTTATTTATAATACACATGTAAACAAATTTGTATGATAACTCTTTG TAAACCCATAGCATGTACACACATAATATTATAATCTTGAAATTATTTCTTACTTTTGTTACATGCAAGGACTGACAATATTTCACTGA AAAATTGAATTGTGGTGATACTTTTTAAATAAAGTGTAAAAAATGAAGCTT
pre-miR-1	GCCCCTAGCTCATAT GAAATGGACACAGGCACACTA TCAAGGAATGGTGATTTACTCTATAGTCCAGTTGCGAATGGGCAAGTCGGG
pre-miR-3	CTCAAGACGTTAATCGCGGACTATAATTTAAGAATGCGCAGAGATGCACTGC TAGGAGAATTAGCGCGGCTTGAT GAGTTGAGAGATA
Primer sequences for constructed lentiviral expression vectors	
mCherry	F: CGGGATCCCCACCGGTCGCCACCAT R: ACGCGTCGACGGCCGCTACTTGTACAGC
*BmRan-3′*UTR	F: ACGCGTCGACCCAGAAGTTACAATGGATCC R: CCCAAGCTTTGTCAGTCCTTGCATGTAAC
3′UTR-miR-1-mut	F: AGAGGCAACCAAGGCTAGCGCGGTGATTGGAGGATCAT GCAAATG R: CTAGCCTTGGTTGCCTCTGTTGATCATATGTCGA CCTTGTACAGC
3′UTR-miR-3-mut	F: AGATACAGAGCCGCGAAGGTTTGGTCACTGTTATTTATA ATACACATGTAA R: TTCGCGGCTCTGTATCTGGCAATCAATGCAAAATGTTTTT ATG
pre-miR-1	F: GGAATTCGCCCCTAGCTCATATG R: TTAATTAACCCGACTTGCCCATTC
pre-miR-3	F: GGAATTCCTCAAGACGTTAATCGC R: TTAATTAATATCTCTCAACTCATCAAGCC

The single-underlined sequence is the restriction site, the double-underlined is the binding site for BmCPV-miR-1, the wavy-underlined is the binding site for BmCPV-miR-3, the boxed sequences are mature miRNAs.

BmN Cell Transfection

To verify the miRNA regulation on target gene expression in BmN cells, miRNA mimics were transfected into the BmN cells to detect the changes in expression of the target gene. miRNA mimics and NC (sequences shown in **Table 3**) were synthesized by Shanghai GenePharma Co., Ltd. BmN cells were inoculated into a six-well plate 16 h before transfection in which the cell density should be over 60%, and they were divided into three groups, i.e., blank control, NC, and mimics, each group was set for three replicates. In a 1.5 mL EP tube, 3.33 μg of mimics or NC was mixed with serum-free TC-100 medium (Sangon Biotech Co., Ltd., Shanghai, China) up to 25 μL. In another tube, 5 μL of transfection reagent (Entranster^{TM}-R4000, Beijing Engreen) was mixed with 20 μL of serum-free medium and kept at room temperature for 5 min. The solution in the two tubes was mixed thoroughly and left to stand for 15 min before transfection. For the transfection, the medium in the six-well cell culture plate was removed, the mixture solution was added to the cells, and culture medium was added up to 2.5 mL. Cells were collected at 24, 48, and 72 h after the transfection for RNA extraction and qRT-PCR detection of the changes in target gene expression with *Bm*β-*actin* as internal reference.

Verification of miRNA Function in Silkworm

To study the regulation of miRNAs on target genes and their influence on virus replication and proliferation in silkworm larvae, the synthesized miRNA mimics, inhibitors (sequence shown in **Table 3**), and NC were respectively injected into the fifth instar larvae of normal silkworm, 2 μg for each larva. The midgut was dissected at 24, 48, 72, and 96 h after the injection. Total RNA was extracted as described above and the expression level of target gene was detected by qRT-PCR with *Bm*β-*actin* as the internal reference gene.

At the same time, the 5th instar larvae of the silkworm were orally infected with BmCPV, 12 h later, miRNA mimics, inhibitors, and NC were injected respectively into the body cavity of the larvae. At 24, 48, 72, and 96 h after the injection, the midgut tissues were dissected for RNA extraction. Then the replication levels of the second, fifth, and tenth segment of BmCPV genomic RNA were detected respectively by qRT-PCR with *Bm*β-*actin* as internal reference.

TABLE 3 | Sequences of miRNA mimics, inhibitors, and NC.

Name		Sequence (5′–3′)
BmCPV-miR-1	Mimic	GAAAUGGACACAGGCACACUA GUGUGCCUGUGUCCAUUUCUU
	Inhibitor	UAGUGUGCCUGUGUCCAUUUC
BmCPV-miR-3	Mimic	UAGGAGAAUUAGCGCGGCUUGAU CAAGCCGCGCUAAUUCUCCUAUU
	Inhibitor	AUCAAGCCGCGCUAAUUCUCCUA
Negative control (NC)		AGAAGCUUAGUCGUGUCGGAUGA

Statistical Analysis Methods

One-way ANOVA analysis in the GraphPad Prism package was used to analyze the experimental data statistically. The results are shown as the mean ± standard error (SE) of three independent treatments. Asterisks denote significant differences as compared with the control group, as indicated by $^{*}p \leq 0.05$, $^{**}p \leq 0.01$, and $^{***}p \leq 0.001$.

RESULTS

Stem-Loop PCR Identification of BmCPV-miR-1 and BmCPV-miR-3

In our previous small RNA sequencing data (data deposited in NCBI Sequence Read Archive Database[4], accession number SRP158739) of the midgut of BmCPV-infected silkworm larvae, we found two miRNA-like small RNAs encoded by the first and third segment of BmCPV genomic RNA, with the sequencing abundances 1375 and 2710, respectively. They were named BmCPV-miR-1 (sequence: GAAAUGGACACAGGCACACUA, located at the 5P arm of its precursor sequence) and BmCPV-miR-3 (sequence: UAGGAGAAUUAGCGCGGCUUGAU, located at the 3P arm of its precursor sequence). With stem-loop RT-PCR detection, obvious bands were detected in midgut tissue of the 5th instar silkworm larvae infected with BmCPV (**Figure 1A**), with a band size of 70–80 bp respectively, while no bands were detected in midgut tissues of normal larvae, indicating that both BmCPV-miR-1 and BmCPV-miR-3 are derived from BmCPV.

Target Gene Prediction

miRanda and Targetscan software were used to predict the target genes of both BmCPV-miR-1 and BmCPV-miR-3 against the silkworm genome[5]. As a result, *B. mori* GTP-binding nuclear protein Ran gene (*BmRan*, NCBI accession number: NM_001046809.1) was predicted to be the common target gene of these two miRNAs. The binding sites for the two miRNAs are all located in the 3′-UTR region of the *BmRan* mRNA sequence with an interval of 284 nt. The binding site of BmCPV-miR-1 is located at 11∼34 nt and that of BmCPV-miR-3 is located at 319∼339 nt, both with an individual specific region complementary to the seed sequence of the miRNAs. The binding free energy of the two miRNAs to their respective target sites is lower than −20 kcal/mol (BmCPV-miR-1: −20.8 kcal/mol, BmCPV-miR-3: −22.7 kcal/mol). GTP-binding nuclear protein Ran is a 25 kDa protein and an important component of exportin-5-mediated nucleocytoplasmic transport. It is mainly involved in the transport of small RNA from nucleus to cytoplasm (Bischoff and Ponstingl, 1991). In the process of nuclear export of pre-miRNA, exportin-5 binds pre-miRNA in a Ran-GTP dependent manner. The depletion of Ran protein level leads to a significant reduction in nuclear export of pre-miRNA (Yi et al., 2003; Bohnsack et al., 2004; Lund et al., 2004; Wang et al., 2011).

[4]http://www.ncbi.nlm.nih.gov/sra/

[5]https://www.ncbi.nlm.nih.gov/genome/?term=silkworm

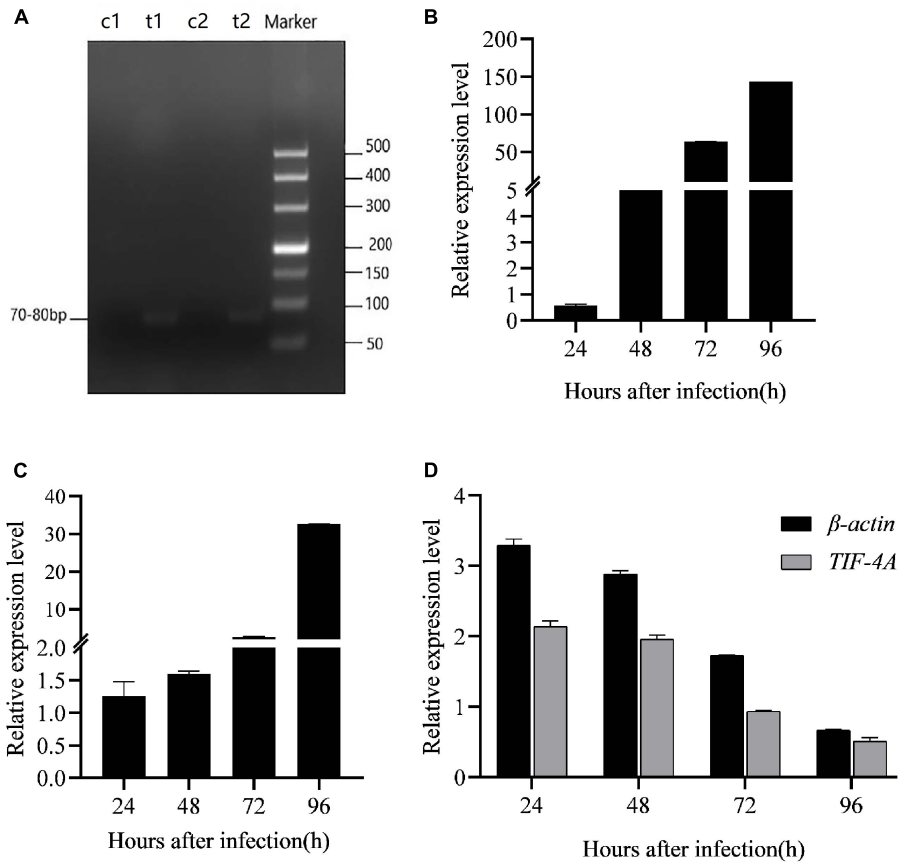

FIGURE 1 | Detection of expression patterns of BmCPV-miRNAs and target gene *BmRan* in the midgut of silkworm larvae infected with BmCPV. **(A)** BmCPV-miR-1 and BmCPV-miR-3 detected by stem-loop RT-PCR. The bands sized about 70–80 bps were the putative miRNAs. c: control; t: BmCPV infected; t1: BmCPV-miR-1; t2: BmCPV-miR-3. **(B)** Expression pattern of BmCPV-miR-1. **(C)** Expression pattern of BmCPV-miR-3. **(D)** Expression pattern of *BmRan* with normalization to different internal reference genes. The expression of BmCPV-miRNAs gradually increased, while the expression of the target gene *BmRan* gradually decreased, as the infection advanced (n = 3 replicate samples, each containing five larvae).

Drosophila exportin-5 can transport pre-miRNA and tRNA (Shibata et al., 2006). However, the mechanism of small RNA transport in the silkworm and its influence factors have not been reported yet. Therefore, the *BmRan* gene of the silkworm was selected in this study to evaluate the function of the two BmCPV-derived miRNAs.

Expression of *BmRan* Is Inversely Correlated With Both BmCPV-miR-1 and BmCPV-miR-3 Levels in the Larvae Infected With BmCPV

Fifth-instar silkworm larvae were inoculated *per os* with BmCPV, and midgut tissues were collected at 12, 24, 48, 72, and 96 h post-infection. Total RNA was extracted for reverse transcription and for detection of the expressional changes of miRNAs and the target gene. The results indicated that the expression level of BmCPV-miR-1 and BmCPV-miR-3 in the virus-infected midgut gradually increased with the advance of infection (**Figures 1B,C**), while the expression of the target gene *BmRan* was gradually downregulated as the time advanced after infection (**Figure 1D**).

To ensure the detection objectivity of the target gene expression, two internal reference genes (*Bm*β*-actin* and *BmTIF-4A*) were used to normalize the qRT-PCR detection data. The overall trend in changes of the target gene expression among the different time points after BmCPV infection was the same, although the calculated expression level of the target genes was slightly different at a specific time point as normalized to different reference genes (**Figure 1D**). It implies that BmCPV-miR-1 and BmCPV-miR-3 might be inversely correlated with the expression of the target gene *BmRan*. It can be speculated that BmCPV-miR-1 and BmCPV-miR-3 have negative regulatory effects on *BmRan*.

BmCPV-miR-1 and BmCPV-miR-3 Negatively Co-regulate Target Gene Expression by Binding to 3′-UTR of *BmRan* mRNA

The constructed expression vectors pLNHX-mCherry-RanUTR and pLNHX-mCherry-RanUTR-mut, both carrying the recombinant target gene consisting of the 731 bp *mCherry* reporter gene and the 570 bp sequence encoding the *BmRan*

mRNA 3′-UTR, were confirmed to be correct by restriction enzyme digestion and sequencing of the inserted fragments. The *mCherry* gene serves here not only as the reporter for successful transfection but also as the substituent target gene for miRNA regulation. On the other hand, the constructed miRNA expression vectors pLKO.3G-miR-1 and pLKO.3G-miR-3 were confirmed by PCR amplification and the specific bands of 87 bp pre-miR-1 and 88 bp pre-miR-3 were detected, then the PCR products were further sequenced as the miRNA precursors of the two miRNAs. These results indicated that the expression vectors were all constructed successfully.

To evaluate the effect of BmCPV-miR-1 and BmCPV-miR-3 bound to the binding sites in 3′-UTR on the expression of the *mCherry* gene (that served as a substituent target gene), HEK293T cells were transfected successively with the above constructed lentiviral expression vectors for mCherry, BmCPV-miR-1, and BmCPV-miR-3. HEK293T cells were firstly co-transfected with the recombinant plasmid pLNHX-mCherry-RanUTR or pLNHX-mCherry-RanUTR-mut and packaging plasmid pVSV-G. After 48 h, about 80% of cells showed red fluorescence (**Figures 2A,B**), indicating that the recombinant expression vector was successfully transfected into the cells and the red fluorescent protein was stably expressed. Then, the HEK293T cells were further transfected with the plasmid pLKO.3G-miR-1 and pLKO.3G-miR-3 respectively, meanwhile another group of cells transfected with the pLKO.3G plasmid were used as NC. The transfection efficiency was about 60% (**Figures 2C–F**) at 20 h post-transfection based on the number of cells showing green fluorescence. Then, cells were collected at 24 and 48 h after transfection of the miRNA expression vectors, and the expression of the miRNAs and the red fluorescent protein gene was quantitatively detected. The expression level of both the miRNAs BmCPV-miR-1 and BmCPV-miR-3 gradually increased with the progression of time

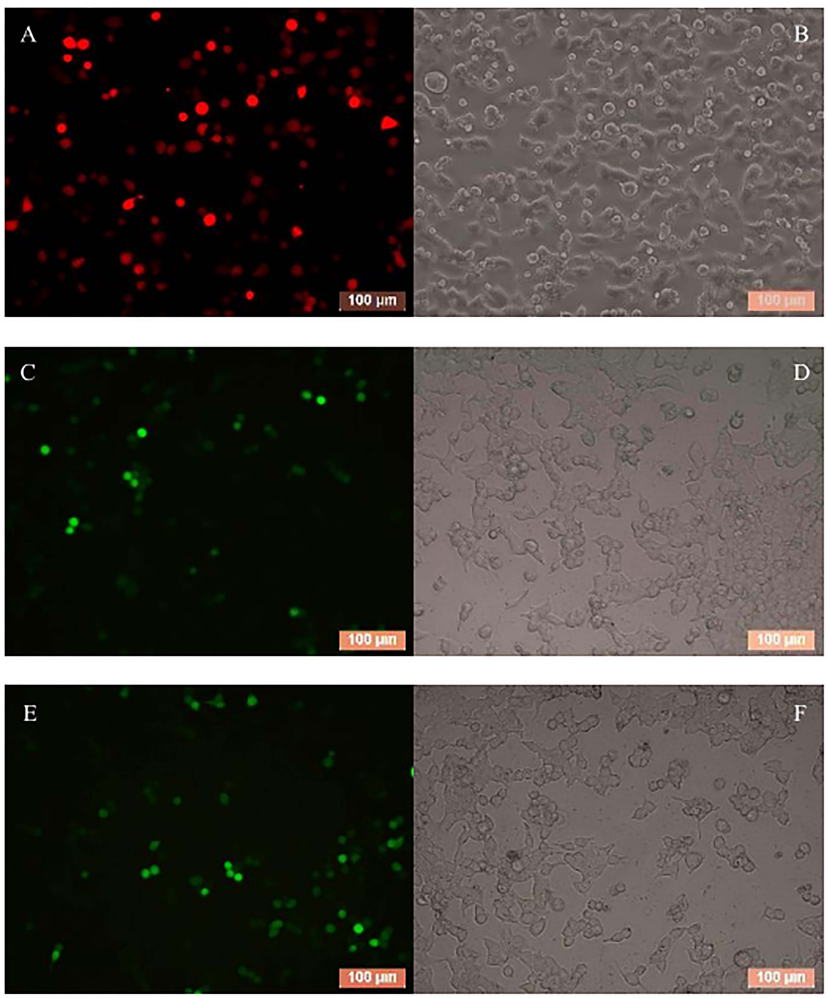

FIGURE 2 | HEK293T cells transfected with the targe gene expression vector pLNHX-mCherry-RanUTR **(A,B)**, the miRNA expression vectors pLKO.3G-miR-1 **(C,D)** and pLKO.3G-miR-3 **(E,F)** respectively. **(A,C,E)** Observed under fluorescent microscope (**A**, under green light; **C,E**, under red light); **(B,D,F)** Observed under optical microscope. Cells showing red fluorescence indicate successful transfection and transfection efficiency of target gene expression vector **(A)**; cells showing green fluorescence indicate the successful transfection and transfection efficiency of miRNA expression vectors **(C,E)**.

after transfection of the miRNA expression vectors as detected by qRT-PCR, indicating that the miRNA expression vectors were not only successfully transfected into HEK293T cells, but the miRNAs were also expressed (**Figure 3A**). At the same time, the expression of the *mCherry* gene in the experimental groups transfected with the miRNA expression vectors decreased (**Figure 3B**), furthermore the downregulated expression of the *mCherry* gene in the cells co-transfected with both pLKO.3G-miR-1 and pLKO.3G-miR-3 was more significant than that in the cells transfected with only pLKO.3G-miR-1 or pLKO.3G-miR-3 (**Figure 4B**). While, the expression level of the *mCherry* gene in the NC cells transfected with pLKO.3G was stable (**Figure 3B**). However, neither pLKO.3G-miR-1 nor pLKO.3G-miR-3 could downregulate the expression of the *mCherry* gene after mutation of the miRNA binding sites on 3′-UTR (**Figure 3B**). These results implied that both pLKO.3G-miR-1 and pLKO.3G-miR-3 could inhibit the expression of the target gene by binding to 3′-UTR of mRNA, and their cooperative action could enhance the repression of the target gene expression.

BmCPV-miR-1 and BmCPV-miR-3 Mimics Negatively Regulate *BmRan* Expression in BmN Cells

In order to validate the regulation effect of the two BmCPV-miRNAs on target gene *BmRan*, BmN cells were transfected respectively with BmCPV-miR-1 and BmCPV-miR-3 mimics or NC. Cells were collected at 24, 48, and 72 h after transfection, and

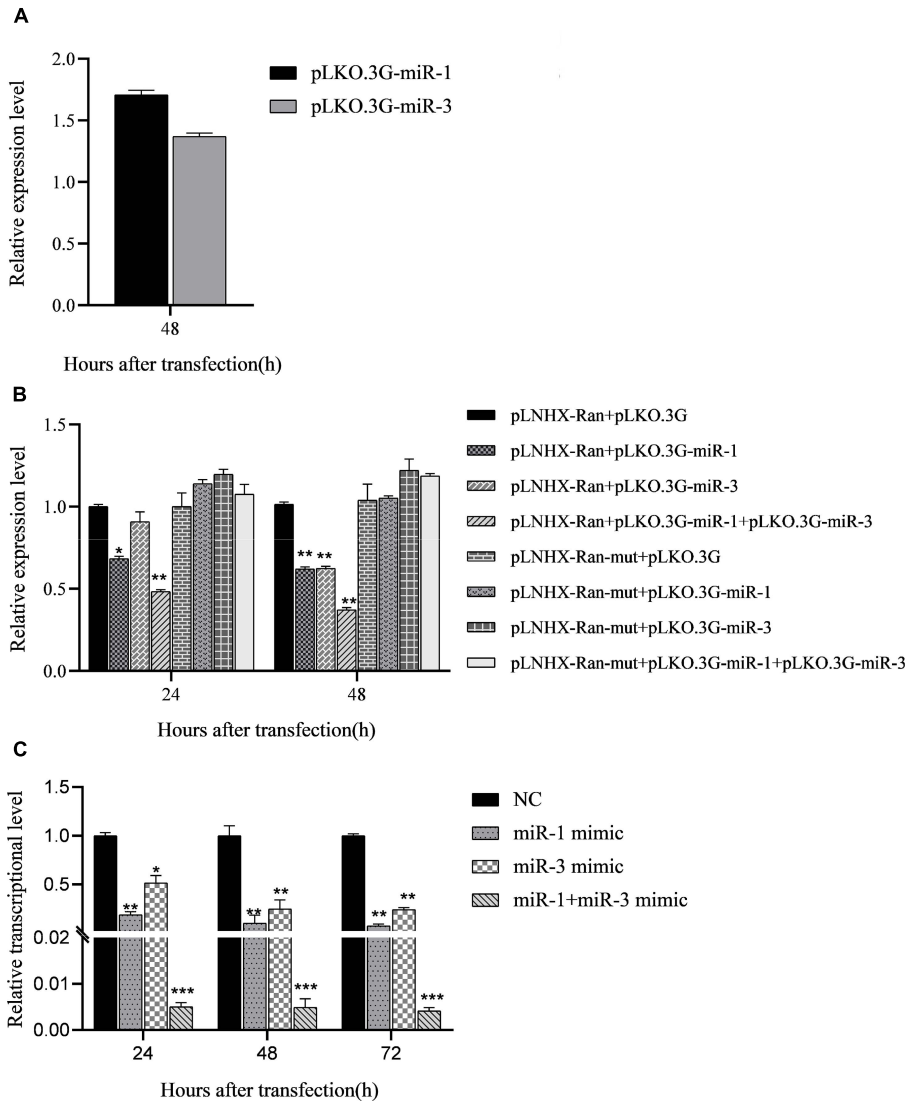

FIGURE 3 | Regulation of BmCPV-miRNAs on the target gene in HEK293T cells and in BmN cells. **(A)** BmCPV-miRNAs were expressed in the transfected HEK293T cells. **(B)** BmCPV-miRNAs downregulate the expression of the substituent target gene *mCherry* in HEK293T cells. pLNHX-Ran: pLNHX-mCherry-RanUTR; pLNHX-Ran-mut: pLNHX-mCherry-RanUTR-mut. **(C)** Regulation of BmCPV-miRNA mimics on expression of target gene *BmRan* in BmN cells ($n = 3$, $^{*}p < 0.05$, $^{**}p < 0.01$, $^{***}p < 0.001$).

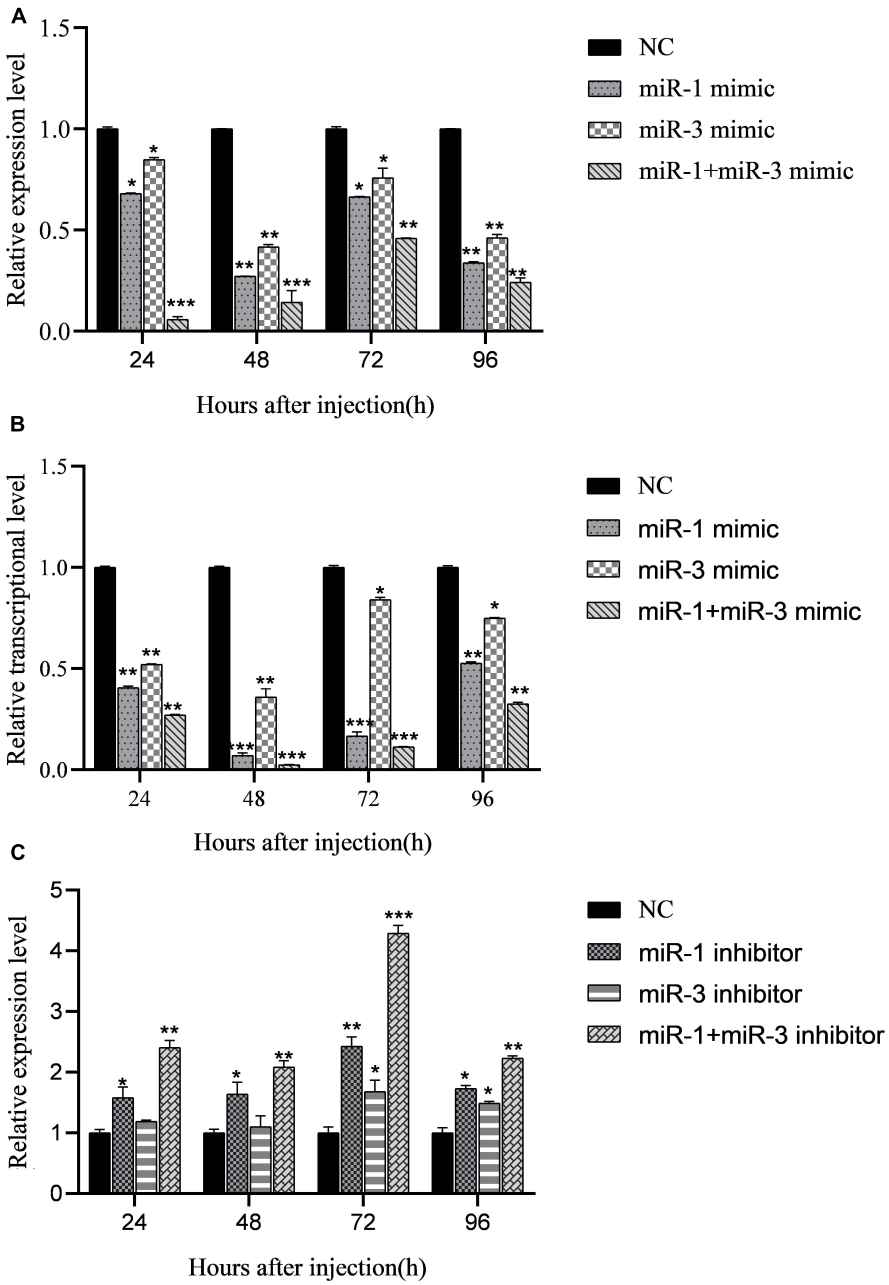

FIGURE 4 | Regulation of miRNA mimics on expression of target gene *BmRan* in midgut of silkworm larvae. Result shows that BmCPV-miRNAs downregulate the expression of *BmRan in vivo* in the silkworm. **(A)** In midgut of normal silkworm larvae. **(B)** In midgut of silkworm larvae infected with BmCPV. **(C)** Regulation of BmCPV-miRNA inhibitors on expression of *BmRan* in midgut of silkworm larvae infected with BmCPV ($n = 3$ replicate samples, each containing five larvae, $^{*}p < 0.05$, $^{**}p < 0.01$, $^{***}p < 0.001$).

the expression changes of the target gene were detected by qRT-PCR. The quantitative detection results (**Figure 3C**) showed that compared with the cells transfected with NC, the expression of the target gene *BmRan* was downregulated in the cells transfected with the BmCPV-miR-1 mimics or BmCPV-miR-3 mimics. At the same time, the expression of the target gene *BmRan* was downregulated more significantly in the cells co-transfected with both the two miRNA mimics (**Figure 3C**). It indicated that the mimics of BmCPV-miR-1 and BmCPV-miR-3 could effectively repress the expression of the *BmRan* gene, and furthermore the repression of the expression was enhanced when the mimics of the two miRNAs acted cooperatively. This is consistent with the regulatory effect of BmCPV-miRNAs on the target gene verified by lentiviral expression vectors in HEK293T cells. These results implied the negative regulation of both BmCPV-miR-1 and BmCPV-miR-3 on expression of the target gene *BmRan*.

BmCPV-miR-1 and BmCPV-miR-3 Downregulate *BmRan* Expression in the Midgut of Silkworm Larvae

To verify the regulatory effects of BmCPV-miR-1 and BmCPV-miR-3 on the expression of the target gene *in vivo* in the silkworm, the mimics of BmCPV-miR-1 and BmCPV-miR-3 were injected into the normal fifth instar larvae separately or jointly to detect the expressional changes of *BmRan*. The larvae injected with NC were used as NC. The results showed that the expression level of the target gene *BmRan* in the midgut of larvae injected with mimics was lower than that in the NC injection group at all the time points of 24, 48, 72, and 96 h after the injection (**Figure 4A**), and further lower in the larvae injected with both the two miRNA mimics. The results indicated that BmCPV-miR-1 and BmCPV-miR-3 could also inhibit the expression of the target gene *BmRan* in silkworm larvae and have a co-operativity in the repression.

At the same time, the mimics and the inhibitors of BmCPV-miR-1 and BmCPV-miR-3 and the NC were injected into the fifth instar larvae infected with BmCPV to further validate the expression changes of the *BmRan* gene. The results showed that the expression level of the *BmRan* gene in the mimic injection groups was also lower than that in the NC group, with the largest decrease of 40.9 times at 48 h (**Figure 4B**), while the expression level in the inhibitor injection groups was higher than that in the NC group (**Figure 4C**) with the highest increase of 4.28 times at 72 h. Furthermore, in the larvae injected with both the two miRNA mimics, the repression of *BmRan* expression was more significantly enhanced, while inhibition of both the miRNAs by injecting both miRNA inhibitors resulted in a much higher *BmRan* expression level. These implied that increasing the level of the BmCPV-miRNAs could inhibit the expression of the *BmRan* gene, while inhibiting the effect of the miRNAs could effectively increase the expression level of the target gene.

Effect of the BmCPV-miRNAs on BmCPV Replication in the Midgut of Silkworm Larvae

The above results verified the negative regulation of the two BmCPV-miRNAs, BmCPV-miR-1 and BmCPV-miR-3, on the target gene *BmRan* both in BmN cells and *in vivo* in the silkworm body. Whether the regulation of BmCPV-miR-1 and BmCPV-miR-3 on the *BmRan* gene affects the replication of the BmCPV genome was also evaluated by injecting the miRNA mimics, inhibitors, and NC into the fifth instar larvae infected with BmCPV and detecting the replication of the second (S2), fifth (S5), and tenth (S10) segment of BmCPV genomic RNA at the time points of 24, 48, 72, and 96 h post-injection. The results showed that the replication levels of the three RNA segments of the viral genome exhibited the same trend, and they all gradually increased with advanced time (**Figure 5**), which indicated viral replication. While, compared with the NC group, the replication level of the three RNA segments in the silkworm larvae injected with the miRNA mimics increased much faster (**Figures 5A1,B1,A2,B2,A3,B3**). However, the replication level of the three RNA segments in the larvae injected with inhibitors was lower than that in the NC group (**Figures 5A1,B1,A2,B2,A3,B3**). Furthermore, increasing the level of both the miRNAs by injecting the two mimics promoted viral replication more significantly than by any single miRNA, while inhibition of both the two miRNAs resulted in further lower replication than inhibition of any single miRNA (**Figures 5C1–C3**). This indicated that the replication of BmCPV was enhanced by increasing the level of miRNAs, but repressed by a decrease of the miRNA level. Therefore, it can be speculated that BmCPV-miR-1 and BmCPV-miR-3 could create a favorable intracellular environment and thus promote virus replication by inhibiting the expression of the target gene *BmRan*.

DISCUSSION

Virus-encoded miRNA plays an important role in the process of virus-host interaction. Its small molecules, non-antigenicity, and target specificity make it a potential strategy for the virus to counter host defense mechanisms. Most of the presently reported viral miRNAs are encoded by DNA viruses, but some RNA viruses can also encode functional miRNAs (Swaminathan et al., 2013; Fani et al., 2018), such as Ebola virus (EBOV) (Liang et al., 2014; Chen et al., 2016; Qiu et al., 2018), hepatitis A virus (HAV) (Shi et al., 2014), bovine leukemia virus (BLV) (Rosewick et al., 2013), and Marek's disease virus (MDV) (Zhao et al., 2011), etc. Studies have shown that one miRNA can target multiple genes, and a target gene can also be regulated by several miRNAs. Generally, miRNA mainly binds to the 3′-UTR of mRNA to repress the target gene translation, and co-operativity between two or more miRNA-binding sites can enhance repression of the mRNA translation (Saetrom et al., 2007; Fang and Rajewsky, 2011; Trobaugh et al., 2014; Liu et al., 2015). On the other hand, some miRNAs bind to the 5′-UTR of mRNA and upregulate the expression of target genes (Jopling et al., 2005; Ørom et al., 2008; Helwak et al., 2013; Hussain et al., 2013). In addition, some miRNAs can also bind to the CDS region and downregulate the expression of the target gene (Hausser et al., 2013; Pan et al., 2017).

Bombyx mori cypovirus has a larger and double-stranded RNA genome, which makes the virus potentially able to encode functional miRNAs, and the miRNAs encoded by the virus might play an important role in the virus-host interaction and in virus replication. In the present study, two miRNAs namely BmCPV-miR-1 and BmCPV-miR-3, which are encoded by the first and third segment of BmCPV genomic RNA, respectively, and their regulatory effects on target genes and then on virus replication and proliferation were studied. BmCPV-miR-1 and BmCPV-miR-3 share a common target gene, *B. mori* GTP-binding nuclear protein Ran (*BmRan*), and their binding sites on *BmRan* mRNA are all located in the 3′-UTR region. qPCR results showed that the expression levels of BmCPV-miR-1 and BmCPV-miR-3 in the midgut of virus-infected larvae gradually increased with the progression of infection, while the expression level of the target gene *BmRan* gradually decreased, indicating that both the two miRNAs were negatively correlated with the expression of target gene *BmRan*. Many virally encoded miRNAs were reported to

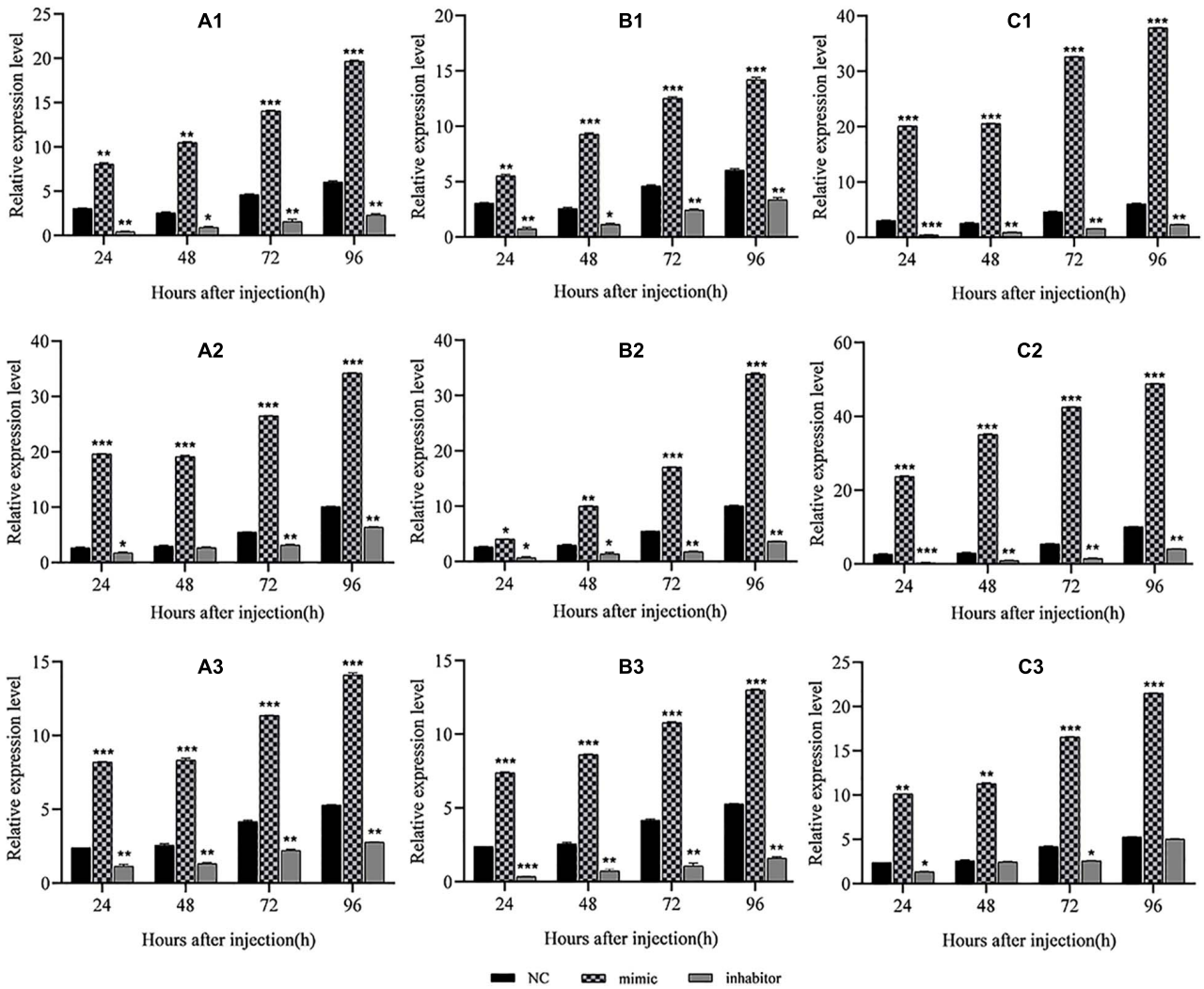

FIGURE 5 | Regulation of miRNA mimics and inhibitors on replication of the BmCPV genome in midgut of silkworm larvae. Result shows that the BmCPV-miRNAs could enhance the replication of BmCPV genomic RNAs. **(A1)** BmCPV-miR-1 to S2; **(B1)** BmCPV-miR-3 to S2; **(C1)** BmCPV-miR-1 + BmCPV-miR-3 to S2; **(A2)** BmCPV-miR-1 to S5; **(B2)** BmCPV-miR-3 to S5; **(C2)** BmCPV-miR-1 + BmCPV-miR-3 to S5; **(A3)** BmCPV-miR-1 to S10; **(B3)** BmCPV-miR-3 to S10; **(C3)** BmCPV-miR-1 + BmCPV-miR-3 to S10. S2, S5, and S10 represent the 2nd, 5th, and 10th segment of BmCPV genomic RNA, respectively ($n = 3$ replicate samples, each containing five larvae, $^{*}p < 0.05$, $^{**}p < 0.01$, $^{***}p < 0.001$).

downregulate the expression of host target genes via binding to the 3′-UTR of their mRNA (Stern-Ginossar et al., 2007; Singh et al., 2012; Skalsky et al., 2012; Fani et al., 2018). Therefore, our results implied that BmCPV-miR-1 and BmCPV-miR-3 might downregulate the expression of the target gene *BmRan*.

At present, the regulation of miRNAs on target genes is mostly verified using the dual luciferase reporter system, but both miRNA and the target gene can only be expressed transiently. However, the lentivirus expression system has the characteristics of high transfection efficiency and expression stability. Therefore, we employed the lentivirus expression vectors to express the miRNAs and the target gene respectively, and to evaluate the interaction between the BmCPV-encoded miRNAs and their shared target gene. In the system, the *mCherry* gene and the cDNA sequence encoding 3′-UTR of *BmRan* mRNA were combined into an expression vector, in which the *mCherry* gene served as both the reporter gene for successful transfection and the substituent target gene for the miRNAs. The results showed that both BmCPV-miR-1 and BmCPV-miR-3 could downregulate the expression of the target gene, and furthermore they had a co-operativity in the regulation.

At the same time, the negative regulation of BmCPV-miR-1 and BmCPV-miR-3 on the target gene *BmRan* was also confirmed in the cultured BmN cells by transfection of miRNA mimics, and *in vivo* in the silkworm by injecting miRNA mimics into both the normal and BmCPV-infected silkworm larvae. Furthermore, injecting miRNA mimics into the larvae enhanced the replication of the tested second, fifth, and tenth segment of the viral genome RNA. This implied that BmCPV-miR-1 and BmCPV-miR-3 encoded by BmCPV might promote the replication and

proliferation of the virus by inhibiting the expression of the target gene *BmRan*.

In plants and invertebrates such as insects, host miRNAs serve as an important antiviral mechanism and degrade viral RNA into siRNAs, which then bind to the virus genome to inhibit viral replication (Ding and Voinnet, 2007; Carl et al., 2013; Bernier and Sagan, 2018). The biological generation of host miRNAs includes the transcription of pri-miRNA containing a stem-loop structure (Lagos-Quintana et al., 2003), which is then digested into pre-miRNA containing a hairpin structure by the Drosha enzyme in the nucleus. Then the pre-miRNA is transported from the nucleus to the cytoplasm, where it is cleaved into mature miRNA by the Dicer enzyme.

GTP-binding nuclear protein Ran is a 25 kDa transporter and serves as an important part of the exportin-5-mediated nucleocytoplasmic transport. It plays an important role in the transport of various non-coding RNAs and proteins from the nucleus to the cytoplasm, and mainly participates in the transport of small RNAs (Bischoff and Ponstingl, 1991). The exportin-5 of Drosophila can transport pre-miRNA and tRNA (Shibata et al., 2006). Research has shown that the nuclear export protein exportin-5 (Exp5) binds specifically to pre-miRNA in a Ran-GTP dependent manner (Yi et al., 2003; Bohnsack et al., 2004; Lund et al., 2004). Then, the pre-miRNA/Exp5/Ran-GTP complex migrates to cytoplasm, where the hydrolysis of Ran-GTP to Ran-GDP induces the release of pre-miRNA. The released pre-miRNA is further processed by the RNase III enzyme called Dicer to release the mature miRNAs (Hutvágner et al., 2001; Ketting et al., 2001). The depletion of Ran results in significant reduction of pre-miRNA export (Yi et al., 2003; Bohnsack et al., 2004; Lund et al., 2004). Other studies have shown that the combination of the pre-miRNA/Exp5/Ran-GTP complex can significantly reduce the efficiency of Dicer cutting pre-miRNA (Kim, 2004; Zeng and Cullen, 2004). In addition, overexpression of the pre-miRNA/Exp5/Ran-GTP complex increased the level of miRNA in the transfected cells, while RNAi-mediated knock-down of the pre-miRNA/Exp5/Ran-GTP complex inhibited the production of mature miRNA. Therefore, the pre-miRNA/Exp5/Ran-GTP complex not only acts as a nuclear export factor for pre-miRNA, but also protects pre-miRNA from degradation, thus promoting the formation of miRNA. Our results indicate that BmCPV-miR-1 and BmCPV-miR-3 may enhance the replication and

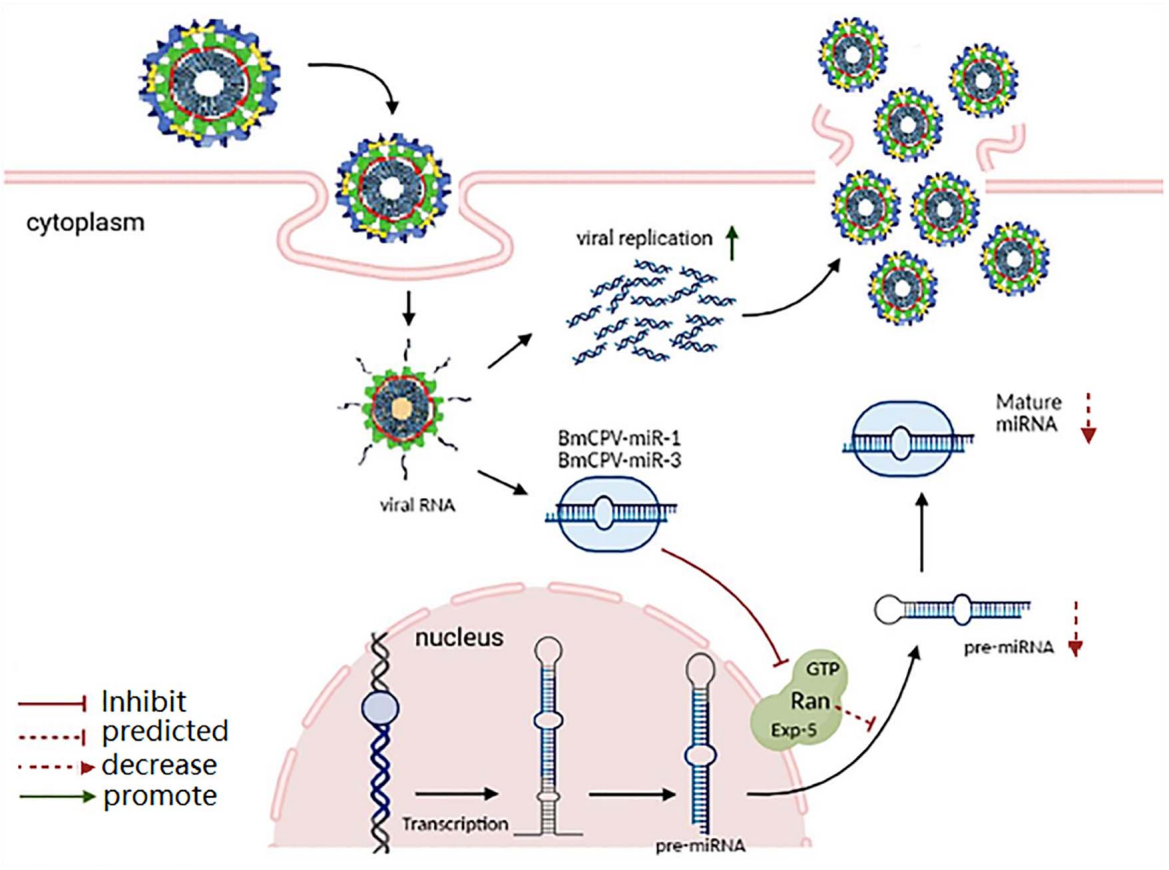

FIGURE 6 | Proposed function mechanism of BmCPV-miR-1 and BmCPV-miR-3 on regulation of the target gene *BmRan* and on replication of BmCPV. BmCPV-miR-1 and BmCPV-miR-3 negatively regulate the translation of the BmRan protein, thus inhibit the transport of pre-miRNA from the nucleus to the cytoplasm in host cells, thereby the population of host miRNAs decreases, consequently creating a favorable intracellular environment for BmCPV genome replication and virus multiplication is enhanced.

proliferation of BmCPV by inhibiting the expression of target gene *BmRan*. The probable reason is that BmCPV-miR-1 and BmCPV-miR-3 bind to the 3′-UTR region of *BmRan* mRNA, negatively regulate the translation of the BmRan protein, thus inhibit the transport of pre-miRNA from the nucleus to the cytoplasm in host cells, reduce the population of host miRNAs, and consequently create a favorable intracellular environment for BmCPV genome replication and virus multiplication. Based on this speculation, the function mechanism of BmCPV-miR-1 and BmCPV-miR-3 on regulation of target gene *BmRan* and on replication of BmCPV is proposed (**Figure 6**). *B. mori* nuclear polyhedrosis virus (BmNPV) is another important virus pathogen of the silkworm, which is a double-stranded DNA virus belonging to *Baculoviridae*. The miRNA bmnpv-miR-1 encoded by BmNPV also represses the expression of *Ran* in the silkworm, leading to the reduction in the host small RNA population, as a consequence, the BmNPV load increases significantly in the infected larvae (Singh et al., 2012). In contrast, blockage of the host miRNA, bmo-miR-8, which targets the immediate-early gene of the virus and whose production was repressed upon bmnpv-miR-1 and Ran dsRNA administration, also resulted in a significant increase in the virus load in the infected silkworm larvae. While inhibition of BmNPV-miR-1 resulted in the significant expression of Ran and the decrease in BmNPV load in the BmNPV-infected larvae (Singh et al., 2012). These results, including those in our present study, provide insights into one of the evasion strategies used by these viruses to counter the host defense for their effective multiplication.

Research on the mechanism of biogenesis of miRNAs by RNA viruses indicated that RNA viruses generate functional miRNAs through non-canonical miRNA biosynthesis pathways. For example, the Drosha enzyme also exists in cytoplasm to cleave pri-miRNA to form pre-miRNA (Shapiro et al., 2012), viruses can encode a protein with the function of the Drosha enzyme to cleave the initial transcripts of miRNA (Kreuze et al., 2005), the tRNase Z in the cytoplasm can cut pri-miRNA into pre-miRNA (Bogerd et al., 2010), and the small stem-loop structure transcripts of the viral genome in the cytoplasm can be directly processed into miRNAs or miRNA-like molecules by the Dicer enzyme (Okamura et al., 2007). Our previous studies identified several miRNAs encoded by BmCPV and have proven that they can regulate the expression of silkworm target genes (Pan et al., 2017; Guo et al., 2020). For example, BmCPV-miR-1 upregulated the expression of another target gene, *B. mori* inhibitor of apoptosis protein (*BmIAP*), by binding to the 5′-UTR of its mRNA and then inhibited the apoptosis of the infected cells, thus facilitating the replication of BmCPV (Pan et al., 2017; Guo et al., 2020). The enhanced replication of the BmCPV genome in the present study should include the contribution from the BmCPV-miR-1 upregulation on *BmIAP*. However, the mechanism with which BmCPV generates the miRNAs requires a further in-depth study in the future.

In summary, the present study revealed the negatively regulatory and co-regulatory function of two BmCPV-encoded putative miRNAs, BmCPV-miR-1 and BmCPV-miR-3, on the host target gene *BmRan*. Furthermore, repression of *BmRan* expression by the two BmCPV-miRNAs enhanced replication of the viral genome. The results might imply one of the strategies employed by the insect virus to modulate miRNA-mediated host antiviral defense by generating miRNAs that inhibits Ran, an important component in miRNA generation.

DATA AVAILABILITY STATEMENT

The original contributions presented in the study are included in the article/supplementary material, further inquiries can be directed to the corresponding author/s.

AUTHOR CONTRIBUTIONS

SL: conceptualization, methodology, investigation, formal analysis, and writing–original draft and editing. YW, ZZ, WW, and YS: methodology, investigation, and formal analysis. ZDZ, MS, and PW: conceptualization, resources, supervision, and writing–original draft. HQ: resources. XG: conceptualization, methodology, funding acquisition, resources, project administration, supervision, and writing–review and editing. All authors contributed to the article and approved the submitted version.

FUNDING

This study was supported by the National Natural Science Foundation of China (Grant No. 31572463).

REFERENCES

Bernier, A., and Sagan, S. M. (2018). The diverse roles of microRNAs at the host-virus interface. *Viruses* 10:440. doi: 10.3390/v10080440

Bischoff, F. R., and Ponstingl, H. (1991). Catalysis of guanine nucleotide exchange on Ran by the mitotic regulator RCC1. *Nature* 354, 80–82.

Bogerd, H. P., Karnowski, H. W., Cai, X., Shin, J., Pohlers, M., and Cullen, B. R. (2010). A mammalian herpesvirus uses noncanonical expression and processing mechanisms to generate viral MicroRNAs. *Mol. Cell* 37, 135–142. doi: 10.1016/j.molcel.2009.12.016

Bohnsack, M. T., Czaplinski, K., and Gorlich, D. (2004). Exportin 5 is a RanGTP-dependent dsRNA-binding protein that mediates nuclear export of pre-miRNAs. *RNA* 10, 185–191. doi: 10.1261/rna.5167604

Cao, G., Meng, X., Xue, R., Zhu, Y., Zhang, X., Pan, Z., et al. (2012). Characterization of the complete genome segments from BmCPV-SZ, a novel *Bombyx mori* cypovirus 1 isolate. *Can. J. Microbiol.* 58, 872–883. doi: 10.1139/w2012-064

Carl, J. W. Jr., Trgovcich, J., and Hannenhalli, S. (2013). Widespread evidence of viral miRNAs targeting host pathways. *BMC Bioinformatics* 14(Suppl. 2):S3. doi: 10.1186/1471-2105-14-S2-S3

Chang, S., Chen, W., and Yang, J. (2009). Another formula for calculating the gene change rate in real-time RT-PCR. *Mol. Biol. Rep.* 36, 2165–2168. doi: 10.1007/s11033-008-9430-1

Chen, C., Ridzon, D. A., Broomer, A. J., Zhou, Z., Lee, D. H., Nguyen, J. T., et al. (2005). Real-time quantification of microRNAs by stem-loop RT-PCR. *Nucleic Acids Res.* 33:e179. doi: 10.1093/nar/gni178

Chen, Z., Liang, H., Chen, X., Ke, Y., Zhou, Z., Yang, M., et al. (2016). An Ebola virus-encoded microRNA-like fragment serves as a biomarker for early diagnosis of Ebola virus disease. *Cell Res.* 26, 380–383. doi: 10.1038/cr.2016.21

Ding, S. W., and Voinnet, O. (2007). Antiviral immunity directed by small RNAs. *Cell* 130, 413–426. doi: 10.1016/j.cell.2007.07.039

Fang, Z., and Rajewsky, N. (2011). The impact of miRNA target sites in coding sequences and in 3′UTRs. *PLoS One* 6:e18067. doi: 10.1371/journal.pone.0018067

Fani, M., Zandi, M., Rezayi, M., Khodadad, N., Langari, H., and Amiri, I. (2018). The Role of microRNAs in the viral infections. *Curr. Pharm. Des.* 24, 4659–4667. doi: 10.2174/1381612825666190110161034

Filipowicz, W., Bhattacharyya, S. N., and Sonenberg, N. (2008). Mechanisms of post-transcriptional regulation by microRNAs: Are the answers in sight?. *Nat. Rev. Genet.* 9, 102–114. doi: 10.1038/nrg2290

Gottwein, E., Mukherjee, N., Sachse, C., Frenzel, C., Majoros, W. H., Chi, J. T., et al. (2007). A viral microRNA functions as an orthologue of cellular miR-155. *Nature* 450, 1096–1099. doi: 10.1038/nature05992

Grimson, A., Farh, K. K., Johnston, W. K., Garrett-Engele, P., Lim, L. P., and Bartel, D. P. (2007). MicroRNA targeting specificity in mammals: determinants beyond seed pairing. *Mol. Cell* 27, 91–105. doi: 10.1016/j.molcel.2007.06.017

Guo, J. Y., Wang, Y. S., Chen, T., Jiang, X. X., Wu, P., Geng, T., et al. (2020). Functional analysis of a miRNA-like small RNA derived from *Bombyx mori* cytoplasmic polyhedrosis virus. *Insect Sci.* 27, 449–462. doi: 10.1111/1744-7917.12671

Hagiwara, K., Rao, S., Scott, S. W., and Carner, G. R. (2002). Nucleotide sequences of segments 1, 3 and 4 of the genome of *Bombyx mori* cypovirus 1 encoding putative capsid proteins VP1, VP3 and VP4, respectively. *J. Gen. Virol.* 83, 1477–1482. doi: 10.1099/0022-1317-83-6-1477

Hausser, J., Syed, A. P., Bilen, B., and Zavolan, M. (2013). Analysis of CDS-located miRNA target sites suggests that they can effectively inhibit translation. *Genome Res.* 23, 604–615. doi: 10.1101/gr.139758.112

Heiss, B. L., Maximova, O. A., Thach, D. C., Speicher, J. M., and Pletnev, A. G. (2012). MicroRNA targeting of neurotropic flavivirus: effective control of virus escape and reversion to neurovirulent phenotype. *J. Virol.* 86, 5647–5659. doi: 10.1128/jvi.07125-11

Helwak, A., Kudla, G., Dudnakova, T., and Tollervey, D. (2013). Mapping the human miRNA interactome by CLASH reveals frequent noncanonical binding. *Cell* 153, 654–665. doi: 10.1016/j.cell.2013.03.043

Hu, X., Chen, F., Zhu, L., Yu, L., Zhu, M., Liang, Z., et al. (2019). *Bombyx mori* cypovirus encoded small peptide inhibits viral multiplication. *Dev. Comp. Immunol.* 96, 51–57. doi: 10.1016/j.dci.2019.02.017

Hussain, M., Walker, T., O'Neill, S. L., and Asgari, S. (2013). Blood meal induced microRNA regulates development and immune associated genes in the Dengue mosquito vector, *Aedes aegypti*. *Insect Biochem. Mol. Biol.* 43, 146–152. doi: 10.1016/j.ibmb.2012.11.005

Hutvágner, G., McLachlan, J., Pasquinelli, A. E., Bálint, E., Tuschl, T., and Zamore, P. D. (2001). A cellular function for the RNA-interference enzyme Dicer in the maturation of the let-7 small temporal RNA. *Science* 293, 834–838. doi: 10.1126/science.1062961

Jiang, L. (2021). Insights into the antiviral pathways of the silkworm *Bombyx mori*. *Front. Immunol.* 12:639092. doi: 10.3389/fimmu.2021.639092

Jopling, C. L., Yi, M., Lancaster, A. M., Lemon, S. M., and Sarnow, P. (2005). Modulation of hepatitis C virus RNA abundance by a liver-specific MicroRNA. *Science* 309, 1577–1581. doi: 10.1126/science.1113329

Ketting, R. F., Fischer, S. E., Bernstein, E., Sijen, T., Hannon, G. J., and Plasterk, R. H. (2001). Dicer functions in RNA interference and in synthesis of small RNA involved in developmental timing in C. elegans. *Genes Dev.* 15, 2654–2659. doi: 10.1101/gad.927801

Kim, V. N. (2004). MicroRNA precursors in motion: exportin-5 mediates their nuclear export. *Trends Cell Biol.* 14, 156–159. doi: 10.1016/j.tcb.2004.02.006

Kreuze, J. F., Savenkov, E. I., Cuellar, W., Li, X., and Valkonen, J. P. (2005). Viral class 1 RNase III involved in suppression of RNA silencing. *J. Virol.* 79, 7227–7238. doi: 10.1128/jvi.79.11.7227-7238.2005

Lagos-Quintana, M., Rauhut, R., Meyer, J., Borkhardt, A., and Tuschl, T. (2003). New microRNAs from mouse and human. *RNA* 9, 175–179.

Liang, H., Zhou, Z., Zhang, S., Zen, K., Chen, X., and Zhang, C. (2014). Identification of Ebola virus microRNAs and their putative pathological function. *Sci. China Life Sci.* 57, 973–981. doi: 10.1007/s11427-014-4759-2

Liu, G., Zhang, R., Xu, J., Wu, C. I., and Lu, X. (2015). Functional conservation of both CDS- and 3′-UTR-located microRNA binding sites between species. *Mol. Biol. Evol.* 32, 623–628. doi: 10.1093/molbev/msu323

Lund, E., Güttinger, S., Calado, A., Dahlberg, J. E., and Kutay, U. (2004). Nuclear export of microRNA precursors. *Science* 303, 95–98. doi: 10.1126/science.1090599

Okamura, K., Hagen, J. W., Duan, H., Tyler, D. M., and Lai, E. C. (2007). The mirtron pathway generates microRNA-class regulatory RNAs in *Drosophila*. *Cell* 130, 89–100. doi: 10.1016/j.cell.2007.06.028

Ørom, U. A., Nielsen, F. C., and Lund, A. H. (2008). MicroRNA-10a binds the 5′UTR of ribosomal protein mRNAs and enhances their translation. *Mol. Cell* 30, 460–471. doi: 10.1016/j.molcel.2008.05.001

Pan, Z. H., Wu, P., Gao, K., Hou, C. X., Qin, G. X., Geng, T., et al. (2017). Identification and characterization of two putative microRNAs encoded by *Bombyx mori* cypovirus. *Virus Res.* 233, 86–94. doi: 10.1016/j.virusres.2017.03.009

Qiu, G. H., Weng, Z. H., Hu, P. P., Duan, W. J., Xie, B. P., Sun, B., et al. (2018). Synchronous detection of ebolavirus conserved RNA sequences and ebolavirus-encoded miRNA-like fragment based on a zwitterionic copper (II) metal-organic framework. *Talanta* 180, 396–402. doi: 10.1016/j.talanta.2017.12.045

Rosewick, N., Momont, M., Durkin, K., Takeda, H., Caiment, F., Cleuter, Y., et al. (2013). Deep sequencing reveals abundant noncanonical retroviral microRNAs in B-cell leukemia/lymphoma. *Proc. Natl. Acad. Sci. U.S.A.* 110, 2306–2311. doi: 10.1073/pnas.1213842110

Saetrom, P., Heale, B. S., Snøve, O. Jr., Aagaard, L., Alluin, J., and Rossi, J. J. (2007). Distance constraints between microRNA target sites dictate efficacy and cooperativity. *Nucleic Acids Res.* 35, 2333–2342. doi: 10.1093/nar/gkm133

Shapiro, J. S., Langlois, R. A., Pham, A. M., and Tenoever, B. R. (2012). Evidence for a cytoplasmic microprocessor of pri-miRNAs. *RNA* 18, 1338–1346. doi: 10.1261/rna.032268.112

Shi, J., Duan, Z., Sun, J., Wu, M., Wang, B., Zhang, J., et al. (2014). Identification and validation of a novel microRNA-like molecule derived from a cytoplasmic RNA virus antigenome by bioinformatics and experimental approaches. *Virol. J.* 11:121. doi: 10.1186/1743-422x-11-121

Shibata, S., Sasaki, M., Miki, T., Shimamoto, A., Furuichi, Y., Katahira, J., et al. (2006). Exportin-5 orthologues are functionally divergent among species. *Nucleic Acids Res.* 34, 4711–4721. doi: 10.1093/nar/gkl663

Singh, C. P., Singh, J., and Nagaraju, J. (2012). A baculovirus-encoded MicroRNA (miRNA) suppresses its host miRNA biogenesis by regulating the exportin-5 cofactor Ran. *J. Virol.* 86, 7867–7879. doi: 10.1128/jvi.00064-12

Skalsky, R. L., Corcoran, D. L., Gottwein, E., Frank, C. L., Kang, D., Hafner, M., et al. (2012). The viral and cellular microRNA targetome in lymphoblastoid cell lines. *PLoS Pathog.* 8:e1002484. doi: 10.1371/journal.ppat.1002484

Stern-Ginossar, N., Elefant, N., Zimmermann, A., Wolf, D. G., Saleh, N., Biton, M., et al. (2007). Host immune system gene targeting by a viral miRNA. *Science* 317, 376–381. doi: 10.1126/science.1140956

Swaminathan, G., Martin-Garcia, J., and Navas-Martin, S. (2013). RNA viruses and microRNAs: challenging discoveries for the 21st century. *Physiol. Genomics* 45, 1035–1048. doi: 10.1152/physiolgenomics.00112.2013

Swevers, L., Feng, M., Ren, F., and Sun, J. (2020). Antiviral defense against Cypovirus 1 (Reoviridae) infection in the silkworm, *Bombyx mori*. *Arch. Insect Biochem. Physiol.* 103:e21616.

Trobaugh, D. W., Gardner, C. L., Sun, C., Haddow, A. D., Wang, E., Chapnik, E., et al. (2014). RNA viruses can hijack vertebrate microRNAs to suppress innate immunity. *Nature* 506, 245–248. doi: 10.1038/nature12869

Wang, X., Xu, X., Ma, Z., Huo, Y., Xiao, Z., Li, Y., et al. (2011). Dynamic mechanisms for pre-miRNA binding and export by Exportin-5. *RNA* 17, 1511–1528. doi: 10.1261/rna.2732611

Yi, R., Qin, Y., Macara, I. G., and Cullen, B. R. (2003). Exportin-5 mediates the nuclear export of pre-microRNAs and short hairpin RNAs. *Genes Dev.* 17, 3011–3016. doi: 10.1101/gad.1158803

Zeng, Y., and Cullen, B. R. (2004). Structural requirements for pre-microRNA binding and nuclear export by Exportin 5. *Nucleic Acids Res.* 32, 4776–4785. doi: 10.1093/nar/gkh824

Zhao, Y., Xu, H., Yao, Y., Smith, L. P., Kgosana, L., Green, J., et al. (2011). Critical role of the virus-encoded microRNA-155 ortholog in the induction of Marek's disease lymphomas. *PLoS Pathog.* 7:e1001305. doi: 10.1371/journal.ppat.1001305

Zhao, Y., Yao, Y., Xu, H., Lambeth, L., Smith, L. P., Kgosana, L., et al. (2009). A functional MicroRNA-155 ortholog encoded by the oncogenic Marek's disease virus. *J. Virol.* 83, 489–492. doi: 10.1128/jvi.01166-08

Conflict of Interest: The authors declare that the research was conducted in the absence of any commercial or financial relationships that could be construed as a potential conflict of interest.

Publisher's Note: All claims expressed in this article are solely those of the authors and do not necessarily represent those of their affiliated organizations, or those of the publisher, the editors and the reviewers. Any product that may be evaluated in this article, or claim that may be made by its manufacturer, is not guaranteed or endorsed by the publisher.

Advantages of publishing in Frontiers

OPEN ACCESS
Articles are free to read for greatest visibility and readership

FAST PUBLICATION
Around 90 days from submission to decision

HIGH QUALITY PEER-REVIEW
Rigorous, collaborative, and constructive peer-review

TRANSPARENT PEER-REVIEW
Editors and reviewers acknowledged by name on published articles

Frontiers
Avenue du Tribunal-Fédéral 34
1005 Lausanne | Switzerland

Visit us: www.frontiersin.org
Contact us: frontiersin.org/about/contact

REPRODUCIBILITY OF RESEARCH
Support open data and methods to enhance research reproducibility

DIGITAL PUBLISHING
Articles designed for optimal readership across devices

FOLLOW US
@frontiersin

IMPACT METRICS
Advanced article metrics track visibility across digital media

EXTENSIVE PROMOTION
Marketing and promotion of impactful research

LOOP RESEARCH NETWORK
Our network increases your article's readership